

# **Colistin: understanding the mechanism of action and the causes of treatment failure**

**Akshay Sabnis**

A thesis submitted for the degree of Doctor of Philosophy

March 2022

MRC Centre for Molecular Bacteriology and Infection

Department of Infectious Disease

Imperial College London

## **Declaration of Originality**

I can confirm that the work in this thesis is my own, and that any work performed by anyone other than myself has been appropriately credited, referenced and acknowledged. Time-of-flight mass spectrometry analysis of BoDipy-labelled polymyxin compounds was performed in collaboration with Lisa Haigh (Department of Chemistry, Imperial College London). MALDI-TOF-based lipidomic mass spectrometry was performed in collaboration with Gerald Larrouy-Maumus and Katheryn Hagart (Department of Life Sciences, Imperial College London). SEM images were obtained in collaboration with Anna Klöckner, Michele Becce and Molly Stevens (Department of Materials, Imperial College London). Mouse experiments were performed in collaboration with Tom Clarke (Department of Infectious Disease, Imperial College London). Strains used in this work were obtained from: Laura Nolan, Alain Filloux, Richard Sequeira, Ali Reza Abdolrasouli, Marc Dionne, Aisha Krishna, Ronan Murphy, Ollie Fletcher, Jane Davies, Hala Abbas, Alison Holmes, Chris Furniss and Despoina Mavridou (all Imperial College London). Fluorescence microscopy was performed using the microscope belonging to Vlad Pelicic. Diagrams were created using BioRender.

## **Copyright Declaration**

The copyright of this thesis rests with the author and is made available under a Creative Commons Attribution-Non-Commercial-No Derivatives 4.0 International Licence (CC BY-NC-ND). Under this licence, researchers are free to copy, distribute or transmit the thesis in any medium or format on the condition that they attribute it to the author, that they do not use it for commercial purposes and that they do not alter, transform or build upon it. For any reuse or redistribution, researchers must make clear to others the licence term of this work by naming the licence and linking to the licence text. Please seek permission from the copyright holder for uses of this work that are not included in this licence or permitted under UK Copyright Law.

~ ~ ~

*“Remember to look up at the stars and not down at your feet. Try to make sense of what you see and wonder about what makes the universe exist. Be curious.”*

~ ~ ~

*“Normal is boring.”*

~ ~ ~

*“The most important thing that I've found, that perhaps you could use, is be passionate and enthusiastic in the direction that you choose in life, and you'll be a winner.”*

~ ~ ~

## Acknowledgements

It will come as little surprise to those who know me that this acknowledgement section is not going to be a short one. There are so many people to thank, so many people who have made this work possible, and so many people who have got me through this PhD that it is difficult to know where even to start. However, the first person I would like to acknowledge is my supervisor, Andy. As you know, Andy, I was very nervous when I first asked you if I could do a PhD in your group, but it was absolutely the best decision and I'm incredibly fortunate that you agreed. Thank you for the trust you showed in me and for believing in my ideas (even when they seemed improbable), thank you for always being so supportive and encouraging, and most of all, thank you for making me smile and laugh every day of my PhD, whether it was about cricket or politics or any old nonsense. Through your amazing supervision, you have given me every opportunity to succeed in my future, and for that I will be eternally grateful. I hope, one day, to be even half the boss you were to me.

Thank you also to my co-supervisor, Ramesh, for allowing me to be independent, but also for being a source of inspiration and help when I needed it. Many thanks must go to Alain and Sophie, my Progress Review Panel – your kind words during my ESA/LSR assessments were highly motivating, and your suggestions for future work and experiments always very helpful. In addition, I would like to give a huge thank you to all the PIs who I collaborated with during my PhD – Tom (for help with the mouse work, LAL assays and general advice), Gerald (for offering his lipidomics expertise), Jane (for providing the clinical angle to my work that I desperately wanted), Alison (for introducing me to her extraordinary CPE Working Group), Freya (for her permanent enthusiasm) and Abhi (for being patient while explaining complex mathematical models). My PhD work would have been much less interesting and exciting without your intellectual contributions, so I am hugely indebted to you all. Additionally, I would like to take this opportunity to thank all the technical/support staff, and especially Alex, who work behind the scenes tirelessly to make doing lab work as easy as possible.

I also wish to acknowledge the people who first got me started on this bacteriology research journey. Thank you to my mentor, John, for offering me my first taste of academic lab life in your group as an undergraduate, and for constantly keeping an eye to make sure I'm doing alright ever since. Thank you to my PhD supervisor for that project, Simren, who was the most patient, but also trusting teacher, with whom I worked on *Pseudomonas* for the very first time – you were a big part of my decision to pursue a PhD myself. Thank you to the two PIs who supervised me during my final-year BSc project, Sandra and Paul, for teaching me all about antimicrobial peptides, and to Jasmeet, for pushing to get the best out of me during those three months. Thank you to Despoina and Chris for your supervision of my Master's research project – I learnt so much from both of you in such a short space of time, and I'm

sure those lessons will prove useful to me throughout my career. And most of all, the biggest thank you to Vera, who guided me right the way through the early stages of this PhD. Vera, you have become like a big sister to me – I'll always remember the endless laughs about Hindi movies, the daily sports catch-up, but also everything you taught me about science and life. Both your humility and your wonderful supervision skills with students stand out in particular to me, and are two of your many exceptional traits that I have always aspired to emulate.

On the subject of supervising students, I absolutely need to dedicate a massive thank you to the brilliant undergraduate and Master's students that I was lucky enough to teach and work alongside during my PhD. Supervising you has been the most enormous joy of the last four years that I have enjoyed every bit as much as my experiments; you are all remarkable in your own unique ways, but absolutely united in your dedication, hard-work, and above all else, your kindness. Thank you to Hina, my very first student, for sharing in that London energy, and for not being too harsh on me whilst I had almost no idea how to supervise. Thank you to Adrianna – I'm not sure I'll ever be able to forget your hilarious grandad stories that made me laugh the most I ever have in the lab. Thank you to Ashim – even though you were 5,000 miles away, your commitment never wavered and you always reminded me of home. Thank you to Dan for your diligent characterisation of a huge panel of clinical isolates. Thank you to Ruta (the bioinformatics expert) and Hugo (a fellow Liverpool fan) – your ability to thrive in the most unusual circumstances with only remote supervision was incredibly impressive. Thank you to Maddy – I'm not sure I've seen anyone spill quite as many bacterial cultures over their clothes on a regular basis, but supervising you was always entertaining and full of smiles, whether you were hurling plates in the bin from a height, or angrily watching the Euros football matches. Thank you to Maddie – as awkward as our first meeting setting up a computer was, I'm so glad we've progressed to be friends who can write stupid riddles about students and cry laughing about what CNR stands for. And lastly, a big thank you to Amber, the only student who was tolerant enough of my nonsense to put up with it for a while longer by coming back to do a PhD. Amber, thanks for always being optimistic and helping me through those tougher days, for being a fellow lab singer/dancer, and for not slapping me after the daily loud "Good morning". To each and every one of these students – I couldn't be more proud seeing how you have all progressed, and I'm so excited to see what the future holds for you all.

I would also like to thank all the members of Andy's group that have formed a giant part of my PhD journey since 2017. The group has always been an environment that is happy, enjoyable and full of funny chats, and that has made it so easy to wake up in the morning looking forward to a day in the lab, even maybe when experiments aren't going to plan. Thank you to Nisha for the cheesy humour. To Aisha for accepting bins falling. To Kam Pou for the lessons on both chopsticks and cloning, maybe at the same time. To Becky for joining the Greg

James fan club. To Anna for the regular supply of Haribo and the chlamydia information. To Lindsay for the chemistry genius. To Brigitte for her knowledge of the Devil and French culinary advice. To Simon for saving me from being the only *Pseudomonas* freak in the lab. And a huge thanks to Lizzie, who has been right there since day one. Lizzie, thank you for bearing my non-stop chatter (even at the expense of missing time-points), for being a fellow swamp monster carer, for listening to our favourite song “Bandages”, and especially for always having an answer to my lab conundrums. To these fabulous colleagues – I’m really going to miss working with all of you, even if I’ve only moved one floor up.

It’s not just Andy’s group that have made the fifth floor of the Flowers Building such a fantastic workplace, and a large acknowledgement must go to the members of the other groups who have also been an absolute joy to have shared the last few years with: Amelia, Ali, Leon, Luis, Louis, Tom, Renad, Becky, Christine, Max, Rekha, Chryso, Nikol, Alec, Joey, Helene, Julien and many, many others... I’ll never forget the days I’ve spent in your company, whether we were gobbling down cake by the food table, fighting over White Elephant presents, or trying to get better at bouldering. There are 3 fifth floor colleagues to whom I would like to express my particular gratitude. To Herb, whose regular presence on the weekends was reassuring and who I could rely on to get the latest football scores from the weekend. To Ricky, who was full of suggestions for podcasts to listen to, who had to put up with my voice droning on as he was trying to dissect mice, who tried (mostly unsuccessfully) to scare me, and who now lives too far away in Australia. And finally to Erin, whose niceness and chattiness was apparent even on a very first impression, who had to face the shame of paying for her Gail’s while I got mine for free, who brightens every day by showing off photos of her golden retriever Link, and who was willing to pay money to feature in this list of acknowledgements. Thank you also to the many members of the CMBI on other floors who have helped me along the way, be that through their questions in seminars, or by taking my mind off work at social events.

Thank you to all the friends from outside work that have been absolutely instrumental in me finishing this PhD, especially friends from College and the Extras. You have all helped to provide perspective and given me an excuse not to be in the lab on weekends. An especially large thank you to the friends from the UK Biocentre in Milton Keynes, who made the truly challenging time during the Covid-19 pandemic a little better – you all turned that experience into an unforgettably awesome one, and I’m thrilled we’ve been able to stay in contact in more normal times. And finally, words alone are entirely insufficient to express how grateful I am to my family for their eternal love and support throughout my education – I’m sure you will all be relieved to know that I have got to the end of this road. Thank you for always being the biggest cheerleaders of my work (even if it didn’t always make sense), for guiding and inspiring me every single day, and for being the rocks I can always count on.

## Abstract

The rapid rise in the prevalence of pathogenic bacteria that are resistant to front-line antibiotic drugs has necessitated a simultaneous upsurge in the use of “last-resort” antimicrobial agents. Colistin is one such antibiotic of last-resort that is increasingly used in the clinic as a salvage therapy to treat infections caused by multi-drug resistant Gram-negative microorganisms, including *Pseudomonas aeruginosa* and *Escherichia coli*. Unfortunately, despite its growing importance, colistin treatment is toxic, frequently fails, and resistance to the antibiotic is an intensifying threat. There is, therefore, a crucial requirement to augment the efficacy of colistin therapy, but efforts to do so are hampered by a lack of understanding about the drug’s mechanism of action.

The work in this thesis initially uncovered a novel process by which colistin-susceptible *P. aeruginosa* cells survive exposure to the antibiotic, through the extracellular release of lipopolysaccharide (LPS) molecules that inactivate colistin in the external environment. In attempting to overcome this mode of drug tolerance by inhibiting LPS biosynthesis, critical insight into colistin’s bactericidal mechanism was obtained – namely, that the antibiotic kills Gram-negative bacteria by targeting LPS in the cytoplasmic membrane, not by interacting with membrane phospholipids, as previously thought. This finding in turn led to investigations about the site where colistin resistance, mediated by cationic chemical modifications to LPS, was conferred. It was shown that resistance to colistin in *P. aeruginosa* and *E. coli*, acquired through the harbouring of diverse plasmid-borne mobile colistin resistance (*mcr*) genes or chromosomal mutations, was in fact conferred at the cytoplasmic membrane, as opposed to the outer membrane of bacterial cells. Subsequent experiments revealed that intrinsic colistin resistance in *Burkholderia cenocepacia* was mediated at the outer membrane, and that strains of *Enterobacter cloacae* possess a unique inducible form of hetero-resistance to colistin.

After characterising the mode of action of colistin and a number of potential causes of colistin treatment failure, new combination treatment strategies were designed to improve the effectiveness of colistin therapy. Using murepavadin, an inhibitor of the LPS transport system in pre-clinical development, to accumulate LPS in the cytoplasmic membrane proved to be particularly potent at amplifying the bactericidal activity of colistin *in vitro* against clinical isolates, in an *in vivo* murine lung infection model, and for overcoming colistin resistance. Furthermore, the capacity for colistin to permeabilise the outer membrane of colistin-resistant bacteria was exploited to re-sensitise Gram-negative pathogenic organisms to rifampicin, an antibiotic which normally cannot traverse the cell envelope. In summary, this work has identified how colistin works and why it often fails clinically, as well as providing urgently-needed novel solutions to enhance colistin efficacy and patient outcomes.

# Table of Contents

<b>Declaration of Originality</b> .....	2
<b>Copyright Declaration</b> .....	2
<b>Acknowledgements</b> .....	4
<b>Abstract</b> .....	7
<b>Table of Contents</b> .....	8
<b>List of Abbreviations</b> .....	13
<b>List of Figures</b> .....	17
<b>List of Tables</b> .....	21
<b>Chapter 1: Introduction</b> .....	22
1.1    The pathogen <i>Pseudomonas aeruginosa</i> .....	22
1.1.1    General characteristics of <i>P. aeruginosa</i> .....	22
1.1.2 <i>P. aeruginosa</i> as an opportunistic pathogen .....	23
1.2    Treatment of <i>P. aeruginosa</i> infections .....	25
1.2.1    Prevention .....	25
1.2.2    Beta-lactam antibiotics.....	26
1.2.3    Quinolone antibiotics .....	27
1.2.4    Aminoglycoside antibiotics .....	27
1.2.5    Combination therapy.....	28
1.2.6    Resistance to front-line antibiotics.....	28
1.3    Lipopolysaccharide as an antibiotic target .....	33
1.3.1    Lipopolysaccharide biosynthesis .....	33
1.3.2    Inhibitors of LPS biosynthesis .....	38
1.3.3    LPS transport.....	41
1.3.4    Inhibitors of LPS transport .....	45
1.4    Colistin, a last-resort antibiotic.....	48
1.4.1    Colistin discovery, structure and chemistry.....	48
1.4.2    Clinical use of colistin.....	50
1.4.3    Colistin dosing and pharmacokinetics .....	51
1.4.4    Colistin toxicity .....	54
1.4.5    Colistin's mechanism of action .....	55
1.5    Colistin resistance .....	59
1.5.1    Intrinsic colistin resistance .....	59
1.5.2    Acquired chromosomal colistin resistance .....	60



1.5.3	Acquired plasmid-mediated colistin resistance.....	64
1.5.4	Prevalence of colistin resistance in <i>P. aeruginosa</i> .....	68
1.6	Colistin treatment failure in <i>P. aeruginosa</i> infections .....	70
1.7	Hypothesis and aims of the project .....	72
<b>Chapter 2: Materials and Methods .....</b>		<b>73</b>
2.1	Bacterial strains and growth conditions .....	73
2.2	Determination of antibiotic MICs .....	73
2.3	Determination of outer membrane disruption .....	76
2.4	Beta-lactamase release assay.....	76
2.5	Cytoplasmic membrane disruption of whole cells .....	77
2.6	Determination of bactericidal activity of antibiotics .....	77
2.7	Determination of lysis in whole cells .....	78
2.8	Emergence of colistin resistance assay .....	78
2.9	Zone of inhibition assay.....	78
2.10	Fluorescent labelling of polymyxin compounds .....	79
2.11	Determination of antibiotic binding to bacterial cells .....	79
2.12	Determination of membrane lipid release from bacteria .....	80
2.13	Bacterial growth assay .....	80
2.14	Limulus amoebocyte lysate assay .....	80
2.15	LPS detection/quantification by silver staining.....	81
2.16	Scanning electron microscopy .....	81
2.17	Isolation of CHIR-090 resistant mutants .....	82
2.18	Determination of surface LPS levels with BoDipy-PMBN.....	82
2.19	Phase-contrast and fluorescence microscopy .....	83
2.20	Generation of spheroplasts .....	83
2.21	Confirmation of successful spheroplast formation .....	83
2.22	Lipidomic analysis by MALDI-TOF mass spectrometry .....	84
2.23	Determination of CM disruption/lysis in spheroplasts .....	85
2.24	Determination of membrane fluidity.....	85
2.25	Determination of membrane charge.....	86
2.26	Population analysis profiling.....	86
2.27	Luria-Delbrück fluctuation test assays .....	86
2.28	Bacterial competition experiments .....	87
2.29	Murine lung infection model.....	87
2.30	Statistical analysis.....	88

<b>Chapter 3: <i>Pseudomonas aeruginosa</i> survives colistin exposure by releasing lipopolysaccharide</b> .....	89
3.1 Introduction .....	89
3.2 Colistin causes sequential disruption of the <i>P. aeruginosa</i> cell membranes .....	90
3.3 Colistin-mediated killing of <i>P. aeruginosa</i> is bi-phasic .....	93
3.4 The bi-phasic killing of <i>P. aeruginosa</i> is not due to the emergence of colistin resistance ....	95
3.5 Colistin activity is lost during exposure of <i>P. aeruginosa</i> .....	96
3.6 <i>P. aeruginosa</i> directly inactivates colistin .....	98
3.7 <i>P. aeruginosa</i> inactivates colistin by releasing a non-lipid, heat-stable factor.....	100
3.8 The colistin inactivator released by <i>P. aeruginosa</i> is not capsular polysaccharide .....	102
3.9 <i>P. aeruginosa</i> releases LPS during exposure to colistin.....	104
3.10 Extracellular LPS reduces colistin activity and promotes survival of <i>P. aeruginosa</i> .....	106
3.11 Colistin-resistant <i>P. aeruginosa</i> cannot inactivate colistin.....	108
3.12 The ability to inactivate colistin is conserved across Gram-negative pathogens .....	109
3.13 Colistin-induced LPS release from <i>P. aeruginosa</i> requires <i>de novo</i> LPS biosynthesis .....	110
3.14 Inactivation of colistin by <i>P. aeruginosa</i> is dependent on active LPS biosynthesis .....	113
3.15 The bactericidal activity of colistin requires <i>de novo</i> LPS biosynthesis .....	114
3.16 Discussion .....	116
<b>Chapter 4: Colistin kills bacteria by targeting lipopolysaccharide in the cytoplasmic membrane</b> .....	121
4.1 Introduction .....	121
4.2 Blocking LPS biosynthesis reduces colistin killing of <i>P. aeruginosa</i> in a dose-dependent manner .....	123
4.3 Inhibiting biosynthesis of LPS prevents colistin-induced morphological changes of <i>P. aeruginosa</i> .....	125
4.4 Inhibiting LPS synthesis specifically blocks colistin killing of <i>P. aeruginosa</i> .....	127
4.5 Colistin's bactericidal activity against <i>P. aeruginosa</i> is not inhibited by growth arrest.....	128
4.6 CHIR-090 and cerulenin do not inactivate colistin directly or indirectly .....	130
4.7 CHIR-090 and cerulenin do not induce stress responses that confer colistin resistance ....	132
4.8 The antagonism of CHIR-090 on colistin killing is not due to off-target effects.....	134
4.9 LPS concentrations in the outer membrane are unaffected by CHIR-090 and cerulenin ...	137
4.10 Inhibiting LPS biosynthesis reduces colistin's binding to <i>P. aeruginosa</i> .....	139
4.11 Polymyxin compounds do not bind to or inhibit growth of Gram-positive bacteria .....	142
4.12 Blocking LPS biosynthesis lowers the abundance of LPS in the cytoplasmic membrane ....	144
4.13 Inhibition of LPS synthesis prevents colistin-induced CM disruption and lysis .....	148

4.14	Colistin's interaction with LPS to disrupt the CM is cation-dependent .....	152
4.15	Polymyxin-mediated CM disruption and lysis requires LPS and the antibiotic's lipid tail..... .....	154
4.16	Blocking LPS synthesis reduces CM disruption, lysis and killing by colistin across Gram-negative pathogens .....	158
4.17	Discussion .....	162
<b>Chapter 5: Acquired colistin resistance in Gram-negative bacteria is mediated at the cytoplasmic membrane.....</b>		<b>166</b>
5.1	Introduction .....	166
5.2	Colistin permeabilises the outer membrane of polymyxin-resistant <i>E. coli</i> expressing <i>mcr-1</i> .. .....	169
5.3	Colistin cannot permeabilise the cytoplasmic membrane of <i>mcr-1</i> -positive <i>E. coli</i> .....	171
5.4	Prevention of CM disruption by colistin in <i>mcr-1</i> -positive <i>E. coli</i> depends on the extent of lipid A modification .....	172
5.5	MCR-1-mediated protection of the <i>E. coli</i> CM is colistin-specific and due to altered membrane charge .....	177
5.6	The CM of <i>mcr-1</i> -positive <i>E. coli</i> has a higher proportion of modified lipid A than the OM .....	179
5.7	Colistin resistance in pathogenic <i>E. coli</i> conferred by <i>mcr</i> genes or chromosomally is mediated at the CM.....	181
5.8	Clinical <i>Enterobacter cloacae</i> isolates harbouring <i>mcr-9</i> do not exhibit classical colistin resistance .....	184
5.9	<i>E. cloacae</i> clinical strains display a novel form of inducible hetero-resistance to colistin..... .....	186
5.10	Colistin hetero-resistance in <i>E. cloacae</i> is mediated by two distinct bacterial populations .....	190
5.11	Chromosomal and intrinsic colistin resistance in bacteria from CF patients are mediated at different membranes.....	195
5.12	Acquired colistin resistance in <i>E. coli</i> is associated with a fitness cost .....	200
5.13	Discussion .....	203
<b>Chapter 6: Novel combination treatment strategies enhance colistin efficacy and overcome colistin resistance.....</b>		<b>208</b>
6.1	Introduction .....	208
6.2	A sub-inhibitory concentration of murepavadin does not affect LPS levels in the OM of <i>P. aeruginosa</i> .....	210
6.3	Murepavadin treatment triggers LPS accumulation in the <i>P. aeruginosa</i> CM.....	213
6.4	Murepavadin enhances colistin-mediated CM disruption and lysis in <i>P. aeruginosa</i> .....	214

6.5	The synergy with murepavadin augments the bactericidal activity of colistin against <i>P. aeruginosa</i> .....	217
6.6	The antibacterial potentiating effects of murepavadin are specific to colistin.....	219
6.7	Murepavadin enhances colistin’s activity against diverse clinical <i>P. aeruginosa</i> isolates ..	223
6.8	Colistin and murepavadin combination therapy promotes bacterial killing against CF isolates and <i>in vivo</i> .....	226
6.9	Colistin and murepavadin synergise against CF isolates of <i>P. aeruginosa</i> that are polymyxin-resistant.....	228
6.10	Colistin synergises with rifampicin against Gram-negative bacteria with acquired polymyxin resistance .....	231
6.11	Discussion .....	233
<b>Chapter 7: Conclusions and Perspectives .....</b>		<b>238</b>
7.1	Key findings.....	238
7.1.1	A new model for colistin’s bactericidal mode of action .....	238
7.1.2	Characterisation of causes of colistin treatment failure.....	239
7.1.3	Design of novel approaches to augment colistin efficacy.....	241
7.2	Future work.....	242
7.2.1	What is the biophysical mechanism by which colistin disrupts cell membranes? .....	242
7.2.2	How do single bacterial cells respond to colistin exposure? .....	244
7.2.3	Do host antimicrobial peptides share a common mode of action with colistin? .....	245
7.2.4	Does released LPS contribute to colistin therapy failure in cystic fibrosis patients? ..	246
7.2.5	Does the host environment influence susceptibility to colistin? .....	247
7.3	Summary .....	248
<b>References.....</b>		<b>249</b>

## List of Abbreviations

<b>A</b>	Absorbance
<b>ABC</b>	ATPase-binding cassette
<b>ADP</b>	Adenosine diphosphate
<b>AKI</b>	Acute kidney injury
<b>AMP</b>	Antimicrobial peptide
<b>ANOVA</b>	Analysis of variance
<b>ATP</b>	Adenosine triphosphate
<b>BALF</b>	Bronchoalveolar lavage fluid
<b>BHI</b>	Brain Heart Infusion broth
<b>BSAC</b>	British Society of Antimicrobial Chemotherapy
<b>c.f.u.</b>	colony forming units
<b>CA-MHB</b>	Cation-adjusted Mueller-Hinton broth
<b>CCCP</b>	Carbonyl cyanide 3-chlorophenylhydrazone
<b>CF</b>	Cystic fibrosis
<b>CI</b>	Competitive Index
<b>CLSI</b>	Clinical and Laboratory Standards Institute
<b>CM</b>	Cytoplasmic membrane
<b>C<sub>max</sub></b>	Peak steady-state plasma concentration
<b>CMP-Kdo</b>	Cytidine monophosphate-ketodeoxyoctonate
<b>DAB</b>	L- $\alpha$ - $\gamma$ -diaminobutyric acid
<b>DDD</b>	Defined daily doses
<b>ddH<sub>2</sub>O</b>	Double-distilled ultra-pure water
<b>DMSO</b>	Dimethyl sulfoxide
<b>DNA</b>	Deoxyribonucleic acid

<b>dTDP</b>	Deoxythymidine diphosphate
<b>EDTA</b>	Ethylenediaminetetraacetic acid
<b>ESPAUR</b>	English Surveillance Programme for Antimicrobial Utilisation and Resistance
<b>EU</b>	Endotoxin units
<b>FDA</b>	U.S. Food and Drug Administration
<b>FEG</b>	Field emission gun
<b>FICI</b>	Fractional inhibitory concentration index
<b>FITC</b>	Fluorescein isothiocyanate
<b>GDP</b>	Guanosine diphosphate
<b>GlcNAc</b>	N-Acetylglucosamine
<b>GMP</b>	Guanosine monophosphate
<b>GP</b>	Generalised Polarisation
<b>Hep</b>	L-glycero-D-manno-heptose
<b>HIV</b>	Human immunodeficiency virus
<b>HPLC</b>	High performance liquid chromatography
<b>IPTG</b>	Isopropyl- $\beta$ -D-thiogalactoside
<b>IU</b>	International units
<b>LAL</b>	Limulus ameocyte lysate
<b>L-Ara4N</b>	4-amino-4-deoxy-L-arabinose
<b>LB</b>	Lysogeny broth
<b>LPS</b>	Lipopolysaccharide
<b>MALDI-TOF</b>	Matrix-assisted laser desorption/ionization time-of-flight
<b>MCR</b>	Mobile colistin resistance
<b>MGE</b>	Mobile genetic element
<b>MHA</b>	Mueller-Hinton agar

<b>MHB</b>	Mueller-Hinton broth
<b>MIC</b>	Minimum inhibitory concentration
<b>mRNA</b>	Messenger ribonucleic acid
<b>NADH/NAD<sup>+</sup></b>	Nicotinamide adenine dinucleotide
<b>NHS</b>	National Health Service
<b>NMR</b>	Nuclear magnetic resonance
<b>NPN</b>	N-phenyl-1-naphtylamine
<b>ns</b>	not significant
<b>OD</b>	Optical density
<b>OM</b>	Outer membrane
<b>OMV</b>	Outer membrane vesicle
<b>PAP</b>	Population analysis profiling
<b>PBP</b>	Penicillin-binding protein
<b>PBS</b>	Phosphate-buffered saline
<b>PC</b>	Phase contrast
<b>pEmpty</b>	Empty plasmid control
<b>PEtN</b>	Phosphoethanolamine
<b>PG</b>	Phosphatidylglycerol
<b>PI</b>	Propidium iodide
<b>PLL</b>	Poly-L-lysine
<b>PMB</b>	Polymyxin B
<b>PMBN</b>	Polymyxin B nonapeptide
<b>pNA</b>	p-Nitroaniline
<b>QRDR</b>	Quinolone resistance determining region
<b>qRT-PCR</b>	Real-Time Quantitative Reverse Transcription PCR
<b>r.f.u.</b>	relative fluorescence units

<b>r.p.m.</b>	rotations per minute
<b>RIFLE</b>	Risk, Injury, Failure, Loss, End-Stage
<b>RNA</b>	Ribonucleic acid
<b>RNAseq</b>	Ribonucleic acid sequencing
<b>rRNA</b>	Ribosomal ribonucleic acid
<b>SAR</b>	Structure-activity relationship
<b>SDS</b>	Sodium dodecyl sulfate
<b>SDS-PAGE</b>	Sodium dodecyl sulfate–polyacrylamide gel electrophoresis
<b>SEM</b>	Scanning electron microscopy
<b>SOD</b>	Superoxide dismutase
<b>T3SS</b>	Type III secretion system
<b>TEM</b>	Transmission electron microscopy
<b>TLR4</b>	Toll-like receptor 4
<b>TSB</b>	Tryptic soy broth
<b>UDP</b>	Uridine diphosphate
<b>UTI</b>	Urinary tract infection
<b>v/v</b>	volume per volume
<b>VAP</b>	Ventilator-associated pneumonia
<b>w/v</b>	weight per volume
<b>WT</b>	Wild-type



## List of Figures

**Figure 1.1:** *P. aeruginosa* causes a diverse range of infections in human patients. (page 24)

**Figure 1.2:** Pathogenesis of *P. aeruginosa* is influenced by a panel of virulence factors. (page 25)

**Figure 1.3:** Front-line antipseudomonal drugs target distinct bacterial processes. (page 26)

**Figure 1.4:** *P. aeruginosa* has a range of mechanisms to resist front-line antibiotics. (page 29)

**Figure 1.5:** Lipopolysaccharides have distinct structural regions with varying functions. (page 34)

**Figure 1.6:** The biosynthetic pathway of the lipid A domain of LPS. (page 36)

**Figure 1.7:** The biosynthetic pathway of the core oligosaccharide domain of LPS. (page 37)

**Figure 1.8:** The biosynthetic pathway of the O-antigen domain of LPS. (page 38)

**Figure 1.9:** The transport pathway of LPS from the cytoplasm to the outer membrane. (page 42)

**Figure 1.10:** Chemical structures of colistin (A and B) and polymyxin B. (page 49)

**Figure 1.11:** The “classic” proposed mechanism of action of colistin is poorly understood. (page 57)

**Figure 1.12:** Alternative proposed mechanisms for colistin’s bactericidal activity. (page 59)

**Figure 1.13:** The interconnected signalling pathways of the PhoPQ and PmrAB two-component systems that regulate the modification of LPS with cationic chemical groups and mediate chromosomal colistin resistance. (page 61)

**Figure 1.14:** The plasmid-borne *mcr-1* gene encodes a phosphoethanolamine transferase enzyme that modifies the lipid A domain of LPS and confers colistin resistance. (page 66)

**Figure 3.1:** Colistin sequentially disrupts the outer membrane (OM) and cytoplasmic membrane (CM) of *P. aeruginosa*. (page 91)

**Figure 3.2:** Colistin causes bi-phasic cell lysis and killing of *P. aeruginosa*. (page 94)

**Figure 3.3:** The recovery of *P. aeruginosa* during colistin exposure is not due to colistin resistance. (page 96)

**Figure 3.4:** Exposure of *P. aeruginosa* causes a loss of colistin activity. (page 97)

**Figure 3.5:** Loss of colistin activity in the *P. aeruginosa* supernatant is not due to binding to bacterial cells. (page 99)

**Figure 3.6:** Inactivation of colistin by *P. aeruginosa* occurs via a heat-stable and non-lipid released factor. (page 101)

**Figure 3.7:** *P. aeruginosa* does not inactivate colistin by releasing the polysaccharide alginate from its capsule. (page 103)

**Figure 3.8:** Colistin exposure induces extracellular release of LPS from *P. aeruginosa*. (page 105)

**Figure 3.9:** The presence of extracellular LPS inactivates colistin and increases the ability of *P. aeruginosa* to tolerate the polymyxin. (page 107)

**Figure 3.10:** Colistin-inactivating properties are lost in colistin-resistant *P. aeruginosa*. (page 109)

**Figure 3.11:** Colistin is inactivated in the supernatant across a diverse panel of Gram-negative pathogens. (page 110)

**Figure 3.12:** LPS release from *P. aeruginosa* in response to colistin is dependent on active LPS biosynthesis. (page 112)

**Figure 3.13:** The ability of *P. aeruginosa* to inactivate colistin extracellularly requires *de novo* LPS biosynthesis. (page 114)

**Figure 3.14:** Colistin's bactericidal activity against *P. aeruginosa* is dependent on active LPS biosynthesis. (page 116)

**Figure 4.1:** Colistin is dependent on *de novo* LPS biosynthesis throughout its bactericidal activity against *P. aeruginosa*. (page 125)

**Figure 4.2:** Alterations to the cell morphology of *P. aeruginosa* caused by colistin require active LPS biosynthesis. (page 126)

**Figure 4.3:** The protective effects of inhibiting LPS biosynthesis on *P. aeruginosa* killing are specific to colistin. (page 128)

**Figure 4.4:** Growth arrest of *P. aeruginosa* does not block the killing of cells by colistin. (page 130)

**Figure 4.5:** Colistin is inactivated neither directly nor indirectly by CHIR-090/cerulenin. (page 131)

**Figure 4.6:** The inhibition of colistin's bactericidal activity by CHIR-090/cerulenin is not due to induction of a stress response that confers polymyxin resistance. (page 133)

**Figure 4.7:** CHIR-090 cannot protect CHIR-090-resistant *P. aeruginosa* from colistin's bactericidal effects. (page 136)

**Figure 4.8:** The LPS synthesis inhibitors CHIR-090/cerulenin do not reduce LPS levels in the OM of *P. aeruginosa*. (page 138)

**Figure 4.9:** Colistin binding to *P. aeruginosa* is reduced by blocking active LPS synthesis. (page 141)

**Figure 4.10:** Colistin is unable to bind to Gram-positive organisms or inhibit their growth. (page 143)

**Figure 4.11:** Spheroplasts generated from *P. aeruginosa* have a spherical morphology, are osmotically-fragile and have no OM contamination in the CM. (page 145)

**Figure 4.12:** Inhibition of LPS biosynthesis with CHIR-090/cerulenin reduces LPS levels in the CM of *P. aeruginosa*. (page 147)

**Figure 4.13:** Reducing CM LPS abundance with CHIR-090/cerulenin blocks colistin from permeabilising the CM and lysing *P. aeruginosa*. (page 151)

**Figure 4.14:** Addition of extracellular Mg<sup>2+</sup> specifically decreases colistin-mediated CM disruption and lysis in *P. aeruginosa* spheroplasts. (page 153)

**Figure 4.15:** Permeabilisation of the CM by polymyxins requires interaction between the polymyxin fatty acid tail and LPS in the CM. (page 156)

**Figure 4.16:** The lytic and bactericidal activity of polymyxins is dependent on the lipid tail of the antibiotic interacting with CM LPS. (page 157)

**Figure 4.17:** Sub-lethal concentrations of CHIR-090/cerulenin reduce colistin-induced CM damage across diverse Gram-negative pathogens. (page 159)

**Figure 4.18:** CHIR-090 and cerulenin block colistin from causing cell lysis and death in a panel of Gram-negative pathogens. (page 160)

**Figure 4.19:** The fatty acid/LPS synthesis inhibitor triclosan blocks *K. pneumoniae* killing by colistin. (page 161)

**Figure 5.1:** Expression of the *mcr-1* gene in polymyxin-resistant *E. coli* does not prevent colistin from disrupting the OM. (page 170)

**Figure 5.2:** The CM of *mcr-1*-expressing *E. coli* is not permeabilised by colistin, protecting cells from being lysed. (page 171)

**Figure 5.3:** Spheroplasts generated from *E. coli* are spherical, with no OM contamination. (page 173)

**Figure 5.4:** LPS modifications in the CM protect *mcr-1*-positive *E. coli* from colistin-mediated CM disruption/lysis in a dose-dependent manner. (page 176)

**Figure 5.5:** MCR-1 increases the positive charge of the *E. coli* CM but specifically inhibits colistin's CM permeabilising and lytic properties. (page 179)

**Figure 5.6:** The ratio of modified:unmodified lipid A is higher in the CM than in the OM of *mcr-1*-expressing *E. coli*. (page 180)

**Figure 5.7:** Colistin resistance in clinical *E. coli* acquired by diverse *mcr* homologues or chromosomal mutations is mediated at the CM. (page 183)

**Figure 5.8:** Pathogenic *E. cloacae* strains display an *mcr-9*-independent “skipped well” phenotype. (page 185)

**Figure 5.9:** Clinical *E. cloacae* strains are colistin hetero-resistant, with a non-susceptible sub-population that is induced by the polymyxin drug. (page 187)

**Figure 5.10:** Inducible colistin non-susceptibility in polymyxin hetero-resistant clinical *E. cloacae* isolates is mediated by lipid A modifications. (page 190)

**Figure 5.11:** Clinical *E. cloacae* strains possess two forms of colistin resistance, one of which is induced by increasing polymyxin concentrations. (page 192)

**Figure 5.12:** High-level colistin resistance in *E. cloacae* isolate IMP14 is associated with stationary phase growth. (page 194)

**Figure 5.13:** Chromosomal colistin resistance is mediated at the CM, but intrinsic colistin resistance is conferred by protection of the OM. (page 197)

**Figure 5.14:** Chromosomal and intrinsic polymyxin resistance provides equal protection from colistin. (page 199)

**Figure 5.15:** Overexpression of *mcr-1* results in a marked fitness cost in *E. coli* cells with acquired colistin resistance. (page 202)

**Figure 6.1:** Blocking LPS transport with a sub-inhibitory murepavadin concentration has a minimal effect on *P. aeruginosa* OM LPS abundance. (page 212)

**Figure 6.2:** LPS molecules accumulate in the CM of *P. aeruginosa* spheroplasts exposed to murepavadin. (page 214)

**Figure 6.3:** Inhibiting LPS transport with murepavadin potentiates the ability of colistin to disrupt the *P. aeruginosa* CM and trigger cell lysis. (page 216)

**Figure 6.4:** Murepavadin enhances colistin-mediated killing of *P. aeruginosa*. (page 219)

**Figure 6.5:** Murepavadin exposure modulates the fluidity and electrostatic charge of the *P. aeruginosa* CM. (page 220)

**Figure 6.6:** Murepavadin specifically amplifies only the capacity of colistin to trigger CM damage and lysis in *P. aeruginosa* spheroplasts. (page 222)

**Figure 6.7:** Sub-lethal murepavadin concentrations potentiate CM disruption induced by colistin in clinical strains of *P. aeruginosa*. (page 224)

**Figure 6.8:** Murepavadin enhances colistin-mediated bacterial lysis and killing against *P. aeruginosa* clinical isolates. (page 225)

**Figure 6.9:** Colistin and murepavadin are synergistic *in vitro* against CF *P. aeruginosa* strains and in an *in vivo* murine lung infection model. (page 227)

**Figure 6.10:** The addition of murepavadin augments colistin-induced CM damage, lysis and killing of polymyxin-resistant *P. aeruginosa* CF isolates. (page 229)

**Figure 6.11:** Murepavadin synergises potently with colistin against polymyxin-resistant *P. aeruginosa* clinical CF strains. (page 230)

**Figure 6.12:** Colistin and rifampicin synergise against *E. coli* and *P. aeruginosa* isolates with acquired polymyxin resistance. (page 232)

**Figure 7.1:** A novel model of how colistin sequentially permeabilises the OM and CM by targeting LPS to kill Gram-negative bacteria. (page 239)

**Figure 7.2:** Acquired and intrinsic resistance to colistin are mediated through two differing mechanisms. (page 240)

**Figure 7.3:** Two new combination treatment strategies that can enhance the activity of colistin and overcome acquired polymyxin resistance. (page 242)

## List of Tables

**Table 1.1:** Antimicrobial resistance rates for *P. aeruginosa* isolates, U.S.A., 1993-2002 (page 32)

**Table 1.2:** Antimicrobial resistance rates for *P. aeruginosa* isolates, Germany, 2004-2010 (page 33)

**Table 1.3:** Inhibitors of LPS biosynthesis in pre-clinical development (page 40)

**Table 1.4:** Inhibitors of LPS transport in pre-clinical development (page 47)

**Table 1.5:** Characteristics of the *mcr* genes that confer colistin resistance (page 67)

**Table 1.6:** Efficacy of colistin treatment against infections caused by *P. aeruginosa* (page 70)

**Table 2.1:** Bacterial strains used in this study (page 74)

# Chapter 1: Introduction

## 1.1 The pathogen *Pseudomonas aeruginosa*

### 1.1.1 General characteristics of *P. aeruginosa*

The bacterium *Pseudomonas aeruginosa* is a Gram-negative, rod-shaped organism that is a member of the Gammaproteobacteria class, and the Pseudomonadaceae family<sup>1</sup>. It was first isolated in 1882 by Carle Gessard, who observed the organism growing on the bandages of patients with cutaneous wounds as a blue-green pus<sup>2</sup>. This pigmentation is typical of *P. aeruginosa* cultures, and is due to the production of the metabolites pyoverdine and pyocyanin, which combine to impart the characteristic blue-green colour<sup>3</sup>. In modern times, the organism is identified diagnostically by being catalase, citrate and oxidase positive, and grows as clear colonies on MacConkey agar due to an inability to ferment lactose<sup>4</sup>.

The genome of *P. aeruginosa* is relatively large, with a large circular chromosome that can be up to 6.8 Mb in size encoding approximately 6000 open reading frames that can undergo translation<sup>5</sup>. However, research on 389 *P. aeruginosa* strains revealed that there is large inter-strain variability between genomes, with only 17.5% sequence homology between these strains<sup>6</sup>. This shared genome is termed the “core” genome, and the sizeable “accessory” genome that remains comprises of numerous genes that can rapidly mutate so that *P. aeruginosa* strains can readily adapt to a wide variety of niches<sup>7</sup>. Hence, this bacterium has evolved to exist in virtually all environments: soil, water, low and high-oxygen atmospheres, on plants, animals and humans (including as a commensal organism as part of the skin microbiota), as well as on artificial surfaces in clinical settings<sup>8</sup>.

The large and versatile genome of this species also confers *P. aeruginosa* with a high metabolic capacity. The bacterium is facultatively aerobic, proliferating in conditions where oxygen is present, but also achieving anaerobic growth when nitrate or nitrite is present as a terminal electron acceptor<sup>9</sup>. Even in the absence of nitrate/nitrite, *P. aeruginosa* can generate ATP for cellular processes by substrate-level phosphorylation through fermentation of pyruvate and arginine<sup>10</sup>. Whilst iron is required as a nutrient source for *P. aeruginosa* growth, the bacterium secretes siderophores (iron-chelating compounds) to obtain iron from its insoluble ferric form and transport it intracellularly<sup>11</sup>.

Adding to its metabolic diversity, many *P. aeruginosa* strains also readily form biofilm structures by releasing extracellular compounds (including exopolysaccharides and DNA) to form an enclosed matrix<sup>12</sup>. Communication between individual bacterial cells in a *P. aeruginosa* community via a process known as quorum sensing, is vital for regulating gene

expression to co-ordinate biofilm formation<sup>13</sup>. In addition to existing in non-motile biofilms, *P. aeruginosa* can also exhibit movement, by swarming in liquid culture or twitching on solid media<sup>14</sup>. In order to display these motile behaviours, the bacterium relies on use of both its polar flagellum and type IV pili<sup>15</sup>. The switch between such a free-swimming lifestyle and a biofilm lifestyle is controlled by the intracellular concentration of a single molecule, cyclic di-GMP, with increased levels of cyclic di-GMP associated with the formation of sessile biofilm communities<sup>16</sup>. Crucially, it is a combination of these abilities – adapting in variable environments, extensive metabolic capabilities and rapid lifestyle changes – that have provided *P. aeruginosa* with the opportunity to thrive as a human pathogen.

### 1.1.2 *P. aeruginosa* as an opportunistic pathogen

In addition to being an extremely prevalent environmental organism, *P. aeruginosa* is also a highly versatile pathogen. Whilst known to cause infections in plant species (*Lactuca sativa*, *Arabidopsis thaliana*) and invertebrate animals (*Drosophila* fruit flies, *Galleria mellonella*, *Caenorhabditis elegans*), the bacterium is best known and studied as an opportunistic pathogen of immunocompromised humans<sup>17–21</sup>. In these individuals, *P. aeruginosa* can colonise a number of different anatomical sites, causing a wide array of infections (**Figure 1.1**). Patients with cystic fibrosis (CF) are especially pre-disposed to lung infections with *P. aeruginosa*, resulting in a virtually chronic diffuse bronchopneumonia<sup>22</sup>. This is due to a mutation causing a loss of function of chloride ion movement across the membranes of airway epithelial cells, which triggers a build-up of mucus in the bronchi/bronchioles and impairs mucociliary clearance (the primary innate immune defence mechanism in the lung)<sup>23</sup>. This accumulation of mucus also occurs in patients with non-CF bronchiectasis, where *P. aeruginosa* infections are frequently observed for similar reasons<sup>24</sup>.

Whilst *P. aeruginosa* can cause community-acquired infections, it is more often associated with being a nosocomial pathogen, with infections usually occurring in healthcare settings. The predominant reason for this is the organism's prolific ability to colonise the moist surfaces of medical devices<sup>25</sup>. For example, *P. aeruginosa* grows readily on the valves and tubes of ventilators, and thus is one of the most common agents responsible for ventilator-associated pneumonia (VAP) in intensive care units<sup>26</sup>. Furthermore, the bacterium can form biofilm structures on catheters, which can lead to urinary tract infections (UTIs) or necrotising enterocolitis in premature infants if orogastric tubes are colonised<sup>27,28</sup>. Patients in hospital with burns or wounds are highly susceptible to *P. aeruginosa* skin and soft tissue infections, and in individuals with deep puncture wounds of the foot (often seen in diabetic patients), such infections can even culminate in osteomyelitis<sup>29–31</sup>. Postoperative infections of the eye with *P. aeruginosa* are also commonly diagnosed, especially following radial keratotomy surgical procedures<sup>32</sup>.

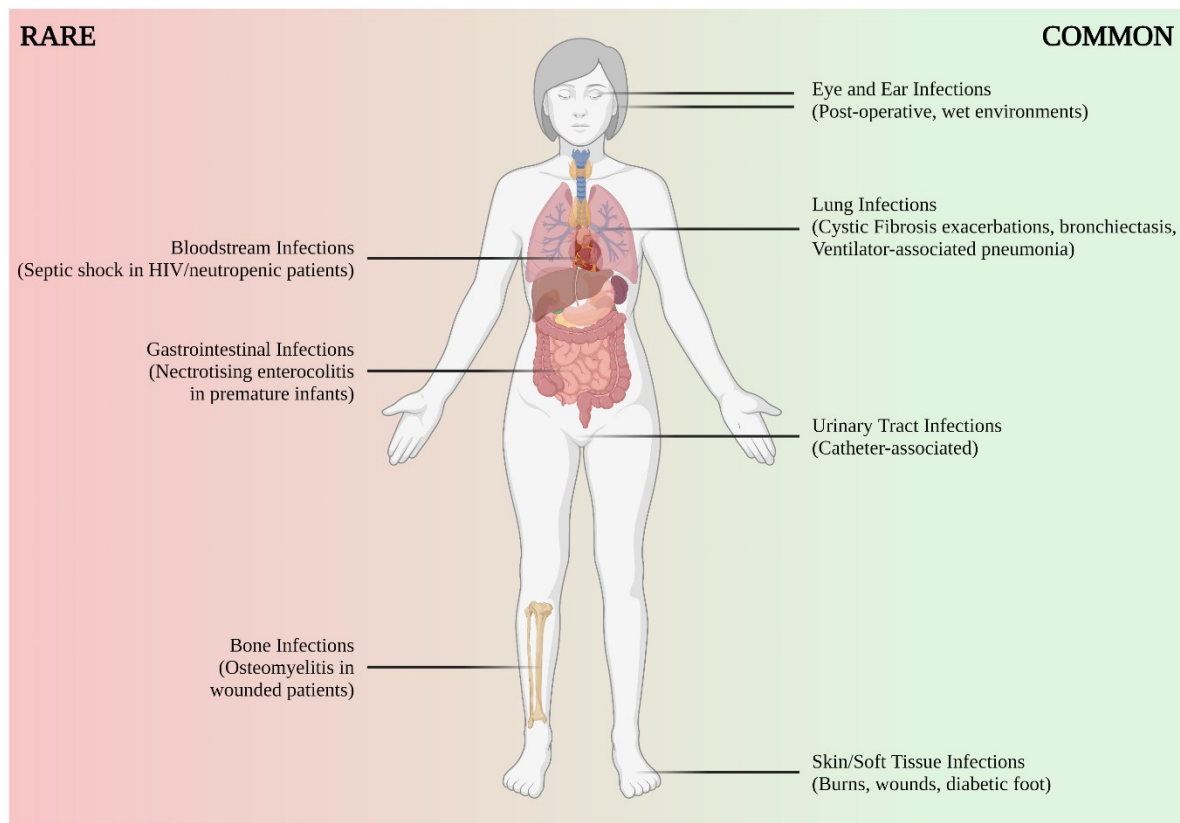


**Figure 1.1: *P. aeruginosa* causes a diverse range of infections in human patients.**

The capacity to thrive in wet environments also makes *P. aeruginosa* a prevalent cause of ear infections and dermatitis acquired from swimming pools or hot tubs where water quality is poor<sup>33,34</sup>. In extremely rare cases where these infections occur in high-risk individuals (e.g. with neutropenia, HIV), the organism can infiltrate the bloodstream and trigger septic shock, which is associated with the formation of pustulic, necrotic skin lesions known as ecthyma gangrenosum<sup>35-37</sup>. Generally, however, *P. aeruginosa* is not an extremely virulent pathogen, especially compared to other bacterial species that are a major source of human infections (*Streptococcus pyogenes*, *Staphylococcus aureus*).

In terms of virulence factors that contribute to *P. aeruginosa* pathogenesis (**Figure 1.2**), the bacterium uses its type III secretion system to release the Exo family of proteins (ExoT, ExoS, ExoY, ExoU), which cause lysis of host eukaryotic cells by degrading their plasma membrane<sup>38</sup>. Additionally, *P. aeruginosa* uses the elastases LasA and LasB to disrupt tight junctions between host epithelial cells, as well as exotoxin A to induce ADP-ribosylation that inactivates eukaryotic elongation factor 2, resulting in host cell necrosis<sup>39,40</sup>. Finally, the pigmented molecules pyocyanin and pyoverdine released by *P. aeruginosa* also possess virulent properties. Pyocyanin alters mitochondrial electron transport in host organisms,



leading to oxidative stress and ultimately cell death<sup>41</sup>. In contrast, pyoverdine via its siderophore activity removes iron from mitochondria, which damages this host organelle<sup>42</sup>. Despite only harbouring this small array of virulence factors, *P. aeruginosa* infections are notoriously challenging to treat.

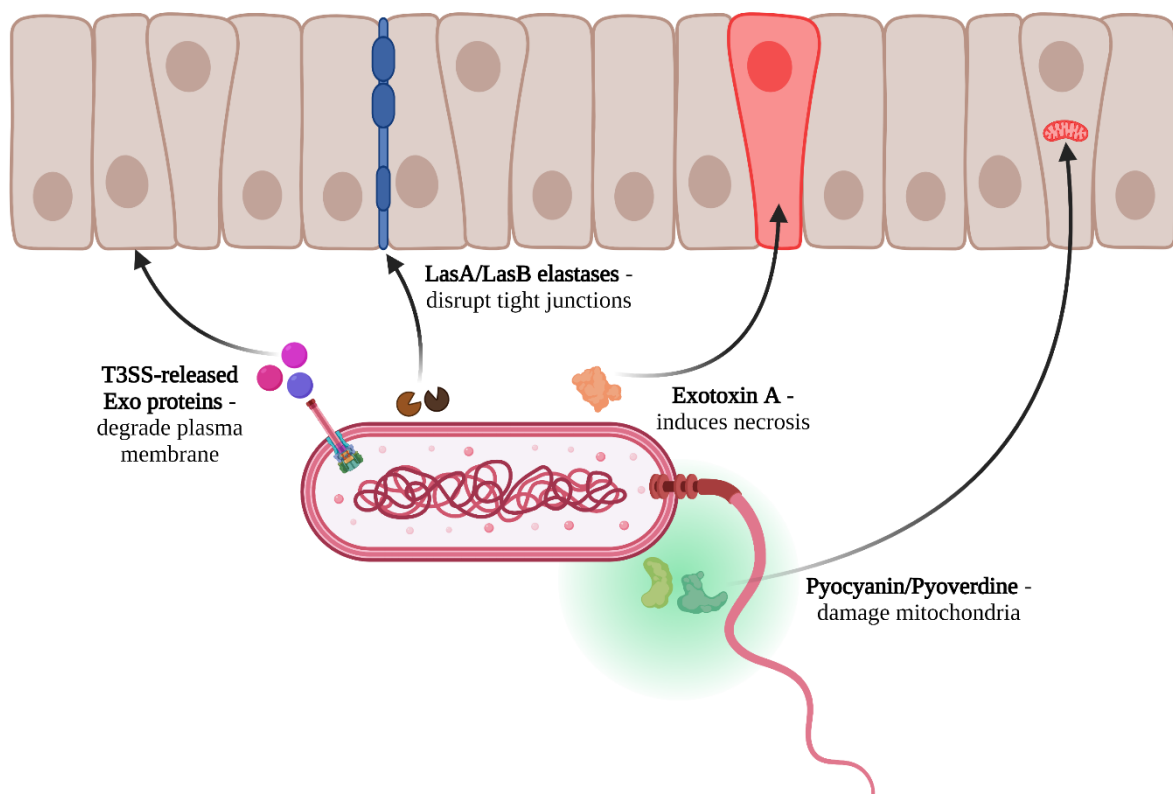


**Figure 1.2: Pathogenesis of *P. aeruginosa* is influenced by a panel of virulence factors.**

## 1.2 Treatment of *P. aeruginosa* infections

### 1.2.1 Prevention

Due to the high rates of hospital-acquired infections caused by *P. aeruginosa*, strategies to overcome this pathogen begin with preventing patients becoming colonised in the first place. This includes extensive good hygiene practices, including regular replacement and/or disinfection of medical equipment that may encounter moisture (catheters, tubing etc.), as well as regular hand washing<sup>43,44</sup>. Since *P. aeruginosa* is also extensively present in the environment, immunocompromised individuals are often advised to avoid swimming pools and other bodies of water where the organism thrives. More recently, oral probiotics

have been investigated as a novel prophylactic treatment strategy in intensive care units to prevent or delay colonisation by *P. aeruginosa*<sup>45</sup>. Furthermore, immunoprophylactic therapeutic options against *P. aeruginosa* are also in development through several vaccine candidates<sup>46,47</sup>. However, very few of these vaccine candidates have reached clinical trial phases, raising doubts over the feasibility and efficacy of this preventative strategy. As such, the use of antibiotic drugs remain the predominant treatment options for combatting *P. aeruginosa* (**Figure 1.3**).

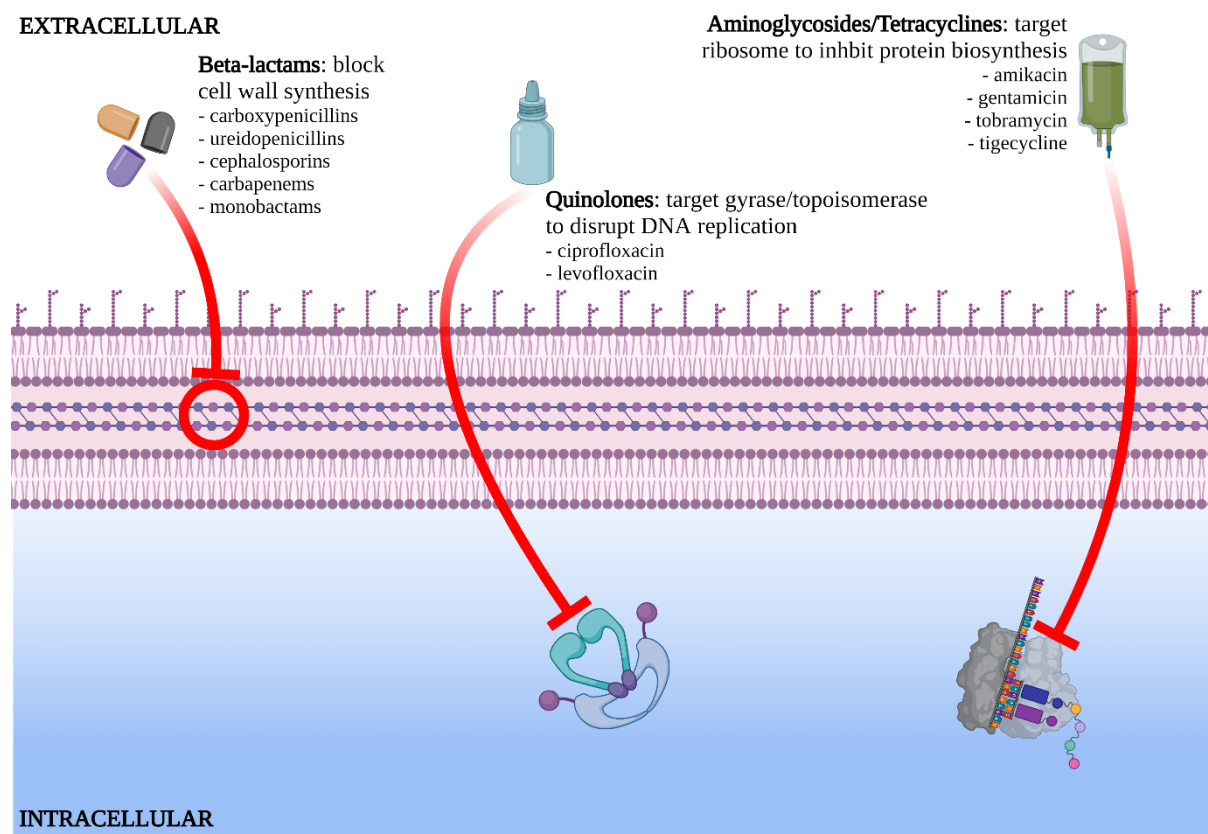


**Figure 1.3: Front-line antipseudomonal drugs target distinct bacterial processes.**

### 1.2.2 Beta-lactam antibiotics

Whilst the list of beta-lactam compounds possessing antipseudomonal activity is small, these antibiotics are still commonly prescribed as a front-line therapy against *P. aeruginosa* infections. These drugs include the carboxypenicillins (ticarcillin, carbenicillin) and the ureidopenicillins (mezlocillin, azlocillin, piperacillin), as well as third-, fourth- and fifth-generation cephalosporin compounds (ceftazidime, cefoperazone, ceftazidime, cefepime, ceftobiprole)<sup>48-50</sup>. Carbapenem antibiotics, including imipenem, doripenem and meropenem, with a broader spectrum of activity are also used to eradicate infections caused by *P. aeruginosa*, as is the monobactam aztreonam, which unlike these other beta-lactams, has no

adjacent second ring fused to its beta-lactam ring<sup>51,52</sup>. It is the beta-lactam ring that confers all these drugs with their antibacterial activity by irreversibly binding to penicillin binding proteins (PBPs), preventing cross-linking of the peptidoglycan layer to disrupt biosynthesis of the cell wall and eventually kill the bacteria<sup>53</sup>. These antibiotics are used to treat infections in virtually all anatomical sites colonised by *P. aeruginosa*, including in VAP, bloodstream infections, intra-abdominal infections, complicated UTIs and skin/soft tissue infections.

### **1.2.3 Quinolone antibiotics**

The quinolone compounds ciprofloxacin and levofloxacin are bactericidal agents used to treat *P. aeruginosa* infections. These drugs are widely effective against most strains of *P. aeruginosa* and are often used topically for superficial, limited bacterial infections, such as those occurring on the skin or in the ear<sup>54–56</sup>. Ciprofloxacin and levofloxacin enter bacteria via their membrane porins and work by inhibiting the ligase activity of DNA gyrase and topoisomerase IV, but have no effect on the nuclease activity of these enzymes<sup>57,58</sup>. As a result, DNA gyrase and topoisomerase IV release their DNA containing single- and double-strand breaks, the presence of which is fatal to bacterial cells<sup>59</sup>. Notably, these quinolone antibiotics have favourable pharmacokinetic/pharmacodynamic properties, which make them a front-line therapeutic strategy against *P. aeruginosa*<sup>60</sup>.

### **1.2.4 Aminoglycoside antibiotics**

As with beta-lactam antibiotics, the aminoglycosides amikacin, gentamicin and tobramycin are used clinically against *P. aeruginosa* infections arising in the majority of human sites colonised, including against sepsis, gastro-intestinal infections, UTIs and deep wound infections<sup>61</sup>. Tobramycin specifically is also extensively used in the treatment of exacerbations of chronic pneumonia by *P. aeruginosa* in CF patients, where a nebulised formulation of this antibiotic has revolutionised therapeutic outcomes<sup>62,63</sup>. The mechanism of action of these aminoglycoside compounds is inhibition of protein synthesis, which occurs when the drugs bind (in some cases irreversibly) to bacterial ribosomes present in the cytosol but associated with cell membranes<sup>64</sup>. This interaction prevents the 30S subunit of the ribosome from elongating, impairing the proofreading process, and therefore mRNA is inaccurately translated. Ultimately, the accumulation of aberrant and prematurely truncated proteins that results from the activity of these aminoglycosides is fatal to the bacterial cell<sup>65</sup>. The tetracycline derivative tigecycline is another protein synthesis inhibitor targeting the bacterial 30S ribosomal subunit that is utilised in the treatment of *P. aeruginosa* infections<sup>66,67</sup>. However, unlike amikacin, gentamicin and tobramycin, tigecycline is bacteriostatic in nature – only preventing bacterial growth, as opposed to initiating bacterial killing.

### 1.2.5 Combination therapy

Medical guidelines for antimicrobial chemotherapy against *P. aeruginosa* infections typically recommend using two antibiotic agents from differing drug classes. This approach is termed the “double coverage effect”, with the rationale being to increase the likelihood that at least one of the chosen antibiotic agents can eradicate the bacterial infection, as opposed to seeking any specific synergistic drug interactions<sup>68,69</sup>. In the clinical setting, it is recommended to administer these combination regimens as early as possible when a *P. aeruginosa* infection is suspected, and subsequently to promptly de-escalate to the single antibiotic with the highest antimicrobial activity *in vitro* when drug susceptibility testing data is available<sup>70</sup>.

The most common combination therapy prescribed is an antipseudomonal beta-lactam antibiotic alongside a second agent from either the aminoglycoside or quinolone classes, with this strategy frequently implemented to combat all serious, invasive *P. aeruginosa* infections (VAP, soft tissue infections, sepsis)<sup>71,72</sup>. Only in cases of contained, superficial infections from *P. aeruginosa* (e.g. ear/eye infections, UTIs) in low-risk patients is single antibiotic therapy considered an adequate treatment option<sup>73</sup>. Unfortunately, despite numerous studies examining the benefits of combination therapy versus monotherapy strategies, there has been no conclusive evidence demonstrating a clear advantage of using two antimicrobials together against *P. aeruginosa*, either for patient mortality, or for delaying the dangerous threat of antibiotic resistance emerging<sup>74–76</sup>. This highlights the extreme clinical challenge of treating patients infected with this pathogen.

### 1.2.6 Resistance to front-line antibiotics

The most threatening characteristic of the pathogen *P. aeruginosa*, and one which makes it especially demanding from a clinical treatment perspective, is its possession of multiple mechanisms that confer high-level drug resistance to the majority of commonly prescribed antimicrobials (**Figure 1.4**). Broadly, these mechanisms can be sub-divided into two types: “intrinsic” antibiotic resistance, where the natural traits of the bacterium render several antibiotic agents entirely ineffective, and “acquired” antibiotic resistance, where chromosomal mutations, or the acquisition of mobile genetic elements by horizontal gene transfer, are involved in blocking the antimicrobial activity of the drugs<sup>77</sup>.

In relation to intrinsic resistance to antibiotics, the first barrier encountered by antimicrobial drugs is the cellular envelope of *P. aeruginosa*. As a Gram-negative pathogen, this envelope consists of two bilayer membranes sandwiching a thin peptidoglycan cell wall: a symmetrical phospholipid cytoplasmic membrane, and an asymmetrical outer membrane with lipopolysaccharide molecules constituting the outermost leaflet, and phospholipids making up the innermost leaflet<sup>78</sup>. It is this outer membrane that is a huge permeability barrier

to many antimicrobial agents, especially hydrophobic antibiotics like rifampicin, ethambutol and isoniazid which have virtually no activity against Gram-negative bacteria<sup>79</sup>. Moreover, the cell envelope of *P. aeruginosa* is studded with numerous and diverse active multidrug efflux pumps encoded chromosomally in all strains of the species by the *mexAB*, *mexXY* and *oprM* genes<sup>80</sup>. The MexB and MexY proteins produced by these genes are located in the cytoplasmic membrane, whilst MexA and MexX are present in the periplasmic space and act as a bridge to the outer membrane<sup>81,82</sup>. OprM is situated in the outer membrane and functions as a pore, through which antibiotics that have entered *P. aeruginosa* cells are expelled, before they can exert their antimicrobial effects<sup>83</sup>. Substrates of these efflux systems include beta-lactams, quinolones, tetracyclines and aminoglycoside compounds<sup>84-86</sup>.

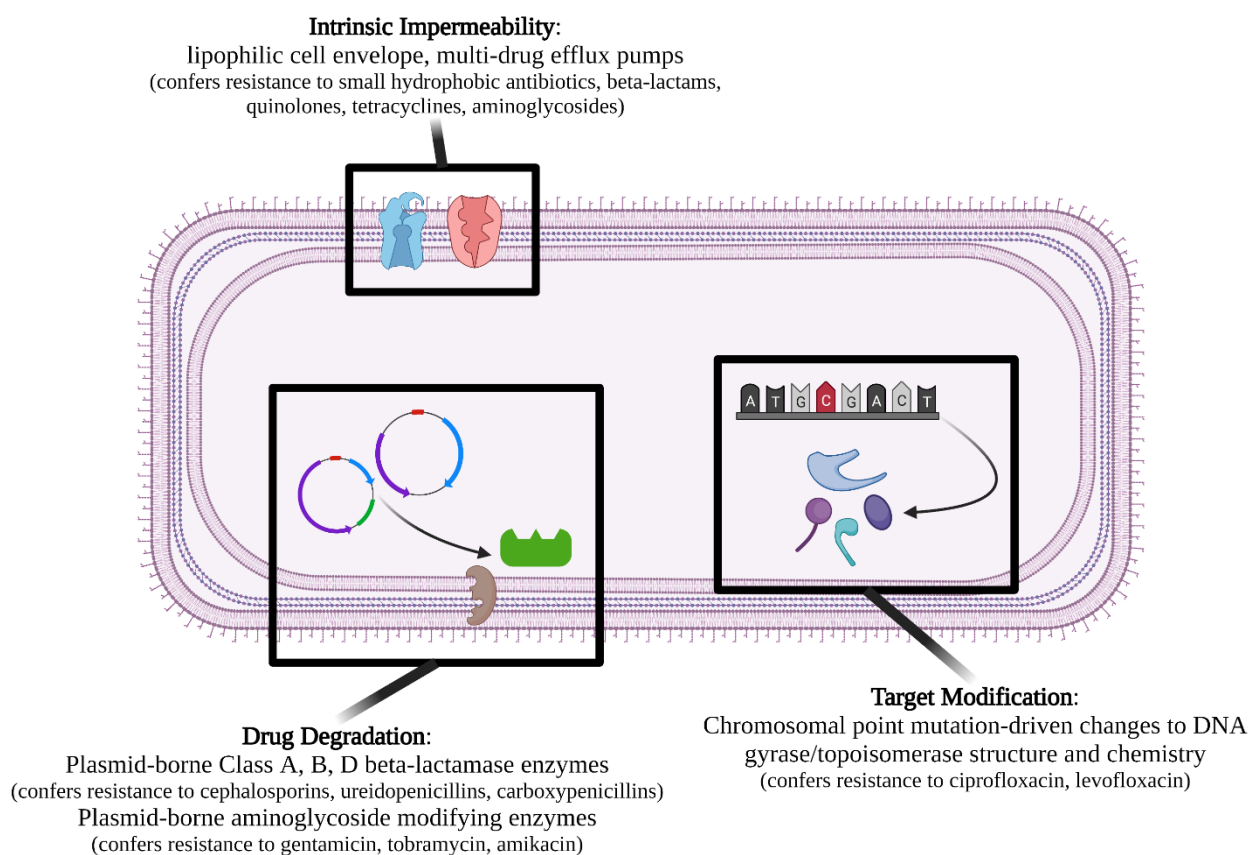


**Figure 1.4: *P. aeruginosa* has a range of mechanisms to resist front-line antibiotics.**

In addition to intrinsic drug resistance mediated by the impermeability of the cell envelope, *P. aeruginosa* strains also encode on their chromosome a beta-lactamase enzyme that degrades a range of beta-lactam-based antibiotics<sup>87</sup>. This enzyme, AmpC, is a class C cephalosporinase, which despite relatively low-level expression, confers resistance to certain first-, second-, and third-generation cephalosporin compounds (notably cefotaxime and ceftriaxone), as well as aminopenicillins and the carbapenem drug ertapenem<sup>88,89</sup>.

Importantly, expression of the *ampC* gene can be induced, leading to over-production of the enzyme, which dramatically increases the range of beta-lactam antibiotics against which *P. aeruginosa* becomes resistant<sup>90</sup>. Induction of the *ampC* gene and subsequent overexpression occurs upon exposure to specific beta-lactam compounds, including ceftiofur and imipenem, which bind and act on their target PBPs, leading to increased levels of peptidoglycan cell wall fragments within the bacterium<sup>91</sup>. These fragments bind to a protein known as AmpR, which undergoes a conformational change and becomes a transcriptional activator that increases expression levels of the *ampC* gene<sup>92</sup>.

With regards to acquired antibiotic resistance in *P. aeruginosa*, chromosomal mutations in the genes or promoter regions of any proteins involved in the induction pathway of *ampC* (including AmpR and AmpD) can lead to derepression of the beta-lactamase gene and constitutive over-production of the resistance determinant<sup>93</sup>. However, the more common mechanism of acquired beta-lactamase resistance observed in *P. aeruginosa* strains is via the acquisition of genes encoding these drug-degrading enzymes on mobile genetic elements (MGEs)<sup>94</sup>. These MGEs can take the form of extrachromosomal plasmids, integrons (chromosomal gene cassettes primed for genetic recombination) or transposable elements containing DNA sequences that readily change position within a genome<sup>95</sup>. The key trait that all these MGEs have in common is the ability to easily and rapidly disseminate throughout bacterial species via the process of horizontal gene transfer.

As a consequence, beta-lactamase enzymes from virtually all Classes have been identified in clinical *P. aeruginosa* strains, including: Class A serine extended spectrum beta-lactamases (e.g. TEM, SHV, CTX-M, PER), Class B metallo-beta-lactamases (e.g. IMP, VIM, NDM, SPM) and Class D oxacillinases (e.g. OXA-1, OXA-2, OXA-10)<sup>96-99</sup>. Together, these enzymes confer resistance to the spectrum of beta-lactams used therapeutically to combat *P. aeruginosa* infections, hydrolysing cephalosporins, ureidopenicillins and carboxypenicillins. To overcome the threat of these resistance determinants, it is typically recommended that antipseudomonal beta-lactams are only prescribed therapeutically in combination with beta-lactamase inhibitors<sup>100</sup>. Tazobactam and clavulanic acid are the two main inhibitor compounds used to block the activity of beta-lactamase enzymes in *P. aeruginosa*, and they work by covalently bonding to residues in the active site of beta-lactamases, preventing hydrolysis of the antibiotics<sup>101-103</sup>. Unfortunately, resistance to beta-lactamase inhibitors, especially tazobactam, has recently emerged, driven by genetic mutations causing structural modifications in horizontally-acquired beta-lactamases<sup>104,105</sup>.

As well as obtaining beta-lactam degrading enzymes by horizontal gene transfer, *P. aeruginosa* can also acquire aminoglycoside modifying enzymes, with the genes encoding these enzymes typically found on plasmids that readily move between bacterial strains<sup>106</sup>.

Aminoglycoside modifying enzymes can be distinguished into three families based on their function – APH phosphotransferases (attach phosphate groups), ANT nucleotidyltransferases (attach adenyl groups) or AAC acetyltransferases (attach acetyl groups)<sup>107–109</sup>. All three families attach their respective chemical moieties on the hydroxyl and amino substituents on aminoglycoside antibiotics, with ANT and AAC enzymes being particularly prevalent in *P. aeruginosa* isolates<sup>110</sup>. As a direct results of these chemical modifications, the aminoglycoside drugs have drastically reduced affinity for their cytoplasmic target, the 30S ribosomal subunit, and thus are unable to exert their antimicrobial activity<sup>111</sup>. The antibiotics gentamicin and tobramycin extensively used against *P. aeruginosa* infections are especially susceptible to this mode of action of the aminoglycoside modifying enzymes.

Whilst *P. aeruginosa* strains can achieve aminoglycoside resistance by harbouring plasmids encoding drug-degrading proteins, an alternative common mechanism of resistance to aminoglycosides in this bacterium is target modification<sup>112</sup>. This resistance mechanism is also conferred by genes carried on MGEs, with plasmids and transposons the major drivers behind the horizontal transfer of the *rmtA* and *rmtB* genes that mediate non-susceptibility to aminoglycosides in *P. aeruginosa*<sup>113</sup>. The enzymes produced from these genes, RmtA and RmtB, are methylases that catalyse the methylation of 16S ribosomal RNA (rRNA)<sup>114,115</sup>. Their activity interferes with the binding of aminoglycoside compounds to the aminoacyl site of the rRNA within the bacterial 30S ribosomal subunit, and thus the antibiotics are no longer able to inhibit protein synthesis<sup>116</sup>. This target modification mechanism confers extremely high-level resistance to gentamicin, tobramycin and amikacin – the three aminoglycoside antimicrobials most frequently used to treat infections from *P. aeruginosa*.

Modification of an antibiotic's bacterial target is also a mechanism used by *P. aeruginosa* to acquire resistance to quinolone compounds. In this case, it is chromosomal mutations in the quinolone resistance determining region (QRDR) of the *gyrA/gyrB* genes and the *parC/parE* genes that leads to antibiotic non-susceptibility<sup>117–119</sup>. The *gyrA/gyrB* genes encode DNA gyrase subunits, whilst the *parC/parE* genes encode subunits of topoisomerase IV, and point mutations in their DNA sequences ultimately result in chemical and structural modifications of these key enzymes involved in DNA replication<sup>120</sup>. This in turn blocks the antipseudomonal quinolones ciprofloxacin and levofloxacin from affecting the ligase activity of DNA gyrase/topoisomerase IV, promoting bacterial survival and resistance even in the presence of the antibiotics.

Concerningly, there is increasing evidence that the rates of resistance to these front-line antibiotics in clinical *P. aeruginosa* isolates is rapidly increasing worldwide<sup>121</sup>. Two important surveillance studies demonstrate this rise in prevalence of antimicrobial resistance over the last three decades. The first of these explored the antibiotic susceptibility profiles of

13,999 nonduplicate *P. aeruginosa* strains obtained from intensive care unit patients across the United States of America from the years 1993 to 2002<sup>122</sup>. Using the Intensive Care Unit Surveillance Study database, it was found that the percentage of bacterial isolates that exhibited resistance to front-line antipseudomonal drugs increased significantly over the ten year period for every single antibiotic examined (**Table 1.1**). Indeed, the study showed that the rate of multidrug-resistance in these *P. aeruginosa* isolates (defined as non-susceptibility to three or more drug classes) rose from just 4% in 1993 to 14% in 2002.

A second similar surveillance study determined how the prevalence of antibiotic resistance changed in *P. aeruginosa* strains isolated from pneumonia patients at a single university hospital centre in Germany between 2004 and 2010<sup>123</sup>. Again, it was observed that rates of non-susceptibility to all commonly prescribed antibiotics against *P. aeruginosa* drastically increased during this seven year timeframe (**Table 1.2**). The most worrisome rises in resistance were seen with ciprofloxacin (15-fold increase in percentage of isolates resistant between 2004 and 2010), gentamicin (12-fold increase) and piperacillin (9-fold increase). Combined, these two studies clearly highlight that resistance to front-line antimicrobial agents in *P. aeruginosa* is a growing, global crisis. Consequently, as the current arsenal of antipseudomonal drugs becomes progressively more ineffectual, interest is increasingly turning towards alternative antibiotics, both old and new, that could be used to treat *P. aeruginosa* infections. A key target of these alternative antibiotics is lipopolysaccharide molecules in the cellular envelope of this Gram-negative pathogen.

**Table 1.1:** Antimicrobial resistance rates for *P. aeruginosa* isolates, U.S.A., 1993-2002<sup>122</sup>

Percentage of <i>P. aeruginosa</i> isolates resistant to antibiotic								
Year	Ceftazidime	Piperacillin	Imipenem	Aztreonam	Ciprofloxacin	Amikacin	Tobramycin	Gentamicin
1993	15	11	15	26	15	7	9	29
1994	16	13	15	29	17	12	11	29
1995	16	11	15	27	19	8	9	26
1996	18	12	15	27	19	8	10	25
1997	18	14	16	29	22	8	9	26
1998	17	13	13	29	25	8	12	32
1999	18	16	17	33	28	9	14	36
2000	19	15	16	33	28	9	12	32
2001	21	19	19	35	34	13	17	NA
2002	19	15	23	32	32	10	16	NA



**Table 1.2:** Antimicrobial resistance rates for *P. aeruginosa* isolates, Germany, 2004-2010<sup>123</sup>

Percentage of <i>P. aeruginosa</i> isolates resistant to antibiotic						
Year	Ceftazidime	Piperacillin	Imipenem	Ciprofloxacin	Tobramycin	Gentamicin
2004	1	1	2	1	1	1
2005	1	2	1	1	1	1
2006	1	1	1	2	1	3
2007	2	3	1	3	3	5
2008	4	5	4	3	2	3
2009	1	3	3	4	2	2
2010	6	9	10	15	11	12

## 1.3 Lipopolysaccharide as an antibiotic target

### 1.3.1 Lipopolysaccharide biosynthesis

Lipopolysaccharide (LPS) is a complex glycolipid molecule that constitutes the principal component of the outermost leaflet of the outer membrane bilayer in Gram-negative bacteria, including *P. aeruginosa*<sup>124</sup>. There are a number of significant functions of LPS in the outer membrane. It is foremost a physical barrier that protects bacteria from damaging extracellular factors (e.g. bacteriophages, host antimicrobial peptides, antibiotics)<sup>125–128</sup>. Moreover, LPS is a vital virulence factor for *P. aeruginosa*, acting as a potent signalling molecule to mediate interactions with host immune cell receptors, which ultimately leads to damage to host tissues and many of the pathologies associated with severe, invasive *P. aeruginosa* infections<sup>129–131</sup>. The biological importance of LPS is highlighted by two key properties. Firstly, the presence of LPS in the outer membrane is essential for the survival of the vast majority of Gram-negative bacteria, sparking significant interest in targeting these molecules as a antimicrobial strategy<sup>132</sup>. Secondly, the structure, biosynthesis and transport pathway of LPS is highly conserved between the diverse range of Gram-negative species<sup>133</sup>. Hence, although these processes have been largely studied and characterized in *Escherichia coli*, it is generally assumed with a great degree of confidence that the pathways are identical in *P. aeruginosa*. This assumption is supported by the extensive sequence homology identified between the genes involved in LPS biosynthesis and transport in *E. coli* and those in the *P. aeruginosa* genome<sup>134</sup>.

The LPS molecule itself is formed of three constituent parts (**Figure 1.5**): a lipid A domain (a disaccharide backbone attached to numerous fatty acid chains anchoring LPS to the outer membrane), a branched nine/ten-sugar core oligosaccharide domain, and the O-antigen domain (a repetitive carbohydrate polymer covalently attached to the core domain)<sup>135–137</sup>.

These three domain structures are synthesised by independent metabolic pathways, and possess distinct biological properties that together contribute to the variable roles of LPS. For example, lipid A is primarily responsible for eliciting an inflammatory response in host immune cells via the human Toll-like receptor 4 (TLR4), and can also confer resistance to environmental stresses (e.g. cationic innate host defence peptides)<sup>138,139</sup>. In contrast, the core oligosaccharide domain mediates the internalisation of bacteria, including *P. aeruginosa*, into host epithelial cells, such as those found in the airways and the cornea<sup>140,141</sup>. Out of all the domains, the O-antigen has the most diverse range of functions, being involved in protection of the bacteria from host immune defence systems (e.g. phagocytosis, complement-mediated killing, oxidative stress), whilst also being essential for virulence traits (e.g. swimming/twitching motility, surface colonisation/attachment, immunogenicity)<sup>142–146</sup>.

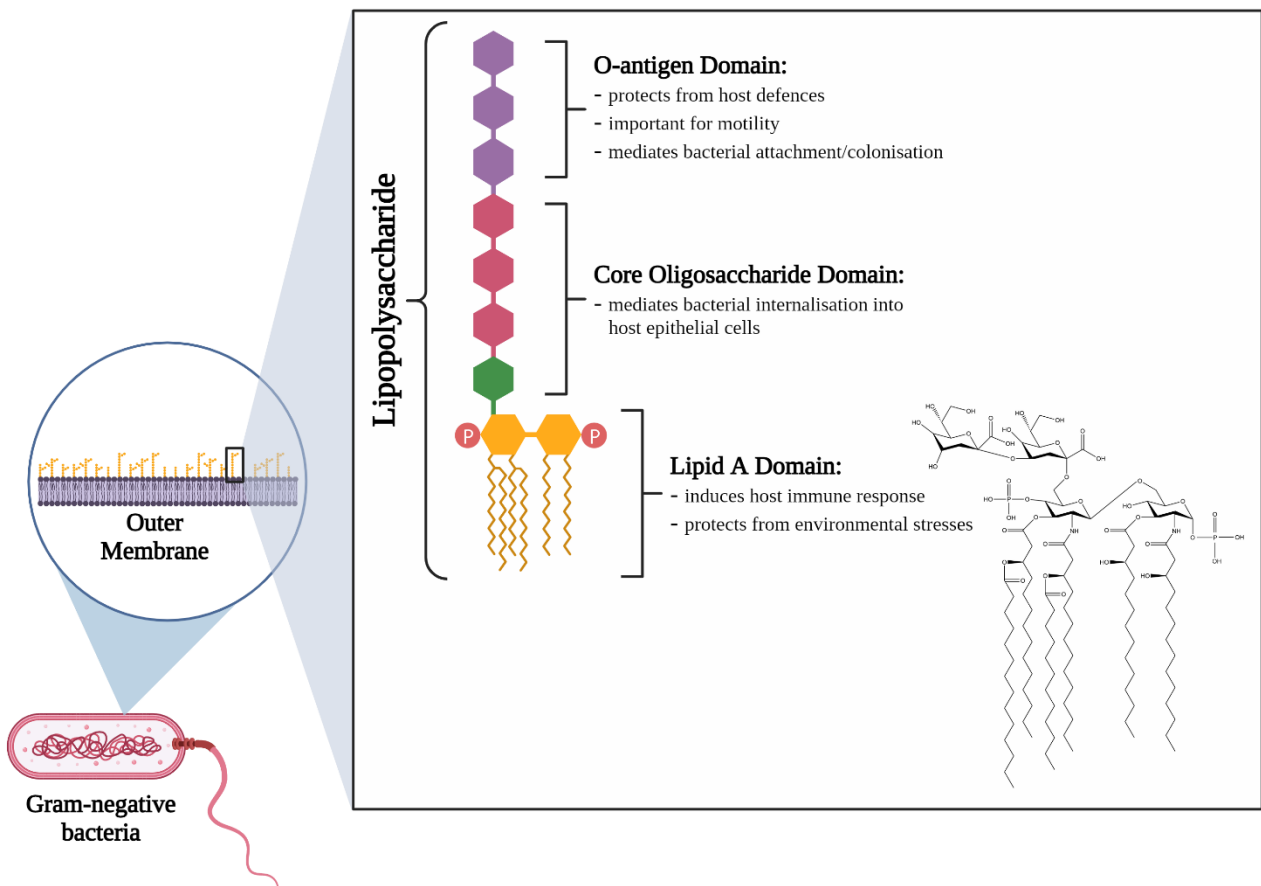


**Figure 1.5: Lipopolysaccharides have distinct structural regions with varying functions.**

Biosynthesis of lipid A occurs in the bacterial cytoplasm and on the innermost surface of the cytoplasmic membrane, and the pathway is mediated by the action of nine highly specific enzymes (**Figure 1.6**)<sup>147</sup>. Lipid A is assembled from the initial building block UDP-GlcNAc, which is converted to UDP-diacyl-GlcN following the addition of two 3-OH fatty acid

chains to the 2- and 3-positions of UDP-GlcNAc<sup>148</sup>. This reaction is catalysed by three soluble enzymes from the Lpx protein family: LpxA, LpxC and LpxD<sup>149–151</sup>. Whilst the first metabolic step mediated by the LpxA homotrimer is reversible, it is the second reaction catalysed by the zinc-dependent enzyme LpxC that represents the first committed step of lipid A biosynthesis. The UDP-diacyl-GlcN intermediate is subsequently hydrolysed through the activity of the peripheral membrane protein LpxH, forming lipid X<sup>152</sup>. Next, the enzyme LpxB, which also only temporarily associates with the cytoplasmic membrane, condenses both lipid X and its precursor compound UDP-diacyl-GlcN, generating disaccharide-1-P as a product<sup>153</sup>. Four enzymes that exist as integral cytoplasmic membrane proteins mediate the ensuing metabolic reactions. The kinase LpxK phosphorylates disaccharide-1-P at its 4'-position, producing lipid IV<sub>A</sub>, which is the minimal LPS structure required for bacterial viability<sup>154</sup>. The bifunctional enzyme KdtA then uses the sugar nucleotide CMP-Kdo as a donor in order to incorporate two Kdo residues (3-deoxy-D-manno-octulosonic acid) at the 6'-position of lipid IV<sub>A</sub><sup>155</sup>. This results in the formation of Kdo<sub>2</sub>-lipid IV<sub>A</sub>, which is chemically modified at its distal glucosamine unit by the action of LpxL (adds a secondary lauroyl residue) and LpxM (adds a myristoyl residue)<sup>156</sup>. Ultimately, the end-product of these catalytic reactions is the compound Kdo<sub>2</sub>-lipid A.

The biosynthetic pathway of the core oligosaccharide domain is a rapid and efficient process involving numerous membrane-associated glycosyltransferase enzymes that act as a co-ordinated complex (**Figure 1.7**)<sup>157</sup>. Together, these proteins use nucleotide sugars as donors to assemble the core oligosaccharide molecules onto Kdo<sub>2</sub>-lipid A. The core oligosaccharide structure can be separated into two chemically distinct regions – a largely conserved inner core directly connected to lipid A, and an outer core that exhibits greater structural diversity attached to the O-antigen domain<sup>158</sup>. The inner core is predominantly composed of Kdo and L-glycero-D-manno-heptose (Hep) residues<sup>159</sup>. Hep biosynthesis is catalysed by the GmhA, GmhB and GmhD enzymes, with the heptosyltransferase proteins WaaC/WaaF responsible for transferring the Hep residues produced onto Kdo<sub>2</sub>-lipid A<sup>160–162</sup>. Biosynthesis of Kdo involves four sequentially acting enzymes (KdsD, KdsA, KdsC, KdsB), and attachment to lipid A occurs via the Kdo transferase WaaA<sup>163,164</sup>. In contrast to the inner core oligosaccharide structure, the outer core is made up of three sugar types: D-glucose (synthesised by Glk, AlgC and GalU), L-rhamnose (synthesised by the RmlABCD pathway) and D-galactosamine<sup>134,165,166</sup>. Attachment of these sugars to the O-antigen domain is performed by the transferase proteins WapG, MigA and WapR<sup>167,168</sup>.

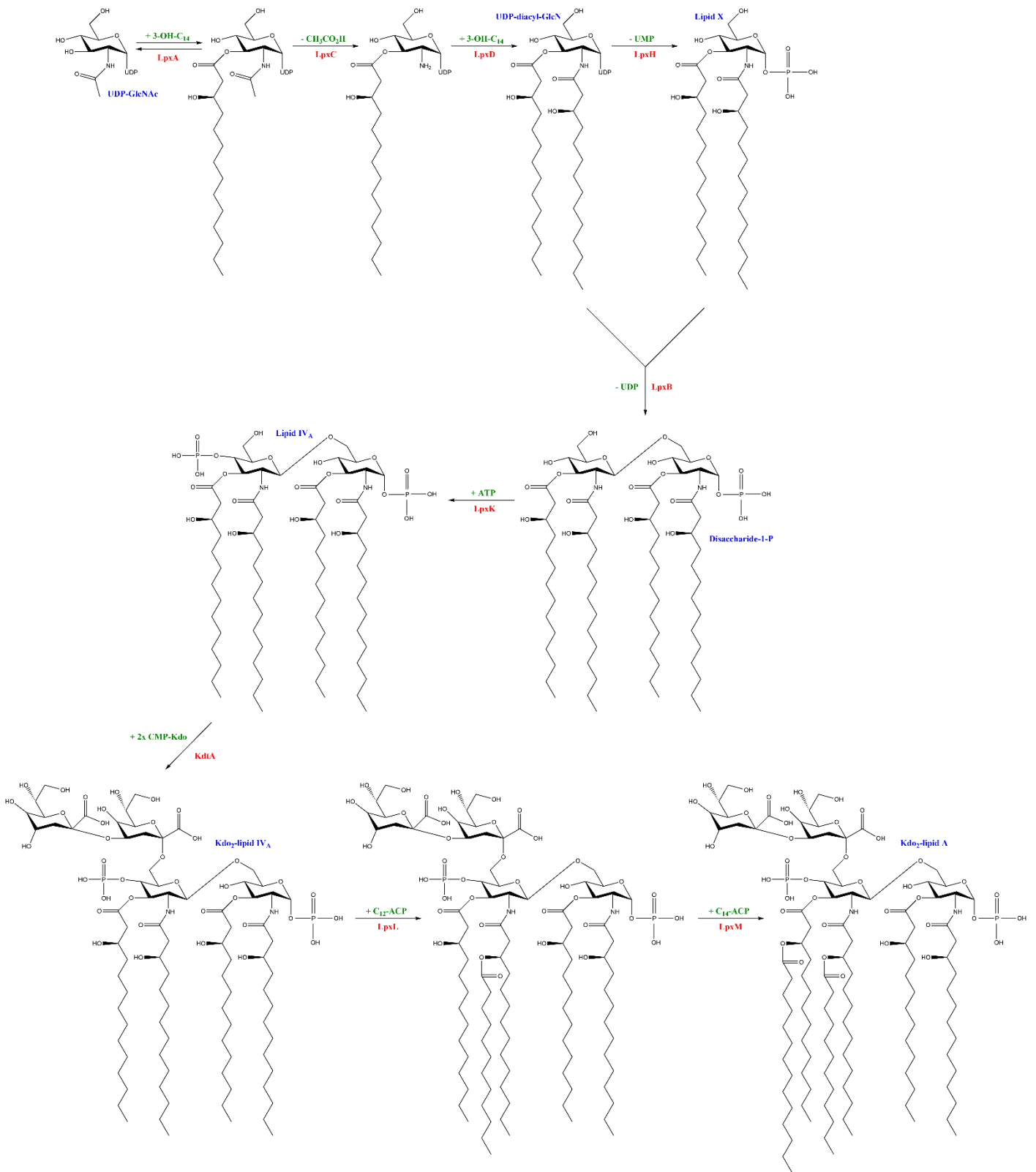


**Figure 1.6: The biosynthetic pathway of the lipid A domain of LPS.**

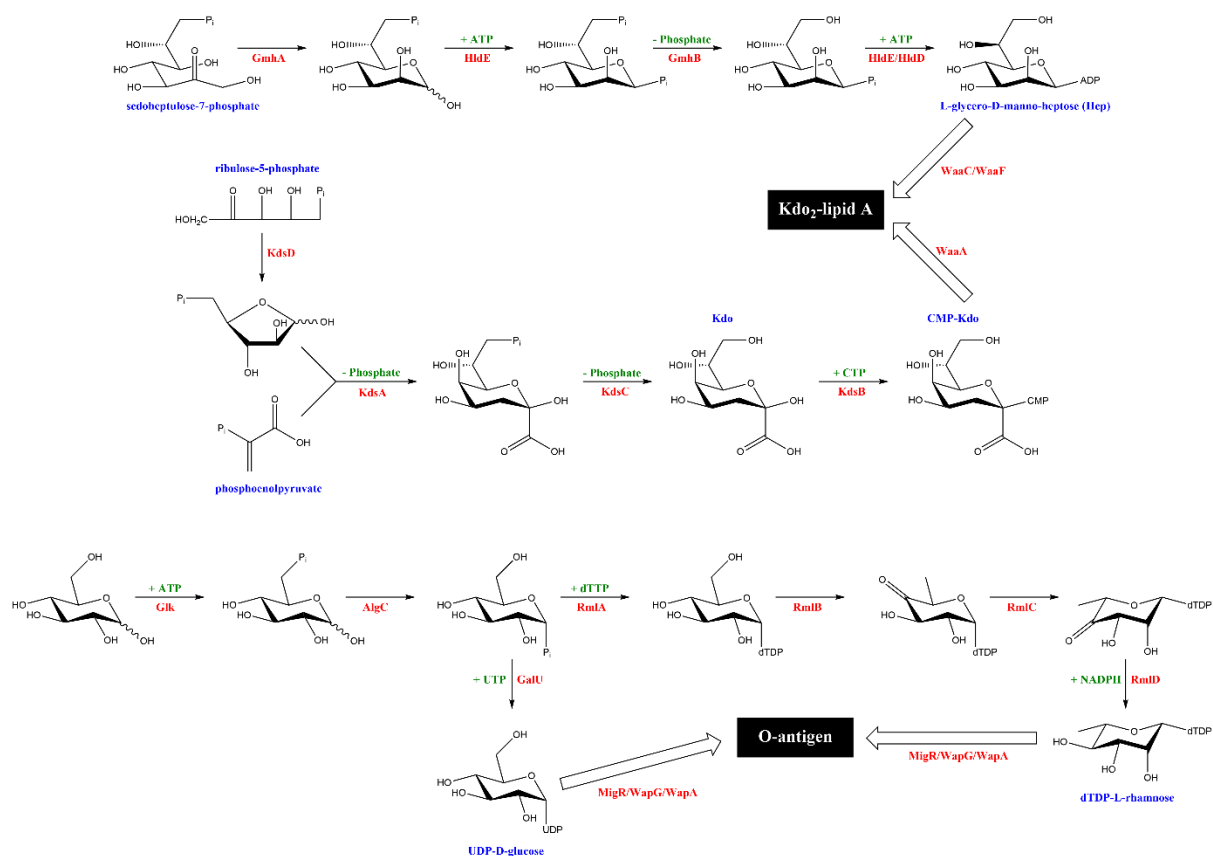


**Figure 1.7: The biosynthetic pathway of the core oligosaccharide domain of LPS.**

Similarly to the core oligosaccharide, the O-antigen domain undergoes biosynthesis at the innermost surface of the cytoplasmic membrane using sugar-based nucleotides as donors<sup>169</sup>. Oligosaccharide units of the O-antigen are assembled on undecaprenyl phosphate (a membrane-bound carrier also used in peptidoglycan and capsular polysaccharide biosynthesis) by glycosyltransferase enzymes<sup>170</sup>. These enzymes, as well as the proteins required for synthesising the unique O-antigen sugar-nucleotide precursor compounds, are encoded by the *rfb* gene cluster<sup>133,147</sup>. This family of genes also produce the polymerase enzymes and other components necessary for complete O-antigen assembly and transfer of O-antigen polymers across the cytoplasmic membrane. Once on the periplasmic outermost leaflet of the cytoplasmic membrane, the O-antigen undergoes further polymerisation by Wzy and Wzz, before being ligated by WaaL onto the core oligosaccharide-lipid A structure to form the final, complete LPS molecule (**Figure 1.8**)<sup>171–173</sup>. Notably, the O-antigen domain of LPS and the enzymes catalysing its biosynthesis exhibit considerable diversity between bacterial species<sup>174</sup>. For instance, the total number of O-antigen subunit groups can differ significantly, and the connections between them may be either linear or branched<sup>175</sup>. Moreover, O-antigens can exist in either a homopolymeric or a heteropolymeric form, and the O-glycosidic linkages

between unit structures can vary in position and/or stereochemistry. The structure of the O-antigen can even be heterogeneous at the level of a single bacterial cell – in *P. aeruginosa* strains, for example, there exist two distinct O-antigen forms on the cellular surface. The first, termed the common polysaccharide antigen (A band), is a simple homopolymer of D-rhamnose molecules, while the second, the O-specific antigen (B band) consists of between three and five unique dideoxy sugars arranged as a heteropolymer<sup>174,175</sup>.

As a consequence of this lack of conservation, inhibition of O-antigen biosynthesis has attracted little attention in terms of novel antibacterial strategies. However, the essential biosynthetic pathway of Kdo<sub>2</sub>-lipid A is a far more conserved metabolic process, and therefore is an attractive target for new antibiotics in development.

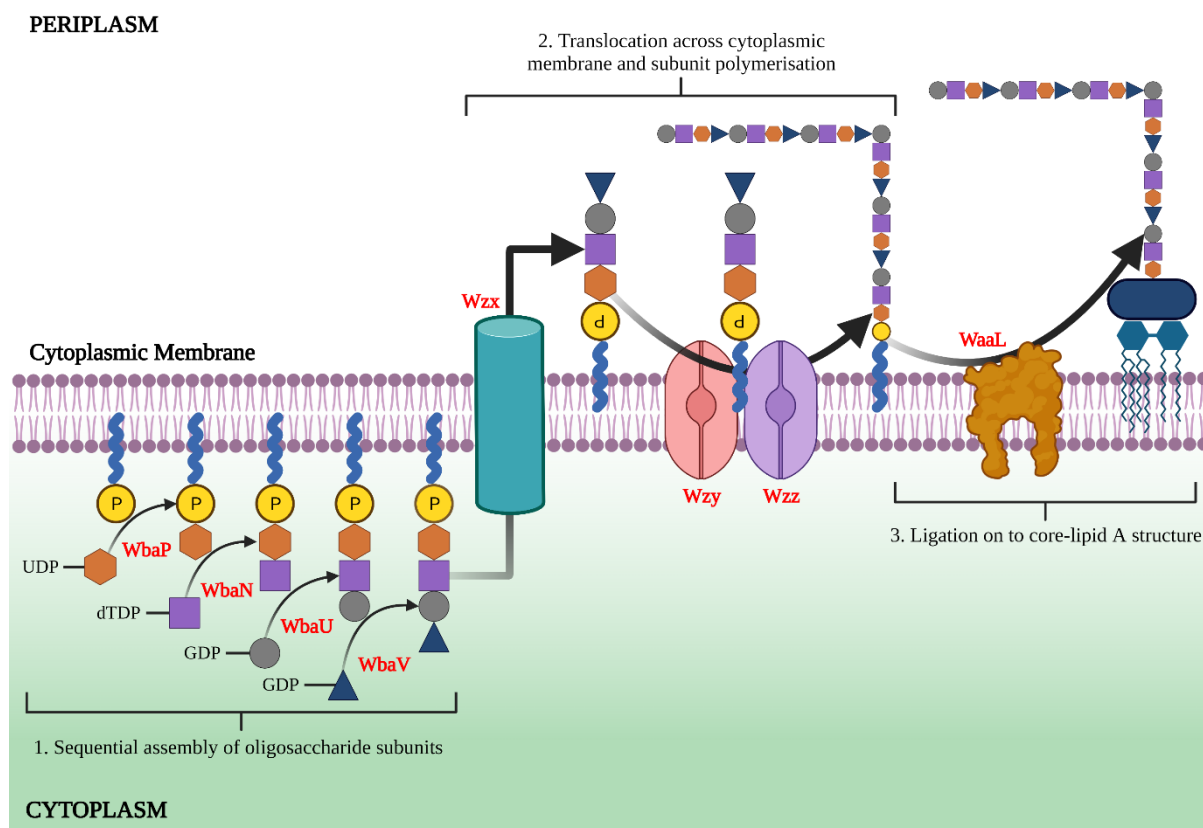


**Figure 1.8: The biosynthetic pathway of the O-antigen domain of LPS.**

### 1.3.2 Inhibitors of LPS biosynthesis

Identification of inhibitors of the enzymes involved in LPS biosynthesis has largely focused on the Lpx family of proteins, and in particular the zinc metalloenzyme LpxC which catalyses the second step (and first irreversible reaction) in the lipid A synthetic pathway (Table 1.3)<sup>176</sup>. The first inhibitor of LpxC, termed L-573,655, was identified in the 1980s by

Merck & Co. by measuring how synthesis of LPS was affected in *Salmonella* bacterial species using a radiolabelled galactose incorporation assay<sup>177</sup>. Optimised derivatives of L-573,655 based around its hydroxamic acid scaffold subsequently displayed potent activity against *E. coli* in a murine septicaemia model. However, a lack of effectiveness of these derivative compounds against other Gram-negative pathogens, including *P. aeruginosa* and *Serratia* species, led to project termination<sup>178</sup>. To overcome this narrow-spectrum activity, hydroxamic acid-containing small molecules were screened against a modified form of LpxC (H19Y), which led to the discovery of two compounds, BB-78484 and BB-78485<sup>179</sup>. These inhibitors reduced the enzymatic activity of LpxC *in vitro*, and also possessed significant antibacterial properties against a wide panel of Enterobacteriaceae, *Burkholderia* and *Serratia* strains. Nevertheless, as with L-573,655, there was unfortunately no further clinical development of these compounds.

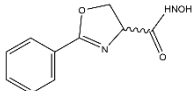
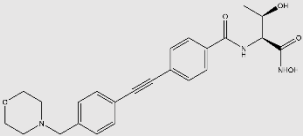
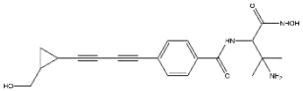
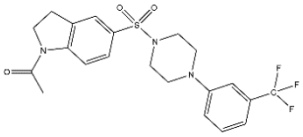
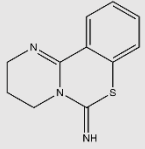
Perhaps the most potent LpxC inhibitor was discovered and characterised in the mid-2000s at Chiron/University of Washington<sup>180</sup>. Known as CHIR-090, this compound is an *N*-aroyl-L-threonine hydroxamic acid that was found to be efficacious against both *P. aeruginosa* and *E. coli*, displaying comparable activity to ciprofloxacin and tobramycin in antibiotic disc diffusion experiments<sup>181,182</sup>. In contrast to other LpxC inhibitors, where binding and dissociation of the small molecule compounds was virtually instantaneous, CHIR-090 is a two-step, slow, tight-binding inhibitor of LpxC, where the molecule undergoes an apparently irreversible isomerisation reaction with the metalloenzyme<sup>183,184</sup>. Despite this, progress of CHIR-090 into pipelines for clinical approval has been slow. Indeed, there has only been one LpxC inhibitor that has entered clinical trials – the small molecule compound ACHN-975<sup>185</sup>. Identified by Achaogen via a high-throughput *in vitro* screen using deacetylation of a radiolabelled UDP-GlcNAc derivative as a read-out, ACHN-975 was shown to possess whole-cell potency in several Gram-negative pathogens, and *in vivo* antimicrobial activity against *Klebsiella pneumoniae* in a murine thigh infection model<sup>186</sup>. However, during the Phase I clinical trial of ACHN-975, there were reports of inflammation at the site where the inhibitor was being infused, which led to the trial being immediately concluded and ACHN-975 being completely withdrawn from the antibiotic discovery pipeline<sup>187</sup>. As such, there remain no LpxC inhibitors approved for therapeutic use, despite decades of research and a highly promising target enzyme.

In addition to LpxC, other enzymes in the lipid A biosynthesis pathway have also been the focus of inhibitor development approaches. Screening of a library of 1.9 billion random 12-amino acid peptides from New England Biolabs identified the compound RJPXD33 that bound with moderate affinity to immobilised LpxD<sup>188</sup>. Interestingly, RJPXD33 was subsequently found to also bind and reduce the activity of LpxA<sup>189</sup>. These two acetyltransferase

enzymes mediate the first and third steps of LPS synthesis, making this dual target activity especially intriguing. In spite of whole-cell activity against a range of Gram-negative bacteria being achieved by fusing RJPXD33 to a membrane-disrupting peptide, it is not clear if this inhibitor will be taken forward to clinical trial stages<sup>190</sup>.

Similar small molecule compounds blocking lipid A biosynthesis that are stuck in pre-clinical development include an LpxH inhibitor (only referred to as Compound 1), and the KdsA inhibitor PD 404,182. The LpxH inhibitor Compound 1 was discovered using a colorimetric outer membrane perturbation assay, and whilst the sulfonyl piperazine molecule was efficacious in an efflux-deficient *E. coli* strain, a lack of activity in the wild-type strain has limited progress of the project<sup>191</sup>. PD 404,182 was identified in a 150,000 compound screen using a continuous coupled phosphatase assay as a potent inhibitor of KdsA, which catalyses Kdo biosynthesis and is required for formation of essential Kdo<sub>2</sub>-lipid A<sup>192</sup>. Although PD 404,182 possessed whole-cell antibacterial activity against wild-type *E. coli* when conjugated to a peptide as a prodrug strategy, it was unfortunately found that human peptidases rapidly degrade such inhibitor-peptide constructs, and thus PD 404,182 is also impractical in a clinical therapeutic setting<sup>193,194</sup>.

**Table 1.3:** Inhibitors of LPS biosynthesis in pre-clinical development

Name	Structure	Mechanism of Action	Stage of Development
L-573,655		Inhibits LpxC in <i>E. coli</i>	Terminated due to narrow-spectrum activity
CHIR-090		Slow, tight-binding inhibition of LpxC in <i>E. coli</i> , <i>P. aeruginosa</i>	In pre-clinical discovery stages
ACHN-975		Inhibits LpxC in <i>K. pneumoniae</i> + other Gram-negative pathogens	Withdrawn after Phase I clinical trials due to toxicity (inflammation)
RJPXD33	TNLYMLPKWDIP	Dual-targeting activity: binds and inhibits LpxA/LpxD in several Gram-negative bacteria	In pre-clinical discovery stages
Compound 1		Inhibits LpxH in efflux-deficient <i>E. coli</i>	In pre-clinical discovery stages
PD 404,182		Inhibits KdsA in <i>E. coli</i>	Abandoned due to rapid degradation by human peptidases



### 1.3.3 LPS transport

Transport of LPS from the cytoplasm to the outer membrane is, analogously to LPS biosynthesis, an essential process required for cell viability in the vast majority of Gram-negative bacteria<sup>195</sup>. If LPS is unable to traverse to the outer membrane, there is a build-up of toxic LPS precursor molecules within the cytoplasmic membrane and a reduction in the integrity of the outer membrane, which ultimately culminates in bacterial death<sup>196</sup>. Hence, the proteins involved in LPS transport have also been an appealing target in the search for urgently-needed, new antibiotic drugs against Gram-negative pathogens. The system by which LPS is exported to the cell surface has been resolved predominantly through investigations in *E. coli*; however, it is again widely accepted that these processes are highly conserved amongst Gram-negative species, with bioinformatic identification of homologous proteins strongly supporting this assumption<sup>197</sup>. Both precursors of LPS, “core oligosaccharide-lipid A” and the O-antigen domain, are synthesised at the innermost surface of the cytoplasmic membrane bilayer, and the first step of LPS transport requires these molecules to be transported across the cytoplasmic membrane<sup>198</sup>. This occurs via two discrete pathways involving separate proteins (**Figure 1.9**).

Core-lipid A transport is performed by the homodimeric enzyme MsbA, which functions as an ATPase-binding cassette (ABC) transporter<sup>199</sup>. As with all members of the ubiquitous ABC transporter superfamily, MsbA has two cytosolic nucleotide-binding domains and two transmembrane domains arranged across its six transmembrane helices<sup>200</sup>. Data from biochemical studies and crystal structures suggests that MsbA flips core-lipid A to the outermost leaflet of the cytoplasmic membrane through an “alternating access” model<sup>201</sup>. In this model, depending on the ATP-binding status of MsbA’s nucleotide-binding domains, the protein exists with its lumen open to either the cytosolic or the periplasmic face of the cytoplasmic membrane<sup>202,203</sup>. As the MsbA flippase enzyme alternates between these two states in an energy-dependent manner, core-lipid A molecules are moved into the outermost leaflet of the cytoplasmic phospholipid bilayer<sup>204</sup>. Interestingly, the ATPase activity of MsbA has been shown to be stimulated by lipid A precursor compounds, as well as by LPS itself<sup>205</sup>. Furthermore, MsbA also has a critical quality-control role, since any core-lipid A constructs that are incorrectly synthesised (e.g. where lipid IV<sub>A</sub> has not been properly converted to lipid A by LpxL/LpxM) act as a poor substrate for the enzymatic activity of MsbA<sup>206,207</sup>. In this manner, MsbA acts as a filter, preventing the flipping and eventual export of unsuitable LPS molecules to the cell surface which may compromise outer membrane integrity.

Transport of the fully synthesised O-antigen domain across the cytoplasmic membrane occurs under the control of another flippase enzyme, the Wzx protein. Key data implicating Wzx in the translocation of O-antigen molecules to the periplasmic face of the cytoplasmic

membrane arose from a study demonstrating that a *wzx* mutant in *Salmonella enterica* accumulates O-antigen subunits in the innermost leaflet of the cytoplasmic phospholipid bilayer<sup>208</sup>. The Wzx enzyme consists of 12 transmembrane segments, and it has been shown that the protein functions by recognising the first sugar phosphate of the O-antigen repeat subunits that is attached to the membrane-bound carrier undecaprenyl phosphate<sup>209–211</sup>. Interestingly, and in opposition to MsbA, there are no ATP-binding domains observed in the primary protein sequences of Wzx<sup>212</sup>. These protein sequences are notably highly variable between different bacteria, with minimal homology or conservation of certain residues detected amongst Wzx enzymes<sup>213</sup>. Nevertheless, Wzx flippases in distinct bacterial species share common hydrophathy profiles, and can even complement each other in the transport of different O-antigen sugar precursors across the cytoplasmic membrane<sup>214–217</sup>.

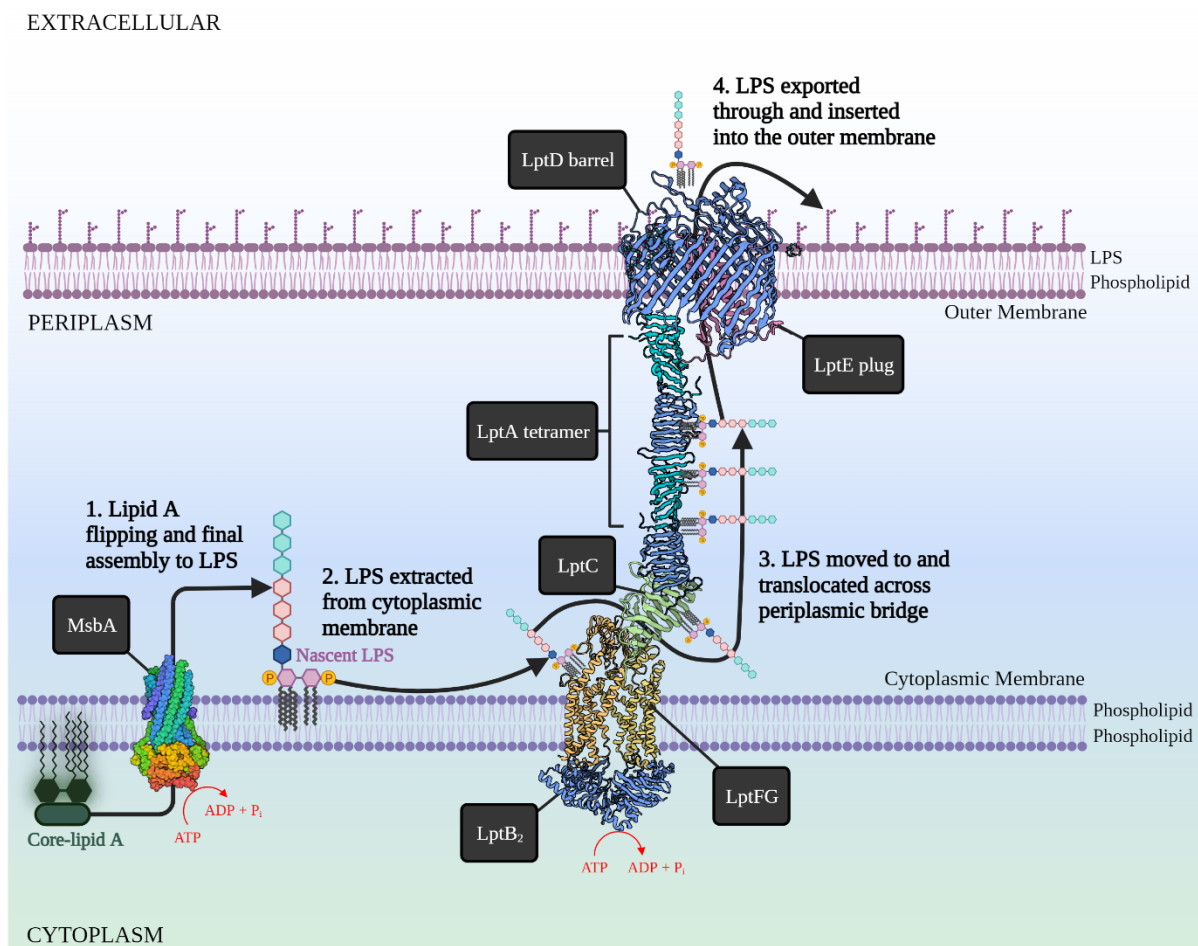


**Figure 1.9: The transport pathway of LPS from the cytoplasm to the outer membrane.**

Once the core-lipid A and O-antigen domains have undergone translocation to the outer leaflet of the cytoplasmic membrane and fusion under the control of WaaL, the nascent LPS molecule produced is ready for export to the outer bacterial membrane<sup>218,219</sup>. This

transport process is entirely dependent on the Lpt family of proteins, which physically interact to form an envelope-spanning bridge between the cytoplasmic and outer membranes<sup>220</sup>. It is this bridge that serves as the complex machinery through which LPS is exported to its ultimate destination on the bacterial surface, in an energy-dependent manner driven by the hydrolysis of ATP<sup>221</sup>. The Lpt system is made up of seven proteins (LptA, LptB, LptC, LptD, LptE, LptF and LptG) that are all essential for cell viability<sup>222</sup>. Depletion of any one of these Lpt transporter proteins results in the entire bridge structure becoming dysfunctional, and the subsequent accumulation of LPS structures in the periplasmic surface of the cytoplasmic membrane leads to bacterial death.

LPS transport mediated by the Lpt machinery can be broadly split into three stages: extraction of LPS from the cytoplasmic membrane, translocation of LPS across the periplasm, and export of LPS across the outer membrane. The first of these stages, LPS extraction away from the periplasmic leaflet of the cytoplasmic phospholipid bilayer, is carried out by the LptB<sub>2</sub>FG protein complex<sup>223</sup>. This complex is an ABC transporter, where the two LptB components are the ATPase nucleotide-binding domains, and LptFG function as the transmembrane domains<sup>224,225</sup>. Since the ATPase activity of LptB<sub>2</sub>FG is significantly higher than that of LptB alone, it is thought that the LptFG transmembrane structure stabilises LptB and facilitates its dimerization, which is a requirement for ATP hydrolysis<sup>226,227</sup>. Evidence from crystallography suggests that during ATP hydrolysis by LptB, there is substantial movement in this nucleotide-binding domain structure, with this movement predicted to lead to the conformational changes in the LptFG transmembrane domains of the ABC transporter that remove LPS molecules away from the cytoplasmic membrane<sup>224</sup>.

The next stage in LPS transport to the outer membrane is the movement of synthesised LPS across a periplasmic bridge fashioned out of the protein LptA. LptA connects to the LptB<sub>2</sub>FG complex through LptC, which spans the cytoplasmic membrane<sup>228</sup>. LptC interacts with LptB<sub>2</sub>FG via the  $\beta$ -jellyroll structure in its amino-terminal edge, with substitution of a single residue in this region sufficient to disrupt this interaction and the formation of the Lpt machinery<sup>229</sup>. By contrast, it is the carboxyl terminus in the transmembrane region of LptC that attaches to the N-terminus of LptA, with this LptCA complex observed to co-purify in size-exclusion chromatography experiments<sup>230-232</sup>. The transfer of LPS molecules from LptB<sub>2</sub>FG to LptA via LptC is another discrete ATP-dependent step in the LPS transport process<sup>233</sup>.

LptA itself exists in a multimeric form, with one crystal structure resolved identifying an LptA tetramer composed of monomeric subunits arranged in an end-to-end manner<sup>234</sup>. Along the backbone of each LptA monomer, there is a 90° twist, which gives a helical conformation to the periplasmic-spanning filament created from the stacking of LptA proteins. It was initially thought that LptA functions as a soluble chaperone molecule,

shielding the six fatty acyl chains in the lipid A domain of LPS molecules during transit across the periplasm<sup>197</sup>. However, the demonstration that LPS is still transported to the outer bacterial membrane even after removal of any soluble periplasmic components through pulse-chase experiments has led to a complete revising of this model<sup>235</sup>. Data from biochemical studies with epitope-tagged versions of the cytoplasmic membrane proteins LptB, LptC and LptF revealed that the LptA structure co-purifies with the outer membrane proteins of the Lpt machinery (LptD and LptE)<sup>236,237</sup>. This provided conclusive evidence that rather than acting as a chaperone for LPS across the periplasm, LptA molecules form a physical bridge that directly connects the two phospholipid bilayers in Gram-negative bacteria. Newly-synthesised LPS moves along this LptA bridge during translocation to the outer membrane, although the precise nature of the interaction between LPS compounds and LptA proteins remains unclear. It is thought that a continuous hydrophobic groove present in certain domains of LptA (the organic solvent tolerance protein A, OstA domains) may be key in periplasmic LPS transit, shielding the lipid A moiety from the surrounding aqueous environment<sup>230</sup>.

The final stage in transport of LPS to the bacterial surface is the export of LPS molecules off the LptA bridge and into the outermost leaflet of the outer membrane. This process is performed by an outer membrane translocon complex containing the proteins LptD and LptE<sup>238–240</sup>. The C-terminus of LptA interacts with the N-terminus of LptD in a conserved manner involving the edges of  $\beta$ -jellyroll structures present in the respective domains of both proteins, with deletion of LptD's amino-terminus disrupting this interaction<sup>230,232</sup>. In turn, the carboxyl-terminus of LptD interacts very strongly with LptE, with an extracellular loop in the  $\beta$ -barrel of LptD's C-terminal region providing the site where the two proteins crosslink<sup>241–243</sup>. LptD is essentially an outer membrane pore, and LptE resides within this pore in a so-called "two-protein, plug-and-barrel conformation"<sup>244</sup>. However, the function of the LptE "plug" is more than simply occluding the lumen of the LptD channel – it also has a role in promoting LptD assembly in a slow-folding pathway requiring disulphide bond rearrangement, and it may even directly interact with LPS molecules and regulate their assembly at the cell surface<sup>245,246</sup>.

The lumen of the crenellated  $\beta$ -barrel structure of LptD is the largest identified thus far for Gram-negative outer membrane proteins, and it is sufficient in size to allow the passage of fully-synthesised LPS molecules across the cell surface bilayer<sup>247,248</sup>. The arrival of LPS molecules after transit along the LptA bridge at the periplasmic amino-terminus of LptD is hypothesised to trigger a conformational change in the LptDE translocon, allowing the entry of LPS molecules to the interior of the  $\beta$ -barrel<sup>247</sup>. It has been proposed that whilst the majority of the LPS structure subsequently moves through the lumen of LptD's  $\beta$ -barrel, the hydrophobic lipid A moiety instead passes through the lipophilic intramembrane opening

between the N-terminal and  $\beta$ -barrel domains of LptD<sup>197,248</sup>. Ultimately, LPS molecules exit the lateral opening of the LptDE translocon complex, where they insert into the outermost leaflet of the outer membrane, facing extracellularly in their final destination. As with the other members of the Lpt family, LptD and LptE are essential, conserved proteins, raising considerable interest in targeting this complex as a novel antibacterial strategy.

### 1.3.4 Inhibitors of LPS transport

Antimicrobial drug discovery approaches seeking to inhibit the LPS transport machinery have predominantly revolved around three proteins: the flippase MsbA, the ATPase LptB, and the outer membrane pore LptD (**Table 1.4**). The first inhibitor of MsbA was identified through an extensive *in vitro* screen of 3 million small molecule compounds that could block the enzymatic activity of the cytoplasmic membrane protein<sup>249</sup>. This led to the discovery of a quinolone-based compound known as G592, which underwent subsequent scaffold optimisation steps to produce G907, a molecule with enhanced potency against MsbA. The mechanism of action of G907 is to uncouple the two cytosolic nucleotide-binding domains of the ABC transporter MsbA by trapping the protein in an inward-facing conformation<sup>250</sup>. As a consequence, core-lipid A structures cannot be flipped across the cytoplasmic membrane, leading to a breakdown in LPS transport and a loss of cell viability, as demonstrated by the extensive bactericidal activity of G907 against both *E. coli* and *K. pneumoniae* strains<sup>249</sup>. Nonetheless, attempts to transfer this *in vitro* efficacy into the clinical setting have failed because G907 binds readily to plasma proteins, resulting in a total alleviation of its potent antibacterial effects<sup>176,249</sup>. Despite numerous attempts to chemically modify G907 to minimise plasma protein binding, the once-promising inhibitor has now been discarded as a lead antimicrobial compound.

Attempts to target MsbA have not been abandoned in spite of the failure of G907, with a whole cell-based screen of 150,000 potential inhibitors investigated using an *Acinetobacter baumannii* strain which, uniquely for Gram-negative pathogens, can tolerate LPS deficiency<sup>251,252</sup>. By looking for hit compounds that could reduce the growth of wild-type *A. baumannii* but not an LPS-deficient form of the bacteria, an unnamed MsbA inhibitor here termed Compound 2 was discovered. In contrast to G907, Compound 2 in fact stimulates ATP hydrolysis by MsbA, however simultaneously decouples this ATPase activity from the flippase protein's effects on core-lipid A translocation across the cytoplasmic membrane<sup>252</sup>. This culminates in the toxic build-up of LPS precursor molecules in the innermost leaflet of the cytoplasmic phospholipid bilayer which interfere with other essential membrane processes. Translational progress of Compound 2 into clinical pipelines has thus far been slow, but the drug is certainly a highly promising inhibitor of the LPS transport pathway.

The first protein in the Lpt LPS translocation complex, LptB, has also been the subject of drug discovery screens for new antimicrobial agents against Gram-negative bacteria. One such screen used 244 kinase inhibitors commercially available from two libraries composed largely of ATP-competitive inhibitor molecules<sup>253</sup>. This identified a compound, also unnamed and here referred to as Compound 3, that blocked the ATPase activity of LptB. Unfortunately, the cytoplasmic nature of LptB has posed a significant barrier to clinical development of inhibitors of this enzyme, since any such molecule needs to cross both the impermeable bacterial membranes in order to exert any potency. Indeed, Compound 3 only displays antibacterial properties against an *E. coli* strain with a hyperpermeable outer membrane, and no efficacy against wild-type *E. coli*. Moreover, the ability of Compound 3 to inhibit LptB-mediated ATP hydrolysis is dramatically reduced when the protein exists as part of the multi-enzyme machinery LptB<sub>2</sub>FGC – its native state in whole bacterial cells<sup>227</sup>. Together, these properties of Compound 3 have proved damaging to its potential use as a therapeutic agent. Interestingly, it has recently been observed that novobiocin, an antibiotic traditionally used to target bacterial DNA gyrase, also binds to LptB and actually stimulates the ATPase activity of this ABC transporter<sup>254,255</sup>. However, the downstream consequences of this effect of novobiocin on LPS transport and cell viability have yet to be fully explored.

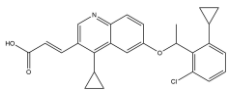
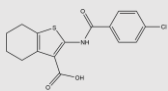
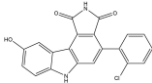
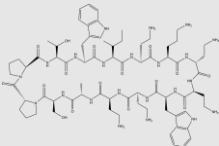
Whilst LptB inhibitors require passage across both bacterial membranes to access their cytoplasmic target, small molecule compounds blocking the activity of the outer membrane translocon structure LptD have a surface-exposed target; LptD has thus been the most studied protein of the LPS transport machinery in terms of novel drug development. A screen of a library containing  $\beta$ -hairpin peptidomimetic compounds based on the chemical structure of protegrin I (a membrane-disrupting host defence peptide) by Polyphor uncovered numerous hit compounds that target LptD and impact bacterial growth<sup>256</sup>. These hit compounds underwent several iterations of library optimisation, focussing especially on stability in plasma, reduced red blood cell haemolysis and potent antimicrobial activity against *P. aeruginosa* strains. This eventually resulted in synthesis of murepavadin (POL7080), a 14-amino-acid cyclical peptide representing a highly-specific, first-in-class novel antipseudomonal antibiotic<sup>257</sup>. Murepavadin interacts with the  $\beta$ -barrel structure of LptD, blocking the movement of LPS molecules across the outer membrane through its lumen and thus interfering with the essential LPS transport process<sup>258</sup>.

Preclinical testing of murepavadin was highly successful, with the inhibitor displaying a great degree of bactericidal activity against more than 1500 strains of *P. aeruginosa* obtained from across the globe, as well as isolates from human CF patients, but no cross-resistance with current front-line antipseudomonal drugs<sup>259,260</sup>. Moreover, studies using murepavadin in a wide range of murine infection models (thigh, lung and sepsis) concluded that the antibiotic

had outstanding *in vivo* efficacy, and from a pharmacokinetic standpoint, exhibited good penetration into epithelial lung fluid<sup>261–263</sup>. This encouraging data enabled murepavadin to enter Phase II clinical trials, where the LptD inhibitor demonstrated efficacy at treating VAP caused by *P. aeruginosa*<sup>264</sup>. Regrettably, in a subsequent Phase III trial of murepavadin, 56% of patients in the treatment group suffered kidney injury, with only 20% of individuals in the control group affected by the same pathology, leading to an immediate and premature termination of the clinical study<sup>176</sup>. It is now being investigated whether delivery of murepavadin via an inhaled route of administration could minimise these nephrotoxic side-effects while maintaining its potency especially in CF patients, with nebulised murepavadin due to enter clinical trials shortly.

As such, despite the wealth of research into inhibitors of LPS biosynthesis and transport, there are no new antibiotics blocking these processes that can currently be clinically used to combat multidrug-resistant *P. aeruginosa*. The urgent requirement for antimicrobial strategies against infections caused by such *P. aeruginosa* strains has led to a renewed interest in physically targeting LPS itself to cause outer membrane disruption and bacterial death. This has led to a resurgence in use of an old class of antibiotics, the polymyxins.

**Table 1.4:** Inhibitors of LPS transport in pre-clinical development

Name	Structure	Mechanism of Action	Stage of Development
G907		Inhibits MsbA in <i>E. coli</i> , <i>K. pneumoniae</i> - traps protein in inward-facing form	Terminated due to significant binding to plasma proteins
Compound 2		Stimulates MsbA ATP hydrolysis in A and decouples protein ATPase activity from flippase activity	In pre-clinical discovery stage
Compound 3		Inhibits ATPase activity of LptB in hyperpermeable <i>E. coli</i>	Abandoned due to lack of activity against native LptB <sub>2</sub> FGC in wild-type <i>E. coli</i>
Murepavadin (POL7080)		Interacts and inhibits the function of the LptD β-barrel	Intravenous form withdrawn after Phase III clinical trials due to toxicity (kidney damage); nebulised form in pre-clinical development

## 1.4 Colistin, a last-resort antibiotic

### 1.4.1 Colistin discovery, structure and chemistry

The polymyxin family of antibiotics consists of five chemical compounds, termed polymyxin A-E, of which two drugs are currently available and prescribed for the treatment of Gram-negative pathogenic infections – polymyxin B and polymyxin E (colistin)<sup>265</sup>. Colistin was first discovered in Japan in 1949, when it was isolated as a secondary metabolite from a flask of fermenting *Paenibacillus polymyxa* var. *colistinus*<sup>266,267</sup>. All polymyxin compounds are produced by strains of *P. polymyxa*, a nitrogen-fixing Gram-positive bacterial species commonly found in soil, plant tissues, hot springs and marine sediments<sup>268–270</sup>. In these bacteria, colistin and polymyxin B are produced by nonribosomal peptide synthetase systems<sup>271</sup>. In order to understand this biosynthetic pathway of the polymyxin antibiotics, it is first important to consider their chemical structure.

Colistin and polymyxin B are both cyclic lipopeptide compounds composed of 10 amino acids, arranged as a circular heptapeptide linked to an exocyclic tripeptide, which in turn is attached to a fatty acid residue (**Figure 1.10**)<sup>272</sup>. In the case of colistin, this fatty acid residue can be either a 6-methyl-octanoic acid group (colistin A) or a 6-methyl-eptanoic acid group (colistin B)<sup>273,274</sup>. In the clinical setting, colistin exists as a complex mixture of colistin A and colistin B, with the relative proportions of these two components varying between pharmaceutical preparations<sup>275,276</sup>. Polymyxin B and colistin differ only by a single amino acid residue at position 6 of the antibiotics' chemical structure – colistin has a D-leucine group at this position, whereas in polymyxin B this is replaced by a D-phenylalanine isomer<sup>277</sup>. The other nine amino acids of polymyxins are a variety of D-leucine and L-threonine residues, as well as five conserved L- $\alpha$ - $\gamma$ -diaminobutyric acid (DAB) residues at positions 1, 3, 5, 8 and 9 of the antibiotic molecules<sup>278</sup>. These DAB residues are crucial for conferring the heptapeptide ring in the C-terminus of polymyxin compounds with a net positive charge at a physiological pH, and the cationic, hydrophilic nature of this macrocycle is essential for colistin's antimicrobial properties<sup>279</sup>. In contrast, the amino-terminus of colistin and polymyxin B, which contains the saturated, branched fatty acyl segment of the antibiotics, is hydrophobic and data from structure-activity relationship (SAR) studies has again revealed that this N-terminal hydrophobicity is critical to the antibacterial effects of polymyxins<sup>280–282</sup>.

Nonribosomal biosynthesis of polymyxin molecules occurs via synthetases with multiple modules, each containing a set of four enzyme domains: an adenylation domain, a peptidyl carrier protein domain, an epimerization domain and a condensation domain<sup>283</sup>. Colistin and polymyxin B synthesis commences with the fatty acyl chain (the loading module) associating with an adenylation domain and a peptidyl carrier protein domain, which leads to



the addition of the first DAB residue<sup>284</sup>. Subsequently, the remaining amino acids are sequentially assembled on this DAB residue, with a linear chain of amino acid groups extending through peptide-bond formation and condensation reactions<sup>285–287</sup>. Once the linear form of the polymyxin compounds is complete, cyclization is accomplished through the action of a thioesterase enzyme situated in the C-terminus of the final synthetase module<sup>288</sup>. This leads to the cyclic lipopeptide molecule being liberated from the enzyme, forming the fully synthesised polymyxin molecule.

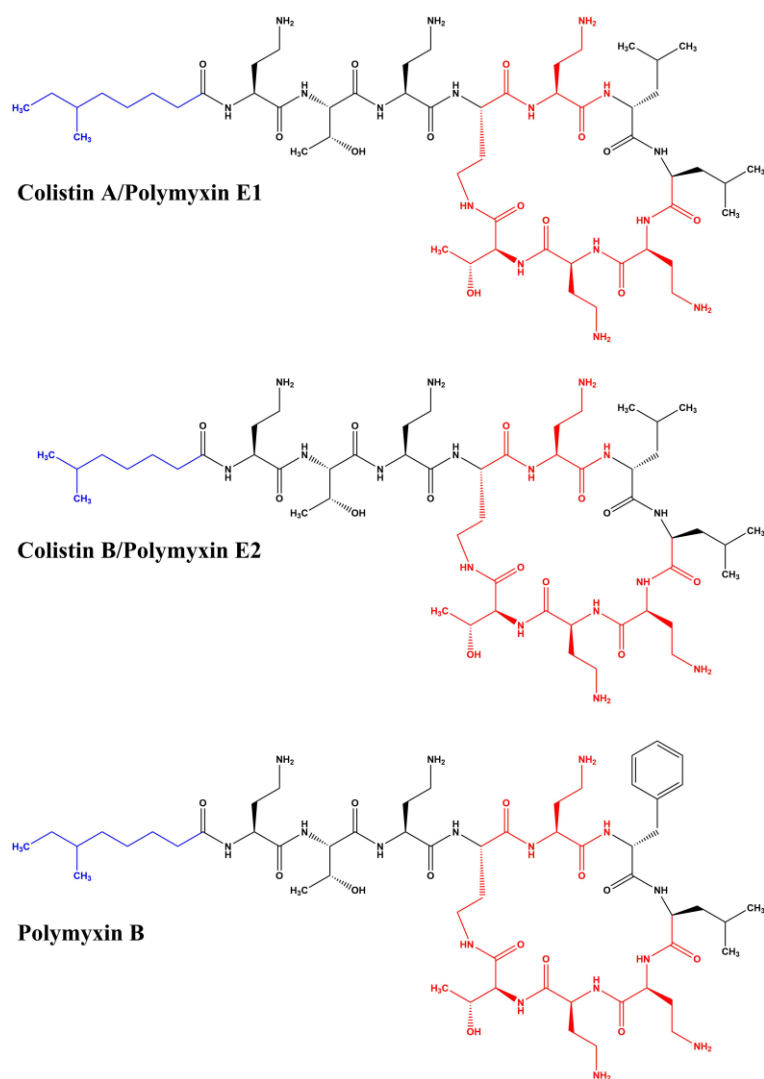


**Figure 1.10: Chemical structures of colistin (A and B) and polymyxin B.** Cationic amino acid residues in the heptapeptide macrocycle are shown in red; the N-terminal lipophilic fatty acyl chain is shown in blue.

### 1.4.2 Clinical use of colistin

As a therapeutic agent against infections caused by Gram-negative pathogens, colistin is available in two different forms – colistin sulfate and colistimethate sodium<sup>289</sup>. Importantly, these two derivatives of the colistin molecule cannot be interchangeably used, since they possess distinct chemical properties. Colistin sulfate is a stable, cationic compound that is active in its native state<sup>290</sup>. It is typically prescribed only as a topical agent for infections of the skin, eye or ear, and in rare cases, it is administered orally to achieve decontamination of the bowels, since colistin sulfate absorption into the gastrointestinal tract is poor<sup>291–293</sup>. In contrast, for the treatment of more invasive infections where parenteral colistin administration is indicated, the antibiotic is given in the form of colistimethate sodium<sup>294</sup>. This formulation, which is prepared by treatment of colistin with sodium bisulfite and formaldehyde, has reduced toxicity compared with colistin sulfate, and hence is thought to be safer for systemic use<sup>295,296</sup>.

Colistimethate sodium is an anionic compound that is highly unstable in both *in vitro* and *in vivo* aqueous solutions, where it readily undergoes hydrolysis to generate colistin sulfate in addition to other partially sulfomethylated colistin derivatives<sup>297,298</sup>. This hydrolytic reaction is vital for the success of the antibiotic, since by itself colistimethate sodium is an inactive prodrug that exerts minimal antibacterial activity. Colistimethate sodium is typically injected intravenously, though occasionally it can be administered intramuscularly, or by intrathecal/intraventricular routes (specifically in the treatment of meningitis or inflammation of the brain's ventricles)<sup>299–302</sup>. More commonly, a nebulised formulation of colistimethate sodium is utilised against VAP and infections from Gram-negative bacteria in CF patients to allow for aerosolised antibiotic administration directly into the lungs<sup>303–305</sup>.

Colistin was first used clinically in the late 1950s across Europe and Japan as a broad-spectrum antimicrobial agent to combat Gram-negative pathogens, with colistimethate sodium achieving FDA approval in the USA in 1959 for the treatment of UTIs and infectious diarrhoea<sup>306,307</sup>. Up until the mid-1970s, colistin was readily prescribed in human medicine for the treatment of a wide range of infections caused by Gram-negative bacteria, and even developed extensive use in veterinary medicine both as a prophylactic agent for livestock growth promotion in agriculture, and as a common therapeutic option<sup>308,309</sup>. However, the development of numerous aminoglycoside antibiotics that exhibited minimal toxic side-effects as front-line antimicrobial drugs meant that the therapeutic use of colistin was virtually abandoned across the globe for two decades across the 1980s and 1990s. Indeed, parenteral administration of colistimethate sodium was severely restricted, with this formulation only remaining in clinical practice as an antipseudomonal agent in patients with CF<sup>310–312</sup>. Since the mid-1990s, the emergence of multi-drug resistant Gram-negative pathogens that exhibit

non-susceptibility to all commonly used front-line antimicrobials has prompted a resurgence in the use of colistin as a so-called “antibiotic of last resort”<sup>313</sup>. This means that in patients infected with bacteria against which beta-lactam, quinolone and aminoglycoside-based therapies are ineffective, colistin is the final treatment option utilised to try and eliminate the pathogen and keep the patient alive.

Indeed, as the prevalence of life-threatening, multi-drug resistant Gram-negative pathogens has rapidly risen over the past two decades, there has been a concurrent increase in the number of doses of colistin being administered in clinical settings. In England, evidence supporting this surge in colistin prescriptions is apparent in two key studies. The first of these, conducted by the Bureau of Investigative Journalism, explored antibiotic use in hospitals in England between 2010 and 2015<sup>314</sup>. Their data revealed that the number of Defined Daily Doses (DDDs) of colistin given to patients rose 23% between 2010 and 2013 (from 237,068 doses to 293,918 doses), before a much more sudden jump of 65% (up to 485,024 doses) in only two years till 2015. The second investigation looking at trends in prescriptions of colistin was the English Surveillance Programme for Antimicrobial Utilisation and Resistance (ESPAUR) study, conducted by Public Health England in 2018<sup>315</sup>. This study reported that colistin consumption increased in the five-year period between 2013 and 2017 in virtually all NHS Acute Trust Types (Small, Large, Multiservice, Specialist and Teaching Trusts). However, this surge was largely driven by changes in Acute Specialist Trusts, where colistin use rose 66.3% between 2016 and 2017, reaching a peak of 315.6 DDDs per 1,000 admissions. A particular increase in inhalational administration of nebulised colistin for the treatment of CF and non-CF bronchiectasis in Trusts specialising in respiratory diseases was likely responsible for this jump, with the use of aerosolised colistin rising more than 6-fold (1.788 to 11.739 DDDs per 1,000 admissions) in the five years till 2017.

### **1.4.3 Colistin dosing and pharmacokinetics**

When colistin was first approved for clinical use in 1959, drug regulatory bodies across the world were not stringent with mandating a pharmacological evidence-based approach for the development of antibiotic dosing strategies. Consequently, there were almost no official guidelines for rational, optimised use of the polymyxin antibiotic to maximise efficacy whilst minimising toxic off-target effects and the emergence of drug resistance<sup>316,317</sup>. The avoidance of colistin as an antimicrobial therapeutic agent in the 1980s and 1990s further compounded this problem. Today, dosing regimens for colistin can vary wildly depending on geographic location, route of administration, the manufacturer of pharmaceutical preparations and any underlying health conditions of patients<sup>318,319</sup>. One of the key hurdles and sources of confusion in terms of colistin dosing is the absence of a universal dosing unit, with certain products providing recommended dosage regimens in milligrams, and other formulations using

international units (IU)<sup>320</sup>. Although a formula for converting milligrams of colistin to IU has been deduced (1 mg = 12,500 IU), further complexity is added by the fact that some manufacturers of colistimethate sodium report dose measurements as milligrams of “colistin base activity”, as opposed to stating milligrams of the colistin derivative compound itself<sup>278</sup>. Colistin base is known to be substantially more active than the inactive prodrug form colistimethate sodium, often necessitating an additional conversion step when deciding on dosage strategies (1 mg of “colistin base” = 2.67 mg of colistimethate sodium)<sup>320</sup>.

In the U.S.A., manufacturers recommend that intravenous colistimethate sodium is administered at a daily dose of 2.5-5 mg/kg, with administration divided into between 2 and 4 doses spread equally across a day<sup>274</sup>. However, this dosing strategy is modified in patients suffering from renal failure. In patients with mild renal dysfunction (serum creatinine level between 1.3 and 1.5 mg/dl), it is recommended that 2 million IU of colistin is administered every 12 hours, with this same dose prescribed every 24 hours for moderate renal failure (serum creatinine level between 1.6 and 2.5 mg/dl), or every 36 hours in severe renal failure (serum creatinine level above 2.6 mg/dl)<sup>321</sup>. If a patient is undergoing dialysis due their renal dysfunction, colistimethate sodium dosing is further adjusted to 2-3 mg/kg (post-haemodialysis) or 2 mg/kg (during peritoneal dialysis)<sup>322,323</sup>.

Contrastingly, in the U.K., it is recommended that colistimethate sodium is given intravenously at a dose of 80-160 mg every 8 hours in individuals with a body weight greater than 60 kg<sup>320</sup>. In children or adults with a body weight less than 60 kg, manufacturers advise a dosing regimen of 4-6 mg/kg of colistimethate sodium per day, administered in three equally-spaced doses across a day<sup>294</sup>. In its nebulised formulation for administration by inhalation, it is recommended that every 12 hours, 40 mg colistimethate sodium is given to patients weighing less than 40 kg, and 80 mg colistimethate sodium is given to patients weighing more than 40 kg<sup>274</sup>. In the rare cases where colistin has been injected directly into cerebrospinal fluid for the treatment of meningitis and ventriculitis, dosage of colistimethate sodium has ranged from 3.2-10 mg given once a day for intrathecal administration, and 1.6-20 mg per day in up to two doses for intraventricular administration<sup>324-330</sup>. In most cases, colistimethate sodium treatment is continued for between 10 and 14 days.

As with the paucity of scientific data regarding optimal colistin dosing, there was also until recently a dearth of studies investigating the pharmacokinetic and pharmacodynamic properties of colistin. It is established that the primary route by which colistin salts are excreted following systemic administration is via glomerular filtration in the kidneys, with no reports in human patients of the antibiotic being excreted via the biliary route<sup>274,298,331</sup>. However, a high performance liquid chromatography (HPLC)-based study in rats revealed that the clearance value of colistimethate sodium following intravenous administration was

0.010 ml/min/kg, which is substantially lower than the expected clearance value for a drug being excreted by glomerular filtration<sup>332</sup>. It was subsequently found that this slow renal excretion of the colistin derivative was due to a high degree of tubular reabsorption of the antibiotic<sup>333</sup>. Interestingly, following clinical administration of colistimethate sodium, not all of the compound is hydrolysed and converted to active colistin salts, with up to 60% of the formulation being excreted in urine in the form of the unchanged inactive prodrug within the first 24 hours after initial dosing<sup>334–336</sup>. In CF patients receiving intravenous colistimethate sodium, it was determined that the prodrug had a mean half-life of  $124 \pm 52$  minutes, whilst the colistin sulfate compound formed from the initial formulation had a mean half-life of  $251 \pm 79$  minutes<sup>331</sup>. Colistin binds tightly and extensively to body tissue in numerous mammalian organs, including to cells in the brain, heart, lung, liver and kidney, as well as to plasma proteins in rats, dogs and calves, where 55% of antibiotic molecules can be found associated with proteins present in blood plasma<sup>337–340</sup>.

The development of novel chromatographic techniques, including HPLC and liquid chromatography-tandem mass spectrometry processes, has enabled accurate and sensitive measurements of plasma colistin levels to be made. One study using these techniques concluded that in rats treated intravenously with a range of colistimethate sodium doses, the active colistin salt formed exhibits linear pharmacokinetic properties<sup>341</sup>. In human patients, the pharmacokinetics of colistin varies markedly between the two key clinical groups where the antibiotic is commonly used – individuals with CF, and critically-ill patients<sup>308</sup>. In CF patients administered with intravenous colistimethate sodium, it was reported that the half-life of the colistin antibacterial agent generated from the prodrug was more than 4 hours. In stark contrast, the half-life in critically-ill individuals is more than 3-times greater (14.4 hours), with this difference hypothesised to be due to reduced conversion of colistimethate sodium to active colistin, or the fact that many of these patients suffer from multi-organ failure, including severe renal dysfunction<sup>342</sup>.

Notably, despite this difference in antibiotic half-life between CF and critically-ill patients, three important studies have revealed that there does not appear to be a significant discrepancy in the peak steady-state plasma concentration ( $C_{\max}$ ) of colistin in these two clinical cohorts. The first investigation of colistin pharmacodynamics in 12 CF individuals in the U.K. found that formed colistin reached a  $C_{\max}$  of 1.2-3.1  $\mu\text{g/ml}$ <sup>331</sup>. Analogously, two studies looking at 13 critically-ill individuals in Italy and 14 intensive care unit patients in Greece established that the  $C_{\max}$  of colistin following intravenous colistimethate sodium was 0.68-4.65  $\mu\text{g/ml}$  and 1.15-5.14  $\mu\text{g/ml}$ , respectively<sup>343,344</sup>. Crucially, and as expected, the dosing regimen of colistin plays a vital role in determining the ultimate  $C_{\max}$  of the antibiotic. In another clinical investigation in Greece, 18 critically-ill subjects were administered an

intravenous infusion of colistimethate sodium in four doses every 8 hours<sup>342</sup>. After the first dose of the antibiotic, the mean formed colistin  $C_{max}$  measured in venous blood samples was only 0.6 µg/ml. However, once patients has been treated with the fourth infusion of colistimethate sodium, the  $C_{max}$  of the polymyxin antibiotic increased nearly four-fold, up to 2.3 µg/ml. This study also indicated that it required 2-3 days of continuous colistimethate sodium dosing before colistin  $C_{max}$  values are achieved in most critically-ill individuals. A study using an *in vitro* pharmacodynamic model also reported that a multi-dosing strategy of colistin was beneficial, since although it did not improve the antibiotic's bactericidal effects, reducing the duration of the delay between doses minimised the emergence of colistin resistance<sup>345-348</sup>.

#### **1.4.4 Colistin toxicity**

The most frequent and serious adverse effect of clinical colistin administration is nephrotoxicity<sup>349</sup>. Indeed, the extensive reports of renal toxicity associated with colistin treatment in the 1970s were a predominant factor in the withdrawal of use of polymyxins as antibiotic therapeutic agents in the 1980s-1990s<sup>350</sup>. A first major trial of colistin safety during 317 cases of therapy reported adverse renal reactions occurring in 20.2% of utilisations<sup>301</sup>. Similar results were observed in intensive care unit patients treated with high doses of colistin, where all fourteen patients enrolled in the study exhibited symptoms of reduced kidney function<sup>351</sup>. These symptoms of nephrotoxicity typically manifest as decreased clearance of creatinine, increased serum creatinine levels and increased serum urea stemming from acute tubular necrosis<sup>352-357</sup>. In most cases, these renal pathologies are reversible and normal kidney function is restored in the weeks and months following cessation of colistin administration, which can occur immediately upon clinical detection of nephrotoxicity<sup>358</sup>. Nonetheless, in rare instances, there have been reports of irreparable damage to the kidneys occurring post-colistin exposure, with symptoms of kidney damage persisting even in the absence of polymyxin therapy<sup>301</sup>. The nephrotoxic side-effects of colistin treatment are dose-dependent, and in fact more related to the total cumulative dose of colistimethate sodium administered, rather than the single or even daily dose<sup>274,294</sup>. This can be particularly important to monitor when colistin is used to treat infections from Gram-negative pathogens in overweight/obese patients, since excessive dosing based on body weight can frequently occur and often leads to renal injury<sup>359</sup>.

It has been suggested that the nephrotoxic adverse consequences of administering colistin therapeutically may have been overstated in the 1970s, potentially due to at the time there being more toxic formulations of the antibiotic, poor monitoring of renal function and a lack of supportive treatments for critically-ill patients<sup>274</sup>. In support of this, more recent studies have identified that rates of nephrotoxicity in individuals receiving intravenous colistin are between 8-14.3%, which is lower than the incidences of renal damage reported in the

1970s<sup>360,361</sup>. However, polymyxin antibiotics remain potently nephrotoxic drugs, and the establishment of the RIFLE (Risk, Injury, Failure, Loss, End-Stage) progressive criteria for accurate diagnosis of Acute Kidney Injury (AKI) has served to highlight this point<sup>362–364</sup>. In 66 patients at the Walter Reed Army Medical Center, the incidence of AKI categorised by the RIFLE system following intravenous administration of colistimethate sodium was 45%, resulting in premature termination of colistin treatment in 21% of subjects<sup>355</sup>. Importantly, although some of these individuals suffering from AKI had evidence of acute tubular necrosis in urine microscopic diagnosis, none of the patients were classified as being in the Loss or End-Stage categories of the RIFLE criteria, suggesting that the nephrotoxic consequences of colistin therapy may be common but not severe. Similar rates of AKI post-colistin treatment have been described in a retrospective cohort study of 71 adult patients in the Samsung Medical Center (53.5% of individuals placed on the RIFLE system), and in 119 patients spread across four tertiary university hospitals in South Korea (54.6% of individuals placed on the RIFLE system)<sup>365,366</sup>.

In addition to nephrotoxicity, colistin use in humans is also associated with neurotoxic side-effects, although the incidence of brain injury following administration of the polymyxin antibiotic is substantially lower than that of renal damage<sup>294</sup>. Two clinical studies have found that the rate of neurotoxicity is as low as 5.9-7.3% in critically-ill patients treated with colistin, with several other investigations observing no cases of neuropathy at all in cohorts<sup>301,367–372</sup>. Unusually, neurotoxic side-effects appear to develop more readily in CF patients administered colistin, with 6 out of 19 individuals (29%) exhibiting such pathologies when treated with intravenous colistimethate sodium<sup>373</sup>. The most frequent symptoms of colistin-induced brain injury include facial and peripheral paraesthesia (the predominant adverse neurotoxic events), as well as vertigo/dizziness, weakness, visual disturbances, confusion, neuromuscular blockade and ataxia<sup>374,375</sup>. As with nephrotoxicity, in the vast majority of cases these neurological effects are only observed during prolonged colistin administration, and usually are readily reversible once antibiotic dosing is halted<sup>376–380</sup>. In extremely rare instances, there have been clinical case studies of colistin causing a range of alternate adverse events, such as allergic/hypersensitivity reactions (skin rash, itching, urticaria), gastrointestinal disorders (e.g. pseudomembranous colitis), and bronchoconstriction/chest tightness following inhaled administration of aerosolised colistin<sup>305,381,382</sup>.

#### **1.4.5 Colistin's mechanism of action**

Polymyxin antibiotics including polymyxin B and colistin are bactericidal compounds, and the first stage by which they exert their effects on killing bacteria is through binding to LPS molecules in the outer membrane of Gram-negative organisms (**Figure 1.11**)<sup>383,384</sup>. More specifically, the primary target of colistin is the negatively-charged phosphate groups within

the lipid A domain of LPS present in the extracellular-facing surface of bacteria, explaining why polymyxin compounds only possess antimicrobial properties against Gram-negative strains<sup>280,385</sup>. The amphipathic nature of colistin's chemical structure is critical to its function, with three-dimensional nuclear magnetic resonance (NMR) experiments revealing that the binding of the antibiotic to LPS is mediated by electrostatic interactions between the positively-charged Dab residues in the polymyxin's heptapeptide macrocycle and the anionic lipid A moiety<sup>282,386-388</sup>. The arrangement of LPS molecules in the outer membrane of Gram-negative bacteria is stabilised by divalent cations, in particular  $Mg^{2+}$  and  $Ca^{2+}$  ions, which form electrostatic bridges between individual lipid A domains in the outermost leaflet of the cell surface bilayer<sup>389-391</sup>. Importantly, the binding affinity of colistin's cationic peptide ring for lipid A is three-times greater than the affinity of  $Mg^{2+}$  and  $Ca^{2+}$  ions for the same moiety<sup>272,392</sup>. Thus, the immediate consequence of colistin binding to LPS is the competitive displacement of these cations away from the negatively-charged lipid A structure, and a loss of the electrostatic bridges between LPS molecules<sup>393-396</sup>. In the absence of these cation bridges, the outer membrane of Gram-negative bacteria is destabilised and disrupted, which is the initial step in colistin's mode of action<sup>397,398</sup>. Crucially, it has been demonstrated that the colistin-induced displacement of  $Mg^{2+}$  and  $Ca^{2+}$  ions is not dependent on the antibiotic's entry into the cell, and that this process can be inhibited when these cations are present extracellularly in excess<sup>399,400</sup>.

Whilst this primary interaction between colistin and LPS is well-established, having been extensively studied and characterised, the subsequent stages in the polymyxin antibiotic's mechanism of bactericidal activity are extremely poorly understood. What is evident is that the initial outer membrane disruption triggered by colistin ultimately leads to damage to the cytoplasmic membrane and leakage of intracellular cytoplasmic contents, with images from transmission electron microscopy (TEM) studies showing cracks in the inner phospholipid bilayer and cytoplasmic material emerging through these cracks in the form of numerous fibrous projections<sup>401-403</sup>. The permeabilisation of the cytoplasmic membrane and loss of intracellular components culminates in cell death, but there is little to no evidence of the precise molecular basis by which disruption of cation bridges by colistin in the outer membrane results in killing of bacteria. Rather, these steps in the mode of action of polymyxins are only postulated in two differing hypothetical models.

The first of these models by which colistin exerts its bactericidal effects is termed "self-directed uptake"<sup>282,404-406</sup>. In this process, the destabilising and weakening of the outer membrane through the binding of the antibiotic's positively-charged peptide ring with LPS creates space that enables colistin to insert its N-terminal fatty acyl chain into the outermost leaflet of the outer membrane<sup>407</sup>. This lipophilic tail of the polymyxin structure then interacts



with the hydrophobic fatty acid residues that comprise the inner portion of the LPS lipid A domain, resulting in further damage to the cell surface bilayer. Permeabilisation of the outer bacterial membrane provides colistin molecules with access to the cytoplasmic membrane, and here, the lipid chain of the antibiotic is again thought to be important for associating with phospholipids in the bilayer and causing membrane disruption<sup>394,408</sup>. It is purported that the deleterious impact of the polymyxin fatty acyl tail on membrane lipids is due to a “detergent-like/surfactant effect”, similar to other structurally-homologous cationic membranolytic antimicrobial peptides<sup>409–412</sup>. In this model of “self-directed uptake”, damage to the entire cell envelope structure through the sequential action of colistin on the outer and cytoplasmic membranes results in the formation of pores in the bacterial bilayers; the consequent loss of cytosolic contents through these pores is what leads to cell death. It is critical to note that virtually none of these stages in the process of “self-directed uptake” have been demonstrated experimentally.

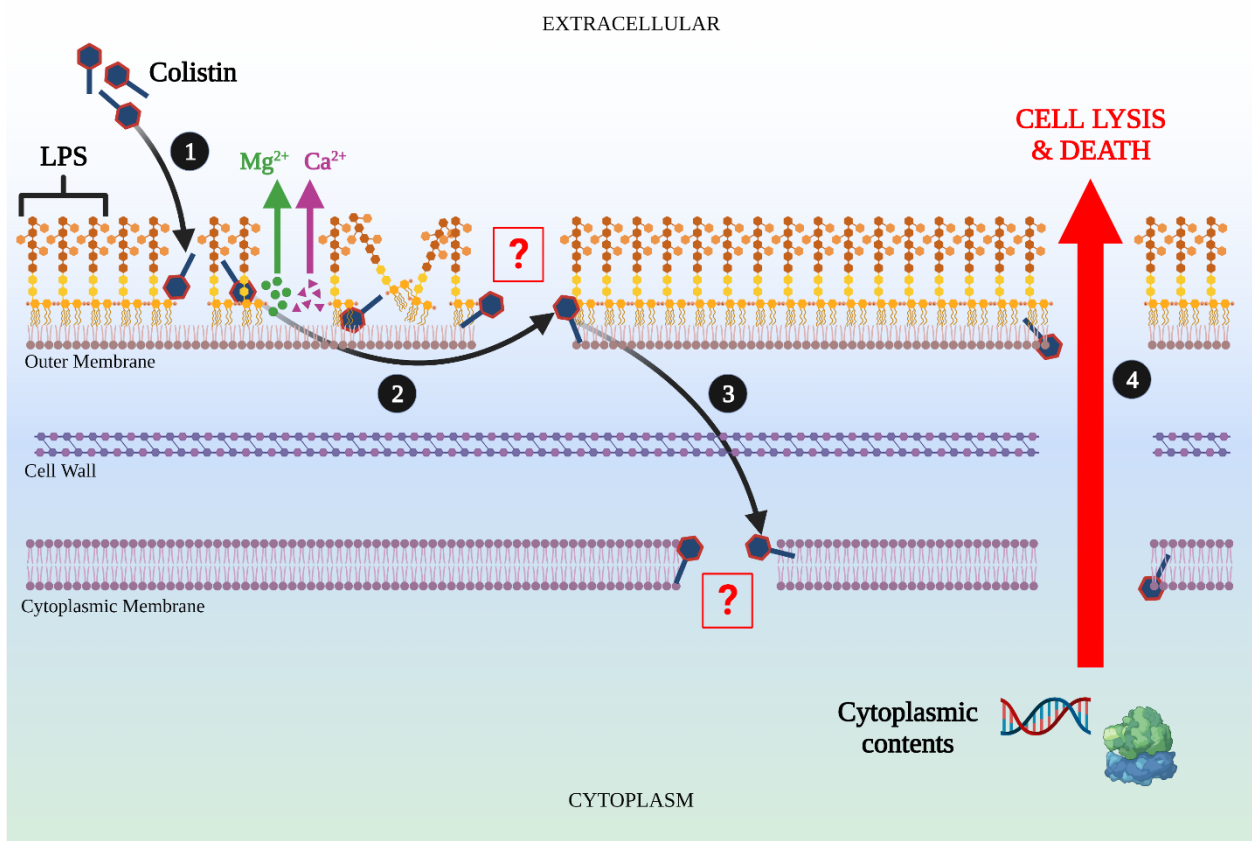


**Figure 1.11: The “classic” proposed mechanism of action of colistin is poorly understood.** (1) Colistin binds to LPS in the outer membrane of Gram-negative bacteria, displacing divalent cationic bridges that stabilise the outer membrane. (2) Colistin traverses the outer membrane through an unknown mechanism termed “self-directed uptake” and permeabilises the outer membrane using its lipid tail. (3) Colistin accesses and damages the cytoplasmic membrane through an unproven process thought to relate to its “detergent-like” properties. (4) Disruption of both cell envelope bilayer leads to loss of cytoplasmic contents, lysis of bacteria and ultimately cell death.

The second hypothesised mechanism for colistin's mode of killing Gram-negative bacteria is by a process known as the "vesicle-vesicle contact pathway", whereby the antibiotic transits the outer membrane after disrupting the cationic bridges between LPS structures and binds to anionic phospholipid vesicles (**Figure 1.12**)<sup>386</sup>. Polymyxin molecules bound to these vesicles then interact with each other, generating stable contacts, and eventually triggering the fusion of the outer membrane with the cytoplasmic membrane<sup>413,414</sup>. The rapid exchange of phospholipids between the two bilayers that ensues is responsible for phospholipid molecules being lost from the bacterial cell envelope, meaning that the osmotic balance necessary for cell viability cannot be maintained and the cell undergoes a lytic cell death. Again, this model of colistin-mediated killing of bacteria remains largely putative, with a distinct lack of experimental scientific evidence.

It has also been proposed that colistin has several cellular targets independent of the outer/cytoplasmic membranes, and may possess its bactericidal properties due to interactions with these. In particular, colistin is reported to have inhibitory activity against essential respiratory enzymes situated in the cytoplasmic membrane<sup>392</sup>. Three protein complexes are responsible for the respiratory chain in bacteria, and they use reduced nicotinamide adenine dinucleotide (NADH) and quinones as carrier compounds to shuttle protons and electrons between each other<sup>415</sup>. Complex 1 therefore contains three respiratory proteins that function as NADH-quinone oxidoreductases: one protein for translocating protons, one protein for translocating sodium, and one protein without an energy-coupling site (NDH-2)<sup>416,417</sup>. Colistin and other polymyxins have been found to inhibit the enzymatic activity of NDH-2 *in vitro* in a panel of Gram-negative organisms (*E. coli*, *K. pneumoniae*, *A. baumannii*), and uniquely in certain Gram-positive species in addition (e.g. *Bacillus subtilis*, *Mycobacterium smegmatis*)<sup>418-420</sup>. However, the links between this inhibition and bacterial killing are yet to be convincingly established in a whole-cell model.

Colistin has furthermore been hypothesised to mediate cell death through reactive oxygen species as part of the "hydroxyl radical death pathway"<sup>421</sup>. These species include superoxide ( $O_2^-$ ) molecules that are converted to hydrogen peroxide ( $H_2O_2$ ) by superoxide dismutase, with  $H_2O_2$  in turn responsible for the formation of hydroxyl radicals ( $\cdot OH$ ) after oxidising ferrous iron in the Fenton reaction<sup>422</sup>. Together, superoxide, hydrogen peroxide and hydroxyl radical species are produced and enter into bacterial cells once colistin has disrupted both the outer and cytoplasmic membranes<sup>423</sup>. These molecules are highly reactive and damage intracellular DNA, proteins and lipids, with this oxidative stress culminating in bacterial killing<sup>424-426</sup>. Finally, it has been suggested that polymyxins may be bactericidal because they display significant affinity to the decoding site (A-site) of prokaryotic 16S rRNA, the cognate target of aminoglycoside antibiotics<sup>427,428</sup>. However, neither colistin nor its

analogues display an ability to block bacterial translation, indicating that despite this binding to ribosomes, it is highly unlikely that polymyxin drugs kill cells via an aminoglycoside-like mechanism of action. In any case, for colistin to have its bactericidal impact by the induction of reactive oxygen species or ribosomal interactions, it is required that the antibiotic first permeabilises the two bilayers of the cell envelope, and the process by which it does this is entirely unclear. Given the ever increasing use and importance of colistin as a last-resort antimicrobial treatment against multi-drug resistant Gram-negative pathogens, there is both an urgent and a pressing need to fully resolve colistin’s mechanism of action on bacterial membranes.

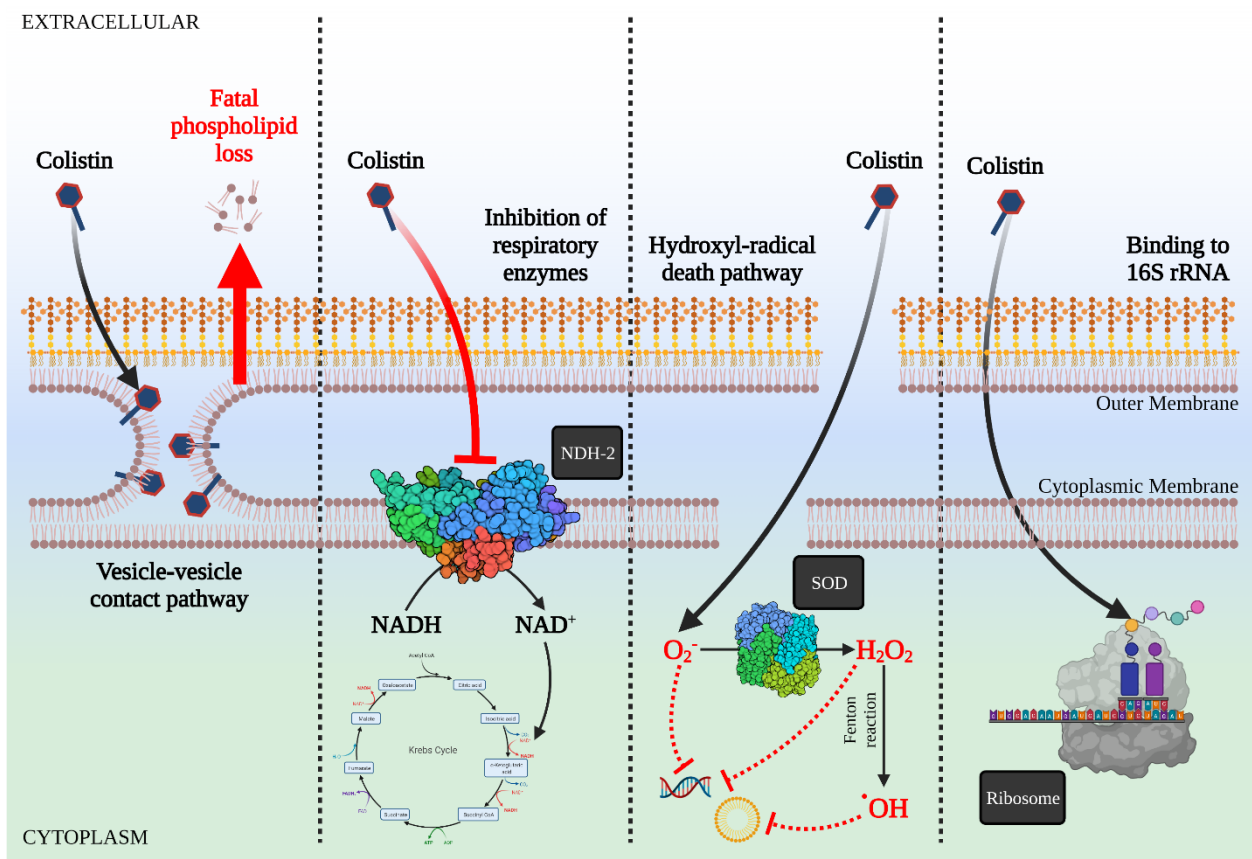


**Figure 1.12: Alternative proposed mechanisms for colistin’s bactericidal activity.**

## 1.5 Colistin resistance

### 1.5.1 Intrinsic colistin resistance

While colistin possesses antimicrobial activity against most Gram-negative pathogens, there are a number of Gram-negative species that have inherent properties making them non-susceptible to polymyxin antibiotics. These organisms include strains of the *Burkholderia*

*cepacia* complex, as well as *Neisseria meningitidis/gonorrhoeae*, *Helicobacter pylori*, *Proteus mirabilis* and bacteria in the *Serratia* genus<sup>429–437</sup>. In all these species, intrinsic colistin resistance is mediated by a target modification strategy – specifically, they constitutively produce LPS modified with the addition of cationic chemical groups<sup>438–440</sup>. These positively-charged chemical moieties added to LPS can take two different forms: phosphoethanolamine (PEtN) and 4-amino-4-deoxy-L-arabinose (L-Ara4N).

Both PEtN and L-Ara4N groups can be added to the lipid A domain of LPS during its biosynthesis, and their cationic nature functions to decrease the net negative charge of lipid A conferred by its phosphate groups<sup>441,442</sup>. Colistin relies on an electrostatic interaction between the polymyxin's positively-charged peptide macrocycle and anionic lipid A in order to bind to LPS and exerts its bactericidal effects. The reduction in lipid A anionicity resulting from the addition of PEtN and L-Ara4N moieties thus severely hampers the colistin-lipid A interaction, blocking the antibiotic from causing membrane disruption that kills the bacteria<sup>443–445</sup>. Interestingly, modification of lipid A with L-Ara4N is more effective as a means of disrupting colistin's binding (reducing the net negative charge of LPS molecules from -1.5 to 0) compared to PEtN modifications, which only lower the anionic charge of LPS from -1.5 to -1<sup>128,441</sup>. The genes responsible for regulating the constitutive production of LPS modified with PEtN and/or L-Ara4N in intrinsically colistin-resistant Gram-negative organisms vary between species – in *Serratia* strains, expression of the *arnBCADTEF* genes confers inherent polymyxin resistance, the *eptA/eptB* genes carry out this role in *Neisseria* and *Proteus* strains, and *H. pylori* is innately non-susceptible to colistin via the action of the *cgt* gene<sup>433,446–451</sup>. Only a single bacterial species, *B. polymyxa* var. *colistinus*, is known to be intrinsically resistant to polymyxin antibiotics through an alternative mechanism than lipid A modification<sup>452,453</sup>. This organism produces the drug-degrading enzyme colistinase as a “self-preservation” process, since colistin is naturally synthesised by *B. polymyxa* var. *colistinus* communities.

### **1.5.2 Acquired chromosomal colistin resistance**

Colistin non-susceptibility mediated by chemical modification of lipid A is not a resistance mechanism that is specific to intrinsically-resistant Gram-negative organisms. The same mode of colistin resistance can also be acquired in bacterial species that are typically sensitive to the polymyxin antibiotic, with the key difference compared to inherently-resistant strains being that modified LPS is not constitutively produced. Rather, the development of colistin resistance in these organisms requires chromosomal mutations, with these mutations predominantly occurring in the two-component systems PhoPQ and PmrAB that are chiefly responsible for the addition of cationic chemical groups to the lipid A moiety of LPS<sup>454</sup>.

The PhoPQ two-component system contains a sensor protein kinase (PhoQ) and a response regulator protein (PhoP)<sup>455</sup>. The function of PhoQ is to sense environmental signals, and the enzyme can detect and be activated via its periplasmic lipid domain by stimuli such as low pH (e.g. when inside the phagosome of a macrophage) or low Mg<sup>2+</sup> in the cell envelope (e.g. through the cationic displacement activity of colistin)<sup>456–461</sup>. Following activation, PhoQ phosphorylates the response regulator PhoP, enhancing its binding capacity to the promoter regions of the genes it transcriptionally controls (**Figure 1.13**)<sup>462–465</sup>. One of the genes that is under PhoP-mediated transcriptional regulation is the *pmrHFIJKLM* operon (also referred to as *arnBCADTEF*), and activation of this genetic element leads to the addition of positively-charged L-Ara4N chemical groups to lipid A structures in the bacterial membrane<sup>466,467</sup>. Chromosomal mutations acquired in the *phoP* and *phoQ* genes that encode this two-component protein complex in Gram-negative bacteria can lead to upregulation of the system, and as a consequence, an increase in the modification of LPS with cationic L-Ara4N moieties. Hence, the electrostatic interaction between colistin and anionic lipid A that is crucial to the antibiotic's bactericidal mechanism of action is blocked, and the polymyxin drug is unable to exercise its antimicrobial effects<sup>468,469</sup>. Mutations in *phoP* and *phoQ* that confer colistin resistance have been reported in several Enterobacteriaceae strains (*E. coli*, *K. pneumoniae*, *Enterobacter* species, *S. enterica*), as well as in *P. aeruginosa*<sup>470–476</sup>.

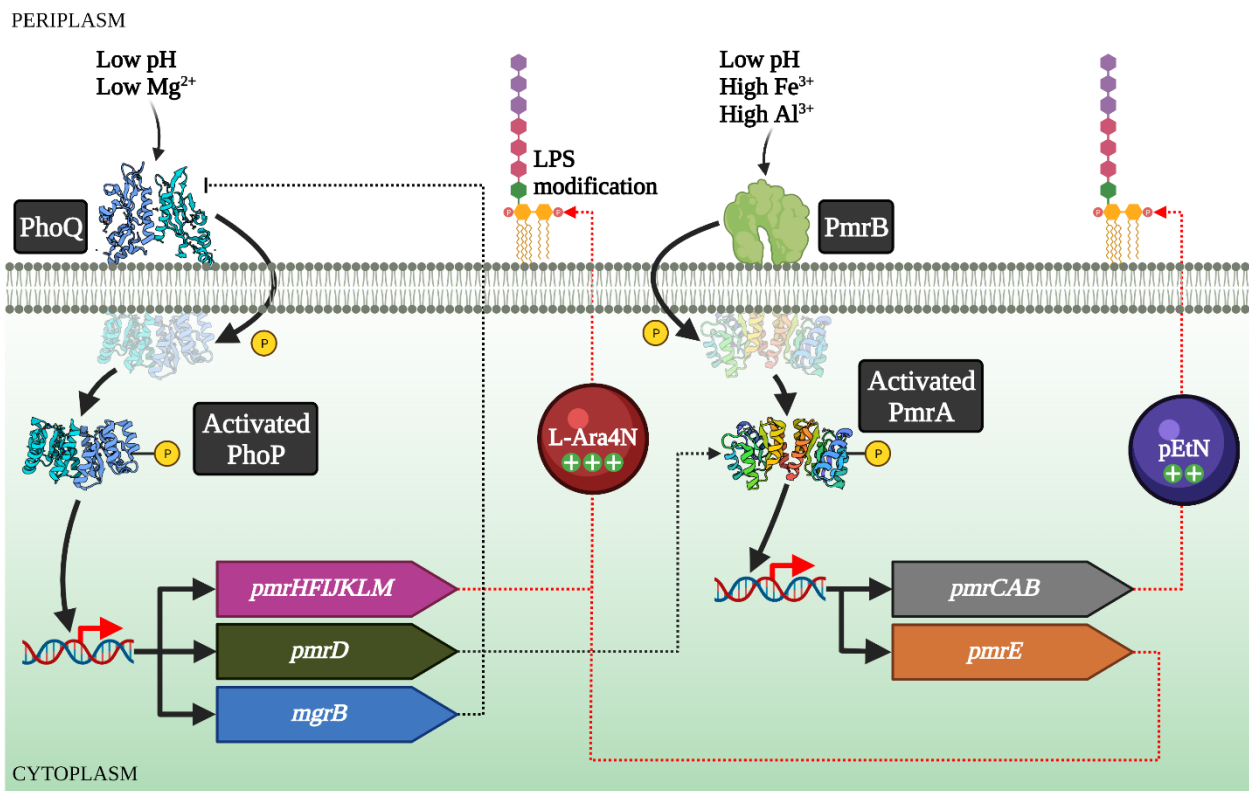


**Figure 1.13: The interconnected signalling pathways of the PhoPQ and PmrAB two-component systems that regulate the modification of LPS with cationic chemical groups and mediate chromosomal colistin resistance.**

Analogously to PhoPQ, the PmrAB two-component system is also comprised of a sensor kinase (PmrB), which in this case responds to low pH and trivalent cations (e.g. Fe<sup>3+</sup>, phagosomal Al<sup>3+</sup>) that are highly toxic to the bacterial membranes<sup>477-479</sup>. Detection of these environmental stimuli triggers PmrB activation, again through its periplasmic domain, and activated PmrB subsequently phosphorylates PmrA via its tyrosine kinase domain<sup>480,481</sup>. As with PhoP, PmrA is a transcriptional regulator, and when phosphorylated is able to bind more strongly to the promoters of a number of target genes, inducing their expression<sup>443</sup>. However, in contrast to the PhoPQ complex, one of the genes transcriptionally-controlled by PmrA is the gene operon *pmrCAB*, which encodes the PmrAB two-component system itself, creating an auto-regulated signal transduction pathway<sup>482,483</sup>. The protein encoded by the *pmrC* gene in this operon is an ethanolamine transferase enzyme that replaces the anionic phosphate groups of lipid A with positively-charged pEtN groups<sup>484</sup>. Additionally, phosphorylated PmrA activates transcription of the *pmrHFIJKLM* operon, as well as the adjacent *pmrE* gene, which together synthesise L-Ara4N moieties and add them to lipid A<sup>485,486</sup>. The acquisition of chromosomal mutations in the *pmrA/pmrB* genes which lead to over-activation of the two-component system can therefore culminate in colistin resistance, due to excess cationic modification of LPS diminishing binding of the polymyxin's positively-charged peptide ring<sup>487,488</sup>. Such chromosomal mutations contributing to reduced colistin susceptibility have been identified in a panel of Gram-negative pathogens, including *K. pneumoniae*, *E. coli*, *Enterobacter aerogenes*, *S. enterica* and *P. aeruginosa*<sup>489-492</sup>.

Notably, the PmrAB and PhoPQ two-components systems can influence one another, since the PmrA transcriptional regulator can be activated by the response protein PhoP, either directly or indirectly through the action of the connector protein PmrD<sup>493,494</sup>. Modulation of the PmrAB system is additionally performed by an alternative regulatory two-component complex termed CrrAB, where CrrA acts as the regulatory protein and CrrB as a sensor kinase enzyme<sup>495-497</sup>. Chromosomal mutations in the *crrB* gene have also been associated with colistin resistance, with six separate resulting amino acid substitutions in the CrrB protein sequence of *K. pneumoniae* clinical isolates (Q10L, Y31H, W140R, N141I, P151S, S195N) identified as being responsible for polymyxin non-susceptibility<sup>498</sup>. It is hypothesised that these substitutions cause an increase in expression of an adjacent gene, *crrC*, which consequently elevates expression of *pmrC* and the *pmrHFIJKLM* operon, ultimately inducing excess modification of lipid A with L-Ara4N and colistin resistance.

The comparable regulator of the PhoPQ two-component system is MgrB, a 47-amino acid transmembrane protein, expression of which is upregulated when PhoP is phosphorylated and activated<sup>499</sup>. The MgrB protein is a negative regulator that suppresses transcription of the *phoQ* gene, thereby inhibiting the enzymatic kinase activity of the PhoQ

protein<sup>500</sup>. In this way, MgrB is the key intermediate in a negative feedback loop that prevents over-activity of the PhoPQ complex. However, chromosomal mutations in the *mgrB* gene that interfere with the function of this transmembrane protein can block its negative regulatory effects, eventually triggering excessive transcriptional induction of the *pmrHFIJKLM* operon, increased addition of cationic L-Ara4N groups to LPS, and a lack of sensitivity to polymyxin antibiotics<sup>501</sup>. These mutations can take the form of mis-sense, nonsense, or insertional alterations to the *mgrB* gene sequence, all of which cause a dysfunctional or truncated version of the MgrB protein to be translated. Colistin resistance mediated through *mgrB* chromosomal mutations have been discovered in *Enterobacter* and *K. pneumoniae* clinical strains<sup>502–504</sup>. In *P. aeruginosa* isolates, gene mutations in several different two-components systems encoded chromosomally have been implicated in polymyxin non-susceptibility, including ParRS, CprRS and ColRS (which is upregulated in the extracellular presence of excess  $Zn^{2+}$ )<sup>505–508</sup>. It is thought that all of these complexes are linked to the *pmrHFIJKLM* operon, and that these chromosomal mutations lead to an increase in the lipid A-modifying activity of the proteins produced from the operon. The precise molecular signalling pathway by which this occurs, however, remains poorly characterised.

In the bacterium *A. baumannii*, colistin resistance can, similarly to other Gram-negative pathogens, occur through chromosomal mutations in the *pmrCAB* gene operon, although this insensitivity to polymyxins can be reversed following the accumulation of additional amino acid substitutions in the PmrAB proteins that downregulate *pmrCAB* expression<sup>509,510</sup>. Importantly, and unlike alternative members of the Enterobacteriaceae family, *A. baumannii* cannot develop resistance to colistin through modification of LPS with L-Ara4N, since the species lacks the *pmrHFIJKLM* operon required for biosynthesis of the cationic chemical group and its addition to lipid A<sup>511</sup>. Nonetheless, non-susceptibility to polymyxin antibiotics can still result in *A. baumannii* from PmrC-mediated LPS modification with pEtN moieties<sup>512,513</sup>.

Uniquely, strains of *A. baumannii* also possess a distinctive mechanism of colistin resistance – chromosomal mutations in the genes responsible for LPS biosynthesis. In particular, mutations in three genes required for synthesis of lipid A (*lpxA*, *lpxC* and *lpxD*) have been identified to spontaneously occur and confer high-level resistance to polymyxin antibiotics in clinical isolates<sup>251,514</sup>. These genes are involved in the very first three steps in the LPS biosynthetic pathway; hence, dysfunction in the enzymes produced from the genes arising from chromosomal mutations means that LPS is unable to be produced<sup>515</sup>. In most Gram-negative organisms, this inhibition of LPS synthesis would be fatal, resulting in bacterial death. However, *A. baumannii* strains are able to tolerate the complete loss of LPS production that stems from mutations in *lpxA*, *lpxC* and *lpxD*<sup>516</sup>. Moreover, in the absence of LPS

molecules in the outer membrane of *A. baumannii* isolates with chromosomal mutations in lipid A biosynthesis genes, colistin has no target sites on the bacterial surface to which its peptide ring can bind. As a direct consequence, the polymyxin antibiotic is unable to disrupt the outer membrane and thus cannot exert its bactericidal effects. The chromosomal mutations in *lpxA*, *lpxC* and *lpxD* that trigger colistin resistance in this manner can be substitutions, frame-shift mutations, truncations, or inactivation via insertion of the transposable element *ISAbal1*<sup>517-519</sup>.

As well as chromosomal mutations inducing resistance to polymyxins through changes to its LPS target (either chemical modification or complete loss), there have also been studies indicating that similar mutations in genes encoding multi-drug efflux pumps can likewise be associated with colistin non-susceptibility. For example, chromosomal mutations causing up-regulation of the MexAB-OprM efflux pump complex have been linked to the ability of metabolically-active *P. aeruginosa* cells to tolerate colistin exposure<sup>520,521</sup>. The small outer membrane pore OprH, which is the major outer membrane protein when the bacterium is starved of Mg<sup>2+</sup> (e.g. after colistin has displaced cation bridges between LPS molecules), has also been proposed as a contributor to polymyxin resistance in *P. aeruginosa*. Studies have demonstrated that overexpression of *oprH*, which can be the outcome of chromosomal mutations, leads to a reduction in susceptibility to colistin<sup>522,523</sup>.

Furthermore, the efflux pumps KpnEF, AcrAB and SapABCDF have all been implicated in polymyxin resistance, with the appearance of mutations in the genes encoding these multi-drug export proteins correlated with colistin non-susceptibility in *E. coli*, *K. pneumoniae* and *P. mirabilis*<sup>524-526</sup>. It has yet to be convincingly proven that colistin is a substrate for these drug efflux systems, and it is postulated that they may modulate susceptibility to the antibiotic via indirect relations to other known mediators of polymyxin resistance. In support of this, activity of the PhoPQ two-component system is dependent on expression of the *acrAB* efflux system genes<sup>527</sup>. Nevertheless, the utilisation of inhibitors of multi-drug efflux pump proteins (e.g. carbonyl cyanide 3-chlorophenylhydrazone, CCCP) decreases resistance to colistin in *P. aeruginosa*, *A. baumannii* and *K. pneumoniae*, suggesting a potential direct involvement of antibiotic export systems in these clinically-important pathogens<sup>528,529</sup>.

### **1.5.3 Acquired plasmid-mediated colistin resistance**

The capacity for Gram-negative bacteria to develop resistance to colistin through chromosomal mutations has been a known phenomenon since the first isolation and genetic characterisation of polymyxin-resistant *Salmonella* strains in the 1970s<sup>480</sup>. Recently however, it has been discovered that Gram-negative organisms can also become colistin-resistant through the acquisition of mobile plasmids harbouring mobile colistin resistance (*mcr*) genes.



The first *mcr* gene was identified in 2015 from a strain of *E. coli* obtained in China from farming animals, and termed *mcr-1*<sup>530</sup>. This *mcr-1* gene was carried on the plasmid pHNSHP45, an approximately 64 kb low-copy member of the IncI plasmid family, and subsequent transformation and conjugation experiments firmly established the ability of plasmid-borne *mcr-1* to move between bacterial cells by horizontal gene transfer. The mobile nature of *mcr-1* is highly concerning, since there is now a distinct prospect of the colistin resistance determinant spreading rapidly and globally, rendering the crucial last-resort polymyxin antibiotic ineffective<sup>531</sup>.

Indeed, despite *mcr-1* only being detected in 2015, it is believed that the gene had been in existence and circulating worldwide for several decades beforehand, with studies indicating *mcr* genes emanated separately in China (identified in samples from poultry in the 1980s) and in France (discovered in samples from veal calves in 2005)<sup>532,533</sup>. Since its first characterisation, the dissemination of *mcr-1* has been widely reported, with the resistance determinant found in more than 40 countries across 5 continents, and in a diverse range of Enterobacteriaceae strains (*E. coli*, *K. pneumoniae*, *S. enterica*, *Shigella sonnei*, *Enterobacter* species, *Citrobacter* species and *Moraxella* species)<sup>534–541</sup>. Although initially detected as being harboured on an IncI plasmid, it has been shown that carriage of the *mcr-1* gene in nature can occur on various plasmid types, including IncF, IncHI2, IncP, IncX4 and IncY plasmids<sup>542–545</sup>. Furthermore, the reservoirs of *mcr-1*-bearing plasmids are similarly wide-ranging, with these mobile genetic elements identified in food (meat/vegetables), aquatic environments, hospital sewage, infected/colonized humans, wild birds/animals and especially predominantly in farm animals<sup>546–553</sup>. It is hypothesised that livestock, particularly cattle and pigs, are a major source and driver of global *mcr-1* spread, and the extensive use of colistin in veterinary medicine as a growth promoter has only served to accelerate and exacerbate this problem<sup>554</sup>. In support, a ban on administration of polymyxin antibiotics to farm animals has led to a drastic reduction in colistin resistance being detected in both livestock and human patients<sup>555,556</sup>. Insect species, in particular houseflies and blowflies, have been proposed to be the intermediate vectors responsible for transmission of *mcr-1*-harbouring bacteria between animals and humans<sup>557</sup>.

The resistance mechanism through which the *mcr-1* gene confers non-susceptibility to polymyxin antibiotics is identical to the mechanisms of intrinsic and chromosomal colistin resistance mediated via LPS modifications. The gene product of *mcr-1* (MCR-1) is a lipid A-modifying phosphoethanolamine transferase enzyme that is a member of the YhjW/YjdB/YijP alkaline phosphatase protein superfamily<sup>558–560</sup>. MCR-1 functions by adding a positively-charged PEtN group to the negatively-charged phosphate groups of lipid A, reducing the overall anionic nature of LPS and interfering with colistin's binding to its cationic polypeptide ring (**Figure 1.14**)<sup>561</sup>. Without the polymyxin compound being able to attach to the lipid A

domain of LPS molecules, colistin cannot disrupt the outer membrane of bacteria to kill the cells, and thus resistance to the antibiotic ensues. Intriguingly, the *mcr-1* gene is thought to have originated from an intrinsically polymyxin-resistant Gram-negative bacteria; whilst the exact source of the resistance determinant has yet to be resolved, *in silico* analyses of amino acid sequences have implicated several bacterial groups in the origins of *mcr-1*, including *Moraxella*, *Vibrio*, *Limnobacter*, *Enhydrobacter* and *Methylophilaceae*<sup>562,563</sup>. Moreover, structural studies of the MCR-1 protein have indicated significant homology to two additional PEtN transferase enzymes from intrinsically-resistant strains: EptC from *Campylobacter jejuni*, and LptA from *N. meningitidis*<sup>430,564–566</sup>. It is believed to be likely that transposable genetic elements caused the initial movement of the parental gene of *mcr-1* from the chromosome of one of these intrinsically colistin-resistant bacteria on to a mobile plasmid, which subsequently disseminated worldwide<sup>534</sup>.

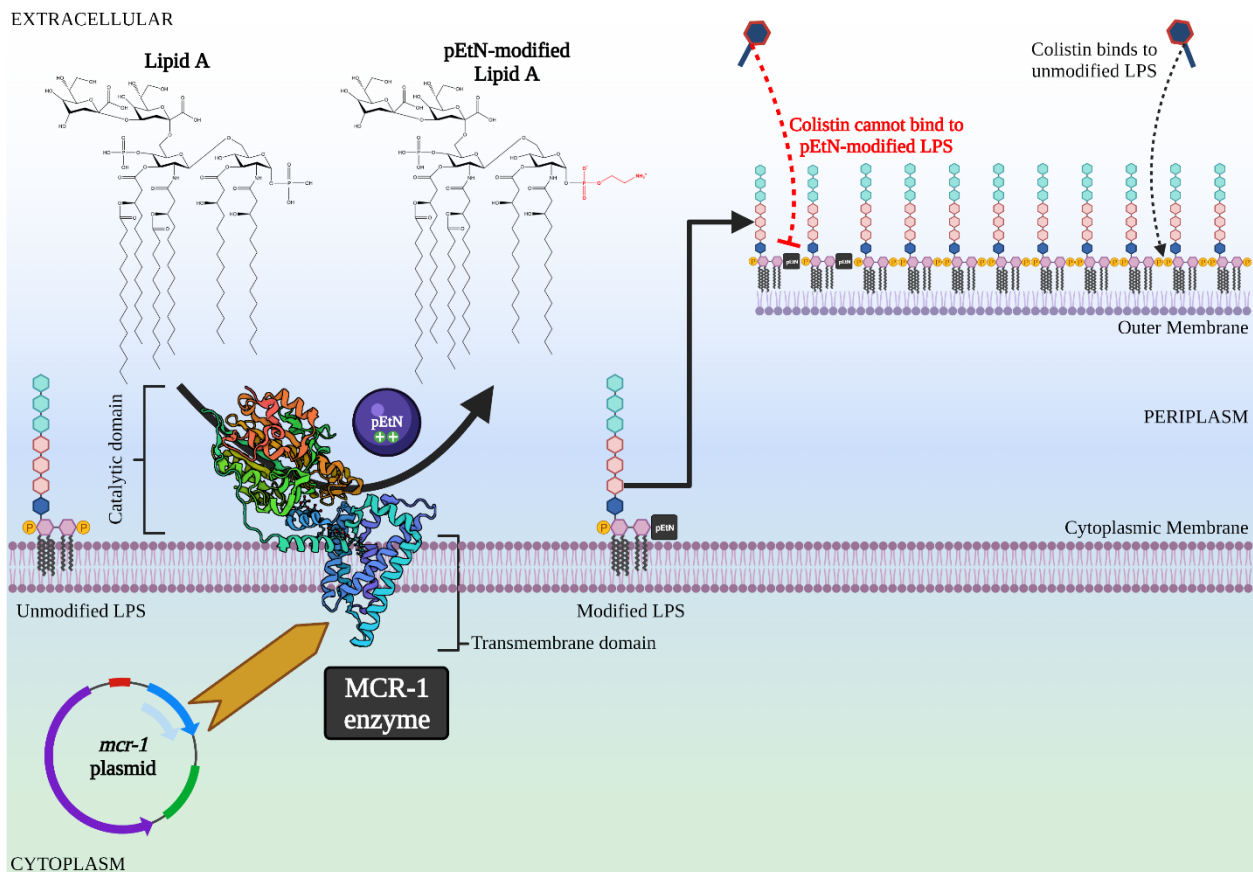


**Figure 1.14:** The plasmid-borne *mcr-1* gene encodes a phosphoethanolamine transferase enzyme that modifies the lipid A domain of LPS and confers colistin resistance.

Alongside the global spread of the *mcr-1* gene, a large number of genetic variants of the original *mcr-1* resistance determinant identified have emerged and expanded internationally. To date, 30 functional variants of *mcr-1* have been discovered, being assigned the classifications of *mcr-1.1* up to *mcr-1.30*<sup>567,568</sup>. All these genetic variants share an overwhelming homology (approximately 99%) in their nucleotide sequences with *mcr-1*, differing by only a few amino acids at most, and hence, the protein products of the resistance determinants all have similar functionality in terms of conferring colistin resistance as the MCR-1 enzyme<sup>569</sup>. However, the mediators of transmissible resistance to polymyxins have also extended more distantly from the original *mcr-1* gene, with the existence of nine other genetic homologues of *mcr-1* reported presently: *mcr-2*, *mcr-3*, *mcr-4*, *mcr-5*, *mcr-6*, *mcr-7*, *mcr-8*, *mcr-9* and *mcr-10* (**Table 1.5**)<sup>570-578</sup>.

**Table 1.5:** Characteristics of the *mcr* genes that confer colistin resistance

Gene	Size	Variants	First Identification	Protein sequence identity to MCR-1
<i>mcr-1</i>	2600 bp	30	<i>E. coli</i> , Pig, China, 2015	100%
<i>mcr-2</i>	1617 bp	7	<i>E. coli</i> , Cattle/Pig, Belgium, 2016	99%
<i>mcr-3</i>	1626 bp	41	<i>E. coli</i> , Pig, China, 2017	76-85%
<i>mcr-4</i>	1626 bp	6	<i>S. enterica</i> , Pig, Italy, 2017	82-99%
<i>mcr-5</i>	1644 bp	4	<i>S. enterica</i> Paratyphi B, Poultry, Germany, 2017	36%
<i>mcr-6</i>	1617 bp	1	<i>Moraxella</i> species, Pig, U.K., 2017	88% (c.f. MCR-2)
<i>mcr-7</i>	1620 bp	1	<i>K. pneumoniae</i> , Poultry, China, 2018	69-81%
<i>mcr-8</i>	1698 bp	5	<i>K. pneumoniae</i> , Pig/Human, China, 2018	31%
<i>mcr-9</i>	2661 bp	3	<i>S. enterica</i> Typhimurium, Human, U.S.A., 2019	84%
<i>mcr-10</i>	1620 bp	1	<i>Enterobacter roggkampii</i> , Human, China, 2020	83% (c.f. MCR-9)

Although all 10 known *mcr* alleles encode PEtN transferase enzymes, the similarity in their amino acid identity compared with *mcr-1* can vary substantially, indicating that they may have originated from disparate genetic sources. The gene products from *mcr-2* and *mcr-6* share the greatest degree of protein homology with MCR-1, with an amino acid identity of between 88% and 99%<sup>541,579,580</sup>. In contrast, the MCR-3, MCR-4, MCR-7 and MCR-9 enzymes translated from their respective *mcr* genes have a high degree of structural resemblance to each other, but less homology with MCR-1 (amino acid identity between 69% and 82%)<sup>392,581</sup>. In fact, the genes encoding these resistance determinants can even differ significantly in size, from the smallest allele *mcr-2* (1617 bp) through to the largest allele *mcr-9* (2661 bp)<sup>577,579</sup>. The impact of these differences in gene/protein sequences on the PEtN transferase activity of the

enzymes, and their capacity to induce colistin non-susceptibility, is not entirely understood. Uniquely and surprisingly, however, it has been found that simply the presence of the *mcr-9* gene does not necessarily confer polymyxin resistance in clinical isolates, despite it being possible to produce a functional lipid A-modifying protein from the gene under laboratory conditions<sup>582,583</sup>. It is hypothesised that *mcr-9* may be a silent, inducible gene that is expressed under certain environmental conditions, although this is yet to be demonstrably proven<sup>584</sup>. Despite this, the *mcr-9* gene is one of the most widely disseminated *mcr* homologue detected in clinical isolates, along with *mcr-1* and *mcr-3*<sup>585-587</sup>. In contrast, the *mcr-2* and *mcr-5* genes are rarely identified in nature, and are therefore viewed as infrequent members of the *mcr* family<sup>588</sup>.

As with *mcr-1*, all the resistance determinants *mcr-2* to *mcr-10* can have genetic variants that are almost identical to the original, parental genes, with minimal amino acid alterations. The number of these variants can dramatically differ amongst the *mcr* alleles – for instance, there are 41 known genetic variants of *mcr-3* (*mcr-3.1* to *mcr-3.41*), 7 variants of *mcr-2* (*mcr-2.1* to *mcr-2.7*), but only single variants of *mcr-6* (*mcr-6.1*) and *mcr-7* (*mcr-7.1*)<sup>589-593</sup>. The *mcr* genes can be borne on a wide range of mobile plasmid types in a diverse panel of Enterobacteriaceae bacteria. However, certain *mcr* alleles are preferentially harboured on specific plasmids and more commonly identified in particular Gram-negative species. For example, the *mcr-3* and *mcr-7.1* genes are especially closely associated with *Aeromonas* strains<sup>594,595</sup>. Similarly, *mcr-2* is typically carried on IncX4 plasmids, while *mcr-9* is often found being transported on mobile IncHI2 plasmids<sup>596,597</sup>. Concerningly, these plasmids can encode many other determinants of antibiotic resistance along with *mcr* genes, including mediators of beta-lactam and fluoroquinolone non-susceptibility; the mobility of such plasmids has the potential to be devastating for the spread of antimicrobial resistance and global public health<sup>598,599</sup>. Moreover, there have been studies demonstrating that *mcr* genes can integrate into the chromosome of *E. coli*, rendering the strain intrinsically resistant to polymyxin drugs<sup>600,601</sup>. The ever-increasing possibility of this occurring as a widespread phenomenon in nature as the prevalence of *mcr* resistance determinants expands globally poses a worrisome threat to the continued efficacy of colistin as an antibiotic of last-resort.

#### **1.5.4 Prevalence of colistin resistance in *P. aeruginosa***

Resistance to polymyxin antibiotics in *P. aeruginosa* strains is mediated almost exclusively by chromosomal mutations in two-component systems, with extremely rare reports of *mcr* carriage in this Gram-negative bacteria<sup>602,603</sup>. Over the last two decades, there have been extensive studies investigating the incidence of colistin non-susceptibility amongst clinical *P. aeruginosa* human isolates, with the majority concluding that resistance to the last-resort antibiotic is relatively infrequent. Perhaps the most significant of these investigations

are two studies from the SENTRY Antimicrobial Surveillance Program conducted ten years apart, in 2001 and again in 2011, where the prevalence of colistin resistance was assessed in *P. aeruginosa* isolates from distinct geographic areas<sup>604,605</sup>. In both these studies, polymyxin non-susceptibility was defined according to the interpretative criteria established by the Clinical and Laboratory Standards Institute (CLSI) as a minimum inhibitory concentration (MIC) greater than the susceptibility breakpoint of 2 µg/ml<sup>606</sup>. Among 80 *P. aeruginosa* bloodstream isolates in the 2001 report, there were no reports of resistance to colistin or polymyxin B at all, with 100% of strains tested displaying susceptibility to the antibiotic<sup>604</sup>. By the time the SENTRY study was repeated in 2011, the scope of the investigation had expanded markedly, and on this occasion, the incidence of colistin resistance was determined in 9,130 *P. aeruginosa* strains isolated from various infection sites (blood, respiratory tract, skin/soft tissue) in patients spread globally across Europe, the U.S.A., Latin-America and the Asia-Pacific region. In this instance, 0.4% of the bacterial strains exhibited non-susceptibility to colistin, indicating that resistance to the polymyxin drug may have risen slightly in the decade between the two studies, but not to a clinically-threatening level<sup>605</sup>.

In addition to the SENTRY Program reports, there have been several smaller studies that have found similar rates of colistin resistance in *P. aeruginosa* clinical strains worldwide. For example, in a 2003 survey of 417 *P. aeruginosa* samples isolated from CF patients in 17 hospitals across the U.K., colistin non-susceptibility, defined as an MIC value greater than 2 µg/ml by the British Society of Antimicrobial Chemotherapy (BSAC), was identified in only 13 strains (3.1%)<sup>607,608</sup>. Likewise, when the polymyxin susceptibility of 77 multi-drug resistant *P. aeruginosa* clinical isolates from intensive care unit patients in Canada in 2008 was measured, just 4% of strains were classified as being resistant to colistin<sup>609</sup>. In 2010, an investigation at a military burn centre in the U.S.A. revealed that out of 703 *P. aeruginosa* clinical strains, only a single isolate exhibited colistin non-susceptibility – a prevalence of 0.14%<sup>610</sup>. As part of the 2011 COMPACT surveillance study, 175 carbapenem-resistant strains of *P. aeruginosa* were isolated from patients across 16 hospitals in Spain and susceptibility to colistin assessed; 6 isolates (0.6%) were found to be resistant to the polymyxin antibiotic<sup>611</sup>. More recently, two surveys in South Korea (2017) and Iran (2020) reported incidence rates of colistin non-susceptibility amongst clinical *P. aeruginosa* samples at 7.4% (16 out of 215 strains) and 3.96% (4 out of 101 strains) respectively<sup>612,613</sup>. Together, all these studies demonstrate that although resistance to polymyxins amongst certain Gram-negative pathogens (e.g. Enterobacteriaceae) is a worsening crisis, actually the incidence of colistin non-susceptibility observed clinically in *P. aeruginosa* strains fortunately continues to be low.

## 1.6 Colistin treatment failure in *P. aeruginosa* infections

Whilst colistin resistance in *P. aeruginosa* conferred by LPS modifications arising from chromosomal mutations is relatively rare, being detected diagnostically in between 0.1-7% of clinical isolates, therapeutic failure of colistin-based antibiotic treatment strategies is significantly more frequent. Studies attempting to accurately quantify the efficacy of colistin therapy against *P. aeruginosa* infections are hindered by a number of different factors, including: the sample sizes of cohorts included in such investigations are often small, patients recruited are typically critically ill and suffering from an array of other co-morbidities, and the fact that colistin is commonly administered alongside various additional antibiotics in treatment regimens<sup>274,278,308</sup>. Furthermore, there are important ethical considerations regarding the appropriateness of performing randomised controlled clinical trials comparing colistin interventions with a placebo, when there is a possibility of saving patient lives using the polymyxin antibiotic. Nevertheless, despite these limitations, the incidence of colistin treatment failure has been assessed in ten key studies since 2003 (**Table 1.6**)<sup>361,614–622</sup>.

**Table 1.6:** Efficacy of colistin treatment against infections caused by *P. aeruginosa*

Year	Route of Administration	Location	Number of Patients	Treatment Failure Rate <sup>†</sup>
2003	Intravenous	Intensive Care Unit, Athens, Greece	18	50%
2003	Intravenous	Intensive Care Unit, Pittsburgh, U.S.A.	23	39%
2007	Intravenous	Cancer Centre, Houston, U.S.A.	18	67%
2008	Intravenous	Calgary Health Region, Alberta, Canada	12	50%
	Nebulised		12	42%
2010	Intravenous	Intensive Care Unit, Athens, Greece	68	25%
2012	Nebulised	13 Cystic Fibrosis Centres, Italy	97	32%
2012	Nebulised	Intensive Care Unit, Paris, France	145	37%
2014	Nebulised	35 Centres across the U.K., Russia and Ukraine	73	49%
2019	Nebulised	Bronchiectasis Outpatient Clinic, A Coruña, Spain	67	60%
2020	Intravenous	Academic Tertiary Care Hospital, Kochi, India	3	67%

<sup>†</sup>Treatment failure: lack of microbiological clearance, exacerbation, poor clinical outcome or death

The largest of these studies investigating the effectiveness of intravenous colistin administration was carried out in 68 patients hospitalised with *P. aeruginosa* infections in an intensive care unit in Greece. Amongst these individuals, therapeutic strategies involving the use of colistin failed to cure the infection in 17 cases (25%), with all these patients experiencing a deterioration of symptoms<sup>617</sup>. In fact, this rate of treatment failure is somewhat low in comparison to the incidence of colistin therapeutic failure reported in similar studies across the world. For example in an earlier survey, again in Greece, of 18 critically-ill individuals

suffering from multi-drug resistant *P. aeruginosa* bloodstream infections, only half of the patients achieved a favourable therapeutic response or outcome when administered colistin<sup>361</sup>. Likewise, in three studies across North America, where intravenous colistin was used in the treatment of 23 postoperative patients, 18 cancer patients and 12 general medicine patients with diverse types of *P. aeruginosa* infection, the frequency of therapeutic failure (defined as no microbiological response, no clinical response or patient death) was 39%, 67% and 50% respectively<sup>614–616</sup>. Although these figures all arise from investigations in high-income countries, the incidence of colistin treatment failure is also thought to be similar in lower/middle-income countries, with a recent small study in India reporting intravenous administration of the polymyxin antibiotic failed to achieve a clinical cure in 67% of *P. aeruginosa* infections<sup>622</sup>.

It was thought that the use of aerosolised colistin for the treatment of *P. aeruginosa* lung infections (e.g. in CF patients/VAP) via an inhaled route of administration may improve the therapeutic efficacy of this important last-resort antibiotic, potentially by ensuring increased concentrations of the polymyxin drug are present at the site of infection<sup>304</sup>. However, data from two large clinical trials conducted in 2012 does not appear to support this idea, with high rates of colistin treatment failure of *P. aeruginosa* infections observed in spite of the antibiotic being delivered in a nebulised form directly into the lungs. The first of these trials, which recruited 97 individuals with CF from 13 clinical centres across Italy, found that 31 patients (32%) experienced treatment failure and were not *P. aeruginosa*-free 180 days post-colistin administration<sup>618</sup>. Analogously, in the second trial on 145 patients with VAP caused by sensitive or multi-drug resistant *P. aeruginosa* strains, it was discovered that the infection was not cured by aerosolised colistin-based therapies in 54 individuals – a treatment failure rate of 37%<sup>619</sup>. Two studies, also predominantly performed in Europe but with smaller cohort sizes, identified comparable levels of therapeutic failure following clinical utilisation of nebulised colistin – in 73 patients with bronchiectasis and chronic *P. aeruginosa* infection, the polymyxin treatment failed and an exacerbation occurred in 36 individuals (49%; placebo-controlled group had therapeutic failure in 59% of patients), while in 67 adults with non-CF bronchiectasis, *P. aeruginosa* was not eradicated from the sputum in 40 cases (60%) even after 12 months of aerosolised colistin administration<sup>620,621</sup>.

Together, all these studies convincingly demonstrate that colistin use against *P. aeruginosa*, regardless of the route by which it is administered, is associated with high levels of treatment failure (25-67%). Considering that the polymyxin drug is an antibiotic of last-resort, and almost exclusively utilised clinically as the final option to keep infected individuals alive, this significant rate of therapeutic failure of colistin often results in an extremely poor prognosis for patients with *P. aeruginosa* infections and a high mortality rate.

## **1.7 Hypothesis and aims of the project**

There is a paradox between the low rates of colistin resistance mediated by chromosomal modification-induced LPS modifications observed in *P. aeruginosa* clinical isolates, and the high incidence of colistin treatment failure when the antibiotic is used therapeutically against *P. aeruginosa* infections. Thus, it is hypothesised that *P. aeruginosa* possesses alternative mechanisms other than classic antimicrobial resistance that enable the pathogen to survive exposure to colistin. However, efforts to comprehend and address these mechanisms are severely hampered by a distinct lack of understanding of the mode of action by which colistin damages the cellular envelope and kills bacteria. It is critical to enhance our knowledge of how colistin exerts its bactericidal effects, in order to design and develop novel treatment strategies that can increase the potency and efficacy of this vital last-resort antibiotic. These new therapeutic approaches will hopefully lead to urgently-required improvements in patient outcomes following colistin treatment.

Therefore, this project has three key aims:

- 1. To resolve the mechanism of action of colistin**
- 2. To understand the causes of colistin treatment failure**
- 3. To develop novel therapeutic strategies to enhance colistin effectiveness**



## Chapter 2: Materials and Methods

### 2.1 Bacterial strains and growth conditions

The bacterial isolates used in this study are listed in **Table 2.1**. For all experiments, bacteria were first grown overnight to stationary-phase; with the exception of the *S. pyogenes* isolate “GAS Mucoid” and the *L. lactis* isolate W2396231, every strain was grown at 37°C with shaking (180 r.p.m.) under aerobic conditions. In contrast, the *S. pyogenes* strain was grown statically at 37°C in 5% CO<sub>2</sub> and the *L. lactis* strain was grown statically at 30°C in air. All the isolates were grown overnight in Lysogeny Broth (LB; Thermo Fisher Scientific, USA), other than the Gram-positive organisms, the *P. aeruginosa* isolate A23 (both grown in Tryptic Soy Broth, TSB; BD Biosciences, USA) and the *K. pneumoniae* isolate KPC (grown in Brain Heart Infusion Broth, BHI; VWR International, USA). Routine culture of these bacteria on solid media was performed by supplementation of the relevant growth media described above with 1.5% technical agar (BD Biosciences). Where necessary, these growth media were additionally supplemented with appropriate compounds, including: gentamicin (15 µg ml<sup>-1</sup>; Sigma-Aldrich, USA), tetracycline (12.5 µg ml<sup>-1</sup>; Sigma-Aldrich), chloramphenicol (25 µg ml<sup>-1</sup>; Sigma-Aldrich) and isopropyl-β-D-thiogalactoside (0.5 mM unless stated otherwise; Melford Laboratories, USA). For enumeration of bacterial colony forming units (c.f.u.), 10-fold serial dilutions of bacterial cultures were plated onto Mueller-Hinton agar (MHA; Thermo Fisher Scientific). All inoculated agar plates were incubated overnight at 37°C statically in air.

### 2.2 Determination of antibiotic MICs

The minimum inhibitory concentrations (MICs) of the antibiotics colistin, cerulenin, ciprofloxacin, EDTA, tetracycline, chloramphenicol, polymyxin B, triclosan (all from Sigma-Aldrich), CHIR-090 (Axon Medchem, Netherlands), gentamicin (Thermo Fisher Scientific), imipenem (Fresenius Kabi, Germany), chlorhexidine (GlaxoSmithKline, UK), murepavadin (DC Chemicals, China) and rifampicin (Molekula Ltd., UK) against relevant bacterial strains were determined using the well-established broth microdilution protocol<sup>623</sup>. Briefly, a 96-well microtitre plate was used to prepare a range of antibiotic concentrations in 200 µl cation-adjusted Mueller-Hinton broth (CA-MHB) through 2-fold serial dilutions. Stationary-phase bacteria were diluted 1000-fold in fresh CA-MHB, and 4 µl was seeded into each well of the microtitre plate to a final inoculum of 5 x 10<sup>5</sup> c.f.u. ml<sup>-1</sup>. Microtitre plates were incubated in air under static conditions at 37°C for 18 hours, except for *S. pyogenes* and *L. lactis* strains, where the plates were incubated in 5% CO<sub>2</sub> or at 30°C respectively. After overnight incubation, the MIC was defined as the lowest antibiotic concentration at which there was no visible bacterial growth. In some cases, the extent of bacterial growth after the 18 hours incubation was also

**Table 2.1: Bacterial strains used in this study**

Strain	Description	Source
<i>Pseudomonas aeruginosa</i>		
PA14	Wild-type reference strain	Lee <i>et al.</i> , 2006
PA14 <i>algP</i> :Tn	PA14 transposon mutant defective for alginate regulatory protein AlgP	Libertati <i>et al.</i> , 2006
PA14 <i>algQ</i> :Tn	PA14 transposon mutant defective for alginate regulatory protein AlgP	Libertati <i>et al.</i> , 2006
PA14 <i>algR</i> :Tn	PA14 transposon mutant defective for alginate regulatory protein AlgQ	Libertati <i>et al.</i> , 2006
PA14 <i>algX</i> :Tn	PA14 transposon mutant defective for alginate biosynthesis protein AlgX	Libertati <i>et al.</i> , 2006
PA14 <i>algZ</i> :Tn	PA14 transposon mutant defective for alginate biosynthesis protein AlgZ	Libertati <i>et al.</i> , 2006
PA14 <i>alg44</i> :Tn	PA14 transposon mutant defective for alginate biosynthesis protein Alg44	Libertati <i>et al.</i> , 2006
PA14 <i>pmrA</i> :Tn	PA14 transposon mutant defective for PmrA two-component system protein	Libertati <i>et al.</i> , 2007
PA14 <i>pmrB</i> :Tn	PA14 transposon mutant defective for PmrB two-component system protein	Libertati <i>et al.</i> , 2008
PA14 <i>phoP</i> :Tn	PA14 transposon mutant defective for PhoP two-component system protein	Libertati <i>et al.</i> , 2009
PA14 <i>phoQ</i> :Tn	PA14 transposon mutant defective for PhoQ two-component system protein	Libertati <i>et al.</i> , 2010
SCT	Human isolate - small colony variant	This study
MS	Human isolate - mucoid strain	This study
A23	Human isolate from blood culture	Medeiros <i>et al.</i> , 1971
AK3	Human cystic fibrosis (CF) isolate - mucoid strain	This study
AK10	Human CF isolate	This study
AK20	Human CF isolate	This study
AK6	Human CF isolate - mucoid strain	This study
AK12	Human CF isolate - mucoid strain	This study
AK8	Human CF isolate - mucoid strain	This study
AK17	Human CF isolate	This study
AK9	Human CF isolate	This study
AK14	Human CF isolate	This study
AK5	Human CF isolate - mucoid strain	This study
AK11	Human CF isolate - mucoid strain	This study
AK13	Human CF isolate	This study
AK18	Human CF isolate	This study
AK22	Human CF isolate	This study
AK1	Human CF isolate - colistin-resistant	This study
AK16	Human CF isolate - colistin-resistant	This study
AK19	Human CF isolate - resistant to colistin and murepavadin	This study
AK24	Human CF isolate - colistin-resistant	This study
<i>Enterobacter cloacae</i>		
IMP08	Human isolate – <i>mcr-9</i> -positive	This study
IMP14	Human isolate – <i>mcr-9</i> -positive	This study
IMP16	Human isolate – <i>mcr-9</i> -positive	This study
IMP48	Human isolate – <i>mcr-9</i> -positive	This study
IMP98	Human isolate – <i>mcr-9</i> -positive	This study
IMP99	Human isolate – <i>mcr-9</i> -positive	This study
IMP15	Human isolate – <i>mcr-9</i> -negative	This study
IMP40	Human isolate – <i>mcr-9</i> -negative	This study
IMP50	Human isolate – <i>mcr-9</i> -negative	This study
IMP83	Human isolate – <i>mcr-9</i> -negative	This study
IMP100	Human isolate – <i>mcr-9</i> -negative	This study

**Table 2.1 (continued):** Bacterial strains used in this study

Strain	Description	Source
<i>Klebsiella pneumoniae</i>		
A73	Human isolate from urine culture	Rasheed <i>et al.</i> , 2000
KPC	Human isolate	This study
<i>Escherichia coli</i>		
CTX-M	Human isolate from blood/urine	Mobley <i>et al.</i> , 1990
UTI1	Human isolate from urine culture	This study
MC1000 pEmpty	Reference strain harbouring the IPTG-inducible pDM1 plasmid	Dortet <i>et al.</i> , 2018
MC1000 <i>mcr-1</i>	MC1000 strain harbouring the pDM1 plasmid encoding the <i>mcr-1</i> gene	Dortet <i>et al.</i> , 2018
KPC BM16	Human isolate - colistin-susceptible	Dortet <i>et al.</i> , 2014
CNR 1745	Human isolate carrying <i>mcr-1</i>	Furniss <i>et al.</i> , 2019
CNR 20140385	Human isolate carrying <i>mcr-1</i>	Furniss <i>et al.</i> , 2019
CNR 1790	Human isolate carrying <i>mcr-1</i>	Furniss <i>et al.</i> , 2019
1078733	Human isolate carrying <i>mcr-1</i>	Wise <i>et al.</i> , 2018
1256822	Human isolate carrying <i>mcr-1.5</i>	Wise <i>et al.</i> , 2018
R11	Human isolate carrying <i>mcr-2</i>	Wise <i>et al.</i> , 2018
1488949	Human isolate carrying <i>mcr-3</i>	Wise <i>et al.</i> , 2018
1267171	Human isolate carrying <i>mcr-3</i>	Wise <i>et al.</i> , 2018
1266877	Human isolate carrying <i>mcr-3.2</i>	Wise <i>et al.</i> , 2018
1144230	Human isolate carrying <i>mcr-5</i>	Wise <i>et al.</i> , 2018
CNR 1728	Chromosomal colistin-resistant human isolate	Dortet <i>et al.</i> , 2014
1195290	Chromosomal colistin-resistant human isolate	Wise <i>et al.</i> , 2018
1272408	Chromosomal colistin-resistant human isolate	Wise <i>et al.</i> , 2018
1262287	Chromosomal colistin-resistant human isolate	Wise <i>et al.</i> , 2018
1252394	Chromosomal colistin-resistant human isolate	Wise <i>et al.</i> , 2018
1150735	Chromosomal colistin-resistant human isolate	Wise <i>et al.</i> , 2018
NCTC 13846	Chromosomal colistin-resistant human isolate	Silva <i>et al.</i> , 2019
<i>Burkholderia cenocepacia</i>		
AK4	Human CF isolate - intrinsic colistin resistance	This study
AK7	Human CF isolate - intrinsic colistin resistance	This study
AK15	Human CF isolate - intrinsic colistin resistance	This study
AK23	Human CF isolate - intrinsic colistin resistance	This study
<i>Acinetobacter baumannii</i>		
N12	Human isolate	This study
<i>Staphylococcus aureus</i>		
SH1000	Wild-type reference strain	Horsburgh <i>et al.</i> , 2002
<i>Streptococcus pyogenes</i>		
GAS Muroid	Human isolate – muroid strain	This study
<i>Lactococcus lactis</i>		
W2396231	Non-pathogenic food-grade organism	This study

quantified by obtaining OD<sub>595nm</sub> measurements using a Bio-Rad iMark microplate absorbance reader (Bio-Rad Laboratories, USA). Where required, the CA-MHB growth media utilised for determination of MICs was also supplemented with purified *E. coli/Salmonella* LPS (Sigma-Aldrich). For certain experiments, checkerboard analyses were performed by preparing 2-fold serial dilutions of two different antibiotics in opposite directions, creating an 8 x 8 matrix to assess the MICs of the antibiotics in combination. The results of these checkerboard broth microdilution assays were used to calculate fractional inhibitory concentration index (FICI) values, using the following previously described formula<sup>624</sup>:

$$FICI = \frac{MIC \text{ of "Drug A" in combination}}{MIC \text{ of "Drug A" alone}} + \frac{MIC \text{ of "Drug B" in combination}}{MIC \text{ of "Drug B" alone}}$$

An FICI value of greater than 1 was interpreted as an “indifferent” effect, an FICI value that was between 0.5 and 1 was interpreted as an “additive” effect, and an FICI value below 0.5 was interpreted as “true synergy”<sup>625</sup>.

### 2.3 Determination of outer membrane disruption

In order to detect damage to the LPS-containing outer membrane (OM) of Gram-negative bacteria, the gold-standard NPN uptake assay was utilised<sup>626</sup>. Briefly, stationary-phase bacterial cells were washed twice by centrifugation (12,300 x *g*, 3 minutes) and resuspension in fresh CA-MHB, then diluted to an optical density (OD<sub>600nm</sub>) of 0.5 in HEPES buffer (5 mM, pH 7.2; Sigma-Aldrich). This suspension of bacteria was added to wells of a black microtitre plate with clear-bottomed wells that contained the relevant antibiotics (also in HEPES buffer), and the phospholipid-reactive fluorescent probe *N*-phenyl-1-naphtylamine (NPN; Acros Organics, USA) at a final concentration of 10 µM. Upon addition of bacteria, fluorescence was measured immediately using a Tecan Infinite 200 Pro multiwell plate reader (Tecan Group Ltd., Switzerland), with an excitation wavelength of 355 nm and an emission wavelength of 405 nm. These fluorescence measurements were obtained every 30 seconds for 10 minutes, and the extent of OM permeabilisation, referred to as the NPN Uptake Factor, was calculated using the following formula:

$$\frac{\text{Fluorescence of sample with NPN} - \text{Fluorescence of sample without NPN}}{\text{Fluorescence of HEPES buffer with NPN} - \text{Fluorescence of HEPES buffer without NPN}}$$

### 2.4 Beta-lactamase release assay

Cells of *P. aeruginosa* were grown overnight to stationary-phase in media containing a sub-inhibitory concentration of imipenem (2 µg ml<sup>-1</sup>), in order to induce expression of its endogenous beta-lactamase enzyme AmpC, as previously established<sup>627</sup>. These stationary-phase cells were washed twice by centrifugation (12,300 x *g*, 3 minutes) and resuspension in

fresh CA-MHB, then added to 3 ml CA-MHB containing the relevant antibiotics at final inoculum of  $10^8$  c.f.u. ml<sup>-1</sup>. The cultures were incubated at 37°C with shaking (180 r.p.m.) for 60 minutes, and every 15 minutes, aliquots were obtained and bacteria removed by centrifugation (12,300 x *g*, 3 minutes). The resulting supernatant was recovered, of which 200 µl was added to the wells of a microtitre plate. Nitrocefin (Abcam, UK) – a chromogenic cephalosporin substrate routinely used to detect and quantify the presence of beta-lactamase enzymes – was added to each well to a final concentration of 250 µM, and this mixture was incubated for 2.5 hours at room temperature<sup>628</sup>. The amount of the periplasmic beta-lactamase AmpC released into the supernatant was expressed by measuring absorbance at 490 nm after this incubation period in a Bio-Rad iMark microplate absorbance reader.

## **2.5 Cytoplasmic membrane disruption of whole cells**

To measure permeabilisation of the cytoplasmic membrane (CM) of whole Gram-negative bacteria, stationary-phase cells were washed twice by centrifugation (12,300 x *g*, 3 minutes) and resuspension in fresh CA-MHB, then inoculated into 3 ml CA-MHB containing the relevant antibiotics at a final inoculum of  $10^8$  c.f.u. ml<sup>-1</sup>. Cultures were incubated at 37°C with shaking (180 r.p.m.) for up to 8 hours, and at regularly interspersed timepoints, aliquots (200 µl) were taken and bacteria isolated by centrifugation (12,300 x *g*, 3 minutes). These cells were washed in sterile phosphate-buffer saline (PBS; VWR International) before being added to the wells of a black-walled microtitre plate. Propidium iodide solution (PI; Sigma-Aldrich) was added to each well at a final concentration of 2.5 µM, and fluorescence was measured immediately in a Tecan Infinite 200 Pro multiwell plate reader (excitation at 535 nm, emission at 617 nm). To account for differences in fluorescence values arising from variations in cell number, the relative fluorescence unit (r.f.u.) measurements were corrected using readings of OD at 600 nm, with the generated number reported as the level of CM damage.

## **2.6 Determination of bactericidal activity of antibiotics**

Stationary-phase bacteria were washed twice by centrifugation (12,300 x *g*, 3 minutes) and resuspension in fresh CA-MHB, before being inoculated into 3 ml CA-MHB containing the relevant antibiotics at a final inoculum of  $10^8$  c.f.u. ml<sup>-1</sup>. These cultures were incubated at 37°C with shaking (180 r.p.m.) for up to 12 hours. Every two hours, the number of surviving bacteria was determined by serially-diluting the cultures in 10-fold steps in 200 µl sterile PBS, before enumeration of c.f.u. counts by plating 10 µl of each dilution onto solid MHA media and subsequent overnight incubation of agar plates.

## **2.7 Determination of lysis in whole cells**

To detect cell lysis in whole Gram-negative bacteria, stationary-phase bacteria were washed twice by centrifugation (12,300 x *g*, 3 minutes) and resuspension in fresh CA-MHB, then inoculated into 3 ml CA-MHB containing the relevant antibiotics at a final inoculum of 10<sup>8</sup> c.f.u. ml<sup>-1</sup>. The cultures were incubated at 37°C with shaking (180 r.p.m.) for up to 12 hours, and at regularly interspersed timepoints, 200 µl aliquots were extracted and transferred to the wells of a microtitre plate. Measurements of OD at 595 nm were obtained using a Bio-Rad iMark microplate absorbance reader.

## **2.8 Emergence of colistin resistance assay**

Stationary-phase cells of *P. aeruginosa* were washed twice by centrifugation (12,300 x *g*, 3 minutes) and resuspension in fresh CA-MHB, before being inoculated into 3 ml CA-MHB containing colistin (2 µg ml<sup>-1</sup>). The cultures were incubated at 37°C with shaking (180 r.p.m.) for 8 hours, and bacterial survival was determined every 2 hours as described above. After the 8 hour incubation, the MIC of colistin against the recovered cell population was immediately determined by the broth microdilution protocol, as detailed above. The recovered bacteria were also washed by centrifugation (12,300 x *g*, 3 minutes) and resuspension in LB media, then inoculated into 3 ml LB media and grown overnight to stationary-phase at 37°C with shaking (180 r.p.m.). This re-grown population was exposed to colistin (2 µg ml<sup>-1</sup>) for a second time, and bacterial viability was again measured over an 8 hour incubation. After this second antibiotic exposure, the colistin MIC against the surviving cell population was determined once again, before these bacteria were grown overnight to stationary-phase and exposed to colistin for a third time, with associated measurements of viability and the colistin MIC of the recovered population obtained as before.

## **2.9 Zone of inhibition assay**

Stationary-phase bacteria were diluted in fresh CA-MHB to an inoculum of 10<sup>6</sup> c.f.u. ml<sup>-1</sup> and 60 µl of this bacterial culture was spread across the surface of a CA-MHA plate. After allowing the plates to air-dry, wells measuring 10 mm in diameter were made in the agar. For some experiments, these wells were filled with the spent supernatant extracted from bacterial cultures exposed to colistin as described above. Recovery of these spent culture supernatants was performed after centrifugation (12,300 x *g*, 3 minutes) of colistin-treated bacteria. In certain cases, fresh colistin was added to the spent culture supernatant and incubated for 4 hours at 37°C with end-over-end rotation, before the wells in the agar plate were filled with this mixture. For other assays, the extracted culture supernatant was pre-treated with heat (80°C, 20 minutes) and allowed to cool prior to the addition of fresh colistin. Where relevant,

antibiotics were added directly into the agar plate wells, either in CA-MHB alone or after 4 hours incubation (37°C, end-over-end rotation) in the presence of purified *E. coli*/*Salmonella* LPS. The CA-MHA plates with filled wells were incubated statically in air at 37°C for 18 hours, and the zone of growth inhibition around each well was measured at 4 perpendicular points. A standard plot was generated that enabled inhibitory zone size to be converted to percentage antibiotic activity using a previously established method<sup>629</sup>.

## **2.10 Fluorescent labelling of polymyxin compounds**

The antibiotics colistin, polymyxin B and polymyxin B nonapeptide (PMBN, Sigma-Aldrich) were labelled with the fluorophore BoDipy FL SE D2184 (Thermo Fisher Scientific) by combining 250 µl of the polymyxin drugs (10 mg ml<sup>-1</sup>) with 100 µl of the BoDipy NHS ester compound (10 mg ml<sup>-1</sup> in DMSO) and 650 µl of sodium bicarbonate (0.2 M, pH 8.5)<sup>630</sup>. This mixture was incubated statically at 37°C for 2 hours. BoDipy molecules that had not bound to the antibiotics were removed by dialysis using a Float-A-Lyser G2 dialysis device (Spectrum Laboratories, USA) with a molecular weight cut-off of 0.5 kDa. Dialysis was carried out against sterile distilled water at 4°C, which was changed four times over the course of a 24 hour period of dialysis. Successful labelling of the three polymyxin compounds with a single fluorescent BoDipy molecule was verified by time-of-flight mass spectrometry. In addition, the impact of BoDipy-labelling on the antibiotic activity of colistin and polymyxin B was measured using the broth microdilution MIC protocol detailed above.

## **2.11 Determination of antibiotic binding to bacterial cells**

Stationary-phase bacteria were washed twice by centrifugation (12,300 x *g*, 3 minutes) and resuspension in fresh CA-MHB, then inoculated at a final density of 10<sup>8</sup> c.f.u. ml<sup>-1</sup> into 3 ml CA-MHB containing fluorescently-labelled BoDipy-colistin, BoDipy-polymyxin B, or BoDipy-PMBN, either alone or in combination with other relevant antibiotics. The cultures were incubated for up to 8 hours at 37°C with shaking (180 r.p.m.), and every 2 hours bacteria were recovered by centrifugation (12,300 x *g*, 3 minutes) and the spent supernatant separately extracted. Pelleted bacterial cells were washed thoroughly by four rounds of centrifugation (12,300 x *g*, 3 minutes) and resuspension in fresh CA-MHB to remove any BoDipy-labelled antibiotic molecules that were not attached to bacteria. The amount of the BoDipy-polymyxin compounds bound to the bacteria or remaining in the culture supernatant was quantified by measuring fluorescence of the samples (200 µl) in a black-walled microtitre plate, with a Tecan Infinite 200 Pro multiwell plate reader (excitation at 490 nm, emission at 525 nm). Relative fluorescence values were corrected using OD<sub>600nm</sub> measurements to account for variations in cell density. Binding of the BoDipy-labelled antibiotics to bacterial cells was also observed by fluorescence microscopy, as described in the relevant section below.

## 2.12 Determination of membrane lipid release from bacteria

Stationary-phase bacteria were washed twice by centrifugation (12,300 x *g*, 3 minutes) and resuspension in fresh CA-MHB, before being inoculated into 3 ml CA-MHB containing the relevant antibiotics at a final inoculum of 10<sup>8</sup> c.f.u. ml<sup>-1</sup>. Cultures were incubated at 37°C with shaking (180 r.p.m.) for 8 hours, and every 2 hours, spent culture supernatants were recovered following centrifugation (12,300 x *g*, 3 minutes). Extracted supernatants (200 µl) were mixed with 5 µl of FM-4-64 styryl dye (Thermo Fisher Scientific) at a final concentration of 5 µg ml<sup>-1</sup> in the wells of a black-walled microtitre plate<sup>631</sup>. Fluorescence was measured using a Tecan Infinite 200 Pro multiwell plate reader (excitation at 565 nm, emission at 660 nm) to quantify the concentration of membrane phospholipids shed into the supernatant.

## 2.13 Bacterial growth assay

Stationary-phase bacteria were diluted 1000-fold in fresh CA-MHB, before 4 µl was seeded at a final inoculum of 5 x 10<sup>5</sup> c.f.u. ml<sup>-1</sup> into the wells of a microtitre plate containing 200 µl CA-MHB and the relevant antibiotics. The microtitre plate was incubated in a Tecan Infinite 200 Pro multiwell plate reader at 37°C with shaking (180 r.p.m.) for up to 24 hours, with measurements of OD<sub>600nm</sub> obtained every 15 minutes. In some cases, bacterial doubling times during logarithmic phase growth were calculated from the generated growth curves.

## 2.14 Limulus amoebocyte lysate assay

The concentration of LPS present in a variety of samples (spent culture supernatants, OM extracts of whole cells, spheroplasts) was quantified using the diagnostic gold-standard chromogenic Limulus amoebocyte lysate (LAL) assay (Thermo Fisher Scientific), as previously described<sup>632,633</sup>. All samples (50 µl) were first equilibrated to 37°C and loaded into the wells of a microtitre plate at the same temperature. LAL reagent (50 µl) – containing the lyophilised lysate prepared from the circulating amoebocytes of the horseshoe crab *Limulus polyphemus* – was added to each well, before the mixture was incubated statically at 37°C for 10 minutes. A colourless chromogenic substrate solution (100 µl, 2 mM) – Ac-Ile-Glu-Ala-Arg-pNA – was added to each well, and the microtitre plate was again incubated statically at 37°C for a further 6 minutes. The enzymatic reaction was stopped by adding 50 µl of 25% acetic acid to each well. The release of yellow *p*-Nitroaniline (pNA) from the chromogenic substrate was determined photometrically by measuring absorbance at 405 nm in a Tecan Infinite 200 Pro multiwell plate reader. A standard curve was generated using known concentrations of an *E. coli* LPS stock solution, which enabled the conversion of A<sub>405nm</sub> values into LPS concentrations. In several cases, samples had to be serially diluted in 10-fold steps in endotoxin-free water to accurately measure LPS levels within the range of the generated standard curve.



## 2.15 LPS detection/quantification by silver staining

LPS was extracted from culture supernatants and visualised on 12% SDS-PAGE gels using previously established protocols<sup>634</sup>. Stationary-phase bacteria (1 ml) were washed twice by centrifugation (12,300 x *g*, 3 minutes) and resuspension in fresh CA-MHB, then inoculated into 9 ml CA-MHB containing the relevant antibiotics at a final inoculum of 10<sup>8</sup> c.f.u. ml<sup>-1</sup>. The bacterial cultures were incubated at 37°C with shaking (180 r.p.m.) for 2, 4, 6 or 8 hours, before 9 ml of spent culture supernatant was recovered following centrifugation (3,270 x *g*, 30 minutes). This supernatant was filter-sterilised using a 0.2 µm filter to ensure removal of any bacterial cells. Absolute ethanol (30 ml) was added to the spent supernatants, and these mixed samples were placed at -20°C for 30 minutes to allow complete precipitation to occur. The precipitate was then pelleted by centrifugation (3,270 x *g*, 30 minutes) and resuspended in 500 µl Laemmli buffer (Sigma-Aldrich). Any precipitated protein was removed by digesting with proteinase K (50 µg, Sigma-Aldrich) overnight, before 25 µl of each sample was run on an acrylamide mini-gel system. Electrophoresis was carried out at 12 mA in the stacking gel, and 25 mA in the separating gel.

The ultrafast silver staining method was used to visualise LPS preparations subjected to SDS-PAGE<sup>635</sup>. Once run, the gel was first oxidised using a 200 ml solution of 40% ethanol-5% acetic acid containing 0.7% sodium periodate (Sigma-Aldrich), incubated with the gel at room temperature for 20 minutes. The gel was then washed three times (5 minutes each time) with distilled water. Fresh silver staining solution was prepared by first adding 4 ml concentrated ammonium hydroxide to 56 ml sodium hydroxide (0.1 M), before adding a further 200 ml of distilled water. Silver nitrate (20% w/v, 10 ml) was then added in drops whilst stirring, before the final addition of 30 ml distilled water. This silver staining solution was then used to stain the oxidised and washed gel for 10 minutes, with the gel subsequently washed in distilled water another three times (5 minutes each time). The silver stained gel was developed with 200 ml of distilled water containing formaldehyde (100 µl of a 37% w/v solution) and 10 mg of citric acid, with development stopped using a 10% acetic acid solution. The gel was then washed once in distilled water and imaged using a Bio-Rad Gel Doc EZ Imager (Bio-Rad Laboratories). The intensity of the silver-stained LPS bands was quantified through densitometry, using the FIJI/ImageJ software as previously detailed<sup>636</sup>.

## 2.16 Scanning electron microscopy

Scanning electron microscope images of bacterial cells were acquired in collaboration with Dr. Anna Klöckner, Dr. Michele Becce and Professor Molly Stevens (Imperial College London). Stationary-phase bacteria were washed twice by centrifugation (12,300 x *g*, 3 minutes) and resuspension in fresh CA-MHB, then inoculated into 3 ml CA-MHB containing

the relevant antibiotics. The cultures were incubated at 37°C with shaking (180 r.p.m.) for 2 hours, after which time 25 µl samples were spotted onto a silicon chip (University Wafer, USA) and allowed to air-dry. The samples were fixed using glutaraldehyde (2.5% in 0.01 M PBS) at room temperature for 30 minutes, and the chip was then washed three times in 0.01 M PBS. The sample was dehydrated with increasing concentrations of ethanol (10%, 30%, 50%, 70%, 90% and 100%) – used for 5 minutes each time – before the application of a coating of 15 nm chromium (Quorum Technologies, UK). Images of bacterial cells were obtained using a LEO Gemini 1525 field emission gun (FEG) scanning electron microscope (Carl Zeiss Microscopy GmbH, Germany).

## **2.17 Isolation of CHIR-090 resistant mutants**

Stationary-phase cells of *P. aeruginosa* PA14 were washed twice by centrifugation (12,300 x *g*, 3 minutes) and resuspension in fresh CA-MHB, before they were diluted 10-fold in CA-MHB to a final inoculum of 10<sup>8</sup> c.f.u. ml<sup>-1</sup>. A 100 µl sample of this inoculum was spread across the surface of a CA-MHA plate, and a well measuring 10 mm in diameter was made in the centre of these agar plates. This well was filled with 130 µl of CHIR-090 (8 µg ml<sup>-1</sup>), and incubated statically at 37°C in air for 18 hours. Mutants with spontaneous resistance to CHIR-090 were isolated by picking colonies that had grown within the zone of inhibition around the well, and grown overnight in LB to stationary-phase. These mutant strains were re-exposed to CHIR-090 (8 µg ml<sup>-1</sup>) in a well as described above to confirm that the bacteria had a reduced susceptibility to the LpxC inhibitor. Measurements of bacterial growth, antibiotic MIC and cell survival were obtained as detailed in the relevant sections to characterise the properties of the CHIR-090-resistant *P. aeruginosa* isolates.

## **2.18 Determination of surface LPS levels with BoDipy-PMBN**

The amount of LPS in the OM of bacterial whole cells and in the CM of spheroplasts was detected and quantified using the BoDipy-labelled form of the compound PMBN as an LPS-specific probe. Samples of whole cells or spheroplasts (10 ml) – pre-exposed to relevant antibiotics in CA-MHB as described in other sections – were centrifuged for 20 minutes at 4°C (3,270 x *g* for whole cells, 2,000 x *g* for spheroplasts) and fixed by resuspending in 10 ml of 4% paraformaldehyde in PBS (with 20% sucrose added for spheroplasts). After fixation for 1 hour at room temperature, samples were washed twice by centrifugation (3,270 x *g*, 4°C, 20 minutes) and re-suspension in 10 ml Tris buffer (0.03 M, pH 8.0; Sigma-Aldrich). BoDipy-PMBN was added at final concentration of 7 µg ml<sup>-1</sup> and the fixed bacterial suspensions were incubated for 30 minutes at 37°C with shaking (180 r.p.m.). To remove any BoDipy-PMBN molecules that were not bound to the cell surface, fixed bacteria were washed twice as stated above. The amount of BoDipy-PMBN bound to the surface of whole cells/spheroplasts was

assessed by seeding 200  $\mu\text{l}$  samples into the wells of a black-walled microtitre plate, and measuring fluorescence in a Tecan Infinite 200 Pro multiwell plate reader (excitation at 490 nm, emission at 525 nm). To account for differences in relative fluorescence arising from variations in cell density, r.f.u. values were corrected for using  $\text{OD}_{600\text{nm}}$  readings. The extent of BoDipy-PMBN binding to the bacterial surface was additionally visualised by fluorescence microscopy, as described below.

## **2.19 Phase-contrast and fluorescence microscopy**

For visualisation of fixed whole bacteria or spheroplasts by phase-contrast/fluorescent microscopy, a 5  $\mu\text{l}$  sample of cells was spotted onto a thin 1.2% agarose gel patch prepared in distilled water on a microscope slide. Bacteria were imaged using an Axio Imager.A2 Zeiss Microscope (Carl Zeiss Microscopy GmbH) at 1000x magnification with an oil immersion objective lens, and processed with the associated ZEN 2012 software. Where relevant, analysis of cell length:width ratios was performed using the FIJI/ImageJ software to measure the size of two perpendicular lines drawn through the centre of bacteria. For all microscopy-based experiments, all images were acquired and processed using identical settings throughout.

## **2.20 Generation of spheroplasts**

Bacterial spheroplasts lacking on OM and cell wall were produced through a previously described and well-established protocol<sup>637</sup>. Stationary-phase whole cells were washed twice by centrifugation (12,300  $\times g$ , 3 minutes) and resuspension in fresh CA-MHB, then inoculated at a final density of  $10^8$  c.f.u.  $\text{ml}^{-1}$  into 9 ml CA-MHB, containing the relevant antibiotics where required. Cultures were incubated with shaking (180 r.p.m.) at 37°C for 2 hours, before the bacteria were washed twice by centrifugation (3,270  $\times g$ , 20 minutes, 4°C) and resuspension first into 10 ml Tris buffer (0.03 M, pH 8.0), and subsequently into Tris buffer containing 20% sucrose. EDTA (250  $\mu\text{l}$ , 10  $\text{mg ml}^{-1}$ ) and lysozyme (1 ml, 10  $\text{mg ml}^{-1}$ ; Roche, Switzerland) were added to remove the OM and cell wall structures respectively, and this cell suspension was incubated for 1 hour in a water bath shaker at 30°C. Next, trypsin (500  $\mu\text{l}$ , 10  $\text{mg ml}^{-1}$ ; Sigma-Aldrich) was added, and the mixture incubated at 30°C for a further 15 minutes in a water bath shaker. The resulting spheroplasts formed were harvested by mild centrifugation (2,000  $\times g$ , 20 minutes, 4°C), and the supernatant containing the extracted OM isolated for later analysis.

## **2.21 Confirmation of successful spheroplast formation**

The successful removal of the OM from whole cells during spheroplasts conversion was validated by demonstrating the loss of fluorescently-labelled outer membrane proteins. Whole bacterial cells in stationary-phase were washed twice by centrifugation (12,300  $\times g$ , 3 minutes) and resuspension in fresh CA-MHB, before inoculation into 9 ml CA-MHB at a final density of

$10^8$  c.f.u. ml<sup>-1</sup>. After this incubation period, proteins in the OM of the bacteria were labelled with fluorescein isothiocyanate (FITC; Sigma-Aldrich) using a previously described method – cells were washed twice by centrifugation (3,270 x *g*, 20 minutes, 4°C) and resuspension in 10 ml Labelling Buffer (50 mM Na<sub>2</sub>CO<sub>3</sub>, 100 mM NaCl, pH 8.0), FITC at a final concentration of 0.5 mg ml<sup>-1</sup> was added, and the mixture incubated statically at room temperature for 30 minutes<sup>638</sup>. Fluorescently-labelled whole cells were washed three times by centrifugation (3,270 x *g*, 20 minutes, 4°C) and resuspension in 10 ml Tris buffer (0.03 M, pH 8.0) containing 20% sucrose. At this point, 1 ml of FITC-tagged bacteria was extracted, centrifuged (12,300 x *g*, 3 minutes), and fixed in 4% paraformaldehyde in PBS. The remaining 9 ml cell suspension was converted into spheroplasts as detailed above, before 1 ml of these spheroplasts was fixed in the same manner as with whole cells. The amount of FITC fluorescence on the surface of whole bacteria and spheroplasts was observed by fluorescence microscopy (as described above), and quantified by seeding 200 µl samples of the fixed cell suspensions into the wells of a black-walled microtitre plate, and measuring fluorescence in a Tecan Infinite 200 Pro multiwell plate reader (excitation at 490 nm, emission at 525 nm). Successful conversion of whole cells into spheroplasts was also confirmed by measuring the length:width ratio of bacteria after phase-contrast microscopy, and showing lysis of spheroplasts in the absence of the sucrose osmoprotective environment, with these assays described in the relevant sections.

## **2.22 Lipidomic analysis by MALDI-TOF mass spectrometry**

To determine LPS concentrations or modifications in whole bacterial cells (grown to stationary-phase in liquid culture, or obtained directly from an agar plate) or spheroplasts, a matrix-assisted laser desorption/ionization time-of-flight (MALDI-TOF) mass spectrometry approach was utilised in collaboration with Katheryn Hagart and Dr. Gerald Larrouy-Maumus (Imperial College London)<sup>639</sup>. Whole cell/spheroplast samples were washed and resuspended in ddH<sub>2</sub>O (200 µl), before a mild acid hydrolysis was performed to enrich for lipid A via the addition of 200 µl of 2% (v/v) acetic acid in ddH<sub>2</sub>O and incubation at 100°C for 30 minutes<sup>640</sup>. Acid-treated bacteria were recovered by centrifugation (17,000 x *g*, 2 minutes), and the pellet was washed then resuspended in 50 µl of ultrapure water. A 0.5 µl sample of this suspension was loaded immediately onto a target plate and overlaid with 1.2 µl of a matrix consisting of 9H-Pyrido[3,4-B]indole (Norharmane; Sigma-Aldrich) dissolved in 90:10 (v/v) chloroform-methanol at a final concentration of 10 mg ml<sup>-1</sup>. The bacterial suspension and matrix were mixed on the target before gentle drying under air at room temperature. A MALDI Biotyper Sirius system (Bruker Daltonics, USA) was then used for MALDI-TOF mass spectrometric analysis, using the linear negative-ion mode as described previously<sup>641</sup>. Manual peak picking at masses relevant to phospholipids or lipid A was performed on the mass spectra obtained, and the corresponding signal intensities at these defined masses was determined. Peaks were

only considered if their ratio of signal:noise was more than 5. To determine the relative abundance of LPS, the sum of the area under the lipid A peaks was divided by the sum of the area under a representative phosphatidylglycerol phospholipid peak (PG 34:2). To determine the ratio of modified lipid A:unmodified lipid A, the area under cationically-modified (pEtN/L-Ara4N) peaks was divided by the area under peaks for native, unaltered lipid A.

## 2.23 Determination of CM disruption/lysis in spheroplasts

Bacterial spheroplasts, pre-exposed or not to the relevant antibiotics, were generated as detailed above, then washed by centrifugation (4,000 x *g*, 5 minutes) and resuspension in 1 ml Tris buffer (0.03 M, pH 8.0) containing 20% sucrose. To measure antibiotic-induced CM permeabilisation in these spheroplasts, 20 µl samples were added in the wells of a black-walled microtitre plate to 180 µl Tris buffer containing 20% sucrose, the relevant antibiotics/chemical compounds, and the fluorescent dye PI at a final concentration of 0.25 µM. The microtitre plate was incubated at 37°C with shaking (180 r.p.m.) for up to 18 hours in a Tecan Infinite 200 Pro multiwell plate reader. Every 15 minutes, fluorescence was measured (excitation at 535 nm, emission at 617 nm) to quantify the extent of PI uptake as a marker of CM damage. To detect antibiotic-triggered spheroplast lysis, the cell forms were exposed to the relevant drugs in a microtitre plate as described above, and every 15 minutes, readings of OD at 600 nm were obtained.

## 2.24 Determination of membrane fluidity

The fluidity of the OM of whole bacterial cells and the CM of spheroplasts was assessed by the gold-standard technique using the fluorescent dye Laurdan (Sigma-Aldrich), as described previously<sup>642</sup>. Stationary-phase whole cells or spheroplasts generated as detailed above were washed, and 500 µl samples were incubated for 5 minutes at room temperature in Tris buffer (0.03 M, pH 8.0, with 20% sucrose added for spheroplasts) containing Laurdan at a final concentration of 100 µM. After the incubation, samples were washed by three rounds of centrifugation (4,000 x *g*, 5 minutes) and resuspension in Tris buffer. Washed cells (200 µl) were transferred to the wells of a black-walled microtitre plate, and fluorescence from Laurdan measured in a Tecan Infinite 200 Pro multiwell plate reader (excitation at 330 nm, emission at both 460 nm and 500 nm). The degree of membrane fluidity was determined by calculating the Generalised Polarisation (GP) based on r.f.u. values using the formula:

$$\text{Generalised Polarisation} = \frac{\text{Emission intensity at 460 nm} - \text{Emission intensity at 500 nm}}{\text{Emission intensity at 460 nm} + \text{Emission intensity at 500 nm}}$$

The higher the GP value, the more rigid the membrane was – with altered water penetration into the membrane affecting the fluorescence of the Laurdan dye.

## **2.25 Determination of membrane charge**

The net electrostatic charge of the OM of whole bacteria and the CM of spheroplasts was measured by a well-established approach using FITC-labelled Poly-L-Lysine (PLL; Sigma-Aldrich)<sup>643</sup>. Samples (300 µl) of whole cells or spheroplasts produced as described above were washed and incubated at room temperature for 10 minutes in Tris buffer (0.03 M, pH 8.0, with 20% sucrose added for spheroplasts) containing FITC-PLL at a final concentration of 20 µg ml<sup>-1</sup>. To remove any FITC-PLL that had not bound to the cellular surface, the samples were washed thoroughly by three rounds of centrifugation (4,000 x *g*, 5 minutes) and resuspension in Tris buffer. Washed cells (200 µl) were seeded into the wells of a black-walled microtitre plate, and the amount of FITC-PLL attached to the samples was quantified by measuring the fluorescence in a Tecan Infinite 200 Pro multiwell plate reader (excitation at 490 nm, emission at 525 nm). The less FITC-PLL binding to the surface of whole cells/spheroplasts, the more positively-charged the membrane was – with the cationic FITC fluorophore having reduced affinity for the membrane bilayer.

## **2.26 Population analysis profiling**

Bacteria were incubated in liquid LB media at 37°C overnight with shaking (180 r.p.m.) to reach stationary-phase growth, and then serially-diluted in 10-fold steps in sterile PBS. From each of these dilutions, 10 µl was plated onto CA-MHA plates containing increasing concentrations of colistin (0, 4, 16 and 64 µg ml<sup>-1</sup>). The colistin-containing agar plates were incubated at 37°C statically for 24 hours, before enumeration of the surviving cells at each colistin concentration by c.f.u. counts.

## **2.27 Luria-Delbrück fluctuation test assays**

Stationary-phase bacterial cultures grown overnight were diluted and seeded into the wells of a microtitre plate containing 200 µl CA-MHB such that each well was inoculated, on average, with 0.5 cells. The microtitre plate was incubated at 37°C with shaking (180 r.p.m.) in a Tecan Infinite 200 Pro multiwell plate reader for, as required, 10 hours (to the start of logarithmic phase), 14 hours (to mid-logarithmic phase), 18 hours (to early stationary phase), or 24 hours (to late stationary phase). Bacteria from every well in which growth had occurred were serially-diluted in 10-fold steps in sterile PBS, and 10 µl of these dilutions was plated on CA-MHA plates containing the relevant concentration of colistin (4, 16 or 64 µg ml<sup>-1</sup>). The agar plates were incubated statically at 37°C for 24 hours, after which time the number of bacteria capable of tolerating colistin exposure from each individual population grown from a single cell was established based on c.f.u. counts.

## 2.28 Bacterial competition experiments

The relative fitness of the *E. coli* MC1000 strain carrying the plasmid-borne *mcr-1* colistin resistance gene was compared to MC1000 bacteria harbouring only an empty plasmid control by means of a well-established growth competition assay<sup>644</sup>. Stationary-phase cultures of both strains were mixed in a 1:1 ratio, diluted 1000-fold in 3 ml LB broth (containing 0.5 mM IPTG or 250 mM IPTG), and incubated at 37°C with shaking (180 r.p.m.) for 24 hours. After this incubation period, the mixed culture was again diluted 1000-fold into 3 ml LB containing either 0.5 mM or 250 mM IPTG, and re-incubated for another 24 hours at 37°C with shaking (180 r.p.m.) to initiate a second growth cycle. This procedure was repeated on a further two occasions, such that the competition experiment was conducted over 4 growth cycles lasting 96 hours. At the half-way stage of each growth cycle (i.e. at 12, 36, 60 and 84 hours), samples of the mixed culture were extracted and serially-diluted in 10-fold steps in sterile PBS. These serial dilutions (10 µl) were plated onto CA-MHA plates containing no colistin, as well as CA-MHA plates containing colistin at a final concentration of 2 µg ml<sup>-1</sup>. Following incubation of the agar plates statically at 37°C overnight, c.f.u. counts were enumerated, and the competitive index (CI) value – a numerical read-out of the relative fitness of the *mcr-1* strain versus the pEmpty strain – was calculated using the following formula:

$$CI = \frac{\log_{10}(\text{Total Colonies}_{t=x}) - \log_{10}(\text{Total Colonies}_{t=0})}{\log_{10}(\text{Resistant Colonies}_{t=x}) - \log_{10}(\text{Resistant Colonies}_{t=0})}$$

where  $\text{Total Colonies}_{t=x}$  is the c. f. u. counts on the No Colistin agar plates at a timepoint  
where  $\text{Total Colonies}_{t=0}$  is the c. f. u. counts on the No Colistin agar plates at 0 hours  
where  $\text{Resistant Colonies}_{t=x}$  is the c. f. u. counts on the Colistin agar plates at a timepoint  
where  $\text{Resistant Colonies}_{t=0}$  is the c. f. u. counts on the Colistin agar plates at 0 hours

A CI value greater than 1 was representative of the fact that the *mcr-1* strain had enhanced fitness relative to the pEmpty control strain. By contrast, a CI value below 1 was representative of the fact that the *mcr-1* strain had a relative fitness cost compared to the pEmpty strain.

## 2.29 Murine lung infection model

An *in vivo* model of an acute, high-burden *P. aeruginosa* infection in the mouse lung was undertaken in collaboration with Dr. Thomas Clarke (Imperial College London). The use of mice was performed under the authority of the UK Home Office outlined in the Animals (Scientific Procedures) Act 1986, after ethical review by the Imperial College London Animal Welfare and Ethical Review Body (PPL 70/7969). Wild-type C57BL/6 mice were purchased from Charles River (UK); all mice were female and aged between 6 and 8 weeks. Mice were housed with five per cage, using “Aspen Chips 2” bedding and 12 hour light/dark cycles at 20-22°C. Water was provided *ad libitum* and mice were fed RM1 (Special Diet Services, UK). Mice

were randomly assigned to experimental groups. To establish bacterial colonisation of the lungs, mice were first anaesthetised and then inoculated via the intranasal route with  $10^7$  c.f.u. of *P. aeruginosa* PA14 cells in 50  $\mu$ l of PBS, as described previously<sup>645,646</sup>. The infection was allowed to establish for 5 hours, before mice were anaesthetised again and treated intranasally with 50  $\mu$ l of PBS alone, or PBS containing either colistin alone (5 mg kg<sup>-1</sup>), murepavadin alone (0.25 mg kg<sup>-1</sup>), or a combination of colistin and murepavadin. After 3 hours post-treatment, mice were humanely sacrificed, both lungs were removed and homogenised in PBS, before plating of 10-fold serial dilutions on to *Pseudomonas* isolation agar (Thermo Fisher Scientific). These agar plates were incubated overnight statically at 37°C, and the bacterial load in the lungs was enumerated by c.f.u. counts.

### **2.30 Statistical analysis**

All experiments were performed on at least three independent occasions, and the resulting data are presented as the arithmetic means of these biological replicates, unless otherwise stated. Where error bars are shown, these represent the standard deviation of the arithmetic mean of the data. For single comparisons, a two-tailed Student's *t*-test (parametric data) or a Mann-Whitney test (nonparametric data) was used to analyse the data. For multiple comparisons at a single timepoint/concentration, data were analysed by a one-way analysis of variance test (ANOVA; parametric data) or a Kruskal-Wallis test (nonparametric data). Where data were obtained across several different timepoints or concentrations, a two-way ANOVA test was used for statistical analyses. Correlations between datasets were analysed by a simple linear regression. Appropriate post-hoc tests (Dunnett's, Sidak's, Holm-Sidak's, Dunn's, or Tukey's) were performed to correct for multiple comparisons, with details provided in figure legends. Statistically-significant differences between data are indicated by asterisks on graphs, and the corresponding p-values are reported in the figure legends. All statistical analyses were performed using GraphPad Prism 9 software (GraphPad Software Inc., USA).



## Chapter 3: *Pseudomonas aeruginosa* survives colistin exposure by releasing lipopolysaccharide

### 3.1 Introduction

The Gram-negative bacterial pathogen *P. aeruginosa* is responsible for causing a diverse range of opportunistic infections in immunocompromised human patients, including serious, invasive infections in the lungs, soft tissue and the bloodstream<sup>647</sup>. Historically, such infections were treated with a combination of beta-lactam, quinolone and aminoglycoside antibiotics<sup>648</sup>. However, the rise in the prevalence of multi-drug resistant *P. aeruginosa* isolates exhibiting non-susceptibility to several antibiotic classes has rendered many of these front-line antimicrobial agents ineffectual<sup>649</sup>. As a result, attention has increasingly turned to alternative antibiotics that could be used to combat *P. aeruginosa* infections in the clinic, and in particular, to the last-resort polymyxin compound colistin.

Colistin is a cyclic lipopeptide antibiotic that was discovered and used extensively in the mid-20<sup>th</sup> century, before its clinical administration was abandoned owing to concerns over neurotoxicity and nephrotoxicity<sup>308</sup>. In spite of these side-effects, as resistance rates to front-line antipseudomonal drugs has soared globally over the previous three decades, there has been a concurrent rise in prescriptions of colistin, which is often used as the final treatment option to keep patients infected with multi-drug resistant *P. aeruginosa* alive<sup>274</sup>. Although it is a “therapeutic of last resort”, concerningly colistin is not an effective antibiotic, and treatment failure is a frequent outcome following clinical use of the polymyxin drug. Studies have reported that colistin administered either intravenously or in nebulised form is unable to clear *P. aeruginosa* infections and prevent patient death in up to 67% of cases<sup>615,622</sup>. With the pipeline for novel antibiotics against Gram-negative bacteria extremely limited to the point of being virtually non-existent, there is a critical, pressing need to identify, understand and ultimately mitigate the causes of colistin therapy failure in order to maintain the ability to treat multi-drug resistant *P. aeruginosa* infections.

There have been numerous hypotheses postulated regarding how *P. aeruginosa* is able to survive colistin exposure and cause antibiotic treatment failure, including the capacity of the bacteria to readily form biofilm structures<sup>520,630</sup>. It is suggested that the principal components of the enclosed biofilm matrix released by the pathogen, namely the alginate exopolysaccharide, mucins and extracellular DNA, may bind colistin and restrict its ability to access bacterial cells, leading to tolerance to the polymyxin antibiotic<sup>650–652</sup>. Additionally, it has been proposed that colistin therapeutic failure against *P. aeruginosa* infections could arise from the phenomenon of antibiotic persistence, where a quiescent, non-growing

subpopulation of cells survive drug exposure due to their dormant state<sup>653–655</sup>. However, the molecular mechanisms underlying *P. aeruginosa* persister cells that tolerate colistin are poorly established. In fact, the predominant reason for colistin treatment failing in the clinical setting is believed to be classical resistance to the polymyxin antibiotic, mediated by chromosomal mutations.

The first step in colistin's bactericidal mode of action is binding to LPS in the outer membrane of Gram-negative bacteria, with electrostatic attractions between the polymyxin's cationic peptide ring and the anionic lipid A domain of LPS crucial for this interaction<sup>398</sup>. Genetic mutations in several chromosomally-encoded two-component systems (e.g. PhoPQ, PmrAB) of *P. aeruginosa* leads to lipid A being modified with positively-charged chemical groups, including phosphoethanolamine and 4-amino-4-deoxy-L-arabinose, which consequently blocks the binding of colistin to LPS and culminates in polymyxin resistance<sup>492</sup>. Whilst this mechanism of resistance to colistin in *P. aeruginosa* is well-characterised, the prevalence of non-susceptibility to the polymyxin antibiotic in clinical isolates of the pathogen is notably low. Large-scale surveillance studies conducted worldwide have identified that colistin resistance occurs in only between 0.1% and 7% of *P. aeruginosa* strains isolated from infected humans<sup>604–613</sup>.

Given that colistin fails to effectively treat patients and clear *P. aeruginosa* infections in more than 60% of individuals, there is an obvious discord between rates of resistance to the polymyxin drug and the frequency of therapeutic failure. This clearly suggests that the pathogen *P. aeruginosa* is able to survive colistin exposure through a process divergent from classical antibiotic resistance. In this chapter, a novel mechanism by which *P. aeruginosa* inactivates colistin and survives treatment with the antibiotic is first identified and then characterised.

### **3.2 Colistin causes sequential disruption of the *P. aeruginosa* cell membranes**

In order to understand how *P. aeruginosa* survives exposure to colistin, a panel of assays to track the polymyxin antibiotic's purported mode of action were first established. The *P. aeruginosa* strain PA14 was used for these experiments since it is a well-characterised virulent reference strain isolated from a human patient and representative of the most common clonal group of *P. aeruginosa* circulating worldwide<sup>656,657</sup>. In addition, *P. aeruginosa* PA14 is susceptible to colistin, with a minimum inhibitory concentration (MIC) value of 1 µg ml<sup>-1</sup>, which is below the resistance breakpoint threshold of 2 µg ml<sup>-1</sup> (**Figure 3.1A**). Therefore, using this strain allowed for investigations of alternate processes that enabled *P. aeruginosa* to survive colistin treatment other than resistance to the polymyxin drug.

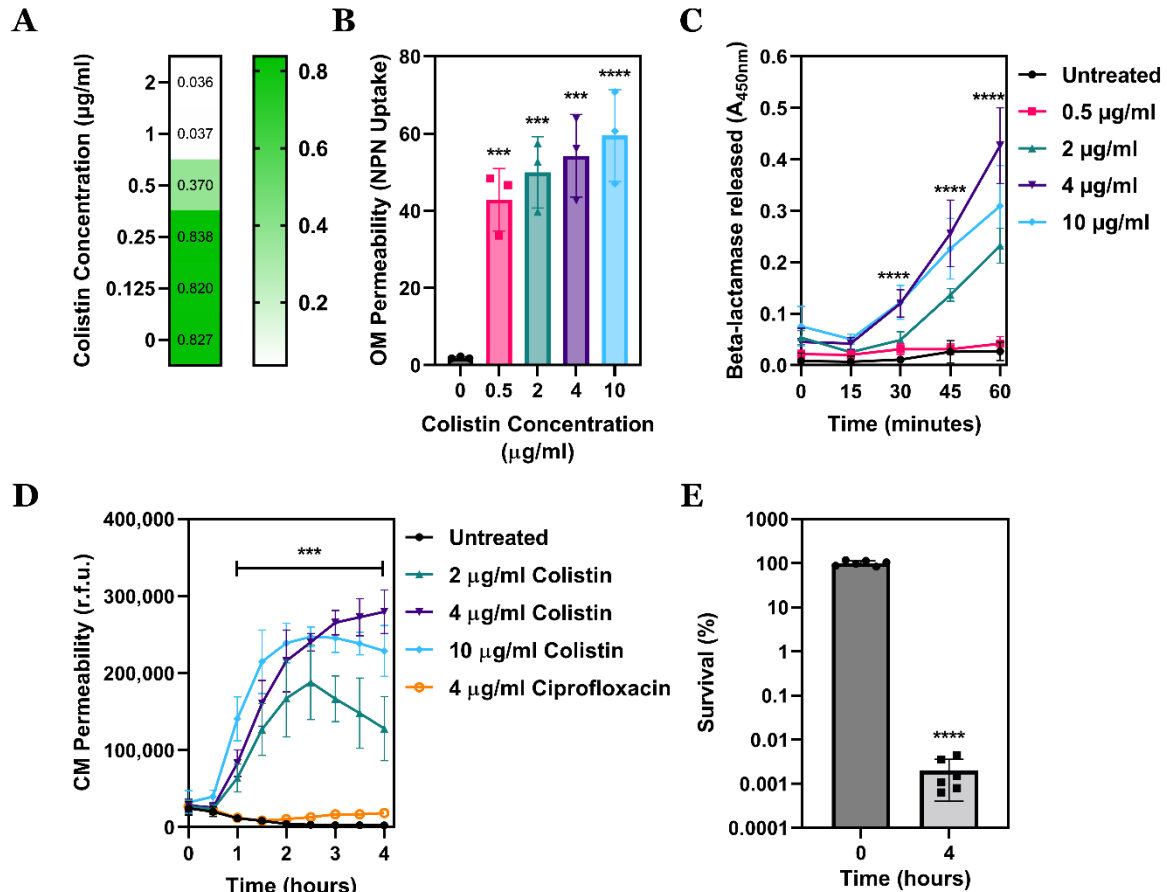


**Figure 3.1: Colistin sequentially disrupts the outer membrane (OM) and cytoplasmic membrane (CM) of *P. aeruginosa*.** **A**, The minimum inhibitory concentration (MIC) of colistin against *P. aeruginosa* PA14 cells, as determined by measuring bacterial growth after 18 hours incubation using OD<sub>595nm</sub> readings (n=4). **B**, Minor permeabilisation of the OM of *P. aeruginosa* PA14 cells exposed to a range of colistin concentrations, as determined by measuring uptake of the NPN fluorophore (10 µM) over 10 minutes (n=3, each data point represents the arithmetic mean of 20 replicate measurements; \*\*\*p<0.001, \*\*\*\*p<0.0001 relative to untreated cells). **C**, Major permeabilisation of the OM of *P. aeruginosa* PA14 cells exposed to a range of colistin concentrations, as determined by measuring release of periplasmic beta-lactamase into the culture supernatant using nitrocefin (250 µM) over 60 minutes (n=4; \*\*\*\*p<0.0001 for 4 and 10 µg ml<sup>-1</sup> colistin relative to untreated cells). **D**, Permeabilisation of the CM of *P. aeruginosa* PA14 cells exposed to a range of colistin concentrations, as determined by measuring fluorescence from PI (2.5 µM) over 4 hours (n=3 in duplicate; \*\*\*p<0.001 for 2, 4 and 10 µg ml<sup>-1</sup> colistin relative to untreated cells). **E**, Survival of *P. aeruginosa* PA14 cells exposed to ciprofloxacin (4 µg ml<sup>-1</sup>) for 4 hours, as determined by c.f.u. counts (n=3 in duplicate; \*\*\*\*p<0.0001 relative to 0 hours). Data in **B** were analysed by a one-way ANOVA with Dunnett's post-hoc test. Data in **C**, **D** were analysed by a two-way ANOVA with Dunnett's post-hoc test. Data in **E** were analysed by a two-tailed unpaired Student's *t*-test. Data are presented as the arithmetic mean, and error bars represent the standard deviation of the mean.

The first stage by which colistin is hypothesised to exert its bactericidal activity is via disruption of the outer membrane (OM) following binding of the antibiotic to lipid A and displacement of intra-LPS stabilising cation bridges. To examine if colistin damaged the OM of *P. aeruginosa* PA14, changes in OM permeability after exposure to the polymyxin drug were

measured using the gold-standard fluorescent dye *N*-phenyl-1-naphthylamine (NPN). This fluorophore is membrane-impermeant, and only emits a fluorescent signal when bound to membrane phospholipids that are exposed once the LPS monolayer in the outermost leaflet of the OM is disrupted<sup>626</sup>. The *P. aeruginosa* PA14 strain was treated with a range of clinically-relevant concentrations of colistin (0.5-10  $\mu\text{g ml}^{-1}$ ) that resembled typical peak steady-state plasma concentrations of the antibiotic observed in human patients<sup>342,344</sup>. Upon exposure to even a sub-inhibitory colistin concentration (0.5x MIC), there was an immediate and marked increase in uptake and fluorescence of the NPN dye in *P. aeruginosa* cells within 10 minutes, indicating that the polymyxin had permeabilised the OM (**Figure 3.1B**). This effect was dose-dependent, with the degree of NPN uptake and OM disruption increasing as the concentration of colistin used to treat *P. aeruginosa* PA14 was increased. Thus, it was confirmed that damage of the bacterial OM was indeed one step in colistin's mechanism of action.

It is postulated that colistin-mediated disruption of the OM of Gram-negative bacteria is a two-stage process, where minor permeabilisation of the outermost bilayer structure enables the polymyxin antibiotic to access and interact further with lipophilic domains within the OM, triggering additional membrane damage<sup>280</sup>. Since NPN is a relatively small molecule (219 Daltons), fluorescence from this dye is only indicative of low-level OM disruption, sufficient to provide the fluorophore with the capacity to bind to membrane phospholipids in the innermost leaflet of the OM. To determine whether colistin subsequently caused more extensive damage to the OM structure of *P. aeruginosa* cells, it was necessary to make use of a much larger molecule. The *P. aeruginosa* PA14 strain intrinsically produces a large beta-lactamase enzyme (AmpC) situated in the periplasmic space and bound to the OM that is approximately 35 Kilodaltons in size<sup>90,658</sup>. Hence, extracellular release of the AmpC beta-lactamase can be used as a marker for significant OM permeabilisation.

Cells of *P. aeruginosa* PA14 were again treated with the same range of colistin concentrations, and AmpC release into the supernatant was quantified using nitrocefin, a chromogenic cephalosporin substrate routinely utilised to detect the presence of beta-lactamase enzymes<sup>628</sup>. At the sub-inhibitory concentration of 0.5  $\mu\text{g ml}^{-1}$  colistin, there was no observable increase in beta-lactamase release compared to untreated bacteria, showing that the polymyxin compound did not induce large-scale OM damage (**Figure 3.1C**). However, in *P. aeruginosa* cells exposed to higher colistin concentrations (2, 4 and 10  $\mu\text{g ml}^{-1}$ ), within 30 minutes, a dose-dependent increase in AmpC release into the supernatant was detected, demonstrating that the antibiotic was extensively damaging the OM. This data revealed that colistin-mediated minor disruption of the OM (detected using NPN) in *P. aeruginosa* was followed by significant OM permeabilisation (marked by periplasmic beta-lactamase release) at inhibitory antibiotic concentrations.

Once the OM of bacteria is significantly damaged by colistin, the next step in the model of the antibiotic's bactericidal mode of action is interaction with and disruption of the cytoplasmic membrane (CM). In order to explore if after permeabilisation of the OM of *P. aeruginosa* PA14 by colistin, the polymyxin drug damaged the CM, the fluorophore propidium iodide (PI) was used<sup>659</sup>. The PI dye is normally unable to cross the bacterial surface envelope, and can only enter the cytoplasm of cells when both the OM and the CM are disrupted. In the cytoplasm, PI molecules bind to DNA at which point they become fluorescent, and thus the intensity of this fluorescent signal is a read-out for the degree of CM permeabilisation<sup>660</sup>. When exposed to a range of inhibitory colistin concentrations, *P. aeruginosa* PA14 cells displayed a dose-dependent increase in fluorescence from the PI dye after 60 minutes, indicating that the antibiotic was damaging the CM (**Figure 3.1D**).

It has previously been stated that PI fluorescence is a marker for bacterial cell death, as opposed to CM disruption. To confirm that the fluorophore specifically detected permeabilisation of the *P. aeruginosa* cell envelope and not simply bacterial killing, PA14 cells were additionally treated with 4  $\mu\text{g ml}^{-1}$  ciprofloxacin and PI fluorescence was quantified. At this concentration, the quinolone antibiotic caused significant death of the bacteria over 4 hours (more than 4-log reduction in survival), but no PI signal was observed (**Figure 3.1DE**). Therefore, fluorescence from the PI dye was a specific indicator of CM damage, rather than a generic marker of killed bacteria. Together, these data provide a time-scale for the sequential disruption of the OM and CM of *P. aeruginosa* by colistin.

### **3.3 Colistin-mediated killing of *P. aeruginosa* is bi-phasic**

In order to investigate the consequences of the permeabilisation of the OM and CM by colistin on *P. aeruginosa* cells, optical density (OD) measurements at 595 nm were obtained during 8 hours for PA14 bacteria treated with a range of clinically-relevant concentrations of the polymyxin antibiotic. Untreated bacteria exhibited an increase in OD<sub>595nm</sub> readings over time, as the bacteria were expectedly able to grow in the absence of any antibiotic pressure (**Figure 3.2A**). By contrast, in *P. aeruginosa* PA14 cells exposed to the highest colistin concentrations tested (4 and 10  $\mu\text{g ml}^{-1}$ ), there was a steady decline in OD<sub>595nm</sub> measurements after 60 minutes. A decrease in OD<sub>595nm</sub> readings is a well-established marker of bacterial lysis, and in this case indicated that rupture of the surface membranes induced by the polymyxin drug culminated in the bursting and disintegration of *P. aeruginosa* cells<sup>661</sup>. Interestingly, in PA14 bacteria treated with 2  $\mu\text{g ml}^{-1}$  colistin, only a modest drop in OD<sub>595nm</sub> measurements was detected during the first 4 hours of antibiotic exposure, before these readings began to increase to above their starting level over the subsequent 4 hours. This suggested that at lower concentrations of colistin, there may be two stages in the response of *P. aeruginosa* to the polymyxin compound.

Whilst measurements of OD<sub>595nm</sub> provided a marker for the cellular response of *P. aeruginosa* to colistin, they did not specifically quantify the changes in bacterial number during antibiotic treatment. To do this, counts of bacterial colony forming units (c.f.u.) were made over 8 hours of exposure of PA14 cells to the same range of colistin concentrations used in the lysis experiments. At all three concentrations, there was a dose-dependent decrease in cell survival after 2 hours of colistin treatment, with the polymyxin drug causing bacterial killing (**Figure 3.2B**). However, at 2 µg ml<sup>-1</sup> colistin, during the next 6 hours of antibiotic exposure, the population of *P. aeruginosa* recovered, with c.f.u. counts increasing back to the starting inoculum by 8 hours. In opposition, bacteria treated with 4 and 10 µg ml<sup>-1</sup> colistin continued to be significantly killed by colistin over the first 6 hours of the assay (4 to 6-log reduction in survival), at which point cell death stopped completely, revealing a polymyxin-tolerant *P. aeruginosa* sub-population. These bi-phasic killing kinetic results firmly demonstrated that a colistin-susceptible strain of *P. aeruginosa* was able to survive exposure to bactericidal colistin concentrations, and even begin to re-grow and recover in the presence of the antibiotic.

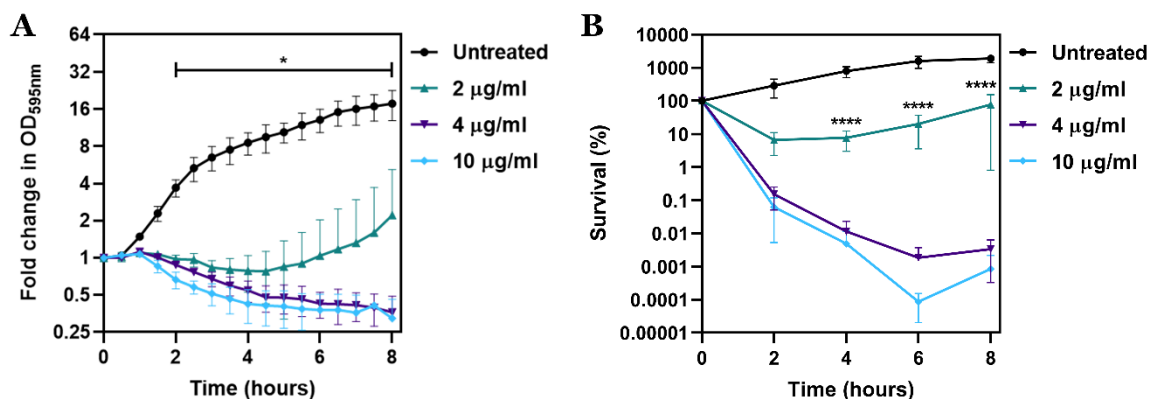


**Figure 3.2: Colistin causes bi-phasic cell lysis and killing of *P. aeruginosa*.** **A**, Lysis or growth of *P. aeruginosa* PA14 cells exposed to a range of colistin concentrations, as determined by measuring OD<sub>595nm</sub> over 8 hours (n=4; \*p<0.05 for 2, 4 and 10 µg ml<sup>-1</sup> colistin relative to untreated cells). **B**, Survival of *P. aeruginosa* PA14 cells exposed to a range of colistin concentrations, as determined by c.f.u. counts over 8 hours (n=4; \*\*\*\*p<0.0001 for 2, 4 and 10 µg ml<sup>-1</sup> colistin relative to untreated cells). Data in **A**, **B** were analysed by a two-way ANOVA with Dunnett's post-hoc test. Data are presented as the arithmetic mean, and error bars represent the standard deviation of the mean.

### 3.4 The bi-phasic killing of *P. aeruginosa* is not due to the emergence of colistin resistance

One potential explanation for how *P. aeruginosa* was able to tolerate colistin treatment and recover after an initial period of killing was that the bacteria developed spontaneous resistance to the polymyxin antibiotic, through chromosomal mutations in two-component systems causing lipid A modifications as previously reported<sup>506</sup>. Alternatively, the bi-phasic nature of the killing kinetic phenotype could also have been due to the presence of a colistin-resistant sub-population of cells within the overall *P. aeruginosa* population (as identified in *Enterobacter cloacae* and *K. pneumoniae*), with this sub-population emerging and growing during exposure to the polymyxin antibiotic, whilst the colistin-susceptible cells were killed<sup>662,663</sup>. To investigate these possibilities that *P. aeruginosa* PA14 was surviving treatment with colistin via the classic mechanisms of antibiotic resistance, bacteria were first exposed to the polymyxin compound for 8 hours, at which point surviving cells were isolated, re-grown overnight, and then treated with colistin over 8 hours for a second time. Throughout these exposures, measurements of bacterial survival were obtained, in addition to measures of the colistin MIC of the surviving *P. aeruginosa* population after each 8 hour period of antibiotic treatment.

During the first exposure to colistin, *P. aeruginosa* PA14 cells were killed initially, before almost recovering to the starting inoculum as observed in previous experiments (**Figure 3.3A**). Importantly, the colistin MIC of these *P. aeruginosa* cells that had survived the first antibiotic treatment was identical to the MIC of the bacteria at the start of the assay ( $0.5 \mu\text{g ml}^{-1}$ ), and crucially this MIC value was below the clinically-established threshold of colistin resistance (**Figure 3.3B**). Therefore, the recovery phenotype of *P. aeruginosa* PA14 during colistin exposure was not due to the acquisition of antibiotic resistance, or the emergence of a colistin-resistant bacterial sub-population.

In keeping with this, the killing kinetics of the PA14 cells that survived the initial colistin treatment was equally bi-phasic upon a second period of colistin exposure, further confirming that *P. aeruginosa* re-growth during treatment with the polymyxin drug was not related to the development of resistance (**Figure 3.3A**). It was only after this second exposure to colistin that the surviving *P. aeruginosa* PA14 population exhibited an increase in MIC to  $2 \mu\text{g ml}^{-1}$ , meeting the resistance breakpoint value, with a subsequent reduction in colistin-mediated killing detected during a third period of antibiotic treatment (**Figure 3.3AB**). In summary, while colistin non-susceptibility readily emerged in *P. aeruginosa* following multiple rounds of antibiotic treatment, the bi-phasic pattern of bacterial killing then recovery in a single colistin exposure was not due to polymyxin resistance.

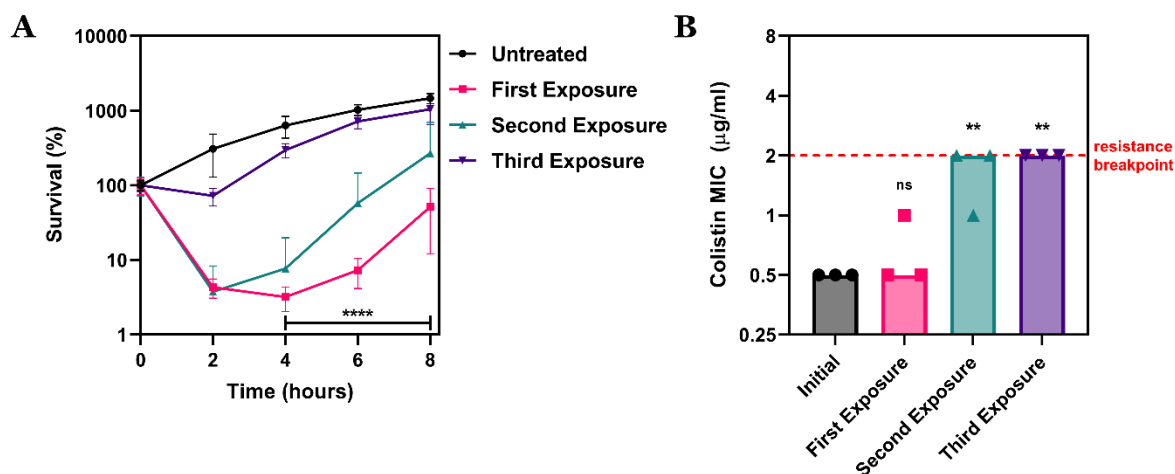


**Figure 3.3: The recovery of *P. aeruginosa* during colistin exposure is not due to colistin resistance.** **A**, Survival of *P. aeruginosa* PA14 cells exposed to colistin ( $2 \mu\text{g ml}^{-1}$ ) for 8 hours in three successive rounds, as determined by c.f.u. counts ( $n=3$  in duplicate; \*\*\*\* $p<0.0001$  for first and second colistin exposures relative to untreated cells). **B**, MIC of colistin against the *P. aeruginosa* PA14 cells that had survived each round of colistin exposure, as determined using the broth microdilution assay ( $n=3$  in triplicate, data are presented as the median value; \*\* $p<0.01$  for second and third exposures relative to initial MIC at the start of the experiment). Data in **A** were analysed by a two-way ANOVA with Dunnett's post-hoc test. Data in **B** were analysed by a one-way ANOVA with Dunnett's post-hoc test. Unless otherwise stated, data are presented as the arithmetic mean, and error bars represent the standard deviation of the mean.

### 3.5 Colistin activity is lost during exposure of *P. aeruginosa*

Having established that the ability of *P. aeruginosa* to survive colistin treatment was not due to the emergence of antibiotic resistance, in order to develop new hypotheses to explain this phenotype of bacterial recovery, the activity of colistin in the spent culture supernatant of PA14 cells exposed to the polymyxin drug was assessed using a zone of inhibition assay<sup>629</sup>. At the start of the assay, the colistin present in the culture supernatant possessed antibacterial activity, as confirmed by a dose-dependent increase in the size of the clear zone of cell growth inhibition around the well where the antibiotic was added (**Figure 3.4A**). However, following 8 hours of incubation with *P. aeruginosa* PA14, it was observed that there was a loss of colistin activity in the spent culture supernatant, with a smaller inhibition zone appearing at all three drug concentrations tested.

By measuring the size of the zones of inhibition over time during exposure of *P. aeruginosa* to colistin, the kinetics of this decrease in colistin activity were quantified. This revealed that colistin activity loss occurred rapidly, with a complete reduction in antibacterial activity at  $2 \mu\text{g ml}^{-1}$  colistin within 2 hours, and a 90% decrease in activity of colistin at  $4 \mu\text{g ml}^{-1}$  within the same time period (**Figure 3.4B**). Notably, in *P. aeruginosa* cells treated with  $10 \mu\text{g ml}^{-1}$  colistin, there was a smaller drop in the polymyxin's antibacterial activity, with the



antibiotic retaining 60% of its initial activity after 8 hours. A plausible explanation for this reduction in colistin activity over time was that the polymyxin compound was unstable, and degradation during the 37°C incubation in culture media was causing the observed decrease in the antibiotic's activity. Moreover, it has been previously discovered that colistin activity can be extensively lost in standard *in vitro* experimental conditions, largely due to significant adherence to labware materials and especially plastics, providing an additional mechanism to potentially explain the drop in polymyxin activity during *P. aeruginosa* treatment<sup>664</sup>. To explore these hypotheses, the activity of colistin was measured over 8 hours incubation in media alone, in the same plastic culture vessels used for preceding experiments, but critically in the absence of any bacteria. In this instance, there was no significant reduction in colistin activity at any concentration tested during the 8 hour assay (**Figure 3.4C**). This indicated that colistin activity loss was not due to degradation or adherence to plastic surface materials; rather, the presence of *P. aeruginosa* bacteria was essential for the loss of activity of colistin.

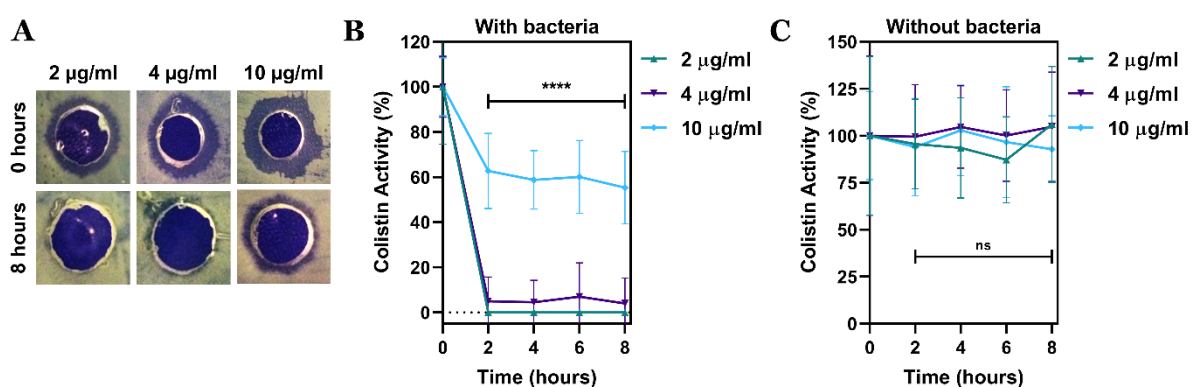


**Figure 3.4: Exposure of *P. aeruginosa* causes a loss of colistin activity.** **A**, The growth inhibitory activity of colistin in the spent culture supernatant of *P. aeruginosa* PA14 cells exposed to a range of colistin concentrations for 8 hours, as determined by a zone of inhibition assay (images are representative of 3 independent experiments). **B**, Quantification of colistin activity in the spent culture supernatant of *P. aeruginosa* PA14 cells exposed to a range of colistin concentrations, as determined by measuring the size of the zone of inhibition over 8 hours (n=4 with 4 replicate measurements of each zone; \*\*\*\*p<0.0001 for 2, 4 and 10 µg ml<sup>-1</sup> colistin relative to activity at 0 hours). **C**, Quantification of activity of a range of colistin concentrations during incubation in culture media alone, as determined by measuring the size of the zone of inhibition over 8 hours (n=4 with 4 replicate measurements of each zone; ns: p>0.05 for 2, 4 and 10 µg ml<sup>-1</sup> colistin relative to activity at 0 hours). Data in **B**, **C** were analysed by a two-way ANOVA with Dunnett's post-hoc test. Data are presented as the arithmetic mean, and error bars represent the standard deviation of the mean.

### 3.6 *P. aeruginosa* directly inactivates colistin

The loss of activity of colistin observed in the spent culture supernatant of *P. aeruginosa* cells exposed to the polymyxin drug could be explained by the fact that all of the antibiotic molecules were binding to the bacterial surface, leaving no colistin molecules in the supernatant to produce an inhibitory effect. In order to examine if this was the case, a fluorescently-labelled version of colistin was synthesised using a BoDipy tag, to enable tracking of the amount of antibiotic attached to *P. aeruginosa* cells, versus the amount present in the culture supernatant<sup>630</sup>. Successful labelling of colistin was confirmed via mass spectrometry, which identified structures corresponding to the predicted masses of both forms of the polymyxin compound (colistin A and colistin B) tagged with a single BoDipy molecule (**Figure 3.5A**).

To determine whether the tagging of colistin with the BoDipy fluorophore affected the drug's antibacterial properties, the MIC of colistin and BoDipy-colistin against *P. aeruginosa* PA14 was assessed. BoDipy-colistin exhibited a two-fold increase in MIC relative to unlabelled colistin, revealing that although there was a small, and not unexpected, reduction in antibiotic activity following fluorescent-labelling, the BoDipy-tagged version of the polymyxin compound retained significant growth inhibitory properties against *P. aeruginosa* (**Figure 3.5B**). Furthermore, there was an extremely strong and linear positive correlation when the fluorescence of BoDipy-colistin was measured across a range of antibiotic concentrations, demonstrating the suitability of using the labelled polymyxin to quantify the amount of drug in the supernatant or bound to bacterial cells (**Figure 3.5C**). As a final control, it was also established that the phenotype of a loss of antibiotic activity in the supernatant during *P. aeruginosa* exposure still occurred with BoDipy-colistin, with a complete loss of activity after 8 hours incubation seen with 2 and 4  $\mu\text{g ml}^{-1}$  BoDipy-colistin, and a partial loss seen at 10  $\mu\text{g ml}^{-1}$  BoDipy-colistin (**Figure 3.5D**).

Having verified the accuracy and sensitivity of the synthesised BoDipy-colistin as a tool for understanding why polymyxin activity was lost in the supernatant of *P. aeruginosa* cultures, the presence of the fluorescent antibiotic in the supernatant or attached to bacteria was evaluated after 8 hours incubation alongside PA14 cells. At the concentrations where a total loss of colistin activity was observed in the *P. aeruginosa* spent supernatant (2 and 4  $\mu\text{g ml}^{-1}$ ), following the 8 hour period of BoDipy-colistin exposure, the vast majority of the fluorescent antibiotic molecules (more than 85%) remained in the culture supernatant, with only a small fraction detected as being cell-bound (**Figure 3.5E**). At a concentration of 10  $\mu\text{g ml}^{-1}$  BoDipy-colistin, there was a greater degree of antibiotic attachment to bacteria; however, more than 80% of the total amount of the fluorescent polymyxin compound was still present in the spent *P. aeruginosa* supernatant, despite a 75% reduction in the antibacterial activity

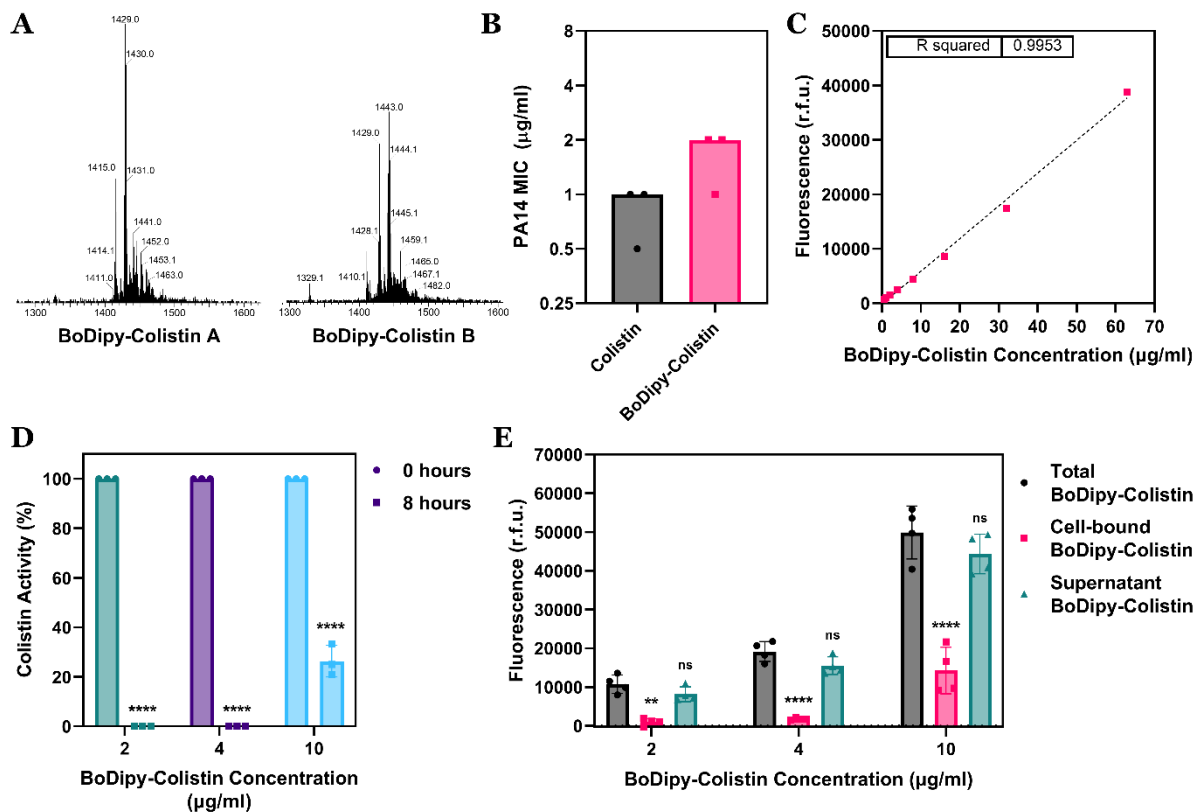


**Figure 3.5: Loss of colistin activity in the *P. aeruginosa* supernatant is not due to binding to bacterial cells.** **A**, Mass spectra of colistin A and colistin B tagged with a single BoDipy fluorophore, as obtained using time-of-flight mass spectrometry, with successful BoDipy-labelling confirmed by detection of chemical species at the expected molecular masses (1430.3 g mol<sup>-1</sup> for BoDipy-colistin A, 1443.8 g mol<sup>-1</sup> for BoDipy-colistin B). **B**, MIC of colistin and BoDipy-colistin against *P. aeruginosa* PA14 cells, as determined using the broth microdilution assay (n=3, data are presented as the median value). **C**, Standard curve of fluorescence measured across a range of BoDipy-colistin concentrations. **D**, Quantification of BoDipy-colistin activity in the spent culture supernatant of *P. aeruginosa* PA14 cells exposed to a range of BoDipy-colistin concentrations for 8 hours, as determined by a zone of inhibition assay (n=3 with 4 replicate measurements of each zone; \*\*\*\*p<0.0001 relative to activity at 0 hours). **E**, Quantity of BoDipy-colistin adhered to bacteria or present in the culture supernatant of *P. aeruginosa* PA14 cells exposed to a range of BoDipy-colistin concentrations, as determined by measuring fluorescence after 8 hours of antibiotic treatment (n=4; \*\*p<0.01, \*\*\*\*p<0.0001, ns: p>0.05 relative to total BoDipy-colistin for each drug concentration). Data in **C** were analysed by a simple linear regression. Data in **D** were analysed by a two-way ANOVA with Sidak's post-hoc test. Data in **E** were analysed by a two-way ANOVA with Dunnett's post-hoc test. Unless otherwise stated, data are presented as the arithmetic mean, and error bars represent the standard deviation of the mean.

of colistin in the supernatant at this drug concentration (**Figure 3.5DE**). Therefore, this data explicitly confirmed that the loss of colistin activity during *P. aeruginosa* treatment was not a consequence of all the antibiotic molecules binding to the bacterial surface. Moreover, this experiment provided additional evidence that there was no significant adherence of colistin molecules to the plastic culture vessels. Instead, colistin was abundantly present in the culture supernatant following exposure of PA14 cells, but the antibiotic had no antibacterial activity. It was hence concluded that *P. aeruginosa* must possess a mechanism by which it directly inactivated colistin.

### 3.7 *P. aeruginosa* inactivates colistin by releasing a non-lipid, heat-stable factor

Two hypotheses were considered for how *P. aeruginosa* cells were able to inactivate colistin – firstly, that the bacteria degraded the antibiotic via a cell-associated factor, and secondly, that *P. aeruginosa* released an extracellular compound that inactivated the polymyxin drug. To test whether *P. aeruginosa* PA14 was releasing a factor extracellularly that caused colistin activity to be lost, the bacteria were exposed to colistin for 8 hours, before the culture supernatant was recovered. Fresh doses of colistin were added to this extracted supernatant, and the ability of the supernatant alone, in the absence of any cells, to inactivate these additional polymyxin doses was assessed. With all three colistin concentrations added, exposure to just the spent culture supernatant from *P. aeruginosa* cells pre-treated with the antibiotic caused a marked decrease in the inhibitory activity of the polymyxin drug (**Figure 3.6A**). This showed that during treatment with colistin, *P. aeruginosa* PA14 released an extracellular compound into the supernatant that inactivated the antibiotic.

Previous studies have identified that extracellular factors released by bacteria can take three different forms: proteinaceous compounds (e.g. lipocalins), lipid-based molecules (e.g. monomeric phospholipids, outer membrane vesicles) or polysaccharides<sup>665–670</sup>. To further characterise the nature of the extracellular compound released by *P. aeruginosa* to inactivate colistin, and in particular examine whether this compound was a protein, the supernatant of PA14 cells pre-exposed to colistin was again extracted, and on this occasion treated with heat to denature any protein-based molecules present in the spent culture supernatant. Even after this heat treatment, the *P. aeruginosa* supernatant retained its ability to inactivate all three concentrations of colistin added to the supernatant alone, with no significant differences in the loss of polymyxin activity observed between the untreated and heat-treated supernatants (**Figure 3.6B**). Therefore, the colistin-inactivating extracellular factor released by *P. aeruginosa* was heat-stable, and highly unlikely to be proteinaceous.

Having established that *P. aeruginosa* was not inactivating colistin through a protein-based molecule, it was next investigated if the factor released into the supernatant responsible for the loss of polymyxin activity was a heat-stable lipid compound. During exposure of PA14 cells to a range of colistin concentrations, the culture supernatant was extracted, and the presence of lipids in this supernatant quantified using the highly selective, lipophilic styryl fluorescent dye FM 4-64. In the absence of any antibiotic treatment, *P. aeruginosa* constitutively shed lipid into the spent supernatant, with an 8-fold increase in fluorescence from the FM 4-64 dye detected after 8 hours (**Figure 3.6C**). This constitutive lipid release is a widely-reported phenomenon in Gram-negative bacteria, and in this case, was likely due to the shedding of outer membrane vesicles (OMVs)<sup>671,672</sup>. In bacteria exposed to a sub-inhibitory

colistin concentration ( $0.5 \mu\text{g ml}^{-1}$ ), whilst lipid release into the supernatant still increased over the 8 hour incubation, there was a reduction in the amount of lipid present in the culture supernatant compared to untreated *P. aeruginosa* cells, suggesting the colistin treatment may in fact block lipid shedding. Importantly, this was further confirmed when *P. aeruginosa* PA14 was treated with higher concentrations of colistin, with no lipid release occurring at all at any time point following exposure of bacteria to 2, 4 and  $10 \mu\text{g ml}^{-1}$  colistin. Together, these results ruled out the possibility that *P. aeruginosa* inactivated colistin through a lipid-based factor, either monomeric or in the form of OMVs, since the supernatant capable of causing a loss of polymyxin activity contained no detectable lipid.

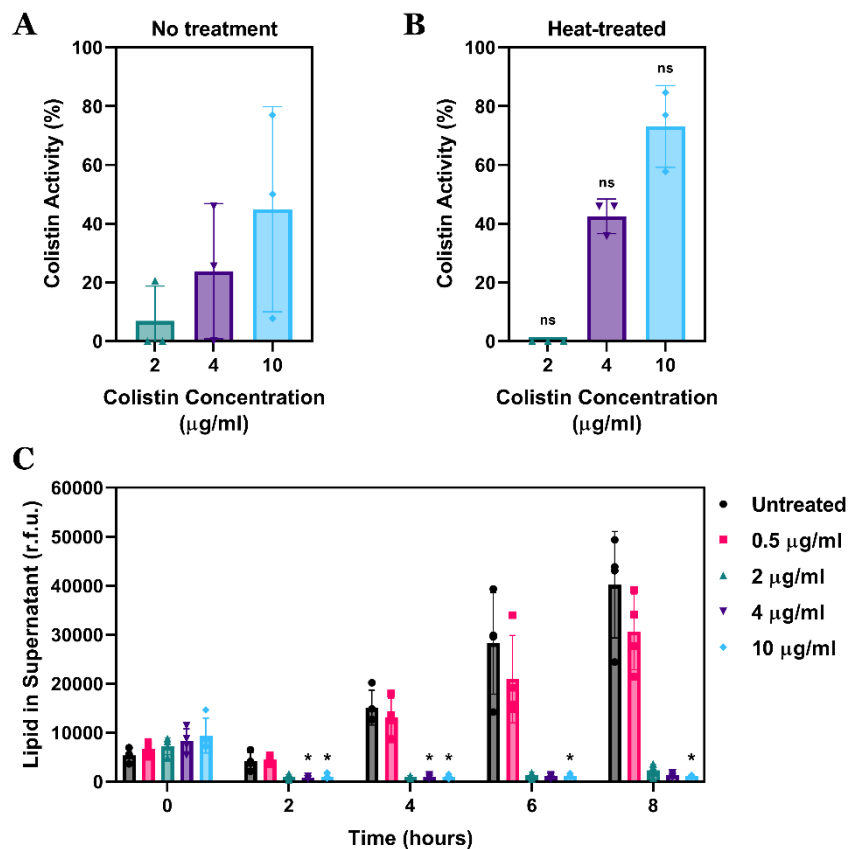


**Figure 3.6: Inactivation of colistin by *P. aeruginosa* occurs via a heat-stable and non-lipid released factor.** **A**, Quantification of activity of a range of colistin concentrations after 4 hours exposure to only the spent culture supernatant of *P. aeruginosa* PA14 cells pre-treated with  $2 \mu\text{g ml}^{-1}$  colistin for 8 hours prior to the addition of subsequent colistin doses, as determined by a zone of inhibition assay ( $n=3$  with 4 replicate measurements of each zone). **B**, Quantification of activity of a range of colistin concentrations after 4 hours exposure to the heat-treated ( $80^\circ\text{C}$ , 20 minutes) culture supernatant of *P. aeruginosa* PA14 cells pre-treated with  $2 \mu\text{g ml}^{-1}$  colistin for 8 hours prior to the addition of subsequent colistin doses, as determined by a zone of inhibition assay ( $n=3$  with 4 replicate measurements of each zone; ns:  $p>0.05$  relative to colistin activity in the untreated supernatants for each drug concentration). **C**, The concentration of lipids in the spent culture supernatant of *P. aeruginosa* PA14 cells exposed to a range of colistin concentrations, as determined by measuring fluorescence from lipophilic dye FM 4-64 over 8 hours ( $n=4$ ;  $*p<0.05$  for reduction in fluorescence relative to 0 hours for each drug concentration). Data in **B** were analysed by a two-way ANOVA with Sidak's post-hoc test. Data in **C** were analysed by two-way ANOVA with Dunnett's post-hoc test. Data are presented as the arithmetic mean, and error bars represent the standard deviation of the mean.

### 3.8 The colistin inactivator released by *P. aeruginosa* is not capsular polysaccharide

After determining that *P. aeruginosa* released a heat-stable and non-lipid factor extracellularly that caused a loss of colistin activity, it was postulated that this inactivating factor may be polysaccharide-based, since such molecules are resistant to heat treatment and have previously been implicated in extracellular inactivation of antibiotics<sup>673</sup>. In particular, Gram-negative bacteria have been found to shed polysaccharides in their capsule away from the cell surface, with these released capsular polysaccharides subsequently sequestering and inactivating polymyxin compounds in the extracellular space<sup>670</sup>. To explore whether the release of capsular polysaccharides from *P. aeruginosa* contributed to the colistin-inactivating properties of the bacterial culture supernatant, a panel of mutants obtained from the PA14 transposon library with transposon insertions in key alginate biosynthesis genes was utilised<sup>674</sup>. Alginate is the primary component and key polysaccharide of the *P. aeruginosa* capsule, and in the absence of alginate biosynthesis, the mucoid capsular biofilm structure is incorrectly formed<sup>675,676</sup>. Hence, the transposon mutants with disrupted alginate biosynthetic genes were optimal for studying the role of capsular polysaccharide in extracellular colistin inactivation.

It was first assessed whether transposon-mediated disruption of the genes involved in alginate biosynthesis caused any notable defects in growth of *P. aeruginosa* PA14 that may compromise use of the transposon mutants in experiments. All six transposon mutants deficient in biosynthesis of alginate displayed virtually identical growth kinetics to the parental PA14 wild-type (WT) strain, verifying that these mutant strains were suitable for using in ensuing assays without concerns that phenotypic effects observed were due to alterations in growth rate (**Figure 3.7A**). In addition, crucially, the MIC of colistin against the panel of transposon mutants was also identical to the colistin MIC of wild-type PA14 cells (**Figure 3.7B**). As well as being an important control for colistin-exposure experiments, this result provided the first piece of evidence that the released colistin inactivator was unlikely to be the capsular polysaccharide alginate, since the MIC of colistin would be expected to decrease in the alginate-deficient transposon mutants if this were the case. These data were further corroborated when the *P. aeruginosa* strains were exposed to 4 µg ml<sup>-1</sup> colistin for 8 hours and bacterial survival enumerated, with no significant differences in killing by the polymyxin antibiotic seen compared to the PA14 WT population (**Figure 3.7C**).

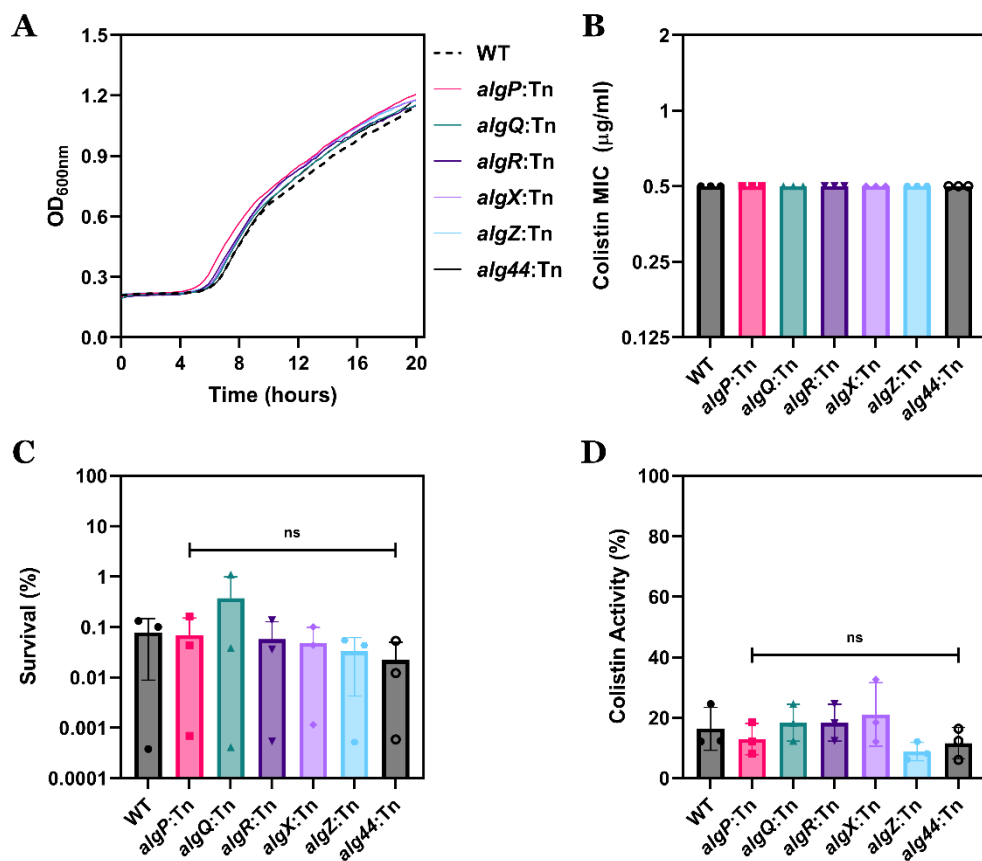


**Figure 3.7: *P. aeruginosa* does not inactivate colistin by releasing the polysaccharide alginate from its capsule.** **A**, Growth kinetics of the *P. aeruginosa* PA14 wild-type (WT) strain and six PA14 transposon insertion mutants deficient in alginate biosynthesis, as determined by measuring OD<sub>600nm</sub> over 20 hours incubation (n=3 in duplicate; error bars omitted for clarity). **B**, MIC of colistin against the *P. aeruginosa* PA14 WT strain and six PA14 alginate-deficient transposon mutants, as determined using the broth microdilution assay (n=3). **C**, Survival of the *P. aeruginosa* PA14 WT strain and six PA14 alginate-deficient transposon mutants exposed to colistin (4 µg ml<sup>-1</sup>) for 8 hours, as determined by c.f.u. counts (n=3 in duplicate; ns: p>0.05 relative to PA14 WT cells). **D**, Quantification of colistin activity in the spent culture supernatant of the *P. aeruginosa* PA14 WT strain and six PA14 alginate-deficient transposon mutants exposed to colistin (4 µg ml<sup>-1</sup>) for 8 hours, as determined by a zone of inhibition assay (n=3 with 4 replicate measurements of each zone; ns: p>0.05 relative to PA14 WT cells). Data in **C**, **D** were analysed by a one-way ANOVA with Dunnett's post-hoc test. Data are presented as the arithmetic mean, and error bars shown represent the standard deviation of the mean.

The most critical assay for testing the involvement of capsular polysaccharide in the extracellular inactivation of colistin by *P. aeruginosa* was measuring the capacity of the alginate-deficient transposon mutants to cause a loss of colistin activity in their culture supernatants relative to the parental strain. Every one of the six transposon mutants inactivated colistin to the same extent as PA14 WT cells, firmly ruling out the possibility that the polysaccharide alginate, the principal component of the *P. aeruginosa* capsule, was the factor released extracellularly by the bacteria that was responsible for the loss of polymyxin activity in the spent culture supernatant (**Figure 3.7D**).

### 3.9 *P. aeruginosa* releases LPS during exposure to colistin

Once it was identified that the extracellular factor released by *P. aeruginosa* to inactivate colistin was not capsular polysaccharide, the involvement of alternative polysaccharide-based compounds was considered. LPS is a polysaccharide molecule that is abundantly present in the cell envelope of Gram-negative bacteria, and several studies have found that this LPS can be released away from the bacterial cell surface<sup>677–679</sup>. Moreover, LPS is a heat-stable compound that is not significantly detected by the lipid-specific fluorescent dye FM 4-64, supporting the characterisation of the released colistin inactivator in previous experiments<sup>680</sup>. Finally, LPS is the molecular target of colistin, with the polymyxin drug attaching to the structure in the first step of its bactericidal mode of action, providing the potential mechanistic explanation that colistin may be inactivated in the *P. aeruginosa* culture supernatant through binding to released LPS.

To examine whether LPS was the released factor that caused the loss of colistin activity, it was first tested if LPS was present in the spent culture supernatant of *P. aeruginosa* PA14 cells during exposure to the polymyxin antibiotic. Two approaches were undertaken to specifically detect and quantify the amount of LPS released by bacteria treated with colistin. The first approach implemented was the Limulus amoebocyte lysate (LAL) assay, the highly accurate, gold-standard technique for LPS quantification which employed the blood cells extracted from the Atlantic horseshoe crab to trigger a measurable chromogenic reaction in the presence of LPS<sup>633</sup>. A reliable standard curve was generated using known concentrations of LPS, with this curve then used to interpolate the amount of LPS present in the supernatant of *P. aeruginosa* populations exposed to sub-inhibitory concentrations of colistin (**Figure 3.8A**). Untreated PA14 cells extensively shed LPS into the culture supernatant after 4 hours of incubation, with this LPS almost certainly indicative of the constitutive extracellular release of OMVs (of which LPS is a predominant constituent part) observed in the lipid release experiments (**Figure 3.8B**). Importantly, however, whilst shedding of OMVs appeared to decrease following sub-inhibitory colistin exposure, the amount of LPS released into the spent supernatant of *P. aeruginosa* treated with 0.25 or 0.5  $\mu\text{g ml}^{-1}$  for 4 hours in fact increased compared to unexposed bacteria. This data strongly implied that LPS was released by *P. aeruginosa* PA14 in response to colistin, and that this LPS shed extracellularly was not in the form of OMVs.

In order to further differentiate between colistin-induced LPS release through OMV shedding or not, the presence of LPS in the *P. aeruginosa* supernatant was analysed by the LAL assay over 8 hours exposure to a bactericidal concentration of colistin (2  $\mu\text{g ml}^{-1}$ ) at which lipid release was completely blocked. Through the course of the 8 hour incubation of PA14 cells with colistin, there was a marked and significant increase in the amount of LPS released



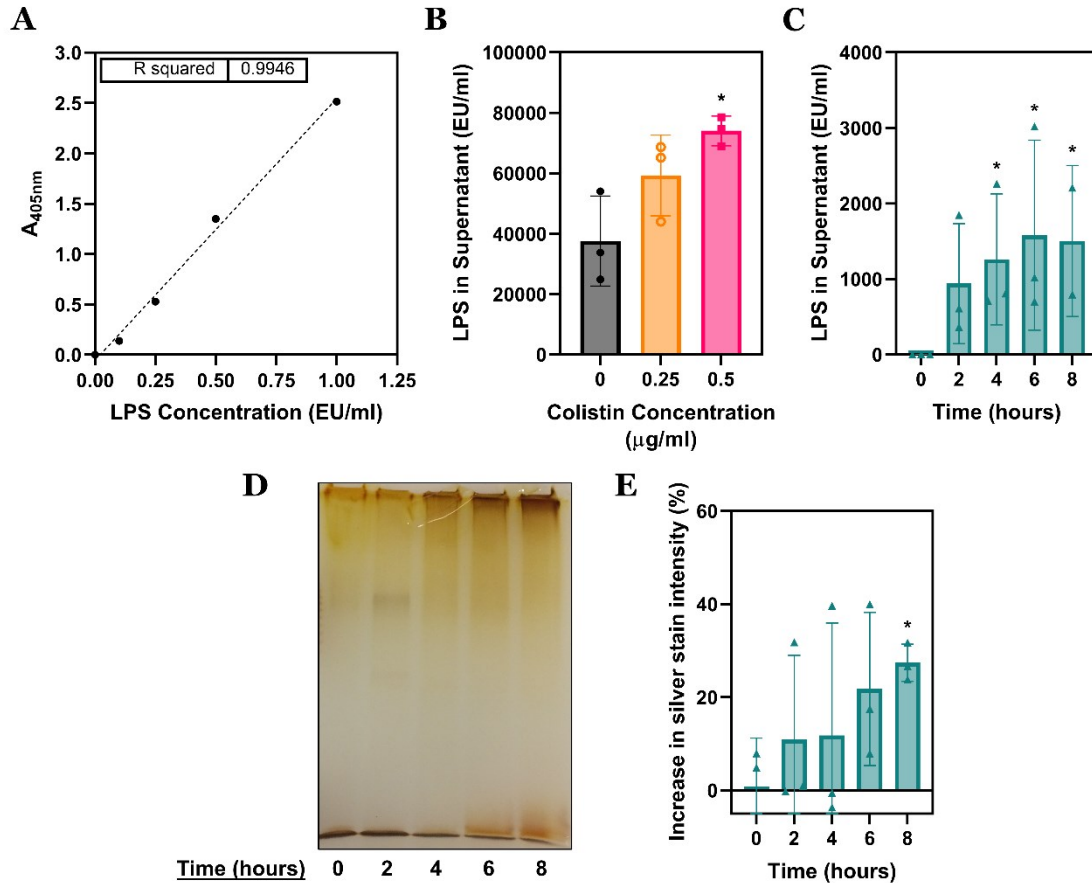


**Figure 3.8: Colistin exposure induces extracellular release of LPS from *P. aeruginosa*.** **A**, Standard curve of intensity of a chromogenic substrate molecule (detected by absorbance values at 405 nm) measured across a range of LPS concentrations for use in the Limulus amoebocyte lysate (LAL) assay. **B**, Concentration of LPS in the spent culture supernatant of *P. aeruginosa* PA14 cells exposed to a range of sub-inhibitory colistin concentrations for 4 hours, as determined using the LAL assay (n=3; \*p<0.05 relative to untreated cells). **C**, Concentration of LPS in the spent culture supernatant of *P. aeruginosa* PA14 cells exposed to a bactericidal colistin concentration (2 µg ml<sup>-1</sup>) over 8 hours, as determined using the LAL assay (n=3; \*p<0.05 relative to 0 hours). **D**, Visualisation of LPS extracted from the spent culture supernatant of *P. aeruginosa* PA14 cells exposed to 2 µg ml<sup>-1</sup> colistin over 8 hours by silver staining of an SDS-PAGE gel (image is representative of 3 independent experiments). **E**, Quantification of silver staining intensity, presented relative to intensity at 0 hours, of LPS extracted from the spent culture supernatant of *P. aeruginosa* PA14 cells exposed to 2 µg ml<sup>-1</sup> colistin over 8 hours (n=3; \*p<0.05 relative to 0 hours). Data in **A** were analysed by a simple linear regression. Data in **B**, **C** were analysed by a Kruskal-Wallis test with Dunn's post-hoc test. Data in **E** were analysed by a one-way ANOVA with Dunnett's post-hoc test. Data are presented as the arithmetic mean, and error bars represent the standard deviation of the mean.

into the culture supernatant, confirming that treatment with the polymyxin antibiotic triggered *P. aeruginosa* to shed non-OMV-associated LPS molecules extracellularly (**Figure 3.8C**). This key finding was subsequently solidified by performing an LPS extraction protocol on the spent supernatants collected from *P. aeruginosa* PA14 bacteria during 8 hours of colistin exposure, and detecting the presence of LPS through a second routinely-used and sensitive approach – silver staining<sup>635</sup>. Extracted LPS visualised by silver staining of an SDS-

PAGE gel has often been shown to appear as a long smear, with the multimeric nature of LPS and the varying number of repeating units in its O-antigen domain producing a ladderlike band pattern<sup>681,682</sup>. By this silver staining method, it was discovered that there was an increase over time of extracellular LPS released into the culture supernatant by *P. aeruginosa* cells treated with 2 µg ml<sup>-1</sup> colistin for 8 hours (**Figure 3.8D**). Quantification of the band intensity of this extracted LPS visualised by silver staining through densitometry clearly demonstrated that *P. aeruginosa* PA14 responded to exposure with bactericidal concentrations of colistin by shedding LPS, raising the distinct prospect that LPS was the released polymyxin inactivating factor (**Figure 3.8E**).

### **3.10 Extracellular LPS reduces colistin activity and promotes survival of *P. aeruginosa***

The fact that LPS was released by *P. aeruginosa* cells in response to colistin treatment did not necessarily definitively implicate the polysaccharide compound in the extracellular inactivation of colistin. In order to establish whether LPS was indeed responsible for the loss of colistin activity in the culture supernatant of PA14 bacteria exposed to the polymyxin drug, purified extracellular LPS obtained from an *E. coli* strain was incubated alongside 2 µg ml<sup>-1</sup> colistin for 4 hours, before the residual growth inhibitory activity of the antibiotic was assessed. A range of concentrations of exogenous LPS was used for this experiment, with the concentrations chosen closely resembling physiologically-relevant LPS concentrations that have been found to be released into bacterial cultures during cell growth<sup>683</sup>. Incubation of colistin with just purified *E. coli* LPS caused a dose-dependent decrease in activity of the polymyxin compound after 4 hours, with a total loss of colistin activity when the antibiotic was in the presence of 20 µg ml<sup>-1</sup> LPS (**Figure 3.9A**).

To eliminate the possibility that these colistin-inactivating properties were restricted only to *E. coli* LPS, the assay was repeated using extracellular LPS isolated from a *Salmonella* species. As previously, incubating colistin along with the purified *Salmonella* LPS again resulted in a dose-dependent reduction in the antibiotic's growth inhibitory effects, with no colistin activity retained at all with the highest LPS concentration tested (**Figure 3.9B**). Having previously identified that the colistin-inactivating factor released by *P. aeruginosa* was insensitive to heat, to provide additional evidence that LPS was this extracellular factor, it was important to verify that the polysaccharide molecule maintained its ability to inactivate colistin even after heat treatment. In spite of being treated with heat, both *E. coli* and *Salmonella* purified LPS continued to induce a decrease in colistin activity in a dose-dependent manner following 4 hours incubation (**Figure 3.9C**). Together, these experiments proved that LPS was a heat-stable compound that inactivated colistin extracellularly, and was thus highly likely to be the colistin inactivator released by *P. aeruginosa*.

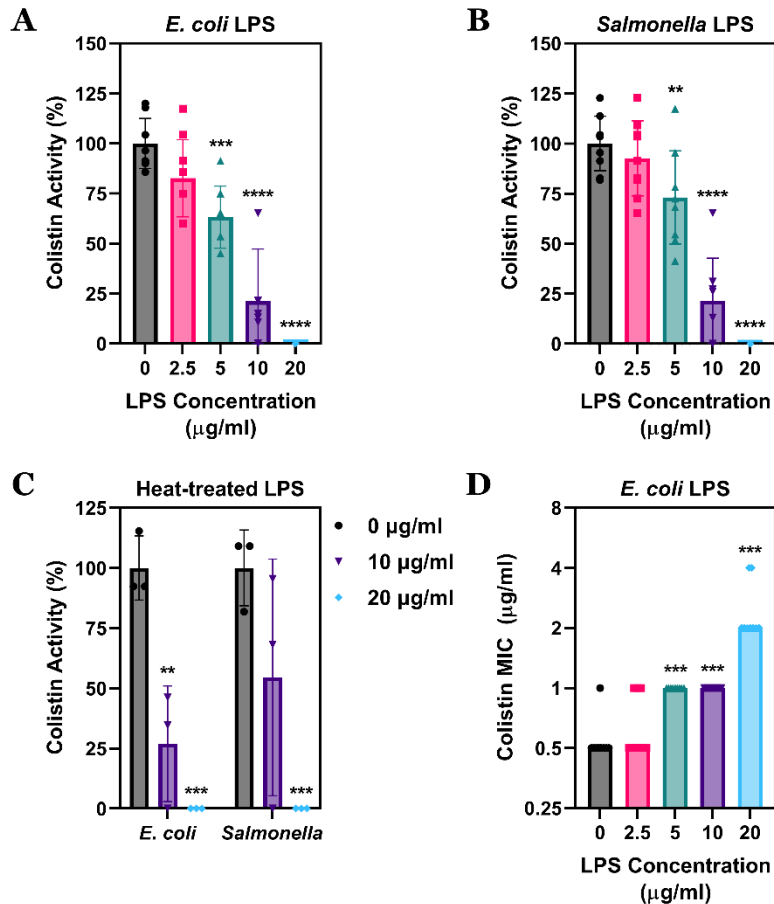


**Figure 3.9: The presence of extracellular LPS inactivates colistin and increases the ability of *P. aeruginosa* to tolerate the polymyxin.** **A**, Quantification of activity of colistin ( $2 \mu\text{g ml}^{-1}$ ) after 4 hours incubation with a range of concentrations of extracellular purified *E. coli* LPS, as determined by a zone of inhibition assay (n=3 in triplicate with 4 replicate measurements of each zone; \*\*\*p<0.001, \*\*\*\*p<0.0001 compared to no LPS). **B**, Quantification of activity of colistin ( $2 \mu\text{g ml}^{-1}$ ) after 4 hours incubation with a range of concentrations of extracellular purified *Salmonella* LPS, as determined by a zone of inhibition assay (n=3 in triplicate with 4 replicate measurements of each zone; \*\*p<0.01, \*\*\*\*p<0.0001 compared to no LPS). **C**, Quantification of activity of colistin ( $2 \mu\text{g ml}^{-1}$ ) after 4 hours incubation with a range of concentrations of extracellular purified *E. coli* and *Salmonella* LPS that had undergone a heat pre-treatment ( $80^{\circ}\text{C}$ , 20 minutes), as determined by a zone of inhibition assay (n=3 with 4 replicate measurements of each zone; \*\*p<0.01, \*\*\*p<0.001 compared to no LPS). **D**, MIC of colistin against *P. aeruginosa* PA14 cells in the presence of a range of concentrations of extracellular purified *E. coli* LPS, as determined using the broth microdilution assay (n=3 in triplicate, data are presented as the median value; \*\*\*p<0.001 compared to no LPS). Data in **A-B**, **D** were analysed by a one-way ANOVA with Dunnett's post-hoc test. Data in **C** were analysed by a two-way ANOVA with Dunnett's post-hoc test. Unless otherwise stated, data are presented as the arithmetic mean, and error bars represent the standard deviation of the mean.

The discovery that LPS was the factor released by *P. aeruginosa* that caused colistin activity to be lost in the culture supernatant during polymyxin treatment led to it being hypothesised that it was this inactivation of colistin that enabled the bacteria to survive and begin re-growing when exposed to the antibiotic. To explore if extracellular LPS that was known to inactivate colistin affected the ability of *P. aeruginosa* to tolerate exposure to the

polymyxin, the MIC of colistin against PA14 cells was measured in the presence of a range of concentrations of exogenous purified *E. coli* LPS. As the concentration of extracellular LPS in the culture media was increased, there was a simultaneous and dose-dependent rise in the colistin MIC of *P. aeruginosa* bacteria, with the MIC value four-fold higher when 20  $\mu\text{g ml}^{-1}$  LPS was present relative to when exogenous LPS was absent (**Figure 3.9D**). Hence, it was apparent that the extracellular LPS released by *P. aeruginosa* in response to colistin not only inactivated the antibiotic, but also enhanced the ability of PA14 bacteria to survive and grow at otherwise bactericidal polymyxin concentrations. In summary, the shedding of LPS appeared to be a protective defence mechanism by *P. aeruginosa* to tolerate colistin, offering a credible explanation for both the bi-phasic killing kinetics of the pathogen by the polymyxin antibiotic, as well as for clinical colistin treatment failure.

### **3.11 Colistin-resistant *P. aeruginosa* cannot inactivate colistin**

For further confirmation that LPS was the factor released by *P. aeruginosa* PA14 cells to reduce colistin activity extracellularly and confer polymyxin tolerance, it was proposed that the colistin-inactivating properties of a *P. aeruginosa* strain that was resistant to the antibiotic should be explored. Since the only known mechanism of colistin resistance in *P. aeruginosa* is via chemical modifications of LPS that diminish its electrostatic affinity with polymyxin molecules, a reduction in the ability of colistin-resistant PA14 cells to inactivate colistin relative to wild-type, colistin-susceptible PA14 bacteria would offer additional conclusive evidence that LPS was the colistin inactivator<sup>441</sup>. A colistin-resistant *P. aeruginosa* PA14 strain was generated by exposing the bacterial population to the polymyxin antibiotic (4  $\mu\text{g ml}^{-1}$ ) for 24 hours, plating the surviving population onto solid culture media, and growing a colony that emerged overnight. The capacity of both this polymyxin-resistant PA14 cell population and the parental PA14 wild-type population to inactivate a range of colistin concentrations following 2 hours of antibiotic treatment was then tested.

Colistin-susceptible *P. aeruginosa* bacteria rapidly and efficiently caused a loss of colistin activity in the spent culture supernatant across the range of polymyxin concentrations as previously observed, with a near-complete inactivation of the antibiotic at 2 and 4  $\mu\text{g ml}^{-1}$  colistin after 2 hours (**Figure 3.10A**). In stark contrast, colistin-resistant PA14 cells displayed almost no ability to inactivate colistin extracellularly, with more than 75% of polymyxin activity retained in the spent supernatant following exposure of the bacteria to 2 or 4  $\mu\text{g ml}^{-1}$  colistin (**Figure 3.10B**). Therefore, the development of resistance to colistin in *P. aeruginosa* was associated with a reduced propensity to inactivate the antibiotic via the released factor. With the only characterised method of colistin non-susceptibility of *P. aeruginosa* strains being LPS modifications, this data offered a convincing indication that LPS was the molecule released by the bacteria to bind and inactivate colistin extracellularly.

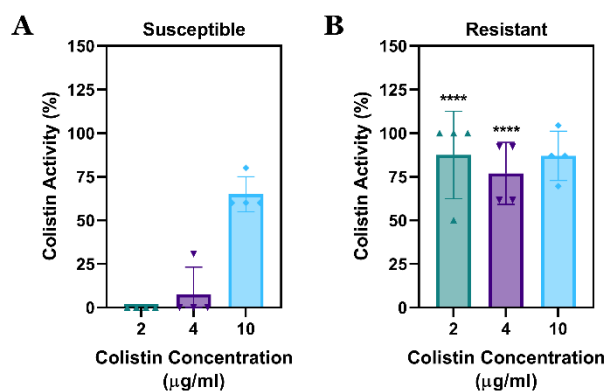


**Figure 3.10: Colistin-inactivating properties are lost in colistin-resistant *P. aeruginosa*.** **A, B**, Colistin activity in the spent supernatants of colistin-susceptible (**A**) and colistin-resistant (**B**) *P. aeruginosa* PA14 cells after 2 hours exposure to a range of polymyxin concentrations, as determined by a zone of inhibition assay (n=4; \*\*\*\*p<0.0001 relative to colistin activity with the susceptible strain). Data were analysed by a two-way ANOVA with Sidak's post-hoc test. Data are presented as the arithmetic mean, and error bars represent the standard deviation of the mean.

### 3.12 The ability to inactivate colistin is conserved across Gram-negative pathogens

The finding that extracellular LPS purified from several different Gram-negative organisms, including *Salmonella* species and *E. coli*, was able to inactivate colistin suggested that the mechanism of tolerance to the polymyxin antibiotic in *P. aeruginosa* PA14 through the release of LPS may not be solely restricted to this laboratory reference strain. In order to investigate if this colistin-inactivating phenotype was seen in other *P. aeruginosa* strains and across diverse, important Gram-negative pathogens, a panel of clinical isolates obtained from infected human patients was exposed to 4 µg ml<sup>-1</sup> colistin for 8 hours, before the residual activity of the polymyxin drug in the spent bacterial culture supernatant was calculated. The clinical isolate panel consisted of *P. aeruginosa*, *K. pneumoniae*, *E. coli* and *A. baumannii* strains from a range of sites, with these species chosen because colistin is commonly used as a last-resort treatment option to combat infections from these multi-drug resistant pathogens.

In the culture supernatants of all eight clinical strains treated with colistin, there was a significant decrease in the inhibitory activity of the antibiotic after 8 hours (**Figure 3.11**). Two strains (*P. aeruginosa* A23 and *K. pneumoniae* KPC) almost completely inactivated colistin, and there was a greater than 50% loss of polymyxin activity across the other isolates compared to the activity of colistin at the start of the assay. Notably, there were no clear patterns in the ability of any one of the bacterial species tested to cause extracellular colistin inactivation to a greater extent than others, with all organisms displaying a similar propensity to interfere with the polymyxin's antibacterial effects. Therefore, the phenotype of colistin inactivation was not only observed in *P. aeruginosa* PA14, but rather conserved throughout genetically-distinct Gram-negative organisms, implying that the release of LPS to tolerate colistin exposure may be a common mechanism by which bacteria survive the antibiotic.

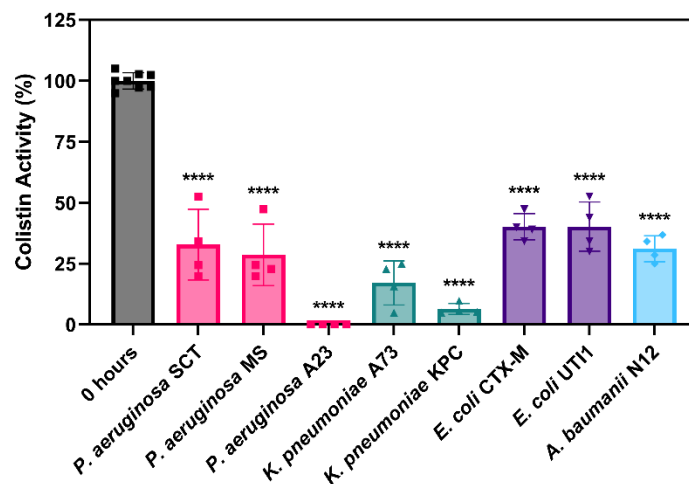


**Figure 3.11: Colistin is inactivated in the supernatant across a diverse panel of Gram-negative pathogens.** Quantification of colistin activity in the spent culture supernatant of three *P. aeruginosa* clinical isolates, two *K. pneumoniae* clinical isolates, two *E. coli* clinical isolates and an *A. baumannii* clinical isolate before and after exposure to colistin ( $4 \mu\text{g ml}^{-1}$ ) for 8 hours, as determined by a zone of inhibition assay ( $n=4$  with 4 replicate measurements of each zone; \*\*\*\* $p<0.0001$  relative to activity at 0 hours). Data were analysed by a one-way ANOVA with Dunnett's post-hoc test. Data are presented as the arithmetic mean, and error bars represent the standard deviation of the mean.

### 3.13 Colistin-induced LPS release from *P. aeruginosa* requires *de novo* LPS biosynthesis

Having determined that *P. aeruginosa* released LPS to inactivate colistin extracellularly, enabling the bacteria to survive polymyxin exposure, it was next decided to investigate the mechanism by which the pathogen was able to shed LPS from its cell surface, and in particular the biological processes upon which LPS release was dependent. The first hypothesis examined was that LPS shedding in response to colistin required active LPS biosynthesis, and to test this suggestion, small molecule inhibitors of the LPS biosynthetic pathway in *P. aeruginosa* were utilised as a combination treatment of PA14 cells alongside colistin. To minimise the possibility that any phenotypes observed were due to off-target effects, two LPS biosynthesis inhibitors were chosen that targeted distinct steps during the synthesis of LPS: CHIR-090, a tight-binding inhibitor of the LpxC enzyme that catalyses the first committed stage of lipid A biosynthesis, and cerulenin, a naturally-occurring compound that blocks the synthesis of fatty acids, and thus that of LPS<sup>181,184,684,685</sup>.

The biosynthesis of LPS is an essential process in *P. aeruginosa*, which when fully inhibited, leads to a complete loss of bacterial viability and cell death<sup>132,134</sup>. Hence, in order to employ CHIR-090 and cerulenin in assays to establish the mechanism of LPS release following colistin exposure, both inhibitors had to be used at sub-inhibitory concentrations that were

not lethal to *P. aeruginosa* PA14 cells. To identify appropriate sub-inhibitory doses for each LPS biosynthesis inhibitor, the growth kinetics of *P. aeruginosa* bacteria were measured across a range of CHIR-090 and cerulenin concentrations. It was found that at concentrations of 0.125  $\mu\text{g ml}^{-1}$  CHIR-090 and 32  $\mu\text{g ml}^{-1}$  cerulenin, these small molecule inhibitors caused a small defect in growth of the PA14 population relative to untreated cells, but did not fully block bacterial growth (**Figure 3.12AB**). Importantly, the modest reduction in *P. aeruginosa* growth in the presence of CHIR-090/cerulenin indicated that the compounds were partially inhibiting the essential LPS biosynthetic pathway. However, the fact that bacterial growth was not fully prevented by either inhibitor served as a crucial control, ensuring that growth arrest could not be the reason for the effects of CHIR-090 and cerulenin in future experiments.

To assess whether colistin-induced LPS release by *P. aeruginosa* in response to colistin was related to *de novo* biosynthesis of LPS, PA14 bacteria were exposed for 4 hours to colistin (4  $\mu\text{g ml}^{-1}$ ), either alone or in combination with the previously identified sub-inhibitory concentrations of CHIR-090/cerulenin, before the concentration of LPS shed into the culture supernatant was quantified by the LAL assay. To begin with, it was confirmed that none of the three antimicrobial agents (colistin, CHIR-090 or cerulenin) interfered significantly with the ability of the LAL assay to accurately detect the amount of LPS present in a sample. As has been demonstrated in other studies, colistin caused a slight reduction in  $A_{405\text{nm}}$  readings across a range of known LPS concentrations extracted from bacterial supernatants; however, there remained a clear, strong and linear positive correlation (R-squared value of 0.95) between concentrations of LPS and  $A_{405\text{nm}}$  values, showing that valid calculations of LPS levels released extracellularly from *P. aeruginosa* could be made, even in the presence of colistin (**Figure 3.12C**)<sup>686</sup>. In addition, neither CHIR-090 nor cerulenin had any effect on the  $A_{405\text{nm}}$  reading at a known LPS concentration, verifying that the LPS biosynthesis inhibitors were compatible for use with the LAL assay.

Quantifying the amount of LPS shed by *P. aeruginosa* cells into the spent culture supernatant after 4 hours exposure to colistin in combination with CHIR-090/cerulenin revealed that there was a drastic drop in LPS release when LPS biosynthesis was inhibited, relative to bacteria treated with colistin alone (**Figure 3.12D**). With PA14 cells exposed to colistin along with a sub-inhibitory concentration of cerulenin, there was virtually no LPS detectable at all in the bacterial supernatant following 4 hours incubation. Therefore, shedding of LPS by *P. aeruginosa* during colistin treatment appeared to be dependent on active biosynthesis of LPS.

To corroborate this data, extracted LPS from the supernatant of *P. aeruginosa* PA14 bacteria exposed to colistin with and without CHIR-090/cerulenin was run on an SDS-PAGE gel and silver stained (**Figure 3.12E**). The reduction in LPS release triggered by colistin from

cells treated with either LPS biosynthesis inhibitor was evidently visible, and densitometric quantification substantiated the discovery that the colistin-induced shedding of LPS by *P. aeruginosa* required *de novo* synthesis of LPS (Figure 3.12F).

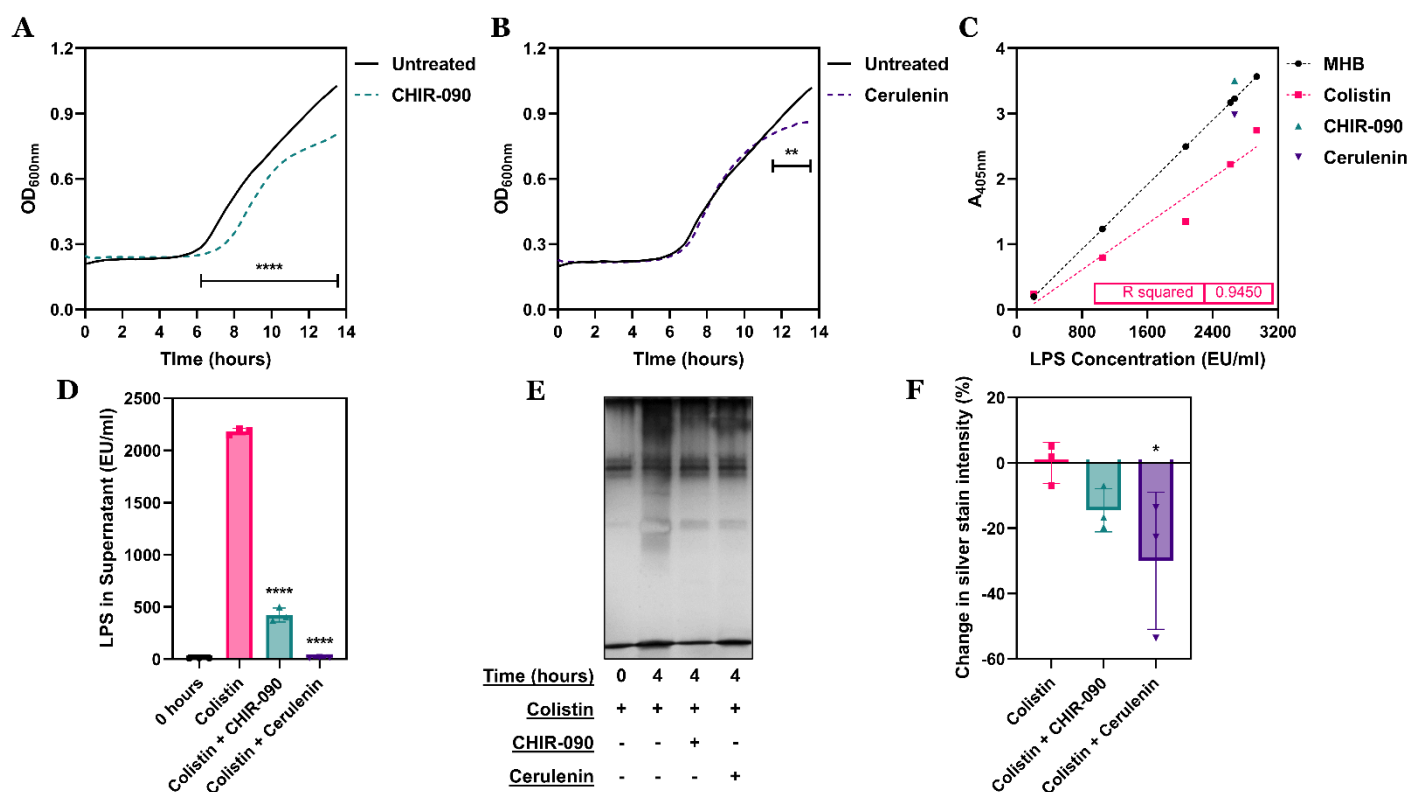


**Figure 3.12: LPS release from *P. aeruginosa* in response to colistin is dependent on active LPS biosynthesis.** **A**, Growth kinetics of *P. aeruginosa* PA14 cells during exposure, or not, to the LpxC inhibitor CHIR-090 (0.125  $\mu\text{g ml}^{-1}$ ), as determined by measuring OD<sub>600nm</sub> over 14 hours incubation (n=3; \*\*\*\*p<0.0001 relative to untreated cells, error bars omitted for clarity). **B**, Growth kinetics of *P. aeruginosa* PA14 cells during exposure, or not, to the fatty acid synthesis inhibitor cerulenin (32  $\mu\text{g ml}^{-1}$ ), as determined by measuring OD<sub>600nm</sub> over 14 hours incubation (n=3; \*\*p<0.01 relative to untreated cells, error bars omitted for clarity). **C**, Standard curve of intensity of the chromogenic substrate molecule used in the LAL assay (detected by A<sub>405nm</sub> readings) across a range of known LPS concentrations, in MHB culture media alone or in the presence of colistin (4  $\mu\text{g ml}^{-1}$ ), CHIR-090 (0.125  $\mu\text{g ml}^{-1}$ ) and cerulenin (32  $\mu\text{g ml}^{-1}$ ). **D**, Concentration of LPS in the spent culture supernatant of *P. aeruginosa* PA14 cells exposed for 4 hours to colistin (4  $\mu\text{g ml}^{-1}$ ) alone, or colistin in combination with CHIR-090 (0.125  $\mu\text{g ml}^{-1}$ ) and cerulenin (32  $\mu\text{g ml}^{-1}$ ), as determined using the LAL assay (n=3; \*\*\*\*p<0.0001 relative to bacteria treated with colistin alone). **E**, Visualisation of LPS extracted from the spent culture supernatant of *P. aeruginosa* PA14 cells exposed for 4 hours to colistin (4  $\mu\text{g ml}^{-1}$ ) alone, or colistin in combination with CHIR-090 (0.125  $\mu\text{g ml}^{-1}$ ) and cerulenin (32  $\mu\text{g ml}^{-1}$ ), by silver staining of an SDS-PAGE gel (image is representative of 3 independent experiments). **F**, Quantification of silver staining intensity of LPS extracted from the spent culture supernatant of *P. aeruginosa* PA14 cells exposed for 4 hours to colistin (4  $\mu\text{g ml}^{-1}$ ) alone, or colistin in combination with CHIR-090 (0.125  $\mu\text{g ml}^{-1}$ ) and cerulenin (32  $\mu\text{g ml}^{-1}$ ), presented relative to intensity of cells exposed only to colistin (n=3; \*p<0.05 relative to bacteria treated with colistin alone). Data in **A**, **B** were analysed by a two-way ANOVA with Sidak's post-hoc test. Data in **C** were analysed by a simple linear regression. Data in **D** were analysed by a one-way ANOVA with Dunnett's post-hoc test. Data in **F** were analysed by a Kruskal-Wallis test with Dunn's post-hoc test. Data are presented as the arithmetic mean, and error bars shown represent the standard deviation of the mean.



### 3.14 Inactivation of colistin by *P. aeruginosa* is dependent on active LPS biosynthesis

Since the LPS biosynthesis inhibitors CHIR-090 and cerulenin reduced the shedding of LPS into the supernatant by PA14 cells treated with colistin, and this released LPS had been identified to inactivate the polymyxin drug extracellularly, it was postulated that inhibition of LPS biosynthesis would decrease the capacity of *P. aeruginosa* bacteria to cause a drop in colistin's antibacterial activity. In order to experimentally test this hypothesis, the residual inhibitory activity of colistin in the spent culture supernatant of *P. aeruginosa* PA14 exposed over 8 hours to the polymyxin compound in combination with sub-inhibitory concentrations of CHIR-090/cerulenin was evaluated.

As previously demonstrated, *P. aeruginosa* cells markedly inactivated colistin at a concentration of 4  $\mu\text{g ml}^{-1}$  within 2 hours of polymyxin treatment (**Figure 3.13A**). However, in the presence of CHIR-090, which had the effect of decreasing LPS shedding in response to colistin, there was a significant reduction in the extent to which the antibiotic was inactivated, and colistin maintained more than 50% of its original growth inhibitory activity in the culture supernatant between 2 and 6 hours of incubation with PA14 bacteria. Similar findings were obtained when the *P. aeruginosa* population was exposed to 10  $\mu\text{g ml}^{-1}$  colistin with and without CHIR-090, where the polymyxin compound retained approximately 25% more activity during co-treatment with the LPS biosynthesis inhibitor, compared to during treatment with colistin alone (**Figure 3.13B**).

Analogously, the colistin-inactivating properties of *P. aeruginosa* PA14 were severely mitigated when cerulenin was present alongside the polymyxin antibiotic (4 or 10  $\mu\text{g ml}^{-1}$ ) throughout the 8 hour incubation. Colistin's residual activity was 50% higher at the end of the assay when cerulenin was added to bacteria exposed to the polymyxin at 4  $\mu\text{g ml}^{-1}$  relative to when the fatty acid/LPS synthesis inhibitor was absent, and more than 25% higher at 10  $\mu\text{g ml}^{-1}$  colistin (**Figure 3.13CD**). Together, these data showed that the ability of *P. aeruginosa* to inactivate colistin extracellularly required the active biological process of *de novo* LPS biosynthesis. Moreover, because it had been illustrated that both CHIR-090 and cerulenin reduced colistin-triggered LPS shedding into the supernatant, the fact that these inhibitors of LPS synthesis also diminished colistin inactivation by *P. aeruginosa* was yet further proof that LPS was indeed the released factor responsible for colistin activity being lost in the extracellular space.

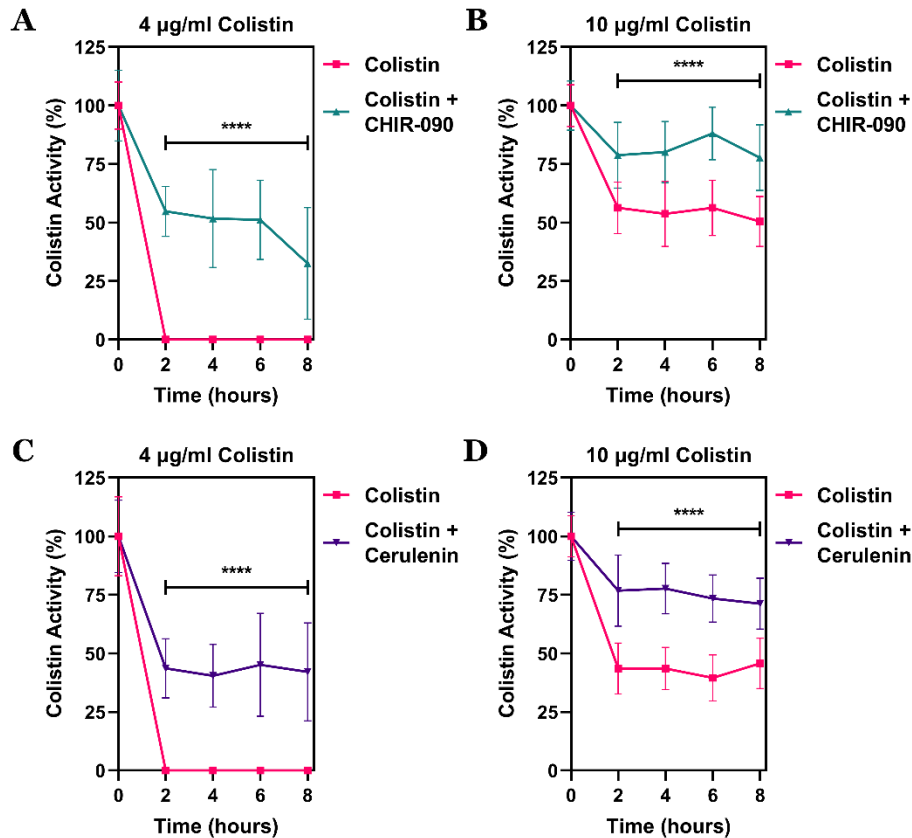


**Figure 3.13: The ability of *P. aeruginosa* to inactivate colistin extracellularly requires *de novo* LPS biosynthesis.** **A, B**, Quantification of colistin activity in the spent culture supernatant of *P. aeruginosa* PA14 cells exposed to **(A)** 4 µg ml<sup>-1</sup> or **(B)** 10 µg ml<sup>-1</sup> colistin alone, or in combination with CHIR-090 (0.125 µg ml<sup>-1</sup>), as determined by measuring the size of the zone of inhibition over 8 hours (n=4 with 4 replicate measurements of each zone; \*\*\*\*p<0.0001 relative to bacteria exposed to colistin alone). **C, D**, Quantification of colistin activity in the spent culture supernatant of *P. aeruginosa* PA14 cells exposed to **(C)** 4 µg ml<sup>-1</sup> or **(D)** 10 µg ml<sup>-1</sup> colistin alone, or in combination with cerulenin (32 µg ml<sup>-1</sup>), as determined by measuring the size of the zone of inhibition over 8 hours (n=4 with 4 replicate measurements of each zone; \*\*\*\*p<0.0001 relative to bacteria exposed to colistin alone). Data in **A-D** were analysed by a two-way ANOVA with Sidak's post-hoc test. Data are presented as the arithmetic mean, and error bars represent the standard deviation of the mean.

### 3.15 The bactericidal activity of colistin requires *de novo* LPS biosynthesis

Due to the protective effects of extracellular LPS released from bacteria on the survival of *P. aeruginosa* exposed to colistin, combined with the discovery that blocking LPS biosynthesis reduces LPS shedding and increased the activity of colistin in the supernatant, it was proposed that inhibiting the synthesis of LPS with CHIR-090/cerulenin could enhance polymyxin-mediated killing of PA14 bacteria. This theory was assessed by treating *P. aeruginosa* cells with a range of therapeutically-relevant colistin concentrations (2, 4 and 10 µg ml<sup>-1</sup>), either alone or alongside sub-inhibitory concentrations of CHIR-090 and cerulenin

that blocked LPS release, with bacterial survival measured during 8 hours incubation by enumeration of colony counts. Firstly, it was verified that the concentration of the LPS biosynthesis inhibition CHIR-090 used ( $0.125 \mu\text{g ml}^{-1}$ ) did not affect PA14 bacterial growth, with the CHIR-090-exposed *P. aeruginosa* population exhibiting identical growth kinetics over 8 hours to untreated cells (**Figure 3.14A**).

Next, the impact of inhibiting LPS biosynthesis with CHIR-090 on the viability of *P. aeruginosa* cells treated with  $2 \mu\text{g ml}^{-1}$  colistin was calculated. Interestingly, and in a strikingly direct contradiction to the original hypothesis, exposing a PA14 population to colistin in combination with CHIR-090 did not increase the killing of bacteria by the polymyxin antibiotic, but rather blocked the bactericidal effects of colistin completely. Whilst there was an initial 10-fold reduction in *P. aeruginosa* survival in cells incubated with  $2 \mu\text{g ml}^{-1}$  colistin alone after 2 hours (before the subsequent recovery of the population characterized earlier), when a sub-inhibitory concentration of CHIR-090 was present, no reduction in the viability of PA14 bacteria was observed at all, even following 8 hours of colistin exposure (**Figure 3.14A**). This phenotype of diminished polymyxin-mediated killing of *P. aeruginosa* if *de novo* LPS biosynthesis was blocked became notably more apparent when CHIR-090 was used in the treatment of PA14 cells along with  $4 \mu\text{g ml}^{-1}$  colistin, which alone reduced bacterial counts by more than 5-logs after 4 hours, but which was unable to kill bacteria by even 1-log in the presence of the LPS synthesis inhibitor (**Figure 3.14B**). Thus, the ability of colistin to kill *P. aeruginosa* appeared to be dependent on the active biosynthesis of LPS. This requirement of *de novo* LPS biosynthesis for the polymyxin's bactericidal properties was partially overcome at the highest colistin concentration tested ( $10 \mu\text{g ml}^{-1}$ ); however, there remained following 4 hours of treatment a 5-log difference between the survival of PA14 cells exposed to colistin alone and those exposed to both colistin and CHIR-090 (**Figure 3.14C**).

To confirm this fundamental finding that colistin relied on active LPS biosynthesis for exerting its bactericidal effects against *P. aeruginosa*, these time-kill experiments were repeated using the fatty acid/LPS synthesis inhibitor cerulenin, as opposed to CHIR-090. Again, cerulenin was used in these assays at a sub-inhibitory concentration ( $32 \mu\text{g ml}^{-1}$ ), which had a minimal impact on the rate of growth of a PA14 cell population compared to untreated bacteria (**Figure 3.14D**). Across the range of colistin concentrations investigated, in all cases exposure of *P. aeruginosa* PA14 to the polymyxin antibiotic in combination with cerulenin caused a significant reduction in the killing kinetics of bacteria, relative to when treated with colistin alone (**Figure 3.14DEF**). This consequence of inhibiting LPS biosynthesis was most evident at 4 and  $10 \mu\text{g ml}^{-1}$  colistin, where the reduction in bacterial killing by the polymyxin when cerulenin was present was 4- and 3-logs respectively after 4 hours. Hence, it was concluded that the killing of *P. aeruginosa* by colistin required active LPS biosynthesis.

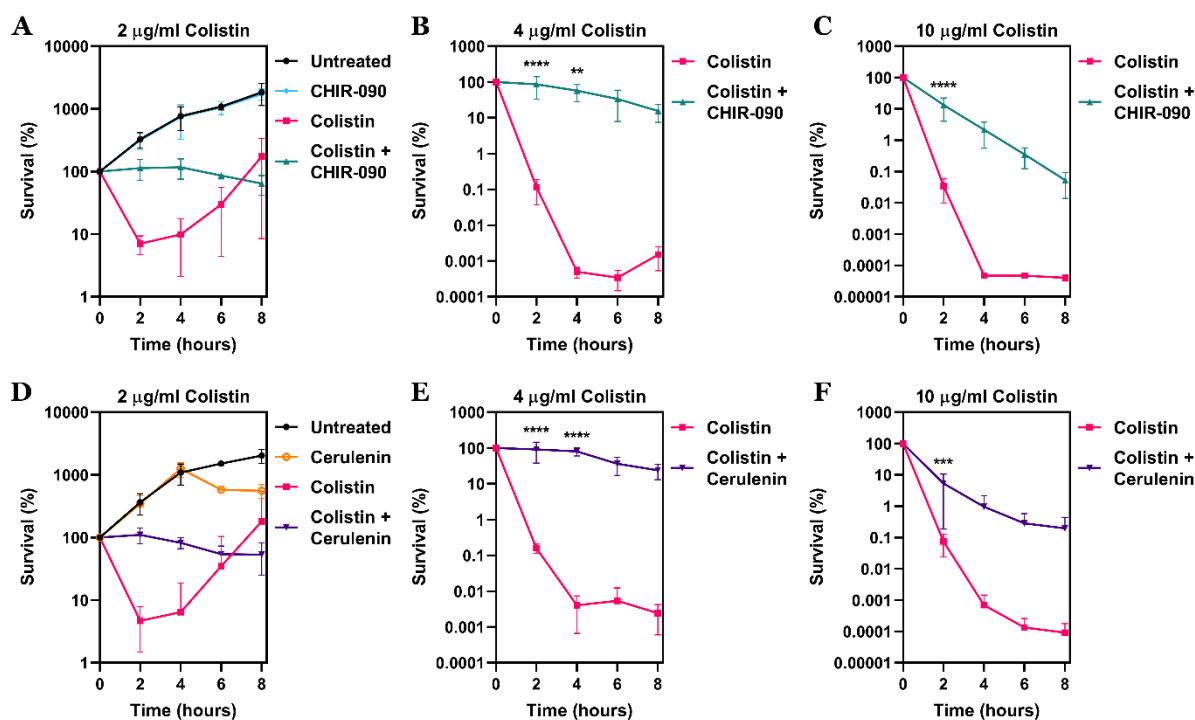


**Figure 3.14: Colistin’s bactericidal activity against *P. aeruginosa* is dependent on active LPS biosynthesis.** A-C, Survival of *P. aeruginosa* PA14 cells exposed to (A) 2 µg ml<sup>-1</sup>, (B) 4 µg ml<sup>-1</sup> or (C) 10 µg ml<sup>-1</sup> colistin alone, or in combination with CHIR-090 (0.125 µg ml<sup>-1</sup>), as determined by c.f.u. counts over 8 hours (n=4; \*\*p<0.01, \*\*\*\*p<0.0001 relative to bacteria exposed to colistin alone). D-F, Survival of *P. aeruginosa* PA14 cells exposed to (D) 2 µg ml<sup>-1</sup>, (E) 4 µg ml<sup>-1</sup> or (F) 10 µg ml<sup>-1</sup> colistin alone, or in combination with cerulenin (32 µg ml<sup>-1</sup>), as determined by c.f.u. counts over 8 hours (n=4; \*\*\*p<0.001, \*\*\*\*p<0.0001 relative to bacteria exposed to colistin alone). Data in A, D were analysed by a two-way ANOVA with Dunnett’s post-hoc test. Data in B-C, E-F were analysed by a two-way ANOVA with Sidak’s post-hoc test. Data are presented as the arithmetic mean, and error bars represent the standard deviation of the mean.

### 3.16 Discussion

Colistin is a vital last-resort antibiotic commonly and increasingly used in the treatment of individuals infected with multi-drug resistant *P. aeruginosa* as the final option to keep patients alive<sup>392</sup>. Unfortunately, however, despite its importance, the clinical utilisation of colistin is associated with extremely high rates of therapeutic failure (in up to two-thirds of cases), with patient mortality frequently occurring as a result<sup>615,622</sup>. There is, therefore, an urgent necessity to understand the causes of colistin treatment failure, in order to develop novel strategies to improve the efficacy of the polymyxin drug and ultimately enhance patient outcomes following colistin administration. Resistance to colistin, mediated by chromosomal genetic mutations that give rise to chemical modifications to LPS (the bacterial target of polymyxins), has been detected in *P. aeruginosa*, but remains rare in the clinical setting, with non-susceptibility to the polymyxin diagnosed in less than 10% of clinical

*P. aeruginosa* isolates<sup>687</sup>. Hence, there must exist alternative explanations for the high rate of colistin therapy failure, other than classical antibiotic resistance. Experiments in this chapter identified a new mechanism by which *P. aeruginosa* survives colistin exposure through the release of LPS molecules, which inactivate the polymyxin drug extracellularly, promoting bacterial survival and population recovery during treatment with colistin. However, attempts to reduce this extracellular inactivation of colistin by inhibiting LPS biosynthesis decreased polymyxin-induced LPS shedding by *P. aeruginosa*, but surprisingly also blocked colistin's bactericidal activity completely.

While characterising for the first time the precise timeframe for successive disruption of the outer and cytoplasmic membranes of Gram-negative bacteria by colistin, a bi-phasic pattern of cell lysis and killing was observed in *P. aeruginosa* populations exposed to the polymyxin. Such bi-phasic killing kinetics have been reported before with diverse antibiotics and bacterial strains, including for *E. coli* strains treated with ampicillin, *K. pneumoniae* treated with ciprofloxacin and mycobacterial cells treated with rifampicin/isoniazid<sup>688-691</sup>. The reasons why a bactericidal antibiotic kills a bacterial population in a bi-phasic manner can vary, but this phenotype is commonly associated with the existence of persister cells – bacteria that enter a dormant-state that confers tolerance to multiple antimicrobial drugs<sup>655</sup>. In the case of the bi-phasic killing of *P. aeruginosa* by colistin discovered here, when the polymyxin compound was present at a concentration of 2 µg ml<sup>-1</sup>, the initial period of bacterial killing was followed by immediate re-growth of cells, and recovery to meet or even exceed the starting inoculum by the time the assay was terminated. Since persister cells are believed to be quiescent, the ability of *P. aeruginosa* bacteria to immediately begin replicating after surviving exposure to 2 µg ml<sup>-1</sup> colistin means that the antibiotic persistence phenomenon is unlikely to be relevant in this instance, and polymyxin tolerance was caused by an alternative explanation.

This explanation was found to be the complete loss of colistin activity in the spent culture supernatant of *P. aeruginosa* treated with 2 or 4 µg ml<sup>-1</sup> colistin, with this extracellular inactivation of the polymyxin rapidly occurring within 2 hours of antibiotic exposure. Intriguingly, whilst there was a significant reduction (40-50%) in the inhibitory activity of colistin in the supernatant of *P. aeruginosa* cells exposed to the polymyxin drug at 10 µg ml<sup>-1</sup>, the residual concentration of the antibiotic even by the end of the experiment would have been approximately 5 µg ml<sup>-1</sup>, which represents what should be a bactericidal concentration of colistin. Nevertheless, a small sub-population of *P. aeruginosa* cells remained alive and able to survive the presence of this otherwise bactericidal polymyxin concentration, raising key questions about the mechanism of this colistin tolerance. In the absence of notable re-growth of these bacteria treated with 10 µg ml<sup>-1</sup> colistin, it is possible that dormant antibiotic persister cells were responsible for this survival capability. The formation of colistin persister cells has

been experimentally proven in past studies, and in support of their involvement in this case, emergence of resistance experiments revealed that after a single exposure to colistin, surviving *P. aeruginosa* cells were killed by the polymyxin identically to previously unexposed cells – a characteristic defining trait of antibiotic persistence<sup>653,654</sup>. However, future studies are needed to isolate the surviving population, and potentially perform metabolic and transcriptomic analyses on the antibiotic tolerant cells before the phenotype of colistin persistence can be firmly demonstrated in *P. aeruginosa*<sup>692,693</sup>.

The basis for the loss of activity of colistin in the culture supernatant of *P. aeruginosa* cells during polymyxin treatment was established as being due to the extracellular release of LPS from bacteria, which inactivated colistin molecules before they could target and kill the pathogen. Crucial data implicating LPS as the shed colistin-inactivating factor arose from experiments that showed the polysaccharide was released into the *P. aeruginosa* supernatant both as a response to exposure to increasing sub-inhibitory colistin concentrations, and over time during incubation with a bactericidal concentration of the antibiotic. Furthermore, the addition of purified LPS to culture media had the effect of directly reducing colistin activity even in the absence of whole bacterial cells, as well as increasing the MIC of colistin against *P. aeruginosa* in a dose-dependent manner, clearly highlighting the protective capacity of extracellular LPS against the polymyxin's antibacterial properties.

The recognition of LPS as the released colistin inactivator is corroborated by recent studies, which found that the inhibitory activity of polymyxin compounds was decreased by extracellular LPS present either in artificial sputum or in the cell wash fluid of Gram-negative bacteria<sup>694,695</sup>. Moreover, OMVs (of which LPS forms a predominant component) shed from pathogenic *E. coli* have been shown to mitigate the bactericidal activity of polymyxin drugs, and the colistin-inactivating behaviour of LPS illustrated in this chapter now provides a mechanistic explanation for this finding<sup>668</sup>. Interestingly, LPS release from *P. aeruginosa* cells treated with an inhibitory colistin concentration did not seem to be in the form of OMVs, since no lipid was detected in these spent culture supernatants in spite of abundant quantification of LPS molecules. Although this may initially appear in opposition to previous investigations that indicated OMV production can be induced by polymyxin compounds, the antibiotic concentrations used in those studies were markedly lower (0.5  $\mu\text{g ml}^{-1}$  rather than 2  $\mu\text{g ml}^{-1}$ ), and it is probable that the LPS release phenotype varies depending on whether colistin is used at sub-inhibitory or lethal concentrations<sup>668</sup>.

There is a growing appreciation that bacteria can tolerate antibiotic exposure by releasing extracellular factors that bind and inactivate antimicrobial agents extracellularly, and the use of extracellular LPS shed from *P. aeruginosa* to enable the pathogen to survive colistin treatment fits with and contributes to this increased understanding of “antibiotic

interception” strategies<sup>665</sup>. Other similar modes of extracellular antibiotic inactivation by bacteria include the release of proteinaceous lipocalins from *B. cenocepacia*, which confer tolerance to rifampicin, norfloxacin and ceftazidime, the shedding of capsular polysaccharide molecules that sequester the human neutrophil antimicrobial peptide HNP-1 by *K. pneumoniae* and *S. pneumoniae*, and the release of DNA into biofilms by *S. epidermidis* as a defence against vancomycin exposure<sup>666,670,696</sup>.

DNA, lipocalins and capsular polysaccharides have all also been linked to the inactivation of polymyxin drugs; however, the prospect of either lipocalins or capsular polysaccharides having a role in the loss of colistin activity in the supernatant of *P. aeruginosa* cultures was eliminated by the fact that the released inactivating factor was insensitive to heat (therefore unlikely to be protein), and still shed in transposon mutants deficient in the production of alginate (the principal capsular polysaccharide). Nonetheless, there is a small possibility that in addition to released LPS, a heat-stable protein/peptide (e.g. secreted enterotoxins) may be involved in extracellular colistin inactivation by *P. aeruginosa*, as well as the minor secreted capsular polysaccharides Psl and Pel, particularly on solid culture media<sup>697</sup>. To overwhelmingly prove that LPS was the only released factor responsible for colistin inactivation by *P. aeruginosa*, future experiments could utilise LPS-degrading enzymes from bacteriophages or human immune cells (e.g. acyloxyacyl hydrolase) to attempt to reduce the polymyxin-inactivating effects of the *P. aeruginosa* spent supernatant<sup>698,699</sup>.

Perhaps the most convincing detail substantiating that LPS was the shed colistin inactivator is that the primary bacterial target of polymyxin antibiotics is the lipid A domain of LPS molecules in the OM of Gram-negative pathogens. Hence, it would be expected that extracellular LPS molecules released by *P. aeruginosa* would be bound by colistin in the culture supernatant, and that the resulting colistin-LPS complexes would have severely reduced antibacterial activity. Indeed, mechanisms of tolerance by extracellular antibiotic interception have often been found to entail shedding of a drug’s target compound, with the inactivation of daptomycin by the membrane phospholipid phosphatidylglycerol in *S. aureus* serving as a perfect example<sup>629</sup>.

Critically, it was observed in this chapter that the development of colistin resistance in *P. aeruginosa*, which is only known to occur through chemical modifications that alter the charge of LPS, was associated with the loss of the bacteria’s colistin-inactivating properties, presumably because the modified LPS molecules released by the pathogen no longer retained their electrostatic affinity for polymyxin drugs. This leads to fascinating questions about whether LPS shedding by *P. aeruginosa* is a defensive strategy against colistin-mediated cell killing, that is simply not required and easily lost without any ensuing cost in polymyxin-resistant bacteria since they possess an alternate mode of antibiotic tolerance.

To understand the mechanism of LPS release by *P. aeruginosa* cells during colistin exposure, and in particular whether this was an active defence process, it was assessed whether shedding of LPS in response to the polymyxin drug was dependent on *de novo* LPS biosynthesis. Whilst it was shown that the extracellular release of LPS was diminished when LPS synthesis was inhibited, with higher levels of colistin activity expectedly maintained in the culture supernatant as a consequence, the subsequent discovery that blocking biosynthesis of LPS simultaneously blocked colistin's bactericidal activity complicates resolving the notion that LPS shedding is an active mode of defence. Colistin is known to disrupt the cationic bridges between LPS molecules in the outer membrane, and ultimately trigger cell lysis, and both these events could feasibly lead to extracellular LPS release<sup>700</sup>. Therefore, it is not clear that the reduction in LPS shedding into the supernatant of *P. aeruginosa* cultures exposed to colistin was not simply a downstream consequence of the antibiotic being unable to exert its bactericidal effects, displacing intra-LPS cation bridges and inducing bacterial lysis.

Notably, sub-inhibitory concentrations of colistin (0.25 and 0.5  $\mu\text{g ml}^{-1}$ ) that would not cause lysis of *P. aeruginosa* cells did stimulate an increase in LPS release extracellularly, as did a colistin concentration of 2  $\mu\text{g ml}^{-1}$ , which initiated bacterial death in the absence of significant detectable cell lysis. These data suggest that LPS shedding was not the outcome of colistin's lytic activity against *P. aeruginosa*. However, even at sub-inhibitory or sub-lytic concentrations, colistin was able to partially disrupt the bacterial OM to a sufficient degree as to allow the uptake of the fluorescent NPN dye, and this damage to the cell envelope, which is thought to be due to displacement of the cation bridges between LPS molecules, could well be the basis for extracellular LPS release.

At higher colistin concentrations (4-10  $\mu\text{g ml}^{-1}$ ), *P. aeruginosa* cells underwent marked lysis when treated with the polymyxin, and thus distinguishing between shedding of LPS as an active defence versus the culmination of lysed bacterial contents leaking into the supernatant is challenging. One key certainty about the LPS shedding phenomenon is that it has a limited capacity to inactivate colistin, and if sufficient polymyxin molecules are present (e.g. at 10  $\mu\text{g ml}^{-1}$ ), substantial antibiotic activity is retained. Nonetheless, further studies are essential to comprehend how and when *P. aeruginosa* releases LPS during colistin exposure, and whether additional cellular processes (e.g. LPS transport) are a requirement for this to occur. By elucidating the mechanism of LPS shedding, novel therapeutic approaches could be developed to minimise this event, for instance by inhibiting LPS transport with murepavadin, which may improve colistin efficacy, overcome colistin tolerance, and lead to enhanced patient outcomes.

In summary, the results in this chapter described a new mechanism by which *P. aeruginosa* survives colistin treatment. Attempts to mitigate this also attenuated colistin's bactericidal activity, and the reasons for this will be explored in the next chapter.



# Chapter 4: Colistin kills bacteria by targeting lipopolysaccharide in the cytoplasmic membrane

## 4.1 Introduction

The mechanism of action by which the vital, last-resort lipopeptide antibiotic colistin kills Gram-negative bacteria is very poorly understood<sup>392,701</sup>. Given colistin's increasing importance and use in clinical settings, there is an urgent demand to resolve this gap in knowledge, with the ultimate aim of using this information of how the polymyxin drug exerts its bactericidal effects to design new treatment strategies that could surmount colistin therapy failure – a concerningly frequent occurrence in patients<sup>374</sup>. Whilst the initial interactions of colistin molecules with bacteria, binding to target LPS molecules in the outer membrane (OM) of Gram-negative organisms, have been well documented, it is the subsequent steps in the antibiotic's mode of action, and in particular how these result in cell death, that remain largely unknown<sup>280</sup>.

Colistin has an amphipathic structure consisting of a positively-charged polypeptide ring connected to a hydrophobic fatty acid tail, and it is believed that these two chemically-distinct regions are responsible for different processes during the antibiotic's preliminary attachment to and disruption of the bacterial OM, although this has never been convincingly demonstrated experimentally<sup>702</sup>. The cationic peptide macrocycle is thought to attach to the negatively-charged phosphate groups in the lipid A domain of LPS through an electrostatic attraction, which causes the displacement of the  $Mg^{2+}/Ca^{2+}$  cationic bridges that stabilise the arrangement of LPS molecules in the OM outermost leaflet<sup>264</sup>. Loss of these cation bridges leads to weakening of the OM, and this disruption is proposed to be exploited by colistin's lipophilic acyl tail to insert itself into the OM structure, where it interacts with the fatty acyl chains that form the inner portion of lipid A, instigating further OM damage via an unproven “surfactant-like” mechanism<sup>408,703,704</sup>.

How this disruption of the extracellular-facing bilayer of the cell envelope by colistin culminates in the killing of Gram-negative bacteria is one of the key unanswered questions in terms of the polymyxin's mode of action. Numerous suggestions have been put forward for how colistin-induced OM permeabilisation could lead to cell death, including: the fatal leakage of cytosolic contents, the generation of reactive oxygen species that damage essential intracellular components, the inhibition of cytoplasmic respiratory enzymes and the binding to protein-synthesising ribosomes inside the bacteria<sup>418,428,705,706</sup>. Regardless of which of these postulated processes confers colistin with its bactericidal properties, before the polymyxin antibiotic can kill Gram-negative organisms by any of these means, it first needs to disrupt

and damage the cytoplasmic membrane (CM). Despite more than six decades of colistin being used clinically, and extensive laboratory research, the mechanism of CM permeabilisation by the polymyxin compound is purely theoretical, with almost no practical evidence of how the antibiotic disrupts the inner phospholipid bilayer of the bacterial cell envelope.

The structural and chemical similarities between colistin and other antimicrobial peptides (AMPs) that disrupt bacterial phospholipid membranes has contributed to the widespread belief that the polymyxin drug permeabilises the CM through a comparable mode of action as bactericidal membranolytic AMPs<sup>707</sup>. These peptides often possess detergent-like characteristics, and their insertion into phospholipid bilayers severely damages the membranes, producing pores in the cell envelope to trigger bacterial death<sup>708,709</sup>. The N-terminal fatty acid tail of colistin molecules is thought to harbour homologous surfactant effects, with the CM of Gram-negative pathogens disrupted by the polymyxin compound as a direct consequence. Data supporting the notion that colistin-mediated permeabilisation of the CM occurs by this detergent behaviour of the antibiotic arises from studies showing that colistin has a degree of antimicrobial activity against the Gram-positive pathogen *S. pyogenes*, and also that polymyxin molecules interfere with mammalian epithelial cell membranes, where in both cases the CM is composed only of a phospholipid bilayer<sup>710,711</sup>. Indeed, the nephrotoxic and neurotoxic side-effects of clinical colistin administration have previously been associated with the antibiotic's ability to disrupt phospholipid bilayers<sup>712,713</sup>.

However, in contrast to these reports of colistin acting as a surfactant to damage the CM, there is also an abundance of evidence indicating that the polymyxin cannot permeabilise phospholipid bilayers. Firstly, while colistin may exhibit some CM-disrupting activity in mammalian epithelial cells and the bacterium *S. pyogenes*, this is only apparent when the polymyxin drug is present at doses (8-16  $\mu\text{g ml}^{-1}$ ) that are far above typical clinical serum concentrations, raising doubts about whether the antibiotic can damage phospholipid bilayer structures at therapeutically-relevant concentrations<sup>710,711</sup>. Moreover, the Gram-negative pathogen *A. baumannii* has a unique method of developing colistin resistance by completely removing LPS from its OM; in this instance, the outermost bilayer of the organism is formed solely of phospholipids, but it is insensitive to polymyxin permeabilisation<sup>516</sup>. In addition, molecular dynamic simulations conducted *in silico* have discovered that, unlike the traditional killing mechanism of AMPs, polymyxin compounds stiffen the CM rather than disrupting it<sup>714</sup>. Perhaps most convincingly, investigations with synthetic vesicles found minimal membrane permeation of vesicles formed only of membrane phospholipids, with vesicle membranes only significantly damaged when the bilayers contained LPS<sup>715</sup>.

Whilst the final destination of LPS molecules in Gram-negative bacteria is the outer extracellular-facing leaflet of the OM, prior to their arrival on the cell surface there exists a

complex process where LPS is synthesised intracellularly and transported across the bacterial cell envelope<sup>223</sup>. The biosynthesis of the “core-lipid A” domain and the O-antigen domain of LPS occurs independently on the innermost cytoplasmic-facing surface of the CM, before these structures are flipped to the periplasmic-facing surface of the CM and ligated to create the complete LPS molecule<sup>716–718</sup>. From the outermost leaflet of the CM, this fully-synthesised LPS is shuttled straight to the OM extracellular-facing leaflet by the Lpt protein family, the members of which extract LPS from the CM, translocate it across the periplasm on a bridge, and insert the polysaccharide compounds into the outermost leaflet of the OM<sup>221</sup>. At any one point in time, therefore, in Gram-negative organisms, LPS is present in notable quantities in the periplasmic-facing leaflet of the CM, awaiting transport to the OM<sup>719</sup>.

Considering the facts that: (i) colistin is unable to permeabilise phospholipid bilayers in the absence of LPS; (ii) the CM of Gram-negative organisms contains LPS molecules in transit; and (iii) colistin has a high affinity and well-established ability to bind/disrupt LPS, it is hypothesised in this chapter that colistin targets LPS molecules in the CM of bacteria in order to damage the bilayer and exert its bactericidal activity. In particular, it is investigated whether the effects of inhibiting LPS biosynthesis on blocking colistin’s ability to kill *P. aeruginosa* observed in previous experiments were due to diminishing the amount of LPS in the CM.

## **4.2 Blocking LPS biosynthesis reduces colistin killing of *P. aeruginosa* in a dose-dependent manner**

Having discovered that the bactericidal activity of colistin against *P. aeruginosa* PA14 cells was abolished when *de novo* LPS biosynthesis was inhibited, it was decided to characterise this phenotype in greater detail, firstly by examining if this effect was dose-dependent. Specifically, the killing kinetics of colistin on a PA14 population co-treated with a range of concentrations of CHIR-090 and cerulenin were measured in order to determine whether their protective effects on polymyxin killing would be reduced at lower concentrations of the LPS synthesis inhibitors than those used in previous assays.

At the highest, but nonetheless sub-inhibitory, concentration of CHIR-090 tested (0.125 µg ml<sup>-1</sup>), addition of the LpxC inhibitor to *P. aeruginosa* cells treated with 4 µg ml<sup>-1</sup> colistin completely stopped bacterial killing by the polymyxin drug as seen earlier, with no reduction in cell survival detected at all over 8 hours (**Figure 4.1A**). As the concentration of CHIR-090 was lowered, there was a small degree (less than 1-log) of killing of PA14 bacteria by colistin over the initial 2-4 hours of antibiotic exposure; however, even at a CHIR-090 concentration that was 25-fold higher than that utilised in initial experiments (0.005 µg ml<sup>-1</sup>),

by 8 hours, there was no noticeable drop in cell numbers relative to the starting inoculum, and a 4-log difference compared to bacteria treated with colistin alone. Therefore, CHIR-090 was a highly potent compound in terms of preventing colistin-mediated killing of *P. aeruginosa*, with striking effects observed even at nanomolar doses. Only when the concentration of the LPS biosynthesis inhibitor was reduced to 0.0025  $\mu\text{g ml}^{-1}$  was any significant death of the PA14 population quantified during colistin exposure, although the killing kinetics of the bacteria remained markedly slower than *P. aeruginosa* cells treated only with the polymyxin drug.

This dose-dependent nature of CHIR-090's protective capacity on colistin-induced bacterial killing was also evident with the fatty acid/LPS synthesis inhibitor cerulenin. While at the highest sub-inhibitory cerulenin concentration used (32  $\mu\text{g ml}^{-1}$ ), the killing of *P. aeruginosa* PA14 by colistin was entirely abrogated, when the concentration of cerulenin was reduced, there was a simultaneous and step-wise increase in the polymyxin's bactericidal activity (**Figure 4.1B**). Indeed, at cerulenin concentrations of 8 and 16  $\mu\text{g ml}^{-1}$ , the number of surviving cells following 8 hours of colistin exposure was essentially identical to bacteria exposed to the polymyxin antibiotic alone, although the rate of killing was appreciably slower. Hence, the abilities of the LPS biosynthesis inhibitors CHIR-090 and cerulenin to block the killing of *P. aeruginosa* by colistin was dependent on the concentration at which they were present. The fact that CHIR-090 appeared to block colistin's bactericidal effects much more efficaciously than cerulenin may suggest that directly targeting the Lpx family of enzymes in the LPS biosynthetic pathway had greater power at stopping polymyxin killing than targeting the upstream process of fatty acid synthesis more generally.

To assess if colistin required *de novo* LPS biosynthesis for only its initial binding and killing of *P. aeruginosa*, or for the on-going continuous killing activity of the polymyxin, PA14 cells were first exposed to 4  $\mu\text{g ml}^{-1}$  colistin alone for 2 hours, before CHIR-090/cerulenin were added to the culture media and bacterial survival enumerated over the subsequent 8 hours of incubation. Under all three conditions, there was a 3-log decrease in survival of *P. aeruginosa* cells after 2 hours colistin treatment; in the PA14 population where the polymyxin was not supplemented with either inhibitor of LPS biosynthesis, bacterial counts continued to drop by another 3-logs during the next 4 hours of the experiment (**Figure 4.1C**). However, the addition of CHIR-090 to the cell culture after 2 hours dramatically reduced the killing rate of *P. aeruginosa* by colistin (2-log difference at 4 hours), and in the case of cerulenin, polymyxin-mediated killing was totally halted. Thus, this data revealed that colistin was not just dependent on active LPS biosynthesis to bind and cause cell death in PA14 cells preliminarily; rather, the polymyxin required *de novo* biosynthesis of LPS throughout its bactericidal mode of action in order to continue killing *P. aeruginosa* even once the antibiotic had bound.

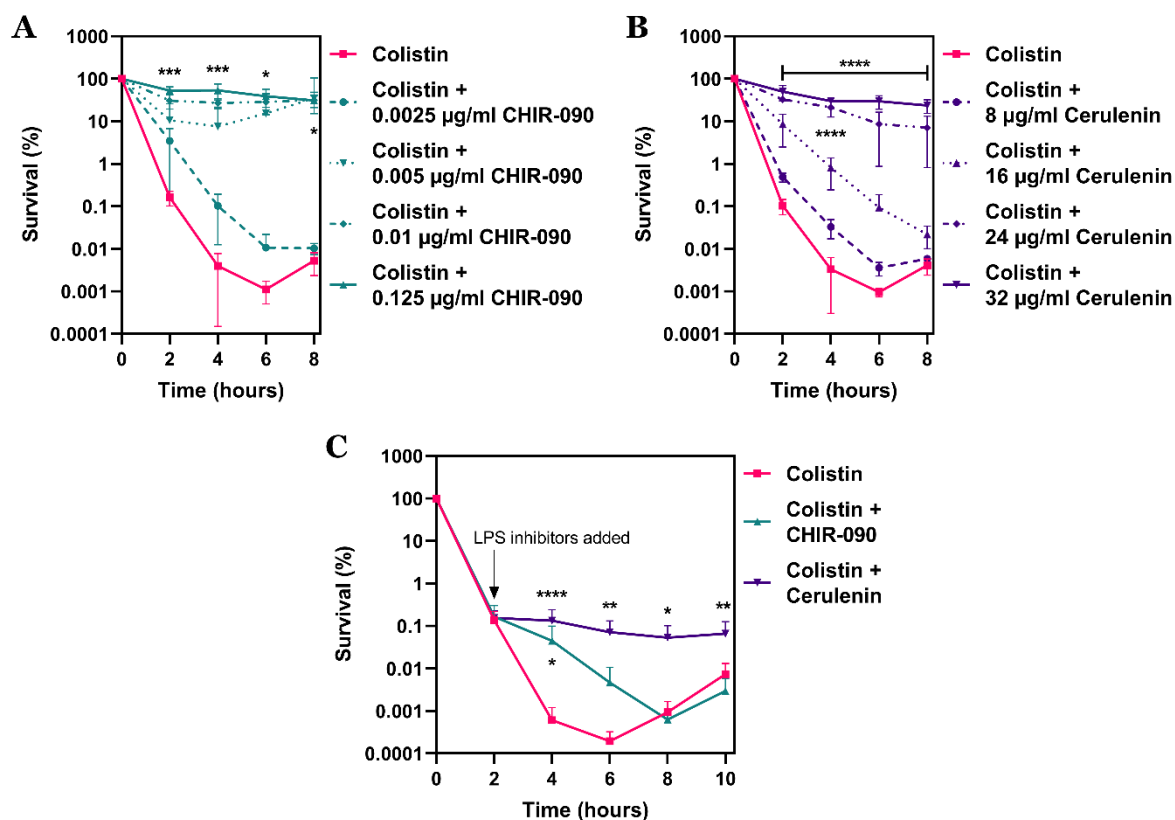


**Figure 4.1: Colistin is dependent on *de novo* LPS biosynthesis throughout its bactericidal activity against *P. aeruginosa*.** **A**, Survival of *P. aeruginosa* PA14 cells exposed to colistin alone ( $4 \mu\text{g ml}^{-1}$ ), or colistin in combination with a range of concentrations of the LPS biosynthesis inhibitor CHIR-090, as determined by c.f.u. counts over 8 hours ( $n=4$ ;  $*p<0.05$ ,  $***p<0.001$  relative to bacteria exposed to colistin alone). **B**, Survival of *P. aeruginosa* PA14 cells exposed to colistin alone ( $4 \mu\text{g ml}^{-1}$ ), or colistin in combination with a range of concentrations of the fatty acid/LPS synthesis inhibitor cerulenin, as determined by c.f.u. counts over 8 hours ( $n=4$ ;  $****p<0.001$  relative to bacteria exposed to colistin alone). **C**, Survival of *P. aeruginosa* PA14 exposed to colistin alone ( $4 \mu\text{g ml}^{-1}$ ) for 2 hours, followed by no further treatment, or the addition of CHIR-090 ( $0.125 \mu\text{g ml}^{-1}$ ) or cerulenin ( $32 \mu\text{g ml}^{-1}$ ), as determined by c.f.u. counts over 10 hours ( $n=3$  in duplicate;  $*p<0.05$ ,  $**p<0.01$ ,  $****p<0.0001$  relative to bacteria exposed to colistin alone). Data in **A**, **B** were analysed by a two-way ANOVA with Dunnett's post-hoc test. Data in **C** were analysed by a two-way ANOVA with Holm-Sidak's post-hoc test. Data are presented as the arithmetic mean, and error bars represent the standard deviation of the mean.

### 4.3 Inhibiting biosynthesis of LPS prevents colistin-induced morphological changes of *P. aeruginosa*

It has previously been established that colistin's bactericidal mode of action through successive disruption of the OM and CM of Gram-negative organisms results in extensive morphological changes to bacterial cells<sup>720</sup>. To further explore the phenomenon of blocking colistin-mediated killing of *P. aeruginosa* by reducing LPS biosynthesis, and in particular to see how the use of the inhibitors CHIR-090 and cerulenin affected the alterations to cell morphology caused by the polymyxin, scanning electron microscopy (SEM) images of PA14 bacteria exposed to the antibiotics for two hours were obtained.

Since the LPS synthesis inhibitors CHIR-090 and cerulenin were being utilised at sub-inhibitory concentrations, treatment of *P. aeruginosa* with either compound alone had no impact at all on the surface morphology of PA14 cells, with these bacteria appearing entirely unchanged in comparison to untreated cells (**Figure 4.2ABC**). In stark contrast, after 2 hours incubation with a bactericidal colistin concentration ( $4 \mu\text{g ml}^{-1}$ ), the morphology of *P. aeruginosa* bacteria was profoundly affected, with the cells found to be greatly distorted and deflated (**Figure 4.2D**). This is in keeping with past reports that exposure of Gram-negative pathogens to colistin is associated with significant alterations to bacterial surface morphology, including the aggregation of cells as observed here, and is likely due to the lytic properties of the polymyxin drug<sup>496,721</sup>. Crucially, however, when *P. aeruginosa* PA14 was treated with this lethal colistin concentration alongside sub-inhibitory doses of either CHIR-090 or cerulenin, the polymyxin antibiotic was unable to trigger these same morphological changes (**Figure 4.2EF**). In fact, bacteria exposed to colistin while *de novo* biosynthesis of LPS was blocked appeared virtually identical to untreated *P. aeruginosa* cells, with no visible signs of the deflation, distortion and aggregation typical of polymyxin-treated bacteria. Hence, it was concluded that inhibition of active LPS biosynthesis compromised colistin's ability to alter bacterial morphology and initiate cell lysis/death in *P. aeruginosa* PA14.

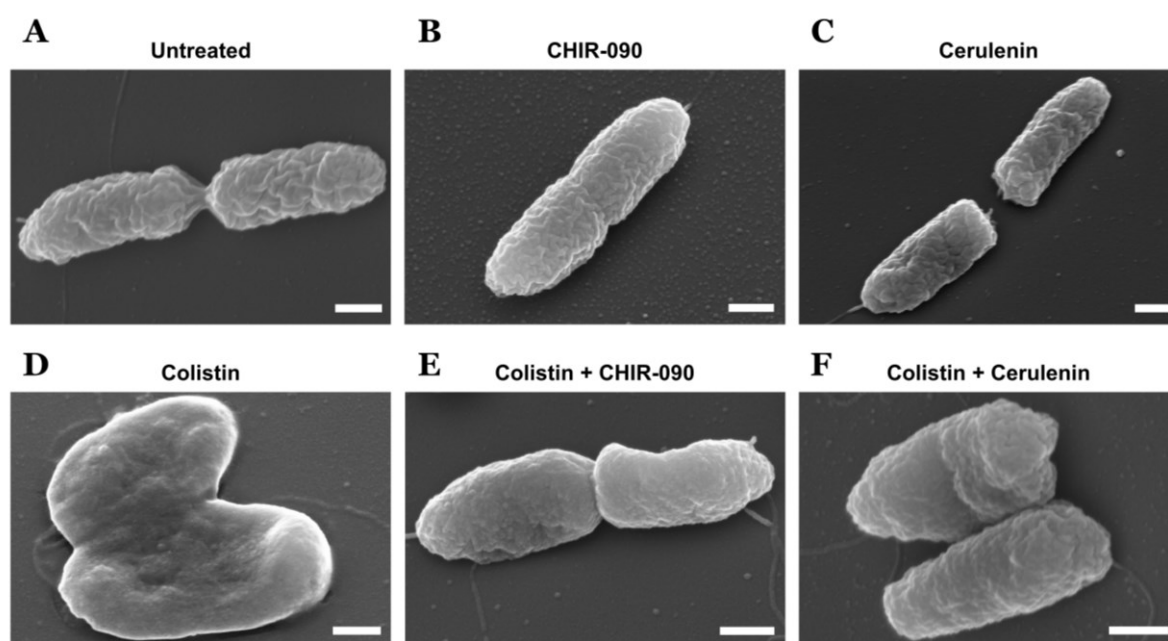


**Figure 4.2: Alterations to the cell morphology of *P. aeruginosa* caused by colistin require active LPS biosynthesis.** A-F, Scanning electron microscopy (SEM) images of *P. aeruginosa* PA14 cells following 2 hours incubation in (A) media alone, or cells exposed to (B)  $0.125 \mu\text{g ml}^{-1}$  CHIR-090 alone, (C)  $32 \mu\text{g ml}^{-1}$  cerulenin alone, (D)  $4 \mu\text{g ml}^{-1}$  colistin alone, (E) colistin in combination with CHIR-090, or (F) colistin in combination with cerulenin (Scale bars: 200 nm). All images are representative of 3 independent experiments.

#### 4.4 Inhibiting LPS synthesis specifically blocks colistin killing of *P. aeruginosa*

Because the effects of blocking biosynthesis of LPS with CHIR-090/cerulenin on preventing colistin's bactericidal activity were so unexpected and prominent, it was resolved to undertake a series of control experiments to ensure the validity of this finding. The first of these control assays performed involved studying whether the two LPS biosynthesis inhibitors modulated the physiology of *P. aeruginosa* in a way that made the bacteria less susceptible to all manner of antibiotic stresses, rather than being a phenotype that was specific to colistin. In order to investigate this, the MIC against PA14 cells was determined for four bactericidal antibiotics commonly-used clinically against *P. aeruginosa* infections, each with distinct bacterial targets and mechanisms of action: the quinolone ciprofloxacin (DNA gyrase inhibitor), the aminoglycoside gentamicin (protein synthesis inhibitor), the beta-lactam imipenem (cell wall synthesis inhibitor) and the membrane-disrupting drug chlorhexidine (**Figure 4.3A**). Having ascertained these MICs, the survival of PA14 bacteria exposed to bactericidal concentrations of the four antibiotics (8-fold higher than the MIC) was measured over 8 hours in the absence or presence of CHIR-090/cerulenin, to see if the LPS synthesis inhibitors triggered a generic stress response in *P. aeruginosa* that compromised killing by all antimicrobial agents.

Individually, each of the four antibiotic drugs killed PA14 cells both rapidly and abundantly, with ciprofloxacin and imipenem reducing viable bacterial counts by more than 4-logs after 8 hours of treatment, whilst gentamicin and chlorhexidine were responsible for a 6-log decrease in *P. aeruginosa* survival (**Figure 4.3BCDE**). Importantly, the addition of either CHIR-090 or cerulenin in combination with the four bactericidal antimicrobials had no impact whatsoever on the killing kinetics of PA14 bacteria by ciprofloxacin, gentamicin, imipenem or chlorhexidine, with the rate of cell death induced by the antibiotics completely unaffected by the inhibitors of LPS biosynthesis. This firmly indicated that the compounds CHIR-090 and cerulenin did not block the bactericidal effects of numerous different antimicrobial agents, but instead only specifically mitigated killing of *P. aeruginosa* by polymyxins.

These time-kill experiments were next repeated using a lethal concentration (8-fold greater than the MIC) of the molecule ethylenediaminetetraacetic acid (EDTA), which shares certain functional similarities with colistin in that it is also a chelating agent, which disrupts the bacterial cell envelope by displacing intra-LPS cationic bridges from the OM of Gram-negative organisms<sup>722,723</sup>. The killing rate of *P. aeruginosa* PA14 cells by EDTA was unaltered in the presence of CHIR-090/cerulenin, further confirming the specificity of these inhibitors for only blocking colistin's ability to kill bacteria (**Figure 4.3F**). Furthermore, this data

provides key mechanistic insight into the requirement of *de novo* LPS biosynthesis for the polymyxin to be bactericidal by showing that displacement of cation bridges to damage the outermost LPS monolayer of the Gram-negative OM (the first stage in colistin's mode of action) was not a process that was dependent on active synthesis of LPS.

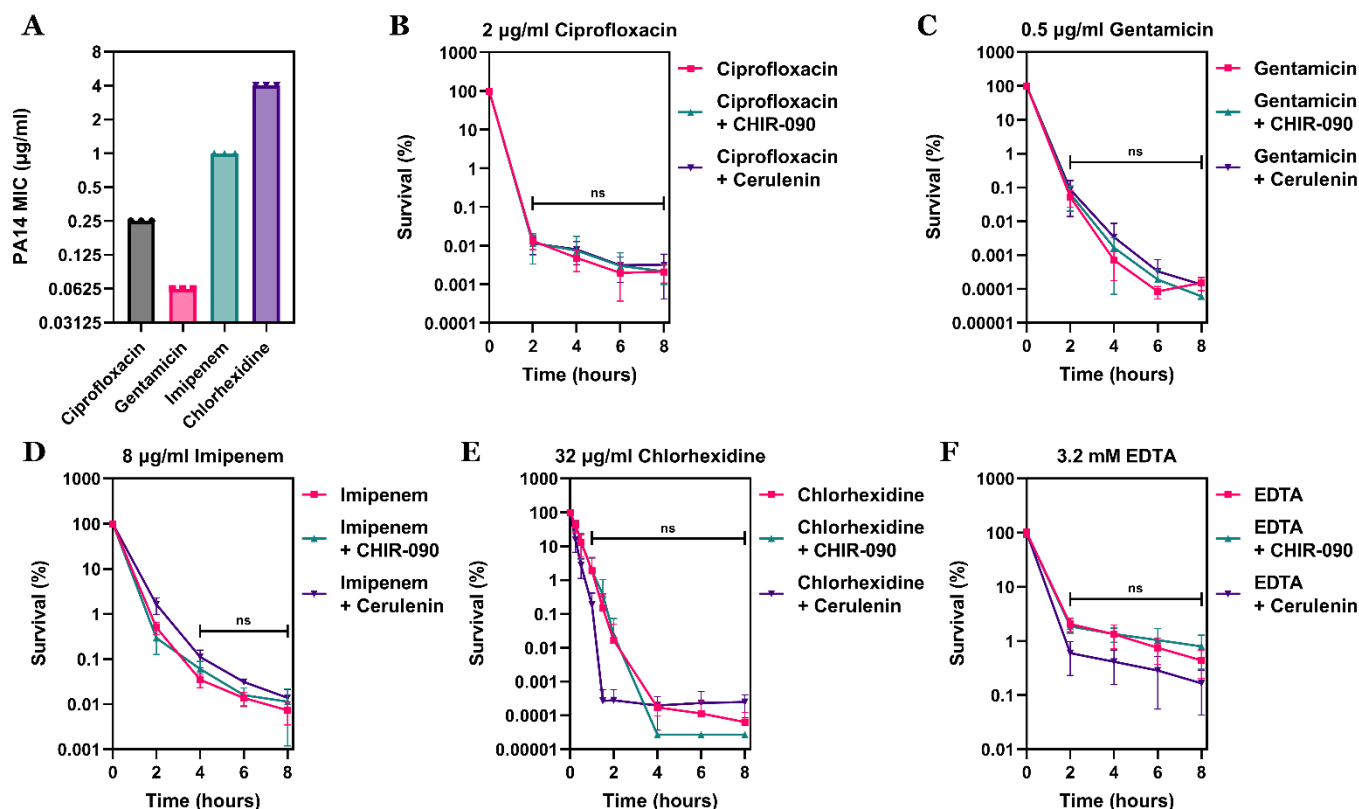


**Figure 4.3: The protective effects of inhibiting LPS biosynthesis on *P. aeruginosa* killing are specific to colistin.** **A**, MIC of ciprofloxacin, gentamicin, imipenem and chlorhexidine against *P. aeruginosa* PA14 cells, as determined using the broth microdilution assay ( $n=3$ ). **B-F**, Survival of *P. aeruginosa* PA14 cells exposed to **(B)** 2  $\mu\text{g ml}^{-1}$  ciprofloxacin, **(C)** 0.5  $\mu\text{g ml}^{-1}$  gentamicin, **(D)** 8  $\mu\text{g ml}^{-1}$  imipenem, **(E)** 32  $\mu\text{g ml}^{-1}$  chlorhexidine, or **(F)** 3.2 mM EDTA, in each case either alone, or in combination with CHIR-090 (0.125  $\mu\text{g ml}^{-1}$ ) or cerulenin (32  $\mu\text{g ml}^{-1}$ ), as determined by c.f.u. counts over 8 hours ( $n=4$  for **B-E**,  $n=3$  in duplicate for **F**; ns:  $p>0.05$  relative to bacteria exposed to the antibiotic alone without CHIR-090/cerulenin). Data in **B-F** were analysed by a two-way ANOVA with Dunnett's post-hoc test. Data are presented as the arithmetic mean, and error bars represent the standard deviation of the mean.

#### 4.5 Colistin's bactericidal activity against *P. aeruginosa* is not inhibited by growth arrest

Having verified that the antibacterial-blocking properties of CHIR-090 and cerulenin were specific to colistin, the second control experiment carried out examined whether these LPS biosynthesis inhibitors affected polymyxin-mediated killing of *P. aeruginosa* through modulation of the bacterial growth rate. This was especially imperative as the arrest of growth



in bacteria has previously been shown to reduce susceptibility to many different antibiotics, including polymyxin compounds, and in spite of being used in all assays at sub-inhibitory doses, both CHIR-090 and cerulenin did at these concentrations have a partial negative impact on the growth of *P. aeruginosa* cells<sup>724–727</sup>. To determine the potential consequences of growth inhibition by CHIR-090/cerulenin on colistin's bactericidal activity, PA14 bacteria were exposed to colistin in combination with two bacteriostatic protein synthesis inhibitors – the antibiotics tetracycline and chloramphenicol. In each case, these antimicrobial agents were utilised alongside 4 µg ml<sup>-1</sup> colistin at numerous concentrations, ranging from sub-inhibitory to fully bacteriostatic, and cell viability was calculated over 8 hours incubation.

When a sub-inhibitory concentration of tetracycline (4 µg ml<sup>-1</sup>, 2-fold lower than the MIC), which had only a minor influence on growth relative to untreated bacteria, was added to *P. aeruginosa* cells along with colistin, there was no perceivable reduction in the killing kinetics of a PA14 population by the polymyxin drug (**Figure 4.4A**). Comparably, even the addition of tetracycline at a concentration that caused absolute growth arrest (32 µg ml<sup>-1</sup>, 4-fold higher than the MIC) had no significant effect on the rate of colistin-induced bacterial death, with colony counts of surviving *P. aeruginosa* cells after 8 hours combination treatment closely resembling the counts of cells treated with the polymyxin alone (**Figure 4.4B**). There did not exist, in fact, any “sweet spot” at which arrest of bacterial growth by tetracycline concurrently blocked colistin's bactericidal tendencies against PA14, since across a range of concentrations of the protein synthesis inhibitor tested, its rapid killing (4 to 5-logs within 6 hours) of *P. aeruginosa* was maintained (**Figure 4.4C**).

Almost identical results were obtained with another bacteriostatic protein synthesis inhibitor, chloramphenicol, which at the sub-inhibitory concentration of 32 µg ml<sup>-1</sup> (4-fold less than the MIC) exhibited no ability to reduce colistin's rate of PA14 killing to a noteworthy extent (**Figure 4.4D**). Once again, even at a totally bacteriostatic dose of 256 µg ml<sup>-1</sup> (2-fold greater than the MIC), viable *P. aeruginosa* cell counts dropped by between 3 and 4-logs in both the population exposed to colistin in combination with chloramphenicol, and the population exposed to colistin alone (**Figure 4.4E**). Throughout all the chloramphenicol concentrations investigated, bacterial growth arrest initiated by the protein synthesis inhibitor was unable to wholly abrogate polymyxin killing, although at the highest dose used (256 µg ml<sup>-1</sup>), the rate of cell death triggered by colistin was moderately, albeit insignificantly, diminished (**Figure 4.4F**). Crucially, however, this phenotype of slower killing by colistin of PA14 cells co-treated with a supraphysiological chloramphenicol concentration was nowhere near the degree to which CHIR-090/cerulenin at sub-lethal doses entirely inhibited the polymyxin antibiotic's bactericidal activity. Together, these data conclusively demonstrated that the LPS biosynthesis inhibitors did not block colistin killing by impacting cell growth.

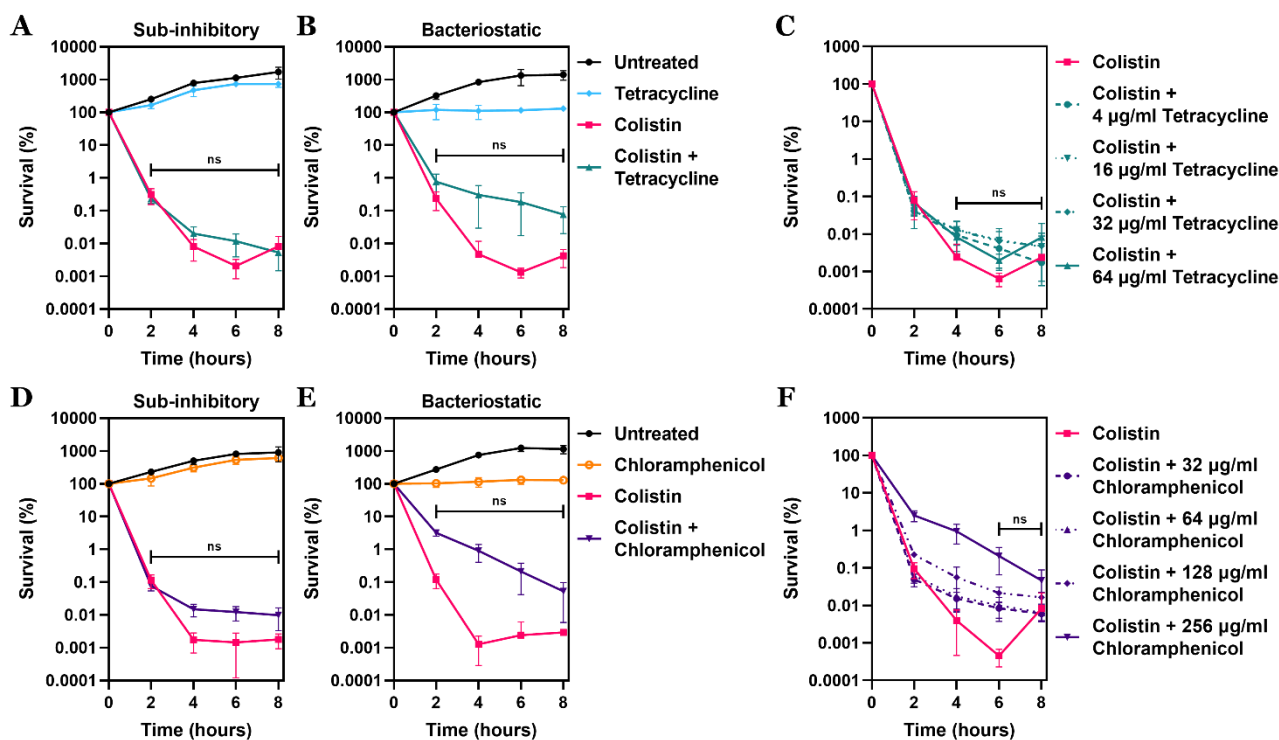


**Figure 4.4: Growth arrest of *P. aeruginosa* does not block the killing of cells by colistin.**

**A-C**, Survival of *P. aeruginosa* PA14 cells exposed to colistin ( $4 \mu\text{g ml}^{-1}$ ), either alone or in combination with **(A)** a sub-inhibitory concentration of tetracycline ( $4 \mu\text{g ml}^{-1}$ ), **(B)** a bacteriostatic concentration of tetracycline ( $32 \mu\text{g ml}^{-1}$ ), or **(C)** a range of tetracycline concentrations, as determined by c.f.u. counts over 8 hours ( $n=4$ ; ns:  $p>0.05$  for colistin and tetracycline-exposed bacteria relative to bacteria exposed to colistin alone). **D-F**, Survival of *P. aeruginosa* PA14 cells exposed to colistin ( $4 \mu\text{g ml}^{-1}$ ), either alone or in combination with **(D)** a sub-inhibitory concentration of chloramphenicol ( $32 \mu\text{g ml}^{-1}$ ), **(E)** a bacteriostatic concentration of chloramphenicol ( $256 \mu\text{g ml}^{-1}$ ), or **(F)** a range of tetracycline concentrations, as determined by c.f.u. counts over 8 hours ( $n=4$ ; ns:  $p>0.05$  for colistin and chloramphenicol-exposed bacteria relative to bacteria exposed to colistin alone). Data in **A-F** were analysed by a two-way ANOVA with Dunnett's post-hoc test. Data are presented as the arithmetic mean, and error bars represent the standard deviation of the mean.

## 4.6 CHIR-090 and cerulenin do not inactivate colistin directly or indirectly

The next plausible confounding factor to control for that could explain the ability of CHIR-090 and cerulenin to block killing of *P. aeruginosa* by colistin was that these inhibitors of LPS biosynthesis directly interfered with the polymyxin drug, for example by binding to the antibiotic. To establish if this hypothesis was correct, checkerboard broth microdilution assays were performed, which allowed detection of any interactions between colistin and CHIR-090/cerulenin that compromised the polymyxin's antibacterial activity against PA14 cells. If indeed either LPS synthesis inhibitor was binding and thereby inactivating colistin, these checkerboard experiments would be expected to reveal an antagonistic growth-inhibitory interaction, with the MICs of the two antimicrobial agents higher in combination than they

were independently. However, it was found that the MICs of colistin and CHIR-090 in combination across the whole range of concentrations tested in the checkerboard matrix were the same as their MICs against *P. aeruginosa* bacteria alone, with a fractional inhibitory concentration index (FICI) value of 2 indicating an “indifferent” effect (**Figure 4.5A**)<sup>625</sup>.

Analogously, the FICI value computed from the checkerboard experiment with colistin and cerulenin was also 2, with no change in the respective MICs of either compound against PA14 cells when used in combination, as opposed to when used alone (**Figure 4.5B**). Thus, the lack of an antagonistic interaction between colistin and either CHIR-090 or cerulenin strongly suggested that the LPS biosynthesis inhibitors were not hindering the polymyxin’s antipseudomonal killing through direct binding/inactivation. It is worth noting that there was also an absence of synergistic growth-inhibitory interactions between colistin and the two LPS synthesis inhibitors, which ruled out the prospect that, in combination with the polymyxin drug, CHIR-090/cerulenin had an enhanced capacity to arrest the growth of *P. aeruginosa* and reduce bacterial killing in the process.

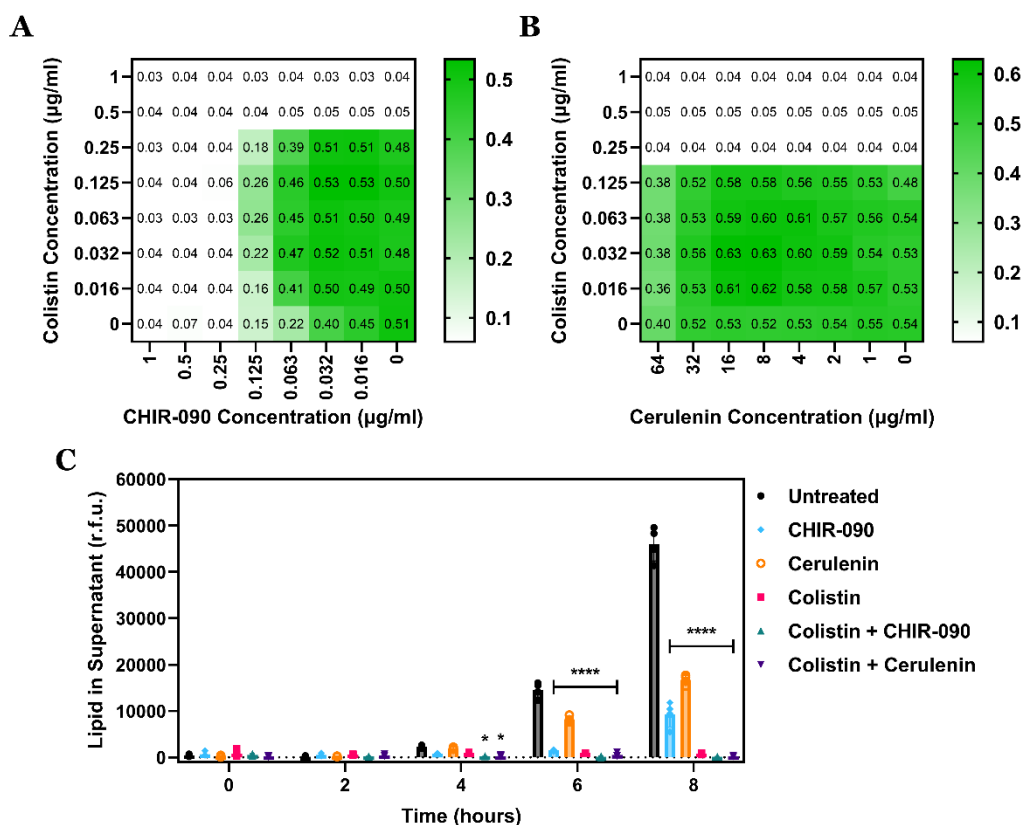


**Figure 4.5: Colistin is inactivated neither directly nor indirectly by CHIR-090/cerulenin.** **A, B**, Checkerboard broth microdilution assays of colistin in combination with **(A)** CHIR-090, or **(B)** cerulenin against *P. aeruginosa* PA14 cells, as determined by measuring bacterial growth after 18 hours incubation using OD<sub>595nm</sub> readings (n=4). **C**, Concentration of lipids in the spent culture supernatant of *P. aeruginosa* PA14 cells exposed to CHIR-090 (0.125 µg ml<sup>-1</sup>), cerulenin (32 µg ml<sup>-1</sup>) or colistin (4 µg ml<sup>-1</sup>), both alone and in combination, as determined by measuring fluorescence from the lipophilic dye FM 4-64 (5 µg ml<sup>-1</sup>) over 8 hours (n=4; \*p<0.05, \*\*\*\*p<0.0001 relative to untreated cells). Data in **C** were analysed by a two-way ANOVA with Dunnett’s post-hoc test. Data are presented as the arithmetic mean, and error bars represent the standard deviation of the mean.

While it was vital to consider and eliminate the likelihood of direct inactivation of colistin by the inhibitors of LPS biosynthesis, it was equally critical to explore the notion that both CHIR-090 and cerulenin may be involved in the indirect and extracellular inactivation of the polymyxin antimicrobial by *P. aeruginosa* cells. In particular, OMVs known to be shed from the majority of Gram-negative organisms, including those in the Pseudomonadaceae family, have been implicated in past studies in causing a loss of colistin activity by binding to antibiotic molecules prior to their attachment to the bacterial surface<sup>668,728</sup>. It was postulated that exposure to CHIR-090/cerulenin could trigger an increase in OMV shedding by PA14 bacteria, augmenting the extracellular inactivation of colistin and hence inhibiting its bactericidal behaviour. In clear opposition to this proposal however, no increase in the release of lipids into the culture supernatant of *P. aeruginosa* was quantified relative to untreated bacteria when the cells were treated with CHIR-090 or cerulenin, either alone or alongside colistin for 8 hours (**Figure 4.5C**). Rather, PA14 cells exposed to either LPS biosynthesis inhibitor had a reduction in the amount of OMVs shed extracellularly compared to when they were not present, undoubtedly excluding even indirect inactivation of colistin as the reason for CHIR-090 and cerulenin's polymyxin-inhibiting properties.

#### **4.7 CHIR-090 and cerulenin do not induce stress responses that confer colistin resistance**

One conceivable basis for the protection conferred by the LPS biosynthesis inhibitors CHIR-090/cerulenin against the killing of *P. aeruginosa* by colistin was that these two antimicrobial compounds produced a stress response in the bacteria that activated the two-component systems PmrAB and PhoPQ. Both these two-component systems function to detect and respond to external environmental signals, for instance the presence of antibiotics that disrupt the cell envelope, through the sensor kinases PmrB and PhoQ respectively<sup>729,730</sup>. In turn, these kinase proteins phosphorylate the transcriptional regulators of the two-component systems, PmrA and PhoP, with these proteins subsequently initiating the expression of a wide variety of genes, including (notably, in this case) operons involved in the addition of the cationic L-Ara4N/pEtN moieties to LPS that mediate colistin non-susceptibility<sup>731,732</sup>. Therefore, there was a direct pathway by which CHIR-090 and cerulenin could elicit damage to the *P. aeruginosa* surface membranes that served as the stimuli for activation of the PmrAB and/or PhoPQ two-component systems, ultimately leading to polymyxin resistance. In order to test whether either inhibitor of LPS synthesis blocked colistin's bactericidal activity through such a stress-induced response, a control assay was undertaken using mutants from the PA14 transposon library with disrupted *pmrA*, *pmrB*, *phoP* and *phoQ* genes<sup>674</sup>.

The suitability of the four transposon mutants for utilisation in experiments was first confirmed by showing that none of the PA14 strains with transposon insertions in the *pmrAB* or *phoPQ* genes displayed any observable growth defects relative to the parental wild-type (WT) strain over 22 hours (**Figure 4.6A**). Moreover, the MICs of the antimicrobial agents colistin, CHIR-090 and cerulenin against the *pmrAB/phoPQ* transposon mutant strains were largely unchanged compared to their MICs against WT PA14 cells, with only a small two-fold increase in the MIC of CHIR-090 identified for the *pmrA:Tn* and *phoP:Tn* strains (**Figure 4.6B**). Thus, the panel of *P. aeruginosa* transposon mutants could be exposed in time-kill experiments to all three antimicrobial compounds at the same concentrations implemented for past assays to assess if the LPS biosynthesis inhibitors antagonised bacterial killing by colistin via interacting with the PmrAB/PhoPQ polymyxin resistance determinants.

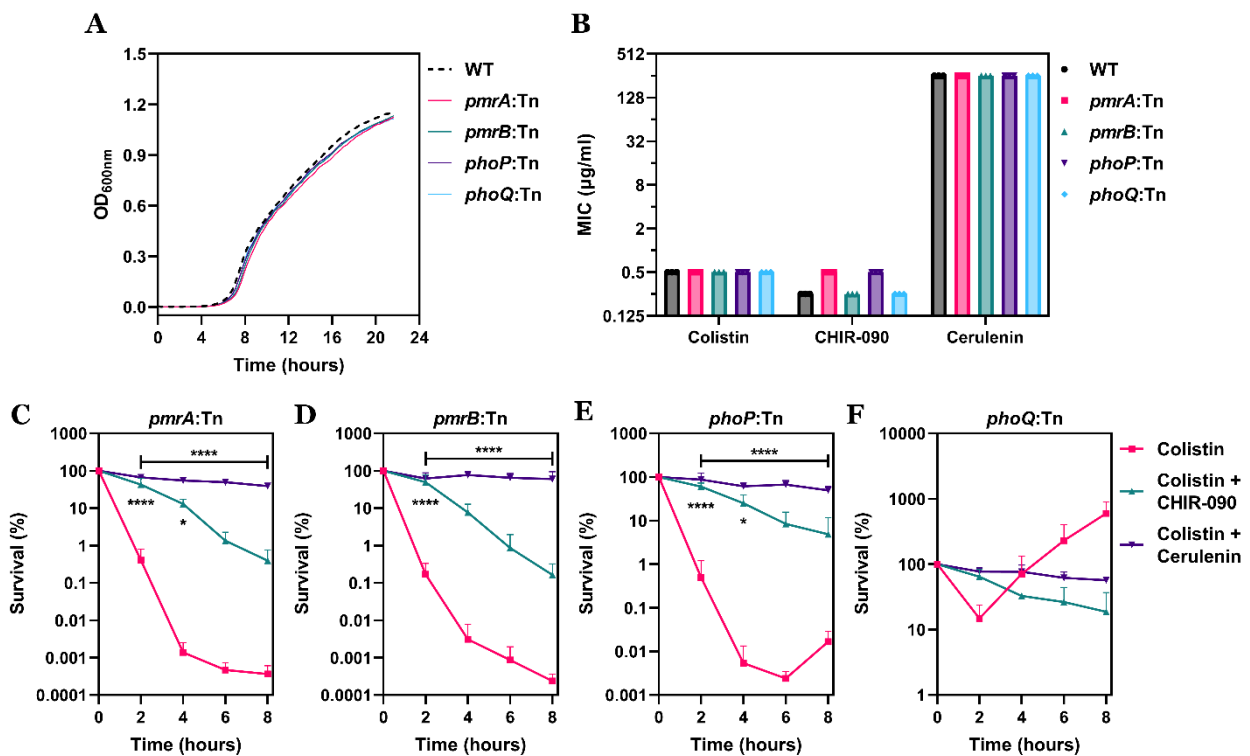


**Figure 4.6: The inhibition of colistin’s bactericidal activity by CHIR-090/cerulenin is not due to induction of a stress response that confers polymyxin resistance.** **A**, Growth kinetics of the *P. aeruginosa* PA14 wild-type (WT) strain, and four PA14 transposon insertion mutants with disrupted *pmrAB* and *phoPQ* genes, as determined by measuring OD<sub>600nm</sub> over 22 hours incubation (n=4; error bars omitted for clarity). **B**, MIC of colistin, CHIR-090 and cerulenin against the *P. aeruginosa* PA14 WT strain, and four PA14 transposon insertion mutants with disrupted *pmrAB* and *phoPQ* genes, as determined using the broth microdilution assay (n=3). **C-F**, Survival of four *P. aeruginosa* PA14 transposon insertion mutants with disrupted genes in **(C)** *pmrA*, **(D)** *pmrB*, **(E)** *phoP* or **(F)** *phoQ* exposed to colistin (4 µg ml<sup>-1</sup>) alone, or in combination with CHIR-090 (0.125 µg ml<sup>-1</sup>) or cerulenin (32 µg ml<sup>-1</sup>), as determined by c.f.u. counts over 8 hours (n=4; \*p<0.05, \*\*\*\*p<0.0001 relative to bacteria exposed to colistin alone). Data in **C-F** were analysed by a two-way ANOVA with Dunnett’s post-hoc test. Data are presented as the arithmetic mean, and error bars shown represent the standard deviation of the mean.

Treatment with colistin alone (4 µg ml<sup>-1</sup>) resulted in marked killing of the *pmrA*:Tn, *pmrB*:Tn and *phoP*:Tn mutant PA14 strains, with a between 5 and 6-log reduction in cell viability following 6 hours of incubation with the polymyxin drug alone (**Figure 4.6CDE**). However, with all three transposon mutants, the addition of sub-inhibitory concentrations of either CHIR-090 or cerulenin caused a significant reduction in colistin's bacterial killing kinetics. This demonstrated that the inhibitors of LPS synthesis were not blocking the polymyxin antibiotic's bactericidal effects by activating the PmrAB/PhoPQ two-component systems, since even when these systems were made dysfunctional by the insertion of transposons into their encoding genes, both CHIR-090 and cerulenin retained their capabilities to prevent colistin-mediated killing of *P. aeruginosa*.

In the mutant strain lacking a functional copy of the *phoQ* gene, colistin possessed considerably less bactericidal activity – a phenotype which has been previously reported (**Figure 4.6F**)<sup>476</sup>. Nevertheless, whilst the polymyxin compound reduced bacterial counts in the *phoQ*:Tn strain by nearly 90% within 2 hours of exposure, when the strain was co-treated with colistin and CHIR-090/cerulenin, there was no cell killing measured at all. This data provided further validation that neither LPS biosynthesis inhibitor impacted colistin's ability to induce *P. aeruginosa* cell death via a PmrAB or PhoPQ-related stress response that culminated in polymyxin resistance.

#### **4.8 The antagonism of CHIR-090 on colistin killing is not due to off-target effects**

Small molecule inhibitor compounds, such as the LpxC inhibitor CHIR-090, are widely understood to often exhibit off-target effects due to non-specific binding to factors other than their primary target<sup>733</sup>. It was hence essential to determine whether the capabilities of CHIR-090 to abrogate killing of *P. aeruginosa* by colistin were a result of the inhibitor's direct action on blocking LPS biosynthesis, or because of any indirect off-target activity of the small molecule compound. This control experiment was performed by first generating strains of PA14 bacteria that had become spontaneously resistant to the antimicrobial properties of CHIR-090. In such CHIR-090-resistant *P. aeruginosa* strains, it is highly likely that non-susceptibility to the LPS synthesis inhibitor's antibacterial effects would have been conferred by mutations to the primary cellular target of the compound (in this instance, the LPS biosynthetic pathway). If CHIR-090 blocked polymyxin-induced killing by acting on the LPS synthesis pathway, it would consequently be expected that the LpxC inhibitor would lose its ability to antagonise colistin killing in CHIR-090-resistant cells. Conversely, if CHIR-090 inhibited colistin's bactericidal activity via an off-target effect, this phenotype would almost certainly be maintained, even in a CHIR-090-resistant *P. aeruginosa* strain.

To produce strains of *P. aeruginosa* PA14 that were resistant to CHIR-090, the bacteria was exposed to a bactericidal concentration of the inhibitor ( $8 \mu\text{g ml}^{-1}$ , 32-fold greater than the MIC) in a well-diffusion assay, which brought about the appearance of spontaneously resistant bacterial colonies within the clear zone of inhibition (**Figure 4.7A**). Two of these colonies were isolated, grown overnight in the absence of CHIR-090, before again being exposed in a well-diffusion experiment to the same concentration of the LPS biosynthesis inhibitor. With one strain, CHIR-090 still produced a zone of inhibition, although this zone was significantly smaller in size than that produced in the wild-type, susceptible PA14 strain, indicating an “intermediate” level of CHIR-090 resistance in this bacterial population. In contrast, in the second isolated strain, no inhibitory zone was produced at all by the LpxC inhibitor, establishing that these *P. aeruginosa* cells were fully resistant to CHIR-090.

As carried out previously with mutant PA14 strains, the growth kinetics and MICs of colistin were measured for the generated CHIR-090-resistant cell populations to check that the acquisition of resistance to the inhibitor was not associated with any fundamental changes in bacterial physiology that could interfere with the reliable use of these strains in assays. Importantly, both the fully CHIR-090-resistant *P. aeruginosa* strain and the strain with intermediate CHIR-090 resistance had a very similar rate of bacterial growth as WT PA14 cells (**Figure 4.7B**). In addition, whilst the MIC of CHIR-090 increased in an expectedly step-wise manner in the two *P. aeruginosa* strains with reduced susceptibility to the LpxC inhibitor (4-fold increase for intermediate-resistant strain, 32-fold increase for fully resistant strain relative to PA14 WT bacteria), there was only a minimal two-fold change in the colistin MIC against both cell populations (**Figure 4.7C**). Having thereby verified that the CHIR-090-resistant strains produced could be acceptably and accurately utilised in experiments, the capacity of the LPS biosynthesis inhibitor to block colistin killing of these *P. aeruginosa* isolates was investigated through time-kill assays.

In the WT PA14 population, the killing of *P. aeruginosa* bacteria by colistin ( $4 \mu\text{g ml}^{-1}$ ) was entirely halted by CHIR-090 even at nanomolar concentrations, with no reduction in cell survival when the strain was co-treated for 8 hours with  $0.005 \mu\text{g ml}^{-1}$  CHIR-090, consistent with past experiments (**Figure 4.7D**). In stark opposition, when the PA14 strain with an intermediate level of CHIR-090 resistance was exposed to colistin along with  $0.005 \mu\text{g ml}^{-1}$  CHIR-090, the killing kinetics were virtually indistinguishable compared to cells treated only with the polymyxin antibiotic, with a loss in bacterial viability of more than 4-logs in both populations (**Figure 4.7E**). Thus, the protective effects of the LPS biosynthesis inhibitor against polymyxin killing were diminished in a CHIR-090-resistant strain. When the concentration of the LpxC inhibitor used in combination with colistin to treat this *P. aeruginosa* isolate with intermediate CHIR-090 resistance was increased to  $0.125 \mu\text{g ml}^{-1}$ ,

colistin's bactericidal activity was once again abolished. However, in the fully CHIR-090-resistant PA14 strain, even this higher inhibitor concentration was unable to stop the polymyxin drug from killing bacteria, with cell counts lowered by 2-logs following 8 hours incubation with colistin (**Figure 4.7F**). In summary, these data together revealed that CHIR-090 did not block colistin-mediated bacterial killing in CHIR-090-resistant *P. aeruginosa*, firmly implying that this LpxC inhibitor prevented the polymyxin from exerting its bactericidal effects not through an off-target effect, but by directly targeting the LPS biosynthetic pathway.

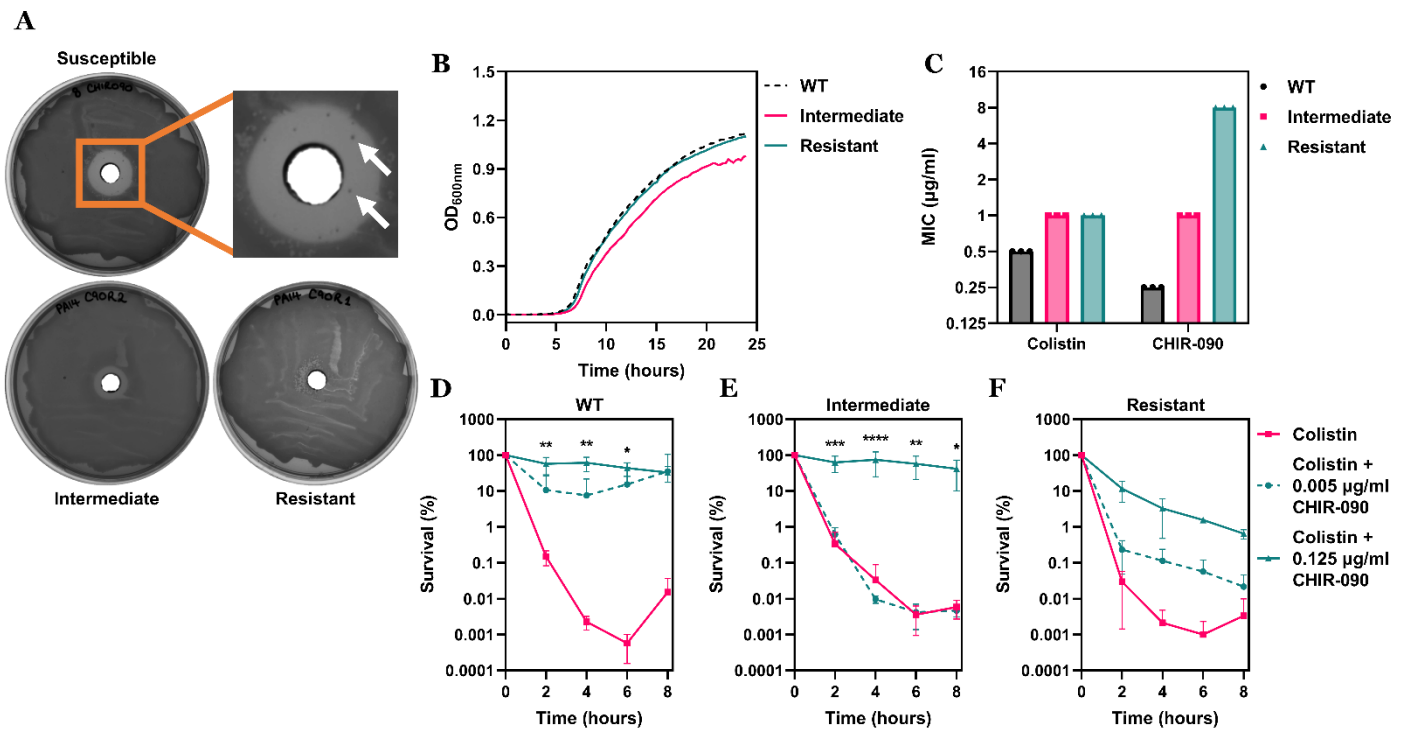


**Figure 4.7: CHIR-090 cannot protect CHIR-090-resistant *P. aeruginosa* from colistin's bactericidal effects.** **A**, Generation of mutants resistant to CHIR-090 by exposing a lawn of *P. aeruginosa* PA14 cells to 8 µg ml<sup>-1</sup> CHIR-090 in a well, before selecting two spontaneously resistant colonies that grew within the zone of inhibition (indicated with white arrows). These colonies consisted of a strain with intermediate resistance to CHIR-090 ("Intermediate"), and a strain that was fully resistant to CHIR-090 ("Resistant"), as confirmed by re-exposing the strains to 8 µg ml<sup>-1</sup> CHIR-090 in a well. **B**, Growth kinetics of the *P. aeruginosa* PA14 wild-type (WT) strain, the "Intermediate" CHIR-090-resistant strain and the fully CHIR-090-resistant strain, as determined by measuring OD<sub>600nm</sub> over 24 hours incubation (n=4; error bars omitted for clarity). **C**, MIC of colistin and CHIR-090 against the *P. aeruginosa* PA14 WT strain, the "Intermediate" CHIR-090-resistant strain and the fully CHIR-090-resistant strain, as determined using the broth microdilution assay (n=3). **D-F**, Survival of **(D)** the *P. aeruginosa* PA14 WT strain, **(E)** the "Intermediate" CHIR-090-resistant strain, or **(F)** the fully CHIR-090-resistant strain exposed to colistin alone (4 µg ml<sup>-1</sup>), or colistin in combination with a range of concentrations of CHIR-090, as determined by c.f.u. counts over 8 hours (n=4; \*p<0.05, \*\*p<0.01, \*\*\*p<0.001, \*\*\*\*p<0.0001 relative to bacteria exposed to colistin alone). Data in **D-F** were analysed by a two-way ANOVA with Dunnett's post-hoc test. Data are presented as the arithmetic mean, and error bars shown represent the standard deviation of the mean.



## 4.9 LPS concentrations in the outer membrane are unaffected by CHIR-090 and cerulenin

After completing these control experiments to prove that the small molecule compounds CHIR-090 and cerulenin modulated colistin killing of *P. aeruginosa* specifically and not through off-target effects (growth arrest, antibiotic inactivation, induction of resistance), it was hypothesised that the blocking of *de novo* LPS biosynthesis by the two inhibitors reduced LPS levels in the OM of the bacteria in order to prevent the polymyxin's antipseudomonal activity. LPS molecules that constitute the extracellular-facing outermost leaflet of the OM bilayer structure are the principal cellular target to which colistin binds in the initial step of its bactericidal mode of action. It was considered that the direct impact of CHIR-090/cerulenin on the LPS biosynthetic pathway could lower the concentration of LPS present in the OM, decreasing the number of bacterial targets to which colistin could attach to and, in the process, inhibit killing of cells by the polymyxin antibiotic. To examine this hypothesis, it was decided to measure LPS amounts in the OM of *P. aeruginosa* PA14 exposed to sub-inhibitory concentrations of CHIR-090/cerulenin through two distinct approaches.

The first method involved the extremely sensitive and widely-used immunogenic Limulus amoebocyte lysate (LAL) assay<sup>633</sup>. Following treatment of *P. aeruginosa* with CHIR-090 and cerulenin for 2 hours, the bacterial OM was extracted using EDTA, and the concentration of LPS in the OM of these cells compared to LPS levels in the OM of untreated bacteria. No significant differences were observed in the amount of LPS, quantified by the LAL assay, in the OM of PA14 cells exposed to either inhibitor of LPS biosynthesis, indicating that at the sub-lethal concentrations used, CHIR-090 and cerulenin were not affecting OM LPS levels (**Figure 4.8A**).

In order to corroborate this key data, a second technique for measuring LPS concentrations directly on whole bacterial cells (as opposed to extracted OM samples) was developed by synthesising a fluorescently-labelled LPS-specific probe, BoDipy-PMBN. PMBN (polymyxin B nonapeptide) is a modified form of colistin and polymyxin B that lacks the characteristic fatty acyl tail of polymyxin antibiotic drugs, and therefore possess no antibacterial activity<sup>734</sup>. Nonetheless, PMBN molecules still have a cationic polypeptide macrocycle structure, meaning they retain a strong affinity for LPS molecules even in the absence of a hydrophobic lipid tail<sup>735</sup>. By labelling PMBN with a fluorescent BoDipy tag, a non-toxic probe was generated with a very high degree of specificity for LPS that could be utilised for not only detecting, but also quantifying, LPS levels on the bacterial cell surface. Indeed, fluorescently-tagged forms of PMBN (e.g. dansyl-PMBN) have previously been used to specifically determine the spatial distribution of LPS in whole cells<sup>736,737</sup>. Mass spectrometry confirmed successful labelling of PMBN with a single BoDipy fluorophore (**Figure 4.8B**).

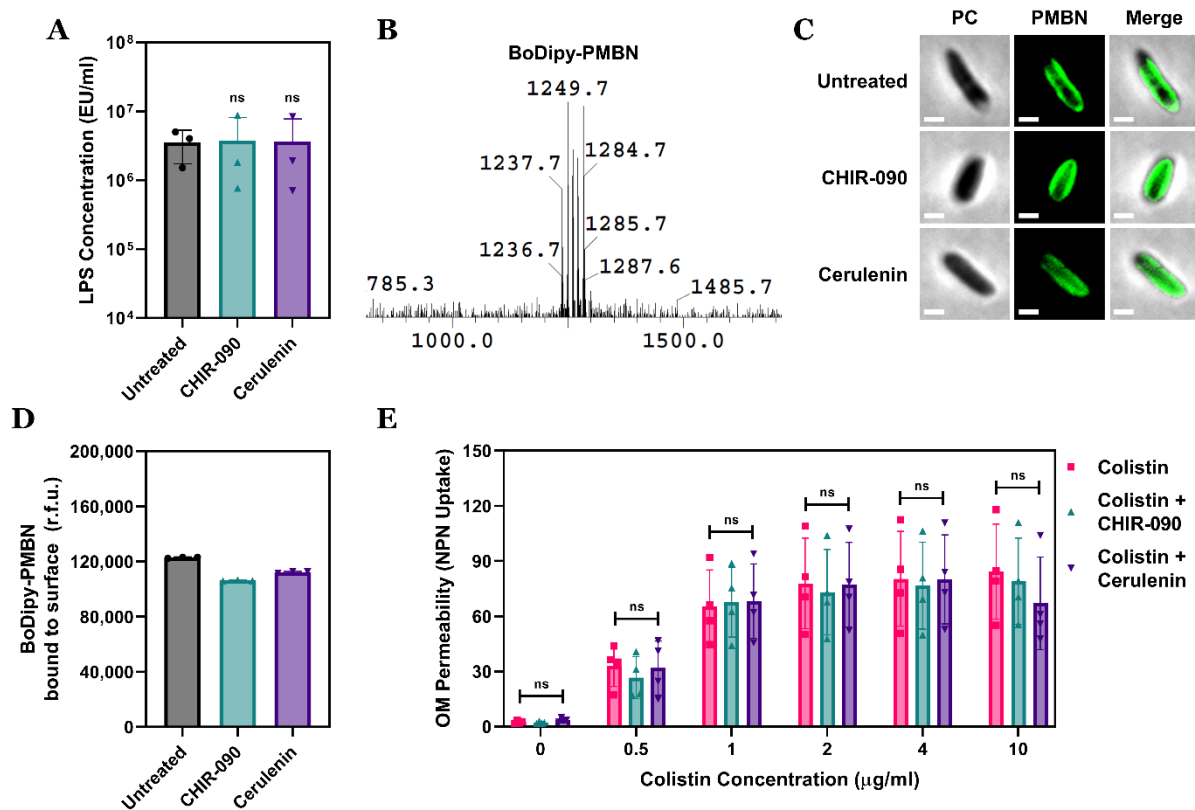


**Figure 4.8: The LPS synthesis inhibitors CHIR-090/cerulenin do not reduce LPS levels in the OM of *P. aeruginosa*.** **A**, Concentration of LPS in the OM extracted from *P. aeruginosa* PA14 cells exposed, or not, to CHIR-090 (0.125  $\mu\text{g ml}^{-1}$ ) and cerulenin (32  $\mu\text{g ml}^{-1}$ ) for 2 hours, as determined using the LAL assay ( $n=3$ ; ns:  $p>0.05$  relative to untreated cells). **B**, Mass spectrum of polymyxin B nonapeptide (PMBN) tagged with a single BoDipy fluorophore, with successful BoDipy-labelling confirmed by detection of chemical species at the expected molecular mass (1237.7  $\text{g mol}^{-1}$  for BoDipy-PMBN). **C**, Visualisation using the LPS-specific fluorescent probe BoDipy-PMBN (7  $\mu\text{g ml}^{-1}$ ) of LPS molecules in the bacterial surface of *P. aeruginosa* PA14 cells exposed, or not, to CHIR-090 (0.125  $\mu\text{g ml}^{-1}$ ) and cerulenin (32  $\mu\text{g ml}^{-1}$ ) for 2 hours, by fluorescence microscopy (images are representative of multiple cells visualised across 3 independent experiments; PC: phase contrast; Scale bars: 5  $\mu\text{m}$ ). **D**, Quantification of BoDipy-PMBN (7  $\mu\text{g ml}^{-1}$ ) bound to the bacterial surface of *P. aeruginosa* PA14 cells exposed, or not, to CHIR-090 (0.125  $\mu\text{g ml}^{-1}$ ) and cerulenin (32  $\mu\text{g ml}^{-1}$ ) for 2 hours ( $n=3$ ). **E**, Permeabilisation of the OM of *P. aeruginosa* PA14 cells exposed to a range of colistin concentrations, either alone or in combination with CHIR-090 (0.125  $\mu\text{g ml}^{-1}$ ) and cerulenin (32  $\mu\text{g ml}^{-1}$ ), as determined by measuring uptake of the NPN fluorophore (10  $\mu\text{M}$ ) over 10 minutes ( $n=4$ , each data point represents the arithmetic mean of 20 replicate measurements; ns:  $p>0.05$  relative to bacteria exposed to colistin alone). Data in **A** were analysed by a one-way ANOVA with Dunnett's post-hoc test. Data in **E** were analysed by a two-way ANOVA with Dunnett's post-hoc test. Data are presented as the arithmetic mean, and error bars represent the standard deviation of the mean.

To assess whether exposure of *P. aeruginosa* to CHIR-090 or cerulenin caused a drop in OM LPS levels using BoDipy-PMBN, PA14 cells were treated with the LPS biosynthesis inhibitors for 2 hours, before the bacteria were incubated alongside the fluorescent PMBN compound for 30 minutes to allow the probe to bind specifically to LPS molecules on the cellular surface. The *P. aeruginosa* bacteria were then visualised by fluorescent microscopy,

where it was found that the BoDipy-PMBN compounds attached to otherwise untreated cells were localised to the external bacterial envelope, substantiating the probe's specificity for surface LPS structures (**Figure 4.8C**). Critically, there was no obvious reduction in the extent of fluorescence from bound BoDipy-PMBN in PA14 cells pre-exposed to either CHIR-090 or cerulenin, suggesting that – at the concentrations used – the inhibitors of LPS synthesis had minimal influence on the concentration of LPS in the OM of bacteria. To overcome any potential biases from looking at individual cells by microscopy, fluorescence from cell-bound BoDipy-PMBN molecules was additionally quantified for all three treatment conditions across the whole *P. aeruginosa* populations using a fluorescent multiwell plate reader. This showed that exposure of PA14 cells to neither of the LPS biosynthesis inhibitors triggered a reduction in BoDipy-PMBN attachment to the bacterial surface, supporting the data from the LAL assay that sub-lethal doses of CHIR-090/cerulenin did not lower the amount of LPS present in the OM (**Figure 4.8D**).

Whilst these results clearly signified that decreasing OM LPS concentrations was very unlikely to be the explanation for CHIR-090 and cerulenin's abilities to block polymyxin-mediated killing, it was crucial to actually explore how colistin's OM-disrupting behaviour against *P. aeruginosa* cells was affected by the LPS biosynthesis inhibitors for this possibility to be conclusively eliminated. This was conducted by measuring uptake of the fluorescent NPN dye, a well-established marker of the OM permeabilisation induced by colistin in the first step of the antibiotic's mechanism of bacterial killing, in PA14 bacteria treated with the polymyxin alone or in combination with CHIR-090/cerulenin<sup>626</sup>. In *P. aeruginosa* populations exposed only to colistin, there was a dose-dependent increase in NPN uptake across a range of antibiotic concentrations, with the polymyxin drug initiating greater permeabilisation of the bacterial OM at higher doses (**Figure 4.8E**). However, in the presence of CHIR-090 or cerulenin, there was no significant reduction in the degree of colistin-induced NPN uptake at any of the antibiotic concentrations tested, definitively demonstrating that the LPS synthesis inhibitors did not abrogate the polymyxin's bactericidal activity against *P. aeruginosa* by lowering the amount of LPS in the OM to prevent colistin from damaging this bilayer structure.

#### **4.10 Inhibiting LPS biosynthesis reduces colistin's binding to *P. aeruginosa***

Although it had been ruled out that CHIR-090 and cerulenin altered polymyxin killing of *P. aeruginosa* by reducing OM LPS levels, it was yet to be illustrated whether or not the two LPS synthesis inhibitors had any effects on colistin's ability to bind to the bacterial cell surface envelope. To investigate this, the fluorescent antibiotic molecule BoDipy-colistin that was

generated and implemented in previous assays was again employed for assessing how attachment of the polymyxin drug to PA14 cells was changed during co-exposure with either CHIR-090 or cerulenin. Prior to this experiment being performed, it was necessary to authenticate that the labelling of colistin with a fluorescent BoDipy tag had not modified the antibiotic's fundamental properties – in this case, the dependence on *de novo* LPS biosynthesis for its antipseudomonal bactericidal activity. To account for the partial reduction in the potency of BoDipy-colistin relative to the untagged polymyxin compound (2-fold increase in MIC), a *P. aeruginosa* population was treated with a slightly higher, but still therapeutically-relevant, concentration of the fluorescent antibiotic ( $5 \mu\text{g ml}^{-1}$ ) than that used in past assays with unlabelled colistin ( $4 \mu\text{g ml}^{-1}$ ), with measurements of bacterial survival obtained over 8 hours in the presence and absence of CHIR-090/cerulenin. Analogously to untagged colistin, both inhibitors of LPS biosynthesis at sub-lethal concentrations strikingly halted BoDipy-colistin-induced killing of PA14 bacteria, with an approximately 5-log difference in viable colony counts compared to cells treated only with BoDipy-colistin at 6 hours (**Figure 4.9A**). Hence, the fluorescently labelled form of colistin was behaving equivalently to the original, unaltered polymyxin compound.

After verifying the appropriateness of BoDipy-colistin for use in binding experiments, the amount of the fluorescent antibiotic attached to the surface of *P. aeruginosa* cells was evaluated over 8 hours exposure to the polymyxin alone, or in combination with CHIR-090 and cerulenin. In bacteria treated only with BoDipy-colistin, there was a rapid, immediate and high level of binding of the fluorescent polymyxin drug to PA14 cells within the first two hours of the assay, which was maintained throughout the subsequent 6 hours (**Figure 4.9B**). By contrast, when active LPS biosynthesis was blocked by either small molecule inhibitor compound, the extent of BoDipy-colistin binding to *P. aeruginosa* was noticeably reduced, with the fluorescently-labelled antibiotic accumulating and attaching to bacterial cells much more slowly. This finding was validated by quantifying the residual amount of BoDipy-colistin left in the culture supernatant following 2 hours exposure of *P. aeruginosa* PA14 to the fluorescent polymyxin under the same three treatment conditions. The decrease in the concentration of BoDipy-colistin in the spent culture supernatant relative to the start of the experiment was the largest and significantly greater when *de novo* LPS biosynthesis was occurring, compared to when it was inhibited with CHIR-090/cerulenin (**Figure 4.9C**). This data provided supplementary proof that blocking the synthesis of LPS caused a drop in the binding of colistin to *P. aeruginosa*.

In summary, the inhibitors CHIR-090 and cerulenin did not lower the amount of LPS present in the bacterial OM (the primary cellular target to which colistin attaches), but they did reduce the binding of colistin to *P. aeruginosa*. The implication of this apparent paradox

is that colistin must additionally bind to the bacteria at a site other than LPS in the OM of the cell envelope. Interestingly, despite the marked differences in the binding of BoDipy-colistin to PA14 cells during combination treatment with CHIR-090/cerulenin, the LPS biosynthesis inhibitors had no impact on the bacterial attachment of BoDipy-PMBN. The lack of the fatty acyl tail in the chemical structure of PMBN is thought to prevent this molecule from penetrating Gram-negative organisms further than their OM, however colistin compounds do possess a hydrophobic lipid tail and thus can access the cell envelope beyond simply the OM bilayer. Because CHIR-090 and cerulenin mediated their influence to decrease bacterial binding on colistin, but not PMBN, attention turned to the role these inhibitors could play on *P. aeruginosa* surface structures below the OM – namely, the cytoplasmic membrane (CM).

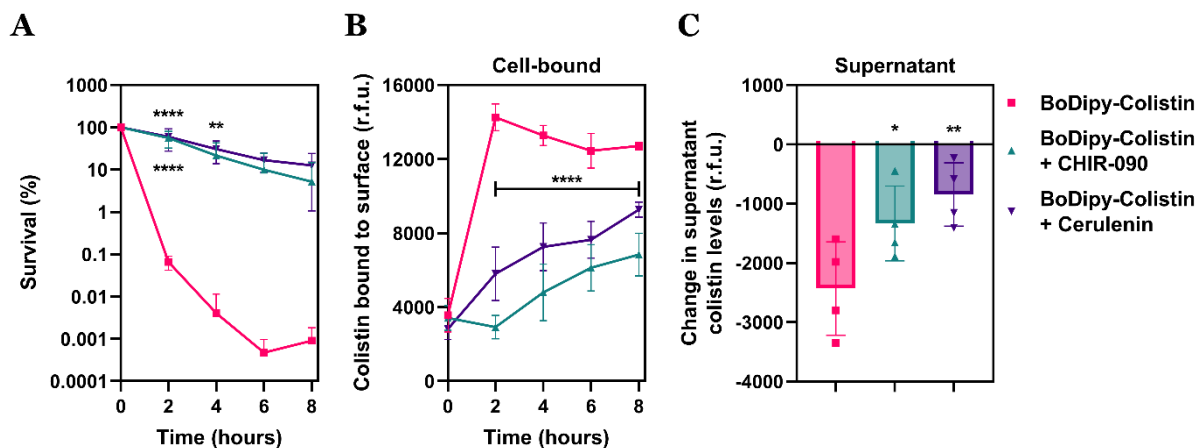


**Figure 4.9: Colistin binding to *P. aeruginosa* is reduced by blocking active LPS synthesis.** **A**, Survival of *P. aeruginosa* PA14 cells exposed to BoDipy-colistin (5 μg ml<sup>-1</sup>), alone and in combination with sub-inhibitory concentrations of CHIR-090 (0.125 μg ml<sup>-1</sup>) or cerulenin (32 μg ml<sup>-1</sup>), as determined by c.f.u. counts over 8 hours (n=4; \*\*p<0.01, \*\*\*\*p<0.0001 relative to bacteria exposed to BoDipy-colistin alone). **B**, Quantification of BoDipy-colistin (5 μg ml<sup>-1</sup>) bound to *P. aeruginosa* PA14 cells exposed to the antibiotic alone and in combination with sub-inhibitory concentrations of CHIR-090 (0.125 μg ml<sup>-1</sup>) or cerulenin (32 μg ml<sup>-1</sup>), as determined by measuring fluorescence of bacteria over 8 hours (n=4; \*\*\*\*p<0.0001 for CHIR-090/cerulenin-treated cells relative to bacteria exposed to BoDipy-colistin alone). **C**, Reduction relative to the start of the assay in the quantity of BoDipy-colistin (5 μg ml<sup>-1</sup>) in the spent culture supernatant of *P. aeruginosa* PA14 cells exposed to the antibiotic alone and in combination with sub-inhibitory concentrations of CHIR-090 (0.125 μg ml<sup>-1</sup>) or cerulenin (32 μg ml<sup>-1</sup>), as determined by measuring fluorescence in the culture supernatant after 2 hours (n=4; \*p<0.05, \*\*p<0.01 relative to bacteria exposed to BoDipy-colistin alone). Data in **A**, **B** were analysed by a two-way ANOVA with Dunnett's post-hoc test. Data in **C** were analysed by a one-way ANOVA with Dunnett's post-hoc test. Data are presented as the arithmetic mean, and error bars represent the standard deviation of the mean.

#### 4.11 Polymyxin compounds do not bind to or inhibit growth of Gram-positive bacteria

It has previously been stated in numerous studies that in colistin's bactericidal mechanism of action against Gram-negative organisms, once the polymyxin antibiotic has bound to LPS and disrupted the OM, it traverses the periplasm and damages the CM through a surfactant-like effect by interacting with membrane phospholipids in the bilayer structure<sup>392</sup>. However, the preceding discoveries here that inhibiting LPS biosynthesis reduced colistin's accumulation at the surface of *P. aeruginosa* and the ensuing bacterial killing, but not by depleting LPS levels at the OM, raised the intriguing possibility that CHIR-090/cerulenin may be mediating this phenotype by modulating the abundance of LPS in the CM, where the polysaccharide molecules reside while in transit to the OM. Before this theory could be fully considered, it was vital to first examine if colistin did indeed bind and permeabilise membrane phospholipid bilayers, as claimed in past literature. To do this, the two synthesised fluorescently-labelled polymyxin compounds (BoDipy-colistin and BoDipy-PMBN) were incubated with the SH1000 reference strain of the Gram-positive pathogen *S. aureus*, where the CM was formed of only a phospholipid bilayer. The capacity for these BoDipy-tagged molecules to bind to the *S. aureus* cell envelope was then compared using fluorescence microscopy to their binding capacity to *P. aeruginosa* PA14 cells, a Gram-negative species where both bacterial surface bilayers (the OM and the CM) contain LPS.

Both BoDipy-colistin and BoDipy-PMBN bound extensively to the cell surface of *P. aeruginosa* bacteria after 4 hours of antibiotic exposure, as evidenced by an accumulation of the fluorescent polymyxin drugs around the perimeter of the PA14 cells (**Figure 4.10A**). In opposition, no binding of either BoDipy-colistin or BoDipy-PMBN was detectable at all by 4 hours in *S. aureus* SH1000 cells, indicating that these polymyxin compounds did not bind to phospholipid bilayer membranes which were absent in LPS molecules. This observation was reinforced by quantifying the binding of the BoDipy-labelled polymyxins over an 8 hour experiment with a wider panel of Gram-positive and Gram-negative organisms, including clinical isolates of *K. pneumoniae* (Gram-negative) and Group A *Streptococcus* (Gram-positive). BoDipy-colistin, as well as BoDipy-PMBN, displayed a high propensity to bind to the Gram-negative strains of *P. aeruginosa* and *K. pneumoniae*, with the attachment of the fluorescent polymyxin compounds to both bacteria rising prominently over the first two hours of the assay (**Figure 4.10BC**). On the other hand, binding of the BoDipy-tagged polymyxin structures to the Gram-positive bacteria *S. aureus* and *S. pyogenes* was virtually non-existent, with no increase in fluorescence from cell-bound BoDipy-colistin/BoDipy-PMBN apparent throughout the 8 hour incubation relative to the start of the experiment. This strongly signalled that polymyxins did not, in fact, interact with membrane phospholipid bilayers.

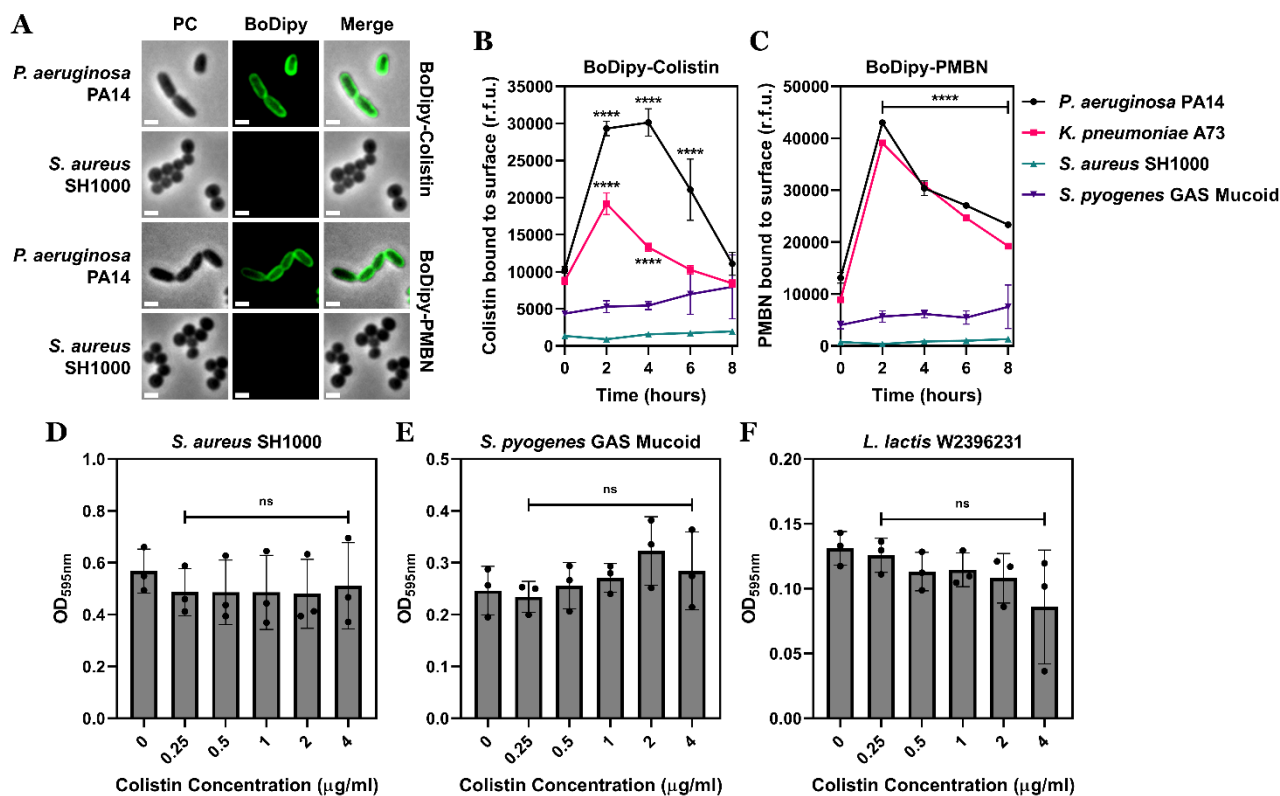


**Figure 4.10: Colistin is unable to bind to Gram-positive organisms or inhibit their growth.**

**A**, Visualisation by fluorescence microscopy of BoDipy-colistin ( $5 \mu\text{g ml}^{-1}$ ) or BoDipy-PMBN ( $7 \mu\text{g ml}^{-1}$ ) bound to the bacterial surface of *P. aeruginosa* PA14 cells or *S. aureus* SH1000 cells after 4 hours incubation (images are representative of cells visualised across 3 independent experiments; PC: phase contrast; Scale bars:  $5 \mu\text{m}$ ). **B**, **C**, Quantification of binding of **(A)** BoDipy-colistin ( $5 \mu\text{g ml}^{-1}$ ), or **(B)** BoDipy-PMBN ( $7 \mu\text{g ml}^{-1}$ ) to a panel of Gram-positive (*S. aureus*, *S. pyogenes*) and Gram-negative (*P. aeruginosa*, *K. pneumoniae*) bacteria, as determined by measuring fluorescence of bacteria over 8 hours ( $n=3$ ;  $****p<0.0001$  for both Gram-negative organisms relative to either Gram-positive species). **D-F**, Growth of **(D)** *S. aureus* SH1000 cells, **(E)** a clinical isolate of Group A *S. pyogenes* or **(F)** *L. lactis* W2396231 cells following 18 hours exposure to a range of therapeutically-relevant colistin concentrations, as determined by obtaining OD<sub>595nm</sub> measurements ( $n=3$  in triplicate; ns:  $p>0.05$  for all colistin concentrations relative to untreated cells). Data in **B**, **C** were analysed by a two-way ANOVA with Tukey's post-hoc test. Data in **D-F** were analysed by a one-way ANOVA with Dunnett's post-hoc test. Data are presented as the arithmetic mean, and error bars represent the standard deviation of the mean.

In order to expand this finding even further, specifically looking at colistin's ability to disrupt rather than simply bind to phospholipid bilayer structures, the antibacterial growth inhibitory properties of the polymyxin drug against three Gram-positive organisms (*S. aureus*, *S. pyogenes*, *Lactococcus lactis*) were tested across a range of clinically-relevant colistin concentrations ( $0.25$  to  $4 \mu\text{g ml}^{-1}$ ) in a broth microdilution assay. None of the colistin concentrations with any of the Gram-positive strains that all had a CM composed of a phospholipid bilayer exhibited an impact on reducing the growth of bacteria, even after 18 hours of antibiotic exposure, with no significant differences in the OD<sub>595nm</sub> readings compared

to the untreated control populations in every case (**Figure 4.10DEF**). Combined, these data patently challenged the widely-held dogma that colistin exerts its bactericidal effects by damaging the CM through a detergent-like interaction with membrane phospholipids within the bilayer, since the polymyxin antibiotic was unable to attach to or permeabilise the phospholipid bilayer CM of Gram-positive bacteria.

#### **4.12 Blocking LPS biosynthesis lowers the abundance of LPS in the cytoplasmic membrane**

Having shown that colistin was unable to disrupt CM bilayers through binding to membrane phospholipids, the postulation that the LPS biosynthesis inhibitors CHIR-090 and cerulenin blocked colistin-induced killing of *P. aeruginosa* by diminishing LPS levels in the bacterial CM could now be explored. Before determining the effect of exposure to CHIR-090/cerulenin on LPS concentrations in the CM of *P. aeruginosa* cells, it was first necessary to produce spheroplasts from PA14 bacteria that lacked an OM and a cell wall, with the cell surface envelope comprised solely of a CM. This conversion of *P. aeruginosa* from whole cells into spheroplasts enabled only LPS abundance in the CM to be specifically probed for, without the confounding factor of LPS present in the OM. Spheroplasts were generated by the well-established technique frequently used for spheroplast formation in other Gram-negative organisms, which involved treating PA14 cells with EDTA (to remove the OM), lysozyme (to digest the cell wall) and trypsin (to remove periplasmic proteins)<sup>637</sup>. The absence of a peptidoglycan cell wall structure meant that the resulting *P. aeruginosa* spheroplasts were osmotically-fragile, and had to be maintained in an hypertonic environment (20% sucrose) for viability. To ensure that PA14 whole cells had been successfully converted to OM/cell wall-lacking spheroplasts, a panel of assays were undertaken.

The most basic, opening experiment to attest the correct formation of *P. aeruginosa* spheroplasts was microscopic visualisation of PA14 cells both before and after exposure to EDTA, lysozyme and trypsin. The untreated *P. aeruginosa* whole cells appeared in their typical rod-shape morphology; contrastingly, however, cells where removal of the bacterial OM and cell wall had been attempted were spherical in nature – a characteristic trait of spheroplasts that was a firm indicator of complete cell wall digestion (**Figure 4.11A**)<sup>738</sup>. Quantification of this revelation by calculating the length:width ratio across 250 PA14 whole cells and spheroplasts demonstrated that while untreated *P. aeruginosa* cells were approximately 2 to 3-fold longer than they were wide, the spheroplasts generated had a mean length:width ratio of exactly 1, suggesting successful spheroplast formation across the entire bacterial population (**Figure 4.11B**). The next validation assay investigated the stability of the *P. aeruginosa*



spheroplasts produced when these cell forms were not maintained in an osmoprotective media. Incubation at 30°C in Tris buffer without additional sucrose resulted in swift and severe lysis of the spheroplasts formed from PA14 whole cells, with OD<sub>595nm</sub> readings reduced more than 8-fold over 4 hours compared to at the start of the experiment (**Figure 4.11C**). Opposingly, when generated *P. aeruginosa* spheroplasts were incubated under the same conditions in Tris buffer containing 20% sucrose, there was no decrease in OD<sub>595nm</sub> measurements whatsoever even by 4 hours, with this stability and lack of lysis in hypertonic solutions convincing proof of proper spheroplast conversion.

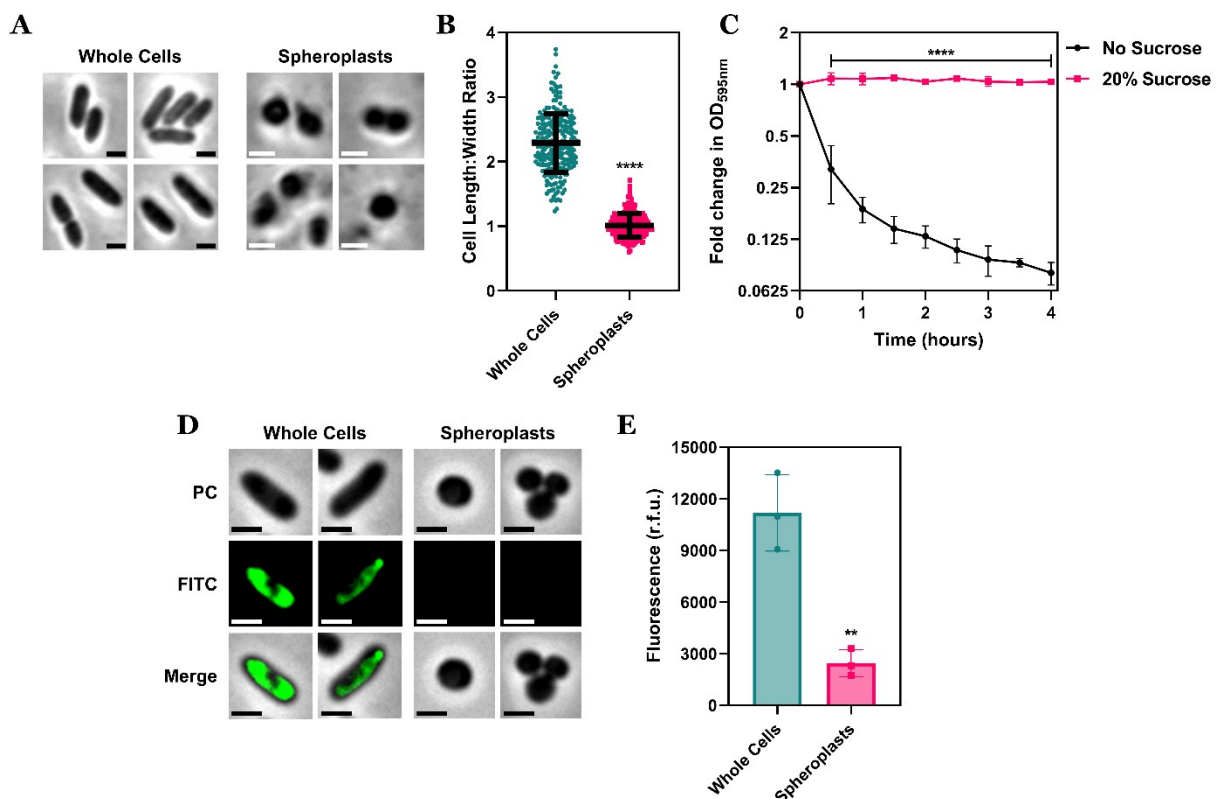


**Figure 4.11: Spheroplasts generated from *P. aeruginosa* have a spherical morphology, are osmotically-fragile and have no OM contamination in the CM.** **A**, Visualisation by phase contrast microscopy of *P. aeruginosa* PA14 whole cells before and after treatment with EDTA (0.25 mg ml<sup>-1</sup>), lysozyme (1 mg ml<sup>-1</sup>) and trypsin (0.5 mg ml<sup>-1</sup>) to produce spheroplasts lacking an OM and cell wall (images are representative of cells visualised across 3 independent experiments; Scale bars: 5 µm). **B**, Quantification of length:width ratio of *P. aeruginosa* PA14 whole cells before/after treatment with EDTA, lysozyme and trypsin to produce spheroplasts (n=250 cells per group; \*\*\*\*p<0.0001 relative to whole cells). **C**, Lysis of *P. aeruginosa* PA14 spheroplasts during exposure to EDTA, lysozyme and trypsin in Tris buffer with and without 20% sucrose, as determined by measuring OD<sub>595nm</sub> over 4 hours incubation at 30°C (n=4; \*\*\*\*p<0.0001 relative to spheroplasts without sucrose). **D**, Visualisation by fluorescence microscopy of *P. aeruginosa* PA14 whole cells labelled with FITC (0.5 mg ml<sup>-1</sup>) to tag OM proteins before/after treatment with EDTA, lysozyme and trypsin to produce spheroplasts (images are representative of cells visualised across 3 independent experiments; PC: phase contrast; Scale bars: 5 µm). **E**, Quantification of fluorescence from FITC-labelled OM proteins in *P. aeruginosa* whole cells before/after treatment with EDTA, lysozyme and trypsin to produce spheroplasts (n=3 in triplicate; \*\*p<0.01 relative to whole cells). Data in **B**, **E** were analysed by a two-tailed unpaired Student's *t*-test. Data in **C** were analysed by a two-way ANOVA with Sidak's post-hoc test. Data are presented as the arithmetic mean, and error bars represent the standard deviation of the mean.

While these data were indicative of cell wall removal during the production of *P. aeruginosa* spheroplasts, it was similarly important to verify that the OM of the bacteria had been removed in the process, especially because future assays required CM LPS amounts to be evaluated when OM LPS was non-existent. To definitively confirm that the OM had been extracted from spheroplasts of PA14 cells, proteins in this extracellular-facing surface bilayer of *P. aeruginosa* whole cells were labelled with a fluorescein isothiocyanate (FITC) fluorophore by a commonly-adopted approach prior to the spheroplast conversion protocol being initiated<sup>638</sup>. Cells were then imaged by fluorescence microscopy at the beginning and end of the EDTA/lysozyme/trypsin treatment, and the degree of fluorescence from FITC-tagged OM proteins was compared. Whereas untreated cells of *P. aeruginosa* PA14 had a strong fluorescent signal around the exterior of bacteria due to the labelling of protein in the OM bilayer, spheroplasts formed from these whole cells had no FITC fluorescence detectable at all (**Figure 4.11D**). Assessing the FITC fluorescent signal in the entire spheroplast/whole cell populations corroborated this microscopic analysis, with a drastically lower level of fluorescence from OM-tagged proteins after the attempted generation of *P. aeruginosa* spheroplasts (**Figure 4.11E**). Together, these data unambiguously depicted that the protocol used for converting whole bacterial cells to spheroplasts was optimal, and successfully removed the cell wall and the OM structures, with no significant contamination of the residual CM with OM material.

To ascertain whether exposure to the LPS biosynthesis inhibitors CHIR-090 or cerulenin caused a depreciation in the amount of LPS present in the CM of *P. aeruginosa*, PA14 whole cells were treated with sub-inhibitory concentrations of the small molecule compounds for 2 hours before they were converted to spheroplasts using the now fully-validated method. The two techniques for quantifying LPS abundance utilised earlier in the OM of whole bacterial cells – namely the LAL assay and binding of BoDipy-PMBN – were then applied to the generated *P. aeruginosa* spheroplasts for computation of the amount of LPS present in the CM when synthesis of LPS was blocked. Through the sensitive immunogenic LAL assay, LPS was, as expected, detected in the CM of untreated PA14 spheroplasts at a concentration that was approximately 100-fold less than LPS levels at bacteria's OM (**Figure 4.12A**). Critically, *P. aeruginosa* cells pre-treated with CHIR-090/cerulenin to inhibit LPS biosynthesis prior to spheroplast conversion had a significant reduction in the amount of LPS in the CM compared to previously untreated spheroplasts. Therefore, the blocking of *de novo* LPS synthesis by either small molecule inhibitor seemed to have the effect of lowering the abundance of CM LPS.

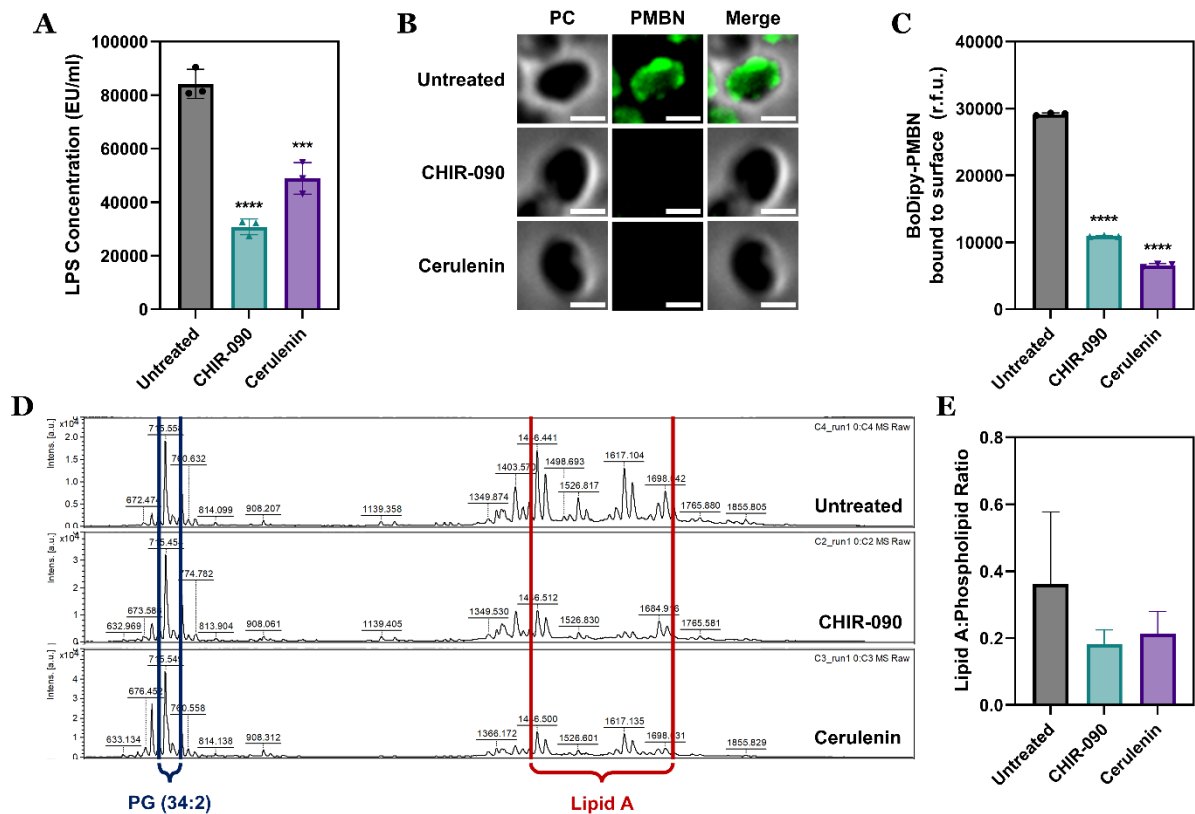


**Figure 4.12: Inhibition of LPS biosynthesis with CHIR-090/cerulenin reduces LPS levels in the CM of *P. aeruginosa*.** **A**, Concentration of LPS in the CM of spheroplasts produced from *P. aeruginosa* PA14 cells pre-exposed, or not, to CHIR-090 (0.125  $\mu\text{g ml}^{-1}$ ) and cerulenin (32  $\mu\text{g ml}^{-1}$ ) for 2 hours before conversion to spheroplasts, as determined using the LAL assay ( $n=3$ ;  $***p<0.001$ ,  $****p<0.0001$  relative to previously untreated spheroplasts). **B**, Visualisation by fluorescence microscopy using BoDipy-PMBN (7  $\mu\text{g ml}^{-1}$ ) of LPS molecules in the CM surface of spheroplasts produced from *P. aeruginosa* PA14 cells pre-exposed, or not, to CHIR-090 (0.125  $\mu\text{g ml}^{-1}$ ) and cerulenin (32  $\mu\text{g ml}^{-1}$ ) for 2 hours before conversion to spheroplasts (images are representative of multiple cells visualised across 3 independent experiments; PC: phase contrast; Scale bars: 5  $\mu\text{m}$ ). **C**, Quantification of fluorescence from BoDipy-PMBN (7  $\mu\text{g ml}^{-1}$ ) bound to the CM surface of spheroplasts produced from *P. aeruginosa* PA14 cells pre-exposed, or not, to CHIR-090 (0.125  $\mu\text{g ml}^{-1}$ ) and cerulenin (32  $\mu\text{g ml}^{-1}$ ) for 2 hours before conversion to spheroplasts ( $n=3$ ;  $****p<0.0001$  relative to previously untreated spheroplasts). **D**, Lipidomic MALDI-TOF mass spectra showing the abundance of lipid A and the membrane phospholipid phosphatidylglycerol (PG) 34:2 in spheroplasts produced from *P. aeruginosa* PA14 cells pre-exposed, or not, to CHIR-090 (0.125  $\mu\text{g ml}^{-1}$ ) and cerulenin (32  $\mu\text{g ml}^{-1}$ ) for 2 hours before conversion to spheroplasts (spectra representative of 3 independent experiments). **E**, Quantification of ratio of lipid A:PG (34:2) in spheroplasts produced from *P. aeruginosa* PA14 cells pre-exposed, or not, to CHIR-090 (0.125  $\mu\text{g ml}^{-1}$ ) and cerulenin (32  $\mu\text{g ml}^{-1}$ ) for 2 hours before conversion to spheroplasts, as determined by measuring the area under the mass spectra peaks ( $n=3$ ). Data in **A**, **C** were analysed by a one-way ANOVA with Dunnett's post-hoc test. Data are presented as the arithmetic mean, and error bars represent the standard deviation of the mean.

Homologous results were obtained using the fluorescence from bound BoDipy-PMBN as a read-out for CM LPS levels, with the membrane-impermeant labelled polymyxin compound having the additional advantage of specifically acting as a marker of LPS on the extracellular-facing outermost leaflet of the CM bilayer, rather than of the total concentration

of LPS within the spheroplast. Visualisation of *P. aeruginosa* spheroplasts formed from otherwise untreated PA14 whole cells via fluorescence microscopy showed an accumulation of BoDipy-PMBN molecules around the spheroplast surface, revealing the widespread presence of LPS structures in the CM (**Figure 4.12B**). However, when whole *P. aeruginosa* bacteria were pre-exposed to either CHIR-090 or cerulenin before their OM/cell wall structures were removed, there was a complete absence of BoDipy-PMBN fluorescence visible throughout the perimeter of the spheroplasts produced, with the decrease in the amount of LPS in the CM likely simultaneously abrogating binding of the LPS-specific fluorescent probe to the spheroplast surface. This phenotype at the level of single cell forms held consistent following quantification of BoDipy-PMBN fluorescence across entire spheroplast populations pre-treated, or not, with the LPS biosynthesis inhibitors, with a notable decrease (greater than 3-fold) in CM LPS abundance/BoDipy-PMBN binding when active synthesis of LPS was blocked (**Figure 4.12C**).

As well as these two approaches for measuring changes to LPS concentrations in the CM, a MALDI-TOF mass spectrometry-based lipidomic method was also implemented for analysing the impact of CHIR-090 and cerulenin on *P. aeruginosa* spheroplasts. This recently developed diagnostic test that specifically detects bacterial membrane lipids was used to evaluate levels of lipid A (the principal domain of LPS) relative to levels of a membrane phospholipid species (phosphatidylglycerol 34:2) in PA14 spheroplasts pre-treated with the LPS synthesis inhibitors<sup>641</sup>. The mass spectra acquired clearly indicated that there was a stark reduction, relative to the reference phospholipid species, in the amount of lipid A within the CM of spheroplasts exposed to CHIR-090/cerulenin (**Figure 4.12D**). By measuring the area under the relevant mass spectra peaks and calculating the ratio of lipid A to the phospholipid PG (34:2), this qualitative observation was semi-quantitatively authenticated, with spheroplasts converted from *P. aeruginosa* cells pre-treated with the inhibitors of LPS biosynthesis having a 2-fold lower phospholipid:lipid A ratio than previously untreated spheroplasts (**Figure 4.12E**). Combined, these three assays evidently implied that although CHIR-090 and cerulenin did not interfere with LPS levels in the OM, they did decrease the concentration of CM LPS, potentially providing an explanation for their antagonism of colistin killing.

### **4.13 Inhibition of LPS synthesis prevents colistin-induced CM disruption and lysis**

In order to examine how permeabilisation of the *P. aeruginosa* CM by colistin was influenced by the CHIR-090/cerulenin-triggered reduction in the abundance of CM LPS, the PI uptake experiment previously utilised for tracking polymyxin-mediated damage to the CM

was repeated on whole PA14 bacterial cells in the presence of the two LPS biosynthesis inhibitors. Relative to an untreated *P. aeruginosa* population, colistin at a concentration of 4  $\mu\text{g ml}^{-1}$  caused extensive disruption of the CM structure, as was made apparent by the prolific increase over the 4 hour assay in fluorescence from the DNA-reactive PI dye, which only gained the intracellular access that was required to produce a fluorescent signal when the CM bilayer was damaged (**Figure 4.13A**). However, when PA14 cells were treated with the same dose of colistin in combination with sub-inhibitory concentrations of either CHIR-090 or cerulenin, there was virtually no increase in PI fluorescence at all during the 4 hour incubation, suggesting that the action of the inhibitors of LPS synthesis on lowering LPS levels in the CM had the downstream consequence of blocking colistin's CM-permeabilising properties. This vital information stood in complete opposition to the impact of CHIR-090/cerulenin on the OM of *P. aeruginosa*, where there was no change in LPS levels and thus no change to colistin-induced OM disruption, and provided support for the first time to the notion that LPS in the CM was a target for colistin's antibacterial effects.

While the data from the PI uptake assay demonstrated that diminishing the amount of LPS in the CM of *P. aeruginosa* whole cells with LPS synthesis inhibitors in turn mitigated CM permeabilisation by colistin, it was not yet clear what the outcome was of this reduced CM damage on bacterial viability. To study this, measurements of cell density by OD<sub>595nm</sub> readings were made over the course of 8 hours treatment of PA14 cells with colistin, CHIR-090 or cerulenin, in each case both alone and in combination, to expose any differences in polymyxin-mediated lysis of bacteria in the presence of the inhibitors of LPS biosynthesis. Because the small molecule compounds CHIR-090 and cerulenin were used at concentrations below their respective MICs, *P. aeruginosa* bacteria grew when treated with either inhibitor; in contrast, the PA14 population incubated with only colistin (4  $\mu\text{g ml}^{-1}$ ) experienced a steady drop in OD<sub>595nm</sub> readings (nearly 4-fold by 8 hours relative to the start of the assay), illustrating that the polymyxin antibiotic was lysing the cells (**Figure 4.13B**). Nevertheless, exposure of *P. aeruginosa* PA14 to colistin alongside CHIR-090/cerulenin wholly blocked bacterial lysis initiated by the polymyxin drug, with absolutely no decrease in OD<sub>595nm</sub> measurements over the 8 hours of treatment compared to the beginning of the experiment. This finding was consistent with the ability of the LPS biosynthesis inhibitors to abrogate colistin's killing of *P. aeruginosa*, and was a strong indication that the polymyxin required LPS in the CM to be a bactericidal, lytic compound.

To firmly establish the effects of CHIR-090 and cerulenin on the CM as the source for this colistin antagonistic phenotype, and eliminate the OM as a potential confounding factor, it was decided to test how depletion of CM LPS with the two inhibitor compounds modulated CM permeabilisation and lysis by colistin on *P. aeruginosa* spheroplasts. Owing to the osmotic

fragility of these OM and cell-wall-lacking cell forms, it was necessary to maintain the spheroplasts in a hypertonic 20% sucrose solution, and hence the capacity for colistin to exert its typical membrane damaging/lytic behaviour within this osmoprotective environment first had to be checked. This was performed by incubating whole PA14 cells with a lethal colistin dose in Tris buffer containing 20% sucrose, and assessing both uptake of the fluorescent PI dye as well as changes in OD<sub>595nm</sub> readings over time.

Treatment of *P. aeruginosa* bacteria with colistin led to a rapid rise over 4 hours in CM disruption in both Tris buffer without sucrose and Tris buffer harbouring 20% sucrose, with no discernible differences in the rate of ensuing PI uptake between the two cell populations (**Figure 4.13C**). Likewise, lysis by colistin of PA14 whole cells occurred to almost the same degree regardless of whether the polymyxin exposure was in hypertonic 20% sucrose media or not, with a 4-fold drop in OD<sub>595nm</sub> measurements by the end of the 8 hour assay (**Figure 4.13D**). These data showed that there was no interference with colistin's propensity to permeabilise the CM bilayer and ultimately lyse bacteria under the same osmoprotective conditions used in spheroplast experiments.

Whilst serving as a key control for later assays with spheroplasts, this discovery also ruled out one hypothesis previously stated that colistin's bactericidal mode of action only involved disruption to the bacterial OM, which when damaged sufficiently compromised the integrity of the cell surface envelope to such an extent that the bacteria simply burst open and lysed. If this proposal were true, it would be expected that exposure of cells to colistin in a hypertonic environment would culminate in reduced bacterial lysis, with the high concentration of solutes in the extracellular media protecting the bursting of cells even once the OM was permeabilised. However, here it was highlighted that colistin-induced lysis of *P. aeruginosa* whole cells was unaffected by being conducted in Tris buffer containing 20% sucrose, from which it could be concluded that the polymyxin antibiotic does not kill Gram-negative organisms through damage to the OM structure alone.

The fragility of spheroplasts formed from *P. aeruginosa* cells was evidenced by that fact that even when not treated with any antimicrobial agent and incubated in hypertonic Tris buffer for 4 hours, there was a slow accumulation of PI fluorescence from within the cytoplasm (**Figure 4.13E**). In spite of this background PI signal, exposure of these spheroplasts to colistin (4 µg ml<sup>-1</sup>) triggered a marked increase in the level of fluorescence from the DNA-reactive dye after 2 hours of polymyxin exposure, revealing that the polymyxin compound was permeabilising the CM. When whole cells of PA14 bacteria were pre-treated with sub-inhibitory concentrations of CHIR-090/cerulenin to decrease the amount of LPS in the CM before being converted to spheroplasts, colistin was no longer able to disrupt the CM bilayer of these cell forms, with the fluorescent PI signal of these spheroplasts no greater than that

observed with previously untreated spheroplasts. Moreover, whereas colistin caused lysis in spheroplasts that had not undergone pre-treatment with either LPS biosynthesis inhibitor, with OD<sub>595nm</sub> readings dropping steadily over the 4 hour incubation period, there was no similar lysis by colistin detected in spheroplasts from *P. aeruginosa* cells pre-exposed to CHIR-090 or cerulenin (**Figure 4.13F**). This result, that colistin-initiated lysis in spheroplasts where the abundance of CM LPS had been lowered was less than lysis in spheroplasts not even exposed to the polymyxin drug, served as the final proof that colistin targeted LPS in the CM of *P. aeruginosa* to lyse and kill the bacteria.

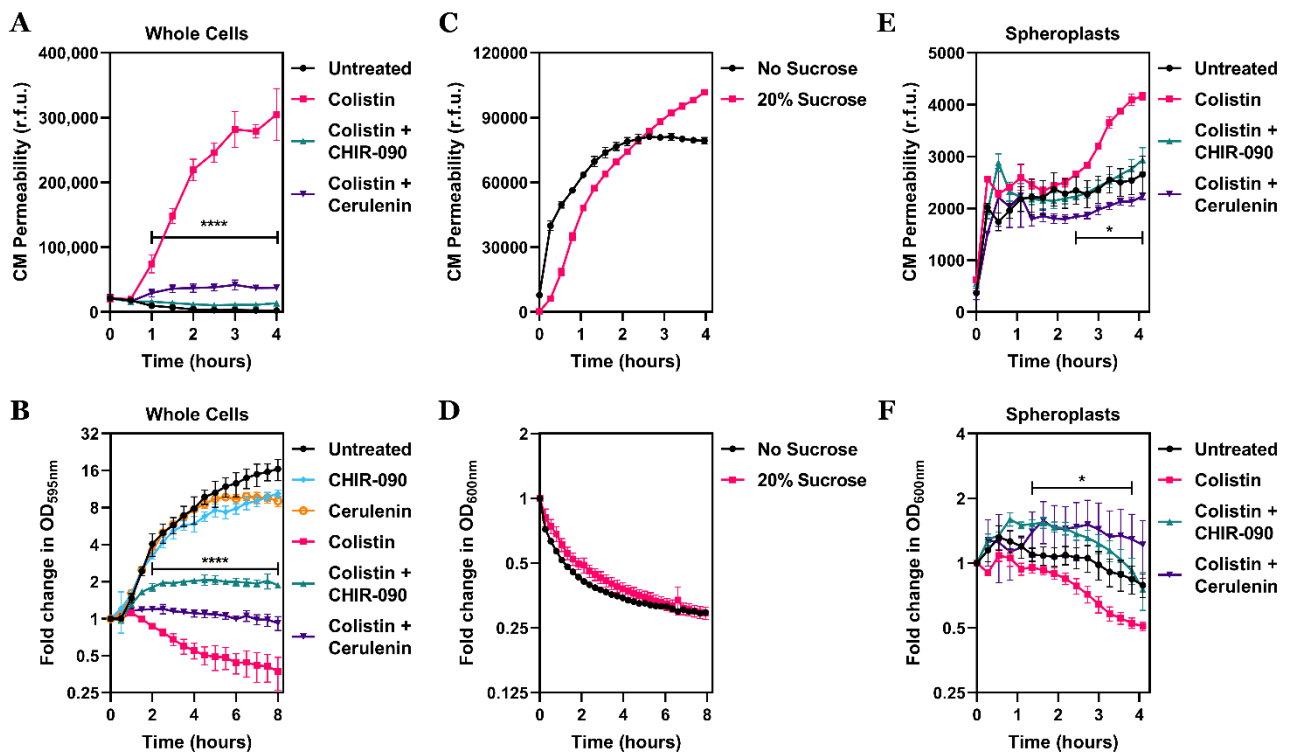


**Figure 4.13: Reducing CM LPS abundance with CHIR-090/cerulenin blocks colistin from permeabilising the CM and lysing *P. aeruginosa*.** **A, B**, Permeabilisation of the CM (**A**) and lysis/growth (**B**) of *P. aeruginosa* PA14 whole cells exposed to colistin (4  $\mu\text{g ml}^{-1}$ ), either alone or in combination with CHIR-090 (0.125  $\mu\text{g ml}^{-1}$ ) and cerulenin (32  $\mu\text{g ml}^{-1}$ ), as determined by measuring fluorescence from PI (2.5  $\mu\text{M}$ ) and measuring OD<sub>595nm</sub> respectively (n=3 in duplicate for **A**; n=4 for **B**; \*\*\*\*p<0.0001 for bacteria treated with colistin and CHIR-090/cerulenin relative to bacteria exposed to colistin alone). **C, D**, Permeabilisation of the CM (**C**) and lysis (**D**) of *P. aeruginosa* PA14 whole cells exposed to colistin (10  $\mu\text{g ml}^{-1}$ ) in Tris buffer with and without 20% sucrose, as determined by measuring fluorescence from PI (2.5  $\mu\text{M}$ ) and measuring OD<sub>600nm</sub> respectively (n=3). **E, F**, Permeabilisation of the CM (**E**) and lysis (**F**) by colistin (4  $\mu\text{g ml}^{-1}$ ) of spheroplasts produced from *P. aeruginosa* PA14 cells pre-exposed, or not, to CHIR-090 (0.125  $\mu\text{g ml}^{-1}$ ) and cerulenin (32  $\mu\text{g ml}^{-1}$ ) for 2 hours before conversion to spheroplasts, as determined by measuring fluorescence from PI (0.25  $\mu\text{M}$ ) and measuring OD<sub>600nm</sub> respectively (n=3, assay performed on 3 independent occasions; \*p<0.05 for spheroplasts pre-treated with CHIR-090/cerulenin relative to previously untreated spheroplasts). Data in **A, B, E, F** were analysed by a two-way ANOVA with Dunnett's post-hoc test. Data are presented as the arithmetic mean, and error bars represent the standard deviation of the mean.

#### 4.14 Colistin's interaction with LPS to disrupt the CM is cation-dependent

Reducing the concentration of LPS in the CM of *P. aeruginosa* spheroplasts to block colistin's permeabilising and lytic effects on these cell forms disclosed that the polymyxin targeted CM LPS for bacterial killing, but not the mechanism by which it did so. In the OM, colistin has been found to damage this outermost cell envelope bilayer by binding to LPS and displacing the  $Mg^{2+}/Ca^{2+}$  cationic bridges between lipid A domains that stabilise this membrane structure<sup>739</sup>. Indeed, colistin-mediated CM permeabilisation and its subsequent antibacterial activity have been shown to be reversed in the presence of these bivalent cations in studies with both whole cells and synthetic model membranes, since displacement of the intra-LPS  $Mg^{2+}/Ca^{2+}$  bridges by the polymyxin antibiotic is less efficient when the ions are excessively abundant in the extracellular environment<sup>715,740</sup>. To investigate whether this same cation-displacing mode of OM disruption by colistin held true for the polymyxin's LPS-dependent process of CM permeabilisation, spheroplasts formed from *P. aeruginosa* PA14 cells were exposed to the antibiotic ( $4 \mu\text{g ml}^{-1}$ ) over 18 hours in media containing increasing concentrations of  $Mg^{2+}$  ions, and measurements of PI uptake and lysis were obtained.

In PA14 spheroplasts treated with colistin in hypertonic Tris buffer with no supplementary  $MgCl_2$  added, the polymyxin drug caused an increase in fluorescence from the PI dye over the course of the assay, as the antibiotic interacted with LPS molecules to damage to CM bilayer (**Figure 4.14A**). However, as the concentration of  $Mg^{2+}$  in the media was augmented, there was a dose-dependent decrease in the amount of PI fluorescence within the *P. aeruginosa* spheroplasts triggered by colistin exposure. At the highest extracellular  $MgCl_2$  concentration tested (5 mM), the PI fluorescent signal barely intensified even following 18 hours of polymyxin treatment, compared to the start of the experiment. This signalled that the permeabilisation of the CM via colistin's interaction with CM LPS was abolished when the bivalent  $Mg^{2+}$  cation essential for stabilising intra-LPS bridges was present in excess in the extracellular milieu. Furthermore, lysis of the generated PA14 spheroplasts by colistin was also blocked by micromolar concentrations of  $MgCl_2$ , with the polymyxin compound inducing a sharp decline in  $OD_{595\text{nm}}$  readings in the absence of any supplemental  $Mg^{2+}$ , but significantly reduced/slower cell lysis when the ion was added to the Tris culture media (**Figure 4.14B**).

Together, these results suggested that, as with the OM, colistin's ability to disrupt the bacterial CM required the displacement of the bivalent  $Mg^{2+}$  species. As well as providing considerable substantiation for the argument that colistin permeabilised the *P. aeruginosa* CM through targeting of LPS – because cationic displacement is fundamental to the polymyxin's interactions with LPS to damage membrane structures – these data also offered the key mechanistic insight that colistin targeted CM LPS in much the same way as LPS in the



OM. As a control that the phenotype of diminishing CM disruption and lysis of PA14 spheroplasts by colistin in the presence of excess  $\text{MgCl}_2$  was specific to the effects of the  $\text{Mg}^{2+}$  ion, as opposed to a more generic protective osmotic effect from the higher salt concentration or a consequence of the chloride ions, these assays were repeated supplementing NaCl into Tris buffer. Importantly, the rates of PI uptake and cell lysis of the spheroplasts during exposure to colistin ( $4 \mu\text{g ml}^{-1}$ ) were entirely unaffected by the addition of a range of NaCl concentrations to the media (**Figure 4.14CD**). Therefore, the antagonistic nature of ions to inhibit colistin's bactericidal and CM-permeabilising activity appeared to be specific to the  $\text{Mg}^{2+}$  species, which is primarily responsible for stabilising adjacent LPS molecules with cationic bridges<sup>389</sup>.

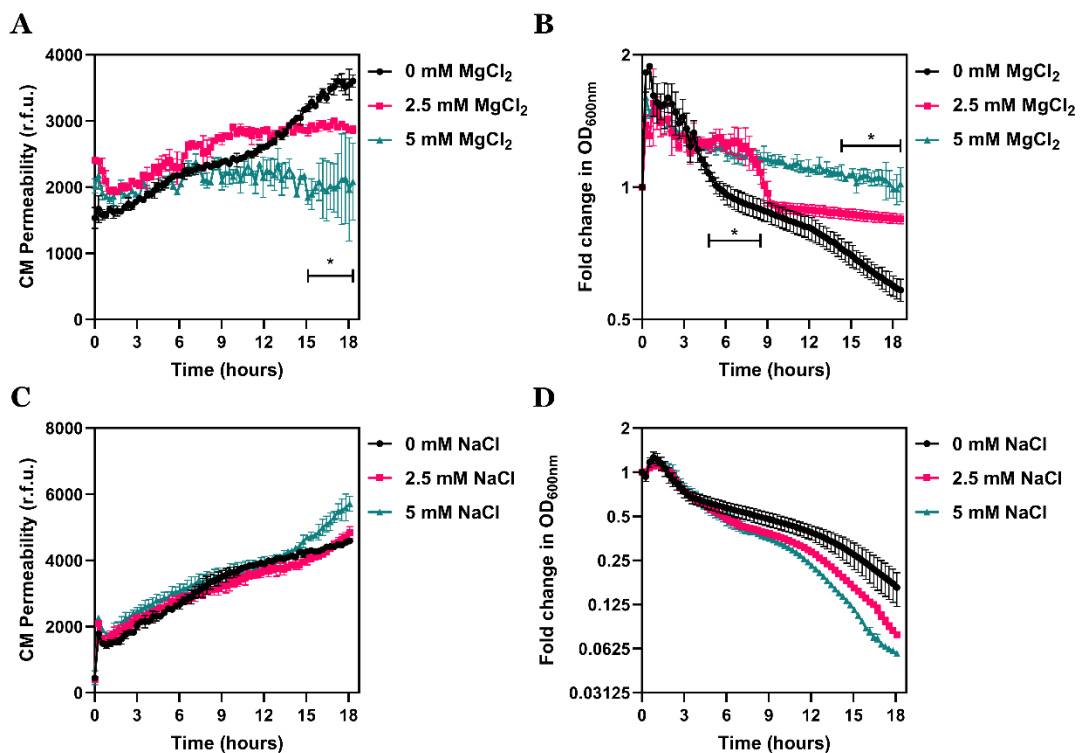


**Figure 4.14: Addition of extracellular  $\text{Mg}^{2+}$  specifically decreases colistin-mediated CM disruption and lysis in *P. aeruginosa* spheroplasts.** **A, B**, Permeabilisation of the CM (**A**) and lysis (**B**) of spheroplasts formed from *P. aeruginosa* PA14 cells during exposure to colistin ( $4 \mu\text{g ml}^{-1}$ ) in the presence or absence of increasing concentrations of  $\text{MgCl}_2$ , as determined by measuring fluorescence from PI ( $0.25 \mu\text{M}$ ) and measuring  $\text{OD}_{600\text{nm}}$  respectively ( $n=2$ , assay performed on 4 independent occasions;  $*p < 0.05$  for spheroplasts in both 2.5 mM and 5 mM  $\text{MgCl}_2$  compared to spheroplasts in no additional  $\text{MgCl}_2$ ). **C, D**, Permeabilisation of the CM (**C**) and lysis (**D**) of spheroplasts formed from *P. aeruginosa* PA14 cells during exposure to colistin ( $4 \mu\text{g ml}^{-1}$ ) in the presence or absence of increasing concentrations of NaCl, as determined by measuring fluorescence from PI ( $0.25 \mu\text{M}$ ) and measuring  $\text{OD}_{600\text{nm}}$  respectively ( $n=3$ , assay performed on 3 independent occasions). Data in **A, B** were analysed by a two-way ANOVA with Dunnett's post-hoc test. Data are presented as the arithmetic mean, and error bars represent the standard deviation of the mean.

#### 4.15 Polymyxin-mediated CM disruption and lysis requires LPS and the antibiotic's lipid tail

Polymyxin antibiotic compounds have two functional domains within their chemical structures: a C-terminal cationic polypeptide ring, and an N-terminal hydrophobic fatty acyl chain<sup>741</sup>. These distinct regions are reported to have contrasting functional effects in terms of the bactericidal mode of action of polymyxin drugs, with the positively-charged heptapeptide macrocycle more commonly associated with electrostatic binding to the anionic lipid A moiety of LPS molecules, whilst the antibiotic's lipid tail is believed to penetrate into and interact with the hydrophobic core of LPS<sup>386,388</sup>. The resultant combination of electrostatic and hydrophobic forces between the polymyxin compounds and the polysaccharide molecules is what is thought to mediate disruption of the LPS-harboring membranes by antibiotic drugs including colistin<sup>280</sup>. Having demonstrated that colistin killed bacteria by sequentially targeting LPS in the OM and CM, leading to permeabilisation of both cell envelope bilayers, it was resolved to understand if the proposed model outlined above of how the structure of colistin enables it to disrupt membranes containing LPS applied identically in the OM and CM. This question was answered through a structure-activity relationship (SAR) approach, incorporating the established panel of assays to track individual stages in the mechanism of action of colistin, but using the structurally-related antimicrobial drug polymyxin B (PMB), and its nonapeptide derivative that lacked a fatty acid tail, PMBN.

The first experiment utilised fluorescent BoDipy-tagged versions of PMB and PMBN to study how binding of the two polymyxin compounds to *P. aeruginosa* whole cells was affected by inhibition of LPS biosynthesis with sub-lethal doses of CHIR-090/cerulenin, which reduced LPS levels at the CM, but not at the OM. At a concentration of 10  $\mu\text{g ml}^{-1}$  of BoDipy-PMB (higher than that used in assays with colistin to account for a partial loss of antibacterial activity following BoDipy labelling), the fluorescent polymyxin drug displayed a steady increase in binding to PA14 cells over 8 hours, which was significantly decreased when *de novo* LPS synthesis was blocked by both CHIR-090 and cerulenin (**Figure 4.15A**). In comparison, there was no accumulation of BoDipy-PMBN (added at an equimolar concentration as BoDipy-PMB) to the *P. aeruginosa* bacterial surface during the 8 hour time course, regardless of whether the two LPS biosynthesis inhibitors were present or absent. This indicated that the polymyxin lipid tail was essential for the antimicrobial compound to access and attach to LPS in the CM bilayer, since either the loss of the antibiotic's N-terminus fatty acyl chain or the lowering of CM LPS abundance abolished polymyxin binding to the cell envelope.

Next, the relevance of the polymyxin fatty acid tail and active LPS biosynthesis for minor OM permeabilisation induced by PMB/PMBN was determined with the fluorescent NPN dye. This revealed that the capacity for PMB (4  $\mu\text{g ml}^{-1}$ ) to initiate low-level disruption to

the extracellular-facing OM bilayer of PA14 cells was unaffected by the presence of CHIR-090 and cerulenin, consistent with the fact that these LPS synthesis inhibitors at sub-inhibitory concentrations had minimal consequences on the amount of LPS in the OM (**Figure 4.15B**). However, an equimolar dose of PMBN caused notably less uptake of the NPN fluorophore into *P. aeruginosa* bacteria, suggesting that although the nonapeptide compound retained a high binding affinity to lipid A in the OM, without an N-terminal acyl chain the polymyxin drug could not even trigger minor OM damage sufficient for NPN fluorescence. The lack of decreased OM disruption when PA14 populations were treated with PMBN in combination with CHIR-090/cerulenin was further validation that neither inhibitor was modulating OM LPS levels.

While fluorescence from the small molecule phospholipid-reactive NPN dye was a read-out for low-level damage to the *P. aeruginosa* OM, the extracellular release of much larger AmpC beta-lactamase enzymes from the periplasm was subsequently used as a marker for more extensive permeabilisation of the OM bilayer. Surprisingly, given that it had been verified that cerulenin did not significantly alter the concentration of LPS in the OM, the fatty acid/LPS synthesis inhibitor did reduce major OM damage induced by PMB (4  $\mu\text{g ml}^{-1}$ ), with a smaller amount of beta-lactamase released into the supernatant over 60 minutes (**Figure 4.15C**). The reasons for this were unclear, and unfortunately the second inhibitor of LPS biosynthesis CHIR-090 cross-reacted with the chromogenic nitrocefin substrate exploited to quantify extracellular beta-lactamase release, meaning this conundrum could not be resolved. Nonetheless, the AmpC release assay crucially illustrated, in corroboration with data from the NPN experiment, that PMBN at an equimolar concentration exhibited no propensity to significantly damage the OM of *P. aeruginosa* PA14 cells, again implicating the lipid tail in the membrane-permeabilising properties of the polymyxin antibiotics.

The final SAR assay exploring membrane disruption by PMB and PMBN when active LPS biosynthesis was inhibited looked specifically at damage during polymyxin exposure to the *P. aeruginosa* CM via the DNA-reactive PI fluorophore. As observed in experiments with colistin, PMB (4  $\mu\text{g ml}^{-1}$ ) instigated an increased in fluorescence from PI over a 4 hour window of antibiotic treatment, as the polymyxin compound permeabilised the CM of PA14 cells (**Figure 4.15D**). This ability to damage the CM bilayer was effectively completely blocked when CHIR-090/cerulenin were added in combination with PMB to lower the abundance of LPS in the CM, with this phenotype implying that this polymyxin antibiotic shared mechanistic similarities with colistin with regards to interacting with CM LPS to disrupt the innermost bilayer of the Gram-negative cell envelope. Moreover, removal of the N-terminal lipid tail of PMB to form PMBN equally abolished the polymyxin's CM permeabilising activity, even in the absence of the LPS biosynthesis inhibitors CHIR-090 and cerulenin.

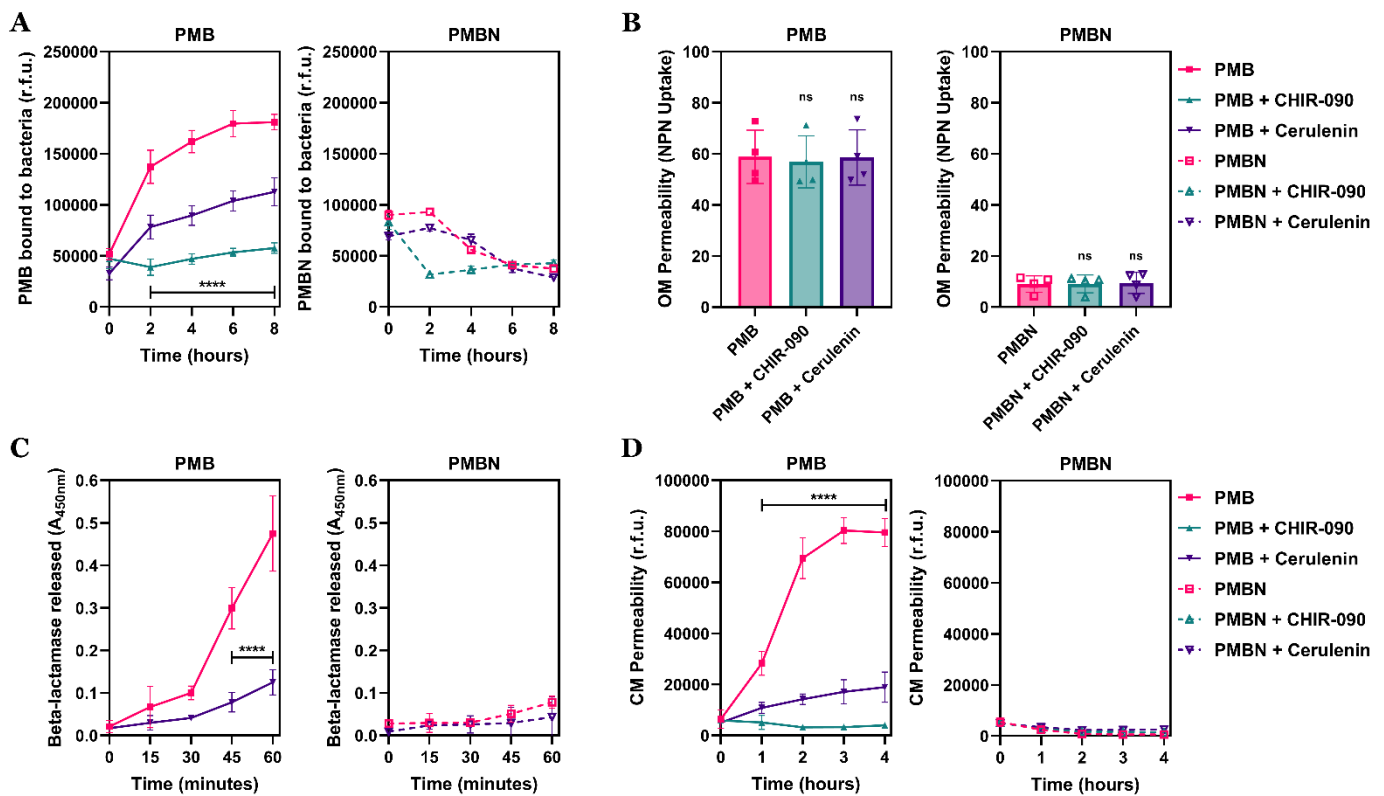


**Figure 4.15: Permeabilisation of the CM by polymyxins requires interaction between the polymyxin fatty acid tail and LPS in the CM.** **A**, Quantification of BoDipy-PMB ( $10 \mu\text{g ml}^{-1}$ ) and an equimolar concentration of BoDipy-PMBN ( $7 \mu\text{g ml}^{-1}$ ) bound to *P. aeruginosa* PA14 cells exposed to the polymyxin compounds alone and in combination with CHIR-090 ( $0.125 \mu\text{g ml}^{-1}$ ) or cerulenin ( $32 \mu\text{g ml}^{-1}$ ), as determined by measuring fluorescence of bacteria over 8 hours ( $n=4$ ; \*\*\*\* $p < 0.0001$  for both CHIR-090 and cerulenin-treated cells relative to bacteria treated with BoDipy-PMB alone). **B**, Minor permeabilisation of the OM of *P. aeruginosa* PA14 cells exposed to PMB ( $4 \mu\text{g ml}^{-1}$ ) and an equimolar concentration of PMBN ( $2.8 \mu\text{g ml}^{-1}$ ), either alone or in combination with CHIR-090 ( $0.125 \mu\text{g ml}^{-1}$ ) and cerulenin ( $32 \mu\text{g ml}^{-1}$ ), as determined by measuring uptake of the NPN fluorophore ( $10 \mu\text{M}$ ) over 10 minutes ( $n=4$ , each data point represents the arithmetic mean of 20 replicate measurements; ns:  $p > 0.05$  relative to bacteria exposed to PMB/PMBN alone). **C**, Major permeabilisation of the OM of *P. aeruginosa* PA14 cells exposed to PMB ( $4 \mu\text{g ml}^{-1}$ ) and PMBN ( $2.8 \mu\text{g ml}^{-1}$ ), alone or in combination with cerulenin ( $32 \mu\text{g ml}^{-1}$ ), as determined by measuring release of periplasmic beta-lactamase into the culture supernatant using nitrocefin ( $250 \mu\text{M}$ ) over 60 minutes ( $n=4$ ; \*\*\*\* $p < 0.0001$  for cerulenin-treated cells relative to bacteria treated with PMB alone). **D**, Permeabilisation of the CM of *P. aeruginosa* PA14 cells exposed to PMB ( $4 \mu\text{g ml}^{-1}$ ) and PMBN ( $2.8 \mu\text{g ml}^{-1}$ ), either alone or in combination with CHIR-090 ( $0.125 \mu\text{g ml}^{-1}$ ) and cerulenin ( $32 \mu\text{g ml}^{-1}$ ), as determined by measuring fluorescence from PI ( $2.5 \mu\text{M}$ ) over 4 hours ( $n=4$ ; \*\*\*\* $p < 0.0001$  for both CHIR-090 and cerulenin-treated cells relative to bacteria treated with PMB alone). Data in **A**, **D** were analysed by a two-way ANOVA with Dunnett's post-hoc test. Data in **B** were analysed by a one-way ANOVA with Dunnett's post-hoc test. Data in **C** were analysed by a two-way ANOVA with Sidak's post-hoc test. Data are presented as the arithmetic mean, and error bars represent the standard deviation of the mean.

From these findings thus far, it was concluded that the mode by which bactericidal polymyxin compounds damaged the CM of *P. aeruginosa* to kill the bacteria was analogous to the process at the OM, requiring the insertion of the antibiotic fatty acyl chain into LPS molecules in order to permeabilise the membrane bilayer structures. To examine the ultimate

outcomes of these differences between PMB and PMBN in membrane disruption when LPS biosynthesis was blocked, measurements of cell lysis and viability were made during treatment of PA14 bacteria with the polymyxin agents alone, as well as in combination with CHIR-090/cerulenin. PMB ( $4 \mu\text{g ml}^{-1}$ ) caused marked lysis of the *P. aeruginosa* population, with a fast decrease in  $\text{OD}_{595\text{nm}}$  readings throughout the 8 hour incubation, which was fully halted by the presence of either LPS synthesis inhibitor (**Figure 4.16A**). The effect of treating PA14 cells with PMBN rather than PMB was even more striking, with bacteria in fact growing in the presence of the polymyxin nonapeptide, as shown by increasing  $\text{OD}_{595\text{nm}}$  readings. Analysing bacterial survival with colony counts produced equivalent results – the rapid killing of *P. aeruginosa* with  $4 \mu\text{g ml}^{-1}$  PMB (4-log decrease in viability by 4 hours) was stopped both by reducing CM LPS levels, and by exposing bacteria to an equimolar PMBN concentration instead of PMB (**Figure 4.16B**). In summary, combined with the data from the membrane disruption SAR experiments, it was deduced that polymyxin-mediated permeabilisation of the Gram-negative CM – a pre-requisite for the antibiotic to be bactericidal – was dependent on the interactions between LPS in the CM and the polymyxin’s fatty acid tail domain.

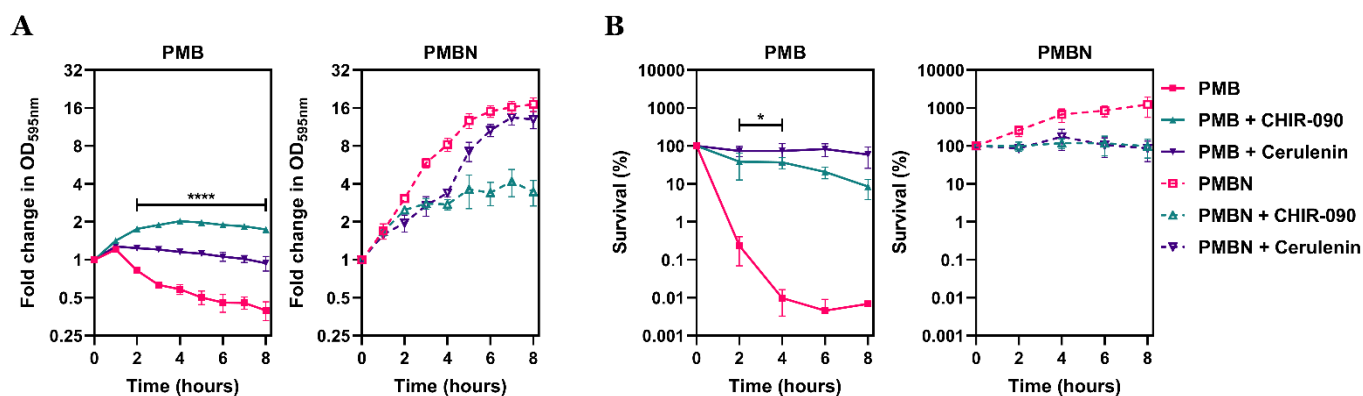


**Figure 4.16: The lytic and bactericidal activity of polymyxins is dependent on the lipid tail of the antibiotic interacting with CM LPS.** **A**, Lysis/growth of *P. aeruginosa* PA14 cells exposed to PMB ( $4 \mu\text{g ml}^{-1}$ ) and an equimolar concentration of PMBN ( $2.8 \mu\text{g ml}^{-1}$ ), either alone or in combination with CHIR-090 ( $0.125 \mu\text{g ml}^{-1}$ ) and cerulenin ( $32 \mu\text{g ml}^{-1}$ ), as determined by measuring  $\text{OD}_{595\text{nm}}$  over 8 hours ( $n=4$ ;  $****p<0.0001$  for both CHIR-090 and cerulenin-treated cells relative to bacteria treated with PMB alone). **B**, Survival of *P. aeruginosa* PA14 cells exposed to PMB ( $4 \mu\text{g ml}^{-1}$ ) and PMBN ( $2.8 \mu\text{g ml}^{-1}$ ), either alone or in combination with CHIR-090 ( $0.125 \mu\text{g ml}^{-1}$ ) and cerulenin ( $32 \mu\text{g ml}^{-1}$ ), as determined by c.f.u. counts over 8 hours ( $n=4$ ;  $**p<0.01$  for both CHIR-090 and cerulenin-treated cells relative to bacteria treated with PMB alone). Data in **A**, **B** were analysed by a two-way ANOVA with Dunnett’s post-hoc test. Data are presented as the arithmetic mean, and error bars represent the standard deviation of the mean.

#### **4.16 Blocking LPS synthesis reduces CM disruption, lysis and killing by colistin across Gram-negative pathogens**

All experiments to this point resolving that colistin's bactericidal mechanism of action relied on interactions with LPS within the CM bilayer had been conducted in the *P. aeruginosa* laboratory reference strain PA14. To expand these discoveries and see their implications in a more clinical context, the three key assays to follow colistin's killing activity (CM permeability, lysis, cell viability) were performed on a panel of Gram-negative strains isolated from human patients in therapeutic settings. These strains consisted of three *P. aeruginosa* clinical isolates, two *K. pneumoniae* species and one *E. coli* isolate, which all possessed resistance mechanisms to multiple classes of antibiotics, and thus represented the class of bacteria against which colistin would be used therapeutically.

In order to test if, as with the PA14 reference strain, the ability of colistin to kill these clinical strains was dependent on interactions with CM LPS, sub-inhibitory concentrations of the LPS biosynthesis inhibitors CHIR-090 and cerulenin were added in combination with the polymyxin antibiotic to deplete the amount of LPS present in the cell envelope's CM structure. For each clinical isolate, both CHIR-090 as well as cerulenin were utilised in colistin combination treatments at a dose that was at least half their respective MICs to reduce the concentration of LPS in the CM without any downstream lethal effects. The sub-lethal nature of these CHIR-090/cerulenin concentrations was confirmed by analysis of bacterial growth over 20 hours in the presence of the two compounds, which showed that the growth rate of the clinical strains was lowered but not absolutely inhibited by either LPS synthesis inhibitor (**Figure 4.17A**). This was noteworthy, since it was indicative that CHIR-090 and cerulenin were partially working to block the essential process of LPS biosynthesis, although any impact they had on colistin's mode of action in future assays could not be due to bacterial growth arrest.

The first experiment tracking colistin's activity against the Gram-negative clinical isolate panel was assessment of the extent of CM damage caused by the polymyxin drug with the fluorescent PI DNA-reactive dye. Exposure to colistin alone produced an obvious increase in uptake of PI in all six bacterial strains, with the antibiotic steadily permeabilising the innermost CM bilayer of the cell envelope over the 4 hour incubation (**Figure 4.17B**). Critically however, when *de novo* biosynthesis of LPS was blocked in these clinical strains with sub-inhibitory concentrations of CHIR-090/cerulenin, which have been shown to diminish CM LPS levels, colistin-induced disruption of the CM structure was simultaneously decreased in every single case. Hence, the requirement for LPS to be present in the CM, and for colistin molecules to interact with this LPS, to enable the polymyxin compound to be bactericidal appeared to be conserved amongst clinically-important Gram-negative pathogens.

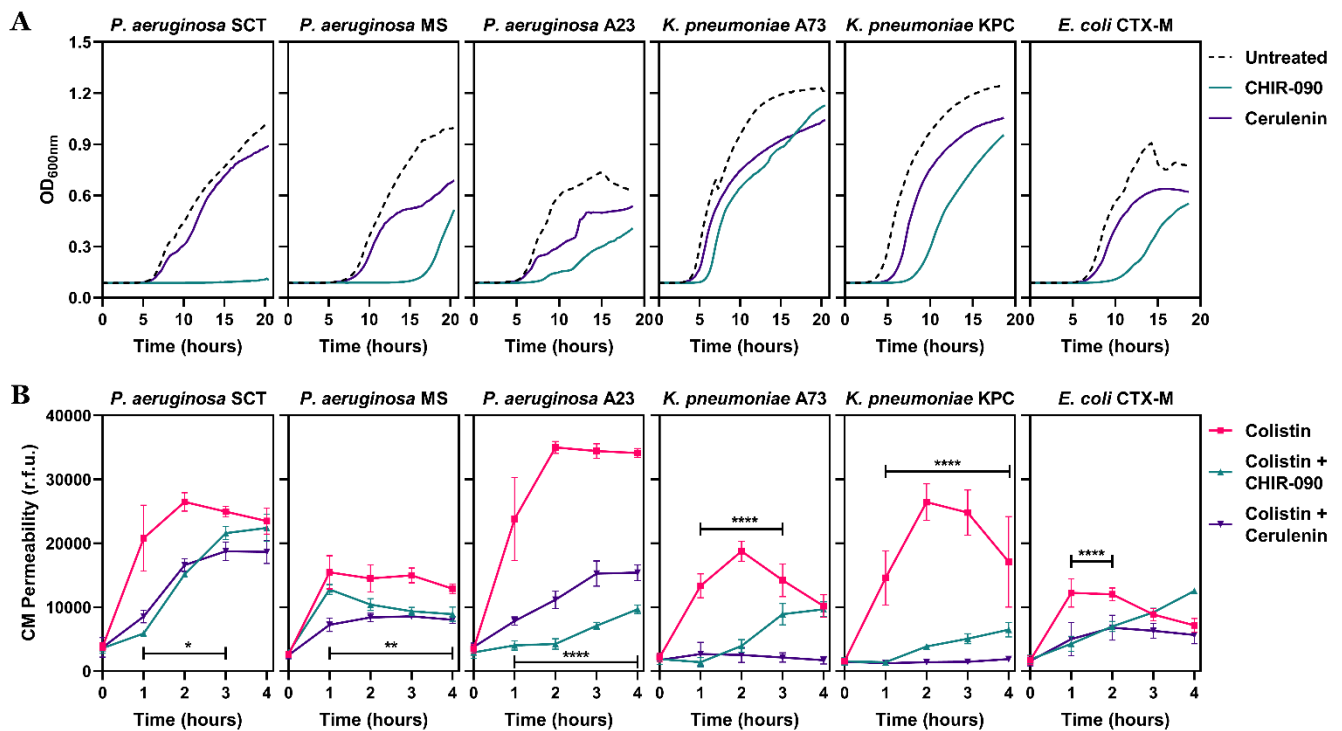


**Figure 4.17: Sub-lethal concentrations of CHIR-090/cerulenin reduce colistin-induced CM damage across diverse Gram-negative pathogens.** **A**, Growth kinetics of 3 *P. aeruginosa* clinical isolates, 2 *K. pneumoniae* clinical isolates and an *E. coli* clinical isolate during exposure, or not, to sub-inhibitory doses of CHIR-090 (0.063  $\mu\text{g ml}^{-1}$  for CTX-M strain; 0.25  $\mu\text{g ml}^{-1}$  for SCT and KPC strains; 0.5  $\mu\text{g ml}^{-1}$  for MS, A23 and A73 strains) and cerulenin (16  $\mu\text{g ml}^{-1}$  for CTX-M strain; 32  $\mu\text{g ml}^{-1}$  for SCT strain; 64  $\mu\text{g ml}^{-1}$  for A23 strain; 128  $\mu\text{g ml}^{-1}$  for MS, A73 and KPC strains), as determined by measuring OD<sub>600nm</sub> over 20 hours incubation. **B**, Permeabilisation of the CM of 3 *P. aeruginosa* clinical isolates, 2 *K. pneumoniae* clinical isolates and an *E. coli* clinical isolate during exposure to colistin (used at 4  $\mu\text{g ml}^{-1}$  for all strains except CTX-M, where used at 2  $\mu\text{g ml}^{-1}$ ), either alone or in combination with the established sub-inhibitory concentrations of CHIR-090 and cerulenin, as determined by measuring fluorescence from PI (2.5  $\mu\text{M}$ ) over 4 hours (n=4; \*p<0.05, \*\*p<0.01, \*\*\*\*p<0.0001 for CHIR-090/cerulenin-treated cells relative to bacteria treated with colistin alone). Data in **B** were analysed by a two-way ANOVA with Dunnett's post-hoc test. Data are presented as the arithmetic mean, and error bars shown represent the standard deviation of the mean.

To relate these differences in CM permeabilisation of the six clinical isolates mediated by colistin during co-exposure with the LPS synthesis inhibitors to the ultimate consequences on bacterial viability, measurements of cell lysis and survival were made throughout an 8 hour treatment period. Colistin on its own triggered bacteria of all six strains to lyse, as evidenced by a drop in OD<sub>595nm</sub> readings over time (**Figure 4.18A**). Despite this, blocking the biosynthesis of LPS with sub-lethal doses of CHIR-090 reduced the rate of bacterial lysis in every clinical strain, whilst the fatty acid/LPS synthesis inhibitor cerulenin was responsible for the same phenotype in four of the six isolates (*P. aeruginosa* MS, *K. pneumoniae* A73, *K. pneumoniae* KPC and *E. coli* CTX-M). When calculating cell survival by colony counts, independently, colistin initiated rapid and extensive bacterial killing (more than 3-logs) in

each case, though interestingly the bi-phasic pattern of cell death detected initially for the *P. aeruginosa* PA14 strain was again apparent with these clinical strains, with a sub-population of bacteria surviving polymyxin exposure before commencing re-growth (**Figure 4.18B**). Nevertheless, in the presence of either CHIR-090/cerulenin, colistin's capacity to kill these Gram-negative pathogenic species was severely lessened, with the most dramatic results reserved for the strains *P. aeruginosa* A23 and *K. pneumoniae* A73, where virtually no bacterial death was observed at all.

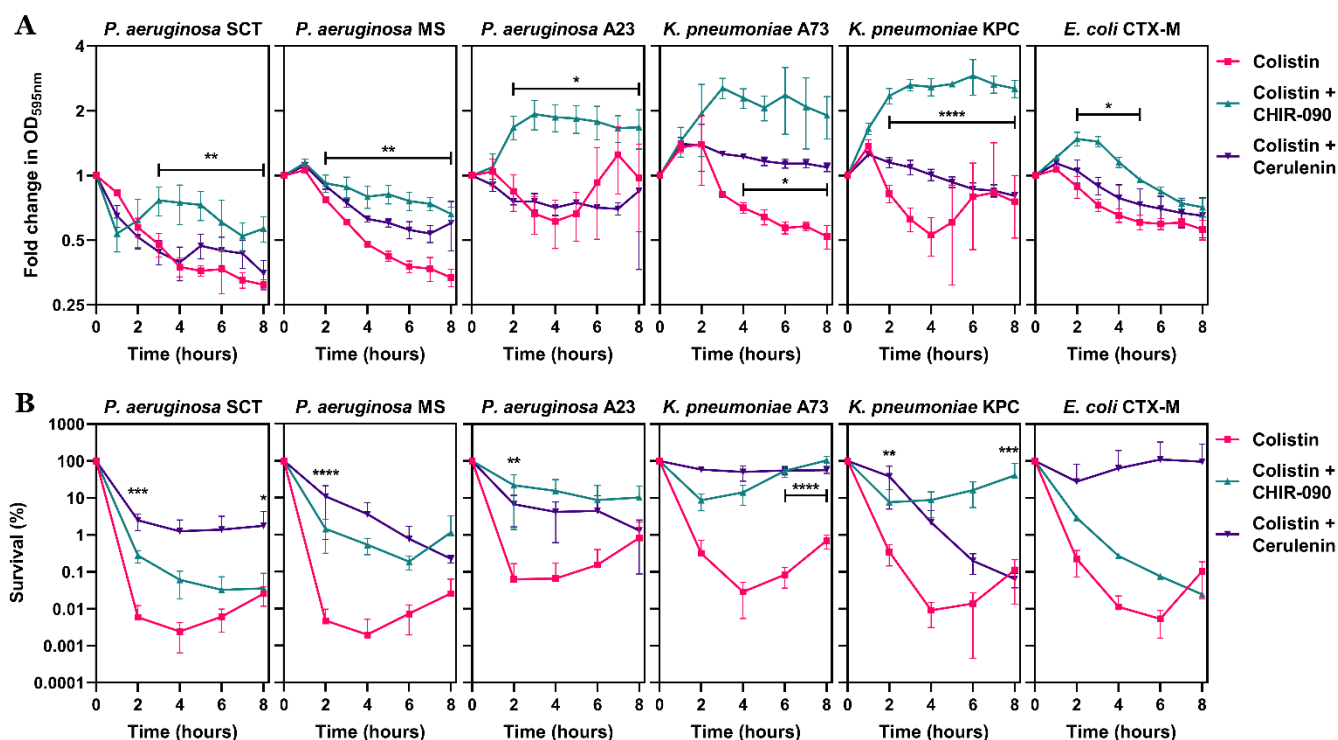


**Figure 4.18: CHIR-090 and cerulenin block colistin from causing cell lysis and death in a panel of Gram-negative pathogens.** **A**, Lysis of 3 *P. aeruginosa* clinical isolates, 2 *K. pneumoniae* clinical isolates and an *E. coli* clinical isolate during exposure to colistin (used at 4  $\mu\text{g ml}^{-1}$  for all strains except CTX-M, where used at 2  $\mu\text{g ml}^{-1}$ ), either alone or in combination with the established sub-inhibitory concentrations of CHIR-090 and cerulenin, as determined by measuring OD<sub>595nm</sub> over 8 hours (n=4; \*p<0.05, \*\*p<0.01, \*\*\*\*p<0.0001 for CHIR-090/cerulenin-treated cells relative to bacteria treated with colistin alone). **B**, Survival of 3 *P. aeruginosa* clinical isolates, 2 *K. pneumoniae* clinical isolates and an *E. coli* clinical isolate during exposure to colistin (used at 4  $\mu\text{g ml}^{-1}$  for all strains except CTX-M, where used at 2  $\mu\text{g ml}^{-1}$ ), either alone or in combination with the established sub-inhibitory concentrations of CHIR-090 and cerulenin, as determined by c.f.u. counts over 8 hours (n=4; \*\*p<0.01, \*\*\*p<0.001, \*\*\*\*p<0.0001 for CHIR-090/cerulenin-treated cells relative to bacteria treated with colistin alone). Data in **A**, **B** were analysed by a two-way ANOVA with Dunnett's post-hoc test. Data are presented as the arithmetic mean, and error bars represent the standard deviation of the mean.

Finally, to extend these findings even beyond the LPS biosynthesis inhibitors widely-used in past assays, a different fatty acid synthesis inhibitor – triclosan – was investigated for its colistin-antagonistic properties. The cellular target of triclosan is the enoyl-acyl carrier protein reductase FabI, and binding of triclosan to this enzyme blocks the essential fatty acid



biosynthetic pathway in which FabI plays an integral part. Because the fatty acids produced from this FabI-dependent synthesis pathway are required for biosynthesis of LPS (in particular the lipid A domain), triclosan, comparably with cerulenin, additionally functions as an LPS synthesis inhibitor<sup>742–744</sup>. Strains of the *P. aeruginosa* species are intrinsically-resistant to the antibacterial effects of triclosan, and thus the *K. pneumoniae* A73 clinical isolate was used to understand if inhibition of LPS biosynthesis by triclosan abrogated colistin killing<sup>745</sup>.

A sub-lethal concentration of triclosan ( $0.125 \mu\text{g ml}^{-1}$ , 4-fold less than the MIC) was identified through a bacterial growth experiment that moderately decreased the growth rate of the *K. pneumoniae* cell population without total growth arrest (**Figure 4.19A**). In a subsequent time-kill assay, this same sub-inhibitory triclosan dose was able to completely block cell death induced even by the highest concentration of colistin achievable therapeutically ( $10 \mu\text{g ml}^{-1}$ ), with no drop in viable bacterial counts at all over the 8 hours of combination treatment with the polymyxin and triclosan, and a greater than 4-log difference in survival relative to *K. pneumoniae* cells exposed to colistin alone (**Figure 4.19B**). In conclusion, the process by which colistin kills bacteria – interacting with LPS in the CM to permeabilise the cell envelope – was not specific to *P. aeruginosa*, but more likely a conserved mechanism of action against all relevant Gram-negative organisms.

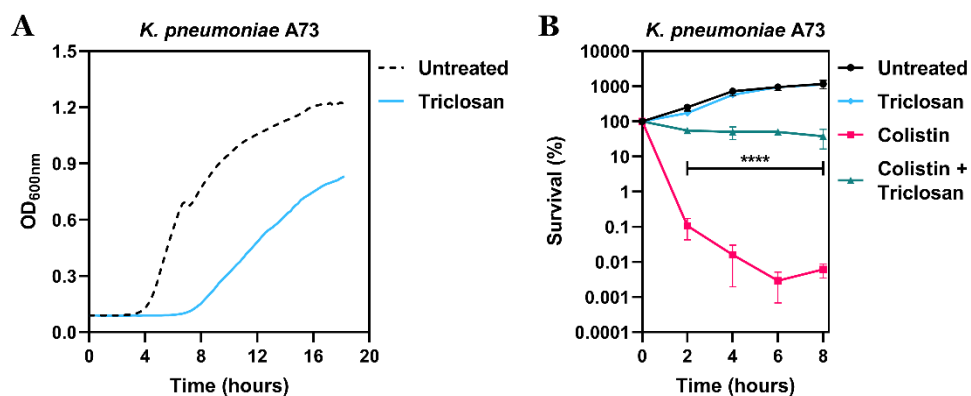


**Figure 4.19: The fatty acid/LPS synthesis inhibitor triclosan blocks *K. pneumoniae* killing by colistin.** **A**, Growth of cells of the clinical isolate *K. pneumoniae* A73 during exposure, or not, to a sub-lethal dose ( $0.125 \mu\text{g ml}^{-1}$ ) of the FabI inhibitor triclosan, as determined by measuring OD<sub>600nm</sub> over 18 hours incubation (n=3; error bars omitted for clarity). **B**, Survival of cells of the clinical isolate *K. pneumoniae* A73 during exposure, or not, to colistin ( $10 \mu\text{g ml}^{-1}$ ) and triclosan ( $0.125 \mu\text{g ml}^{-1}$ ) both alone, and in combination, as determined by c.f.u. counts over 8 hours (n=4; \*\*\*\*p<0.0001 for colistin and triclosan-treated cells relative to bacteria treated with colistin alone). Data in **B** were analysed by a two-way ANOVA with Sidak’s post-hoc test. Data are presented as the arithmetic mean, and error bars shown represent the standard deviation of the mean.

## 4.17 Discussion

Colistin is a vital antibiotic of last-resort that is often used as the final treatment option in patients infected with multi-drug resistant bacterial pathogens, including *P. aeruginosa*<sup>701</sup>. Unfortunately, despite its critical importance, colistin therapy against infections caused by *P. aeruginosa* species frequently fails, and efforts to address and overcome this high rate of treatment failure are hampered by a lack of understanding regarding colistin's bactericidal mechanism of action<sup>294</sup>. In particular, it was entirely unknown how colistin-induced disruption of the bacterial OM following binding of the polymyxin drug to LPS on the cell surface lead to damage to the CM bilayer, permeabilisation of the cellular envelope, and ultimately bacterial death. Work in this chapter has resolved, for the first time, the subsequent steps in colistin's mode of action downstream of OM disruption by showing that the polymyxin compound also interacts with LPS in the CM of *P. aeruginosa* that is awaiting export to the OM, and that this interaction with CM LPS is essential for permeabilisation of the innermost bacterial membrane bilayer and the killing activity of colistin.

The key data confirming the dependence on interactions with LPS molecules in the CM for colistin's bacterial killing effects arose from demonstrating that the inhibition of *de novo* LPS biosynthesis with CHIR-090/cerulenin blocked the CM-damaging and bactericidal properties of the polymyxin antibiotic. That colistin required an active biological process in order to cause death of *P. aeruginosa* cells was a surprising finding in itself. Whilst it is well known that many antibiotics that target fundamental cellular processes (e.g. beta-lactams blocking cell wall synthesis, aminoglycosides inhibiting protein synthesis) rely on active bacterial metabolism to exert their antimicrobial effects, it was long believed that killing by colistin and other similar membrane-damaging antimicrobial compounds (e.g. host defence peptides) was not analogously conditional on any *de novo* bacterial biosynthetic pathways<sup>746,747</sup>. Indeed, the fact that such antimicrobial peptides could display potency even in the absence of active biological processes in bacteria was considered a highly advantageous trait, especially for the eradication of metabolically-dormant bacterial persister cells<sup>748-750</sup>.

However, the conclusions from experiments in this study that killing of *P. aeruginosa* by colistin can be completely halted by inhibition of *de novo* LPS biosynthesis calls into question whether the polymyxin drug would be able to initiate cell death in bacterial persisters. Furthermore, these results provide a mechanistic explanation for previous reports that highlighted the existence and formation of colistin-tolerant persister cells during exposure to the polymyxin, but no molecular basis for this phenotype<sup>653,654</sup>. Although it remains to be confirmed in future investigations if these persister bacteria that can survive colistin treatment do actually have decreased LPS synthesis (for instance through the use of a fluorescent reporter strain that offers a measurable read-out of the rate of LPS biosynthesis), this

hypothesis is supported by proteomic data on colistin-tolerant *P. aeruginosa* cells present in biofilms, which found lower abundance of an LPS assembly protein in biofilm cells that can tolerate polymyxin exposure<sup>751</sup>. In addition, there is some evidence from assays conducted in this chapter that bacterial growth arrest – a defining trait of persister cell populations – may partially reduce the killing efficacy of colistin. While co-treatment with bacteriostatic concentrations of tetracycline or chloramphenicol did not fully abrogate colistin-mediated cell death to the same extent as sub-inhibitory concentrations of CHIR-090/cerulenin, the two protein synthesis inhibitors still lowered by 2-3 logs the extent of polymyxin killing of a *P. aeruginosa* population. It is certainly possible that these growth arrested cells, which are a representative model of bacterial persisters, have increased colistin tolerance due to a diminished metabolic capacity and a slower rate of LPS biosynthesis.

The antagonistic interactions between colistin and other antimicrobial compounds that ultimately inhibit the synthetic pathway of LPS have significant and prominent wider implications in relation to their context in the clinical setting. Colistin is commonly incorporated as part of combination therapy strategies against Gram-negative infections, largely because of its membrane-disrupting abilities that are thought to enhance the uptake and access of intracellularly-acting antibiotics to their cytoplasmic targets<sup>360,752</sup>. The discovery here that numerous antibiotic drugs can lessen the bactericidal activity of colistin when utilised alongside the polymyxin raises obvious concern about the appropriateness of administering such combination treatment to infected patients. Particular caution and attention should be given to direct LPS biosynthesis inhibitors that are in pre-clinical drug development pipelines (e.g. CHIR-090, RJPXD33), but also to antibacterial compounds already extensively used both in and out of the clinic, such as triclosan (shown to block colistin killing of *K. pneumoniae*) and bacteriostatic inhibitors of protein synthesis<sup>184,189</sup>. Interestingly, large-scale clinical trials have revealed that colistin and rifampicin combination therapies do not improve patient outcomes compared to colistin alone; though the reasons for this are unclear and remain to be tested, it may be worth considering the potential impact of rifampicin on LPS synthesis rates in future studies<sup>753,754</sup>.

Analysis of the data presented in this chapter suggests that there are several similarities between how colistin interacts with LPS in the OM versus in the CM. In both bilayer structures, it has now been proven that the permeabilisation of the membranes following the binding of colistin molecules to LPS relies on the displacement of divalent cations, and that this membrane disruption can be overcome when cations are present in excess. Relevantly, the extracellular concentration of Mg<sup>2+</sup> ions (5 mM) necessary to abolish CM permeabilisation and lysis of *P. aeruginosa* spheroplasts in assays here is identical to the Mg<sup>2+</sup> concentration found previously to stop the disruption of synthetic membrane vesicles that resemble the OM of

Gram-negative bacteria<sup>715</sup>. Moreover, experiments performed in this study comparing the membrane-damaging activity of polymyxin B (PMB) with its lipid tail-deficient derivative PMBN clearly indicated that the major disruption of the OM and CM triggered by polymyxin molecules, which was a pre-requisite for their bactericidal effects, was dependent on the hydrophobic fatty acyl tail of the antibiotics. Exactly what role the polymyxin lipid tail plays in the binding and disruption of LPS structures is still unresolved, and should form a focus of subsequent biophysical investigations that could make use of diverse analytical techniques, including electron spin/nuclear magnetic resonance, microscopy (electron/atomic force) and electrophysiological measurements.

In spite of these parallels between how colistin interferes with LPS molecules in the CM compared to in the OM, there also appear to be certain differences in the behaviour of polymyxin compounds at the two discrete membrane bilayers. The most obvious discrepancy relates to the duration of time taken for colistin to permeabilise the cell envelope structures of Gram-negative bacteria. Minor disruption of the OM in response to the presence of the polymyxin antibiotic occurred almost immediately (less than 10 minutes), as quantified by uptake of the phospholipid-reactive NPN fluorophore, with more significant major OM damage, marked by periplasmic beta-lactamase release, arising shortly after (within 30 minutes). By contrast, permeabilisation of the CM of *P. aeruginosa* as detected by fluorescence from the DNA-reaction PI dye was only observed after 2 hours of colistin treatment, and the fact that this timescale was the same in experiments with both whole cells and spheroplasts rules out the possibility that this delay was solely due to the time taken for polymyxin molecules to traverse across the periplasm/cell wall.

The most likely explanation for why colistin damaged the OM much more quickly and efficiently than the CM is the stark disparity in the abundance of LPS between the two bilayer membranes<sup>755</sup>. In the OM, LPS is a predominant component, with the outermost extracellular-facing leaflet of the bilayer comprised exclusively of the polysaccharide structure. Oppositely, LPS exists as a minor fraction in the Gram-negative bacterial CM, with molecules of the polysaccharide only present temporarily en route to their final OM destination. This difference in LPS concentrations was quantified here with both an immunogenic assay (LAL) and a fluorescent LPS-specific probe (BoDipy-PMBN), which showed that the amount of LPS in the CM was approximately 10-fold lower than in the OM. The direct correlation between the efficiency of membrane permeabilisation by colistin and LPS abundance in the membrane has already been established in a past study with synthetic vesicle bilayers, and is the most probable reason for the divergence in the time taken for OM and CM disruption induced by the polymyxin antibiotic<sup>715</sup>. Of absolute bearing on the findings in this chapter, this same study also reported that when LPS is present at low concentrations within membrane bilayers

(around 3%), any further reduction in LPS levels, even as small as lowering the LPS abundance from 3% to 1%, can have dramatic consequences on colistin's capability to permeabilise the membrane structure<sup>715</sup>. The effects here of CHIR-090 and cerulenin on depleting LPS from the CM of *P. aeruginosa* were of roughly the same scale (2 to 3-fold), and together these pieces of information combine to elucidate how the relatively modest decreases in CM LPS caused by the two LPS biosynthesis inhibitors can have such striking impacts on polymyxin killing.

In conclusion, the work in this chapter provides a new model of colistin's bactericidal mode of action against Gram-negative bacteria. Through a series of carefully controlled experiments, it is made evident that colistin damages the CM of the cell envelope not through the previously proposed mechanism of surfactant/detergent-like interactions with membrane phospholipids, but rather by targeting LPS molecules in the CM. This information is especially crucial because it opens the door for the development of therapeutic strategies to enhance the activity and efficacy of colistin, for example by increasing the concentration of CM LPS, and such novel options are urgently-needed to tackle the high rate of clinical treatment failure of the last-resort polymyxin antibiotic.

## Chapter 5: Acquired colistin resistance in Gram-negative bacteria is mediated at the cytoplasmic membrane

### 5.1 Introduction

Owing to the critical importance of colistin as an antibiotic of last-resort against Gram-negative bacterial infections, the discovery that these pathogenic organisms readily develop resistance to the polymyxin drug poses an extremely grave threat to the successful use of colistin as a salvage therapy and patient outcomes<sup>756</sup>. The first reports of polymyxin resistance appeared in 1953 – only four years after colistin was first isolated – with the finding that non-susceptibility to polymyxin B can emerge rapidly in *P. aeruginosa* and *Aerobacter aerogenes* species<sup>757</sup>. However, it was not until 1978 that the first mechanism by which colistin resistance could be acquired was unearthed, with mutations in the chromosome of *Salmonella* strains identified as being responsible for a lack of sensitivity to polymyxin antibiotics<sup>480</sup>.

In the ensuing decades, the dramatic rise in the administration of colistin in clinical settings that has occurred in response to the increased prevalence of multi-drug resistant pathogens has led to a simultaneous upsurge in the rates of colistin non-susceptibility<sup>758</sup>. A temporal analysis of colistin resistance rates between 2010 and 2014 in Brazil revealed that the prevalence of colistin resistance amongst Enterobacteriaceae rose from 6.6% to 9.4% over the five year period<sup>759</sup>. Two key studies looking specifically at *K. pneumoniae* isolates across the globe have reported homologous trends, with three-fold increases in the rates of colistin non-susceptibility observed in Tunisia (3.57% in 2002 to 9.68% in 2013) and Italy (10% in 2010 to 30% in 2014)<sup>760,761</sup>. Concerningly, the investigation in Italy additionally demonstrated that the 30-day mortality in patients infected with colistin-resistant *K. pneumoniae* was as high as 51% (compared with 39.4% in patients infected with susceptible bacteria), highlighting the severe consequences of polymyxin resistance on therapeutic outcomes<sup>761</sup>.

Until 2017, colistin was extensively utilised in the farming industry as a growth promoter, which is thought to have been a major driver in the ever-increasing prevalence of resistance to the last-resort antibiotic<sup>762,763</sup>. In support of this, a report from Taiwan showed an 8-fold rise in the detection of colistin-resistant *E. coli* from market meat samples, from 1.1% in 2012 to 8.7% in 2015<sup>764</sup>. Finally, although polymyxin resistance in clinical *P. aeruginosa* samples has historically been a rare phenotype, according to surveillance data from the European Antimicrobial Resistance Surveillance Network, there has also been a recent escalation in the rates of colistin non-susceptibility in this pathogen, from 1% in 2013 up to 4% in 2016<sup>758,765</sup>. Without doubt, resistance to colistin is a growing crisis compromising the effective use of the polymyxin drug, against which novel solutions are urgently required.

As was the case with the first identified genetic mediator of colistin resistance in the 1970s, polymyxin non-susceptibility in Gram-negative pathogens frequently arises from the acquisition of mutations in the regions of the bacterial chromosome that encode regulatory two-component systems (e.g. PmrAB, PhoPQ, ParRS, CprRS, ColRS)<sup>454,506</sup>. The characteristic traits of all of these two-component systems is the ability to sense environmental stimuli, including changes to the cell envelope Mg<sup>2+</sup> composition triggered by colistin, and initiate a transcriptional response that induces the expression of a number of target genes<sup>766–769</sup>. Among these target genes are the *pmrHFIJKLM* operon (also known as *arnBCADTEF*) and *pmrC*, which function to modify the lipid A domain of LPS with cationic L-Ara4N and pEtN moieties, respectively<sup>435,770</sup>. Addition of these positively-charged chemical groups to the typically anionic lipid A structure interferes with the electrostatic interaction between colistin molecules and LPS that is essential for the polymyxin drug's antibacterial effects. Hence, mutations in the two-component system genes, or in the genes encoding their regulatory proteins (e.g. MgrB, CrrAB), that bring about an upregulation/over-activation of the *pmrHFIJKLM* and *pmrCAB* operons can cause excessive cationic lipid A modification, culminating in a reduction in the capacity of colistin to bind LPS and polymyxin resistance<sup>771</sup>.

Colistin non-susceptibility occurring via this chromosomal mutation mechanism was believed to be the predominant process by which resistance to the lipopeptide antibiotic could be acquired until the startling discovery of the mobile colistin resistance gene, *mcr-1* in 2015<sup>530</sup>. The gene product of *mcr-1* is a pEtN transferase enzyme that shares a common mode of conferring polymyxin resistance with the chromosomally-encoded *pmrC* gene, in terms of adding a positively-charged pEtN group on to lipid A that diminishes colistin's affinity for LPS molecules<sup>558</sup>. However, in stark contrast with chromosomal *pmrC*, the *mcr-1* gene, borne on a wide range of mobile plasmids (e.g. IncI, IncF, IncHI2, IncP, IncX4, IncY), can easily move between distinct bacterial species by horizontal gene transfer<sup>772,773</sup>. As a result, the *mcr-1* colistin resistance determinant has disseminated throughout the world at a vast pace in the last decade, spreading into a diverse panel of pathogenic organisms, including *E. coli*, *K. pneumoniae*, *Shigella*, *Salmonella* and *Enterobacter* strains<sup>534</sup>. Even more concerningly, the existence of nine other pEtN transferase-encoding *mcr* genes (termed *mcr-2* to *mcr-10*) has now been demonstrated, though relatively little is known about the functional activity of these *mcr* homologues in terms of their capacity to mediate colistin resistance<sup>774</sup>. Of particular interest is the *mcr-9* gene variant, which is often detected in clinical isolates but appears to be “silent”, with carriage not associated with expression and a loss of polymyxin sensitivity<sup>582,775</sup>.

Alongside these acquired mechanisms of resistance to colistin, a number of bacteria also exhibit intrinsic colistin resistance – indeed the *mcr* genes themselves are postulated to have originated through a lateral movement event from an intrinsically polymyxin-resistant

species on to a plasmid<sup>560,563</sup>. The process by which resistance to colistin occurs in these organisms, which include *Burkholderia*, *Neisseria* and *Serratia* strains, is again analogous with that previously described for acquired polymyxin non-susceptibility – the modification of LPS with cationic pEtN/L-Ara4N moieties that blocks the first step of binding to lipid A in colistin's mode of action<sup>776</sup>. Whilst it is thought that the constitutive addition of these positively-charged chemical groups to lipid A is what instigates inherent colistin resistance, the molecular bases of the differences between acquired and intrinsic resistance to the antibiotic are not well understood. Providing a further layer of complexity to efforts to comprehend and overcome resistance to polymyxin drugs is the recent description of colistin hetero-resistance. Antibiotic hetero-resistance is a phenotype where the majority of a bacterial population is susceptible to an antimicrobial agent, except for a small sub-population of cells possessing a means of surviving and tolerating exposure to the drug<sup>777</sup>. Hetero-resistance to colistin has been identified in *K. pneumoniae*, *E. coli*, *A. baumannii* and *Enterobacter* species, is proposed to be related to alterations in the PmrAB/PhoPQ two-component systems, and can contribute to *in vivo* polymyxin treatment failure<sup>778–783</sup>. Nonetheless, there remain numerous unanswered questions around how colistin hetero-resistance arises, and in particular the behaviour of the colistin-tolerant sub-population of bacterial cells.

The experiments in the previous chapter confirmed that colistin kills Gram-negative bacteria by targeting LPS molecules in the cytoplasmic membrane (CM) to permeabilise the bilayer structure and induce cell lysis. This finding is highly relevant to the field of colistin resistance because of past studies indicating that the cationic modifications of lipid A conferring polymyxin non-susceptibility take place at the CM, prior to LPS being exported to the outer membrane (OM) bacterial surface<sup>784</sup>. The first piece of evidence that LPS is modified at the CM arose from the revelation that all the enzymes catalysing the addition of positively-charged chemical groups on to lipid A (the MCR/PmrC pEtN transferases and the ArnT L-Ara4N transferase) are located in the CM, with regions that span the innermost membrane bilayer and functional domains that face the periplasmic surface<sup>484,785–787</sup>. Moreover, the modification of LPS with L-Ara4N/pEtN has been shown to be dependent on the MsbA-dependent flipping of lipid A structures from the cytoplasmic-facing innermost leaflet of the CM bilayer to its outermost leaflet, with the accumulation of cationically-modified LPS in the CM only apparent when the MsbA flippase was functional<sup>204</sup>. Given the bactericidal activity of colistin is dependent on interactions with LPS in the CM, and that the LPS modifications resulting in polymyxin non-susceptibility happen within the CM, the hypothesis examined in this chapter is that resistance to colistin in Gram-negative pathogens is mediated not at the OM of cells, but at the CM. Using a combination of *mcr* and chromosomally colistin-resistant bacterial strains, constructed in the laboratory and isolated from patients, misunderstandings in the mechanism of colistin resistance are resolved.



## 5.2 Colistin permeabilises the outer membrane of polymyxin-resistant *E. coli* expressing *mcr-1*

In order to investigate whether colistin non-susceptibility conferred by the widely prevalent mobile resistance determinant MCR-1 was mediated at the bacterial OM or the CM bilayer, cells of the *E. coli* reference strain MC1000 were transformed with the IPTG-inducible plasmid pDM1 harbouring the *mcr-1* gene encoding the pEtN transferase enzyme<sup>788</sup>. In addition, *E. coli* MC1000 cells were also transformed with the pDM1 vector alone for use as an empty plasmid control bacterial population (pEmpty), creating an isogenic strain pair that was optimised for subsequent experiments on the mechanism of colistin resistance. These studies were performed using *E. coli* because the species is the most common host organism for the *mcr-1* gene found in the environment and in veterinary/human medicine<sup>551,789</sup>. Before the isogenic *E. coli* pair generated could be utilised in analytical assays, it was first crucial to determine if expression of *mcr-1* was associated with any notable growth defects that could provide a potential source of bias when interpreting results. However, over a 16 hour incubation, the growth profiles of MC1000 cells harbouring *mcr-1* and empty plasmid control cells were virtually identical, with only a minor reduction in the rate of logarithmic growth observed in *mcr-1*-positive bacteria and no difference in OD<sub>600nm</sub> readings by the end of the experiment (**Figure 5.1A**).

Next, it was important to verify that possession of the *mcr-1* containing pDM1 plasmid in *E. coli* led to successful translation/production of the MCR-1 enzyme, and ultimately bestowed polymyxin resistance on the bacterial cell population. This was done by determining the MIC of colistin against the isogenic pair of strains, which showed that growth of *mcr-1*-harbouring MC1000 cells was only fully inhibited at a colistin concentration of 4 µg ml<sup>-1</sup> – above the CLSI/BSAC breakpoint for polymyxin resistance and 16-fold higher than the colistin MIC of pEmpty *E. coli* (**Figure 5.1B**)<sup>606,790</sup>. Thus, correct expression of the *mcr-1* gene was proven, with the pEtN transferase protein encoded by the resistance determinant responsible for causing colistin non-susceptibility.

To establish which cell envelope membrane structure, the OM or the CM, was the site at which this polymyxin resistance was mediated, the preliminary assay conducted used the well-established phospholipid-reactive fluorescent NPN dye as a marker for colistin-induced OM permeabilisation<sup>626</sup>. Across a range of therapeutically-relevant colistin concentrations (0.5-10 µg ml<sup>-1</sup>), exposure of susceptible *E. coli* MC1000 cells containing only the empty pDM1 plasmid to the antibiotic triggered a dose-dependent increase in uptake of the NPN fluorophore, indicating that, as expected, the polymyxin drug was disrupting the surface OM bilayer (**Figure 5.1C**). Interestingly, however, the same phenotype was also observed with colistin-resistant *E. coli* expressing *mcr-1*, with the polymyxin antibiotic still able to damage

the bacterial OM, and no significant differences in fluorescence from the NPN dye between the pEmpty and *mcr-1* cell populations. It was therefore concluded that resistance to colistin conferred by the *mcr-1* gene could not be due to protection of the OM from the antibiotic's permeabilising effects, because the polymyxin disrupted the outermost cell surface bilayer of susceptible and resistant *E. coli* to equal extents.

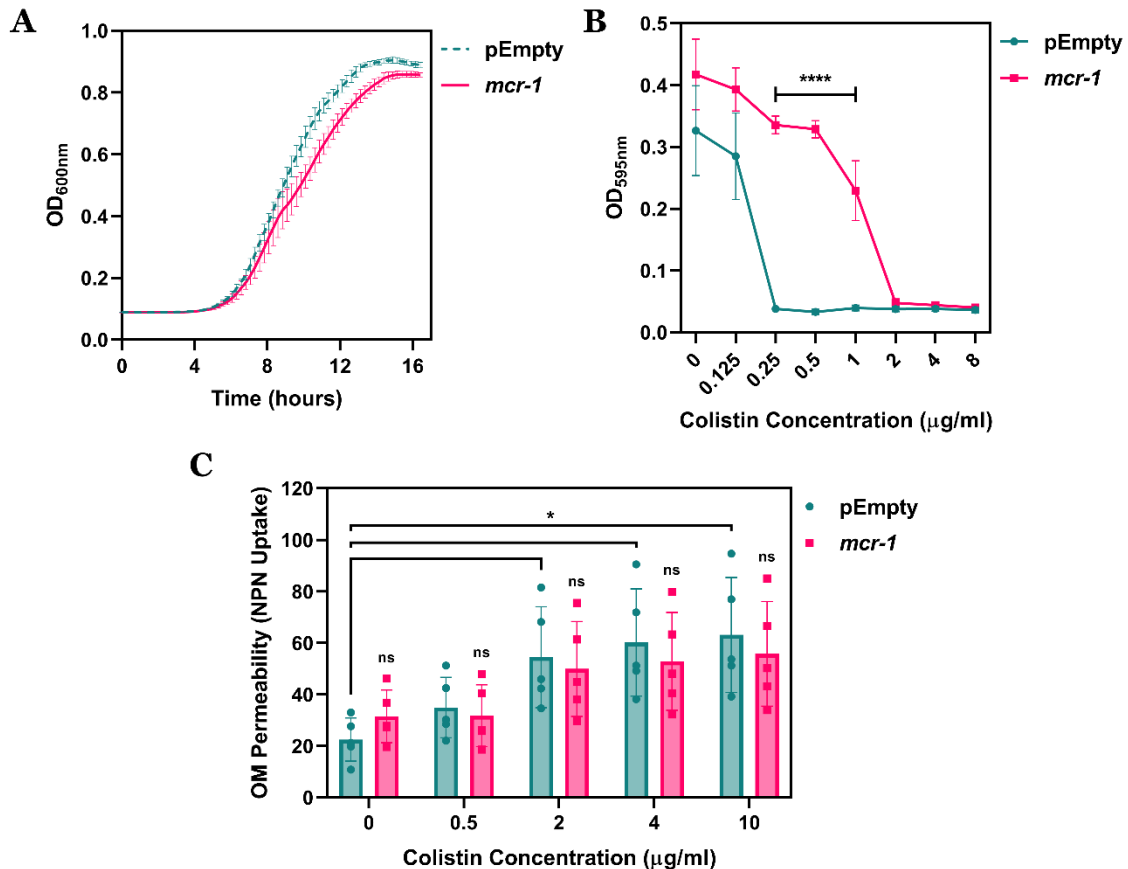


**Figure 5.1: Expression of the *mcr-1* gene in polymyxin-resistant *E. coli* does not prevent colistin from disrupting the OM.** **A**, Growth kinetics of *E. coli* MC1000 cells harbouring the *mcr-1* gene on the pDM1 plasmid and empty plasmid control cells (pEmpty), as determined by measuring OD<sub>600nm</sub> over 16 hours incubation (n=3 in triplicate). **B**, The MIC of colistin against *E. coli* MC1000 cells harbouring *mcr-1* and empty plasmid control cells, as determined by measuring OD<sub>595nm</sub> after 18 hours exposure to a range of clinically-relevant colistin concentrations (n=3 in triplicate; \*\*\*\*p<0.0001 for *mcr-1*-positive bacteria relative to pEmpty bacteria). **C**, Permeabilisation of the OM of *E. coli* MC1000 cells harbouring *mcr-1* and empty plasmid control cells during exposure to a range of concentrations of colistin, as determined by measuring uptake of the NPN fluorophore (10 µM) over 10 minutes (n=5, each data point represents the arithmetic mean of 20 replicate measurements; \*p<0.05 for pEmpty bacteria relative to untreated cells, ns: p>0.05 for *mcr-1*-positive bacteria relative to pEmpty bacteria). Data in **B** were analysed by a two-way ANOVA with Sidak's post-hoc test. Data in **C** were analysed by a two-way ANOVA with both Sidak's and Dunnett's post-hoc tests. Data are presented as the arithmetic mean, and error bars represent the standard deviation of the mean.

### 5.3 Colistin cannot permeabilise the cytoplasmic membrane of *mcr-1*-positive *E. coli*

Having demonstrated that colistin maintained its capacity to damage the OM of even non-susceptible, *mcr-1*-expressing *E. coli* cells, it was decided to measure CM disruption by the antibiotic to explore if the innermost of the two cell envelope bilayers was mediating colistin resistance. Using fluorescence from the DNA-reactive PI dye as a read-out for the degree of CM permeabilisation stimulated by colistin, the isogenic MC1000 strain pair was exposed to the polymyxin drug ( $4 \mu\text{g ml}^{-1}$ ) for 8 hours. As previously observed with colistin-susceptible *P. aeruginosa* cells, the polymyxin antibiotic markedly damaged the CM of empty plasmid-containing *E. coli*, with a rapid increase in the fluorescent PI signal compared to untreated bacteria that peaked following 4 hours of colistin treatment (**Figure 5.2A**). By contrast MC1000 cells expressing the *mcr-1* gene exhibited almost no CM disruption at all during colistin exposure, with the kinetics of PI uptake closely resembling that of bacteria when the polymyxin was not even present. Hence, in spite of colistin's propensity to damage the OM of *E. coli* resistant to the drug due to production of MCR-1, the CM of these same non-susceptible cells was protected from polymyxin permeabilisation, providing the initial evidence that the CM was the critical factor in this mobile form of colistin resistance.

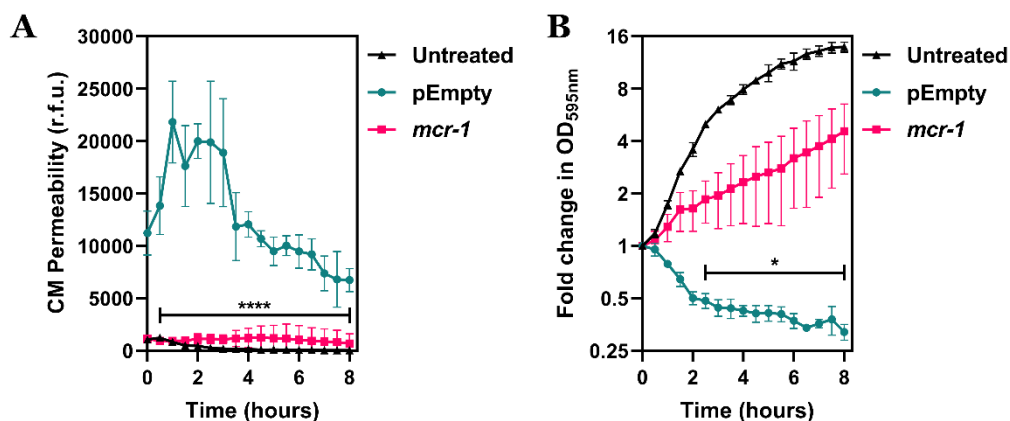


**Figure 5.2: The CM of *mcr-1*-expressing *E. coli* is not permeabilised by colistin, protecting cells from being lysed.** **A**, Permeabilisation of the CM of *E. coli* MC1000 cells harbouring *mcr-1* and empty plasmid control cells during exposure to colistin ( $4 \mu\text{g ml}^{-1}$ ), as determined by measuring fluorescence from PI ( $2.5 \mu\text{M}$ ) over 8 hours ( $n=4$ ; \*\*\*\* $p<0.0001$  for *mcr-1*-positive bacteria relative to pEmpty bacteria). **B**, Lysis/growth of *E. coli* MC1000 cells harbouring *mcr-1* and empty plasmid control cells during exposure to colistin ( $4 \mu\text{g ml}^{-1}$ ), as determined by measuring OD<sub>595nm</sub> over 8 hours ( $n=4$ ; \* $p<0.05$  for *mcr-1*-positive bacteria relative to pEmpty bacteria). Data in **A**, **B** were analysed by a two-way ANOVA with Dunnett's post-hoc test. Data are presented as the arithmetic mean, and error bars represent the standard deviation of the mean.

To understand the downstream consequences on bacterial lysis of the disparity in colistin-triggered CM disruption between *mcr-1*-positive and pEmpty *E. coli* cells, readings of OD<sub>595nm</sub> were obtained during treatment with the polymyxin drug (4 µg ml<sup>-1</sup>) for 8 hours. The striking rise in PI fluorescence and CM permeabilisation detected in the susceptible empty plasmid control bacteria was associated with an expected, but sharp, decrease in OD<sub>595nm</sub> measurements for the duration of colistin exposure, as the MC1000 cells lysed and the culture became clear (**Figure 5.2B**). In opposition, the *E. coli* population expressing *mcr-1* displayed an increase in OD<sub>595nm</sub> readings over 8 hours, implying that the bacteria were able to grow in the presence of colistin, although not at the rate of untreated cells. Together, these data highlighted that the activity of the MCR-1 pEtN transferase enzyme blocked colistin's membranolytic properties against the CM, not the OM, enabling bacteria producing the resistance determinant to not only survive, but also divide during polymyxin exposure.

#### **5.4 Prevention of CM disruption by colistin in *mcr-1*-positive *E. coli* depends on the extent of lipid A modification**

With preliminary data suggesting that colistin resistance conferred by the *mcr-1* gene in *E. coli* whole cells was mediated by protection of the CM rather than the OM from the antibiotic's bilayer-damaging effects, for this finding to be confirmed, it was necessary to examine whether MCR-1-producing *E. coli* spheroplasts, lacking an OM/cell wall and enveloped by only a surface CM, were also resistant to the polymyxin antibiotic. However, prior to undertaking this experiment, as with the *P. aeruginosa* spheroplasts, a number of control assays were carried out to ensure that the standard protocol for generating spheroplasts from whole cells (successive treatment with EDTA, lysozyme and trypsin) did indeed remove the bacterial OM and cell wall structures correctly<sup>637</sup>. First, the morphology of *E. coli* MC1000 populations harbouring *mcr-1* or the empty plasmid alone was assessed by microscopy, both before and after conversion to spheroplasts was attempted. While whole bacterial cells (both *mcr-1* and pEmpty) unexposed to EDTA/lysozyme/trypsin appeared in their conventional rod-like form, the spheroplasts produced from these cells were spherical, with their length and width being approximately equal in size (**Figure 5.3A**). This observation was further strengthened by calculating the length:width ratio of 100 whole cells and spheroplasts from each strain of the isogenic *E. coli* pair, which revealed a transformation from the elongated nature of untreated whole bacteria to cell forms with a length:width ratio of precisely 1 – a firm indicator of successful cell wall digestion in spheroplasts being held in an osmoprotective 20% sucrose environment (**Figure 5.3B**).

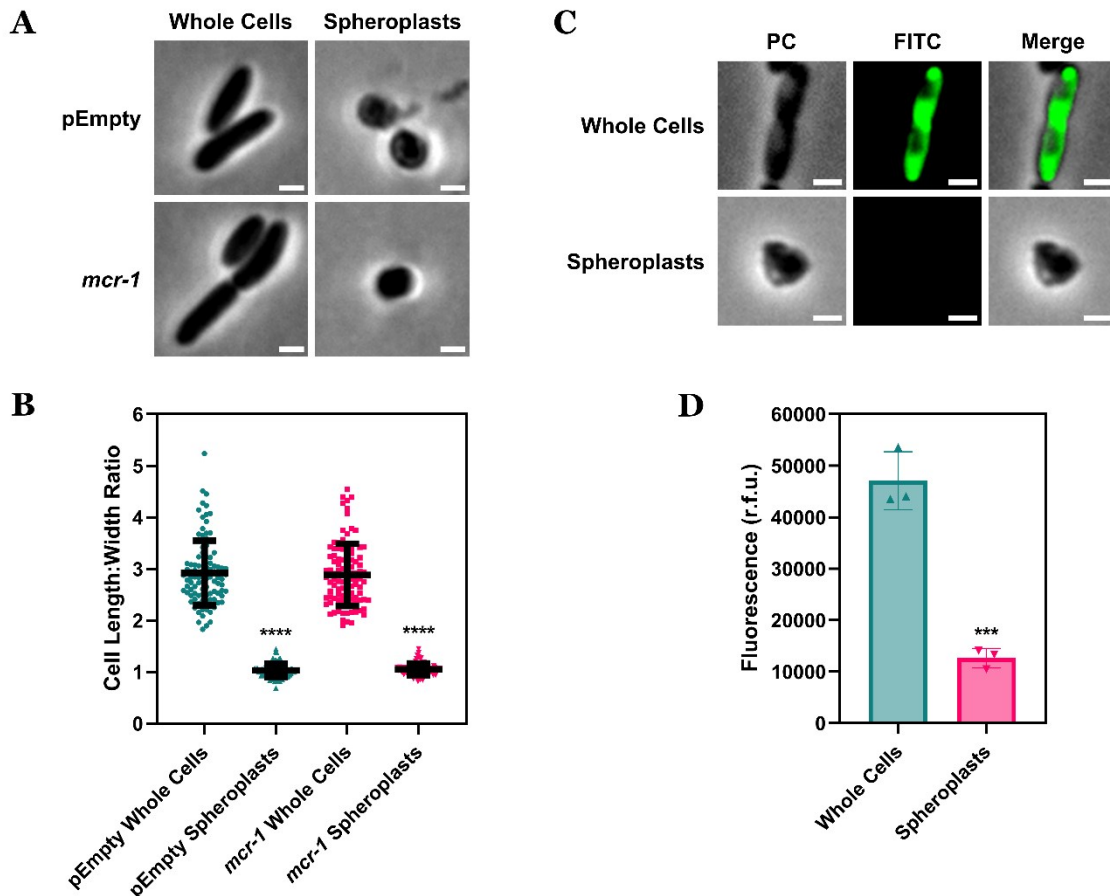


**Figure 5.3: Spheroplasts generated from *E. coli* are spherical, with no OM contamination in the CM.** **A**, Visualisation by phase contrast microscopy of *E. coli* MC1000 whole cells (both the *mcr-1*-expressing strain and the empty plasmid control strain), before and after treatment with EDTA (0.25 mg ml<sup>-1</sup>), lysozyme (1 mg ml<sup>-1</sup>) and trypsin (0.5 mg ml<sup>-1</sup>) to produce spheroplasts lacking an OM and cell wall (images are representative of cells visualised across 3 independent experiments; Scale bars: 5 µm). **B**, Quantification of length:width ratio of *E. coli* MC1000 whole cells before/after treatment with EDTA, lysozyme and trypsin to produce spheroplasts (n=100 cells per group; \*\*\*\*p<0.0001 relative to pEmpty and *mcr-1* whole cells respectively). **C**, Visualisation by fluorescence microscopy of *E. coli* MC1000 pEmpty whole cells labelled with FITC (0.5 mg ml<sup>-1</sup>) to tag OM proteins before/after treatment with EDTA, lysozyme and trypsin to produce spheroplasts (images are representative of cells visualised across 3 independent experiments; PC: phase contrast; Scale bars: 5 µm). **D**, Quantification of fluorescence from FITC-labelled OM proteins in *E. coli* MC1000 pEmpty whole cells before/after treatment with EDTA, lysozyme and trypsin to produce spheroplasts (n=3 in triplicate; \*\*\*p<0.001 relative to whole cells). Data in **B** were analysed by a one-way ANOVA with Tukey's post-hoc test. Data in **D** were analysed by a two-tailed unpaired Student's *t*-test. Data are presented as the arithmetic mean, and error bars represent the standard deviation of the mean.

To investigate if the process for generating MC1000 spheroplasts suitably removed the OM bilayer – a potential confounding factor in assays studying the role of the CM in colistin resistance – proteins in the OM of whole *E. coli* cells were tagged with fluorescent FITC molecules, and changes in FITC fluorescence were evaluated following implementation of the spheroplast conversion protocol<sup>638</sup>. Visualisation by microscopy showed an accumulation of

fluorescently-tagged FITC proteins around the OM surface of MC1000 whole cells, which was entirely lost once the treatment with EDTA, lysozyme and trypsin had occurred (**Figure 5.3C**). Quantification by measuring fluorescence across the entire *E. coli* populations supported this finding, with a prominent and significant decrease in the fluorescent FITC signal after production of spheroplasts from whole cells (**Figure 5.3D**). Combined, these control experiments convincingly proved the appropriateness of the process used for removing the OM and cell wall from Gram-negative bacteria to successfully create spheroplasts.

In order to determine whether the correctly-generated MCR-1-producing spheroplasts were able to tolerate colistin exposure, and in the process make apparent the key role of the CM in mediating polymyxin resistance, these OM/wall-lacking cell forms were exposed for 12 hours to the antibiotic ( $4 \mu\text{g ml}^{-1}$ ) and the capacity of colistin to induce CM permeabilisation and lysis was tested. In *E. coli* MC1000 spheroplasts harbouring only the empty plasmid control, treatment with colistin resulted in an obvious increase in fluorescence from the PI dye relative to untreated spheroplasts – indicative of major damage to the CM caused by the polymyxin drug, which allowed PI molecules to access cytoplasmic DNA and fluoresce (**Figure 5.4A**). Contrastingly, in spheroplasts produced from MC1000 cells expressing the *mcr-1* gene, colistin caused no discernible rise in the fluorescent PI signal compared to spheroplasts where the antibiotic was not present, with a significant decrease in the kinetics of CM disruption relative to pEmpty spheroplasts. Thus, even in the absence of an OM bilayer, MCR-1 protects the CM of cells harbouring the resistance determinant from colistin's membrane-disrupting behaviour. In corroboration, whereas colistin exposure triggered rapid and extensive lysis of spheroplasts from pEmpty *E. coli* cells (nearly 8-fold decrease in  $\text{OD}_{600\text{nm}}$  readings after 12 hours), the rate of cell lysis in *mcr-1*-expressing spheroplasts was less than that of untreated spheroplasts (**Figure 5.4B**). These data served to emphasise that the mechanism by which MCR-1 conferred polymyxin resistance was through blocking of CM permeabilisation by colistin, which prevented lysis and promoted bacterial viability.

It was postulated that the MCR-1 pEtN transferase mediated resistance to colistin at the CM because the enzyme cationically modified the lipid A domain of LPS while it was situated in this innermost membrane bilayer. The importance of the interaction between colistin molecules and CM LPS structures for the antibiotic's bactericidal activity has been previously characterised, leading to the proposal that the addition by MCR-1 of positively-charged pEtN to lipid A in the CM may hamper colistin's ability to bind to CM LPS, culminating in polymyxin resistance. To explore if this was true, by taking advantage of the IPTG-inducible nature of the pDM1 plasmid carrying the *mcr-1* gene, spheroplasts of *E. coli* MC1000 cells were generated with varying levels of *mcr-1* expression and subsequent LPS modification. The extent of lipid A modification by the MCR-1 enzyme was analysed by a

lipidomic approach using MALDI-TOF mass spectrometry, which can distinguish between unmodified LPS and pEtN-modified LPS, where the additional mass of the cationically-altered polysaccharide results in the appearance of a distinct peak<sup>639</sup>. This demonstrated that the LPS in the CM of spheroplasts produced from pEmpty cells unsurprisingly consisted entirely of unmodified lipid A, but also that the ratio of modified:unmodified LPS in the CM of *mcr-1*-harbouring spheroplasts could be manipulated by changing the concentration of IPTG used to induce expression of the gene (**Figure 5.4C**). When expression of *mcr-1* was induced with a high concentration of IPTG, the size of the unmodified lipid A peak decreased compared to when no IPTG was present, implying that more MCR-1 protein was being produced, and more CM LPS was being modified with pEtN moieties. Calculating the area under the respective modified and unmodified LPS peaks enabled this effect to be semi-quantified, and a significant increase in the ratio of modified:unmodified lipid A (from 3:1 to 4:1) was visible as the concentration of IPTG added to induce *mcr-1* expression was increased (**Figure 5.4D**).

Having generated *E. coli* spheroplasts with differing amounts of pEtN-modified LPS in the CM, it was now possible to elucidate the role of this cationic alteration to lipid A on colistin resistance. The three spheroplast populations (no modified lipid A, low-level lipid A modifications, high-level lipid A modifications) were all exposed to colistin (4 µg ml<sup>-1</sup>) for 8 hours, and as before, measurements of CM permeabilisation (via PI fluorescence) and cell lysis (via OD<sub>600nm</sub> readings) were made. Whilst the CM of pEmpty MC1000 spheroplasts with no lipid A modifications was severely damaged by the polymyxin drug, there was a direct correlation between the extent of LPS modification and colistin-induced CM disruption for *mcr-1* spheroplasts (**Figure 5.4E**). Where expression of the *mcr-1* gene was induced with a high concentration of IPTG, and more lipid A was modified with pEtN, no palpable increase in PI uptake was seen; however, in the absence of IPTG induction and a consequential lower level of lipid A modification, permeabilisation of the CM initiated by colistin was no longer abrogated entirely, with an increase in the fluorescent PI signal after 6 hours.

In keeping with these results, observations of changes in OD<sub>600nm</sub> readings in the three *E. coli* spheroplast populations made evident that spheroplasts with no modified LPS were lysed comprehensively by colistin, spheroplasts with high-level LPS modification induced by IPTG displayed no lysis, and spheroplasts with low-level LPS modification without any IPTG induction exhibited an intermediate phenotype, with a slower rate of cell lysis (**Figure 5.4F**). In summary, there was a clear dose-dependent effect between how much CM lipid A was modified by MCR-1, and the protection conferred against polymyxin-induced CM disruption and lysing of bacteria. Hence, it was concluded that the presence of pEtN-modified LPS in the CM on *mcr-1*-expressing *E. coli* is what mediated resistance to the antibiotic.

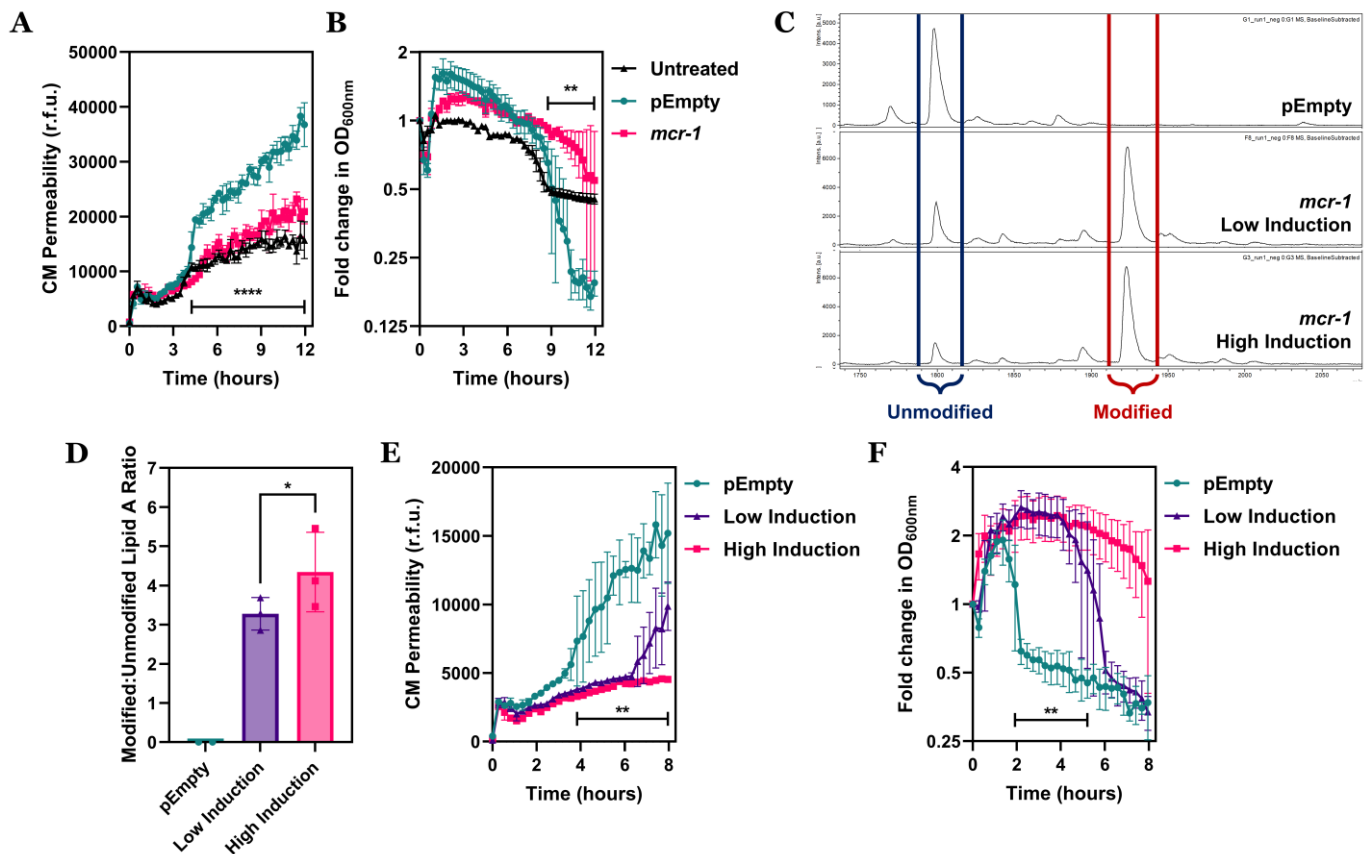


**Figure 5.4: LPS modifications in the CM protect *mcr-1*-positive *E. coli* from colistin-mediated CM disruption/lysis in a dose-dependent manner.** **A**, Permeabilisation of the CM of spheroplasts produced from *E. coli* MC1000 cells harbouring *mcr-1* and empty plasmid control cells during exposure to colistin ( $4 \mu\text{g ml}^{-1}$ ), as determined by measuring fluorescence from PI ( $0.25 \mu\text{M}$ ) over 12 hours ( $n=3$ , assay performed on 4 independent occasions; \*\*\*\* $p<0.0001$  for *mcr-1*-positive bacteria relative to pEmpty bacteria). **B**, Lysis of spheroplasts produced from *E. coli* MC1000 cells harbouring *mcr-1* and empty plasmid control cells during exposure to colistin ( $4 \mu\text{g ml}^{-1}$ ), as determined by measuring  $\text{OD}_{600\text{nm}}$  over 12 hours ( $n=3$ , assay performed on 4 independent occasions; \*\* $p<0.01$  for *mcr-1*-positive bacteria relative to pEmpty bacteria). **C**, Lipidomic MALDI-TOF mass spectra showing the abundance of unmodified lipid A and pEtN-modified lipid A in spheroplasts produced from *E. coli* MC1000 pEmpty cells, *mcr-1*-harbouring cells where IPTG was not used for inducing *mcr-1* gene expression (“Low Induction”), or *mcr-1*-harbouring cells where *mcr-1* gene expression was induced with  $0.5 \text{ mM}$  IPTG (“High Induction”; all spectra representative of 3 independent experiments). **D**, Quantification of ratio of modified lipid A:unmodified lipid A in spheroplasts produced from *E. coli* MC1000 pEmpty cells, *mcr-1*-harbouring cells with a low level of *mcr-1* expression, or *mcr-1*-harbouring cells with a high level of *mcr-1* expression, as determined by measuring the area under the mass spectra peaks ( $n=3$ ; \* $p<0.05$  for “High Induction” compared to “Low Induction”). **E**, Permeabilisation of the CM of spheroplasts produced from *E. coli* MC1000 pEmpty cells, *mcr-1*-harbouring cells with a low level of *mcr-1* expression, or *mcr-1*-harbouring cells with a high level of *mcr-1* expression, as determined by measuring fluorescence from PI ( $0.25 \mu\text{M}$ ) over 8 hours ( $n=3$ , assay performed on 3 independent occasions; \*\* $p<0.01$  for *mcr-1*-positive bacteria relative to pEmpty bacteria). **F**, Lysis of spheroplasts produced from *E. coli* MC1000 pEmpty cells, *mcr-1*-harbouring cells with a low level of *mcr-1* expression, or *mcr-1*-harbouring cells with a high level of *mcr-1* expression, as determined by measuring  $\text{OD}_{600\text{nm}}$  over 8 hours ( $n=3$ , assay performed on 3 independent occasions; \*\* $p<0.01$  for *mcr-1*-positive bacteria relative to pEmpty bacteria). Data in **A**, **B**, **E**, **F** were analysed by a two-way ANOVA with Dunnett’s post-hoc test. Data in **D** were analysed by a two-tailed paired Student’s *t*-test. Data are presented as the arithmetic mean, and error bars represent the standard deviation of the mean.



## 5.5 MCR-1-mediated protection of the *E. coli* CM is colistin-specific and due to altered membrane charge

The fact that the occurrence of pEtN-modified lipid A in the CM was associated with a loss of colistin's CM permeabilising activity and tolerance to the antibiotic did not definitively resolve the mechanism of polymyxin resistance conferred by the *mcr-1* gene. One central possibility to consider was that cationic alterations to CM LPS molecules may affect the biophysical properties of the inner cell envelope bilayer, in particular changing the fluidity or the electrostatic charge of the membrane. Variations in both membrane fluidity and membrane charge have been widely implicated in past studies as causal factors contributing to resistance to antimicrobial peptides such as colistin<sup>791–795</sup>. To understand if the cationic modifications to lipid A mediated by the MCR-1 resistance determinant led to colistin resistance through effects on the fluidity or charge of the *E. coli* CM, gold-standard techniques were applied to measure these membrane attributes in the MC1000 pEmpty/*mcr-1* isogenic strain pair.

Using whole cells and spheroplasts of the *E. coli* bacterial populations, changes in fluidity of the OM as well as the CM resulting from *mcr-1* expression were probed with the fluorescent Laurdan dye<sup>642</sup>. This fluorophore enables calculation of the Generalised Polarisation (GP) value of membrane bilayers, which is an indicator of how much water can penetrate into the membrane and thus a marker of how rigid the bilayer structure is. There was no difference in the GP value between MC1000 whole cells producing MCR-1 and whole cells containing the empty plasmid control alone, showing that the fluidity of the bacterial OM was unaltered by the activity of the pEtN transferase enzyme (**Figure 5.5A**). In comparison to the fluidity of the OM in *E. coli* whole cells, the CM of the spheroplasts formed from these cells had a significantly lower GP value, suggesting that the CM had a much more fluid nature than the OM – perhaps due to the notably lower concentration of LPS molecules in the innermost of the two cell envelope bilayers. Nevertheless, the rigidity of the CM of MC1000 spheroplasts expressing *mcr-1* was found to be identical to that of pEmpty spheroplasts, eliminating alterations in CM fluidity as an explanation for why pEtN modifications of CM lipid A blocked colistin from damaging the bilayer structure.

In order to dissect whether MCR-1 adjusted the electrostatic charge of the *E. coli* OM/CM to confer polymyxin resistance, a fluorescent FITC-labelled derivative of the highly cationic compound Poly-L-Lysine (PLL) was exploited<sup>643</sup>. The capacity for FITC-tagged PLL to bind to the surface of MC1000 whole cells and spheroplasts served as a direct read-out of membrane charge, because a more positively-charged bilayer would have reduced affinity for PLL molecules, and hence a reduced fluorescent signal from FITC-PLL accumulated at the cell surface would be detected. Interestingly, the extent of PLL binding to the OM of *E. coli* whole

cells harbouring the *mcr-1* plasmid was unchanged relative to empty plasmid control cells, revealing that the electrostatic charge of the bacterial OM bilayer was not substantially affected by MCR-1 activity (**Figure 5.5B**). In contrast, the amount of fluorescent PLL bound to the CM of MC1000 spheroplasts expressing *mcr-1* was significantly lower than the amount bound to pEmpty spheroplasts, which demonstrated that the MCR-1 enzyme functioned to make the *E. coli* CM more positively-charged. Indeed, this was not a surprising finding, and was almost certainly reflective of the presence of cationically-modified LPS in the CM of *mcr-1*-positive bacteria that was previously presented. However, this data did provide key mechanistic insight insofar as it implied that colistin resistance mediated by the protection MCR-1 conferred on the CM may be a consequence of electrostatic repulsion of positively-charged colistin molecules away from the CM bilayer. Moreover, the discovery that expression of *mcr-1* did not correlate with changes in the charge of the *E. coli* OM offered the first indication of why colistin was still able to disrupt the OM of these polymyxin-resistant bacteria.

To test if the increase in the net positive charge of the CM in *mcr-1*-expressing bacterial cells provided protection specifically to colistin's membrane permeabilising effects, or to cationic antimicrobial peptides in general, *E. coli* MC1000 spheroplasts were exposed to daptomycin or nisin (both added at 20  $\mu\text{g ml}^{-1}$ ) for 8 hours. These two antibacterial agents are positively-charged, with modulations in membrane charge a common mode of resistance to the peptide compounds<sup>796,797</sup>. When assessing CM disruption in the spheroplasts by uptake of the DNA-reactive PI fluorophore, daptomycin and nisin induced a dramatic increase in the fluorescent PI signal of both MCR-1-producing spheroplasts and empty plasmid control spheroplasts (**Figure 5.5CD**). Therefore, unlike colistin, these cationic antimicrobial peptides were able to damage the *E. coli* CM irrespective of whether its electrostatic charge was made more positive by the pEtN-transferring action of MCR-1.

Similarly, when observing cell lysis during treatment with daptomycin/nisin, the two antibacterial compounds triggered an equally rapid drop in OD<sub>600nm</sub> readings in pEmpty and *mcr-1* spheroplasts over the 8 hour incubation period (**Figure 5.5EF**). Again, this was in complete opposition to the phenotype with colistin, and it was inferred that the increase in the CM's net positive charge in *mcr-1*-positive *E. coli* did not promote tolerance to all cationic polypeptide antibiotics. Rather, the polymyxin-specific quality of the antimicrobial antagonising behaviour of the MCR-1 enzyme strongly insinuated that colistin did not share the same CM target as daptomycin and nisin (typically thought to bind to membrane phospholipids), and thus was wholly in keeping with the earlier conclusion that colistin killed Gram-negative bacteria by targeting LPS in the CM<sup>798,799</sup>. Together, these results established a model by which *mcr-1* expression instigated polymyxin resistance via cationic pEtN modifications to CM LPS and subsequent repulsion of colistin molecules away from the CM.

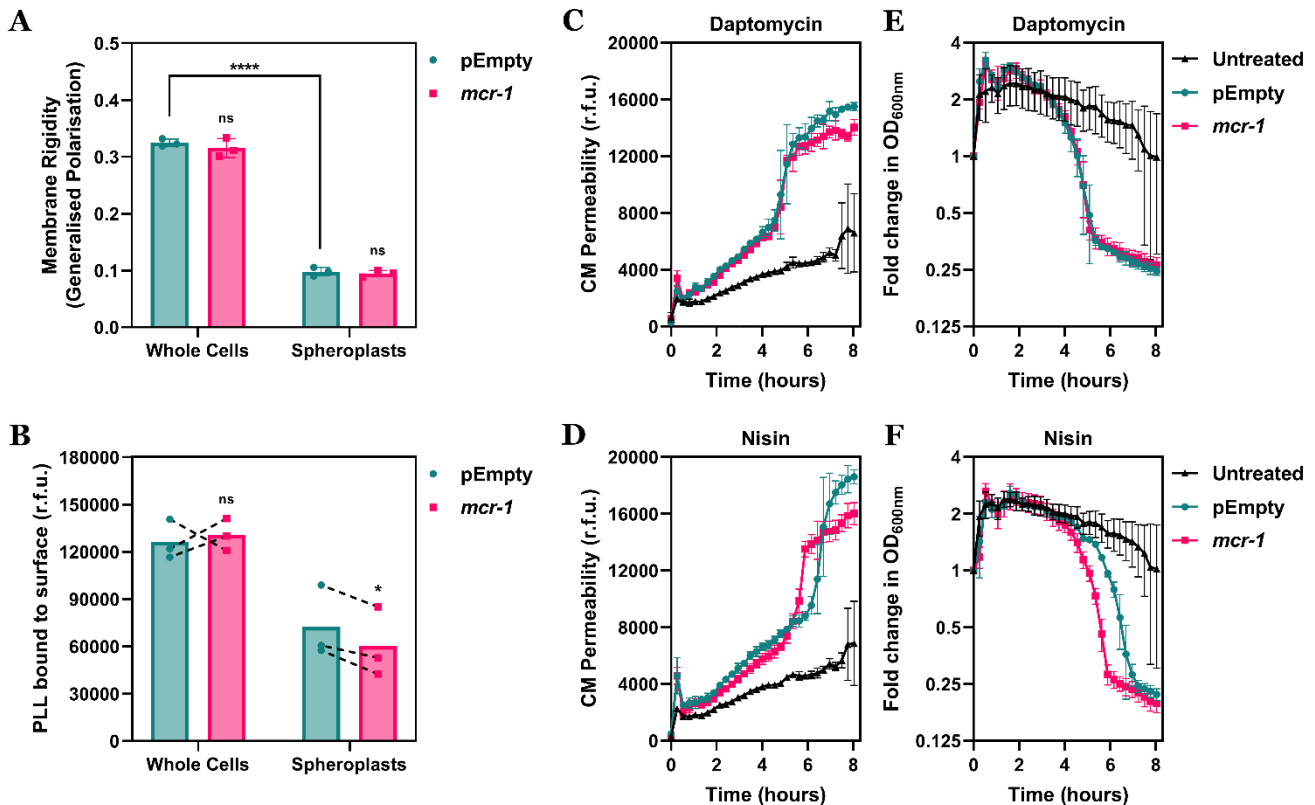


**Figure 5.5: MCR-1 increases the positive charge of the *E. coli* CM but specifically inhibits colistin's CM permeabilising and lytic properties.** **A**, Rigidity of the OM/CM of *E. coli* MC1000 whole cells and spheroplasts, in each case either harbouring *mcr-1* or an empty plasmid control, as determined using the fluorescent Laurdan dye (100  $\mu$ M) to generate Generalised Polarisation values ( $n=3$  in duplicate; ns:  $p>0.05$  for *mcr-1*-positive bacteria relative to pEmpty bacteria, \*\*\*\* $p<0.0001$  for pEmpty spheroplasts relative to pEmpty whole cells). **B**, Net negative charge of the OM/CM of *E. coli* MC1000 whole cells and spheroplasts, in each case either harbouring *mcr-1* or an empty plasmid control, as determined by measuring binding of highly cationic FITC-labelled Poly-L-Lysine (PLL, 20  $\mu$ g ml<sup>-1</sup>) to the cell surface ( $n=3$ ; ns:  $p>0.05$ , \* $p<0.05$  for *mcr-1*-positive bacteria relative to pEmpty bacteria). **C**, **D**, Permeabilisation of the CM of spheroplasts produced from *E. coli* MC1000 cells harbouring *mcr-1* and empty plasmid control cells during exposure to **(C)** daptomycin (20  $\mu$ g ml<sup>-1</sup> with 1.25 mM Ca<sup>2+</sup> ions), or **(D)** nisin (20  $\mu$ g ml<sup>-1</sup>), as determined by measuring fluorescence from PI (0.25  $\mu$ M) over 8 hours ( $n=3$ , assay performed on 4 independent occasions). **E**, **F**, Lysis of spheroplasts produced from *E. coli* MC1000 cells harbouring *mcr-1* and empty plasmid control cells during exposure to **(E)** daptomycin (20  $\mu$ g ml<sup>-1</sup> with 1.25 mM Ca<sup>2+</sup> ions), or **(F)** nisin (20  $\mu$ g ml<sup>-1</sup>), as determined by measuring OD<sub>600nm</sub> over 8 hours ( $n=3$ , assay performed on 4 independent occasions). Data in **A** were analysed by a two-way ANOVA with Tukey's post-hoc test. Data in **B** were analysed by two-tailed paired Student's *t*-tests. Data are presented as the arithmetic mean, and error bars shown represent the standard deviation of the mean.

## 5.6 The CM of *mcr-1*-positive *E. coli* has a higher proportion of modified lipid A than the OM

To further comprehend why *mcr-1*-conferred colistin non-susceptibility was mediated at the CM of *E. coli* cells, and why the antibiotic was able to permeabilise the OM of these polymyxin-resistant bacteria, MALDI-TOF mass spectrometry-based lipidomic analysis was performed on both whole cells and spheroplasts of MC1000 populations expressing *mcr-1*,

allowing for the computation of the ratio between unmodified and pEtN-modified LPS in the OM and CM respectively. The mass spectra obtained from this experiment depicted the presence of unaltered lipid A and lipid A with an additional pEtN chemical group in both whole cells and spheroplasts of MCR-1-producing *E. coli*; however, it was immediately apparent that the proportion of pEtN-modified lipid A relative to unmodified lipid A was much higher in MC1000 spheroplasts compared to whole cells (**Figure 5.6A**). The fact that the difference in the size of the unaltered and cationically-altered LPS peaks was greater in *mcr-1*-positive spheroplasts than in whole cells suggested that the ratio of modified:unmodified lipid A was larger in the bacterial CM bilayer than in the OM.

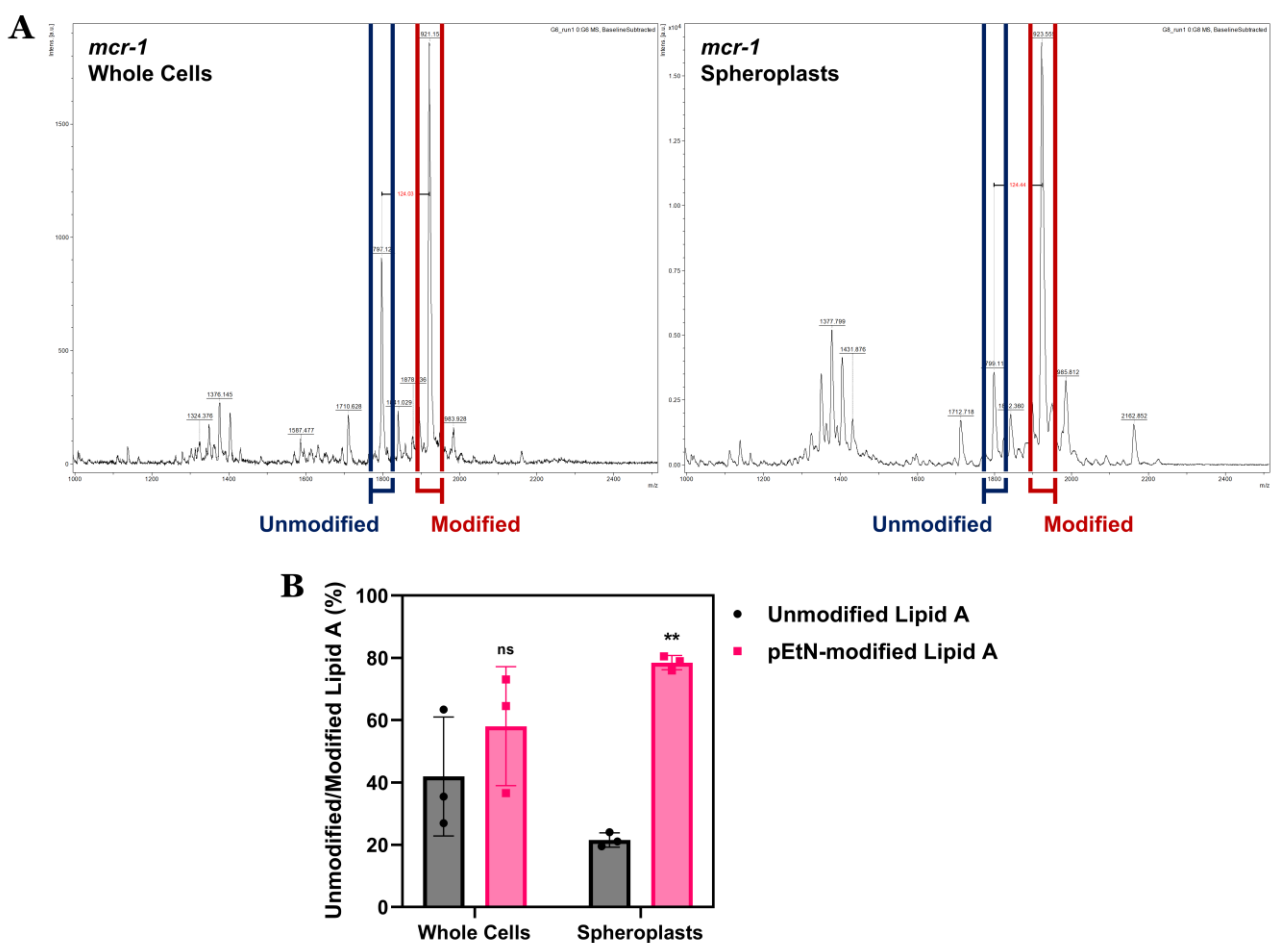


**Figure 5.6: The ratio of modified:unmodified lipid A is higher in the CM than in the OM of *mcr-1*-expressing *E. coli*.** **A**, Lipidomic MALDI-TOF mass spectra showing the abundance of unmodified lipid A and pEtN-modified lipid A in the OM/CM of MCR-1-positive *E. coli* MC1000 whole cells and spheroplasts (spectra representative of 3 independent experiments). **B**, Quantification of percentage of unmodified lipid A and pEtN-modified lipid A in the OM/CM of MCR-1-positive *E. coli* MC1000 whole cells and spheroplasts, as determined by measuring the area under the mass spectra peaks (n=3 in duplicate; ns: p>0.05, \*\*p<0.01 for pEtN-modified lipid A relative to unmodified lipid A). Data in **B** were analysed by a two-way ANOVA with Sidak's post-hoc test. Data are presented as the arithmetic mean, and error bars represent the standard deviation of the mean.

This was validated semi-quantitatively by measuring the area under the relevant mass spectra peaks, which highlighted that in the OM of *E. coli* whole cells expressing the *mcr-1* gene, there was an almost equal amount (40% compared to 60%) of unmodified and pEtN-modified LPS (**Figure 5.6B**). In stark contrast, when looking specifically at the CM in MCR-1-producing spheroplasts, there was 4-fold more cationically-modified lipid A than there was unaltered lipid A (80% compared to 20%). In combination, these outcomes of the lipidomic assay offered a likely explanation for why colistin can disrupt the OM of *E. coli* cells that are not susceptible to the antibiotic through the action of *mcr-1* – because the outermost cell surface bilayer of these bacteria has a high proportion of unmodified LPS structures that can be targeted by the polymyxin. In the CM of these *mcr-1*-positive cells, there are far fewer unmodified lipid A molecules for colistin to bind to, and a high proportion of LPS altered with a cationic pEtN moiety, meaning colistin is electrostatically repelled from the innermost membrane bilayer, the CM remains intact, and polymyxin resistance ensues.

## **5.7 Colistin resistance in pathogenic *E. coli* conferred by *mcr* genes or chromosomally is mediated at the CM**

The experiments undertaken thus far proved that colistin non-susceptibility in the *E. coli* laboratory reference strain MC1000 conferred by expression of the *mcr-1* resistance determinant resulted in protection of the bacterial CM, not the OM, from the polymyxin's membranolytic properties. However, in clinical settings, resistance to colistin can occur through diverse methods (such as harbouring of various plasmid-borne MCR homologues other than MCR-1, or chromosomal mutations) in bacterial isolates that are genetically distinct from MC1000 cells. Therefore, in order to expand the therapeutic relevance of the investigation into the mechanism of polymyxin resistance, it was essential to study pathogenic *E. coli* strains isolated from human patients that exhibited non-susceptibility to polymyxin antibiotics through a combination of *mcr* or chromosomally-mediated processes. A panel of such *E. coli* clinical isolates was assembled, consisting of a colistin-susceptible control strain (KPC BM16), five strains expressing the *mcr-1* gene, five strains expressing homologues of the *mcr-1* gene (*mcr-2*, *mcr-3*, *mcr-3.2* or *mcr-5*), and six strains with chromosomal mutations that induced polymyxin resistance.

To understand if acquired colistin resistance in this clinical isolate panel was conferred at the cellular CM, all the *E. coli* strains were first converted into spheroplasts using the previously described method of successive treatment with EDTA, lysozyme and trypsin<sup>637</sup>. This allowed for the protective nature of the CM in these polymyxin-resistant *E. coli* isolates to be assessed specifically, without the confounding presence of the OM. All 17 clinical strains were

exposed, or not, to colistin ( $4 \mu\text{g ml}^{-1}$ ) for 12 hours, and the kinetics of fluorescent PI uptake measured as a read-out of the extent of CM permeabilisation. Using the respective values for PI fluorescence in untreated and polymyxin-treated spheroplast populations, the percentage increase in CM disruption triggered by colistin over 12 hours was calculated for each clinical isolate (**Figure 5.7A**). The colistin-susceptible control *E. coli* strain displayed a large increase (nearly 80%) in uptake of the PI fluorophore following polymyxin exposure, as the CM was expectedly damaged by the antibiotic. However, there was almost no amplification of the PI signal in the five *mcr-1*-positive isolates after treatment with colistin, with the less than 15% rise in fluorescence in these clinical strains indicating that the ability of the polymyxin drug to permeabilise their CM bilayer was largely lost. Hence, the manner in which the MCR-1 protein blocked colistin-mediated damage to the CM in *E. coli* MC1000 cells was equally apparent in *E. coli* cells isolated from patients.

Analysing spheroplast CM disruption of the five clinical strains harbouring plasmids that expressed homologues of the *mcr-1* gene (*mcr-2* to *mcr-5*) revealed a more heterogeneous phenotype. Whereas two of these isolates (R11 and 1488949) were impervious to any increase in PI uptake induced by colistin, in the other three strains (1267171, 1266877 and 1144230), exposure to colistin produced a larger rise (30-35%) in CM permeabilisation and PI fluorescence. Whilst these values were far lower than that of the polymyxin-susceptible control clinical isolate, suggesting that these variants of the MCR-1 protein partially prevented colistin from damaging the CM, this data also implied that the propensity for *mcr* homologues to mediate resistance to the antibiotic at the innermost membrane bilayer may vary between different members of the pEtN transferase enzyme family. When examining spheroplasts of the six chromosomally colistin-resistant *E. coli* strains, the effects of the antibiotic on initiating CM disruption were far more consistent, with the increase in uptake of the fluorescent PI dye post-polymyxin treatment no greater than 20%, and as low as 4%. It was concluded that non-susceptibility to colistin conferred by chromosomal mutations was, as with *mcr*-conferred polymyxin resistance, also mediated at the bacterial CM. In summary, carriage of the *mcr-1* gene and mutations in the chromosome were associated with the greatest degree of antagonism against colistin-induced CM permeabilisation, while genetic variants of MCR-1 protected the *E. coli* CM bilayer to a lesser, but still notable, extent.

It was previously shown that *mcr-1* expression in *E. coli* MC1000 cells led to colistin resistance because of the high prevalence of pEtN modified lipid A relative to unmodified lipid A in the bacterial CM. To study if this were also the case with polymyxin non-susceptibility conferred by divergent MCR homologues or chromosomal mutations in clinical *E. coli* samples, lipidomics using MALDI-TOF-based mass spectrometry was carried out on spheroplasts produced from the 17 isolates in the strain panel. This enabled determination of

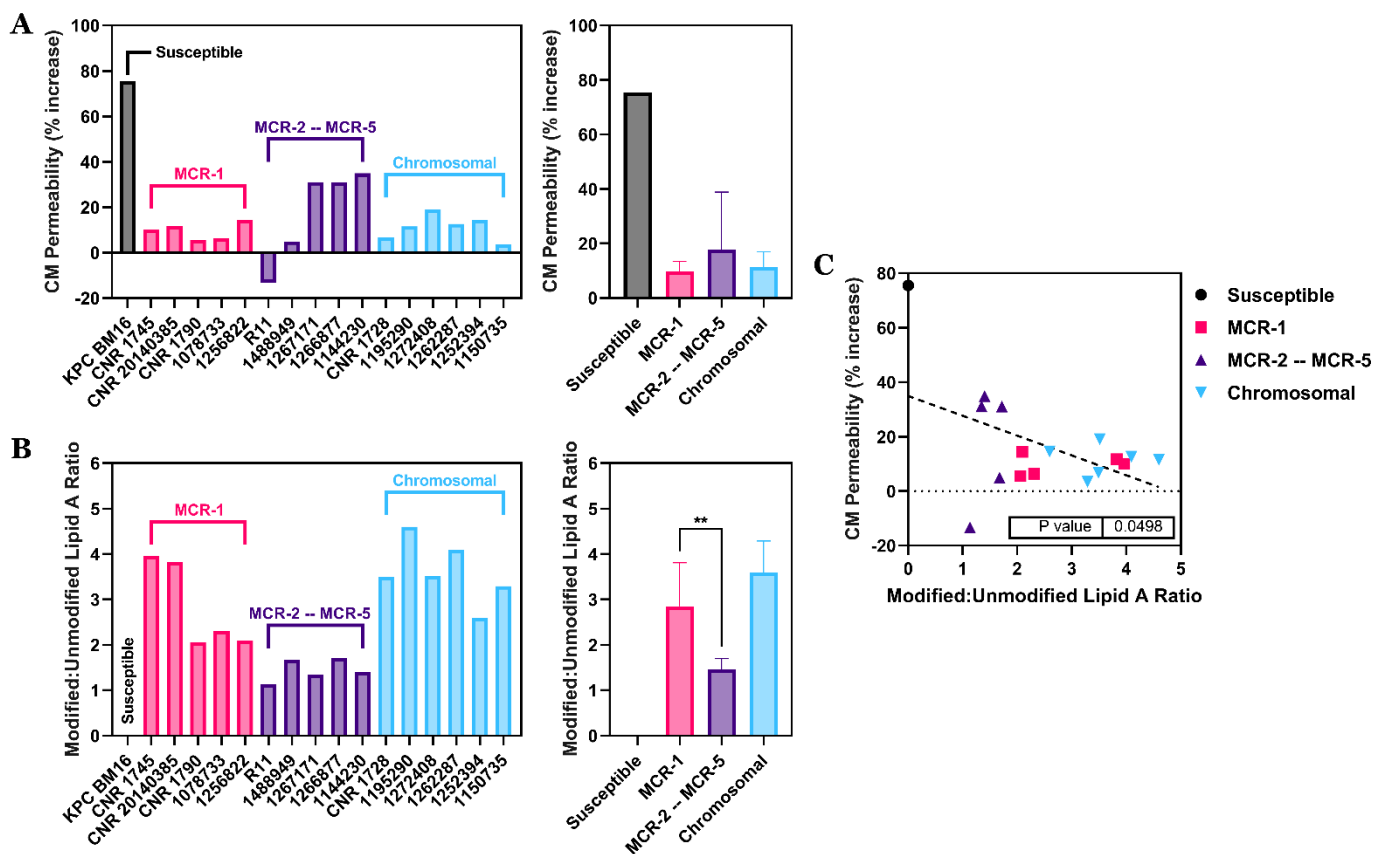


**Figure 5.7: Colistin resistance in clinical *E. coli* acquired by diverse *mcr* homologues or chromosomal mutations is mediated at the CM.** **A**, Permeabilisation of the CM of spheroplasts produced from a panel of pathogenic *E. coli* strains isolated from patients (1 colistin-susceptible isolate, 5 *mcr-1*-expressing isolates, 5 isolates harbouring *mcr* homologues, and 6 isolates with chromosomal colistin resistance) during exposure to colistin (4  $\mu\text{g ml}^{-1}$ ), as determined by measuring fluorescence from PI (0.25  $\mu\text{M}$ ) over 12 hours (data are presented as the percentage increase relative to untreated spheroplasts; second graph depicts the arithmetic mean of values from the 4 indicated strain groups). **B**, Quantification of the ratio of cationically-modified lipid A to unmodified lipid A in the CM of spheroplasts produced from the strains in the pathogenic *E. coli* clinical isolate panel, as determined by measuring the area under the relevant mass spectra peaks following MALDI-TOF-based lipidomics (second graph depicts the arithmetic mean of values from the 4 indicated strain groups; \*\* $p < 0.01$  for MCR homologues relative to MCR-1). **C**, Correlation between colistin-induced CM permeabilisation and the ratio of modified:unmodified lipid A in the CM of spheroplasts produced from the strains in the pathogenic *E. coli* clinical isolate panel (each data point represents an individual bacterial isolate;  $p < 0.05$  indicates a significant negative correlation). Data in **B** were analysed by a one-way ANOVA with Sidak's post-hoc test. Data in **C** were analysed by a simple linear regression. Error bars shown represent the standard deviation of the mean.

the ratio of cationically-modified LPS:unmodified LPS in the CM of these clinical isolates by dividing the area under the relevant mass peaks for native lipid A and lipid A with a positively-charged chemical group added (pEtN only for *mcr* strains; pEtN and L-Ara4N for chromosomally resistance strains). As anticipated, the colistin-sensitive clinical strain possessed no modified lipid A in its CM, providing a molecular basis for why the polymyxin

drug was able to markedly damage this innermost membrane bilayer structure (**Figure 5.7B**). However, in the CM of all five *E. coli* isolates producing MCR-1, high levels of LPS cationic modification were observed, with pEtN-altered lipid A being between 2 and 4-fold more abundant than unaltered lipid A in these spheroplasts. Comparable ratios of modified:unaltered LPS were seen in the six clinical *E. coli* strains that were chromosomally resistant to colistin, where cationically-modified LPS was present at 2.5 to 4.5-fold greater amounts in the CM than unmodified LPS. This finding resolved that polymyxin non-susceptibility arising from carriage of the MCR-1 enzyme or chromosomal mutations in pathogenic *E. coli* samples prevented colistin from permeabilising the CM and promoted antibiotic resistance via extensive modification of CM LPS molecules.

It was hypothesised that the fact that certain homologues of *mcr-1* (*mcr-2* to *mcr-5*) did not confer protection of the *E. coli* CM from colistin-triggered disruption to the same magnitude as chromosomal polymyxin resistance, or the MCR-1 pEtN transferase itself, may be due to a lower rate of cationic modifications to LPS in the CM of these bacteria. In support of this, the ratio of pEtN-altered lipid A:unaltered lipid A in spheroplasts generated from the five clinical isolates harbouring the *mcr-1* gene variants was visibly reduced relative to all the other colistin-resistant strains in the panel, with the prevalence of cationically-modified LPS only between 1.1 and 1.7-fold higher than the prevalence of unmodified LPS. Indeed, the mean proportion of pEtN-modified lipid A amongst the *E. coli* strains expressing the *mcr* homologues was significantly lower compared to the mean amongst the *mcr-1*-positive isolates, serving to explain why MCR-1 was, on average, more capable of inhibiting colistin from damaging the CM than the MCR-2 to MCR-5 variants. This discovery firmly denoted that the extent of cationic modification of CM lipid A in these clinical *E. coli* isolates may be directly correlated with the susceptibility of the CM to permeabilisation initiated by colistin. Confirmation of this theory was achieved by plotting the percentage increase in PI uptake in response to colistin exposure against the ratio of modified:unaltered LPS in the CM of the spheroplasts formed from the 17 strains (**Figure 5.7C**). This uncovered a statistically significant ( $p=0.0498$ ) negative correlation between the proportion of CM lipid A that was cationically-altered, and the degree of CM disruption caused by colistin.

## **5.8 Clinical *Enterobacter cloacae* isolates harbouring *mcr-9* do not exhibit classical colistin resistance**

Having characterised the mechanism by which colistin resistance occurs in Gram-negative bacteria expressing the plasmid-borne *mcr-1*, *mcr-2*, *mcr-3* and *mcr-5* genes, it was decided to extend the scope of this study to include pathogenic clinical isolates that harboured



the *mcr-9* polymyxin resistance determinant, since – uniquely – this genetic homologue of the *mcr* family has in past studies been postulated to be carried silently in bacterial cells, not conferring colistin non-susceptibility despite its widespread global dissemination<sup>587,775,800</sup>. In order to test this proposal, a panel of 11 *E. cloacae* clinical strains was acquired, isolated from patients during a recent (2016-2019) outbreak of carbapenemase-producing Enterobacterales across a London regional hospital network. Constituting this panel were six *mcr-9*-positive *E. cloacae* isolates, all harbouring an IncHI2 plasmid encoding the resistance determinant, and five *E. cloacae* strains from the same outbreak but not carrying the *mcr-9* gene for use as comparative controls. To detect whether or not *mcr-9*-carriage in these isolates was associated with a loss of polymyxin susceptibility, the MIC of colistin against each strain was measured using the gold-standard diagnostic broth microdilution technique (**Figure 5.8**).

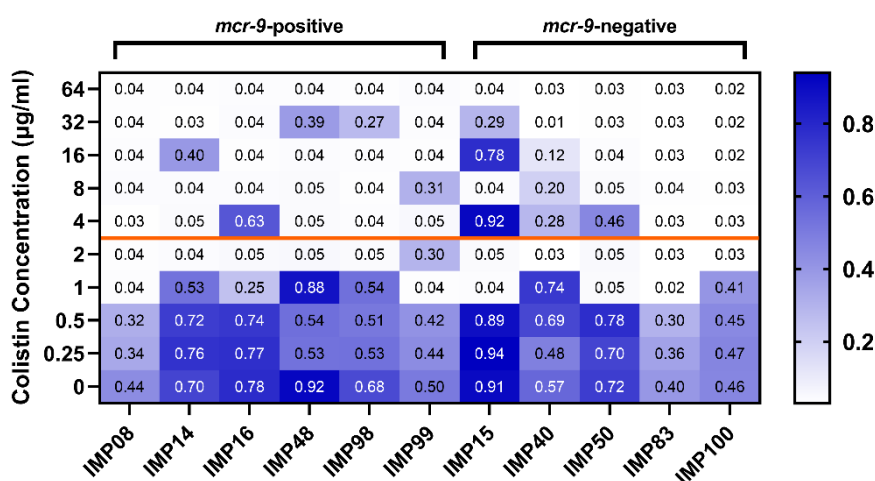


**Figure 5.8: Pathogenic *E. cloacae* strains display an *mcr-9*-independent “skipped well” phenotype.** The MIC of colistin against a panel of 11 *E. cloacae* strains isolated from human patients (six isolates carrying the *mcr-9* gene, and five *mcr-9*-negative isolates), as determined using the broth microdilution method to measure bacterial growth (OD<sub>595nm</sub>) across a range of colistin concentrations after 18 hours incubation. Data presented are representative of 3 individual experiments; the orange line above 2 µg ml<sup>-1</sup> indicates the CLSI/BSAC-defined threshold for polymyxin resistance.

With all six *mcr-9*-positive strains of *E. cloacae*, using the classical definition of an antibiotic’s MIC as the lowest drug concentration at which bacterial growth was fully inhibited, the MIC of colistin was between 1 µg ml<sup>-1</sup> and 2 µg ml<sup>-1</sup> – below the CLSI/BSAC-established breakpoint for colistin resistance<sup>606,790</sup>. This same range of colistin MICs, lower than the resistance threshold, was also seen with the *mcr-9*-negative clinical isolates, and, consistently with previous reports, authenticated the hypothesis that harbouring the *mcr-9* gene was not sufficient for conventional colistin resistance to be induced. However, in five out of the six *mcr-9*-carrying *E. cloacae* strain (all except IMP08), a “skipped well” phenotype was observed

at concentrations above the colistin resistance breakpoint, where bacterial growth was blocked at certain antibiotic doses, but as the concentration was increased, bacteria were once again capable of replicating, before cell division was inhibited a second, or even third time as the polymyxin dose was raised further. Importantly, the appearance of these “skipped wells” was random, with the colistin concentrations at which *E. cloacae* cells were able to grow altering when the experiment was repeated.

It is worth noting that the “skipped well” phenomenon was not an *mcr-9*-specific one, since three out of the five clinical isolates not carrying the gene (IMP15, IMP40 and IMP50) also had a seemingly random ability to begin replicating at colistin doses greater than the polymyxin resistance threshold. This phenotype of “skipped wells” has been identified in previous studies both with polymyxin drugs and other distinct antimicrobial agents, and is thought to be associated with antibiotic hetero-resistance, with cells from the small non-susceptible bacterial sub-population inoculated by chance into wells containing a high antibiotic concentration at which they can divide and grow<sup>801–805</sup>. Thus, the prospect of a colistin hetero-resistance existing in this panel of clinical *E. cloacae* strains warranted further investigation.

## **5.9 *E. cloacae* clinical strains display a novel form of inducible hetero-resistance to colistin**

To determine whether or not the “skipped well” phenotype observed in the panel of pathogenic *E. cloacae* clinical isolates was due to colistin hetero-resistance, all 11 bacterial strains (both *mcr-9*-positive and negative) were subjected to population analysis profiling (PAP). This PAP experiment is well-established in the literature as the ideal method for identifying hetero-resistance to an antibiotic in diverse species of bacteria, and involved plating of an overnight *E. cloacae* culture on increasing concentrations of colistin, contained in solid media (Mueller-Hinton Agar), enabling enumeration of the number of cells within the overall bacterial population that could grow at each polymyxin dose<sup>806–808</sup>. Through this assay, the presence of hetero-resistance becomes apparent if a sub-population of bacteria emerges capable of replicating at concentrations above the clinical breakpoint threshold for antibiotic resistance (2 µg ml<sup>-1</sup> in the case of colistin).

Using two control *E. coli* strains – a colistin-susceptible isolate (MC1000) and a chromosomally colistin-resistant isolate (NCTC 13846) – it was first validated that the PAP technique was producing appropriate results. With polymyxin-sensitive MC1000 cells, the entire bacterial population (between 10<sup>9</sup> and 10<sup>10</sup> c.f.u. ml<sup>-1</sup>) grew when plated on media containing no colistin, but the number of cells that could replicate on plates containing 4 µg

ml<sup>-1</sup>, 16 µg ml<sup>-1</sup> or 64 µg ml<sup>-1</sup> colistin dropped below the limit of detection (10<sup>2</sup> c.f.u. ml<sup>-1</sup>) of the assay (**Figure 5.9A**). However, when examining the polymyxin-resistant NCTC 13846 strain, all cells in the bacterial population appeared to be able to grow on 4 µg ml<sup>-1</sup> colistin-containing media, with no decrease in the number of colonies compared to media absent in the antibiotic (**Figure 5.9B**). Hence, the PAP method correctly distinguished colistin susceptibility from conventional polymyxin resistance, where every bacteria in a population of cells could replicate at a concentration above the clinical breakpoint. Notably, increasing the dose of colistin to which the resistant isolate NCTC 13846 was exposed to 16 µg ml<sup>-1</sup> or 64 µg ml<sup>-1</sup> resulted in a complete drop in the number of surviving cells to below the limit of detection, with no sub-population of bacteria materialising that could grow at these higher antibiotic concentrations.

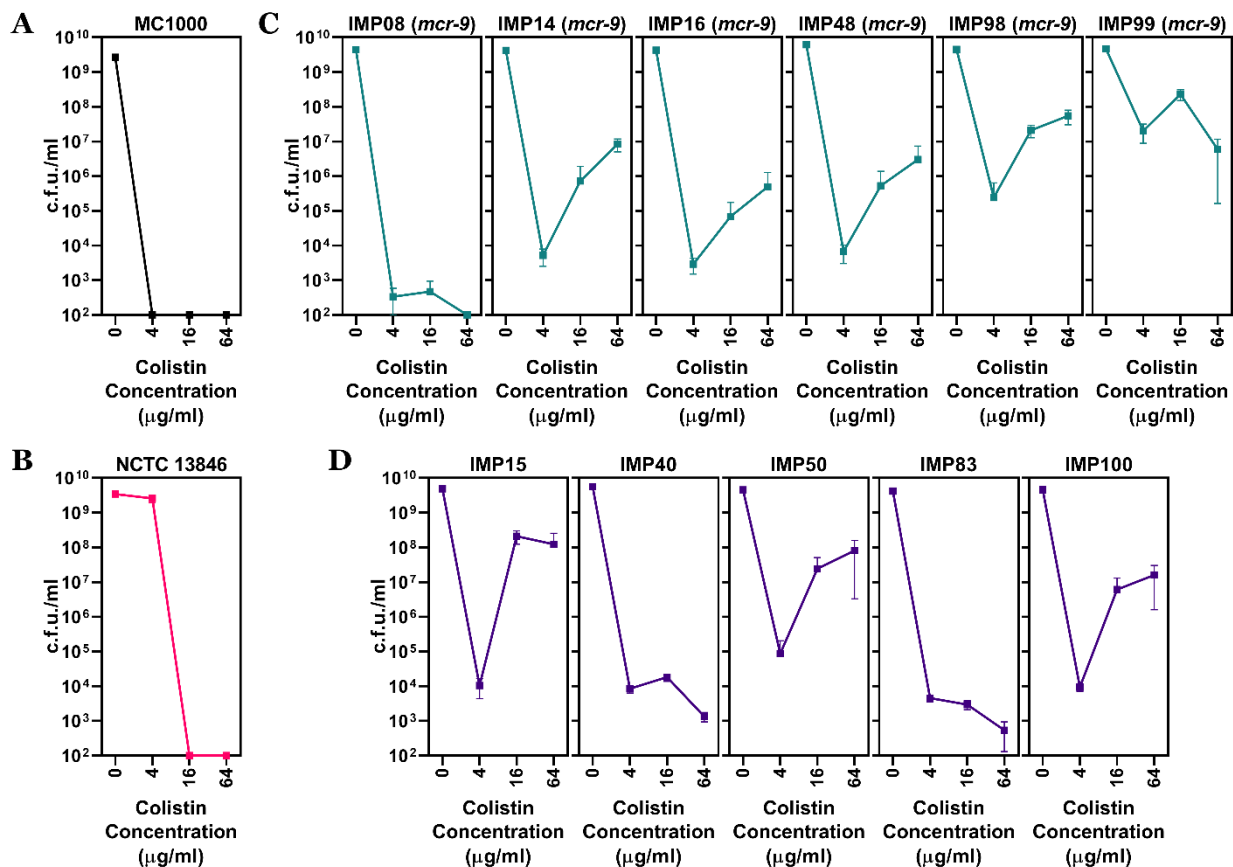


**Figure 5.9: Clinical *E. cloacae* strains are colistin hetero-resistant, with a non-susceptible sub-population that is induced by the polymyxin drug.** A-D, Population analysis profiling (PAP) to detect colistin hetero-resistance in (A) the colistin-susceptible control strain MC1000 (black), (B) a chromosomally colistin-resistant control strain NCTC 13846 (magenta), (C) six *mcr-9*-harbouring *E. cloacae* clinical isolates (cyan), and (D) five *mcr-9*-negative *E. cloacae* clinical isolates (purple), as determined by plating of bacterial cultures on increasing concentrations of colistin contained in Mueller-Hinton agar and enumeration of colony forming units (n=3). Data are presented as the arithmetic mean, and error bars represent the standard deviation of the mean.

Having verified the applicability of the PAP assay, this technique was next performed on the *E. cloacae* clinical strain panel. With all 11 bacterial isolates, regardless of the presence of the *mcr-9* gene, as the concentration of colistin on which they were plated was increased from 0  $\mu\text{g ml}^{-1}$  to 4  $\mu\text{g ml}^{-1}$ , the number of colonies that grew decreased sharply, but crucially did not drop below the assay's limit of detection (**Figure 5.9CD**). It was therefore clear that a sub-population of cells existed within the overall population of bacteria that tolerated and replicated at a polymyxin concentration greater than the resistance threshold – indicating conclusively that all the *E. cloacae* strains exhibited colistin hetero-resistance. This size of this sub-population that grew at 4  $\mu\text{g ml}^{-1}$  colistin varied dramatically between the strains, from as low as 0.0001% of the total number of cells in isolate IMP08, up to approximately 1% of the whole bacterial population for isolate IMP99.

When plating overnight cultures of these same 11 *E. cloacae* clinical strains on 16  $\mu\text{g ml}^{-1}$  and 64  $\mu\text{g ml}^{-1}$  colistin, an unexpected effect became visible in a number of the isolates. In nine of the strains (all except IMP08 and IMP83), raising the polymyxin concentration to which the bacteria were exposed above 4  $\mu\text{g ml}^{-1}$  actually caused an increase in the number of colonies that grew on the colistin-containing media. In most instances, this increase was vast in nature (between 3 and 5-log rise in cell counts relative to 4  $\mu\text{g ml}^{-1}$  colistin), and counter-intuitively implied that the phenotype of polymyxin hetero-resistance in these *E. cloacae* isolates was uniquely inducible, with the size of the sub-population not susceptible to the antibiotic becoming larger when treated with a higher concentration of colistin. Conspicuously, the two clinical strains that did not display this inducible behaviour (IMP08 and IMP83) also had no signs of “skipped wells” when MIC assays were carried out earlier, suggesting that these two effects may be interconnected. Additionally, although *mcr-9* has in previous studies been reported to be an inducible colistin resistance determinant, it is vital to note that the inducible hetero-resistance characterised here occurred in both *mcr-9*-harbouring and *mcr-9*-absent *E. cloacae*, ruling out the involvement of the gene in this novel phenotype<sup>584</sup>.

To further understand this effect of inducible polymyxin hetero-resistance in clinical *E. cloacae*, a colony from each bacterial strain that grew on solid media plates containing 64  $\mu\text{g ml}^{-1}$  colistin was isolated. These colonies were resuspended in liquid media, before being spread on the surface of an agar plate in which a well containing a high concentration of colistin (50  $\mu\text{g ml}^{-1}$ ) had been created. Analysis of the zone of inhibition formed around this well following incubation of the agar plates uncovered another previously undescribed phenotype in a number of the clinical strains. As indicated by isolates IMP50, IMP98, IMP99 and IMP100, furthest away from the colistin-containing well, where the antibiotic concentration was lower, bacteria were able to grow in a manner typical of such zone of

inhibition assays (**Figure 5.10A**). Moving closer to the well containing colistin, to a site where the polymyxin dose was higher, resulted in bacterial replication being inhibited, and thus a clear zone where growth of the *E. cloacae* cells had been blocked. Remarkably, however, closest and directly around the well in which 50  $\mu\text{g ml}^{-1}$  colistin had been added – at the location where the concentration of the polymyxin drug was at its highest – *E. cloacae* bacteria were again able to grow, meaning that the clear zone of inhibition appeared in a “halo-like” ring shape, as opposed to the complete clear circle usually seen<sup>809</sup>. This finding supported the notion that colistin non-susceptibility was being induced in these hetero-resistant clinical isolates, with a higher dose of the antibiotic promoting rather than inhibiting bacterial growth. Moreover, it was inferred from this experiment that resistance to colistin in the non-susceptible sub-populations of the *E. cloacae* strains was not stable, since if this were the case, no zone of inhibition around the colistin-containing well would have been apparent at all.

For extended characterisation of the stability, inducibility and mechanism of colistin hetero-resistance in the panel of *E. cloacae* isolates, colonies of strains that grew on plates containing 64  $\mu\text{g ml}^{-1}$  colistin in the PAP assay were first transferred to an agar plate containing no colistin, and then after a period of overnight growth, moved back and grown on solid media supplemented with 64  $\mu\text{g ml}^{-1}$  colistin. The previously used lipidomic technique based on MALDI-TOF mass spectrometry was thereafter employed on the bacterial populations that had grown on both the colistin-absent media and the colistin-containing media to detect the presence of cationically-modified lipid A in these *E. cloacae* cells that was likely responsible for mediating the polymyxin non-susceptibility. As represented by the strain IMP14, upon transfer of cells encompassing the colistin resistant bacterial sub-population to media absent in colistin, several isolates exhibited no modification of their LPS structures, with only peaks representing unaltered lipid A discerned (**Figure 5.10B**). This was in keeping with the hypothesis that colistin non-susceptibility in the hetero-resistant sub-population was unstable, and immediately lost when the polymyxin compound was not present.

Nonetheless, when these same IMP14 cells were moved on to media containing 64  $\mu\text{g ml}^{-1}$  colistin, mass spectra peaks corresponding to cationically-modified lipid A were again observed, backing up that colistin hetero-resistance in the *E. cloacae* was a trait induced by polymyxin exposure, and one that was conferred by chemical alterations to LPS. Critically, the difference in mass-charge ratio between the unmodified and modified lipid A structures detected here was +131, which is the size of an L-Ara4N moiety<sup>640</sup>. Because this cationic group can only be added to the lipid A domain of LPS by chromosomally-encoded proteins, and not MCR enzymes, it was concluded that *mcr-9* played no role in the induced colistin hetero-resistance of the *E. cloacae* isolates, but chromosomal L-Ara4N transferases were almost certainly involved<sup>641</sup>.

The reverse of this experiment was also performed, with resistant *E. cloacae* colonies isolated from their respective 64  $\mu\text{g ml}^{-1}$  colistin plates in the PAP assay transferred initially to another plate containing 64  $\mu\text{g ml}^{-1}$  colistin, and later after an overnight incubation, to solid media with no colistin added – MALDI-TOF mass spectrometry-based lipidomics was then undertaken on these cell populations. As represented in this case by strain IMP48, in bacteria moved first on to agar into which colistin was supplemented, cationic modifications to lipid A were maintained (**Figure 5.10C**). However, transfer of these *E. cloacae* cells to media not containing any colistin caused an immediate and complete loss of any cationically-altered LPS, reinforcing the necessity for high concentrations of the polymyxin to be present in order to induce polymyxin non-susceptibility in the hetero-resistant bacterial sub-population.

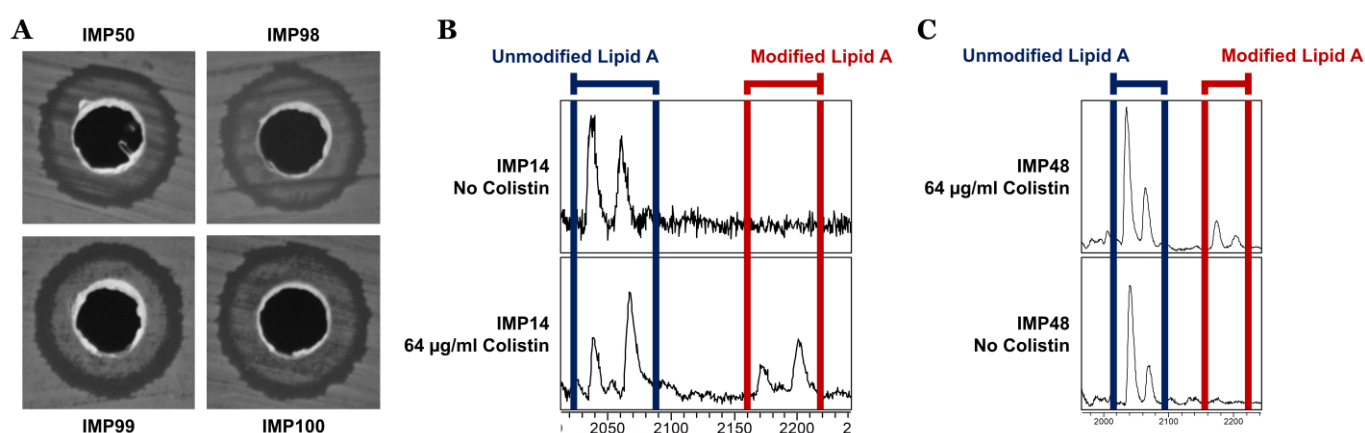


**Figure 5.10: Inducible colistin non-susceptibility in polymyxin hetero-resistant clinical *E. cloacae* isolates is mediated by lipid A modifications.** **A**, Growth on solid media of *E. cloacae* cells isolated from the hetero-resistant sub-population growing at 64  $\mu\text{g ml}^{-1}$  colistin of four clinical strains (IMP50, IMP98, IMP99, IMP100) around a well containing 50  $\mu\text{g ml}^{-1}$  colistin, revealing a unique “ring-like” zone of inhibition (images are representative of 3 independent experiments). **B**, Lipidomic MALDI-TOF mass spectra showing the abundance of unmodified lipid A and lipid A cationically modified with an L-Ara4N chemical group in cells of *E. cloacae* strain IMP14 isolated from the hetero-resistant sub-population growing at 64  $\mu\text{g ml}^{-1}$  colistin, before being moved to media containing no colistin (top spectrum) and then to media containing 64  $\mu\text{g ml}^{-1}$  colistin (bottom spectrum). **C**, Lipidomic MALDI-TOF mass spectra showing the abundance of unmodified lipid A and lipid A cationically modified with an L-Ara4N chemical group in cells of *E. cloacae* strain IMP48 isolated from the hetero-resistant sub-population growing at 64  $\mu\text{g ml}^{-1}$  colistin, before being moved to media containing 64  $\mu\text{g ml}^{-1}$  colistin (top spectrum) and then to media containing no colistin (bottom spectrum). All spectra are representative of 3 independent experiments.

## 5.10 Colistin hetero-resistance in *E. cloacae* is mediated by two distinct bacterial populations

In order to investigate the novel phenotype of inducible colistin hetero-resistance amongst the *E. cloacae* isolate panel at the level of a single bacterial cell, the classic Luria-Delbrück fluctuation test experiment was carried out on representative clinical strains<sup>810,811</sup>. In this fluctuation test assay, an overnight bacterial culture is diluted down and re-inoculated

into multiple wells containing media in such a way that ensures each well contains only one bacterial cell. Allowing the bacteria in these wells to grow thus produces multiple populations, each grown from a different cell from the original overnight culture. Subsequently exposing these different populations to an antibiotic stress and measuring bacterial viability then enables an assessment of how tolerance to the antimicrobial agent varies between individual cells, and the results of this can offer an insight into the process by which drug resistance is occurring. If non-susceptibility to an antibiotic was mediated by genetic mutations arising in the absence of the selective pressure – as is true for most of the characterised forms of antimicrobial resistance – it would be expected that the majority of the populations grown from individual bacterial cells would not be able to tolerate exposure to the antibiotic, but a small number of populations grown from cells where relevant mutations had randomly occurred would display a high propensity for surviving the same treatment<sup>812–814</sup>. In other words, the viability of the different populations following antibiotic exposure would be highly variable, and not normally distributed. If, however, resistance to an antibiotic was caused by a cellular response induced in the presence of the drug, it would be expected that all of the different populations grown from individual bacterial cells would exhibit an equal capacity to tolerate antimicrobial treatment, and measurements of bacterial survival would be distributed normally.

Utilising this approach to comprehend the mechanism and potential inducible nature of colistin resistance in sub-populations of clinically-isolated *E. cloacae* bacteria, cultures of strains IMP14, IMP40 and IMP99 were diluted down to individual cells, re-grown, and finally plated on solid agar media containing 64  $\mu\text{g ml}^{-1}$  colistin to quantify bacterial viability by colony counts. These three strains were chosen because they each showed distinct profiles of colistin hetero-resistance in the PAP experiment - whilst the small colistin-tolerant sub-population of cells in isolate IMP14 greatly increased in size at higher drug concentrations, the polymyxin-resistant sub-population of isolate IMP40 was largely unaffected by increasing doses of the antibiotic, and the size of the much larger colistin-tolerant sub-population in isolate IMP99 only partially grew at higher polymyxin concentrations. The output of the fluctuation test assay on *E. cloacae* strain IMP14 was remarkable, in that a number of cells from every population generated from a single bacteria were able to survive and replicate on an agar plate containing 64  $\mu\text{g ml}^{-1}$  colistin, but the colistin-tolerant nature of these different populations varied dramatically, with a more than 3-log difference in colony counts between populations started from different single cells of the same original bacterial culture (**Figure 5.11A**). Whereas viable cell counts on solid media with 64  $\mu\text{g ml}^{-1}$  colistin added were between  $10^3$  and  $10^4$  c.f.u.  $\text{ml}^{-1}$  for many of the populations started from individual IMP14 cells, the concentration of polymyxin-resistant cells was as high as  $10^5$  or even  $10^6$  c.f.u.  $\text{ml}^{-1}$  in a small number of these populations.

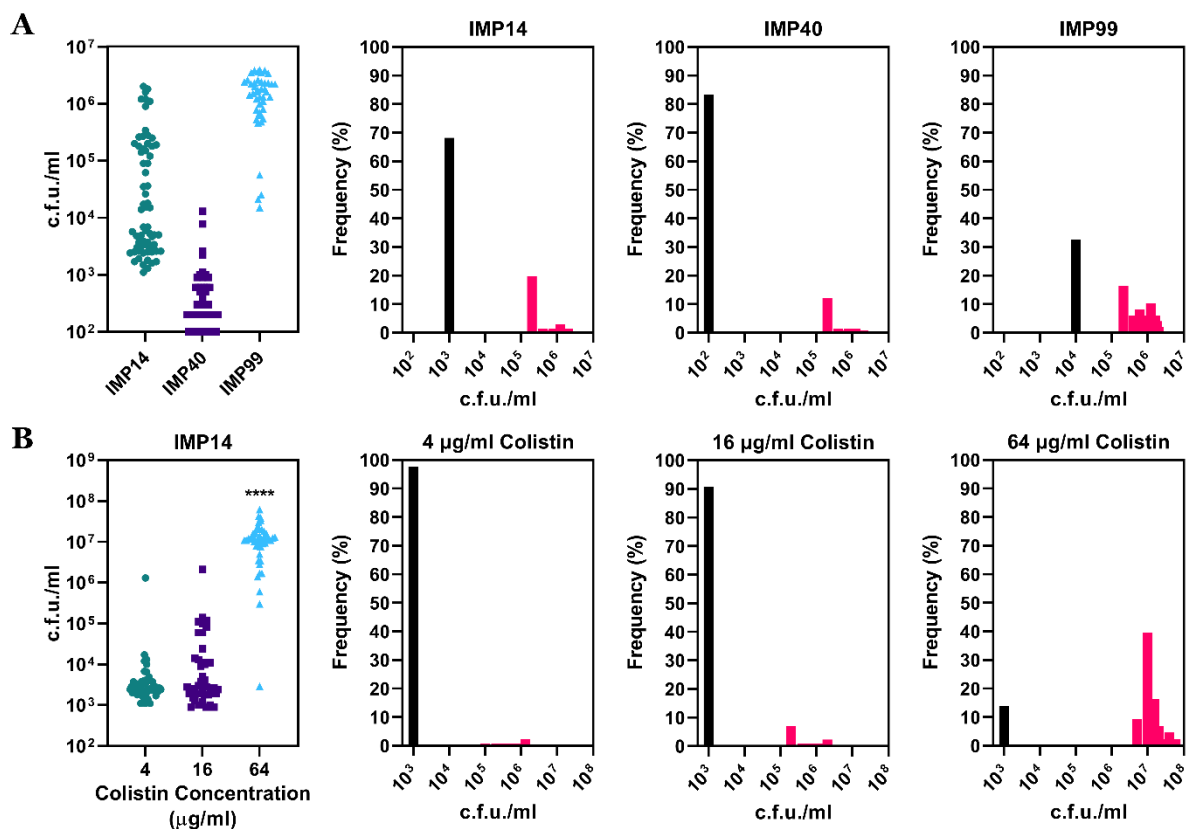


**Figure 5.11: Clinical *E. cloacae* strains possess two forms of colistin resistance, one of which is induced by increasing polymyxin concentrations.** **A**, Fluctuation test results on three clinical *E. cloacae* isolates (IMP14, IMP40, IMP99) diluted down to single cells, re-grown to stationary phase, and plated on solid media containing 64 µg ml<sup>-1</sup> colistin before enumeration of colony counts (n=66 populations for IMP14, 48 populations for IMP40, 43 populations for IMP99). **B**, Fluctuation test results on *E. cloacae* isolate IMP14, which was diluted down to single cells, re-grown to stationary phase, and plated on solid media containing 4, 16 or 64 µg ml<sup>-1</sup> colistin before enumeration of colony counts (n=43 populations; \*\*\*\*p<0.0001 relative to 4 and 16 µg ml<sup>-1</sup> colistin). Data in **B** were analysed by a one-way ANOVA with Tukey's post-hoc test. Data are presented both as the raw c.f.u. data (where each data point represents a different bacterial population grown from a single cell), and as a histogram showing the distribution of the c.f.u. data for each individual strain/colistin concentration, with populations showing low-level colistin resistance shown in black and populations with high-level colistin resistance in pink.

This diversity in the response of the different IMP14 cell populations to colistin exposure became more apparent when analysing the distribution of viable colony counts by visualisation of the data on a histogram, which revealed a bimodal pattern. In 70% of the bacterial populations generated from individual *E. cloacae* IMP14 cells, a low-level ability to survive treatment with 64 µg ml<sup>-1</sup> colistin was seen, but the remaining 30% of cell populations had a much greater capacity for tolerating colistin exposure. This finding suggested that within cultures of isolate IMP14, there existed two forms of colistin resistance. The fact that every single population grown from an individual *E. cloacae* cell had at least a partial ability to survive treatment with the polymyxin strongly implied, according to the Luria-Delbrück



hypothesis, that exposure to colistin was inducing low-level antibiotic resistance. However, the colony count data were certainly not normally distributed, indicating that genetic mutations may be involved in mediating the higher degree of polymyxin tolerance in 30% of the IMP14 populations. Interestingly, the relative proportions of the low-level and high-level colistin resistant populations shifted when the fluctuation test experiment was done on isolates IMP40 (85% low-level tolerance, 15% high-level tolerance) and IMP99 (35% low-level tolerance, 65% high-level tolerance). Since the PAP experiment had previously identified that these three *E. cloacae* clinical strains IMP14, IMP40 and IMP99 differed in the extent to which the size of their colistin-resistant sub-populations are induced by the polymyxin drug, it was hypothesised that colistin inducibility could have a role in these inter-strain variations observed in the fluctuation tests.

To examine this hypothesis, the fluctuation test experiment was repeated with the *E. cloacae* isolate IMP14, but rather than plating the separate populations all grown from single bacterial cells only on media containing 64  $\mu\text{g ml}^{-1}$  colistin, these same populations were also plated on 4  $\mu\text{g ml}^{-1}$  and 16  $\mu\text{g ml}^{-1}$  colistin before enumeration of viable colony counts (**Figure 5.11B**). Again, the distribution of the raw cell count data was additionally visualised by plotting of a histogram, which highlighted that when the IMP14 populations were exposed to a colistin concentration of 4  $\mu\text{g ml}^{-1}$ , the vast majority of the populations (more than 95%) only displayed low-level colistin resistance (resistant cells at a density of  $10^3$  c.f.u.  $\text{ml}^{-1}$ ). Increasing the polymyxin dose used to treat the *E. cloacae* populations started from single cells up to 16  $\mu\text{g ml}^{-1}$  caused a slight shift down to 90% in the proportion of populations that had low-level tolerance to the antibiotic, with the remaining 10% of IMP14 populations exhibiting a much greater degree of colistin resistance (density of resistant cells around  $10^6$  c.f.u.  $\text{ml}^{-1}$ ). This insinuated that the ability of the populations of *E. cloacae* to be highly-resistant to colistin may be dependent on the concentrations of the polymyxin drug to which they were exposed, with increased doses of the antibiotic having an inducible effect. In support of this postulation, plating of the same IMP14 populations on agar plates supplemented with 64  $\mu\text{g ml}^{-1}$  colistin resulted in a complete swing in the relative proportions of the low-level and high-level polymyxin-resistant populations, with only 15% of populations with colony counts of  $10^3$  c.f.u.  $\text{ml}^{-1}$ , and 85% where the colony counts were  $10^7$  c.f.u.  $\text{ml}^{-1}$  or higher.

The last fluctuation test assay undertaken involved growing populations of the clinical *E. cloacae* strain IMP14 started from individual bacterial cells in an overnight culture for different lengths of time, in order to ascertain whether being in a different growth phase would have an impact on the populations being highly colistin-resistant or only partially so. These populations were grown for either 10 hours to early logarithmic phase, 14 hours to mid-logarithmic phase, or 18 hours to early stationary phase, then plated on solid media containing

64  $\mu\text{g ml}^{-1}$  colistin to assess the distribution of viable bacterial cells across the distinct populations as before (**Figure 5.12ABC**). When the IMP14 populations were only allowed to replicate for 10 hours – at a stage where they had only just commenced exponential growth – none of the populations had any colistin-tolerating properties, with colony counts in 100% of the *E. cloacae* populations at, or below, the assay’s  $10^2$  c.f.u.  $\text{ml}^{-1}$  limit of detection (**Figure 5.12A**).

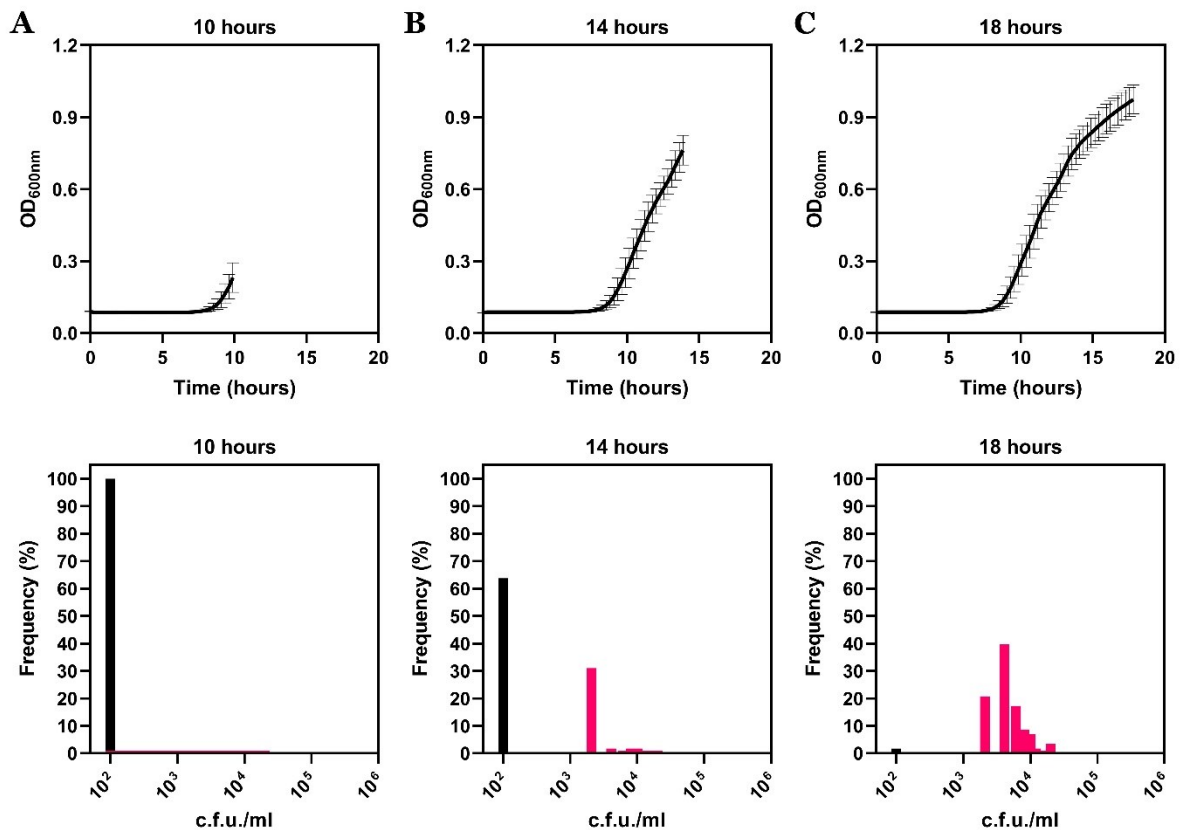


**Figure 5.12: High-level colistin resistance in *E. cloacae* isolate IMP14 is associated with stationary phase growth.** A-C Growth curves (top graphs) and histograms (bottom graphs) showing the results of fluctuation test experiments on *E. cloacae* strain IMP14 diluted down to single cells, then re-grown to (A) early logarithmic phase (10 hours), (B) mid-logarithmic phase (14 hours), or (C) early stationary phase (18 hours), before plating on solid media containing 64  $\mu\text{g ml}^{-1}$  colistin to enumerate colony counts (n=48 populations for A, 58 populations for B, 58 populations for C). Growth curve data was generated by measuring OD<sub>600nm</sub> readings. Histogram data shows the distribution of the raw c.f.u. data for each different incubation time, with populations showing low-level colistin resistance shown in black and populations with high-level colistin resistance in pink.

By contrast, increasing the time of incubation of the IMP14 populations to 14 hours triggered a change in the proportion of populations with this low-level or non-existent colistin resistance, with only 65% of populations producing cell counts around the limit of detection, and the remaining 35% possessing a higher level of polymyxin tolerance, with colony counts

of approximately  $10^4$  c.f.u. ml<sup>-1</sup> (**Figure 5.12B**). Continuing this trend, when the growth period of the *E. cloacae* populations was further extended up to 18 hours (the start of the stationary phase), the proportion of these populations with low-level resistance to colistin dropped to nearly 0%, and nearly all of the populations were found to be of the more highly polymyxin-tolerant variety (**Figure 5.12C**). In summary, the conclusions from these set of Luria-Delbrück experiments were that whilst colistin does induce a low-level of colistin resistance in all *E. cloacae* cells, a subset of these cells emerges as the bacterial population enters stationary phase growth with high-level colistin resistance, and the size of this subset of cells increases upon exposure to higher polymyxin concentrations. However, the precise mechanism and molecular basis of inducible colistin hetero-resistance in these clinical *E. cloacae* samples remains to be fully understood.

### **5.11 Chromosomal and intrinsic colistin resistance in bacteria from CF patients are mediated at different membranes**

Having resolved the mechanism by which polymyxin non-susceptibility was mediated in *mcr*-carrying and chromosomally-resistant pathogens, as well as discovering a new form of colistin hetero-resistance that was induced by the antibiotic itself, the final form of polymyxin resistance to study was intrinsic colistin non-susceptibility. More specifically, to characterise the site where resistance to colistin was conferred in bacteria that were inherently insensitive to the polymyxin drug, and explore if this was the same site (i.e. the innermost CM bilayer) as in the previously established modes of plasmid-borne or chromosomal mutation-based colistin resistance, another panel of 13 pathogenic clinical isolates were obtained. All these bacterial strains were multi-drug resistant, and isolated from sputum samples during chronic airway infections in cystic fibrosis (CF) patients at the Royal Brompton Hospital CF Centre (London). The panel of 13 clinical strains was comprised of five susceptible *P. aeruginosa* isolates (used as controls for making comparisons), four *P. aeruginosa* isolates that were chromosomally-resistant to colistin, and four *Burkholderia cenocepacia* isolates with intrinsic colistin resistance, where non-susceptibility to the polymyxin was not dependent on the acquisition of any mutations or additional resistance determinants.

The primary assay conducted to comprehend the location where polymyxin resistance was mediated in this clinical isolate panel made use of the phospholipid-reactive fluorescent NPN dye to test if colistin exposure initiated permeabilisation of the extracellular-facing bacterial OM bilayer. All 13 strains were either left untreated, or exposed to 4 µg ml<sup>-1</sup> colistin, and the resulting values generated for uptake of the NPN fluorophore were subtracted to produce a final numerical read-out for polymyxin-induced OM disruption. Expectedly, the OM

structure of the five susceptible *P. aeruginosa* strains was extensively damaged by colistin, with a marked degree of NPN fluorescence within 10 minutes of antibiotic treatment (**Figure 5.13A**). The polymyxin compound also caused similar levels of uptake of the NPN dye in three out of the four chromosomally colistin-resistant *P. aeruginosa* isolates (all except strain AK19), and importantly, the mean average of colistin-triggered OM permeabilisation in these “chromosomal” strains was not significantly different from the susceptible strains. This implied that colistin non-susceptibility arising from chromosomal mutations in *P. aeruginosa* was not conferred by protection of the OM, reinforcing the earlier finding in *E. coli* clinical isolates that resistance to polymyxin is rather mediated at the CM bilayer. Notably, however, in the four intrinsically colistin-resistant *B. cenocepacia* CF isolates, there was no increased uptake of the NPN fluorophore whatsoever in response to colistin exposure, showing that the OM of these strains was entirely impervious to the polymyxin’s membrane-damaging effects. It appeared, therefore, that intrinsic colistin resistance in *B. cenocepacia* strains may be conferred by protection of the cell surface OM structure, unlike *mcr* or chromosomally-mediated polymyxin resistance.

Next, to further unravel the seemingly divergent modes of colistin non-susceptibility within this strain panel at the level of the CM, the 13 bacterial isolates were again treated, or not, with the polymyxin antibiotic ( $4 \mu\text{g ml}^{-1}$ ) for 2 hours, but this time in the presence of the DNA-reactive PI dye instead of the NPN fluorophore. Deducting the amount of PI fluorescence in unexposed cells from their corresponding values following colistin treatment thus provided an indication of the degree of CM permeabilisation induced by the drug. All five polymyxin-susceptible *P. aeruginosa* strains had a high level of PI uptake after 2 hours of colistin exposure, confirming that the CM of these bacteria was being damaged, allowing PI molecules to enter the intracellular cytoplasm and fluoresce (**Figure 5.13B**). By comparison, the CM of the four *P. aeruginosa* isolates that were chromosomally colistin-resistant remained intact and undisrupted in spite of polymyxin treatment. The complete absence of a fluorescent PI signal in these samples clearly portrayed that colistin non-susceptibility occurring via chromosomal mutations was a consequence of protection of the CM from colistin’s membranolytic activity, and that this was likely a conserved mechanism of resistance in Gram-negative pathogens including *E. coli* and *P. aeruginosa*. The four *B. cenocepacia* clinical strains with inherent insensitivity to polymyxins also displayed no PI fluorescence post-colistin exposure, which was unsurprising considering that the antibiotic was unable to damage the OM in these strains, and hence did not even have access to the inner CM bilayer.

In order to gain additional insight exclusively into the colistin antagonistic properties of the bacterial CM structure in the resistant isolates of this panel of CF bacteria, all 13 strains were converted into spheroplasts lacking a cell wall/OM by treatment with EDTA, lysozyme

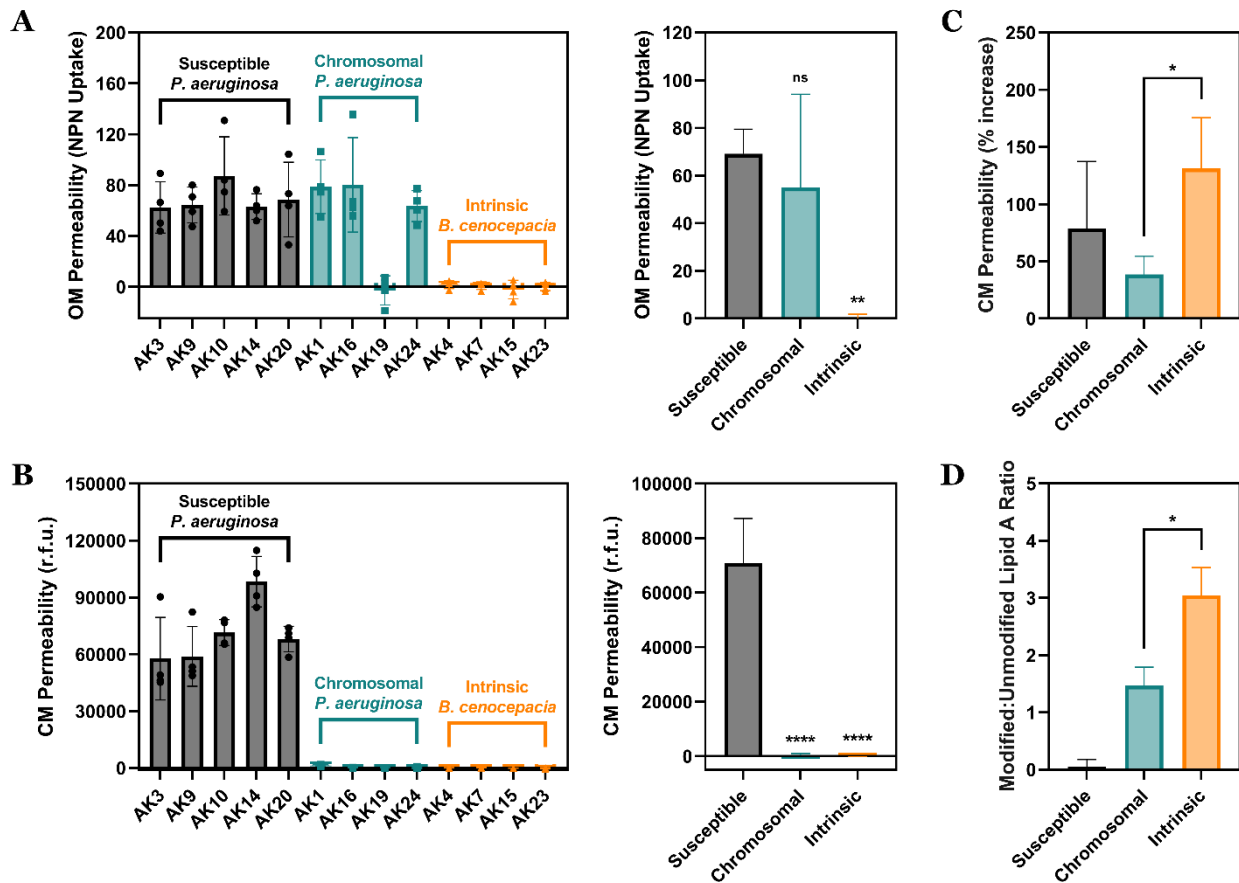


**Figure 5.13: Chromosomal colistin resistance is mediated at the CM, but intrinsic colistin resistance is conferred by protection of the OM.** **A**, Permeabilisation of the OM by colistin ( $4 \mu\text{g ml}^{-1}$ ) in a panel of clinical strains isolated from CF patients (5 polymyxin-susceptible *P. aeruginosa* isolates, 4 chromosomally-resistant *P. aeruginosa* isolates and 4 intrinsically-resistant *B. cenocepacia* isolates), as determined by measuring uptake of the NPN fluorophore ( $10 \mu\text{M}$ ) over 10 minutes ( $n=4$ , each data point represents the arithmetic mean of 20 replicate measurements; data are presented as the increase relative to untreated cells; second graph depicts the arithmetic mean of values from the 3 indicated strain groups; ns:  $p>0.05$ ,  $**p<0.01$  relative to “Susceptible” bacteria). **B**, Permeabilisation of the CM by colistin ( $4 \mu\text{g ml}^{-1}$ ) in whole cells of the clinical CF isolate panel, as determined by measuring fluorescence from PI ( $2.5 \mu\text{M}$ ) after 2 hours ( $n=4$ ; data are presented as the increase relative to untreated cells; second graph depicts the arithmetic mean of values from the 3 indicated strain groups;  $****p<0.0001$  relative to “Susceptible” bacteria). **C**, Permeabilisation of the CM by colistin ( $4 \mu\text{g ml}^{-1}$ ) in spheroplasts produced from the clinical CF isolate panel, as determined by measuring fluorescence from PI ( $0.25 \mu\text{M}$ ) over 12 hours (data are presented as the percentage increase relative to untreated spheroplasts, with the graph depicting the arithmetic mean of values from the 3 strain groups;  $*p<0.05$  for “Intrinsic” bacteria relative to “Chromosomal” bacteria). **D**, Quantification of the ratio of cationically-modified lipid A to unmodified lipid A in the CM of spheroplasts produced from the clinical CF isolate panel, as determined by measuring the area under the relevant mass spectra peaks following MALDI-TOF-based lipidomics (graphs depicts the arithmetic mean of values from the 3 strain groups;  $*p<0.05$  for “Intrinsic” bacteria relative to “Chromosomal” bacteria). Data in **A**, **B** were analysed by a one-way ANOVA with Dunnett’s post-hoc test. Data in **C**, **D** were analysed by a one-way ANOVA with Sidak’s post-hoc test. Data are presented as the arithmetic mean, and error bars represent the standard deviation of the mean.

and trypsin. By either incubating these generated spheroplasts with no colistin, or exposing them to 4  $\mu\text{g ml}^{-1}$  colistin (in both cases for 12 hours in an osmoprotective environment of 20% sucrose), the percentage increase in PI uptake could be calculated as a sign of the polymyxin's CM permeabilising behaviour without any confounding cell envelope structures being present. This experiment revealed that whilst the mean percentage increase in colistin-initiated spheroplast CM disruption in the five susceptible *P. aeruginosa* isolates was predictably high (nearly 80%), the average amongst the chromosomally-resistant *P. aeruginosa* strains was much lower (less than 40%), with this phenotype entirely consistent with that observed in past assays with *E. coli* spheroplasts (**Figure 5.13C**). These data provided the final validation that polymyxin non-susceptibility conferred by mutations acquired in the chromosome of Gram-negative bacteria was indeed mediated at the CM bilayer.

Interestingly, the average damage to the CM of spheroplasts formed from the four intrinsically colistin-resistant *B. cenocepacia* strains was significantly higher than that of the isolates with chromosomal polymyxin resistance, with a mean percentage increase in the fluorescent PI signal after colistin treatment as high as 130%. The fact that this value was greater than even the average of the susceptible strains strongly suggested that the CM of these intrinsically-resistant *B. cenocepacia* isolates was not at all protected from colistin-triggered damage, and that the inherent polymyxin non-susceptibility was mediated only at the bacterial OM structure. The reasons for this were unclear, but one possibility considered was that the efficiency of cationic lipid A modifications culminating in colistin insensitivity was much higher in the OM of strains with intrinsic, as opposed to acquired, polymyxin resistance, and because colistin could not even permeabilise the surface OM bilayer of these cells, there was no evolutionary requirement for these bacteria to maintain modified LPS in their CM as a means of defence against polymyxin molecules.

To investigate this proposal, the 13 strains in the panel of clinical CF isolates were subjected to the MALDI-TOF mass spectrometry-based lipidomic method for quantifying the ratio of modified lipid A to unmodified lipid A by measuring the area under the relevant mass spectra peaks. This analysis disclosed that there was virtually no modified LPS in the five susceptible *P. aeruginosa* strains, but much elevated levels of lipid A modification in cells of the four chromosomally polymyxin-resistant *P. aeruginosa* isolates, where cationically-altered LPS structures were 1.5-fold more prevalent than unaltered LPS structures (**Figure 5.13D**). However, the modified:unmodified lipid A ratio was far higher in the intrinsically-resistant *B. cenocepacia* strains, with modified LPS 3-times more abundant relative to unmodified LPS. As detailed above, this result offered one plausible explanation as to why acquired and inherent colistin non-susceptibility were mediated at independent cell envelope membranes.

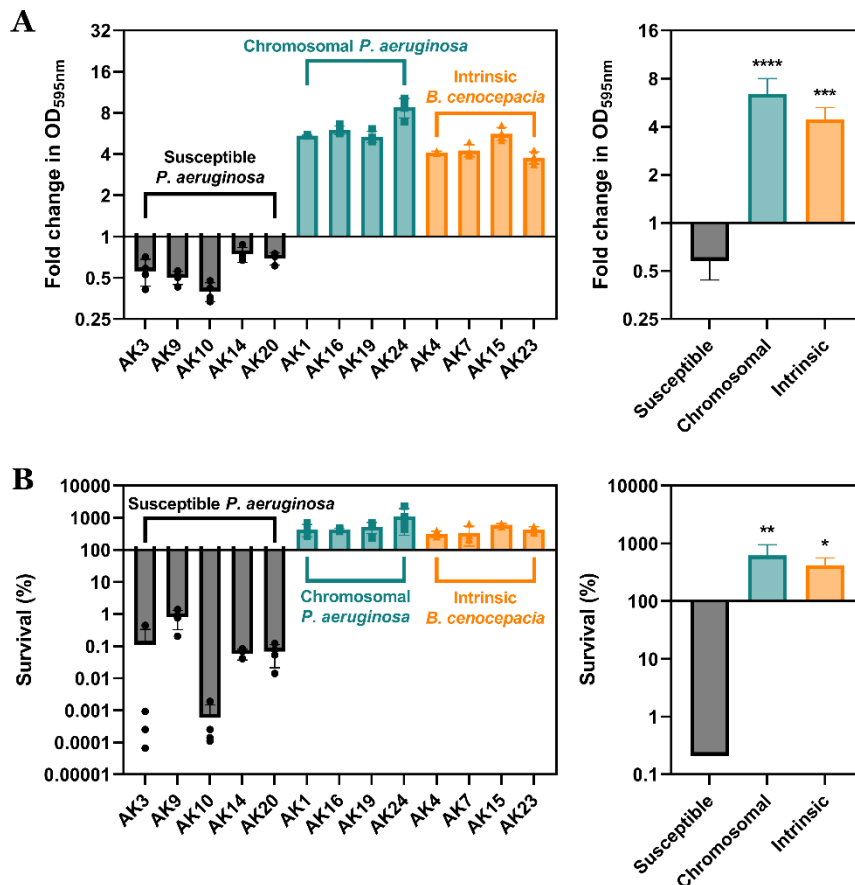


**Figure 5.14: Chromosomal and intrinsic polymyxin resistance provides equal protection from colistin.** **A**, Lysis/growth in whole cells of the clinical CF isolate panel following exposure to colistin ( $4 \mu\text{g ml}^{-1}$ ), as determined by measuring  $\text{OD}_{595\text{nm}}$  after 4 hours ( $n=4$ ; second graph depicts the arithmetic mean of values from the 3 indicated strain groups;  $***p<0.001$ ,  $****p<0.0001$  relative to “Susceptible” bacteria). **B**, Survival of whole cells of the clinical CF isolate panel following exposure to colistin ( $4 \mu\text{g ml}^{-1}$ ), as determined by c.f.u. counts after 4 hours ( $n=4$ ; second graph depicts the arithmetic mean of values from the 3 indicated strain groups;  $*p<0.05$ ,  $**p<0.01$  relative to “Susceptible” bacteria). Data in **A**, **B** were analysed by a one-way ANOVA with Dunnett’s post-hoc test. Data are presented as the arithmetic mean, and error bars represent the standard deviation of the mean.

The downstream outcomes of these variations in colistin-induced OM and CM permeabilisation within the clinical strain panel on bacterial lysis and survival were assessed after 4 hours of exposure to the polymyxin compounds ( $4 \mu\text{g ml}^{-1}$ ) by measuring  $\text{OD}_{595\text{nm}}$  and counting viable colonies, respectively. In the five polymyxin-susceptible *P. aeruginosa* CF isolates, where both the OM and the CM were damaged during colistin treatment, the cell cultures had a drop in  $\text{OD}_{595\text{nm}}$  readings of between 2 and 4-fold compared to the start of the assay, demonstrating that the progressive disruption of the two cell envelope bilayers caused ultimately the bacteria to lyse (**Figure 5.14A**). Contrastingly, in chromosomally colistin-resistant *P. aeruginosa* cells (where the polymyxin permeabilised the OM but not the CM), or inherently non-susceptible *B. cenocepacia* cells (where the polymyxin could not even damage

the OM), an increase in OD<sub>595nm</sub> readings of 4 to 8-fold was apparent following treatment with colistin for 4 hours, signifying that these bacteria were growing in the antibiotic's presence. Analogous findings were made when measuring cell counts, with the susceptible strains being drastically killed by colistin (4 to 6-log reduction in colonies by 4 hours), whilst the isolates with chromosomal/intrinsic resistance to the polymyxin drug were able to replicate by up to 1-log despite colistin exposure (**Figure 5.14B**). Put together, these results proved that although polymyxin non-susceptibility was conferred at different membrane sites in acquired versus intrinsic colistin resistance, both mechanisms provided bacteria with an equal capacity to tolerate and survive the polypeptide antibiotic.

### **5.12 Acquired colistin resistance in *E. coli* is associated with a fitness cost**

A hypothesis to rationalise why acquired polymyxin non-susceptibility (arising from carriage of *mcr* genes or chromosomal mutations) was mediated at the CM of Gram-negative bacteria, while intrinsic colistin resistance was mediated at the cellular OM, related to disparities in the ability of the LPS transport machinery to export modified lipid A structures. In typically colistin-susceptible strains, the sudden acquisition of plasmid-borne *mcr* variants or mutations in the chromosome may mean that the LPS molecules situated in the CM are excessively cationically-modified, but the Lpt protein complex responsible for moving LPS from the CM to the extracellular-facing leaflet of the OM may not have adapted to transport electrostatically-altered lipid A as efficiently as unaltered lipid A. If this were true, and there was a fitness cost to exporting modified LPS, it would consequently be expected that the CM of these bacteria with acquired colistin resistance would be enriched for cationically-altered lipid A relative to the OM. In fact, the MALDI-TOF experiment previously performed on whole cells and spheroplasts of *mcr-1*-positive *E. coli* showed this to be the case, with the higher ratio of modified:unmodified LPS in the CM compared to the OM a key piece of evidence hinting that cationically-altered lipid A may be a weaker substrate for the enzymes of the Lpt transport machinery than unaltered lipid A.

On the other hand, in bacteria with intrinsic polymyxin resistance, it is possible that due to the constitutive production of cationically-modified LPS in these cells, their LPS export proteins have evolved to proficiently move electrostatically-altered lipid A structures from the CM to the OM<sup>845</sup>. Hence, the OM of these inherently non-susceptible strains may contain a higher proportion of modified LPS than the OM of strains with acquired colistin resistance. This concept of there being a cost to transporting cationically-altered LPS in bacteria with *mcr*/chromosomal colistin non-susceptibility that did not exist in intrinsically-resistant strains presented a logical solution for the distinct membrane locations where resistance to the polymyxin was conferred between these two cell types.



To delve deeper into whether this hypothesis was correct, it was essential to test if there was a fitness cost in bacteria that had acquired colistin resistance where there was an excess presence of modified lipid A in the CM bilayer. This was done by returning to the *E. coli* MC1000 isogenic strain pair, consisting of one strain harbouring the *mcr-1* gene on an IPTG-inducible pDM1 plasmid, and another control strain carrying the empty plasmid alone. In order to examine the potential cost of *mcr-1*-mediated polymyxin non-susceptibility, the growth kinetics of the two isogenic MC1000 isolates were compared under conditions where *mcr-1* expression was induced at a basal level (0.5 mM IPTG) – where CM lipid A modification would occur at physiological levels – and under conditions of *mcr-1* overexpression (250 mM IPTG), where LPS in the CM would be excessively cationically-modified. The doubling times of these two cell populations (pEmpty and *mcr-1*) at the start of exponential-phase growth was calculated using OD<sub>600nm</sub> readings during both basal and high-level IPTG induction, and compared to detect any growth defects associated with *mcr* activity.

When expression of *mcr-1* was induced at basal levels, there was a small but significant increase in the doubling time of bacteria carrying the resistance determinant relative to empty plasmid control bacteria treated with the same IPTG concentration, with the duration taken for the OD<sub>600nm</sub> measurements to double increasing by 20% in *mcr-1*-positive cells (**Figure 5.15A**). However, when *mcr-1* was overexpressed, there was a far more striking increase in the bacterial doubling time (more than 250%) compared to the pEmpty cell population (**Figure 5.15B**). It was obvious, therefore, that the activity of the MCR enzyme led to a defect in *E. coli* growth, and that this effect was much larger when the protein was over-produced and excessively modifying CM LPS. This suggested that there may well be a fitness cost in bacteria with acquired colistin resistance, where a reduced ability to efficiently transport vast quantities of cationically-altered lipid A structures from the CM to the OM could have been important in the slower rate of replication.

For further analysis of the loss of fitness in *mcr-1*-expressing *E. coli* MC1000 cells, a well-established competition experiment was set up, where the colistin-resistant strain was co-cultured at a 1:1 ratio alongside the empty plasmid control strain, and this mixed population induced basally with a low concentration of IPTG (0.5 mM), or over-induced with a much greater amount of IPTG (250 mM)<sup>644</sup>. These two co-cultures were incubated initially for 12 hours, at which point the mixture of the isogenic strains was diluted and then re-inoculated so that the competition could be continued for 24 hours; this procedure was repeated on another 2 occasions so samples could be extracted at time points of 12, 36, 60 and 84 hours after the start of the assay. These samples were plated on solid agar media containing no colistin, or containing colistin at a concentration of 2 µg ml<sup>-1</sup> and after enumeration of the number of colonies that grew on the respective plates, a competitive index (CI) value was

generated through dividing the colony counts on colistin-absent media by colony counts on colistin-containing media. A CI value of greater than 1 obtained using this standardised technique for fitness experiments would indicate that the *mcr-1*-positive strain was out-competing the pEmpty strain, and thus had a relative growth advantage. Opposingly, CI values below 1 would show that pEmpty cells were becoming dominant within the mixed bacterial population, and axiomatically, expression of *mcr-1* conferred a fitness cost<sup>644</sup>.

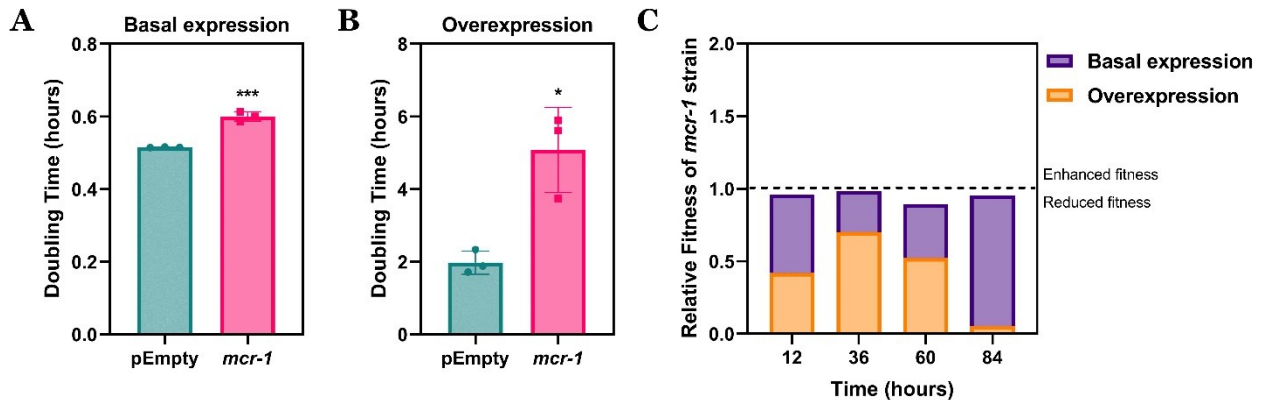


**Figure 5.15: Overexpression of *mcr-1* results in a marked fitness cost in *E. coli* cells with acquired colistin resistance.** **A, B,** Doubling time of *E. coli* MC1000 cells expressing *mcr-1* on the IPTG-inducible pDM1 plasmid, or cells harbouring the empty plasmid alone, during induction with **(A)** 0.5 mM IPTG, or **(B)** 250 mM IPTG, as determined by calculating the rate of increase in OD<sub>600nm</sub> readings at the start of logarithmic phase growth (n=3 in triplicate; \*p<0.05, \*\*\*p<0.001 relative to pEmpty bacteria). **C,** Competition experiment in co-cultures of *E. coli* MC1000 pEmpty cells and *mcr-1*-positive cells (1:1 ratio) induced with 0.5 mM IPTG (“Basal expression”) or 250 mM IPTG (“Overexpression”), as determined by plating cultures on colistin-free media or media containing 2 µg ml<sup>-1</sup> colistin and enumerating c.f.u. counts to generative competitive index (CI) values (n=3; CI value above 1 indicates growth advantage of *mcr-1* bacteria, CI value below 1 indicates fitness cost of *mcr-1* bacteria). Data in **A, B** were analysed by a two-tailed unpaired Student’s *t*-test. Data are presented as the arithmetic mean, and error bars shown represent the standard deviation of the mean.

In the *E. coli* co-culture where IPTG was added to only induce the *mcr-1* gene at basal levels, across the four time points, the CI values remained constant and around 1, revealing that physiological *mcr-1* expression resulted in no significant drop in fitness (**Figure 5.15C**). Nevertheless, in the co-culture exposed to high levels of IPTG to over-express *mcr-1*, the CI value was approximately 0.5 at the 12, 36 and 60 hour time points, before dropping as low as 0.05 by 84 hours (the end of the assay). This data highlighted that when the *mcr* resistance determinant was excessively induced, a noteworthy defect in bacterial fitness ensued. In this instance, then, acquired colistin non-susceptibility contributed to both a growth defect and a competitive fitness cost, and although here it was not absolutely verified that a diminished

capacity to export modified LPS from the CM to the OM via the Lpt transport machinery was the driver behind this phenotype, such findings substantiated this explanation for why intrinsic polymyxin resistance was mediated at the outermost cell envelope bilayer, but resistance arising through the acquisition of *mcr* genes or chromosomal mutations was not.

### 5.13 Discussion

With colistin becoming an increasingly critical therapeutic of last-resort in the treatment of multi-drug resistant bacterial infections, the expanding prevalence of non-susceptibility to the antibiotic is a public health emergency that requires immediate attention<sup>816</sup>. Unfortunately, attempts to mitigate and overcome colistin resistance are hampered by key gaps in the understanding of the molecular mechanisms by which bacteria survive exposure to the polymyxin<sup>442,454</sup>. The experiments in this chapter answered a number of questions about the basis of polymyxin non-susceptibility, showing that the two major forms of acquired colistin resistance detected clinically (*mcr* genes and chromosomal mutations) are both mediated at the level of the CM, not the OM, in diverse Gram-negative organisms. It was also found that intrinsic polymyxin resistance in *B. cenocepacia* was not conferred in the same manner as acquired non-susceptibility to colistin, but rather by protection of the OM from the antibiotic's membrane permeabilising behaviour, with preliminary data implying that this difference compared to *mcr*/chromosomal resistance may be due to a transport cost of moving modified lipid A to the cell surface OM bilayer. Finally, the work presented here also characterised a unique and new form of inducible colistin heteroresistance in *E. cloacae* isolates, which may play a role in clinical polymyxin treatment failure.

That colistin resistance conferred by activity of the *mcr-1* gene in *E. coli* was mediated at the CM might at first appear contradictory to the widely-held dogma that polymyxin non-susceptibility was a consequence of the antibiotic being unable to interact with and disrupt LPS molecules in the OM<sup>817,818</sup>. However, two previous studies looking at the mechanism through which the MCR-1 protein blocks colistin killing of *E. coli* offer key supporting evidence that the OM is not an important mediator of polymyxin resistance. Firstly, it has been reported using the identical NPN assay performed here that the OM of *mcr-1*-expressing *E. coli* undergoes polymyxin-induced permeabilisation to a similar extent as its respective wild-type strain, in spite of having a colistin MIC that was 32-fold higher<sup>819</sup>. Secondly, an investigation into the protective effects of secreted outer membrane vesicles (OMVs) concluded that the vesicles shed from *mcr-1*-positive *E. coli* cells maintained an ability to absorb extracellular colistin and promote bacterial survival<sup>820</sup>. These results, together with the work in this chapter, emphasise the irrelevance of the OM in polymyxin resistance.

Confirmation that the CM, not the OM, was the membrane site mediating colistin non-susceptibility arose from experiments with *E. coli* whole cells and spheroplasts producing MCR-1, which served to demonstrate that the polymyxin drug was unable to damage the innermost cell envelope bilayer and initiate uptake of the DNA-reactive PI fluorescent dye. The spheroplasts assays were especially crucial, exposing the lack of colistin's bactericidal and lytic activity against *mcr-1*-expressing cells, even when the OM structure had been removed. In combination with data from the previous chapter, this finding also reinforced that LPS in the CM was the central target in colistin's mode of bacterial killing, and that if CM LPS is either depleted (as done earlier) or cationically-modified to diminish the electrostatic interaction with polymyxin molecules (as done here), then the bactericidal behaviour of colistin can be wholly inhibited.

The reason why colistin could permeabilise the OM of *mcr-1*-positive *E. coli* but not the CM is likely due to discrepancies in the relative proportions of pEtN-modified lipid A to unmodified lipid A structures between the two bilayers. As identified using MALDI-TOF-based lipidomics, in the OM of MCR-1-producing *E. coli* whole cells, 60% of the total LPS was modified with a cationic pEtN chemical group, and 40% remained unaltered. In contrast, 80% of the lipid A molecules in the CM of *mcr-1*-expressing *E. coli* spheroplasts had a pEtN moiety added, with only 20% of total CM lipid A not modified. Colistin is dependent on binding to unmodified LPS molecules in order to damage membrane bilayers, and whilst the drop in the percentage of unaltered lipid A from 40% in the OM to 20% in the CM may seem somewhat small, it is absolutely vital to note that the abundance of LPS in the OM is far higher than that in the CM bilayer<sup>745</sup>. Previous assays measuring the concentration of LPS in the two membranes of *P. aeruginosa* cells showed that the quantity of the LPS in the OM is approximately 100-fold greater compared to the CM, and it is almost certain that this is also the case in *E. coli* strains, since past studies with the closely-related *S. typhimurium* species have reported comparable concentrations<sup>755</sup>. Therefore, in the OM of *E. coli* cells expressing *mcr-1*, there are a vast amount of LPS molecules (approximately  $10^7$  EU ml<sup>-1</sup>), and 40% of these have no lipid A modifications, meaning they can be targeted by colistin. On the other hand, in the CM of these same bacteria, there are much fewer LPS structures (less than  $10^5$  EU ml<sup>-1</sup>), 80% of which are pEtN-modified and not susceptible to colistin binding and disruption. This dissimilarity in the prevalence of unmodified LPS molecules (the fundamental molecular target of polymyxin antibiotics) in the CM versus the OM explains why colistin resistance was not mediate equally at the two bilayer membranes.

One of the major determinations from these set of experiments was that the degree to which colistin could permeabilise the CM of Gram-negative bacteria was directly correlated and proportional to the ratio of cationically-modified lipid A to unaltered lipid A within the

bilayer. This was made apparent by altering the proportion of LPS that was modified with pEtN in the CM of *E. coli* spheroplasts using an IPTG-inducible vector, and also by assessing colistin-triggered CM disruption in spheroplasts generated from a panel of *E. coli* clinical isolates that were polymyxin-resistant through diverse processes, including the expression of *mcr-1/mcr-2/mcr-3/mcr-5* genes, or via chromosomal mutations. In this clinical strain panel, it was deduced that bacteria harbouring the *mcr-1* resistance determinant had high levels of CM lipid A modification, and hence low levels of CM damage during colistin exposure. Conversely, bacteria carrying other *mcr* variants (in particular *mcr-3* or *mcr-5*) possessed a relatively low ratio of modified:unmodified LPS in the CM, meaning colistin permeabilised the CM of these spheroplasts to a greater extent. The fact that *mcr-1*-expression was associated with the highest degree of protection of the CM from colistin's membranolytic tendencies may provide a justification as to why the gene is the most widely disseminated of the *mcr* variants globally, being identified more frequently than other gene homologues in clinical samples<sup>789</sup>. It was, perhaps, surprising that colistin non-susceptibility conferred by chromosomal mutations in the *E. coli* strains did not block disruption of the CM by the polymyxin compound more than *mcr*-mediated resistance, considering chromosomal colistin resistance is typically linked to a double modification of lipid A with both pEtN and L-Ara4N domains<sup>821</sup>.

Quite why the *mcr-3* and *mcr-5* genes were less efficient at cationically-altering LPS and inhibiting colistin's permeabilisation of the CM remains unclear. Notably, these two homologues have been shown in previous analyses to be phylogenetically distant from the *mcr-1/mcr-2* variants that exhibited a more proficient form of colistin resistance at the level of the CM, existing in a separate family when categorising the *mcr* genes by their amino acid sequence identity<sup>572,581</sup>. However, the outcomes of differences in protein sequence between *mcr* homologues on their catalytic activity as pEtN transferase enzymes is poorly characterised and should be a focus of future work. In particular, these resistance determinants could be sequenced, and any polymorphisms relative to a reference *mcr-1* strain mapped on to their protein structures to understand if there are changes in the active sites or residues of the enzymes that may impact their function as pEtN transferases.

Disparities in enzyme activity may not be the only cause of the reduced lipid A modification in the *mcr-3* and *mcr-5*-harbouring isolates, with lower gene expression, protein production or protein stability (all factors that have previously been established as relevant in levels of resistance to other antibiotics) potential contributors to this phenotype<sup>822-824</sup>. This could be resolved by conducting a combination of qRT-PCR and RNAseq experiments (to test gene expression levels), as well as Western blotting (to test enzyme stability), in subsequent investigations. It would also be worth addressing the small sample size of particular *mcr* variants (e.g. *mcr-5*, where only a single isolate was tested) by expanding the collection of

clinical isolates included in the strain panel. Indeed, the discovery here that intrinsic colistin resistance was mediated at the cellular OM, not the CM as in bacteria with acquired polymyxin non-susceptibility, was achieved solely through assays with *B. cenocepacia* strains, and this clinical isolate panel should also be augmented to include additional species that have inherent resistance to colistin, such as *Neisseria* and *Serratia*.

New diagnostic approaches for rapidly detecting colistin resistance in clinical bacterial samples rely on the MALDI-TOF mass spectrometry-based method implemented often in this chapter to distinguish the presence of cationically-modified lipid A, as an alternate technique to traditional antibiotic susceptibility testing by broth microdilution<sup>641,788</sup>. A concern regarding this assay is that the results from this chapter imply polymyxin non-susceptibility is not as simple as modified LPS being present or not – rather, it is the ratio of cationically-altered:unaltered LPS specifically in the CM that dictates whether a bacteria will be colistin-sensitive or not. Thus, MALDI-TOF-based diagnostics for polymyxin resistance may need to be partially optimised to make the technique more quantitative, with a cut-off defined for what proportion of modified lipid A culminates in colistin becoming ineffective above its specified resistance breakpoint.

Another worry from a diagnostic standpoint is the recognition in the work presented here of colistin hetero-resistance in clinical *E. cloacae* isolates. This phenotype is likely to be highly challenging to detect, only suspected by the appearance of “skipped wells” during MIC testing, which are random and inconsistent due to the nature of hetero-resistance<sup>777,801</sup>. Hetero-resistance to colistin is now a widely-reported phenomenon, and *in vivo* studies using *E. cloacae* strains have proved that the resistant sub-population mediating this behaviour can be responsible for polymyxin treatment failing<sup>662,778</sup>. Disparate from any previous reports with any antibiotics, however, the sub-population of *E. cloacae* cells that were colistin non-susceptible actually increased in size during exposure to higher concentrations of the polymyxin drug itself. The molecular basis for this inducible trait is completely unknown, but future work should commence by isolation of the resistant sub-population (by PAP experiments), followed by comparative whole genome sequencing to comprehend how these bacteria become more colistin-tolerant when treated with increased amounts of the antibiotic.

An unexpected conclusion from this chapter’s data is that polymyxin-resistant bacteria appeared to tolerate and replicate despite permeabilisation of the OM by colistin. This is not to say that these cells were entirely unaffected by the damage incurred to their outermost surface bilayer, because bacterial growth, though not halted, was significantly slower than in otherwise untreated cell populations. Moreover, the OM disruption characterised here is, in fact, only a marker of relatively minor permeabilisation of the extracellular-facing membrane, sufficient for the small NPN dye to access membrane phospholipids and fluoresce. However,

with colistin treatment enabling the intracellular access of even a low molecular-weight compound into colistin-resistant bacteria, the fascinating prospect of using the polymyxin drug to promote uptake of other small hydrophobic antibiotics that normally cannot cross the Gram-negative OM (e.g. rifampicin) is raised. In summary, the work here not only describes and differentiates the mechanisms by which acquired and intrinsic polymyxin resistance are mediated, it also opens opportunities for the design of novel combination therapies that are desperately needed to combat colistin non-susceptibility.

## Chapter 6: Novel combination treatment strategies enhance colistin efficacy and overcome colistin resistance

### 6.1 Introduction

The high rate of treatment failure during clinical colistin administration to patients infected with Gram-negative bacterial pathogens, combined with the rising prevalence of polymyxin resistance, has necessitated the development of new therapeutic options that can improve the antibiotic's effectiveness<sup>782,825</sup>. Recently, there has been considerable interest amongst the medical community about increasing the efficacy of colistin by administering the drug alongside a second antimicrobial agent<sup>294</sup>. It is thought that such combination therapies may be preferable to polymyxin monotherapy, because as well as augmenting the ability of colistin to clear bacteria, they may allow for a reduction in the dosage of the antibiotic used to treat infected patients<sup>826</sup>. This is of particular importance due to the frequent nephrotoxic and neurotoxic side-effects closely associated with colistin therapy, which could be kept in check by limiting the polymyxin concentration administered in combination treatments<sup>827,828</sup>. Moreover, by administering lower doses of colistin, there is a potential that the emergence of polymyxin non-susceptibility may be slowed, and it has been suggested that the utilisation of another antimicrobial drug in addition to colistin could even be advantageous in overcoming the problem of hetero-resistance observed in Gram-negative bacterial populations exposed to the polymyxin alone<sup>752,829</sup>. On the other hand, combination therapy approaches that include colistin do have increased expenditure, and there remains a lack of conclusive evidence about whether polymyxin combination treatments actually have a therapeutic superiority over monotherapy in clinical settings, despite the fact that colistin would now rarely be administered as a sole, independent antibiotic by most medical practitioners.

The majority of research into antibiotics to be used in combination with colistin has been conducted through *in vitro* synergy testing experiments, with various methods such as E-test, time-kill and checkerboard assays employed predominantly on *P. aeruginosa* and *A. baumannii* species. One key study reported that the adding colistin along with several typical front-line antipseudomonal agents (ceftazidime, aztreonam, meropenem, ciprofloxacin) to cultures of *P. aeruginosa* resulted in significantly greater and more rapid bacterial killing, even at low, sub-inhibitory colistin concentrations ( $0.5 \mu\text{g ml}^{-1}$ )<sup>830</sup>. However, this phenotype was inconsistent in another similar study, which found a synergistic interaction between colistin and ceftazidime, but no effect with ciprofloxacin on enhancing polymyxin activity<sup>831</sup>. Data on *in vitro* combinations of carbapenem compounds with colistin has been more reproducible, with two reports highlighting the colistin-potentiating properties of meropenem and imipenem against multi-drug resistant *P. aeruginosa* isolates<sup>832,833</sup>. A critical



investigation examining colistin combinations under anaerobic and biofilm conditions interestingly noted that ciprofloxacin, ceftazidime, co-trimoxazole and azithromycin all displayed a degree of synergy with the polymyxin antibiotic in these clinically-relevant environments<sup>834</sup>. Perhaps the best characterised antibiotic for administration alongside colistin is rifampicin, with many *in vitro* studies in *P. aeruginosa* and *A. baumannii* concluding that colistin plus rifampicin is a much more potent bactericidal treatment option than polymyxin monotherapy<sup>835–839</sup>. The synergistic nature of the drugs meropenem, azithromycin and doxycycline with colistin against *A. baumannii* strains has also been demonstrated in a landmark report<sup>832</sup>. It is generally considered that the mechanism mediating the improved antibacterial activity of these polymyxin combinations is amplified access of the secondary antibiotic compounds to intracellular targets once colistin has disrupted and permeabilised the cell envelope bilayers, although this has not been conclusively proven experimentally<sup>840</sup>.

Whilst the *in vitro* analysis of antimicrobial molecules to incorporate in novel colistin combination therapeutic strategies has been extensive, the subsequent investigation of these using *in vivo* models that more closely resemble the human host environment has been comparatively lacking. A historic study on septic monkeys infected with *P. aeruginosa* found no obvious benefit to mortality with a colistin and carbenicillin combination treatment relative to colistin alone, but two more recent reports from Italy uncovered that overall mortality in a rat *P. aeruginosa* sepsis model was halved when either imipenem or rifampicin were included in the treatment regimen along with colistin, again relative to treatment with the polymyxin alone<sup>833,841,842</sup>. In two mouse infection experiments with *A. baumannii* – one pneumonia model and one thigh infection model – it was shown that combining colistin with rifampicin resulted in an approximately 30% improvement in outcomes (reduced bacterial load in the lungs in the pneumonia model, improved mortality in the thigh model) in comparison to colistin monotherapy<sup>843,844</sup>. One single study on an *E. coli* strain that was inoculated intraperitoneally into adult rats identified a similar level of reduced mortality (33%) with colistin plus piperacillin therapy, compared to treatment with only the polymyxin compound<sup>845</sup>.

This information, though only obtained from a small number of *in vivo* studies, may indicate an advantage of these proposed drug combinations that could translate to clinical settings. Unfortunately, however, clinical trial data assessing the efficacy of these treatment regimens has been both limited and disappointing. Combining colistin with a wide range of front-line antibiotics (aztreonam, azlocillin, piperacillin, ceftazidime, imipenem, amikacin, ciprofloxacin, rifampicin) across three clinical studies (in Italy, U.S.A., U.K.) on human patients infected with *P. aeruginosa* caused no significant differences in microbiological responses, therapeutic outcomes or toxicity rates relative to colistin treatment alone<sup>311,614,846</sup>. In a retrospective trial comparing colistin plus meropenem therapy with only colistin therapy,

patients infected with diverse Gram-negative pathogens (*P. aeruginosa*, *A. baumannii*, *E. coli*, *E. cloacae*, *Stenotrophomonas maltophilia*) actually had significantly higher levels of survival when treated with the polymyxin monotherapy<sup>827</sup>. Finally, the most recent large, multicentre, randomized clinical trial on colistin combination treatments against extremely drug-resistant *A. baumannii* infections concluded that there was no impact on 30-day mortality in patients where rifampicin was added alongside the polymyxin antibiotic<sup>753</sup>.

To summarise, in spite of years of substantial research, there are no clear and evident combination strategies in routine clinical use that can make colistin a more effective antibiotic. Nevertheless, there still exists an urgent demand to develop such approaches that can reduce polymyxin treatment failure, mitigating colistin's toxic side-effects and enhancing outcomes in infected patients. In this chapter, by exploiting previous findings, two new therapeutic options are presented that not only improve colistin's activity against susceptible strains, they also overcome the ever-growing threat of polymyxin resistance.

## **6.2 A sub-inhibitory concentration of murepavadin does not affect LPS levels in the OM of *P. aeruginosa***

Having established earlier that the bactericidal activity of colistin is dependent on the targeting of LPS molecules in the CM of Gram-negative bacteria, and that the polymyxin's killing capacity could be blocked by depleting LPS from the innermost membrane bilayer, the first possibility considered for improving the efficacy of colistin was increasing the abundance of LPS structures within the cellular CM. Murepavadin is a novel antimicrobial agent in pre-clinical developmental pipelines that functions by interacting with the  $\beta$ -barrel of the LPS transport protein LptD, disrupting the essential process of LPS export from the CM to the OM of bacteria to ultimately induce cell death<sup>256–258</sup>. It was hypothesised that exposing bacteria to sub-inhibitory concentrations of murepavadin could lead to partial inhibition of LptD and a reduction in the speed by which the Lpt protein machinery transported LPS out of the CM and into the OM, without any significant loss of cell viability. As a consequence, the postulation was that LPS molecules would accumulate within the CM bilayer, because they were still being synthesised within the bacterial cytoplasm by the Lpx enzymes and flipped to the outermost leaflet of the CM by the MsbA enzyme, but their subsequent movement to the extracellular-facing leaflet of the OM bilayer was obstructed by murepavadin<sup>203,223</sup>. To examine this proposal, it was first necessary to identify a sub-inhibitory concentration of murepavadin, and since the LptD inhibitor is a *Pseudomonas*-specific antibiotic, experiments were performed using the reference *P. aeruginosa* strain PA14<sup>259,260</sup>.

Determination of what constituted a sub-lethal concentration of murepavadin against *P. aeruginosa* PA14 cells was undertaken by exposing bacterial populations to a range of doses of the LPS transport inhibitor, and measuring the growth kinetics by OD<sub>600nm</sub> readings over 16 hours incubation. It was discovered that addition of murepavadin at a concentration of 0.05 µg ml<sup>-1</sup> had a barely noticeable impact on the rate of growth of PA14 bacteria throughout the treatment period relative to untreated cells, confirming that this was a suitable dose of the compound to be used in all further experiments with the strain, allowing partial blocking of LPS transport without compromising viability (**Figure 6.1A**). Prior to exploring whether murepavadin-mediated inhibition of LptD triggered the build-up of LPS molecules in the CM, it was vital to test the inhibitor's effects on LPS levels in the OM, as modulations in OM LPS abundance even with a sub-inhibitory murepavadin concentration could confound the future interpretation of results. The amount of LPS present in the extracellular-facing OM bilayer of *P. aeruginosa* whole cells was quantified using the two approaches employed previously – namely, the diagnostic gold-standard immunogenic LAL assay, and via the LPS-specific fluorescently-labelled probe BoDipy-PMBN<sup>633</sup>.

For the LAL experiment, PA14 bacteria were either exposed or not to the verified sub-inhibitory concentration of murepavadin, before the OM was extracted by EDTA treatment and the LPS abundance in this sample calculated. There was no significant difference between the amount of LPS within the OM of untreated and murepavadin-treated cells, indicating that sub-lethal doses of the compound could be used to inhibit LPS transport with minimal impact on the outermost cell surface bilayer (**Figure 6.1B**). Likewise, when these two *P. aeruginosa* populations were incubated alongside BoDipy-PMBN for 30 minutes after their respective treatments (unexposed or murepavadin-exposed), the fluorescent signal from molecules of the PMBN probe bound to LPS in the OM bacterial surface was identical, irrespective of the presence of the LptD inhibitor or not (**Figure 6.1C**). This provided supplementary validation that the levels of LPS in the OM of PA14 cells were largely unaffected when treated with sub-lethal murepavadin doses.

In order to substantiate these data, the ability of colistin to permeabilise the OM of *P. aeruginosa* cells exposed to a sub-inhibitory murepavadin concentration was assessed, with the hypothesis being that if the LPS transport inhibitor did indeed exhibit no propensity for lowering OM LPS abundance, then the extent of colistin-induced OM damage should also be unchanged by the inclusion of murepavadin in the assay. Populations of PA14 bacteria were treated with two clinically-relevant colistin concentrations (1 and 2 µg ml<sup>-1</sup>), in each case either alone or in combination with murepavadin, and OM disruption initiated by the polymyxin drug was analysed using the phospholipid-reactive NPN fluorescent dye<sup>626</sup>. Exposure to colistin alone caused a marked increase in NPN uptake, revealing the polypeptide antibiotic

was permeabilising the OM bilayer, although notably, murepavadin treatment alone did not have the same effect, with no rise in NPN fluorescence over the course of the experiment (**Figure 6.1D**). More crucially, NPN uptake into *P. aeruginosa* bacteria treated with the combination of colistin and murepavadin was equal to cells treated only with the polymyxin, highlighting that colistin-triggered disruption to the OM was not altered by the activity of the LptD inhibitor. Together, these results proved that, at the concentration used, blocking LPS transport from the CM with murepavadin had no impact on the amount of LPS in the OM.

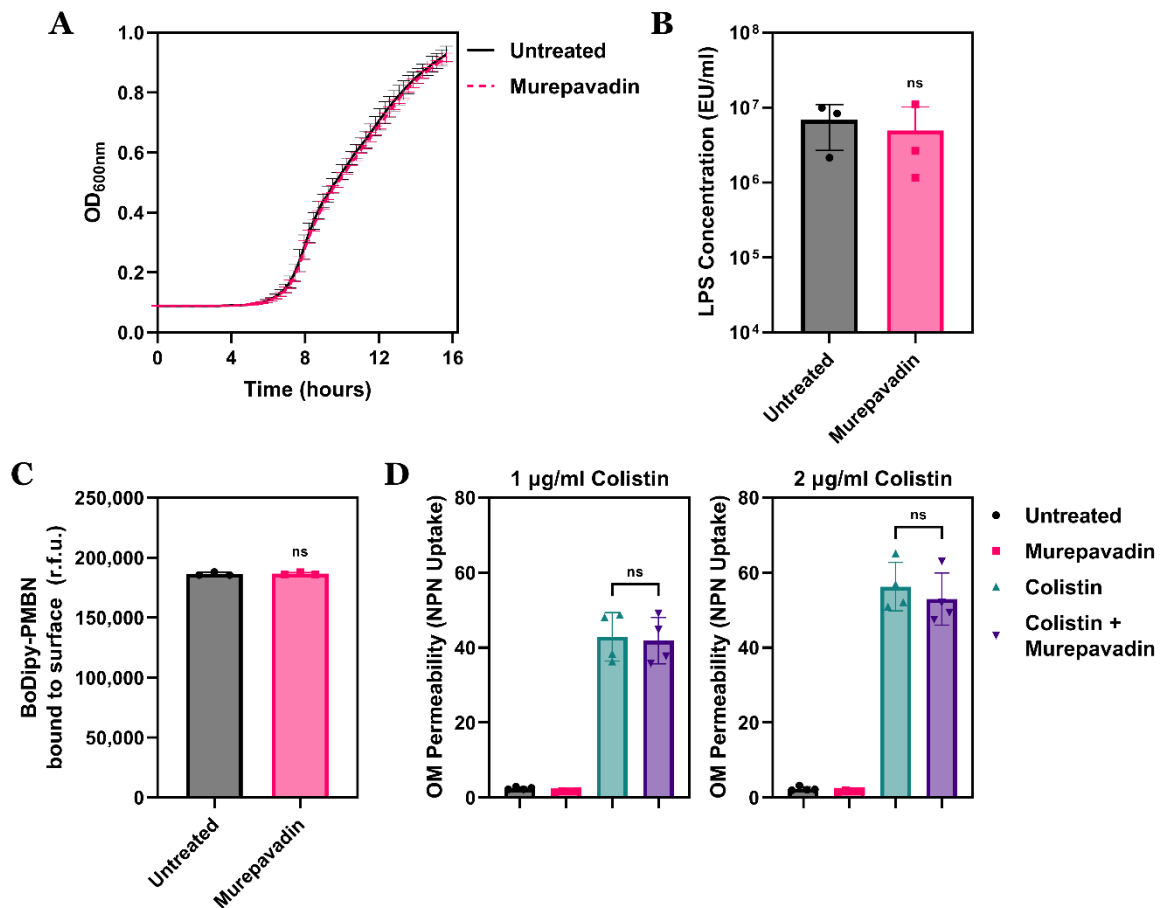


**Figure 6.1: Blocking LPS transport with a sub-inhibitory murepavadin concentration has a minimal effect on *P. aeruginosa* OM LPS abundance.** **A**, Growth kinetics of *P. aeruginosa* PA14 cells during exposure, or not, to the LptD inhibitor murepavadin (0.05 µg ml<sup>-1</sup>), as determined by measuring OD<sub>600nm</sub> over 16 hours incubation (n=4). **B**, Concentration of LPS in the OM extracted from *P. aeruginosa* PA14 cells exposed, or not, to murepavadin (0.05 µg ml<sup>-1</sup>) for 2 hours, as determined using the LAL assay (n=3; ns: p>0.05 relative to untreated cells). **C**, Quantification of BoDipy-PMBN (7 µg ml<sup>-1</sup>) bound to the bacterial surface of *P. aeruginosa* PA14 cells exposed, or not, to murepavadin (0.05 µg ml<sup>-1</sup>) for 2 hours (n=3; ns: p>0.05 relative to untreated cells). **D**, Permeabilisation of the OM of *P. aeruginosa* PA14 cells exposed, or not, to two colistin concentrations (1 µg ml<sup>-1</sup> and 2 µg ml<sup>-1</sup>), in each case either alone or in combination with murepavadin (0.05 µg ml<sup>-1</sup>), as determined by measuring uptake of the NPN fluorophore (10 µM) over 10 minutes (n=4, each data point represents the arithmetic mean of 20 replicate measurements; ns: p>0.05 relative to bacteria exposed to colistin alone). Data in **B**, **C** were analysed by a two-tailed unpaired Student's *t*-test. Data in **D** were analysed by a one-way ANOVA with Sidak's post-hoc test. Data are presented as the arithmetic mean, and error bars represent the standard deviation of the mean.

### 6.3 Murepavadin treatment triggers LPS accumulation in the *P. aeruginosa* CM

After deducing a sub-inhibitory concentration of murepavadin that could be used to block LPS transport in *P. aeruginosa* PA14 cells with minimal effects on LPS abundance in the OM, it was next investigated whether this same dose of the LptD inhibitor could bring about an accumulation of LPS molecules in the bacterial CM bilayer, with the ultimate aim being to potentiate the activity of colistin. To specifically measure LPS levels exclusively in the CM, without the contaminating presence of the OM, PA14 bacteria were pre-treated with the sub-lethal murepavadin dose for 2 hours, and then converted into spheroplasts, removing the OM and cell wall structures through the successive addition of EDTA, lysozyme and trypsin in the protocol validated by earlier experiments<sup>637</sup>. These murepavadin-exposed spheroplast forms, maintained in an osmoprotective 20% sucrose buffer, were subjected to three techniques for quantifying the amount of CM LPS, with otherwise untreated spheroplasts serving as the comparative controls.

The first technique implemented MALDI-TOF mass spectrometry lipidomics on the *P. aeruginosa* spheroplasts treated with murepavadin to detect the ratio of lipid A to a membrane phospholipid (phosphatidylglycerol 34:2) within the cellular CM<sup>687</sup>. It was immediately apparent from visual inspection of the generated mass spectra alone that the proportion of lipid A relative to the PG 34:2 peak was larger in the spheroplasts pre-exposed to murepavadin than when the LPS transport inhibitor was absent (**Figure 6.2A**). This was supported semi-quantitatively by analysing the area under the peaks of lipid A and the reference phospholipid, which showed that the ratio of lipid A:phospholipid was approximately 50% higher in the CM of PA14 cells incubated with murepavadin, offering a preliminary sign that the LptD inhibitor did trigger a build-up of LPS molecules in the innermost membrane bilayer (**Figure 6.2B**).

To corroborate these data, the two LPS quantification approaches used in the OM of murepavadin-treated whole cells of *P. aeruginosa* were repeated with PA14 spheroplasts at the level of the CM. With the immunogenic LAL assay, it was found that the concentration of LPS molecules in the CM of untreated spheroplasts was 100-fold lower than that in the OM of whole bacteria, but there was a significant increase in the abundance of CM LPS in the cell population pre-exposed to murepavadin before spheroplast conversion (**Figure 6.2C**). Using the lipid A-specific fluorescent BoDipy-PMBN probe as a marker of surface LPS amounts, analogous results were obtained – in the CM of *P. aeruginosa* spheroplasts that had been treated with the LPS transport antagonist, the binding of BoDipy-PMBN was patently higher than in the CM of unexposed spheroplasts (**Figure 6.2D**). Hence, while a sub-inhibitory dose of murepavadin did not alter LPS abundance in the OM, it did initiate an accumulation of LPS molecules in the PA14 CM.

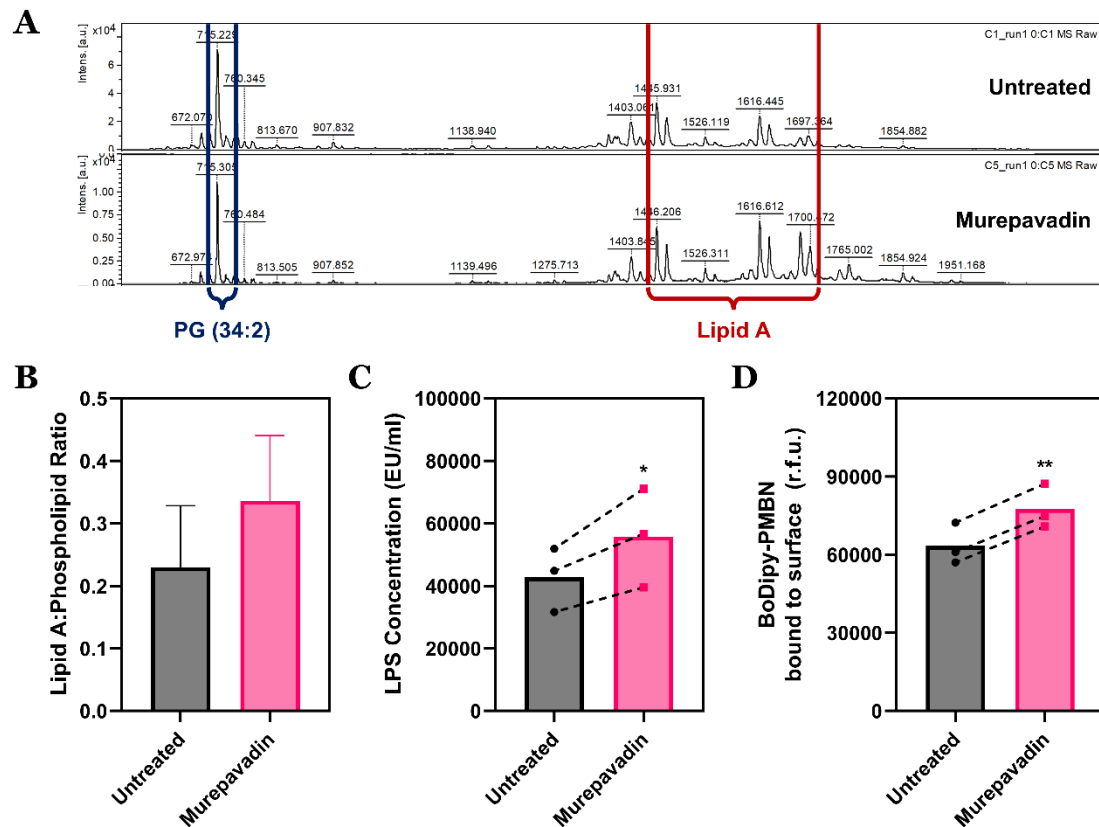


**Figure 6.2: LPS molecules accumulate in the CM of *P. aeruginosa* spheroplasts exposed to murepavadin.** **A**, Lipidomic MALDI-TOF mass spectra showing the abundance of lipid A and the membrane phospholipid phosphatidylglycerol (PG) 34:2 in spheroplasts produced from *P. aeruginosa* PA14 cells pre-treated, or not, with murepavadin ( $0.05 \mu\text{g ml}^{-1}$ ) for 2 hours prior to conversion into spheroplasts (spectra representative of 3 independent experiments). **B**, Quantification of ratio of lipid A:PG (34:2) in spheroplasts from *P. aeruginosa* PA14 cells pre-exposed, or not, to murepavadin ( $0.05 \mu\text{g ml}^{-1}$ ) for 2 hours prior to conversion into spheroplasts, as determined by measuring the area under the mass spectra peaks ( $n=3$  in duplicate). **C**, Concentration of LPS in the CM of spheroplasts produced from *P. aeruginosa* PA14 cells pre-exposed, or not, to murepavadin ( $0.05 \mu\text{g ml}^{-1}$ ) for 2 hours prior to conversion into spheroplasts, as determined using the LAL assay ( $n=3$ ; \* $p<0.05$  relative to previously untreated spheroplasts). **D**, Quantification of fluorescence from BoDipy-PMBN ( $7 \mu\text{g ml}^{-1}$ ) bound to the CM surface of spheroplasts produced from *P. aeruginosa* PA14 cells pre-exposed, or not, to murepavadin ( $0.05 \mu\text{g ml}^{-1}$ ) for 2 hours prior to conversion into spheroplasts ( $n=3$ ; \*\* $p<0.01$  relative to previously untreated spheroplasts). Data in **C**, **D** were analysed by a two-tailed paired Student's *t*-test. Data are presented as the arithmetic mean, and error bars shown represent the standard deviation of the mean.

## 6.4 Murepavadin enhances colistin-mediated CM disruption and lysis in *P. aeruginosa*

Once an appropriate concentration of murepavadin had been established that, through blocking LPS transport, caused an accumulation of LPS molecules in the cellular CM without affecting LPS levels in the OM, it was now possible to test the initial proposal that colistin's bactericidal activity could be enhanced by the LptD inhibitor. To do this, *P. aeruginosa* PA14 whole cells were exposed to two therapeutically-relevant doses of the polymyxin antibiotic ( $1$  and  $2 \mu\text{g ml}^{-1}$ ), both with and without the supplemental addition of murepavadin at a sub-

lethal concentration ( $0.05 \mu\text{g ml}^{-1}$ ), and the capacity for colistin to permeabilise the CM bilayer – the key step in its killing mode of action – was compared. Using fluorescence from the DNA-reactive PI dye as a read-out for colistin-induced CM damage, it was observed that in PA14 bacteria treated with the lower polymyxin concentration ( $1 \mu\text{g ml}^{-1}$ ) alone, there was a negligible increase in PI uptake during the 8 hour antibiotic exposure relative to untreated cells, implying that colistin was only minimally disrupting the CM structure (**Figure 6.3A**). Whilst exposure to murepavadin alone triggered a small rise in the fluorescent PI signal, there was significantly higher PI fluorescence measured in the *P. aeruginosa* population co-treated with the LPS transport inhibitor and murepavadin, signifying for the first time that initiating a build-up of LPS molecules in the bacterial CM with the LptD antagonist potentiated colistin's CM permeabilising behaviour. This phenotype was exacerbated in PA14 whole cells exposed to the higher colistin concentration ( $2 \mu\text{g ml}^{-1}$ ), which independently was responsible for a limited increase in CM disruption and PI uptake over the first 2 hours of the assay, but in combination with murepavadin damaged the CM bilayer much more strikingly, with the PI fluorescent signal at least 3-fold higher than bacteria treated with colistin/murepavadin alone.

Although it had already been verified that the presence of murepavadin did not impact colistin-mediated OM disruption through the NPN experiment, in order to definitively eliminate any contribution of the outermost cell surface bilayer to the polymyxin-potentiating effects of the LptD inhibitor, the CM permeabilisation assays were repeated with spheroplasts of *P. aeruginosa* that had been pre-treated, or not, with murepavadin. This approach had the additional advantage of distinguishing between whether colistin was enhancing murepavadin-induced CM damage, or murepavadin was enhancing colistin-induced CM damage, because cells were incubated with the LPS transport antagonist initially, before any residual molecules of murepavadin were washed out and the spheroplasts generated from these whole cells were exposed to colistin ( $1$  or  $2 \mu\text{g ml}^{-1}$ ) alone. Colistin-treated spheroplasts from PA14 cells that had not been pre-exposed to murepavadin displayed a slow increase in fluorescence from the PI dye that was entirely in line with untreated spheroplasts, revealing that the polymyxin drug at these concentrations did not permeabilise the CM structure at all (**Figure 6.3B**). By contrast, when spheroplasts pre-treated with murepavadin to accumulate LPS in the CM bilayer were then exposed to the same two colistin doses, in each case uptake of PI occurred both more rapidly and to a greater degree. These data demonstrated irrefutably that the inhibition of LPS transport with murepavadin augmented the ability of colistin to disrupt the *P. aeruginosa* CM.

To assess the downstream consequences of murepavadin's influence on polymyxin-induced CM damage on the viability of PA14 whole cells and spheroplasts, optical density readings were made in cultures incubated with colistin to detect bacterial lysis. Whole cells of

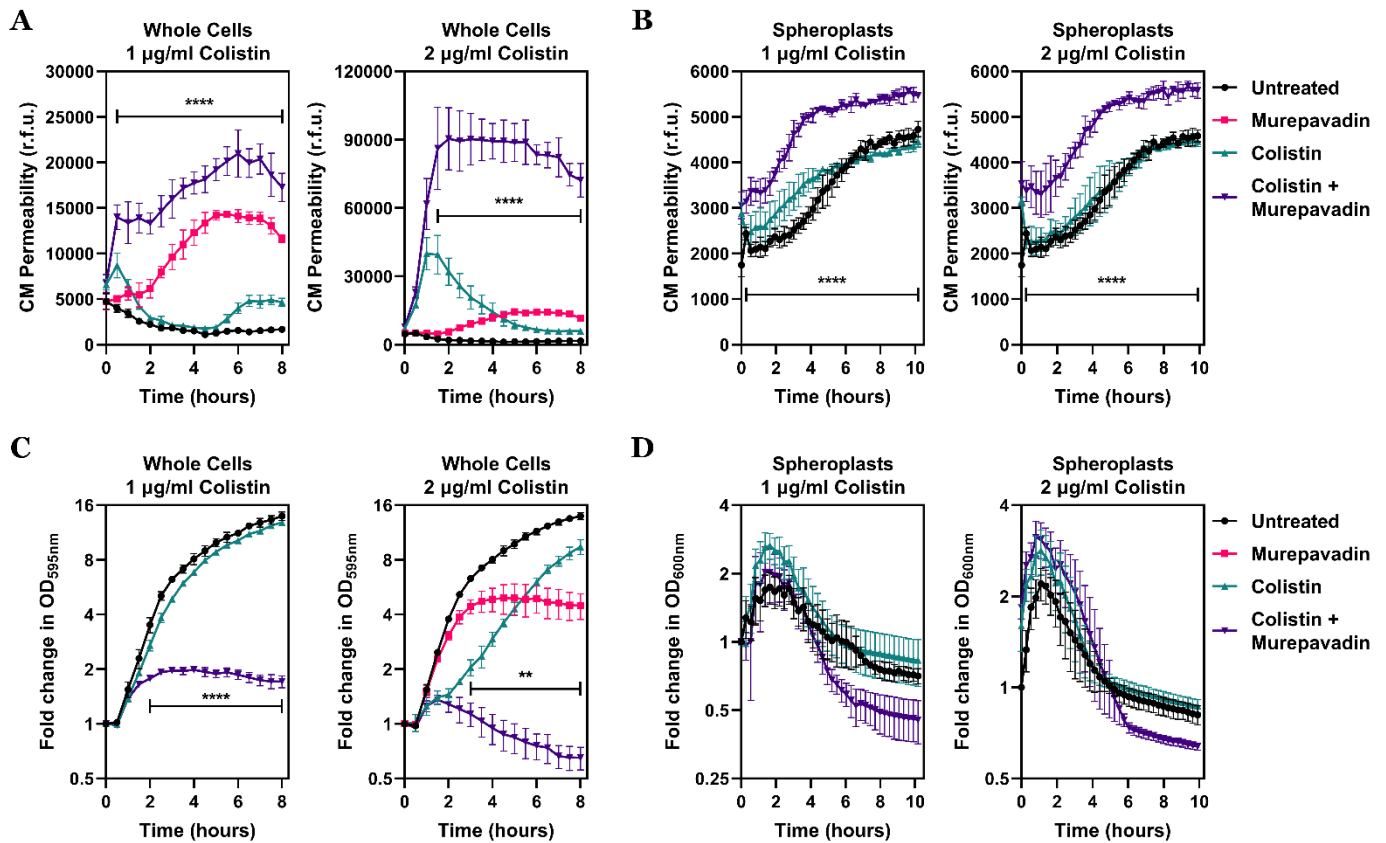


**Figure 6.3: Inhibiting LPS transport with murepavadin potentiates the ability of colistin to disrupt the *P. aeruginosa* CM and trigger cell lysis.** **A**, Permeabilisation of the CM of *P. aeruginosa* PA14 whole cells exposed, or not, to two colistin concentrations (1  $\mu\text{g ml}^{-1}$  and 2  $\mu\text{g ml}^{-1}$ ), in each case either alone or in combination with murepavadin (0.05  $\mu\text{g ml}^{-1}$ ), as determined by measuring fluorescence from PI (2.5  $\mu\text{M}$ ) over 8 hours ( $n=4$ ; \*\*\*\* $p<0.0001$  for bacteria exposed to colistin and murepavadin relative to all other conditions). **B**, Permeabilisation of the CM by colistin (1 or 2  $\mu\text{g ml}^{-1}$ ) of spheroplasts produced from *P. aeruginosa* PA14 cells pre-treated, or not, with murepavadin (0.05  $\mu\text{g ml}^{-1}$ ) for 2 hours prior to conversion into spheroplasts, as determined by measuring fluorescence from PI (0.25  $\mu\text{M}$ ) over 10 hours ( $n=3$ , assay performed on 4 independent occasions; \*\*\*\* $p<0.0001$  for bacteria exposed to colistin and murepavadin relative to all other conditions). **C**, Lysis of *P. aeruginosa* PA14 whole cells exposed, or not, to two colistin concentrations (1  $\mu\text{g ml}^{-1}$  and 2  $\mu\text{g ml}^{-1}$ ), in each case either alone or in combination with murepavadin (0.05  $\mu\text{g ml}^{-1}$ ), as determined by measuring  $\text{OD}_{595\text{nm}}$  over 8 hours ( $n=4$ ; \*\* $p<0.01$ , \*\*\*\* $p<0.0001$  for bacteria exposed to colistin and murepavadin relative to all other conditions). **D**, Lysis by colistin (1 or 2  $\mu\text{g ml}^{-1}$ ) of spheroplasts produced from *P. aeruginosa* PA14 cells pre-treated, or not, with murepavadin (0.05  $\mu\text{g ml}^{-1}$ ) for 2 hours prior to conversion into spheroplasts, determined by measuring  $\text{OD}_{600\text{nm}}$  over 10 hours ( $n=3$ , assay performed on 4 independent occasions). Data in **A-C** were analysed by a two-way ANOVA with Dunnett's post-hoc test. Data are presented as the arithmetic mean, and error bars represent the standard deviation of the mean.

*P. aeruginosa* treated only with 1  $\mu\text{g ml}^{-1}$  colistin grew in the presence of the polypeptide antibiotic, with  $\text{OD}_{595\text{nm}}$  readings increasing at the same rate as unexposed bacteria over the 8 hour experiment (**Figure 6.3C**). However, when murepavadin was added to the assay, the rise in  $\text{OD}_{595\text{nm}}$  measurements was much smaller, with only a two-fold increase over the first 2 hours of drug exposure. In the absence of any subsequent drop in  $\text{OD}_{595\text{nm}}$  readings, it was



concluded that the LptD inhibitor did not enhance colistin-induced lysis at this lower polymyxin concentration, although there was a much more potent growth inhibitory effect with the combination treatment than with colistin alone.

Increasing the dose of colistin used in the experiment to 2  $\mu\text{g ml}^{-1}$  produced a more noteworthy phenotype, with whole cells of PA14 again replicating during exposure to the polymyxin drug alone (8-fold rise in OD<sub>595nm</sub> measurements over 8 hours), but prominent lysis of *P. aeruginosa* bacteria initiated by colistin clearly discernible when murepavadin was incorporated into the assay (2-fold drop in OD<sub>595nm</sub> measurements over 8 hours). Importantly, there was an increase in OD<sub>595nm</sub> readings in cells treated with murepavadin only, which confirmed that the LPS transport inhibitor was being used at a sub-inhibitory concentration. Consistent results were acquired when repeating the assay with spheroplasts pre-treated, or not, with murepavadin prior to colistin exposure. Lysis of spheroplasts generated from PA14 cells not previously exposed to the LptD antagonist was insignificant when treated to either 1 or 2  $\mu\text{g ml}^{-1}$  colistin, with the kinetics of OD<sub>595nm</sub> readings unchanged relative to spheroplasts that were not even incubated with the polymyxin compound (**Figure 6.3D**). Nonetheless, with both colistin concentrations, lysis triggered by the polymyxin drug was increased in spheroplasts from *P. aeruginosa* bacteria that had been pre-treated with murepavadin to accumulate LPS in the CM, with a faster and larger decrease in OD<sub>595nm</sub> measurements over the course of the experiment. Put together, this set of data showed that the blocking of LPS transport and build-up of CM LPS by murepavadin heightened the efficacy of colistin not only to permeabilise the *P. aeruginosa* CM, but also to lyse the bacterial cells.

## **6.5 The synergy with murepavadin augments the bactericidal activity of colistin against *P. aeruginosa***

Thus far, it had been proven that two distinct steps in colistin's mode of bacterial killing – namely, CM disruption and lysis – were enhanced by murepavadin, but the direct impact of the LptD inhibitor on the polymyxin's bactericidal activity was yet to be quantified. To study this, *P. aeruginosa* PA14 populations were exposed again to the two previously used, clinically-relevant colistin concentrations (1 and 2  $\mu\text{g ml}^{-1}$ ), either alone or in combination with a sub-lethal dose of murepavadin (0.05  $\mu\text{g ml}^{-1}$ ), and the number of viable cells in the population over an 8 hour incubation period was determined via colony counts. Bacteria treated only with 1  $\mu\text{g ml}^{-1}$  colistin grew 10-fold over the course of the experiment, at precisely the same rate as bacteria not exposed to any antibiotic stress (**Figure 6.4A**). Opposingly, in PA14 cells exposed to the same polymyxin concentration in the presence of murepavadin, there was a rapid drop in colony counts, and by 8 hours, a more than 3-log difference in the number of viable bacteria

relative to the colistin monotherapy condition. Conducting this assay with 2  $\mu\text{g ml}^{-1}$  colistin made the potentiating influence of murepavadin even more apparent. Whereas bacteria treated with colistin or murepavadin alone replicated during incubation with the respective antibiotic agents, *P. aeruginosa* cells exposed to both drugs in combination were markedly killed, and the difference in the number of colonies at the 6 hour timepoint compared to the individual antimicrobial treatments was nearly 5-logs in magnitude.

As a control to ensure that the vast increase in bacterial killing with the colistin and murepavadin dual therapy was not due to the polymyxin compound improving the access of the LPS transport inhibitor by damaging the cellular OM, the time-kill experiment was repeated using the modified polymyxin nonapeptide molecule PMBN in place of colistin. Since PMBN possesses similar OM permeabilising properties as colistin but no bactericidal activity, combining the nonapeptide drug with murepavadin enabled the specific testing of whether disruption of the *P. aeruginosa* OM structure was sufficient to augment killing of PA14 cells through enhanced access of murepavadin to its LptD target<sup>847,848</sup>. It was found that combining PMBN, used at a concentration that was equimolar to 2  $\mu\text{g ml}^{-1}$  colistin, with murepavadin did not induce any reduction in the viability of *P. aeruginosa* bacteria whatsoever, with no drop in colony counts seen after 8 hours (**Figure 6.4B**). Therefore, the profound bactericidal phenotype of the colistin and murepavadin treatment condition could not be explained by increased access of the LptD antagonist to its target protein.

As a final authentication of murepavadin's ability to sensitise *P. aeruginosa* to colistin, the classically-established method of analysing possible synergistic interactions between two drugs was performed – the checkerboard broth microdilution assay<sup>625</sup>. This revealed that the MIC of colistin and murepavadin individually against PA14 cells was 1  $\mu\text{g ml}^{-1}$  and 0.8  $\mu\text{g ml}^{-1}$  respectively, but with the antibiotic agents in combination, bacterial growth was fully inhibited at a colistin concentration of 0.125  $\mu\text{g ml}^{-1}$  and a murepavadin concentration of 0.2  $\mu\text{g ml}^{-1}$  (**Figure 6.4C**). These changes in susceptibility of *P. aeruginosa* bacteria exposed to both the polymyxin drug and the LPS transport inhibitor were represented by a fractional inhibitory concentration index (FICI) value of 0.375, which was indicative of “true synergy” between colistin and murepavadin. When this checkerboard experiment was replicated using PMBN instead of colistin, there was no significant change in the MICs of either the nonapeptide compound or murepavadin in combination relative to when the drugs were present alone, with an FICI value of 1 signifying an “indifferent” interaction between the antibacterial agents<sup>849</sup>. This supported the previous discovery that the mechanism of colistin and murepavadin synergy was not enhanced access of murepavadin to its membrane LptD target following polymyxin-mediated OM disruption. Rather, in the context of earlier data, these results imply that murepavadin potentiates the bactericidal action of colistin by accumulating CM LPS.

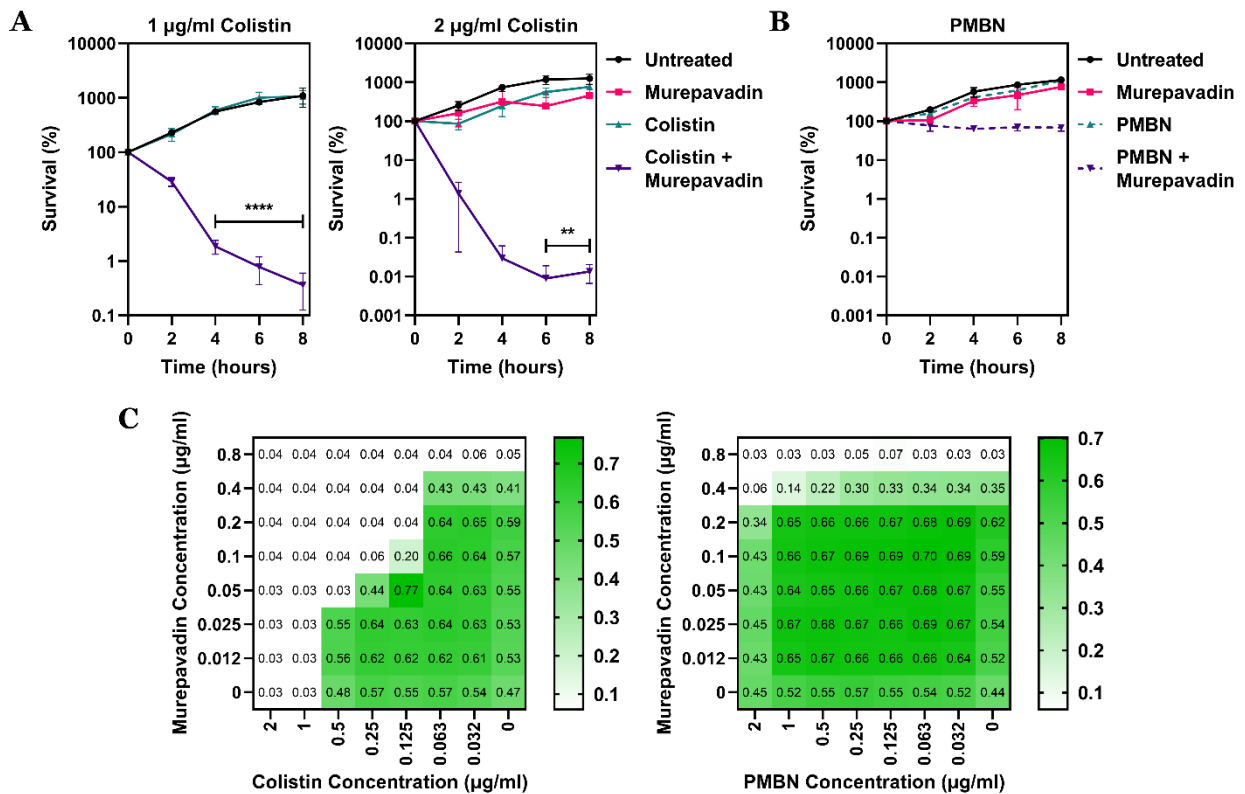


**Figure 6.4: Murepavadin enhances colistin-mediated killing of *P. aeruginosa*.** **A**, Survival of *P. aeruginosa* PA14 cells exposed, or not, to two colistin concentrations (1 µg ml<sup>-1</sup> and 2 µg ml<sup>-1</sup>), in each case either alone or in combination with murepavadin (0.05 µg ml<sup>-1</sup>), as determined by c.f.u. counts over 8 hours (n=4; \*\*p<0.01, \*\*\*\*p<0.0001 for colistin and murepavadin-exposed bacteria relative to bacteria exposed to colistin alone). **B**, Survival of *P. aeruginosa* PA14 cells exposed, or not, to PMBN (1.67 µg ml<sup>-1</sup> – equimolar to 2 µg ml<sup>-1</sup> colistin) alone/in combination with murepavadin (0.05 µg ml<sup>-1</sup>), as determined by c.f.u. counts over 8 hours (n=4). **C**, Checkerboard broth microdilution assays of colistin (left) or PMBN (right) in combination with murepavadin against *P. aeruginosa* PA14 cells, as determined by measuring bacterial growth after 18 hours incubation using OD<sub>595nm</sub> readings (n=4). Data in **A** were analysed by a two-way ANOVA with Dunnett’s post-hoc test. Data are presented as the arithmetic mean, and error bars represent the standard deviation of the mean.

## 6.6 The antibacterial potentiating effects of murepavadin are specific to colistin

Despite finding that the inhibition of LPS transport using murepavadin triggered a build-up of LPS in the CM of *P. aeruginosa*, and that the LptD antagonist enhanced colistin-mediated CM permeabilisation and the polymyxin’s overall bactericidal behaviour, it had yet to be firmly resolved that these two events were linked. Indeed, there remained a possibility that the accumulation of CM LPS induced by colistin may have altered the innermost bilayer’s biophysical properties in a way that made the bacterial membrane structure more susceptible to all manner of CM-damaging agents (including antimicrobial peptides), instead of augmenting colistin’s activity by providing a greater number of LPS molecules to target in the CM. In order to distinguish between these two divergent explanations, first measurements of

two key physical membrane characteristics that are widely known to influence sensitivity to bilayer disrupting stressors, fluidity and electrostatic charge, were made on PA14 spheroplasts that had been pre-exposed, or not, to murepavadin<sup>791–795</sup>. The consequences of treatment with the LPS transport inhibitor on membrane fluidity were examined with the fluorescent Laurdan dye used earlier as an indicator of bilayer rigidity<sup>642</sup>. This showed that the CM of *P. aeruginosa* spheroplasts that had been pre-incubated with murepavadin was significantly less rigid than the CM of previously untreated bacterial cells, with a decidedly lower Generalised Polarisation (GP) value evidencing that the membrane structure was more fluid and thus more disposed to water penetration (**Figure 6.5A**).

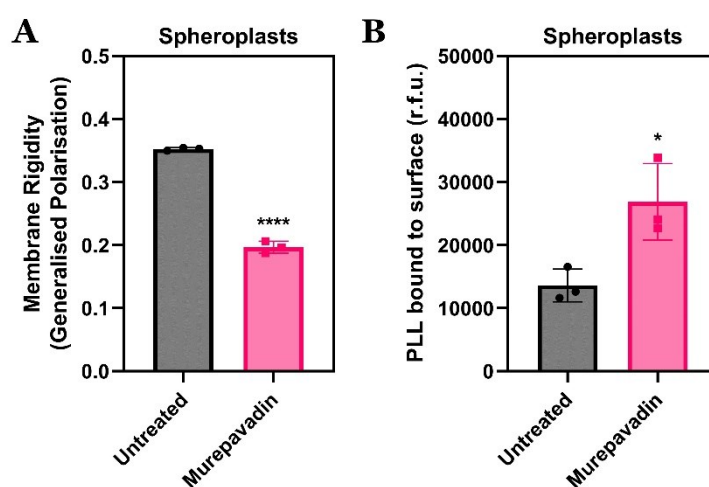


**Figure 6.5: Murepavadin exposure modulates the fluidity and electrostatic charge of the *P. aeruginosa* CM.** **A**, Rigidity of the CM of *P. aeruginosa* PA14 spheroplasts pre-treated, or not, with murepavadin ( $0.05 \mu\text{g ml}^{-1}$ ) for 2 hours prior to conversion into spheroplasts, as determined using the fluorescent Laurdan dye ( $100 \mu\text{M}$ ) to generate Generalised Polarisation values ( $n=3$  in triplicate; \*\*\*\* $p < 0.0001$  relative to untreated cells). **B**, Net negative charge of the CM of *P. aeruginosa* PA14 spheroplasts pre-treated, or not, with murepavadin ( $0.05 \mu\text{g ml}^{-1}$ ) for 2 hours prior to conversion into spheroplasts, as determined by measuring binding of highly cationic FITC-labelled Poly-L-Lysine (PLL,  $20 \mu\text{g ml}^{-1}$ ) to the cell surface ( $n=3$  in triplicate; \* $p < 0.05$  relative to untreated cells). Data in **A**, **B** were analysed by a two-tailed unpaired Student's *t*-test. Data are presented as the arithmetic mean, and error bars represent the standard deviation of the mean.

Investigating changes in the electrostatic charge of the CM following murepavadin exposure by analysing binding of fluorescent FITC-tagged cationic Poly-L-Lysine (PLL) to the spheroplast surface demonstrated a rise in attachment of FITC-PLL molecules to the *P. aeruginosa* CM when LPS transport was blocked (**Figure 6.5B**)<sup>643</sup>. This suggested that treatment of PA14 cells with murepavadin caused an increase in the net negative charge of the CM bilayer. That the LptD antagonist brought about these alterations in CM fluidity and electrostatic charge was not altogether surprising, considering that the antibacterial

compound functioned to accumulate LPS molecules in this innermost membrane structure. The lipid A domain of LPS (and in particular its phosphate groups) confers the polysaccharide with an anionic charge, and hence the increase in the anionicity of the CM of *P. aeruginosa* cells detected after murepavadin exposure was wholly in keeping with an increased abundance of CM LPS<sup>850,851</sup>. Likewise, the fact that CM rigidity was reduced in PA14 spheroplasts pre-treated with murepavadin could be the result of the greater number of LPS molecules present within the bilayer interfering with the typical packing of phospholipids, producing a more fluid membrane structure<sup>852</sup>. However, given that the LPS transport inhibitor was responsible for such large shifts in the bilayer's biophysical traits, it was absolutely imperative to understand how these contributed to the CM's susceptibility to stress-induced damage.

To do this, PA14 spheroplasts produced from cells that had either been treated to a sub-lethal murepavadin concentration ( $0.05 \mu\text{g ml}^{-1}$ ) or not before removal of the OM/cell wall were exposed to a range of different conditions designed to permeabilise the *P. aeruginosa* CM. These conditions included incubation with  $2 \mu\text{g ml}^{-1}$  colistin (used as a control against which comparisons could be made), incubation with the cationic antimicrobial peptides daptomycin and nisin (both added at  $20 \mu\text{g ml}^{-1}$ ), and incubation in purified, distilled water, where the lack of solutes was expected to prove fatal to the osmotically-fragile spheroplasts normally maintained in a 20% sucrose environment. In each case, the extent of CM disruption and lysis was assessed, using the fluorescent PI dye and  $\text{OD}_{600\text{nm}}$  readings respectively, in spheroplasts with basal CM LPS levels, as well as murepavadin-triggered elevated CM LPS levels, over a 15 hour time period. As observed previously, permeabilisation of the spheroplast CM by colistin was distinctly enhanced in murepavadin pre-treated *P. aeruginosa* cells relative to non-murepavadin treated cells, with the rate of uptake of the PI fluorophore substantially raised (**Figure 6.6A**). On the other hand, in PA14 spheroplasts exposed to daptomycin, nisin or distilled water, the intensity of the PI fluorescent signal throughout the 15 hour incubation was largely unaffected by whether or not the cell forms had undergone pre-treatment with murepavadin. This insinuated that although the blocking of LPS transport to accumulate CM LPS did make the membrane less rigid and more negatively-charged, these changes in CM biophysics were insufficient to make the innermost bilayer structure more prone to damage by all membrane-disrupting agents; in fact, murepavadin specifically potentiated only colistin-initiated CM disruption.

Lysis data acquired from  $\text{OD}_{600\text{nm}}$  measurements made over time further supported this notion. Whilst lysis of *P. aeruginosa* spheroplasts by colistin was augmented in cells that had been pre-exposed to murepavadin, with a more rapid and extensive drop in  $\text{OD}_{600\text{nm}}$  readings during the 15 hour antibiotic exposure, there was certainly no increase in the rate of lysis induced by daptomycin, nisin or distilled water in murepavadin-treated spheroplasts

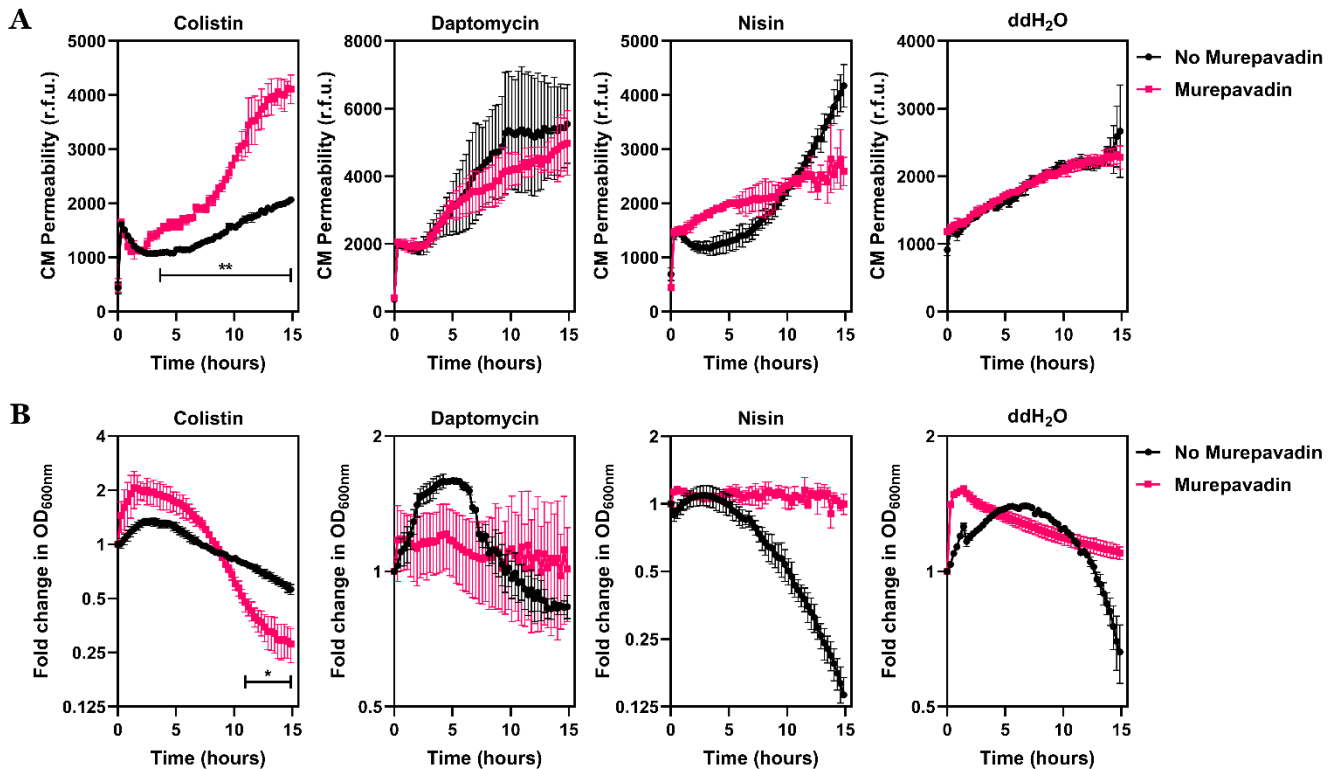


**Figure 6.6: Murepavadin specifically amplifies only the capacity of colistin to trigger CM damage and lysis in *P. aeruginosa* spheroplasts.** **A, B**, Permeabilisation of the CM (**A**) and lysis (**B**) of *P. aeruginosa* PA14 spheroplasts pre-treated, or not, with murepavadin ( $0.05 \mu\text{g ml}^{-1}$ ) for 2 hours prior to conversion into spheroplasts, during exposure to colistin ( $2 \mu\text{g ml}^{-1}$ ), daptomycin ( $20 \mu\text{g ml}^{-1}$  with  $1.25 \text{ mM Ca}^{2+}$  ions), nisin ( $20 \mu\text{g ml}^{-1}$ ), or distilled water ( $\text{ddH}_2\text{O}$ ), as determined by measuring fluorescence from PI ( $0.25 \mu\text{M}$ ) and  $\text{OD}_{600\text{nm}}$  respectively over 15 hours ( $n=3$ , assay performed on 3 independent occasions;  $*p<0.05$ ,  $**p<0.01$  for spheroplasts pre-treated with murepavadin relative to previously untreated spheroplasts). Data in **A, B** were analysed by a two-way ANOVA with Sidak's post-hoc test. Data are presented as the arithmetic mean, and error bars represent the standard deviation of the mean.

compared to those that had been previously untreated (**Figure 6.6B**). Remarkably, it actually appeared that the ability of any of these three stress factors to lyse PA14 spheroplasts was completely abolished when LPS molecules were allowed to build-up in the CM through the inhibition of LPS transport, with no real decrease in  $\text{OD}_{600\text{nm}}$  readings seen in spheroplast populations pre-exposed to murepavadin before incubation with daptomycin, nisin or distilled water. This unexpected result hinted for the first time that there may be a structural role to LPS being present in the CM that was analogous to the polysaccharide's function at the OM of bacteria – preventing membrane permeabilisation and a loss of cell integrity under otherwise membranolytic conditions<sup>389,853</sup>. That this protective effect of elevated CM LPS levels was not applicable to colistin offered conclusive validation of not only the polymyxin's mode of targeting LPS in the Gram-negative CM to kill bacteria, but also the molecular mechanism that murepavadin amplified colistin's bactericidal activity by presenting an increased number of CM LPS molecules to which the antibiotic could bind.

## 6.7 Murepavadin enhances colistin's activity against diverse clinical *P. aeruginosa* isolates

Experiments undertaken so far that uncovered the phenotype and mechanism by which inhibiting LPS transport with murepavadin triggered an accumulation of LPS in the CM and consequently augmented colistin's ability to kill bacteria had all been performed in the laboratory reference type strain of *P. aeruginosa*, PA14. In order to understand the wider implications of this discovery, particularly in terms of whether colistin and murepavadin combination therapy could potentially be of relevance in the clinical setting, it was crucial to investigate if the LptD antagonist also potentiated the polymyxin antibiotic against a wider panel of *P. aeruginosa* strains that had been isolated from infected human patients. Three multi-drug resistant *P. aeruginosa* isolates, representative of the type of strains for which colistin would be prescribed as a last-resort treatment option, were utilised for this analysis.

To identify a sub-lethal concentration of murepavadin to which these three strains of *P. aeruginosa* could be exposed for blocking the essential LPS transport process without any significant growth inhibitory effects, OD<sub>600nm</sub> measurements were obtained during 20 hours incubation of the isolates alongside the LptD inhibitor. It was identified that treatment of the clinical strains with 0.05 µg ml<sup>-1</sup> murepavadin (the same concentration used in assays with PA14 cells) caused at most a minor reduction in the bacterial growth rate, and in the case of the *P. aeruginosa* MS isolate, no impact on the rate of cell replication at all (**Figure 6.7A**). Hence, it was deduced that this was a suitable sub-lethal dose of the LPS transport antagonist that could be incorporated into ensuing experiments in combination with colistin. The first of these experiments explored the polymyxin's capacity to permeabilise the CM structure of the three clinical isolates, either independently or as a dual therapy with murepavadin, by means of the DNA-reactive fluorescent PI dye. In each case, exposure to colistin alone induced a minor increase in uptake of PI into the bacterial cytoplasm after 1 hour of polymyxin treatment, indicating that the polypeptide antibiotic was at least partially damaging the CM of the *P. aeruginosa* strains (**Figure 6.7B**). However, the intensity of the PI fluorescent signal was both significantly greater in magnitude, and notably more sustained over the 4 hour assay, when murepavadin was present along with colistin during treatment of all three isolates. It was therefore inferred that the LptD inhibitor enhanced colistin's membranolytic properties against the CM not only in *P. aeruginosa* PA14, but also in an assorted range of *P. aeruginosa* clinical strains.

Next, to extend these findings regarding amplified CM disruption initiated by colistin in combination with murepavadin to cell viability, both bacterial lysis and killing of the three *P. aeruginosa* isolates were assessed during 8 hours exposure to polymyxin monotherapy, or the dual colistin-murepavadin treatment. With the clinical strain *P. aeruginosa* SCT, readings

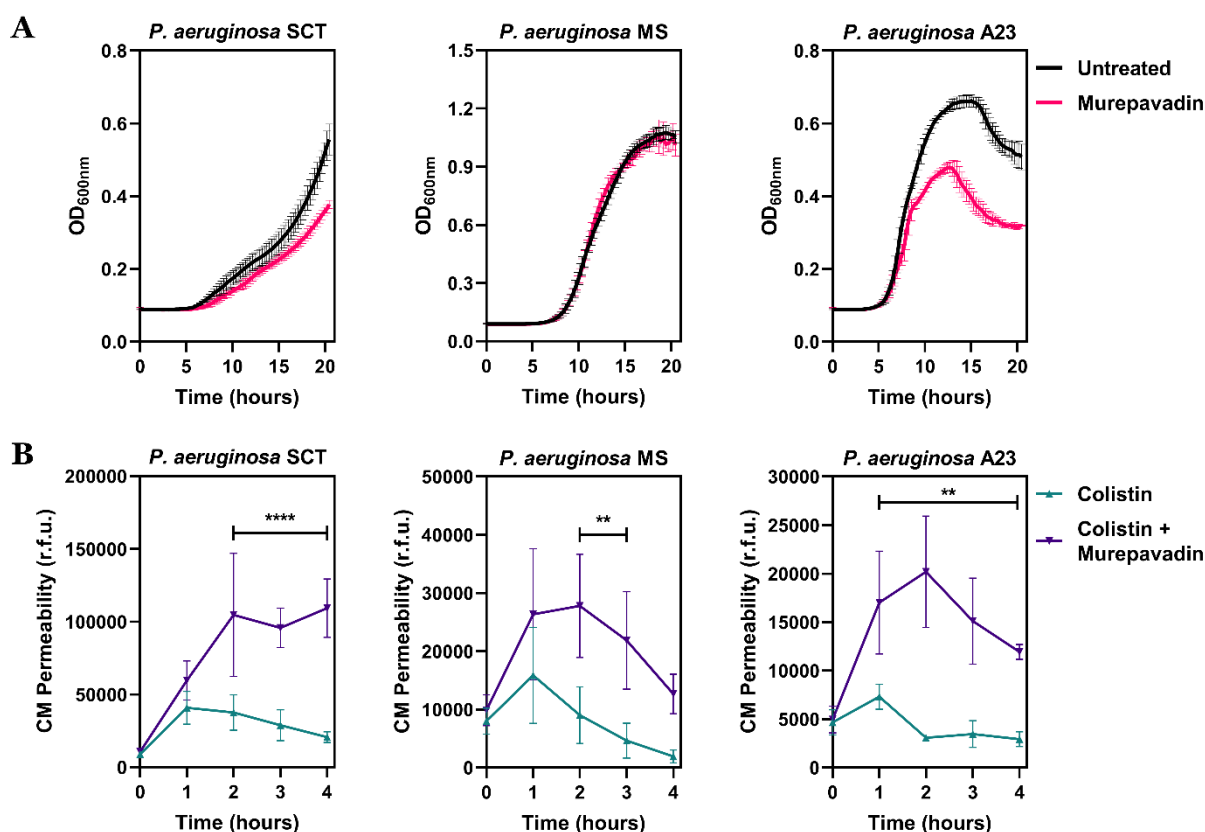


**Figure 6.7: Sub-lethal murepavadin concentrations potentiate CM disruption induced by colistin in clinical strains of *P. aeruginosa*.** **A**, Growth kinetics of 3 *P. aeruginosa* clinical isolates (SCT, MS and A23) during exposure, or not, to murepavadin ( $0.05 \mu\text{g ml}^{-1}$ ), as determined by measuring  $\text{OD}_{600\text{nm}}$  over 20 hours incubation ( $n=3$ ). **B**, Permeabilisation of the CM of 3 *P. aeruginosa* clinical isolates during exposure to colistin (used at  $1 \mu\text{g ml}^{-1}$  for strains SCT/MS and  $2 \mu\text{g ml}^{-1}$  for strain A23), either alone or in combination with murepavadin ( $0.05 \mu\text{g ml}^{-1}$ ), as determined by measuring fluorescence from PI ( $2.5 \mu\text{M}$ ) over 4 hours ( $n=4$ ;  $**p<0.01$ ,  $****p<0.0001$  for colistin and murepavadin-exposed bacteria relative to bacteria exposed to colistin alone). Data in **B** were analysed by a two-way ANOVA with Sidak's post-hoc test. Data are presented as the arithmetic mean, and error bars represent the standard deviation of the mean.

of  $\text{OD}_{595\text{nm}}$  increased over time in the cell population incubated only with colistin (suggestive of bacterial growth), but decreased between two and four-fold by 8 hours relative to the start of the assay in the population treated with colistin along with the LPS transport antagonist, signifying that the bacteria were lysing (**Figure 6.8A**). In terms of the *P. aeruginosa* isolates MS and A23, whilst the same rapid decrease in  $\text{OD}_{595\text{nm}}$  measurements was not observed for the dual polymyxin and murepavadin therapy, these readings of  $\text{OD}_{595\text{nm}}$  were nevertheless significantly lower than in bacteria exposed to colistin alone, confirming the more potent antibacterial activity of the combination treatment.

This phenotype became most apparent when analysing cell killing by colony counts. All three clinical *P. aeruginosa* strains exhibited almost no cell death when incubated only with colistin, with the number of viable cells in the population after 8 hours equalling, or even



exceeding, the number at the experiment's start (**Figure 6.8B**). Contrastingly, these same bacteria exposed to both colistin and murepavadin were abundantly killed, with a drop in colony counts of more than 90% in the strains MS/A23, and a 4-log reduction in the isolate SCT following 8 hours of antibiotic treatment. In summary, murepavadin was able to potentiate all aspects of the bactericidal behaviour of colistin against varied *P. aeruginosa* strains isolated from human patients, highlighting that it may have a novel feasible role as a polymyxin adjuvant for the treatment of infections in the clinic.

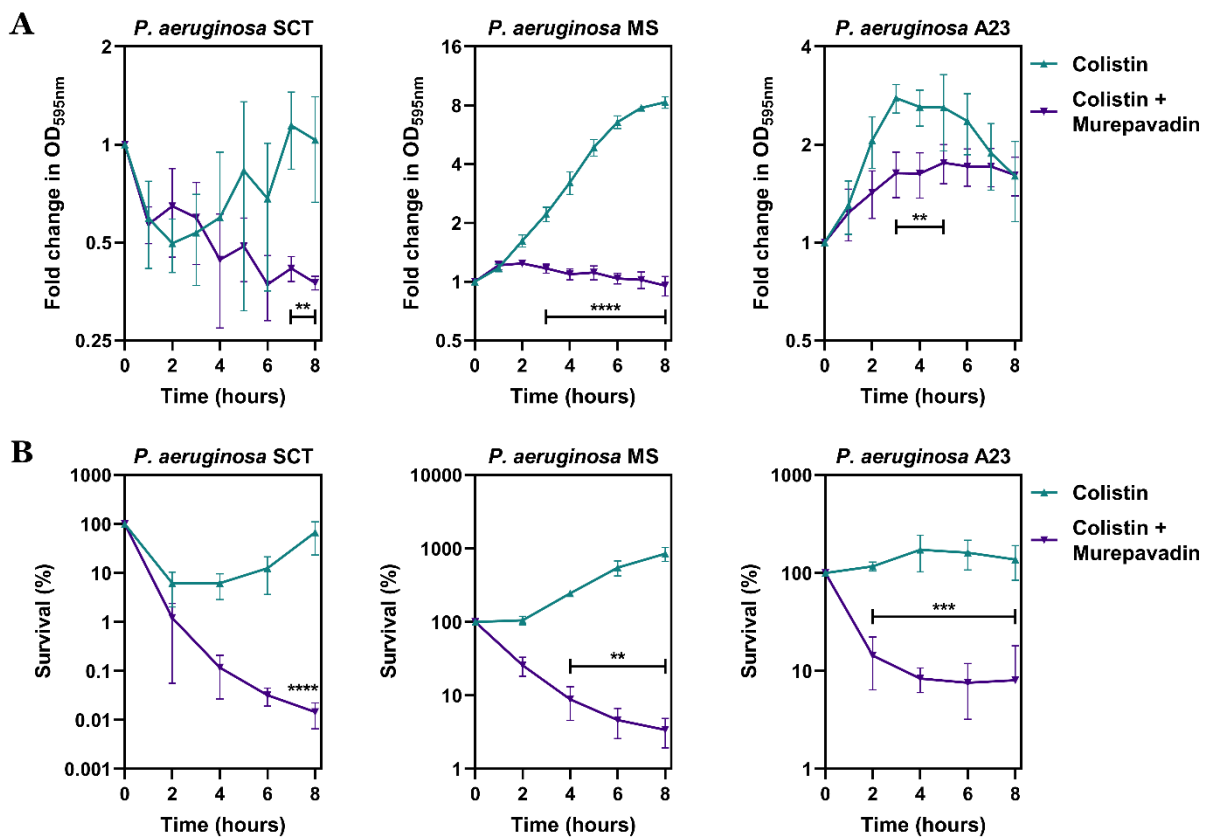


**Figure 6.8: Murepavadin enhances colistin-mediated bacterial lysis and killing against *P. aeruginosa* clinical isolates.** **A**, Lysis/growth of 3 *P. aeruginosa* clinical isolates during exposure to colistin (used at 1  $\mu\text{g ml}^{-1}$  for strains SCT/MS and 2  $\mu\text{g ml}^{-1}$  for strain A23), either alone or in combination with murepavadin (0.05  $\mu\text{g ml}^{-1}$ ), as determined by measuring OD<sub>595nm</sub> over 8 hours (n=4; \*\*p<0.01, \*\*\*\*p<0.0001 for colistin and murepavadin-exposed bacteria relative to bacteria exposed to colistin alone). **B**, Survival of 3 *P. aeruginosa* clinical isolates during exposure to colistin (used at 1  $\mu\text{g ml}^{-1}$  for strains SCT/MS and 2  $\mu\text{g ml}^{-1}$  for strain A23), either alone or in combination with murepavadin (0.05  $\mu\text{g ml}^{-1}$ ), as determined by c.f.u. counts over 8 hours (n=4; \*\*p<0.01, \*\*\*p<0.001, \*\*\*\*p<0.0001 for colistin and murepavadin-exposed bacteria relative to bacteria exposed to colistin alone). Data in **A**, **B** were analysed by a two-way ANOVA with Sidak's post-hoc test. Data are presented as the arithmetic mean, and error bars represent the standard deviation of the mean.

## 6.8 Colistin and murepavadin combination therapy promotes bacterial killing against CF isolates and *in vivo*

Murepavadin is in pre-clinical development as a novel aerosolised antimicrobial agent specifically for the treatment of *P. aeruginosa* infections in cystic fibrosis (CF) patients<sup>260</sup>. Colistin is already frequently prescribed to individuals with CF suffering with exacerbations caused by Gram-negative bacterial pathogens, where a nebulised form of the polymyxin drug is delivered via the inhalatory route directly into the lungs of patients. Given that these two compounds were both strongly associated with CF therapy, to further study whether synergy between colistin and murepavadin was a phenomenon that was applicable in clinical settings, it was critical to test if the LPS transport inhibitor enhanced the bactericidal activity of colistin against *P. aeruginosa* strains isolated directly from sputum samples of patients with CF<sup>316,854,855</sup>. Thus, a panel consisting of 15 multi-drug resistant CF isolates of *P. aeruginosa* was assembled, and exposed for 8 hours to either colistin alone (used at a therapeutically-relevant concentration of 2 µg ml<sup>-1</sup>), or colistin in combination with a sub-inhibitory dose of murepavadin (0.5x MIC), before cell survival was computed by counting viable colonies.

In most cases, incubation with colistin alone produced minimal killing of the bacterial isolates – out of the 15 *P. aeruginosa* strains, 12 displayed less than a 1-log reduction in viable cell counts even after 8 hours of antibiotic treatment, making evident the ineffectiveness of polymyxin monotherapy (**Figure 6.9A**). However, the addition of a sub-lethal murepavadin concentration had a marked and pronounced effect on increasing death of the CF isolates. This amplification of bacterial killing with the colistin-murepavadin combination therapy was vast, ranging from a 2/3-log increase in cell death with strains AK10, AK6, AK8 and AK17, to more than 4-logs in isolates AK14, AK5 and AK22, relative to polymyxin treatment alone. Amongst the 15 CF strains examined, the augmentation in colistin's bactericidal impact in the presence of the LptD antagonist was statistically significant in 12 of the *P. aeruginosa* isolates (80%). Indeed, the only strain in which no additional cell killing was observed following the dual combination treatment (isolate AK19), was found to be resistant to murepavadin. The fact, then, that the LPS transport inhibitor was unable to potentiate polymyxin activity against this non-susceptible strain AK19 served as an important control that the ability of murepavadin to amplify colistin-induced killing in these CF isolates was not due to off-target effects.

Having demonstrated that the colistin and murepavadin synergised potently against strains of *P. aeruginosa* isolated from the sputum of individuals with CF, in order to more comprehensively characterise if this combination of antibiotics could be a useful treatment option for CF lung infections, an *in vivo* murine model of a respiratory tract *P. aeruginosa* infection was employed<sup>646</sup>. Mice were inoculated via the intranasal route with a high density of PA14 cells (10<sup>7</sup> c.f.u.) to ensure that bacterial colonisation was restricted to the lungs, and

this infection was permitted to establish for 5 hours. Subsequently, mice were treated – again, intranasally – with phosphate-buffered saline (PBS) alone as the negative control, or PBS containing only colistin (5 mg kg<sup>-1</sup>), only murepavadin (0.25 mg kg<sup>-1</sup>), or both antimicrobial compounds combined at the same concentrations used for monotherapy. These drug doses were chosen based closely on those used in the treatment of human lung infections, and also corresponded to concentrations of the drugs that were previously utilised for *in vitro* assays<sup>261,856</sup>. After 3 hours of the relevant antibiotic therapies, mice were sacrificed humanely, before the bacterial load in the lungs was enumerated by viable colony counts. In mice treated with either murepavadin alone or colistin alone, there was no significant reduction in the number of *P. aeruginosa* cells present in the lungs relative to either the start of the experiment, or to PBS-treated control mice (**Figure 6.9B**). In striking opposition, the bacterial burden in the lungs of mice that had undergone the dual colistin-murepavadin therapy was distinctly lower than the individual treatment conditions, with a 2 to 3-log reduction in colony counts compared to the untreated negative control population. Together, these results proved that the synergy between colistin and murepavadin was maintained against isolates from CF patients and *in vivo*, indicating that this new combination treatment strategy may have great clinical potential against *P. aeruginosa* CF lung infections.

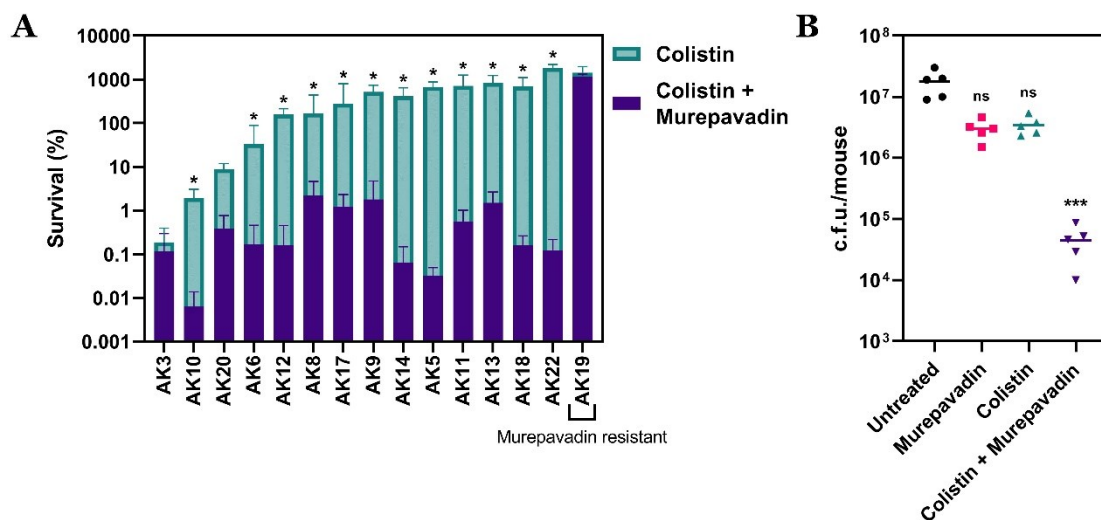


**Figure 6.9: Colistin and murepavadin are synergistic *in vitro* against CF *P. aeruginosa* strains and in an *in vivo* murine lung infection model.** **A**, Survival of 15 *P. aeruginosa* clinical strains isolated from the sputum of CF patients during exposure to colistin (2 µg ml<sup>-1</sup>) alone, or colistin in combination with a sub-lethal concentration of murepavadin (0.4 µg ml<sup>-1</sup> for strains AK3, AK12, AK14 and AK22; 0.8 µg ml<sup>-1</sup> for strains AK5, AK6, AK8, AK9, AK10, AK11, AK13, AK17, AK18 and AK20; 3.2 µg ml<sup>-1</sup> for strain AK19), as determined by c.f.u. counts after 8 hours (n=4; \*p<0.05 for colistin and murepavadin-exposed bacteria relative to cells exposed to colistin alone). **B**, Burden of *P. aeruginosa* PA14 cells in the murine lungs after 3 hours treatment with PBS (untreated control), murepavadin (0.25 mg kg<sup>-1</sup>), colistin (5 mg kg<sup>-1</sup>), or both antibiotics in combination, as determined by c.f.u. counts (n=5 per treatment group, each data points represents a single mouse; ns: p>0.05, \*\*\*p<0.001 relative to mice that were treated only with PBS). Data in **A** were analysed by multiple Mann-Whitney tests. Data in **B** were analysed by a Kruskal-Wallis test with Dunn’s post-hoc correction. Data are presented as the arithmetic mean, and error bars shown represent the standard deviation of the mean.

## 6.9 Colistin and murepavadin synergise against CF isolates of *P. aeruginosa* that are polymyxin-resistant

Preliminary data from the previous chapter had identified that acquired resistance to colistin was associated with a growth cost and a competitive disadvantage, with one hypothesis to explain this finding being that Gram-negative bacteria may not be able to transport LPS that is cationically-modified as efficiently from its CM bilayer to the OM surface as unmodified LPS. Crucially, this postulation was supported substantially by the conclusion from lipidomic analyses that the ratio of modified:unmodified lipid A structures in the cellular CM is much higher than the ratio in the OM bilayer. Key data presented in this chapter has resolved that in *P. aeruginosa* strains exposed to murepavadin to block LPS transport from the CM to the OM, there was a resultant accumulation of LPS structures within the bacterial CM which rendered the cells drastically more susceptible to colistin-induced lysis and death. Combining these discoveries, it was proposed that treatment of colistin-resistant isolates of *P. aeruginosa* with murepavadin would still trigger a build-up of LPS molecules in the CM, and if the lipid A-modifying enzymes that alter the electrostatic charge of LPS were unable to cationically-modify all this CM LPS (due to the associated fitness cost), then murepavadin exposure could even cause an accumulation of unmodified LPS in the CM. If this were true, it was considered that treatment with murepavadin of polymyxin non-susceptible *P. aeruginosa* cells may re-sensitise these otherwise resistant bacteria to colistin, because the polymyxin antibiotic would have a greater number of unmodified CM LPS structures to target.

To test this, three colistin-resistant clinical *P. aeruginosa* strains isolated from the sputum of CF patients were obtained, exposed to the polymyxin drug alone, murepavadin alone, or both compounds in combination, and then subjected to a panel of assays to track the impact of the LptD inhibitor on various distinct stages of colistin's bactericidal mechanism of action. Starting with disruption of the OM bilayer – quantified by means of the phospholipid-reactive NPN dye – it was found that in all three CF isolates, treatment with colistin only (4  $\mu\text{g ml}^{-1}$ ) resulted in an increase in the fluorescent NPN signal, in line with the earlier identification that the polymyxin drug maintained its capacity to damage the OM of chromosomally colistin-resistant bacteria (**Figure 6.10A**). Exposure only to murepavadin on the other hand had no effect on OM permeabilisation of the *P. aeruginosa* cells, and in all cases, the addition of the LPS transport antagonist alongside colistin did not significantly change the extent of NPN uptake into the clinical strains. This revealed that murepavadin did not potentiate the OM-disrupting activity of colistin against polymyxin non-susceptible *P. aeruginosa* isolates.

In contrast, measuring colistin-initiated CM disruption with the DNA-reactive PI fluorophore produced a more noteworthy phenotype. While the CM of bacteria treated with either colistin or murepavadin independently remained largely intact, with no major rise in PI

fluorescence relative to the untreated conditions, cells of the three clinical CF strains exposed to the colistin-murepavadin combination therapy had a much higher degree of CM damage, and PI uptake was more than three-fold greater in every instance by the end of the experiment (**Figure 6.10B**). That permeabilisation of the CM of these colistin-resistant *P. aeruginosa* strains was enhanced in the presence of murepavadin was in keeping with the hypothesis that the LptD antagonist may be inducing a build-up of unmodified LPS structures within the CM, proffering the polymyxin antimicrobial with an augmented number of lipid A domains to which it could bind.

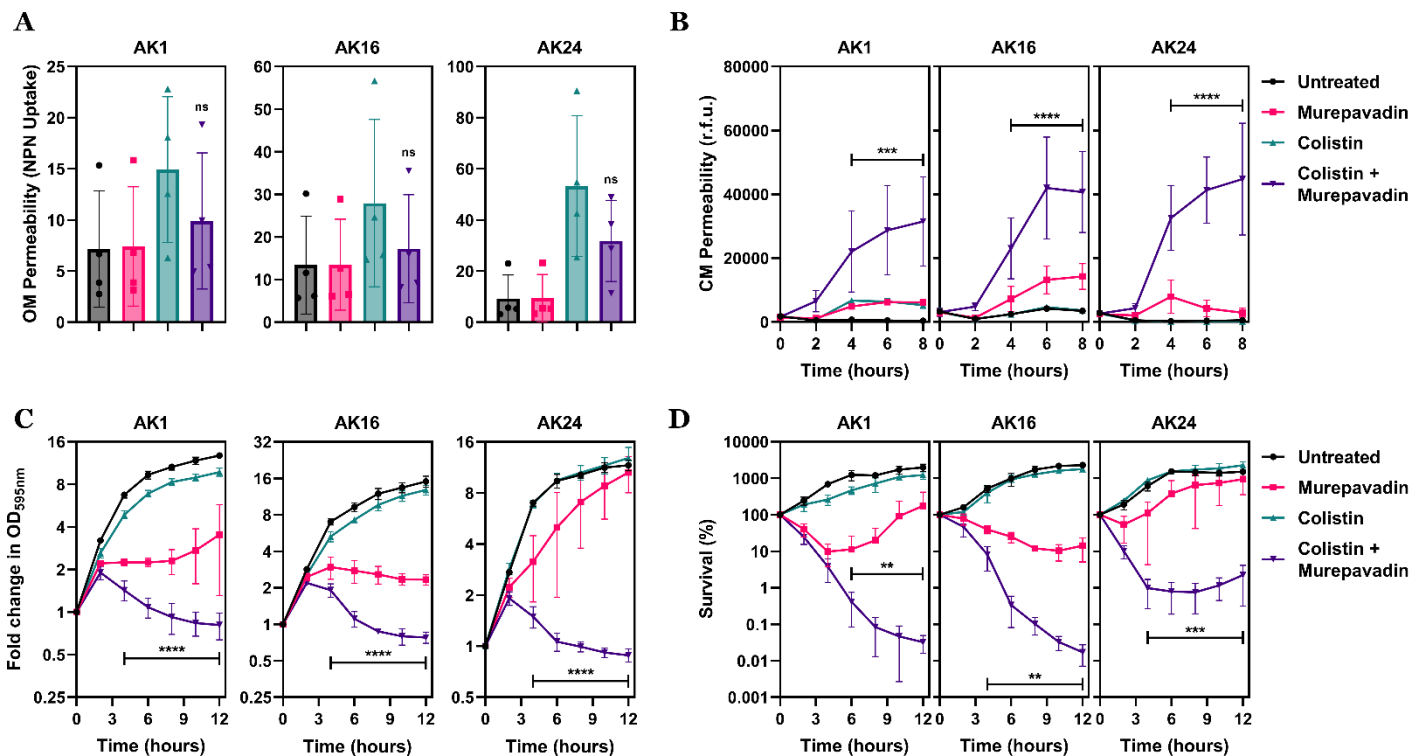


**Figure 6.10: The addition of murepavadin augments colistin-induced CM damage, lysis and killing of polymyxin-resistant *P. aeruginosa* CF isolates.** **A**, Permeabilisation of the OM of 3 chromosomally polymyxin non-susceptible clinical *P. aeruginosa* CF strains (isolates AK1, AK16 and AK24) by colistin alone ( $4 \mu\text{g ml}^{-1}$ ), murepavadin alone ( $3.2 \mu\text{g ml}^{-1}$  for strain AK1,  $6.4 \mu\text{g ml}^{-1}$  for strain AK16, and  $1.6 \mu\text{g ml}^{-1}$  for strain AK24), or both drugs in combination), as determined by measuring uptake of the NPN fluorophore ( $10 \mu\text{M}$ ) over 10 minutes ( $n=4$ , each data point represents the arithmetic mean of 20 replicate measurements; ns:  $p>0.05$  relative to bacteria exposed to colistin alone). **B**, Permeabilisation of the CM of 3 polymyxin-resistant *P. aeruginosa* CF isolates by colistin alone, murepavadin alone, or both drugs in combination, determined by measuring fluorescence from PI ( $2.5 \mu\text{M}$ ) over 8 hours ( $n=4$ ;  $***p<0.001$ ,  $****p<0.0001$  for colistin and murepavadin-exposed bacteria relative to bacteria exposed to colistin alone). **C**, Lysis/growth of 3 polymyxin-resistant *P. aeruginosa* CF isolates by colistin alone, murepavadin alone, or both drugs in combination, determined by measuring  $\text{OD}_{595\text{nm}}$  over 12 hours ( $n=4$ ;  $****p<0.0001$  for colistin and murepavadin-exposed bacteria relative to bacteria exposed to colistin alone). **D**, Survival of 3 polymyxin-resistant *P. aeruginosa* CF isolates by colistin alone, murepavadin alone, or both drugs in combination, determined by c.f.u. counts over 12 hours ( $n=4$ ;  $**p<0.01$ ,  $***p<0.001$ , for colistin and murepavadin-exposed bacteria relative to bacteria exposed to colistin alone). Data in **A** were analysed by a one-way ANOVA with Dunnett's post-hoc test. Data in **B-D** were analysed by a two-way ANOVA with Dunnett's post-hoc test. Data are presented as the arithmetic mean, and error bars shown represent the standard deviation of the mean.

When assessing bacterial lysis through readings of OD<sub>595nm</sub> over 12 hours antibiotic treatment, a rise in OD<sub>595nm</sub> measurements was observed with all three CF isolates during incubation with either colistin or murepavadin alone, implying that the *P. aeruginosa* cells were replicating irrespective of exposure to the drugs (**Figure 6.10C**). Only when the two agents were added in combination was a reduction in OD<sub>595nm</sub> readings seen over time in each strain, which showed that the dual colistin-murepavadin therapy was causing the cells to lyse. These data were of vital importance, since murepavadin has been reported in past studies to have a non-lytic mode of action<sup>257</sup>. Hence, the fact the LPS transport inhibitor and colistin were able to trigger lysis of *P. aeruginosa* in combination firmly suggested it was murepavadin that was amplifying the antibacterial behaviour of the polymyxin compound, and not the other way around. Perhaps the most prominent consequence of the combined colistin and murepavadin treatment condition was detected when investigating viability of the polymyxin-resistant CF *P. aeruginosa* isolates through colony counts. Across the three clinical strains, in isolation neither colistin nor murepavadin exposure had any remarkable influence on killing bacteria, with the number of living cells by the end of the 12 hour experiment reduced by less than 1-log compared to the starting inoculum (**Figure 6.10D**). However, *P. aeruginosa* cells of all three isolates treated with both antibiotics together were quickly and extensively killed, with viable colony counts lowered by more than 3-logs relative to bacteria exposed to murepavadin alone. It was therefore inferred that colistin and the LptD inhibitor synergised even against clinical CF strains that were polymyxin non-susceptible.

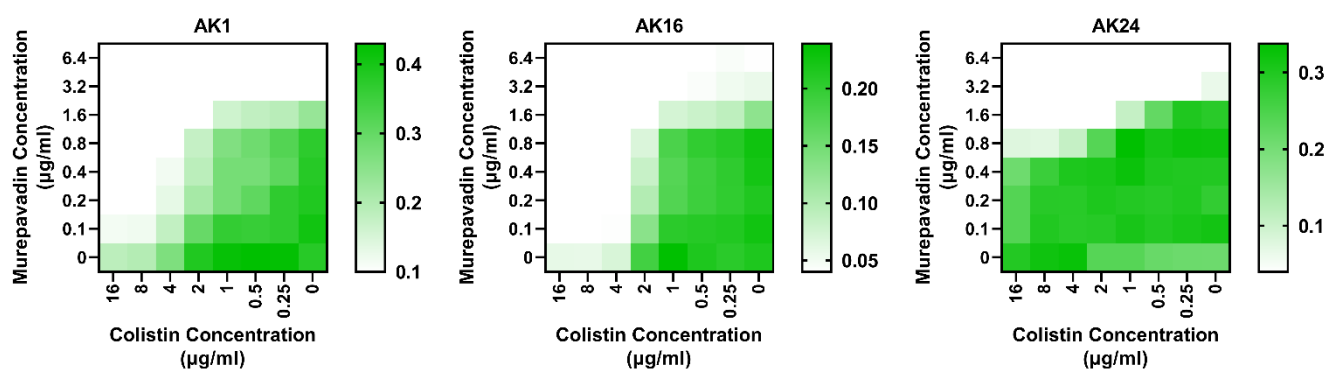


**Figure 6.11: Murepavadin synergises potently with colistin against polymyxin-resistant *P. aeruginosa* clinical CF strains.** Checkerboard broth microdilution assays of colistin alongside murepavadin against cells of 3 chromosomally polymyxin non-susceptible clinical *P. aeruginosa* CF strains (isolates AK1, AK16 and AK24), as determined by measuring bacterial growth after 18 hours incubation using OD<sub>595nm</sub> readings (n=3; a more intense green colour indicates a higher OD<sub>595nm</sub> value and more dense bacterial growth),

As a final validation of the additive nature of these two antimicrobial compounds in combination, checkerboard broth microdilution assays were performed on the clinically-isolated, colistin-resistant *P. aeruginosa* isolates to compare the MICs of the drugs in combination to their MICs when utilised alone. This demonstrated that in every case, the concentration of colistin and murepavadin that could fully inhibit bacterial growth was substantially lower when both antibiotics were present, compared to when they were tested individually, with FICI values of 0.375, 0.5 and 0.3125 for strains AK1, AK16 and AK24 respectively (**Figure 6.11**). It was thereby authenticated that murepavadin re-sensitised polymyxin-resistant *P. aeruginosa* strains to colistin, and although the precise molecular mechanism of this phenotype is yet to be entirely solved (for example, via lipidomic studies), this result served to emphasise the power, applicability and wide clinical scope of this novel combinatory therapeutic option.

### **6.10 Colistin synergises with rifampicin against Gram-negative bacteria with acquired polymyxin resistance**

The LPS monolayer in the extracellular-facing outermost bilayer of the OM of Gram-negative organisms poses a major permeability barrier to small, hydrophobic antibiotics (such as isoniazid, ethambutol and rifampicin) with cytoplasmic targets, and therefore the vast majority of such Gram-negative pathogens are inherently resistant to these antimicrobial agents<sup>247,857</sup>. Work conducted in the previous chapter had uncovered that resistance to colistin in *E. coli* and *P. aeruginosa*, acquired either through carriage of the mobilised *mcr* genes or via chromosomal mutations, was conferred by the presence of modified LPS at the bacteria's CM, and that the polymyxin drug retained its ability to permeabilise the cellular OM. It was postulated that, because exposure of pathogens with acquired polymyxin non-susceptibility to colistin induced OM disruption, this damage to the outermost bacterial bilayer could, in turn, promote the intracellular access of a hydrophobic antibiotic (e.g. rifampicin) that would not typically traverse an otherwise intact LPS monolayer<sup>858</sup>. If this were the case, it would be expected that colistin and rifampicin may exhibit synergy in combination even against colistin-resistant Gram-negative organisms where neither antibiotic in isolation would be effective.

In order to explore this proposal, the isogenic pair of *E. coli* MC1000 strains employed for earlier experiments – consisting of an isolate harbouring the polymyxin resistance gene *mcr-1* on a plasmid, and an isolate carrying only an empty plasmid control – were assayed through the gold-standard checkerboard broth microdilution technique for any additive effect of dual colistin and rifampicin therapy. With the pEmpty control *E. coli* cell population, the MIC of colistin was reduced from 1  $\mu\text{g ml}^{-1}$  in isolation to 0.5  $\mu\text{g ml}^{-1}$  in combination, and the

rifampicin MIC was lowered from 16  $\mu\text{g ml}^{-1}$  in isolation to 4  $\mu\text{g ml}^{-1}$  in combination, generating an FICI value of 0.75 (**Figure 6.12A**). This indicated that against colistin-susceptible bacteria, the polymyxin compound and rifampicin had an “additive” but not “synergistic” interaction – a phenotype that has been commonly observed and is likely linked to a greater number of rifampicin molecules being able to penetrate into the *E. coli* cytoplasm after colistin-mediated cell envelope damage<sup>859,860</sup>. More surprisingly, in the polymyxin-resistant, *mcr-1*-expressing MC1000 population, the MICs of colistin and rifampicin dropped from 8 and 16  $\mu\text{g ml}^{-1}$  respectively in isolation, to 1  $\mu\text{g ml}^{-1}$  and 0.25  $\mu\text{g ml}^{-1}$  respectively for both antibiotics in combination, representing an FICI value as low as 0.141 that revealed “true synergy” between the two antibiotics (**Figure 6.12B**). It was concluded that colistin and rifampicin treatment was a potent dual therapeutic option against *E. coli* cells harbouring the *mcr-1* resistance determinant, even though independently, the two antibacterial agents were wholly ineffectual.

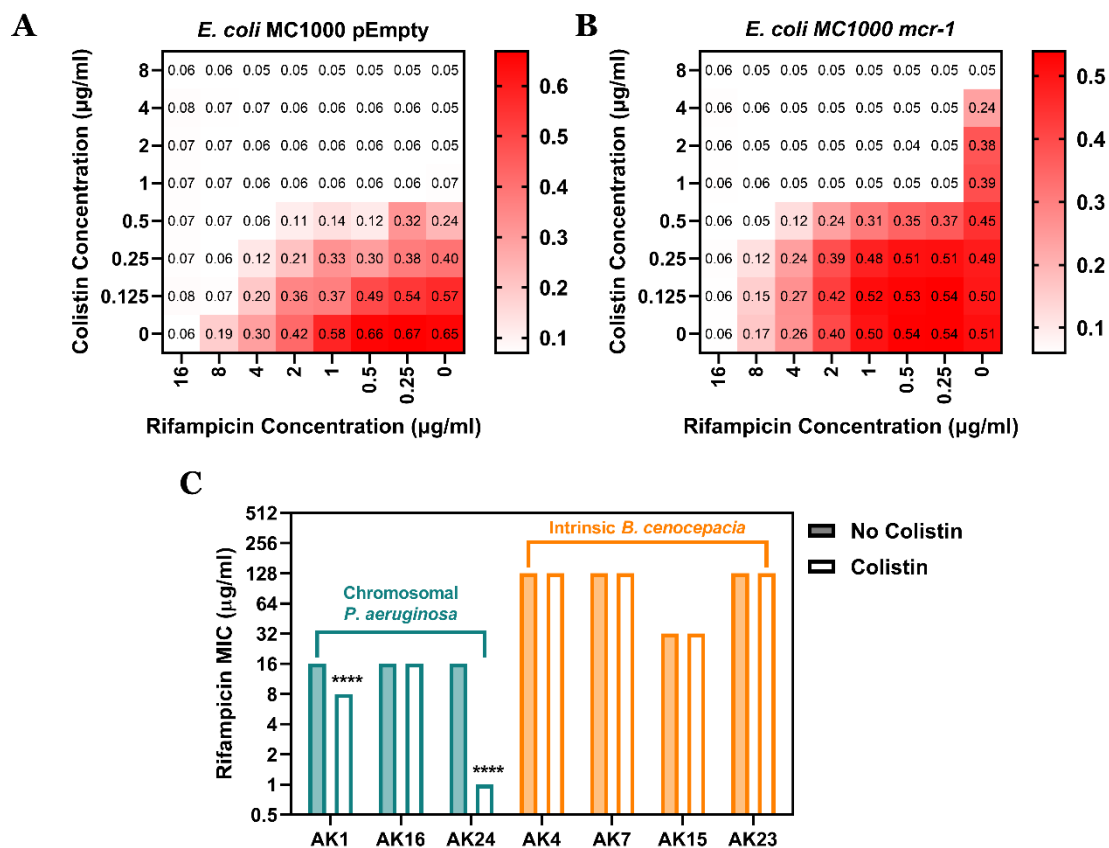


**Figure 6.12: Colistin and rifampicin synergise against *E. coli* and *P. aeruginosa* isolates with acquired polymyxin resistance.** **A, B**, Checkerboard broth microdilution assays of colistin in combination with rifampicin against **(A)** *E. coli* MC1000 cells harbouring an empty plasmid control (pEmpty), or **(B)** *E. coli* MC1000 cells expressing the *mcr-1* gene, as determined by measuring bacterial growth after 18 hours incubation using OD<sub>595nm</sub> readings (n=4). **C**, The MIC of rifampicin against a panel of colistin non-susceptible clinical CF isolates (3 chromosomally-resistant *P. aeruginosa* strains, 4 intrinsically-resistant *B. cenocepacia* strains), either alone or in the presence of a sub-inhibitory colistin concentration (1  $\mu\text{g ml}^{-1}$ ), as determined using the broth microdilution method (n=3, data are presented as the median value; \*\*\*\*p<0.0001 for colistin and rifampicin-exposed bacteria relative to bacteria exposed to colistin alone). Data in **C** were analysed by a two-way ANOVA with Sidak’s post-hoc test. Unless otherwise stated, data are presented as the arithmetic mean.



To expand this central finding to clinical isolates and colistin resistance acquired via chromosomal mutations, the three polymyxin non-susceptible strains of *P. aeruginosa* that had been obtained from the sputum of CF patients and used in past experiments were probed to understand if their sensitivity to rifampicin was modulated in the presence of colistin. For all the CF isolates, the MIC of rifampicin when colistin was absent was 16  $\mu\text{g ml}^{-1}$  – confirming that the *P. aeruginosa* strains were indeed resistant to the RNA synthesis inhibitor (**Figure 6.12C**). In spite of this, the addition of a sub-inhibitory colistin concentration (1  $\mu\text{g ml}^{-1}$ ) to the assay brought about a significant decrease in the rifampicin MIC for two out of the three clinical strains, down to 8  $\mu\text{g ml}^{-1}$  for isolate AK1 (2-fold drop), and down as far as 1  $\mu\text{g ml}^{-1}$  for isolate AK24 (16-fold drop). Thus, it appeared that against chromosomally polymyxin-resistant *P. aeruginosa*, with colistin still able to permeabilise the OM bilayer of these cells, synergy with hydrophobic rifampicin molecules was also apparent. As a control, this assay was carried out in a corresponding manner with four intrinsically colistin non-susceptible CF isolates of *B. cenocepacia*, where it had been proven that this inherent form of polymyxin resistance was mediated at the OM bacterial surface, which was impervious to colistin’s membrane-permeabilising properties. In every instance, the MIC of rifampicin against these *B. cenocepacia* strains was absolutely unchanged when combined with 1  $\mu\text{g ml}^{-1}$  colistin, with this data implicating colistin-initiated OM disruption in *P. aeruginosa*/*E. coli* cells that had acquired polymyxin resistance as the mechanism for the augmented antibacterial effects of the novel “colistin-rifampicin” dual treatment.

## 6.11 Discussion

Colistin is an essential “antibiotic of last-resort” in the fight against infections caused by multi-drug resistant Gram-negative pathogens, but unfortunately its efficacy is limited, with treatment failure a frequent occurrence and resistance rapidly emerging<sup>776,861,862</sup>. Nonetheless, because there is an extremely limited pipeline of new antimicrobial compounds in clinical development, it has become a global health priority to maintain colistin’s value as a “salvage therapy” option in the clinic<sup>863,864</sup>. Resultingly, there have been decades of research to identify antibacterial agents that can be combined with colistin to enhance the polymyxin’s potency and overcome treatment failure. These have, however, largely proved fruitless, and to date there are no colistin combination therapies that have been unambiguously demonstrated to have any clinical benefit, meaning that the search for novel polymyxin adjunctive agents is incomplete. In this chapter, taking inspiration from the previous discoveries regarding the mechanism of action of colistin and how polymyxin resistance is mediated, two combinatory approaches for increasing the effectiveness of the last-resort antibiotic were designed and characterised – namely, amplifying colistin activity using murepavadin to accumulate LPS in the CM, and overcoming polymyxin non-susceptibility by combining colistin with rifampicin.

The revelation that the LPS transport inhibitor murepavadin, in itself undergoing pre-clinical development as an antipseudomonal drug, potentiated the activity of colistin arose from *in vitro* experiments initially with the *P. aeruginosa* type strain PA14, which were then extended to general clinical isolates, clinical strains from the sputum of CF patients, and ultimately to a murine lung infection model<sup>257</sup>. By conducting assays across a diverse range of *P. aeruginosa* strains and *in vivo*, the clinical potential of the “colistin-murepavadin” dual therapy was made evident. Notably, the concentration of murepavadin utilised to amplify the bactericidal effects of colistin were, in all cases, sub-inhibitory, and additionally, the doses of the polymyxin antibiotic dramatically augmented by the LptD antagonist were at the lower end of the range of serum concentrations of colistin achievable in patients (1 – 2 µg ml<sup>-1</sup>)<sup>344</sup>. This was of particular import because both colistin and murepavadin have been found to possess significant toxic side-effects, especially in the kidneys of individuals exposed to these antimicrobials<sup>865–867</sup>. Indeed, the first Phase III clinical trial of intravenous murepavadin had to be terminated prematurely owing to a large incidence of nephrotoxicity in the treatment group of the study, and the LPS transport inhibitor is now being repurposed solely for aerosolised administration via the inhaled route against CF exacerbations.

The fact that a combination of sub-lethal colistin and murepavadin concentrations could together trigger substantial killing in isolates of *P. aeruginosa* is hence highly promising, as it raises the prospect of minimising the side-effects of the two compounds by administering patients with lower doses. Future *in vivo* mouse experiments should focus on whether combining colistin with murepavadin at reduced concentrations produces any further unexpected toxicity, and if these prove successful, studies could progress to the stage of small randomised controlled clinical trials. Colistin is already frequently prescribed and delivered in a nebulised form to treat individuals with CF suffering from *P. aeruginosa* infections, and with murepavadin in development for the identical pathology, the possibility of mixing both agents in a dual aerosolised formulation is one that is simultaneously intriguing and clinically valuable<sup>868</sup>. Moreover, it may also be the case that using lower concentrations of colistin and murepavadin may, as observed with other combination therapies, delay the emergence of resistance to either antibiotic due to a reduced selection pressure, though this is yet to be tested<sup>869,870</sup>.

Mechanistic detail into the molecular process by which murepavadin enhanced the antipseudomonal properties of colistin – through inhibiting LptD and the associated transport machinery to accumulate LPS molecules in the bacterial CM – was obtained chiefly via the measurement of CM LPS levels in murepavadin-exposed *P. aeruginosa* spheroplasts. These assays indicated that the amount of LPS present in the CM bilayer increased by approximately 25-30% after treatment with murepavadin. It may seem surprising that this perhaps moderate

rise in the abundance of LPS within the cellular CM could culminate in a comparatively vast augmentation of colistin's bactericidal effects, where it was seen that polymyxin-mediated killing of PA14 bacteria could be boosted by more than 5-logs in the presence of murepavadin. However, previous studies on synthetic membrane vesicles have highlighted that even minute modulations in the ratio of LPS to phospholipids in bilayer structures can hugely impact the susceptibility of membranes to colistin-induced permeabilisation<sup>745</sup>. That specifically altering CM LPS levels directly influenced the capacity of colistin to disrupt the *P. aeruginosa* CM and initiate cell lysis suggested that the polymyxin-LPS interaction in the CM, not the OM, is the critical and fundamental step in determining whether a Gram-negative cell is killed by colistin. This bolstered the conclusion from earlier chapters, generated by depleting or chemically-modifying CM LPS molecules, that the antibiotic action of polymyxins is dependent on the targeting of lipid A in the innermost bacterial bilayer.

Whilst the work presented here showed that the blocking of LPS transport with murepavadin led to a potentiation of colistin's antimicrobial tendencies, one key past report has described that exposing bacteria to novobiocin (and its analogs) in fact sensitises cells to colistin by stimulating the LptB ATPase enzyme that powers LPS transport<sup>255</sup>. Despite initially appearing contradictory to the data in this chapter, it is worth considering why this may not be the case. Firstly, the study on novobiocin performed experiments largely on the species *A. baumannii*, a pathogen that is unique amongst Gram-negative organisms in relation to its LPS biosynthesis/transport systems and can even tolerate a complete absence of LPS in its cell envelope. It is therefore conceivable that this synergistic nature of novobiocin for colistin activity may be exclusive to *A. baumannii* strains, and future work could examine how the two drugs interact against a wider panel of bacterial species. Likewise, subsequent investigations should assess whether blocking LPS transport in non-pseudomonal strains also leads to an accumulation of CM LPS, and enhanced killing by colistin, when such broader-spectrum inhibitors of the Lpt machinery are available.

The second reason that the novobiocin report is not necessarily conflicting with the results here is that bacteria have a number of systems that tightly regulate the abundance of LPS in the CM when it is too low, for example via the proteins FtsH/LapB/PbgA<sup>719,871,872</sup>. Thus, if the novobiocin-induced stimulation of LPS transport from the CM brought about a reduction in CM LPS levels, it is likely that cells may respond by actually increasing the amount of LPS present in the CM to match the elevated demand of the Lpt enzymes, offering a consistent explanation for the phenotype of amplified colistin activity. A study that found higher expression levels of the *lpxC* gene (the primary regulator of the LPS biosynthesis pathway) in novobiocin-treated *E. coli* cells provides preliminary support for this hypothesis, and future work should analyse precisely how novobiocin exposure affects the amount of CM LPS<sup>873</sup>.

A crucial control experiment enabled the clarification that it was murepavadin that potentiated colistin, and not colistin that was potentiating murepavadin, by disclosing the pre-treatment of *P. aeruginosa* spheroplasts with the LptD antagonist was sufficient to increase polymyxin-induced CM permeabilisation and lysis following subsequent colistin exposure. These set of assays additionally showed that murepavadin's ability to augment antibiotic activity was a colistin-specific phenomenon, with elevated levels of LPS in the CM bilayer having no consequences on membrane disruption triggered by daptomycin, nisin or osmotic stress. Surprisingly, rather, cell lysis was entirely abolished in PA14 spheroplasts exposed to these three non-polymyxin conditions. The mechanism as to why murepavadin treatment was associated with protection of *P. aeruginosa* from antimicrobial peptide/osmotic damage is as yet unclear, but relevantly, it was found that the accumulation of CM LPS post-murepavadin exposure caused an increase in membrane fluidity, which has been linked in a number of previous studies to reduced susceptibility to various membranolytic stressors<sup>874-876</sup>. These data open up fascinating questions about the function of LPS molecules in the bacterial CM. It is well-recognised that in the extracellular-facing, cell surface OM, the outermost LPS leaflet has a vital structural role, greatly contributing to membrane integrity under routine conditions, as well as mitigating the impact of cell envelope-damaging compounds<sup>853</sup>. Forthcoming experiments could seek to understand if the presence of LPS in the innermost CM bilayer shares similar functions, with the now obvious exception of colistin, for instance through biophysical/biomechanical experimentation.

Not only was the “colistin-murepavadin” combination therapy powerfully synergistic against susceptible *P. aeruginosa* strains, the dual treatment also exhibited a propensity for re-sensitising chromosomally colistin-resistant CF isolates of the species to the last-resort polymyxin drug. The basis for reversing polymyxin resistance by blocking LPS transport with murepavadin is postulated to be an accumulation of unmodified LPS structures in the bacterial CM, with the enzymes responsible for cationically-altering lipid A domains at the innermost membrane bilayer unable to keep up with the murepavadin-induced build-up of CM LPS. The imperative next step in comprehending the nature of the interaction between colistin and murepavadin in polymyxin non-susceptible *P. aeruginosa* will be to undertake MALDI-TOF mass spectrometry-based lipidomic analyses on spheroplasts of the CF strains that have been pre-exposed to the LptD antagonist, in order to measure changes in the ratio of modified to unmodified LPS within the CM<sup>687</sup>. Furthermore, the experiments outlined above with colistin-sensitive PA14 cells that distinguished polymyxin-mediated potentiation of murepavadin from murepavadin-mediated potentiation of colistin should be repeated with these resistant clinical isolates. Of note, the three polymyxin non-susceptible *P. aeruginosa* strains were all sensitive to the antimicrobial action of murepavadin, eliminating any suggestions of cross-resistance between colistin and the LPS transport inhibitor that have been proposed<sup>877</sup>.

If the hypothesis were to be proven accurate – that the synergy between murepavadin and colistin in polymyxin-resistant *P. aeruginosa* was a result of unmodified LPS structures accumulating in the CM – this would add weight to the early implication from the past chapter of colistin non-susceptibility being related to a fitness cost. To elaborate, this outcome would indicate that the bacteria may only be able to tolerate a limited amount of cationically-altered lipid A structures within its CM bilayer, perhaps due to a diminished capacity to transport modified LPS molecules to the OM compared to unmodified LPS molecules. Future work to explore the fitness cost of acquired colistin resistance could include bioinformatic searches using established whole-genome sequencing databases to study whether polymyxin non-susceptible strains acquire mutations in their Lpt protein machinery, as a means of evolving to improve export of cationically-modified LPS. This could also similarly be answered by cloning the Lpt system of intrinsically colistin-resistant bacteria (e.g. *Burkholderia/Neisseria* strains) into isolates with acquired polymyxin resistance, to see if transport of modified LPS to the OM cell surface was enhanced.

The conferring of acquired non-susceptibility to colistin (either through *mcr* genes or chromosomal mutations) at the CM as opposed to the OM bilayer was exploited by revealing that polymyxin-induced OM disruption in resistant *E. coli* and *P. aeruginosa* isolates paved the way for rifampicin, a small hydrophobic antibiotic that normally cannot traverse the Gram-negative cell envelope, to display marked antibacterial effects<sup>858</sup>. This was in keeping with a number of previous reports that stated acquired, but not intrinsic, colistin resistance can be overcome by combining the polypeptide antibiotic with other drugs, for which the findings described here now impart a molecular rationalisation<sup>624,819,878</sup>. It will be interesting in ensuing studies to examine whether the synergy between colistin and rifampicin is expandable to other hydrophobic compounds that are typically blocked by the outermost LPS-containing bilayer (including ethambutol and isoniazid), as the arsenal of antimicrobial options available for the treatment of such multi-drug resistant Gram-negative pathogens would be vastly magnified if this were true. It must be stated that although the additive combined interaction between the drugs rifampicin and colistin has been extensively confirmed *in vitro* with polymyxin-sensitive strains, this efficacy of the dual treatment has never translated to clinical settings<sup>753,835–838</sup>. Hence, to validate the therapeutic potential of “colistin-rifampicin” treatment against colistin-resistant bacteria, *in vivo* experiments using murine infection models should be carried out in the same manner as the “colistin-murepavadin” assays represented here.

In conclusion, the results of this chapter highlight two novel therapeutic options that can be utilised both to augment the bactericidal activity of colistin, and even to surmount the emerging crisis of polymyxin resistance. It is hoped that these new treatment strategies may be transferrable to the clinic, improving patient outcomes during last-resort colistin therapy.

## Chapter 7: Conclusions and Perspectives

### 7.1 Key findings

#### 7.1.1 A new model for colistin's bactericidal mode of action

One of the most significant hurdles in attempts to improve the treatment efficacy of the vital last-resort antibiotic colistin against infections caused by Gram-negative pathogens is that the process by which the polymyxin drug kills bacteria is poorly understood<sup>294</sup>. More specifically, there are substantial gaps in understanding the mechanism by which colistin damages the inner cytoplasmic membrane (CM) of Gram-negative bacteria – a key step in triggering the entire permeabilisation of the cell envelope that is a pre-requisite for cell lysis and death. Though once widely accepted that colistin-mediated disruption of the CM occurs through a detergent-like effect on CM phospholipids, replicating the hypothesised surfactant action of structurally-homologous cationic antimicrobial peptides, experiments presented in this study have enabled a rejection of this proposal<sup>386</sup>. Rather, the work here has proved that colistin permeabilises the CM bilayer and kills bacteria by targeting molecules of LPS situated within the CM awaiting transport to the outer membrane (OM) cell surface. This important conclusion was arrived at through the demonstration that the bactericidal activity of colistin could be dramatically modulated by increasing/decreasing the abundance of LPS in the CM, or by cationic chemical modification of CM LPS. Using this data, a novel model that, for the first time, provides a step-wise and complete explanation of how colistin kills Gram-negative bacteria has been constructed, and is detailed below (**Figure 7.1**):

1. Colistin molecules bind to LPS structures in the OM of Gram-negative bacterial cells via an electrostatic interaction between the cationic polypeptide ring of the polymyxin antibiotic and the anionic lipid A domain of LPS.
2. Colistin attaching to OM LPS causes the displacement of the intra-LPS positively-charged divalent ions ( $Mg^{2+}/Ca^{2+}$ ) that stabilise the outermost cell surface monolayer, resulting in minor OM disruption. This low-level damage to the OM structure is again mediated largely by colistin's C-terminal polypeptide macrocycle.
3. The minor damage to the bacterial OM enables the insertion of colistin's lipid tail into the OM, where its hydrophobic interactions with the fatty acyl chains of lipid A trigger a total loss of OM integrity and the leakage of periplasmic contents.
4. Disruption of the OM induced by colistin also leads to the extracellular release of LPS away from the cell's OM surface, which provides the polymyxin antibiotic with access to the CM bilayer where LPS molecules yet to be exported to the OM are situated.

5. Colistin binds and interacts with this CM LPS in a manner entirely analogous with its behaviour at the OM, inducing displacement of cations including  $Mg^{2+}$  and damaging the CM by means of its N-terminal fatty acid tail.
6. Permeabilisation of the CM by colistin means the protective cell envelope is wholly compromised, and essential cytoplasmic components leak out of the cell, culminating in lysis and death of bacteria. It is possible that this significant CM disruption allows for additional downstream bactericidal processes (e.g. the production of damaging reactive oxygen species, or the targeting of ribosomes).

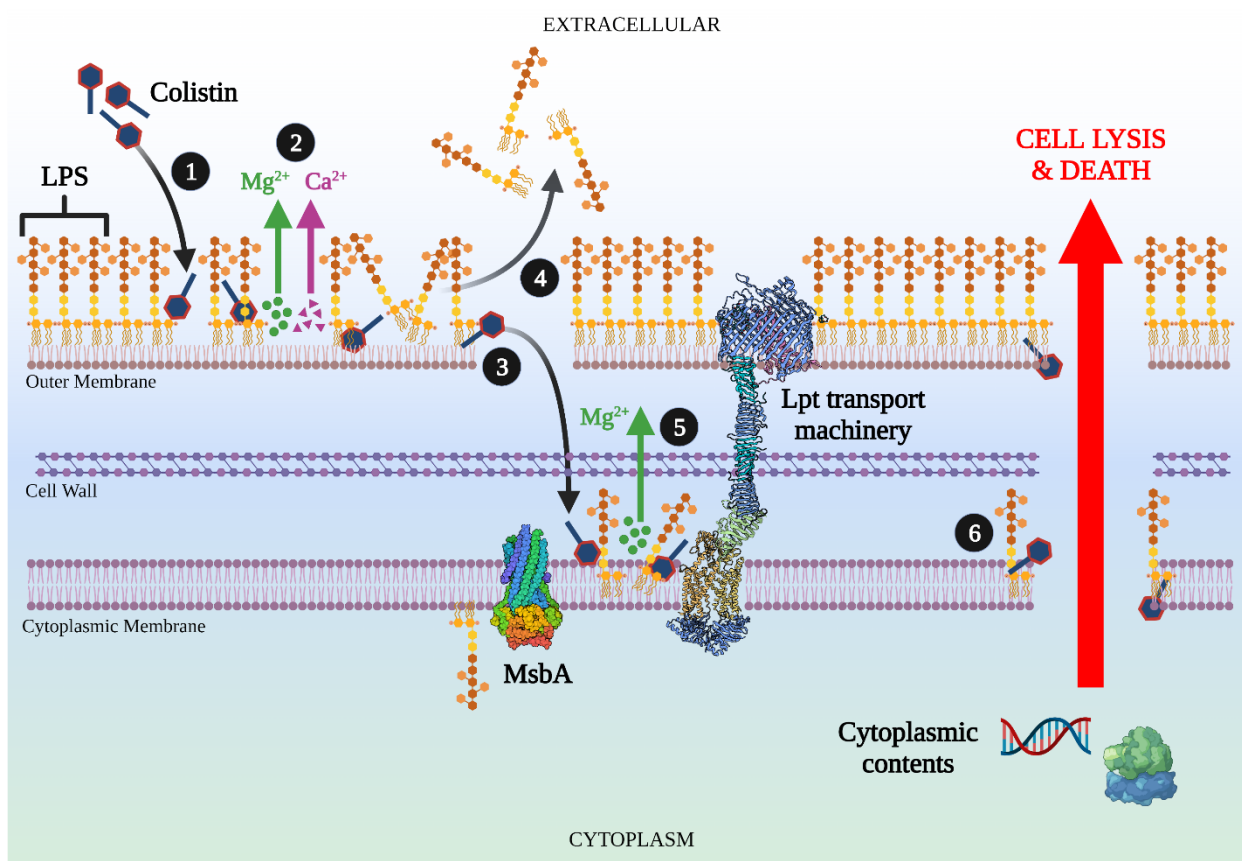


**Figure 7.1: A novel model of how colistin sequentially permeabilises the OM and CM by targeting LPS to kill Gram-negative bacteria.**

### 7.1.2 Characterisation of causes of colistin treatment failure

A grave threat to the clinical effectiveness of “salvage” colistin therapy is the rapidly growing emergence of polymyxin non-susceptibility, which can be conferred in three distinct manners: *mcr* gene-mediated plasmid-borne resistance, chromosomal mutation-mediated resistance, or intrinsic resistance<sup>879</sup>. All these forms of non-susceptibility to colistin result from the addition of positively-charged chemical groups (pEtN/L-Ara4N) to the lipid A domain of LPS, and prior to this work, it was believed that such modifications prevented

colistin from binding to and disrupting the extracellular-facing LPS monolayer of the Gram-negative OM<sup>880</sup>. In this study, however, it has been established that acquired colistin resistance (i.e. conferred by *mcr* homologues or chromosomal mutations) is, in fact, mediated at the bacterial CM, and the polymyxin antibiotic retains its ability to permeabilise the OM of these non-susceptible strains (**Figure 7.2**). It was also found that the mechanism of intrinsic polymyxin resistance in inherently non-susceptible species differs from that in bacteria with acquired resistance, where colistin is unable to damage the cell surface OM structure. The molecular bases of key contributors to the failure of colistin therapy in the clinic have, therefore, been characterised and distinguished through the assays described here.

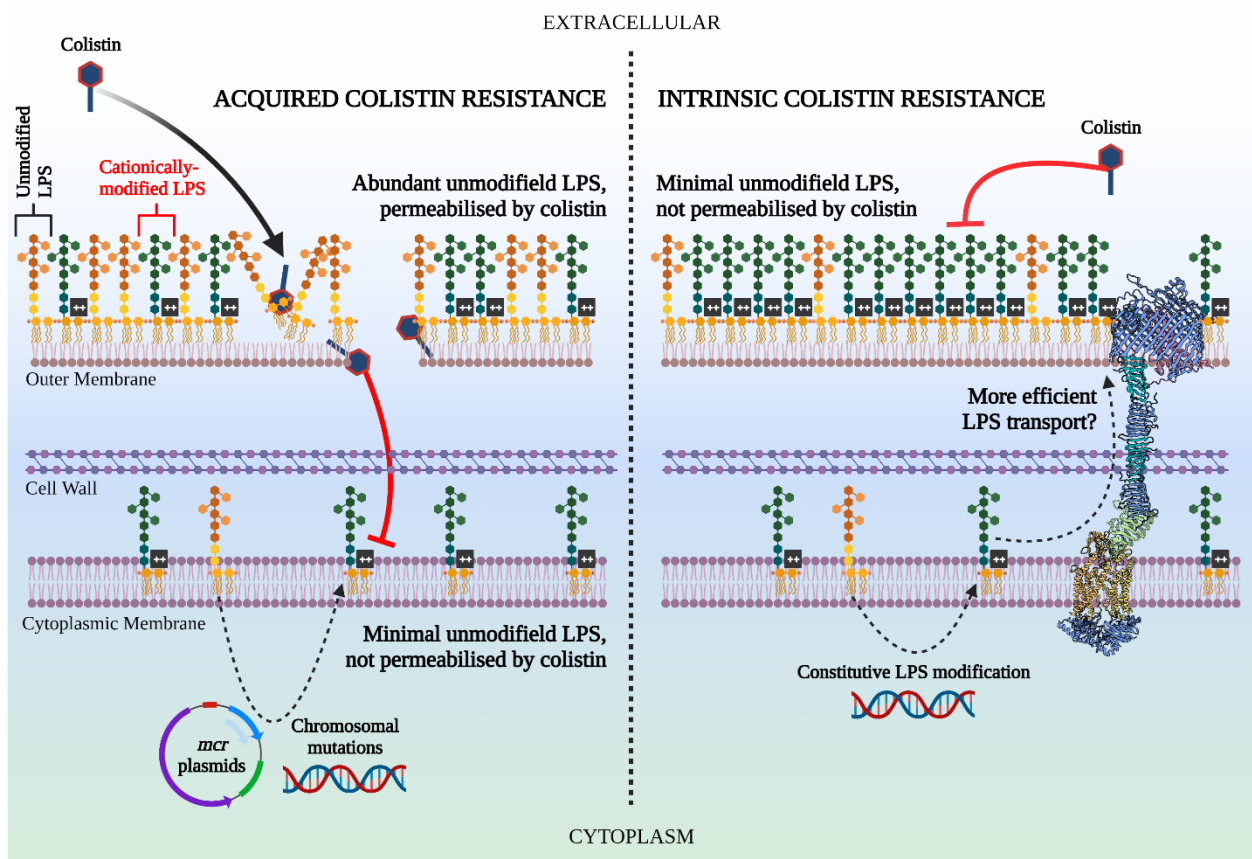


**Figure 7.2: Acquired and intrinsic resistance to colistin are mediated through two differing mechanisms.**

Importantly, “classical” colistin resistance detected diagnostically cannot be the only reason for polymyxin treatment failing, because the prevalence of colistin non-susceptibility amongst clinical Gram-negative isolates remains rare (less than 10%), but the antibiotic is unable to produce a favourable therapeutic outcome on more than 50% of occasions in which it is administered to patients<sup>563,662</sup>. This work has identified two additional processes not falling in the realm of traditional antibiotic non-susceptibility that bacteria use to survive and



tolerate exposure to colistin. Firstly, Gram-negative pathogens that are colistin-sensitive release LPS structures extracellularly in response to polymyxin treatment, and this shed LPS is able to bind and inactivate colistin molecules in the external milieu, impeding the access of the antibiotic to the cell to ensure bacterial survival. Secondly, certain strains harbour a small colistin-resistant sub-population of cells within a much larger population of colistin-sensitive bacteria, and uniquely, the size of this resistant sub-population can drastically increase upon exposure to the polymyxin drug. With both these modes of colistin tolerance being extremely challenging to detect via existing antibiotic susceptibility testing, the value of their extensive characterisation here is of notable import.

### **7.1.3 Design of novel approaches to augment colistin efficacy**

Owing to the poor success rate of clinical colistin administration, it was crucial that this study took advantage of progress made in comprehending the antibiotic's mechanism of action, and elucidating the means by which polymyxin resistance is conferred, to develop therapeutic strategies that potentiate the activity of colistin. To this end, in the work here two new combination treatments were designed and tested against both lab reference and clinical isolates, which both enhanced colistin's antibacterial properties (**Figure 7.3**). The first of these exploited the discovery that colistin relied on interactions with CM LPS in order to kill bacterial cells, and combined the polymyxin drug with the in-development LptD inhibitor murepavadin<sup>257</sup>. It was revealed that blocking the transport of LPS from the CM to the OM with murepavadin induced an accumulation of LPS structures within the CM bilayer, and as a consequence, the ability of colistin to kill bacteria *in vitro* and *in vivo* was increased markedly. Notably, this dual "colistin-murepavadin" therapy was also extremely potent against polymyxin-resistant bacteria, with this result expanding the potential scope and use of this combination approach in clinical settings.

The second dual treatment strategy developed utilised the fact that acquired colistin resistance is mediated at the CM, not the OM, meaning polymyxin-induced OM disruption in these non-susceptible bacteria could enable hydrophobic antibiotics to traverse the Gram-negative cell envelope and enter the cytoplasm. An example of one such hydrophobic drug is rifampicin, which alone is entirely ineffective against Gram-negative pathogens since it is not able to cross the external OM LPS monolayer<sup>858</sup>. Nonetheless, here it was made evident that by combining rifampicin and colistin against bacterial cells with *mcr*/chromosomally-conferred polymyxin resistance, a high degree of synergy can be observed after colistin permeabilises the OM structure, granting rifampicin access to its intracellular RNA polymerase target. The data in this work, therefore, raise the prospect of both potentiating colistin, and overcoming polymyxin non-susceptibility through these two novel and exciting approaches which may be able to improve patient outcomes.

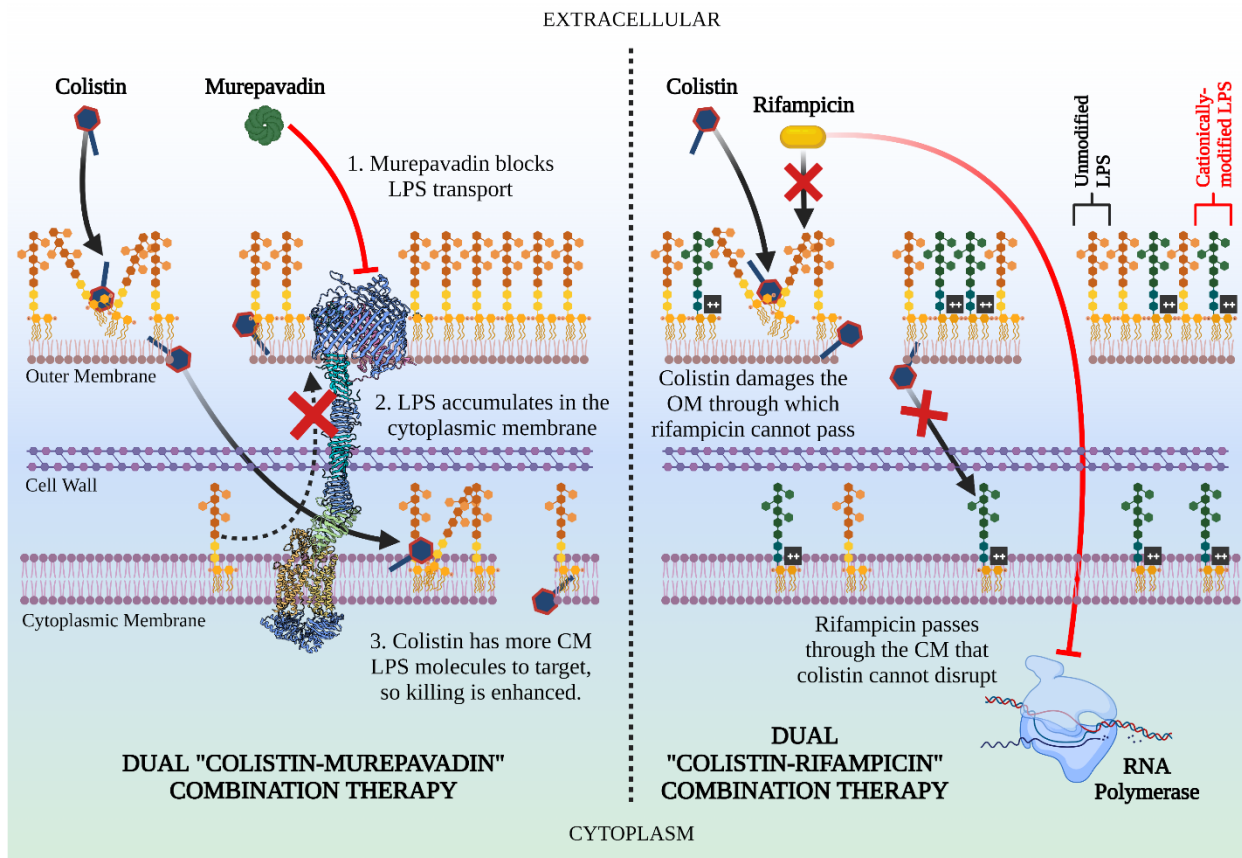


**Figure 7.3: Two new combination treatment strategies that can enhance the activity of colistin and overcome acquired polymyxin resistance.**

## 7.2 Future work

### 7.2.1 What is the biophysical mechanism by which colistin disrupts cell membranes?

Whilst this study identified that colistin-mediated killing of Gram-negative bacterial pathogens was dependent on the interaction of the polymyxin antibiotic with LPS in the CM, there are still a number of critical questions regarding the precise biophysical nature of this membrane permeabilisation process that are unresolved. It was demonstrated that damage to the CM induced by colistin binding to LPS was a cation-dependent effect, and thus shared some commonalities with the polymyxin's OM-disrupting behaviour, where the antibiotic's positively-charged peptide ring has been implicated in the displacement of the intra-LPS  $Mg^{2+}/Ca^{2+}$  ions that stabilise the OM's outermost monolayer<sup>280</sup>. In contrast to the OM however, further investigations are required to elucidate the relationship between colistin's chemical structure and its ability to permeabilise the CM. This could be studied by comparing

the CM-damaging capacity of polymyxin B and PMBN in bacterial spheroplasts to assess whether the polypeptide macrocycle is responsible for the displacement of cations between CM LPS molecules, and whether this cation displacement is sufficient to trigger CM permeabilisation and cell lysis.

It is also not clear why the loss of cations from LPS structures within the CM would compromise the structural integrity of this innermost membrane bilayer to such an extent that the entire CM would be lethally damaged. One hypothesis to explain this is that CM LPS molecules cluster in the bilayer at certain sites (potentially in the proximity of the Lpt protein transport machinery), and that the cationic bridges that form between the individual LPS structures in these aggregates provide essential structural stability to the CM. Indeed, in this work, preliminary data indicated that LPS in the CM had a vital structural role, conferring greater protection against membranolytic stress factors when its abundance was increased. In order to examine this proposal, previously developed nanomaterial-based approaches that selectively detect LPS molecules could be used. These include gold/silver metal nanomaterial biosensors that rapidly and specifically bind to the lipid A domain of CM LPS, which can be utilised in combination with electron microscopy to test whether LPS structures aggregate in the innermost membrane bilayer of Gram-negative bacteria<sup>881</sup>. The fluorescently-tagged form of colistin, BoDipy-colistin, synthesised in this study could also be exploited alongside such LPS biosensors to characterise the interactions between the polymyxin drug and molecules of LPS situated within the CM.

There is a possibility that though colistin's binding to LPS is a primary, fundamental step in the antibiotic's membrane-damaging properties, other components of the bacterial membrane – most notably phospholipids – may also be involved downstream of the initial colistin-LPS interaction. Earlier reports have shown that membrane-perturbing compounds, including EDTA and SDS that strip away intra-LPS cationic bridges (analogously to colistin), trigger glycerophospholipids to flip from the innermost leaflet of the OM bilayer to the outermost leaflet via symmetric lipid rafts which connect the two membrane monolayers<sup>882</sup>. This accumulation of glycerophospholipids in the outermost leaflet of the OM is known to result in an increase in membrane permeability that can ultimately be lethal, and it is worth considering that colistin-induced displacement of cation bridges between LPS molecules in both the OM and the CM may similarly lead to loss of membrane integrity through a phospholipid flipping process<sup>883,884</sup>. To analyse this hypothesis, proteins that have been demonstrated to be important for removing mislocalised phospholipids from the outermost leaflet of membrane bilayers (e.g. the MlaABCDEF protein complex and the phospholipase PldA) could be manipulated by genetic techniques, and the impact on colistin susceptibility determined<sup>882</sup>.

In addition, the interaction between colistin and mammalian phospholipid bilayers warrants further study following the outcome of this work. It has been a widely-held dogma that the significant toxic side-effects of clinical polymyxin administration are related to the fact that the drug disrupts phospholipid membranes through a detergent, surfactant-like effect<sup>867</sup>. However, the findings depicted here – that colistin causes minimal damage to bilayers containing phospholipids in the absence of LPS molecules – call into question whether the nephrotoxicity and neurotoxicity associated with polymyxin treatment may not, in fact, be a direct outcome of the antibiotic permeabilising mammalian cell membranes. Of relevance is the discovery that other antimicrobial drugs not believed to bind to the phospholipid bilayers of mammalian host cells, such as beta-lactam agents, can also bring about nephrotoxic side effects in patients<sup>885</sup>. It is imperative, therefore, to reassess how mammalian cell membranes are affected by colistin exposure, which in turn will allow for a greater comprehension of the mechanisms of polymyxin toxicity.

### **7.2.2 How do single bacterial cells respond to colistin exposure?**

A key finding of this work is that colistin treatment induces LPS structures to be shed from the cell envelope of Gram-negative pathogens, and that the active LPS biosynthesis is required for the polymyxin drug to be able to cause bacterial cell death. It is plausible that these two phenotypes may be linked, and actually contribute to colistin's bactericidal mode of action. There is likely to be an intracellular response to the bacteria's extracellular release of LPS molecules, with Gram-negative organisms possessing a number of systems to sense and regulate membrane LPS levels, meaning that cells may upregulate their LPS biosynthetic pathway to overcome the loss of LPS initiated by polymyxin exposure<sup>886,887</sup>. If this were true, an increase in the rate of LPS biosynthesis by the Lpx family of enzymes could elevate the abundance of LPS structures within the bacterial cell envelope bilayer (both the OM and the CM), providing colistin molecules with a greater number of targets to bind and disrupt. More simply, there may exist a positive feedback loop driving polymyxin-mediated killing, where the antibiotic triggers LPS release, the cell consequently enhances LPS production, and this further potentiates colistin activity. To examine this postulation, LPS levels in the OM/CM of bacteria could be measured after exposure to colistin through the panel of LPS quantification assays (LAL, BoDipy-PMBN, lipidomics) established in the study here. Furthermore, any changes in abundance of the Lpx enzymes in the LPS biosynthetic pathway following colistin treatment could be probed by Western blotting.

A second notable conclusion from this work is that the susceptibility to colistin of different single cells in a bacterial population can vary dramatically. In the case of clinical isolates of *Enterobacter cloacae* exhibiting signs of colistin hetero-resistance, populations of bacteria each grown from an individual cell in a stationary-phase culture as part of the Luria-

Delbrück fluctuation test experiment, differed by 3 to 4-logs in their ability to survive colistin exposure. It would be of interest to understand if this effect was specific to the strain panel tested, or more broadly representative of the behaviour of individual bacterial cells in whole populations of diverse polymyxin-resistant and susceptible Gram-negative pathogens. The molecular bases of these variations in the single cell response to colistin should additionally form an area of future research. With a decrease in the rate of LPS biosynthesis shown here to be a cause of diminished killing by the polymyxin drug, a conceivable explanation for the divergence in colistin activity at the level of a single bacterium is fluctuations in the activity of the Lpx enzymes between cells. This could be tested by separating and growing individual bacterial cells into distinct populations as before, and then assessing the expression levels of the *lpx* genes by qRT-PCR or RNAseq-based transcriptomics.

An alternative reason for the vastly differing colistin susceptibility of single cells in a bacterial population could be connected to the two-component systems involved in cationic lipid A modifications in Gram-negative organisms (e.g. PmrAB and PhoPQ)<sup>476,485</sup>. It is certainly possible that alterations between individual bacteria in the activity of these two-component regulatory protein complexes, or their downstream target genes (including the *arn* operon and the *pmrCAB* operon), may dictate the proportion of LPS in their membrane bilayers that is cationically-altered, and thus the ability of cells to tolerate colistin exposure. Two separate methods could be implemented to resolve this proposal. Firstly, a lipidomic approach based on the MALDI-TOF mass spectrometry technique described here could allow for quantifying the ratio of modified:unmodified lipid A in the surface membranes of bacterial populations grown up from individual single cells<sup>641</sup>. Secondly, the genetic construction of reporter strains in which expression of two-component systems/operons engaged in cationic LPS alterations produced a detectable fluorescent signal could be used to identify through flow cytometry if there were any cells in a whole bacterial population with an increased propensity to modify lipid A. The outputs of both these two methods could then be correlated to the bactericidal efficacy of colistin against populations grown from individual bacterial cells, offering greater insight into colistin activity at the single cell level.

### **7.2.3 Do host antimicrobial peptides share a common mode of action with colistin?**

In the same manner as the historic belief that colistin permeabilises the bacterial CM through a surfactant-like effect on phospholipids in the bilayer, it is generally thought that the host antimicrobial peptides which form a prominent part of the innate immune defence system amongst all classes of life, kill microbial organisms by deleteriously interacting with membrane phospholipids<sup>411,888</sup>. Most host antimicrobial peptides consist of abundant cationic and hydrophobic amino acid residues, and it is considered that their insertion into bacterial

cell membranes leads to the formation of lethal pores in the bilayers<sup>889,890</sup>. However, this proposed mechanism of action for certain host antimicrobial peptides, including the cecropins DAN<sub>1/2</sub> and several *Drosophila* peptides, is called into doubt by the fact that they have antibacterial properties only against Gram-negative pathogens<sup>891,892</sup>.

The implication from this information is that such antimicrobial peptides cannot be solely interacting with membrane phospholipids, which are equally present in both Gram-positive and Gram-negative bacteria. Rather, it should now be considered, particularly in the light of this work, that Gram-negative-specific host defence peptides function by targeting LPS in both the OM and CM of bacterial cells. This could be investigated by examining how the killing effect of antimicrobial peptides (obtained in a purified form, or isolated from the degranulation of host neutrophils/macrophages) is affected by modulating membrane LPS levels via the antagonists of LPS biosynthesis/transport used here. Intriguingly, there is a prospect that elevating the abundance of CM LPS with the LptD inhibitor murepavadin may not only be clinically relevant for potentiating colistin, but also therapeutically useful if it augments the activity of host antimicrobial peptides.

In support of the notion that Gram-negative-specific host defence peptides target LPS to kill bacteria, non-susceptibility to polymyxin antibiotics occurring through modifications of lipid A can result in cross-resistance to some antimicrobial peptides, including LL-37,  $\alpha$ -defensin 5 and  $\beta$ -defensin 3<sup>893</sup>. This finding may provide evolutionary context for how colistin resistance – both chromosomally and MCR-conferred – was selected for in the decades prior to its routine administration in clinical settings. On a related evolutionary note, the novel process of colistin tolerance by extracellular LPS shedding reported in this study may also have developed in response to bacterial exposure to LPS-targeting antimicrobial peptides in the environment, as well as during infections of host organisms. With this in mind, it may be of relevance to explore whether Gram-negative pathogens also release LPS into their external milieu when treated with antimicrobial peptides, and whether this shed LPS can compromise the bactericidal tendencies of these peptides.

#### **7.2.4 Does released LPS contribute to colistin therapy failure in cystic fibrosis patients?**

Colistin is one of the most frequently administered antibiotics in individuals with CF that are chronically infected with multi-drug resistant Gram-negative pathogens, where the polymyxin drug is often delivered in a nebulised formulation directly into the patients' lungs<sup>316</sup>. Concerningly, but perhaps not surprisingly, it has been identified that in the bronchoalveolar lavage fluid (BALF) of CF patients, there exists a significant amount of LPS which may, based on the results portrayed here, interfere with the antibacterial activity of colistin<sup>894</sup>. In order to test if this is the case, samples of sputum/BALF from individuals with

CF, as well as non-CF individuals for use as a control population, could be obtained. Using these samples and the immunogenic LAL assay, the concentration of LPS in the lungs of CF/non-CF patients could be quantified, allowing a correlation to be made between LPS levels and the ability of colistin to kill bacteria, with polymyxin susceptibility testing conducted directly in sputum/BAL lung fluids. If true, that colistin's antibacterial effects are diminished in the CF lung due to higher amounts of extracellular LPS, novel therapeutic strategies could be developed to overcome this contributor to polymyxin treatment failure. These include the use of PMBN, a compound with an extremely high specificity and binding capacity to LPS, that could be administered as a pre-treatment to individuals with CF to "soak up" released LPS molecules in the lung prior to the delivery of aerosolised colistin<sup>895</sup>. Notably, this combined approach may be of additional advantage because PMBN is believed to have reduced mammalian cell toxicity owing to the lack of a fatty acyl lipid tail, although this would need to be confirmed via haemolysis or cell culture-based toxicity testing<sup>896</sup>.

Somewhat counterintuitively, nebulised colistin therapy in CF patients can actually be often comparatively efficacious in mitigating the symptoms of lung disease experienced by these individuals, despite the high LPS concentrations in the environment<sup>897</sup>. One explanation for this beneficial influence of colistin could be that the polymyxin drug is not acting as an antibiotic at all, but rather binding to highly immunogenic LPS molecules in the lung, and thereby blocking the damaging activation of an inflammatory response in immune cells residing in the airways<sup>898</sup>. It is plausible that the rapidly decreasing lung function observed in individuals with CF that are chronically infected with bacteria is not directly related to the carriage of microbial pathogens, but more indirectly caused by LPS-mediated stimulation of tissue-damaging inflammation which can be downregulated by the binding of molecules of colistin to this exogenous LPS<sup>899</sup>. To study this hypothesis, the inflammatory response to BALF or sputum samples obtained from CF patients could be determined in the absence/presence of added colistin using, for example, a human TLR4 reporter cell line in which LPS-driven activation of TLR4 results in the secretion of alkaline phosphatase that can be both detected and quantified<sup>900</sup>.

### **7.2.5 Does the host environment influence susceptibility to colistin?**

In addition to the role extracellular LPS may play in how effectively colistin can work in the CF lung, it is of absolute import to consider the impact of the host environment more generally in terms of elucidating why polymyxin therapy fails to treat human infections. The majority of experiments presented in this work were undertaken in media optimised for bacterial growth, which was nutrient-rich and not wholly representative of the conditions to which Gram-negative pathogens are exposed inside infected patients. It is, therefore, worth exploring how pre-incubation of bacteria in a host fluid, for example human serum, affects the

ability of colistin to exert its bactericidal effects. Any differences arising in the killing activity of colistin in such host environments could be further investigated by fractionation of the fluids used, combined with a mass spectrometry-based approach to identify if there were any specific host molecules that interacted with bacterial cells to modulate susceptibility to polymyxin antibiotics.

Particular attention should be paid to exogenous host lipids (for instance by utilising delipidated serum), since it is known that bacteria can take up these extracellular fatty acid intermediates and feed them into biosynthetic pathways, such as the synthesis of the LPS lipid A domain. With this study highlighting how the rate of LPS biosynthesis is intricately interconnected with the activity of colistin, uptake of host lipid molecules by pathogenic bacteria could be one mechanism by which the host environment shapes the efficaciousness of polymyxin treatment<sup>901,902</sup>. Finally, it is possible that certain host stressors and factors could trigger the activation of determinants of polymyxin resistance in bacteria, including the PhoPQ/PmrAB two-component systems, or the potentially inducible plasmid-borne gene *mcr-9*. This suggestion could be analysed by performing colistin susceptibility assays on relevant pathogenic strains in host fluids which more closely resemble the environmental conditions encountered by bacteria in infected host organisms.

### 7.3 Summary

In conclusion, this study aimed to provide an in-depth characterisation of colistin, an antibiotic of last-resort that is extremely crucial in the treatment of multi-drug resistant Gram-negative pathogens, but one that is associated with a high frequency of therapeutic failure. This work uncovered key insight into the mechanism of action of colistin – revealing that the polymyxin compound kills bacteria by targeting LPS molecules in the cytoplasmic membrane of cells. Moreover, three potential causes for why colistin treatment can fail in the clinic were identified and described here: the extracellular release of LPS that can inactivate the antibiotic, the acquisition of colistin resistance mediated by modified LPS in the bacterial cytoplasmic membrane, and a novel phenotype of inducible colistin hetero-resistance in sub-populations of bacterial cells. New combination therapy approaches were designed that can overcome these grounds for colistin therapy being ineffective, including the utilisation of an LPS transport inhibitor murepavadin that potentiates the polymyxin drug even against non-susceptible bacteria, and dual “colistin-rifampicin” treatment to target pathogens resistant to both antimicrobial agents individually. These findings offer clinically feasible routes to enhance the efficacy of colistin and improve the therapeutic outcomes in infected patients undergoing salvage colistin therapy.



## References

1. Diggle, S. P. & Whiteley, M. Microbe Profile: *Pseudomonas aeruginosa*: opportunistic pathogen and lab rat. *Microbiology (N Y)* **166**, 30–33 (2020).
2. Moore, N. M. & Flaws, M. L. Introduction: *Pseudomonas aeruginosa*. *American Society for Clinical Laboratory Science* **24**, 41–42 (2011).
3. Etymologia: *Pseudomonas*. *Emerging Infectious Diseases* **18**, 1241–1241 (2012).
4. Banerjee, S. *et al.* Detection and characterization of pathogenic *Pseudomonas aeruginosa* from bovine subclinical mastitis in West Bengal, India. *Veterinary World* **10**, 738–742 (2017).
5. Stover, C. K. *et al.* Complete genome sequence of *Pseudomonas aeruginosa* PAO1, an opportunistic pathogen. *Nature* **406**, (2000).
6. Freschi, L. *et al.* Clinical utilization of genomics data produced by the international *Pseudomonas aeruginosa* consortium. *Frontiers in Microbiology* **6**, (2015).
7. Kung, V. L., Ozer, E. A. & Hauser, A. R. The Accessory Genome of *Pseudomonas aeruginosa*. *Microbiology and Molecular Biology Reviews* **74**, (2010).
8. de Smet, J., Hendrix, H., Blasdel, B. G., Danis-Wlodarczyk, K. & Lavigne, R. *Pseudomonas* predators: Understanding and exploiting phage-host interactions. *Nature Reviews Microbiology* vol. 15 (2017).
9. Schobert, M. & Jahn, D. Anaerobic physiology of *Pseudomonas aeruginosa* in the cystic fibrosis lung. *International Journal of Medical Microbiology* vol. 300 (2010).
10. Arai, H. Regulation and function of versatile aerobic and anaerobic respiratory metabolism in *Pseudomonas aeruginosa*. *Frontiers in Microbiology* **2**, (2011).
11. Buckling, A. *et al.* Siderophore-mediated cooperation and virulence in *Pseudomonas aeruginosa*. *FEMS Microbiology Ecology* vol. 62 (2007).
12. Jennings, L. K. *et al.* Pel is a cationic exopolysaccharide that cross-links extracellular DNA in the *Pseudomonas aeruginosa* biofilm matrix. *Proc Natl Acad Sci U S A* **112**, (2015).
13. Diggle, S. P., Griffin, A. S., Campbell, G. S. & West, S. A. Cooperation and conflict in quorum-sensing bacterial populations. *Nature* **450**, (2007).
14. Cai, Y. Ming *et al.* Differential impact on motility and biofilm dispersal of closely related phosphodiesterases in *Pseudomonas aeruginosa*. *Scientific Reports* **10**, (2020).
15. Murray, T. S. & Kazmierczak, B. I. *Pseudomonas aeruginosa* exhibits sliding motility in the absence of type IV pili and flagella. *Journal of Bacteriology* **190**, (2008).
16. Valentini, M. & Filloux, A. Biofilms and Cyclic di-GMP (c-di-GMP) signaling: Lessons from *Pseudomonas aeruginosa* and other bacteria. *Journal of Biological Chemistry* vol. 291 (2016).
17. Walker, T. S. *et al.* *Pseudomonas aeruginosa*-Plant Root Interactions. Pathogenicity, Biofilm Formation, and Root Exudation. *Plant Physiology* **134**, (2004).
18. Rahme, L. G. *et al.* Use of model plant hosts to identify *Pseudomonas aeruginosa* virulence factors. *Proc Natl Acad Sci U S A* **94**, (1997).
19. Mahajan-Miklos, S., Tan, M. W., Rahme, L. G. & Ausubel, F. M. Molecular mechanisms of bacterial virulence elucidated using a *Pseudomonas aeruginosa*-*Caenorhabditis elegans* pathogenesis model. *Cell* **96**, (1999).
20. D'Argenio, D. A., Gallagher, L. A., Berg, C. A. & Manoil, C. *Drosophila* as a model host for *Pseudomonas aeruginosa* infection. *Journal of Bacteriology* **183**, (2001).

21. Miyata, S., Casey, M., Frank, D. W., Ausubel, F. M. & Drenkard, E. Use of the *Galleria mellonella* caterpillar as a model host to study the role of the type III secretion system in *Pseudomonas aeruginosa* pathogenesis. *Infection and Immunity* **71**, (2003).
22. Johnson, P. A. Novel understandings of host cell mechanisms involved in chronic lung infection: *Pseudomonas aeruginosa* in the cystic fibrotic lung. *Journal of Infection and Public Health* **12**, (2019).
23. Robinson, M. & Bye, P. T. B. Mucociliary clearance in cystic fibrosis. *Pediatric Pulmonology* **33**, (2002).
24. Davies, G., Wells, A. U., Doffman, S., Watanabe, S. & Wilson, R. The effect of *Pseudomonas aeruginosa* on pulmonary function in patients with bronchiectasis. *European Respiratory Journal* **28**, (2006).
25. Khatoon, Z., McTiernan, C. D., Suuronen, E. J., Mah, T. F. & Alarcon, E. I. Bacterial biofilm formation on implantable devices and approaches to its treatment and prevention. *Heliyon* vol. 4 (2018).
26. Ramírez-Estrada, S., Borgatta, B. & Rello, J. *Pseudomonas aeruginosa* ventilator-associated pneumonia management. *Infection and Drug Resistance* vol. 9 (2016).
27. Ferreiro, J. L. L. *et al.* *Pseudomonas aeruginosa* urinary tract infections in hospitalized patients: Mortality and prognostic factors. *PLoS ONE* **12**, (2017).
28. Leigh, L., Stoll, B. J., Rahman, M. & McGowan, J. *Pseudomonas aeruginosa* infection in very low birth weight infants: A case-control study. *Pediatric Infectious Disease Journal* **14**, (1995).
29. Bielecki, P., Glik, J., Kawecki, M. & Martins Dos Santos, V. A. P. Towards understanding *Pseudomonas aeruginosa* burn wound infections by profiling gene expression. *Biotechnology Letters* vol. 30 (2008).
30. Sivanmaliappan, T. S. & Sevanan, M. Antimicrobial susceptibility patterns of *Pseudomonas aeruginosa* from diabetes patients with foot ulcers. *International Journal of Microbiology* (2011).
31. Laghmouche, N. *et al.* Successful treatment of *Pseudomonas aeruginosa* osteomyelitis with antibiotic monotherapy of limited duration. *Journal of Infection* **75**, (2017).
32. Procope, J. A. Delayed-onset *Pseudomonas* keratitis after radial keratotomy. *Journal of Cataract and Refractive Surgery* **23**, (1997).
33. Llor, C., McNulty, C. A. M. & Butler, C. C. Ordering and interpreting ear swabs in otitis externa. *BMJ (Online)* **349**, (2014).
34. Jacob, J. S. & Tschén, J. Hot Tub-Associated *Pseudomonas* Folliculitis: A Case Report and Review of Host Risk Factors. *Cureus* (2020).
35. Albasanz-Puig, A. *et al.* Impact of antibiotic resistance on outcomes of neutropenic cancer patients with *Pseudomonas aeruginosa* bacteraemia (IRONIC study): Study protocol of a retrospective multicentre international study. *BMJ Open* **9**, (2019).
36. Diekema, D. J. *et al.* Survey of bloodstream infections due to gram-negative bacilli: Frequency of occurrence and antimicrobial susceptibility of isolates collected in the United States, Canada, and Latin America for the SENTRY Antimicrobial Surveillance Program, 1997. *Clinical Infectious Diseases* **29**, (1999).
37. Koo, S. H., Lee, J. H., Shin, H. & Lee, J. I. Ecthyma gangrenosum in a previously healthy infant. *Archives of Plastic Surgery* **39**, (2012).
38. Matz, C. *et al.* *Pseudomonas aeruginosa* uses type III secretion system to kill biofilm-associated amoebae. *ISME Journal* **2**, (2008).

39. Toder, D. S., Ferrell, S. J., Nezezon, J. L., Rust, L. & Iglewski, B. H. *lasA* and *lasB* genes of *Pseudomonas aeruginosa*: Analysis of transcription and gene product activity. *Infection and Immunity* **62**, (1994).
40. Michalska, M. & Wolf, P. *Pseudomonas* Exotoxin A: Optimized by evolution for effective killing. *Frontiers in Microbiology* vol. 6 (2015).
41. Managò, A. *et al.* *Pseudomonas aeruginosa* Pyocyanin Induces Neutrophil Death via Mitochondrial Reactive Oxygen Species and Mitochondrial Acid Sphingomyelinase. *Antioxidants and Redox Signaling* **22**, (2015).
42. Kirienko, N. v., Ausubel, F. M. & Ruvkun, G. Mitophagy confers resistance to siderophore-mediated killing by *Pseudomonas aeruginosa*. *Proc Natl Acad Sci U S A* **112**, (2015).
43. Spagnolo, A. M., Sartini, M. & Cristina, M. L. *Pseudomonas aeruginosa* in the healthcare facility setting. *Reviews in Medical Microbiology* **32**, (2021).
44. Wiehlmann, L. *et al.* Effective prevention of *Pseudomonas aeruginosa* cross-infection at a cystic fibrosis centre - Results of a 10-year prospective study. *International Journal of Medical Microbiology* **302**, (2012).
45. Forestier, C. *et al.* Oral probiotic and prevention of *Pseudomonas aeruginosa* infections: A randomized, double-blind, placebo-controlled pilot study in intensive care unit patients. *Critical Care* **12**, (2008).
46. Döring, G. & Pier, G. B. Vaccines and immunotherapy against *Pseudomonas aeruginosa*. *Vaccine* vol. 26 (2008).
47. Cabral, M. P. *et al.* A live auxotrophic vaccine confers mucosal immunity and protection against lethal pneumonia caused by *Pseudomonas aeruginosa*. *PLoS Pathogens* **16**, (2020).
48. Slack, M. P. E. Antipseudomonal  $\beta$ -lactams. *Journal of Antimicrobial Chemotherapy* **8**, (1981).
49. Paul, M., Yahav, D., Bivas, A., Fraser, A. & Leibovici, L. Anti-pseudomonal beta-lactams for the initial, empirical, treatment of febrile neutropenia: Comparison of beta-lactams. *Cochrane Database of Systematic Reviews* vol. 2010 (2010).
50. Horita, N., Shibata, Y., Watanabe, H., Namkoong, H. & Kaneko, T. Comparison of antipseudomonal  $\beta$ -lactams for febrile neutropenia empiric therapy: systematic review and network meta-analysis. *Clinical Microbiology and Infection* vol. 23 (2017).
51. Mushtaq, S., Ge, Y. & Livermore, D. M. Doripenem versus *Pseudomonas aeruginosa* in vitro: Activity against characterized isolates, mutants, and transconjugants and resistance selection potential. *Antimicrobial Agents and Chemotherapy* **48**, (2004).
52. Walton, M. A., Villarreal, C., Herndon, D. N. & Hegggers, J. P. The use of aztreonam as an alternate therapy for multi-resistant *Pseudomonas aeruginosa*. *Burns* **23**, (1997).
53. Smith, P. W. *et al.* Pharmacokinetics of  $\beta$ -Lactam Antibiotics: Clues from the Past to Help Discover Long-Acting Oral Drugs in the Future. *ACS Infectious Diseases* vol. 4 (2018).
54. Morissey, L. & Smith, J. T. Activity of 4-quinolones against *Pseudomonas aeruginosa*. *Arzneimittel-Forschung/Drug Research* **44**, (1994).
55. Guzek, J. P., Chacko, D., Kettering, J. D., Wessels, I. F. & Apreccio, R. M. Comparison of topical ciprofloxacin to conventional antibiotic therapy in the treatment of experimental *Pseudomonas aeruginosa* keratitis. *Cornea* **13**, (1994).
56. Jang, C. H. & Park, S. Y. Emergence of ciprofloxacin-resistant *Pseudomonas* in chronic suppurative otitis media. *Clinical Otolaryngology and Allied Sciences* vol. 29 (2004).
57. Wohlkonig, A. *et al.* Structural basis of quinolone inhibition of type IIA topoisomerases and target-mediated resistance. *Nature Structural and Molecular Biology* **17**, (2010).

58. Laponogov, I. *et al.* Structural insight into the quinolone-DNA cleavage complex of type IIA topoisomerases. *Nature Structural and Molecular Biology* **16**, (2009).
59. Aldred, K. J., Kerns, R. J. & Osheroff, N. Mechanism of quinolone action and resistance. *Biochemistry* vol. 53 (2014).
60. Drusano, G. *et al.* Pharmacokinetics and pharmacodynamics of fluoroquinolones. in *Clinical Microbiology and Infection* vol. 4 (1998).
61. Gonzalez, L. S. & Spencer, J. P. Aminoglycosides: A practical review. *American Family Physician* vol. 58 (1998).
62. Olivares, E. *et al.* Tobramycin and amikacin delay adhesion and microcolony formation in *Pseudomonas aeruginosa* cystic fibrosis isolates. *Frontiers in Microbiology* **8**, (2017).
63. Ratjen, F., Brockhaus, F. & Angyalosi, G. Aminoglycoside therapy against *Pseudomonas aeruginosa* in cystic fibrosis: A review. *Journal of Cystic Fibrosis* vol. 8 (2009).
64. Krause, K. M., Serio, A. W., Kane, T. R. & Connolly, L. E. Aminoglycosides: An overview. *Cold Spring Harbor Perspectives in Medicine* **6**, (2016).
65. Davis, B. D., Chen, L. & Tai, P. C. Misread protein creates membrane channels: An essential step in the bactericidal action of aminoglycosides. *Proc Natl Acad Sci U S A* **83**, (1986).
66. Krasnanova, V. & Kovacikova, L. Tigecycline Therapy for Multi-drug-Resistant *Pseudomonas aeruginosa* Sepsis Associated with Multi-organ Failure in an Infant with Persistent Arterial Duct. Case Report. *SN Comprehensive Clinical Medicine* **2**, (2020).
67. Greer, N. D. Tigecycline (Tygacil): The First in the Glycylcycline Class of Antibiotics. *Baylor University Medical Center Proceedings* **19**, (2006).
68. Bassetti, M., Vena, A., Croxatto, A., Righi, E. & Guery, B. How to manage *Pseudomonas aeruginosa* infections. *Drugs in Context* vol. 7 (2018).
69. Deshpande, A. *et al.* Empiric Double Coverage for Healthcare-Associated Pneumonia: Is It Still Necessary? *Open Forum Infectious Diseases* **3**, (2016).
70. Hughes, J. *et al.* Benefits and unintended consequences of antimicrobial de-escalation: Implications for stewardship programs. *PLoS ONE* **12**, (2017).
71. Bliziotis, I. A., Petrosillo, N., Michalopoulos, A., Samonis, G. & Falagas, M. E. Impact of definitive therapy with Beta-Lactam monotherapy or combination with an Aminoglycoside or a Quinolone for *Pseudomonas aeruginosa* bacteremia. *PLoS ONE* **6**, (2011).
72. Kalil, A. C. *et al.* Management of Adults With Hospital-acquired and Ventilator-associated Pneumonia: 2016 Clinical Practice Guidelines by the Infectious Diseases Society of America and the American Thoracic Society. *Clinical Infectious Diseases* vol. 63 (2016).
73. Rossolini, G. M. & Mantengoli, E. Treatment and control of severe infections caused by multiresistant *Pseudomonas aeruginosa*. *Clinical Microbiology and Infection, Supplement* vol. 11 (2005).
74. Tschudin-Sutter, S., Fosse, N., Frei, R. & Widmer, A. F. Combination therapy for treatment of *Pseudomonas aeruginosa* bloodstream infections. *PLoS ONE* **13**, (2018).
75. Paul, M., Benuri-Silbiger, I., Soares-Weiser, K. & Leibovici, L.  $\beta$  lactam monotherapy versus  $\beta$  lactam-aminoglycoside combination therapy for sepsis in immunocompetent patients: Systematic review and meta-analysis of randomised trials. *British Medical Journal* vol. 328 (2004).
76. Peña, C. *et al.* Effect of adequate single-drug vs combination antimicrobial therapy on mortality in *Pseudomonas aeruginosa* bloodstream infections: A post hoc analysis of a prospective cohort. *Clinical Infectious Diseases* **57**, (2013).

77. Pang, Z., Raudonis, R., Glick, B. R., Lin, T. J. & Cheng, Z. Antibiotic resistance in *Pseudomonas aeruginosa*: mechanisms and alternative therapeutic strategies. *Biotechnology Advances* vol. 37 (2019).
78. Delcour, A. H. Outer membrane permeability and antibiotic resistance. *Biochimica et Biophysica Acta - Proteins and Proteomics* vol. 1794 (2009).
79. Savage, P. B. Multidrug-resistant bacteria: Overcoming antibiotic permeability barriers of Gram-negative bacteria. *Annals of Medicine* vol. 33 (2001).
80. Dreier, J. & Ruggerone, P. Interaction of antibacterial compounds with RND efflux pumps in *Pseudomonas aeruginosa*. *Frontiers in Microbiology* vol. 6 (2015).
81. Daury, L. *et al.* Tripartite assembly of RND multidrug efflux pumps. *Nature Communications* 7, (2016).
82. Morita, Y., Tomida, J. & Kawamura, Y. MexXY multidrug efflux system of *Pseudomonas aeruginosa*. *Frontiers in Microbiology* vol. 3 (2012).
83. Hancock, R. E. W. & Brinkman, F. S. L. Function of *Pseudomonas* porins in uptake and efflux. *Annual Review of Microbiology* vol. 56 (2002).
84. Masuda, N. *et al.* Substrate specificities of MexAB-OprM, MexCD-OprJ, and MexXY-OprM efflux pumps in *Pseudomonas aeruginosa*. *Antimicrobial Agents and Chemotherapy* 44, (2000).
85. Dupont, P., Hocquet, D., Jeannot, K., Chavanet, P. & Plésiat, P. Bacteriostatic and bactericidal activities of eight fluoroquinolones against Mex-AB-OprM-overproducing clinical strains of *Pseudomonas aeruginosa*. *Journal of Antimicrobial Chemotherapy* 55, (2005).
86. Hocquet, D. *et al.* MexXy-OprM efflux pump is necessary for adaptive resistance of *Pseudomonas aeruginosa* to aminoglycosides. *Antimicrobial Agents and Chemotherapy* 47, (2003).
87. Livermore, D. M. & Yang, Y. J.  $\beta$ -lactamase lability and inducer power of newer  $\beta$ -lactam antibiotics in relation to their activity against  $\beta$ -lactamase-inducibility mutants of *Pseudomonas aeruginosa*. *Journal of Infectious Diseases* 155, (1987).
88. Berrazeg, M. *et al.* Mutations in  $\beta$ -lactamase AmpC increase resistance of *Pseudomonas aeruginosa* isolates to antipseudomonal cephalosporins. *Antimicrobial Agents and Chemotherapy* 59, (2015).
89. Masuda, N. *et al.* Interplay between chromosomal  $\beta$ -lactamase and the MexAB-OprM efflux system in intrinsic resistance to  $\beta$ -lactams in *Pseudomonas aeruginosa*. *Antimicrobial Agents and Chemotherapy* 43, (1999).
90. Torrens, G. *et al.* Regulation of AmpC-Driven  $\beta$ -Lactam Resistance in *Pseudomonas aeruginosa*: Different Pathways, Different Signaling. *mSystems* 4, (2019).
91. Lee, M. *et al.* Muropeptides in *Pseudomonas aeruginosa* and their Role as Elicitors of  $\beta$ -Lactam-Antibiotic Resistance. *Angewandte Chemie - International Edition* 55, (2016).
92. Lodge, J. M., Minchin, S. D., Piddock, L. J. V. & Busby, J. W. Cloning, sequencing and analysis of the structural gene and regulatory region of the *Pseudomonas aeruginosa* chromosomal ampC  $\beta$ -lactamase. *Biochemical Journal* 272, (1990).
93. Juan, C. *et al.* Molecular mechanisms of  $\beta$ -lactam resistance mediated by AmpC hyperproduction in *Pseudomonas aeruginosa* clinical strains. *Antimicrobial Agents and Chemotherapy* 49, (2005).
94. Ruppé, É., Woerther, P. L. & Barbier, F. Mechanisms of antimicrobial resistance in Gram-negative bacilli. *Annals of Intensive Care* vol. 5 (2015).

95. Pereira, S. G. & Cardoso, O. Mobile genetic elements of *Pseudomonas aeruginosa* isolates from hydrotherapy facility and respiratory infections. *Clinical Microbiology and Infection* **20**, (2014).
96. Rawat, D. & Nair, D. Extended-spectrum  $\beta$ -lactamases in gram negative bacteria. *Journal of Global Infectious Diseases* **2**, (2010).
97. Weldhagen, G. F., Poirel, L. & Nordmann, P. Ambler class A extended-spectrum  $\beta$ -lactamases in *Pseudomonas aeruginosa*: Novel developments and clinical impact. *Antimicrobial Agents and Chemotherapy* vol. 47 (2003).
98. Hong, D. J. *et al.* Epidemiology and characteristics of metallo- $\beta$ -lactamase-producing *Pseudomonas aeruginosa*. *Infection and Chemotherapy* **47**, (2015).
99. Maveyraud, L. *et al.* Insights into class D  $\beta$ -lactamases are revealed by the crystal structure of the OXA10 enzyme from *Pseudomonas aeruginosa*. *Structure* **8**, (2000).
100. Drawz, S. M. & Bonomo, R. A. Three decades of  $\beta$ -lactamase inhibitors. *Clinical Microbiology Reviews* vol. 23 (2010).
101. Yang, Y., Rasmussen, B. A. & Shlaes, D. M. Class A  $\beta$ -lactamases - Enzyme-inhibitor interactions and resistance. *Pharmacology and Therapeutics* vol. 83 (1999).
102. Pagan-Rodriguez, D. *et al.* Tazobactam inactivation of SHV-1 and the inhibitor-resistant Ser 130  $\rightarrow$  Gly SHV-1  $\beta$ -lactamase: Insights into the mechanism of inhibition. *Journal of Biological Chemistry* **279**, (2004).
103. Cole, M. Biochemistry and action of clavulanic acid. *Scottish Medical Journal* **27**, (1982).
104. MacVane, S. H., Pandey, R., Steed, L. L., Kreiswirth, B. N. & Chen, L. Emergence of ceftolozane-tazobactam-resistant *Pseudomonas aeruginosa* during treatment is mediated by a single AmpC structural mutation. *Antimicrobial Agents and Chemotherapy* **61**, (2017).
105. Javiya, V., Ghatak, S., Patel, K. & Patel, J. Antibiotic susceptibility patterns of *Pseudomonas aeruginosa* at a tertiary care hospital in Gujarat, India. *Indian Journal of Pharmacology* **40**, (2008).
106. Ramirez, M. S. & Tolmasky, M. E. Aminoglycoside modifying enzymes. *Drug Resistance Updates* **13**, (2010).
107. Hächler, H., Santanam, P. & Kayser, F. H. Sequence and characterization of a novel chromosomal aminoglycoside phosphotransferase gene, *aph(3')-IIb*, in *Pseudomonas aeruginosa*. *Antimicrobial Agents and Chemotherapy* **40**, (1996).
108. Jacoby, G. A. *et al.* Appearance of amikacin and tobramycin resistance due to 4'-aminoglycoside nucleotidyltransferase [ANT(4')-II] in gram-negative pathogens. *Antimicrobial Agents and Chemotherapy* **34**, (1990).
109. Kitao, T., Miyoshi-Akiyama, T. & Kirikae, T. AAC(6')-Iaf, a novel aminoglycoside 6'-N-acetyltransferase from multidrug-resistant *Pseudomonas aeruginosa* clinical isolates. *Antimicrobial Agents and Chemotherapy* **53**, (2009).
110. Vaziri, F., Peerayeh, S. N., Nejad, Q. B. & Farhadian, A. The prevalence of aminoglycoside-modifying enzyme genes (*aac (6')-I*, *aac (6')-II*, *ant (2'')-I*, *aph (3')-VI*) in *Pseudomonas aeruginosa*. *Clinics* **66**, (2011).
111. Poole, K. Aminoglycoside resistance in *Pseudomonas aeruginosa*. *Antimicrobial Agents and Chemotherapy* vol. 49 (2005).
112. Langendonk, R. F., Neill, D. R. & Fothergill, J. L. The Building Blocks of Antimicrobial Resistance in *Pseudomonas aeruginosa*: Implications for Current Resistance-Breaking Therapies. *Frontiers in Cellular and Infection Microbiology* vol. 11 (2021).

113. Yamane, K., Wachino, J. I., Doi, Y., Kurokawa, H. & Arakawa, Y. Global spread of multiple aminoglycoside resistance genes. *Emerging Infectious Diseases* **11**, (2005).
114. Yamane, K. *et al.* Genetic environments of the *rmtA* gene in *Pseudomonas aeruginosa* clinical isolates. *Antimicrobial Agents and Chemotherapy* **48**, (2004).
115. Yamane, K. *et al.* 16S rRNA methylase-producing, gram-negative pathogens, Japan. *Emerging Infectious Diseases* **13**, (2007).
116. Doi, Y. & Arakawa, Y. 16S ribosomal RNA methylation: Emerging resistance mechanism against aminoglycosides. *Clinical Infectious Diseases* vol. 45 (2007).
117. Lee, J. K., Lee, Y. S., Park, Y. K. & Kim, B. S. Alterations in the GyrA and GyrB subunits of topoisomerase II and the ParC and ParE subunits of topoisomerase IV in ciprofloxacin-resistant clinical isolates of *Pseudomonas aeruginosa*. *International Journal of Antimicrobial Agents* **25**, (2005).
118. Bruchmann, S., Dötsch, A., Nouri, B., Chaberny, I. F. & Häußler, S. Quantitative contributions of target alteration and decreased drug accumulation to *Pseudomonas aeruginosa* fluoroquinolone resistance. *Antimicrobial Agents and Chemotherapy* **57**, (2013).
119. Moshirian Farahi, R., Abdi Ali, A. & Gharavi, S. Characterization of *gyrA* and *parC* mutations in ciprofloxacin-resistant *Pseudomonas aeruginosa* isolates from Tehran hospitals in Iran. *Iranian Journal of Microbiology* **10**, (2018).
120. Jalal, S., Ciofu, O., Høiby, N., Gotoh, N. & Wretling, B. Molecular mechanisms of fluoroquinolone resistance in *Pseudomonas aeruginosa* isolates from cystic fibrosis patients. *Antimicrobial Agents and Chemotherapy* **44**, (2000).
121. Lister, P. D., Wolter, D. J. & Hanson, N. D. Antibacterial-resistant *Pseudomonas aeruginosa*: Clinical impact and complex regulation of chromosomally encoded resistance mechanisms. *Clinical Microbiology Reviews* vol. 22 (2009).
122. Obritsch, M. D., Fish, D. N., MacLaren, R. & Jung, R. National surveillance of antimicrobial resistance in *Pseudomonas aeruginosa* isolates obtained from intensive care unit patients from 1993 to 2002. *Antimicrobial Agents and Chemotherapy* **48**, (2004).
123. Yayan, J., Ghebremedhin, B. & Rasche, K. Antibiotic resistance of *Pseudomonas aeruginosa* in pneumonia at a single university hospital center in Germany over a 10-Year Period. *PLoS ONE* **10**, (2015).
124. Sutcliffe, I. C. A phylum level perspective on bacterial cell envelope architecture. *Trends in Microbiology* vol. 18 (2010).
125. Kim, M. & Ryu, S. Spontaneous and transient defence against bacteriophage by phase-variable glucosylation of O-antigen in *Salmonella enterica* serovar Typhimurium. *Molecular Microbiology* **86**, (2012).
126. Joiner, K. A. Complement evasion by bacteria and parasites. *Annual Review of Microbiology* vol. 42 (1988).
127. Carpenter, T. S., Parkin, J. & Khalid, S. The Free Energy of Small Solute Permeation through the *Escherichia coli* Outer Membrane Has a Distinctly Asymmetric Profile. *Journal of Physical Chemistry Letters* **7**, (2016).
128. Nikaido, H. Molecular Basis of Bacterial Outer Membrane Permeability Revisited. *Microbiology and Molecular Biology Reviews* **67**, (2003).
129. Jeannin, J. F., Sassi, N., Paul, C., Martin, A. & Bettaieb, A. Lipid A-Induced responses *in vivo*. *Advances in Experimental Medicine and Biology* **667**, (2009).

130. Needham, B. D. & Trent, M. S. Fortifying the barrier: The impact of lipid A remodelling on bacterial pathogenesis. *Nature Reviews Microbiology* vol. 11 (2013).
131. Scott, A. J., Oyler, B. L., Goodlett, D. R. & Ernst, R. K. Lipid A structural modifications in extreme conditions and identification of unique modifying enzymes to define the Toll-like receptor 4 structure-activity relationship. *Biochimica et Biophysica Acta - Molecular and Cell Biology of Lipids* vol. 1862 (2017).
132. Zhang, G., Meredith, T. C. & Kahne, D. On the essentiality of lipopolysaccharide to Gram-negative bacteria. *Current Opinion in Microbiology* vol. 16 (2013).
133. Raetz, C. R. H. & Whitfield, C. Lipopolysaccharide endotoxins. *Annual Review of Biochemistry* vol. 71 (2002).
134. King, J. D., Kocíncová, D., Westman, E. L. & Lam, J. S. Lipopolysaccharide biosynthesis in *Pseudomonas aeruginosa*. *Innate Immunity* vol. 15 (2009).
135. Raetz, C. R. H., Reynolds, C. M., Trent, M. S. & Bishop, R. E. Lipid A modification systems in gram-negative bacteria. *Annual Review of Biochemistry* vol. 76 (2007).
136. Bystrova, O. v. *et al.* Structures of the core oligosaccharide and O-units in the R- and SR-type lipopolysaccharides of reference strains of *Pseudomonas aeruginosa* O-serogroups. *FEMS Immunology and Medical Microbiology* **46**, (2006).
137. Rocchetta, H. L., Burrows, L. L. & Lam, J. S. Genetics of O-Antigen Biosynthesis in *Pseudomonas aeruginosa*. *Microbiology and Molecular Biology Reviews* **63**, (1999).
138. Rallabhandi, P. *et al.* Differential Activation of Human TLR4 by *Escherichia coli* and *Shigella flexneri* 2a Lipopolysaccharide: Combined Effects of Lipid A Acylation State and TLR4 Polymorphisms on Signaling. *The Journal of Immunology* **180**, (2008).
139. Drayton, M. *et al.* Host defense peptides: Dual antimicrobial and immunomodulatory action. *International Journal of Molecular Sciences* vol. 22 (2021).
140. Pier, G. B., Grout, M., Zaidi, T. S. & Goldberg, J. B. How mutant CFTR may contribute to *Pseudomonas aeruginosa* infection in cystic fibrosis. in *American Journal of Respiratory and Critical Care Medicine* vol. 154 (1996).
141. Zaidi, T. S., Lyczak, J., Preston, M. & Pier, G. B. Cystic fibrosis transmembrane conductance regulator-mediated corneal epithelial cell ingestion of *Pseudomonas aeruginosa* is a key component in the pathogenesis of experimental murine keratitis. *Infection and Immunity* **67**, (1999).
142. Dasgupta, T. *et al.* Characterization of lipopolysaccharide-deficient mutants of *Pseudomonas aeruginosa* derived from serotypes O3, O5, and O6. *Infection and Immunity* **62**, (1994).
143. Berry, M. C., Mcghee, G. C., Zhao, Y. & Sundin, G. W. Effect of a *waaL* mutation on lipopolysaccharide composition, oxidative stress survival, and virulence in *Erwinia amylovora*: RESEARCH LETTER. *FEMS Microbiology Letters* **291**, (2009).
144. Abeyrathne, P. D., Daniels, C., Poon, K. K. H., Matewish, M. J. & Lam, J. S. Functional characterization of WaaL, a ligase associated with linking O-antigen polysaccharide to the core of *Pseudomonas aeruginosa* lipopolysaccharide. *Journal of Bacteriology* **187**, (2005).
145. Tang, H. B. *et al.* Contribution of specific *Pseudomonas aeruginosa* virulence factors to pathogenesis of pneumonia in a neonatal mouse model of infection. *Infection and Immunity* **64**, (1996).
146. Liu, C. *et al.* Construction of a protective vaccine against lipopolysaccharide-heterologous *Pseudomonas aeruginosa* strains based on expression profiling of outer membrane proteins during infection. *Frontiers in Immunology* **9**, (2018).



147. Wang, X. & Quinn, P. J. Lipopolysaccharide: Biosynthetic pathway and structure modification. *Progress in Lipid Research* vol. 49 (2010).
148. Dotson, G. D., Kaltashov, I. A., Cotter, R. J. & Raetz, C. R. H. Expression cloning of a *Pseudomonas* gene encoding a hydroxydecanoyl- acyl carrier protein-dependent UDP-GlcNAc acyltransferase. *Journal of Bacteriology* **180**, (1998).
149. Williams, A. H. & Raetz, C. R. H. Structural basis for the acyl chain selectivity and mechanism of UDP-N-acetylglucosamine acyltransferase. *Proc Natl Acad Sci U S A* **104**, (2007).
150. Williamson, J. M., Anderson, M. S. & Raetz, C. R. H. Acyl-acyl carrier protein specificity of UDP-GlcNAc acyltransferases from gram-negative bacteria: Relationship to lipid A structure. *Journal of Bacteriology* vol. 173 (1991).
151. Buetow, L., Smith, T. K., Dawson, A., Fyffe, S. & Hunter, W. N. Structure and reactivity of LpxD, the N-acyltransferase of lipid A biosynthesis. *Proc Natl Acad Sci U S A* **104**, (2007).
152. Babinski, K. J., Kanjilal, S. J. & Raetz, C. R. H. Accumulation of the lipid A precursor UDP-2,3-diacetylglucosamine in an *Escherichia coli* mutant lacking the *lpxH* gene. *Journal of Biological Chemistry* **277**, (2002).
153. Crowell, D. N., Anderson, M. S. & Raetz, C. R. H. Molecular cloning of the genes for lipid A disaccharide synthase and UDP-N-acetylglucosamine acyltransferase in *Escherichia coli*. *Journal of Bacteriology* **168**, (1986).
154. Garrett, T. A., Que, N. L. S. & Raetz, C. R. H. Accumulation of a lipid A precursor lacking the 4'-phosphate following inactivation of the *Escherichia coli* *lpxK* gene. *Journal of Biological Chemistry* **273**, (1998).
155. Brozek, K. A., Hosaka, K., Robertson, A. D. & Raetz, C. R. H. Biosynthesis of lipopolysaccharide in *Escherichia coli*. Cytoplasmic enzymes that attach 3-deoxy-D-manno-octulosonic acid to lipid A. *Journal of Biological Chemistry* **264**, (1989).
156. Brozek, K. A. & Raetz, C. R. H. Biosynthesis of lipid A in *Escherichia coli*. Acyl carrier protein-dependent incorporation of laurate and myristate. *Journal of Biological Chemistry* **265**, (1990).
157. Holst, O. Structure of the Lipopolysaccharide Core Region. *Bacterial Lipopolysaccharides* (2011).
158. Whitfield, C. & Stephen Trent, M. Biosynthesis and export of bacterial lipopolysaccharides. *Annual Review of Biochemistry* vol. 83 (2014).
159. Delucia, A. M. *et al.* Lipopolysaccharide (LPS) inner-core phosphates are required for complete lps synthesis and transport to the outer membrane in *Pseudomonas aeruginosa* PAO1. *mBio* **2**, (2011).
160. Roncero, C. & Casadaban, M. J. Genetic analysis of the genes involved in synthesis of the lipopolysaccharide core in *Escherichia coli* K-12: Three operons in the *rfa* locus. *Journal of Bacteriology* **174**, (1992).
161. Schnaitman, C. A. & Klena, J. D. Genetics of lipopolysaccharide biosynthesis in enteric bacteria. *Microbiological Reviews* vol. 57 (1993).
162. Whitfield, C., Amor, P. A. & Köplin, R. Modulation of the surface architecture of Gram-negative bacteria by the action of surface polymer:lipid A-core ligase and by determinants of polymer chain length. *Molecular Microbiology* vol. 23 (1997).
163. Raetz, C. R. H. Biochemistry of endotoxins. *Annual Review of Biochemistry* **59**, (1990).
164. Belunis, C. J. & Raetz, C. R. H. Biosynthesis of endotoxins. Purification and catalytic properties of 3- deoxy-D-manno-octulosonic acid transferase from *Escherichia coli*. *Journal of Biological Chemistry* **267**, (1992).

165. Dean, C. R. & Goldberg, J. B. *Pseudomonas aeruginosa galU* is required for a complete lipopolysaccharide core and repairs a secondary mutation in a PA103 (serogroup O11) *wbpM* mutant. *FEMS Microbiology Letters* **210**, (2002).
166. Blankenfeldt, W. *et al.* The purification, crystallization and preliminary structural characterization of glucose-1-phosphate thymidyltransferase (RmlA), the first enzyme of the dTDP-L-rhamnose synthesis pathway from *Pseudomonas aeruginosa*. *Acta Crystallographica Section D: Biological Crystallography* **56**, (2000).
167. Yethon, J. A., Vinogradov, E., Perry, M. B. & Whitfield, C. Mutation of the lipopolysaccharide core glycosyltransferase encoded by *waaG* destabilizes the outer membrane of *Escherichia coli* by interfering with core phosphorylation. *Journal of Bacteriology* **182**, (2000).
168. Poon, K. K. H., Westman, E. L., Vinogradov, E., Jin, S. & Lam, J. S. Functional characterization of MigA and WapR: Putative rhamnosyltransferases involved in outer core oligosaccharide biosynthesis of *Pseudomonas aeruginosa*. *Journal of Bacteriology* **190**, (2008).
169. Greenfield, L. K. & Whitfield, C. Synthesis of lipopolysaccharide O-antigens by ABC transporter-dependent pathways. in *Carbohydrate Research* vol. 356 (2012).
170. Jiang, X. -M *et al.* Structure and sequence of the *rfb* (O antigen) gene cluster of *Salmonella* serovar Typhimurium (strain LT2). *Molecular Microbiology* **5**, (1991).
171. Kaluzny, K., Abeyrathne, P. D. & Lam, J. S. Coexistence of two distinct versions of O-antigen polymerase, Wzy-alpha and Wzy-beta, in *Pseudomonas aeruginosa* serogroup O2 and their contributions to cell surface diversity. *Journal of Bacteriology* **189**, (2007).
172. Daniels, C., Griffiths, C., Cowles, B. & Lam, J. S. *Pseudomonas aeruginosa* O-antigen chain length is determined before ligation to lipid A core. *Environmental Microbiology* **4**, (2002).
173. Abeyrathne, P. D. & Lam, J. S. WaaL of *Pseudomonas aeruginosa* utilizes ATP in *in vitro* ligation of O antigen onto lipid A-core. *Molecular Microbiology* **65**, (2007).
174. Huszczyński, S. M., Hao, Y., Lam, J. S. & Khursigara, C. M. Identification of the *Pseudomonas aeruginosa* O17 and O15 O-Specific Antigen Biosynthesis Loci Reveals an ABC Transporter-Dependent Synthesis Pathway and Mechanisms of Genetic Diversity. *Journal of Bacteriology* **202**, (2020).
175. Hong, Y. & Reeves, P. R. Diversity of O-antigen repeat unit structures can account for the substantial sequence variation of Wzx translocases. *Journal of Bacteriology* **196**, (2014).
176. MacNair, C. R., Tsai, C. N. & Brown, E. D. Creative targeting of the Gram-negative outer membrane in antibiotic discovery. *Annals of the New York Academy of Sciences* vol. 1459 (2020).
177. Onishi, H. R. *et al.* Antibacterial agents that inhibit lipid A biosynthesis. *Science (1979)* **274**, (1996).
178. Zhou, P. & Barb, A. Mechanism and Inhibition of LpxC: An Essential Zinc-Dependent Deacetylase of Bacterial Lipid A Synthesis. *Current Pharmaceutical Biotechnology* **9**, (2008).
179. Clements, J. M. *et al.* Antibacterial activities and characterization of novel inhibitors of LpxC. *Antimicrobial Agents and Chemotherapy* **46**, (2002).
180. McClerren, A. L. *et al.* A slow, tight-binding inhibitor of the zinc-dependent deacetylase LpxC of lipid A biosynthesis with antibiotic activity comparable to ciprofloxacin. *Biochemistry* **44**, (2005).
181. Barb, A. W. *et al.* Inhibition of lipid A biosynthesis as the primary mechanism of CHIR-090 antibiotic activity in *Escherichia coli*. *Biochemistry* **46**, (2007).

182. Tan, J. H. *et al.* *In vitro* and *In vivo* efficacy of an LpxC inhibitor, CHIR-090, alone or combined with colistin against *Pseudomonas aeruginosa* biofilm. *Antimicrobial Agents and Chemotherapy* **61**, (2017).
183. Barb, A. W., Jiang, L., Raetz, C. R. H. & Zhou, P. Structure of the deacetylase LpxC bound to the antibiotic CHIR-090: Time-dependent inhibition and specificity in ligand binding. *Proc Natl Acad Sci U S A* **104**, (2007).
184. Bodewits, K., Raetz, C. R. H., Govan, J. R. & Campopiano, D. J. Antimicrobial activity of CHIR-090, an inhibitor of lipopolysaccharide biosynthesis, against the *Burkholderia cepacia* complex. *Antimicrobial Agents and Chemotherapy* vol. 54 (2010).
185. Krause, K. M. *et al.* Potent LpxC Inhibitors with *in Vitro* Activity against Multidrug-Resistant *Pseudomonas aeruginosa*. *Antimicrobial Agents and Chemotherapy* **63**, (2019).
186. Kalinin, D. v. & Holl, R. LpxC inhibitors: a patent review (2010-2016). *Expert Opinion on Therapeutic Patents* vol. 27 (2017).
187. Erwin, A. L. Antibacterial drug discovery targeting the lipopolysaccharide biosynthetic enzyme LpxC. *Cold Spring Harbor Perspectives in Medicine* **6**, (2016).
188. Jenkins, R. J. & Dotson, G. D. Dual targeting antibacterial peptide inhibitor of early lipid A biosynthesis. *ACS Chemical Biology* **7**, (2012).
189. Jenkins, R. J., Heslip, K. A., Meagher, J. L., Stuckey, J. A. & Dotson, G. D. Structural basis for the recognition of peptide RJPXD33 by acyltransferases in lipid A biosynthesis. *Journal of Biological Chemistry* **289**, (2014).
190. Postma, T. M. & Liskamp, R. M. J. Triple-targeting Gram-negative selective antimicrobial peptides capable of disrupting the cell membrane and lipid A biosynthesis. *RSC Advances* **6**, (2016).
191. Nayar, A. S. *et al.* Novel antibacterial targets and compounds revealed by a high-throughput cell wall reporter assay. *Journal of Bacteriology* **197**, (2015).
192. Birck, M. R., Holler, T. P. & Woodard, R. W. Identification of a slow tight-binding inhibitor of 3-deoxy-D-manno-octulosonic acid 8-phosphate synthase. *Journal of the American Chemical Society* vol. 122 (2000).
193. Hammond, S. M. *et al.* A new class of synthetic antibacterials acting on lipopolysaccharide biosynthesis. *Nature* **327**, (1987).
194. Goldman, R., Kohlbrenner, W., Lartey, P. & Pernet, A. Antibacterial agents specifically inhibiting lipopolysaccharide synthesis. *Nature* **329**, (1987).
195. Laguri, C. *et al.* Interaction of lipopolysaccharides at intermolecular sites of the periplasmic Lpt transport assembly. *Scientific Reports* **7**, (2017).
196. Balibar, C. J. & Grabowicz, M. Mutant alleles of *lptD* increase the permeability of *Pseudomonas aeruginosa* and define determinants of intrinsic resistance to antibiotics. *Antimicrobial Agents and Chemotherapy* **60**, (2016).
197. Okuda, S., Sherman, D. J., Silhavy, T. J., Ruiz, N. & Kahne, D. Lipopolysaccharide transport and assembly at the outer membrane: The PEZ model. *Nature Reviews Microbiology* vol. 14 (2016).
198. Ruiz, N., Kahne, D. & Silhavy, T. J. Transport of lipopolysaccharide across the cell envelope: The long road of discovery. *Nature Reviews Microbiology* vol. 7 (2009).
199. Karow, M. & Georgopoulos, C. The essential *Escherichia coli msbA* gene, a multicopy suppressor of null mutations in the *htrB* gene, is related to the universally conserved family of ATP-dependent translocators. *Molecular Microbiology* **7**, (1993).

200. Jones, P. M. & George, A. M. The ABC transporter structure and mechanism: Perspectives on recent research. *Cellular and Molecular Life Sciences* vol. 61 (2004).
201. Ward, A., Reyes, C. L., Yu, J., Roth, C. B. & Chang, G. Flexibility in the ABC transporter MsbA: Alternating access with a twist. *Proc Natl Acad Sci U S A* **104**, (2007).
202. Polissi, A. & Georgopoulos, C. Mutational analysis and properties of the *msbA* gene of *Escherichia coli*, coding for an essential ABC family transporter. *Molecular Microbiology* **20**, (1996).
203. Zhou, Z., White, K. A., Polissi, A., Georgopoulos, C. & Raetz, C. R. H. Function of *Escherichia coli* MsbA, an essential ABC family transporter, in lipid A and phospholipid biosynthesis. *Journal of Biological Chemistry* **273**, (1998).
204. Doerrler, W. T., Gibbons, H. S., Christian, R. & Raetz, H. MsbA-dependent translocation of lipids across the inner membrane of *Escherichia coli*. *Journal of Biological Chemistry* **279**, (2004).
205. Doerrler, W. T. & Raetz, C. R. H. ATPase activity of the MsbA lipid flippase of *Escherichia coli*. *Journal of Biological Chemistry* **277**, (2002).
206. Meredith, T. C., Aggarwal, P., Mamat, U., Lindner, B. & Woodard, R. W. Redefining the requisite lipopolysaccharide structure in *Escherichia coli*. *ACS Chem Biol* **1**, (2006).
207. Mamat, U. *et al.* Single amino acid substitutions in either YhjD or MsbA confer viability to 3-deoxy-D-manno-oct-2-ulosonic acid-depleted *Escherichia coli*. *Molecular Microbiology* **67**, (2008).
208. Liu, D., Cole, R. A. & Reeves, P. R. An O-antigen processing function for Wzx (RfbX): A promising candidate for O-unit flippase. *Journal of Bacteriology* **178**, (1996).
209. Rick, P. D. *et al.* Evidence that the *wzxE* gene of *Escherichia coli* K-12 encodes a protein involved in the transbilayer movement of a trisaccharide-lipid intermediate in the assembly of enterobacterial common antigen. *Journal of Biological Chemistry* **278**, (2003).
210. Hong, Y., Cunneen, M. M. & Reeves, P. R. The Wzx translocases for *Salmonella enterica* O-antigen processing have unexpected serotype specificity. *Molecular Microbiology* **84**, (2012).
211. Hvorup, R. N. *et al.* The multidrug/oligosaccharidyl-lipid/polysaccharide (MOP) exporter superfamily. *European Journal of Biochemistry* vol. 270 (2003).
212. Islam, S. T. & Lam, J. S. Synthesis of bacterial polysaccharides via the Wzx/Wzy-dependent pathway. *Canadian Journal of Microbiology* **60**, (2014).
213. Li, Y. *et al.* Molecular detection of all 34 distinct O-antigen forms of *Shigella*. *Journal of Medical Microbiology* **58**, (2009).
214. Macpherson, D. F., Manning, P. A. & Morona, R. Genetic analysis of the *rfbX* gene of *Shigella flexneri*. *Gene* **155**, (1995).
215. Marolda, C. L., Vicarioli, J. & Valvano, M. A. Wzx proteins involved in biosynthesis of O antigen function in association with the first sugar of the O-specific lipopolysaccharide subunit. *Microbiology (NY)* **150**, (2004).
216. Feldman, M. F. *et al.* The activity of a putative polyisoprenol-linked sugar translocase (Wzx) involved in *Escherichia coli* O antigen assembly is independent of the chemical structure of the O repeat. *Journal of Biological Chemistry* **274**, (1999).
217. Alaimo, C. *et al.* Two distinct but interchangeable mechanisms for flipping of lipid-linked oligosaccharides. *EMBO Journal* **25**, (2006).
218. McGrath, B. C. & Osborn, M. J. Localization of the terminal steps of O-antigen synthesis in *Salmonella typhimurium*. *Journal of Bacteriology* **173**, (1991).

219. Cuthbertson, L., Kos, V. & Whitfield, C. ABC Transporters Involved in Export of Cell Surface Glycoconjugates. *Microbiology and Molecular Biology Reviews* **74**, (2010).
220. Sperandeo, P., Dehò, G. & Polissi, A. The lipopolysaccharide transport system of Gram-negative bacteria. *Biochimica et Biophysica Acta - Molecular and Cell Biology of Lipids* vol. 1791 (2009).
221. Sperandeo, P., Martorana, A. M. & Polissi, A. The lipopolysaccharide transport (Lpt) machinery: A nonconventional transporter for lipopolysaccharide assembly at the outer membrane of Gram-negative bacteria. *Journal of Biological Chemistry* vol. 292 (2017).
222. Sperandeo, P. *et al.* Functional analysis of the protein machinery required for transport of lipopolysaccharide to the outer membrane of *Escherichia coli*. *Journal of Bacteriology* **190**, (2008).
223. Simpson, B. W., May, J. M., Sherman, D. J., Kahne, D. & Ruiz, N. Lipopolysaccharide transport to the cell surface: Biosynthesis and extraction from the inner membrane. *Philosophical Transactions of the Royal Society B: Biological Sciences* vol. 370 (2015).
224. Sherman, D. J. *et al.* Decoupling catalytic activity from biological function of the ATPase that powers lipopolysaccharide transport. *Proc Natl Acad Sci U S A* **111**, (2014).
225. Ruiz, N., Gronenberg, L. S., Kahne, D. & Silhavy, T. J. Identification of two inner-membrane proteins required for the transport of lipopolysaccharide to the outer membrane of *Escherichia coli*. *Proc Natl Acad Sci U S A* **105**, (2008).
226. Narita, S. Ichiro & Tokuda, H. Biochemical characterization of an ABC transporter LptBFGC complex required for the outer membrane sorting of lipopolysaccharides. *FEBS Letters* **583**, (2009).
227. Sherman, D. J., Okuda, S., Denny, W. A. & Kahne, D. Validation of inhibitors of an ABC transporter required to transport lipopolysaccharide to the cell surface in *Escherichia coli*. *Bioorganic and Medicinal Chemistry* **21**, (2013).
228. Sperandeo, P. *et al.* Characterization of *lptA* and *lptB*, two essential genes implicated in lipopolysaccharide transport to the outer membrane of *Escherichia coli*. *Journal of Bacteriology* **189**, (2007).
229. Villa, R. *et al.* The *Escherichia coli* *lpt* transenvelope protein complex for lipopolysaccharide export is assembled via conserved structurally homologous domains. *Journal of Bacteriology* **195**, (2013).
230. Freinkman, E., Okuda, S., Ruiz, N. & Kahne, D. Regulated Assembly of the Transenvelope Protein Complex Required for Lipopolysaccharide Export. *Biochemistry* **51**, (2012).
231. Bowyer, A., Baardsnes, J., Ajamian, E., Zhang, L. & Cygler, M. Characterization of interactions between LPS transport proteins of the Lpt system. *Biochemical and Biophysical Research Communications* **404**, (2011).
232. Sperandeo, P. *et al.* New insights into the Lpt machinery for lipopolysaccharide transport to the cell surface: LptA-LptC interaction and LptA stability as sensors of a properly assembled transenvelope complex. *Journal of Bacteriology* **193**, (2011).
233. Okuda, S., Freinkman, E. & Kahne, D. Cytoplasmic ATP hydrolysis powers transport of lipopolysaccharide across the periplasm in *E. coli*. *Science (1979)* **338**, (2012).
234. Suits, M. D. L., Sperandeo, P., Dehò, G., Polissi, A. & Jia, Z. Novel Structure of the Conserved Gram-Negative Lipopolysaccharide Transport Protein A and Mutagenesis Analysis. *Journal of Molecular Biology* **380**, (2008).
235. Tefsen, B., Geurtsen, J., Beckers, F., Tommassen, J. & de Cock, H. Lipopolysaccharide transport to the bacterial outer membrane in spheroplasts. *Journal of Biological Chemistry* **280**, (2005).

236. Chng, S. S., Gronenberg, L. S. & Kahne, D. Proteins required for lipopolysaccharide assembly in *Escherichia coli* form a transenvelope complex. *Biochemistry* **49**, (2010).
237. Ishidate, K. *et al.* Isolation of differentiated membrane domains from *Escherichia coli* and *Salmonella typhimurium*, including a fraction containing attachment sites between the inner and outer membranes and the murein skeleton of the cell envelope. *Journal of Biological Chemistry* **261**, (1986).
238. Bos, M. P., Tefsen, B., Geurtsen, J. & Tommassen, J. Identification of an outer membrane protein required for the transport of lipopolysaccharide to the bacterial cell surface. *Proc Natl Acad Sci U S A* **101**, (2004).
239. Braun, M. & Silhavy, T. J. Imp/OstA is required for cell envelope biogenesis in *Escherichia coli*. *Molecular Microbiology* **45**, (2002).
240. Wu, T. *et al.* Identification of a protein complex that assembles lipopolysaccharide in the outer membrane of *Escherichia coli*. *Proc Natl Acad Sci U S A* **103**, (2006).
241. Chng, S. S., Ruiz, N., Chimalakonda, G., Silhavy, T. J. & Kahne, D. Characterization of the two-protein complex in *Escherichia coli* responsible for lipopolysaccharide assembly at the outer membrane. *Proc Natl Acad Sci U S A* **107**, (2010).
242. Dong, H. *et al.* Structural basis for outer membrane lipopolysaccharide insertion. *Nature* **511**, (2014).
243. Qiao, S., Luo, Q., Zhao, Y., Zhang, X. C. & Huang, Y. Structural basis for lipopolysaccharide insertion in the bacterial outer membrane. *Nature* **511**, (2014).
244. Freinkman, E., Chng, S. S. & Kahne, D. The complex that inserts lipopolysaccharide into the bacterial outer membrane forms a two-protein plug-and-barrel. *Proc Natl Acad Sci U S A* **108**, (2011).
245. Chng, S. S. *et al.* Disulfide rearrangement triggered by translocon assembly controls lipopolysaccharide export. *Science (1979)* **337**, (2012).
246. Malojčić, G. *et al.* LptE binds to and alters the physical state of LPS to catalyze its assembly at the cell surface. *Proc Natl Acad Sci U S A* **111**, (2014).
247. Gu, Y. *et al.* Lipopolysaccharide is inserted into the outer membrane through an intramembrane hole, a lumen gate, and the lateral opening of *lptD*. *Structure* **23**, (2015).
248. Li, X., Gu, Y., Dong, H., Wang, W. & Dong, C. Trapped lipopolysaccharide and LptD intermediates reveal lipopolysaccharide translocation steps across the *Escherichia coli* outer membrane. *Scientific Reports* **5**, (2015).
249. Alexander, M. K. *et al.* Disrupting Gram-negative bacterial outer membrane biosynthesis through inhibition of the lipopolysaccharide transporter MsbA. *Antimicrobial Agents and Chemotherapy* **62**, (2018).
250. Ho, H. *et al.* Structural basis for dual-mode inhibition of the ABC transporter MsbA. *Nature* **557**, (2018).
251. Kamoshida, G. *et al.* Lipopolysaccharide-Deficient *Acinetobacter baumannii* Due to Colistin Resistance Is Killed by Neutrophil-Produced Lysozyme. *Frontiers in Microbiology* **11**, (2020).
252. Zhang, G. *et al.* Cell-based screen for discovering lipopolysaccharide biogenesis inhibitors. *Proc Natl Acad Sci U S A* **115**, (2018).
253. Gronenberg, L. S. & Kahne, D. Development of an activity assay for discovery of inhibitors of lipopolysaccharide transport. *J Am Chem Soc* **132**, (2010).
254. May, J. M. *et al.* The Antibiotic Novobiocin Binds and Activates the ATPase That Powers Lipopolysaccharide Transport. *J Am Chem Soc* **139**, (2017).

255. Mandler, M. D. *et al.* Novobiocin Enhances Polymyxin Activity by Stimulating Lipopolysaccharide Transport. *J Am Chem Soc* **140**, (2018).
256. Srinivas, N. *et al.* Peptidomimetic antibiotics target outer-membrane biogenesis in *Pseudomonas aeruginosa*. *Science (1979)* **327**, (2010).
257. Martin-Loeches, I., Dale, G. E. & Torres, A. Murepavadin: a new antibiotic class in the pipeline. *Expert Review of Anti-Infective Therapy* **16**, (2018).
258. Schmidt, J., Patora-Komisarska, K., Moehle, K., Obrecht, D. & Robinson, J. A. Structural studies of  $\beta$ -hairpin peptidomimetic antibiotics that target LptD in *Pseudomonas* sp. *Bioorganic and Medicinal Chemistry* **21**, (2013).
259. Sader, H. S., Dale, G. E., Rhomberg, P. R. & Flamm, R. K. Antimicrobial activity of murepavadin tested against clinical isolates of *Pseudomonas aeruginosa* from the United States, Europe, and China. *Antimicrobial Agents and Chemotherapy* **62**, (2018).
260. Díez-Aguilar, M. *et al.* Murepavadin antimicrobial activity against and resistance development in cystic fibrosis *Pseudomonas aeruginosa* isolates. *J Antimicrob Chemother* **76**, (2021).
261. Melchers, M. J. *et al.* Pharmacokinetics and pharmacodynamics of murepavadin in neutropenic mouse models. *Antimicrobial Agents and Chemotherapy* **63**, (2019).
262. Wach, A., Dembowsky, K. & Dale, G. E. Pharmacokinetics and safety of intravenous murepavadin infusion in healthy adult subjects administered single and multiple ascending doses. *Antimicrobial Agents and Chemotherapy* **62**, (2018).
263. Amponnawarat, A., Chompunud Na Ayudhya, C. & Ali, H. Murepavadin, a Small Molecule Host Defense Peptide Mimetic, Activates Mast Cells via MRGPRX2 and MrgprB2. *Frontiers in Immunology* **12**, (2021).
264. Upert, G., Luther, A., Obrecht, D. & Ermert, P. Emerging peptide antibiotics with therapeutic potential. *Medicine in Drug Discovery* vol. 9 (2021).
265. Satlin, M. J. & Jenkins, S. G. 151 - Polymyxins. in *Infectious Diseases (Fourth Edition)* (eds. Cohen, J., Powderly, W. G. & Opal, S. M.) 1285-1288.e2 (Elsevier, 2017).
266. Koyama, Y., Kurosasa, A., Tsuchiya, A. & Takakuta, K. A new antibiotic 'colistin' produced by spore-forming soil bacteria. *Antibiot* (1950).
267. Benedict, R. G. & Langlykke, A. F. Antibiotic activity of *Bacillus polymyxa*. *J Bacteriol* **54**, (1947).
268. Mahajan, G. B. & Balachandran, L. Sources of antibiotics: Hot springs. *Biochemical Pharmacology* vol. 134 (2017).
269. Tang, Q., Puri, A., Padda, K. P. & Chanway, C. P. Biological nitrogen fixation and plant growth promotion of lodgepole pine by an endophytic diazotroph *Paenibacillus polymyxa* and its GFP-tagged derivative. *Botany* **95**, (2017).
270. Padda, K. P., Puri, A. & Chanway, C. P. *Paenibacillus polymyxa*: A prominent biofertilizer and biocontrol agent for sustainable agriculture. in *Agriculturally Important Microbes for Sustainable Agriculture* vol. 2 (2017).
271. Li, Y. X., Zhong, Z., Zhang, W. P. & Qian, P. Y. Discovery of cationic nonribosomal peptides as Gram-negative antibiotics through global genome mining. *Nature Communications* **9**, (2018).
272. Rhouma, M., Beaudry, F., Thériault, W. & Letellier, A. Colistin in pig production: Chemistry, mechanism of antibacterial action, microbial resistance emergence, and one health perspectives. *Frontiers in Microbiology* vol. 7 (2016).
273. Storm, D. R., Rosenthal, K. S. & Swanson, P. E. Polymyxin and related peptide antibiotics. *Annual Review of Biochemistry* vol. Vol. 46 (1977).

274. Falagas, M. E. & Kasiakou, S. K. Colistin: The revival of polymyxins for the management of multidrug-resistant gram-negative bacterial infections. *Clinical Infectious Diseases* vol. 40 (2005).
275. Orwa, J. A. *et al.* Isolation and structural characterization of colistin components. *Journal of Antibiotics* **54**, (2001).
276. Decolin, D., Leroy, P., Nicolas, A. & Archimbault, P. Hyphenated Liquid Chromatographic Method for the Determination of Colistin Residues in Bovine Tissues. *Journal of Chromatographic Science* **35**, (1997).
277. Zavascki, A. P., Goldani, L. Z., Li, J. & Nation, R. L. Polymyxin B for the treatment of multidrug-resistant pathogens: A critical review. *Journal of Antimicrobial Chemotherapy* vol. 60 (2007).
278. Li, J. *et al.* Colistin: the re-emerging antibiotic for multidrug-resistant Gram-negative bacterial infections. *Lancet Infectious Diseases* vol. 6 (2006).
279. Azzopardi, E. A., Boyce, D. E., Thomas, D. W. & Dickson, W. A. Colistin in burn intensive care: Back to the future? *Burns* vol. 39 (2013).
280. Velkov, T., Thompson, P. E., Nation, R. L. & Li, J. Structure-activity relationships of polymyxin antibiotics. *Journal of Medicinal Chemistry* vol. 53 (2010).
281. Meredith, J. J., Dufour, A. & Bruch, M. D. Comparison of the structure and dynamics of the antibiotic peptide polymyxin B and the inactive nonapeptide in aqueous trifluoroethanol by NMR spectroscopy. *Journal of Physical Chemistry B* **113**, (2009).
282. Pristovšek, P. & Kidrič, J. Solution structure of polymyxins B and E and effect of binding to lipopolysaccharide: An NMR and molecular modeling study. *Journal of Medicinal Chemistry* **42**, (1999).
283. Dewick, P. M. Peptides, Proteins, and Other Amino Acid Derivatives. in *Medicinal Natural Products* (2009).
284. Tambadou, F. *et al.* Characterization of the colistin (polymyxin E1 and E2) biosynthetic gene cluster. *Archives of Microbiology* **197**, (2015).
285. Ito, M., Aida, K. & Uemura, T. Biosynthesis of colistin by *Bacillus colistinus* Koyama. *BBA Section Nucleic Acids And Protein Synthesis* **213**, (1970).
286. Choi, S. K. *et al.* Identification of a polymyxin synthetase gene cluster of *Paenibacillus polymyxa* and heterologous expression of the gene in *Bacillus subtilis*. *Journal of Bacteriology* **191**, (2009).
287. Shaheen, M., Li, J., Ross, A. C., Vederas, J. C. & Jensen, S. E. *Paenibacillus polymyxa* PKB1 produces variants of polymyxin B-type antibiotics. *Chemistry and Biology* **18**, (2011).
288. Kopp, F. & Marahiel, M. A. Macrocyclization strategies in polyketide and nonribosomal peptide biosynthesis. *Natural Product Reports* vol. 24 (2007).
289. Bergen, P. J., Li, J., Rayner, C. R. & Nation, R. L. Colistin methanesulfonate is an inactive prodrug of colistin against *Pseudomonas aeruginosa*. *Antimicrobial Agents and Chemotherapy* **50**, (2006).
290. Bennett, J. E., Dolin, R. & Blaser, M. J. *Mandell, Douglas, and Bennett's Principles and Practice of Infectious Diseases* vols. 1–2 (2014).
291. Conly, J. M. & Johnston, B. L. Colistin: The phoenix arises. *Canadian Journal of Infectious Diseases and Medical Microbiology* **17**, (2006).
292. Rhouma, M. *et al.* Gastric stability and oral bioavailability of colistin sulfate in pigs challenged or not with *Escherichia coli* O149: F4 (K88). *Research in Veterinary Science* **102**, (2015).



293. Mead, A., Richez, P., Azzariti, S. & Pelligand, L. Pharmacokinetics of Colistin in the Gastrointestinal Tract of Poultry Following Dosing via Drinking Water and Its Bactericidal Impact on Enteric *Escherichia coli*. *Frontiers in Veterinary Science* **8**, (2021).
294. Biswas, S., Brunel, J. M., Dubus, J. C., Reynaud-Gaubert, M. & Rolain, J. M. Colistin: An update on the antibiotic of the 21st century. *Expert Review of Anti-Infective Therapy* vol. 10 (2012).
295. Barnett, M., Bushby, S. R. M. & Wilkinson, S. Sodium sulphomethyl derivatives of polymyxins. *British Journal of Pharmacology and Chemotherapy* **23**, (1964).
296. Beveridge, E. G. & Martin, A. J. Sodium sulphomethyl derivatives of polymyxins. *British Journal of Pharmacology and Chemotherapy* **29**, (1967).
297. Li, J., Milne, R. W., Nation, R. L., Turnidge, J. D. & Coulthard, K. Stability of colistin and colistin methanesulfonate in aqueous media and plasma as determined by high-performance liquid chromatography. *Antimicrobial Agents and Chemotherapy* **47**, (2003).
298. Li, J. *et al.* Pharmacokinetics of colistin methanesulphonate and colistin in rats following an intravenous dose of colistin methanesulphonate. *Journal of Antimicrobial Chemotherapy* **53**, (2004).
299. Wahby, K., Chopra, T. & Chandrasekar, P. Intravenous and inhalational colistin-induced respiratory failure. *Clinical Infectious Diseases* **50**, (2010).
300. Michalopoulos, A., Kasiakou, S. K., Rosmarakis, E. S. & Falagas, M. E. Cure of multidrug-resistant *Acinetobacter baumannii* bacteraemia with continuous intravenous infusion of colistin. *Scandinavian Journal of Infectious Diseases* **37**, (2005).
301. Koch-Weser, J. *et al.* Adverse effects of sodium colistimethate. Manifestations and specific reaction rates during 317 courses of therapy. *Ann Intern Med* **72**, (1970).
302. Karaiskos, I., Galani, L., Baziaka, F. & Giamarellou, H. Intraventricular and intrathecal colistin as the last therapeutic resort for the treatment of multidrug-resistant and extensively drug-resistant *Acinetobacter baumannii* ventriculitis and meningitis: A literature review. *International Journal of Antimicrobial Agents* vol. 41 (2013).
303. Karvouniaris, M. *et al.* Nebulised colistin for ventilator-associated pneumonia prevention. *European Respiratory Journal* **46**, (2015).
304. Aygun, F. *et al.* Can nebulised colistin therapy improve outcomes in critically ill children with multi-drug resistant gram-negative bacterial pneumonia? *Antibiotics* **8**, (2019).
305. Cunningham, S. *et al.* Bronchoconstriction following nebulised colistin in cystic fibrosis. *Archives of Disease in Childhood* **84**, (2001).
306. Evans, M. E., Feola, D. J. & Rapp, R. P. Polymyxin B sulfate and colistin: Old antibiotics for emerging multiresistant gram-negative bacteria. *Annals of Pharmacotherapy* vol. 33 (1999).
307. Kumazawa, J. & Yagisawa, M. The history of antibiotics: The Japanese story. *Journal of Infection and Chemotherapy* vol. 8 (2002).
308. Nation, R. L. & Li, J. Colistin in the 21st century. *Current Opinion in Infectious Diseases* vol. 22 (2009).
309. Kempf, I., Jouy, E. & Chauvin, C. Colistin use and colistin resistance in bacteria from animals. *International Journal of Antimicrobial Agents* **48**, (2016).
310. Li, J., Turnidge, J., Milne, R., Nation, R. L. & Coulthard, K. In vitro pharmacodynamic properties of colistin and colistin methanesulfonate against *Pseudomonas aeruginosa* isolates from patients with cystic fibrosis. *Antimicrobial Agents and Chemotherapy* **45**, (2001).
311. Conway, S. P. *et al.* Intravenous colistin sulphomethate in acute respiratory exacerbations in adult patients with cystic fibrosis. *Thorax* **52**, (1997).

312. Ledson, M. J., Gallagher, M. J., Cowperthwaite, C., Convery, R. P. & Walshaw, M. J. Four years' experience of intravenous colomycin in an adult cystic fibrosis unit. *European Respiratory Journal* **12**, (1998).
313. Giamarellou, H. & Poulakou, G. Multidrug-resistant gram-negative infections: What are the treatment options? *Drugs* vol. 69 (2009).
314. Davies M & Wasley A. Summary of Antibiotic Use in Hospitals, England, 2010-2015. (2017).
315. Public Health England. English Surveillance Programme for Antimicrobial Utilisation and Resistance (ESPAUR) Report 2018. (2018).
316. Beringer, P. & Shapiro, B. J. The clinical use of colistin in patients with cystic fibrosis. *Current Opinion in Pulmonary Medicine* vol. 7 (2001).
317. Goodwin, N. J. Colistin and Sodium Colistimethate. *Medical Clinics of North America* **54**, (1970).
318. Bergen, P. J., Li, J. & Nation, R. L. Dosing of colistin - Back to basic PK/PD. *Current Opinion in Pharmacology* vol. 11 (2011).
319. Ortwine, J. K., Kaye, K. S., Li, J. & Pogue, J. M. Colistin: Understanding and applying recent Pharmacokinetic advances. *Pharmacotherapy* vol. 35 (2015).
320. Lim, L. M. *et al.* Resurgence of colistin: A review of resistance, toxicity, pharmacodynamics, and dosing. *Pharmacotherapy* vol. 30 (2010).
321. Falagas, M. E., Kasiakou, S. K., Tsiodras, S. & Michalopoulos, A. The use of intravenous and aerosolized polymyxins for the treatment of infections in critically ill patients: A review of the recent literature. *Clinical Medicine and Research* vol. 4 (2006).
322. Curtis, J. R. & Eastwood, J. B. Colistin Sulphomethate Sodium Administration in the Presence of Severe Renal Failure and During Haemodialysis and Peritoneal Dialysis. *British Medical Journal* **1**, (1968).
323. Michalopoulos, A. & Falagas, M. E. Colistin and Polymyxin B in Critical Care. *Critical Care Clinics* vol. 24 (2008).
324. Kasiakou, S. K., Rafailidis, P. I., Liaropoulos, K. & Falagas, M. E. Cure of post-traumatic recurrent multiresistant Gram-negative rod meningitis with intraventricular colistin. *Journal of Infection* **50**, (2005).
325. Quinn, A. L., Parada, J. P., Belmares, J. & O'Keefe, J. P. Intrathecal colistin and sterilization of resistant *Pseudomonas aeruginosa* shunt infection. *Annals of Pharmacotherapy* **39**, (2005).
326. Bukhary, Z., Mahmood, W., Al-Khani, A. & Al-Abdely, H. M. Treatment of nosocomial meningitis due to a multidrug resistant *Acinetobacter baumannii* with intraventricular colistin. *Saudi Medical Journal* **26**, (2005).
327. Ng, J., Gosbell, I. B., Boyle, M. J. & Ferguson, J. K. Cure of multiresistant *Acinetobacter baumannii* central nervous system infections with intraventricular or intrathecal colistin: Case series and literature review. *Journal of Antimicrobial Chemotherapy* **58**, (2006).
328. Benifla, M., Zucker, G., Cohen, A. & Alkan, M. Successful treatment of *Acinetobacter* meningitis with intrathecal polymyxin E. *Journal of Antimicrobial Chemotherapy* vol. 54 (2004).
329. Fernandez-Viladrich, P., Corbella, X., Corral, L., Tubau, F. & Mateu, A. Successful treatment of ventriculitis due to carbapenem-resistant *Acinetobacter baumannii* with intraventricular colistin sulfomethate sodium. *Clinical Infectious Diseases* **28**, (1999).
330. Vasen, W., Desmery, P., Ilutovich, S. & di Martino, A. Intrathecal use of colistin. *Journal of Clinical Microbiology* vol. 38 (2000).

331. Li, J. *et al.* Steady-state pharmacokinetics of intravenous colistin methanesulphonate in patients with cystic fibrosis. *Journal of Antimicrobial Chemotherapy* **52**, (2003).
332. Li, J. *et al.* Use of high-performance liquid chromatography to study the pharmacokinetics of colistin sulfate in rats following intravenous administration. *Antimicrobial Agents and Chemotherapy* **47**, (2003).
333. Ma, Z. *et al.* Renal disposition of colistin in the isolated perfused rat kidney. *Antimicrobial Agents and Chemotherapy* **53**, (2009).
334. Sorlí, L. *et al.* Colistin for the treatment of urinary tract infections caused by extremely drug-resistant *Pseudomonas aeruginosa*: Dose is critical. *Journal of Infection* **79**, (2019).
335. Luque, S. *et al.* Urinary concentrations of colistimethate and formed colistin after intravenous administration in patients with multidrug-resistant gram-negative bacterial infections. *Antimicrobial Agents and Chemotherapy* **61**, (2017).
336. Zhao, M. *et al.* Pharmacokinetics of colistin methanesulfonate (CMS) in healthy Chinese subjects after single and multiple intravenous doses. *International Journal of Antimicrobial Agents* **51**, (2018).
337. Kunin, C. M. & Bugg, A. Binding of polymyxin antibiotics to tissues: The major determinant of distribution and persistence in the body. *Journal of Infectious Diseases* **124**, (1971).
338. Craig, W. A. & Kunin, C. M. Significance of serum protein and tissue binding of antimicrobial agents. *Annual review of medicine* vol. 27 (1976).
339. al Khayyat, A. A. & Aronson, A. L. Pharmacologic and toxicologic studies with the polymyxins. III. Considerations regarding clinical use in dogs. *Chemotherapy* **19**, (1973).
340. Ziv, G., Nouws, J. F. M. & van Ginneken, C. A. M. The pharmacokinetics and tissue levels of polymyxin B, colistin and gentamicin in calves. *Journal of Veterinary Pharmacology and Therapeutics* vol. 5 (1982).
341. Marchand, S., Lamarche, I., Gobin, P. & Couet, W. Dose-ranging pharmacokinetics of colistin methanesulphonate (CMS) and colistin in rats following single intravenous CMS doses. *Journal of Antimicrobial Chemotherapy* **65**, (2010).
342. Plachouras, D. *et al.* Population pharmacokinetic analysis of colistin methanesulfonate and colistin after intravenous administration in critically ill patients with infections caused by gram-negative bacteria. *Antimicrobial Agents and Chemotherapy* **53**, (2009).
343. Imberti, R. *et al.* Steady-state pharmacokinetics and BAL concentration of colistin in critically ill patients after IV colistin methanesulfonate administration. *Chest* **138**, (2010).
344. Markou, N. *et al.* Colistin serum concentrations after intravenous administration in critically ill patients with serious multidrug-resistant, gram-negative bacilli infections: A prospective, open-label, uncontrolled study. *Clinical Therapeutics* **30**, (2008).
345. Mohamed, A. F., Cars, O. & Friberg, L. E. A pharmacokinetic/pharmacodynamic model developed for the effect of colistin on *Pseudomonas aeruginosa in vitro* with evaluation of population pharmacokinetic variability on simulated bacterial killing. *Journal of Antimicrobial Chemotherapy* **69**, (2014).
346. Bergen, P. J. *et al.* Pharmacokinetic/pharmacodynamic investigation of colistin against *Pseudomonas aeruginosa* using an *in vitro* model. *Antimicrobial Agents and Chemotherapy* **54**, (2010).
347. Bergen, P. J. *et al.* Comparison of once-, twice- and thrice-daily dosing of colistin on antibacterial effect and emergence of resistance: Studies with *Pseudomonas aeruginosa* in an *in vitro* pharmacodynamic model. *Journal of Antimicrobial Chemotherapy* **61**, (2008).

348. Tam, V. H. *et al.* Pharmacodynamics of polymyxin B against *Pseudomonas aeruginosa*. *Antimicrobial Agents and Chemotherapy* **49**, (2005).
349. Li, J., Nation, R. L., Milne, R. W., Turnidge, J. D. & Coulthard, K. Evaluation of colistin as an agent against multi-resistant Gram-negative bacteria. *International Journal of Antimicrobial Agents* vol. 25 (2005).
350. Falagas, M. E. & Kasiakou, S. K. Toxicity of polymyxins: A systematic review of the evidence from old and recent studies. *Critical Care* vol. 10 (2006).
351. Price, D. J. E. & Graham, D. I. Effects of Large Doses of Colistin Sulphomethate Sodium on Renal Function. *British Medical Journal* **4**, (1970).
352. Wolinsky, E. & Hines, J. D. Neurotoxic and Nephrotoxic Effects of Colistin in Patients with Renal Disease. *New England Journal of Medicine* **266**, (1962).
353. Hopper, J., Jawetz, E. & Hinman, F. Polymyxin B in chronic pyelonephritis: observations on the safety of the drug and on its influence on the renal infection. *Am J Med Sci* **225**, (1953).
354. Falagas, M. E. *et al.* Toxicity after prolonged (more than four weeks) administration of intravenous colistin. *BMC Infectious Diseases* **5**, (2005).
355. Hartzell, J. D. *et al.* Nephrotoxicity associated with intravenous colistin (colistimethate sodium) treatment at a tertiary care medical center. *Clinical Infectious Diseases* **48**, (2009).
356. Falagas, M. E., Fragoulis, K. N., Kasiakou, S. K., Sermaidis, G. J. & Michalopoulos, A. Nephrotoxicity of intravenous colistin: A prospective evaluation. *International Journal of Antimicrobial Agents* **26**, (2005).
357. Kim, J., Lee, K. H., Yoo, S. & Pai, H. Clinical characteristics and risk factors of colistin-induced nephrotoxicity. *International Journal of Antimicrobial Agents* **34**, (2009).
358. Randall, R. E., Bridi, G. S., Setter, J. G. & Brackett, N. C. Recovery from colistimethate nephrotoxicity. *Ann Intern Med* **73**, (1970).
359. Gauthier, T. P. *et al.* Incidence and predictors of nephrotoxicity associated with intravenous colistin in overweight and obese patients. *Antimicrobial Agents and Chemotherapy* **56**, (2012).
360. Kasiakou, S. K. *et al.* Combination therapy with intravenous colistin for management of infections due to multidrug-resistant gram-negative bacteria in patients without cystic fibrosis. *Antimicrobial Agents and Chemotherapy* **49**, (2005).
361. Markou, N. *et al.* Intravenous colistin in the treatment of sepsis from multiresistant Gram-negative bacilli in critically ill patients. *Crit Care* **7**, (2003).
362. Lopes, J. A. & Jorge, S. The RIFLE and AKIN classifications for acute kidney injury: A critical and comprehensive review. *Clinical Kidney Journal* vol. 6 (2013).
363. Hoste, E. A. J. *et al.* RIFLE criteria for acute kidney injury are associated with hospital mortality in critically ill patients: A cohort analysis. *Critical Care* **10**, (2006).
364. van Biesen, W., Vanholder, R. & Lameire, N. Defining acute renal failure: RIFLE and beyond. *Clinical journal of the American Society of Nephrology : CJASN* vol. 1 (2006).
365. Kwon, J. A. *et al.* Predictors of acute kidney injury associated with intravenous colistin treatment. *International Journal of Antimicrobial Agents* **35**, (2010).
366. Ko, H. J. *et al.* Early acute kidney injury is a risk factor that predicts mortality in patients treated with colistin. *Nephron - Clinical Practice* **117**, (2011).
367. Molina, J., Cordero, E. & Pachón, J. New information about the polymyxin/colistin class of antibiotics. *Expert Opinion on Pharmacotherapy* vol. 10 (2009).

368. Falagas, M. E., Kasiakou, S. K., Kofteridis, D. P., Roditakis, G. & Samonis, G. Effectiveness and nephrotoxicity of intravenous colistin for treatment of patients with infections due to polymyxin-only-susceptible (POS) gram-negative bacteria. *European Journal of Clinical Microbiology and Infectious Diseases* **25**, (2006).
369. Michalopoulos, A. S., Tsiodras, S., Rellos, K., Mentzelopoulos, S. & Falagas, M. E. Colistin treatment in patients with ICU-acquired infections caused by multiresistant Gram-negative bacteria: The renaissance of an old antibiotic. *Clinical Microbiology and Infection* **11**, (2005).
370. Pintado, V. *et al.* Intravenous colistin sulphomethate sodium for therapy of infections due to multidrug-resistant gram-negative bacteria. *Journal of Infection* **56**, (2008).
371. Reina, R. *et al.* Safety and efficacy of colistin in *Acinetobacter* and *Pseudomonas* infections: A prospective cohort study. *Intensive Care Medicine* **31**, (2005).
372. Levin, A. S. *et al.* Intravenous colistin as therapy for nosocomial infections caused by multidrug-resistant *Pseudomonas aeruginosa* and *Acinetobacter baumannii*. *Clinical Infectious Diseases* **28**, (1999).
373. Seilheimer, D. K. & Harrison, G. M. Toxicity of colistin in cystic fibrosis patients. *Annals of Pharmacotherapy* **25**, (1991).
374. Babar, Z. U., Dodani, S. K. & Nasim, A. Treatment outcome and adverse effects of colistin in adult patients with carbapenem-resistant gram-negative bacteremia from Pakistan. *International Journal of Infectious Diseases* **106**, (2021).
375. Garnacho-Montero, J. *et al.* Treatment of multidrug-resistant *Acinetobacter baumannii* ventilator-associated pneumonia (VAP) with intravenous colistin: A comparison with imipenem-susceptible VAP. *Clinical Infectious Diseases* **36**, (2003).
376. Wadia, S. & Tran, B. Colistin-mediated neurotoxicity. *BMJ Case Reports* **2014**, (2014).
377. Nigam, A., Kumari, A., Jain, R. & Batra, S. Colistin neurotoxicity: Revisited. *BMJ Case Reports* **2015**, (2015).
378. Duncan, D. A. Colistin toxicity. Neuromuscular and renal manifestations. Two cases treated by hemodialysis. *Minnesota Medicine* **56**, (1973).
379. Spapen, H., Jacobs, R., van Gorp, V., Troubleyn, J. & Honoré, P. M. Renal and neurological side effects of colistin in critically ill patients. *Annals of Intensive Care* **1**, (2011).
380. Radhakrishnan, R. C., Jacob, S., Pathak, H. R. & Tamilarasi, V. Colistin Induced Neurotoxicity in a Patient with End Stage Kidney Disease and Recovery with Conventional Hemodialysis. *The Open Urology & Nephrology Journal* **8**, (2015).
381. Tosi, M. F., Konstan, M. W. & Paschall, V. L. Rapid intravenous desensitization to colistin. *Annals of Allergy, Asthma and Immunology* **109**, (2012).
382. Lee, H. Y. *et al.* Risk factors and outcomes of *Clostridium difficile* infection in hospitalized patients. *Biomedical Journal* **42**, (2019).
383. Schindler, M. & Osborn, M. J. Interaction of Divalent Cations and Polymyxin B with Lipopolysaccharide. *Biochemistry* **18**, (1979).
384. Hancock, R. E. Antibacterial peptides and the outer membranes of gram-negative bacilli. *Journal of Medical Microbiology* vol. 46 (1997).
385. Hancock, R. E. W. & Lehrer, R. Cationic peptides: A new source of antibiotics. *Trends in Biotechnology* vol. 16 (1998).
386. Clausell, A. *et al.* Gram-negative outer and inner membrane models: Insertion of cyclic cationic lipopeptides. *Journal of Physical Chemistry B* **111**, (2007).

387. Melo, M. N., Ferre, R. & Castanho, M. A. R. B. Antimicrobial peptides: Linking partition, activity and high membrane-bound concentrations. *Nature Reviews Microbiology* **7**, (2009).
388. Powers, J. P. S. & Hancock, R. E. W. The relationship between peptide structure and antibacterial activity. *Peptides (N.Y.)* **24**, (2003).
389. Clifton, L. A. *et al.* Effect of divalent cation removal on the structure of gram-negative bacterial outer membrane models. *Langmuir* **31**, (2015).
390. Rice, A. & Wereszczynski, J. Atomistic Scale Effects of Lipopolysaccharide Modifications on Bacterial Outer Membrane Defenses. *Biophysical Journal* **114**, (2018).
391. Rahnamoun, A., Kim, K., Pedersen, J. A. & Hernandez, R. Ionic Environment Affects Bacterial Lipopolysaccharide Packing and Function. *Langmuir* **36**, (2020).
392. El-Sayed Ahmed, M. A. E. G. *et al.* Colistin and its role in the Era of antibiotic resistance: an extended review (2000–2019). *Emerging Microbes and Infections* vol. 9 (2020).
393. Mularski, A. *et al.* A nanomechanical study of the effects of colistin on the *Klebsiella pneumoniae* AJ218 capsule. *European Biophysics Journal* **46**, (2017).
394. Dupuy, F. G. *et al.* Selective Interaction of Colistin with Lipid Model Membranes. *Biophysical Journal* **114**, (2018).
395. Zhang, L., Dhillon, P., Yan, H., Farmer, S. & Hancock, R. E. W. Interactions of bacterial cationic peptide antibiotics with outer and cytoplasmic membranes of *Pseudomonas aeruginosa*. *Antimicrobial Agents and Chemotherapy* **44**, (2000).
396. Elias, R., Duarte, A. & Perdigão, J. A molecular perspective on colistin and *Klebsiella pneumoniae*: Mode of action, resistance genetics, and phenotypic susceptibility. *Diagnostics* vol. 11 (2021).
397. Hancock, R. E. W. The bacterial outer membrane as a drug barrier. *Trends in Microbiology* vol. 5 (1997).
398. Bialvaei, A. Z. & Samadi Kafil, H. Colistin, mechanisms and prevalence of resistance. *Current Medical Research and Opinion* vol. 31 (2015).
399. Gales, A. C., Jones, R. N. & Sader, H. S. Global assessment of the antimicrobial activity of polymyxin B against 54 731 clinical isolates of Gram-negative bacilli: Report from the SENTRY antimicrobial surveillance programme (2001-2004). *Clinical Microbiology and Infection* **12**, (2006).
400. Falagas, M. E., Rafailidis, P. I. & Matthaïou, D. K. Resistance to polymyxins: Mechanisms, frequency and treatment options. *Drug Resistance Updates* **13**, (2010).
401. Davis, S. D., Iannetta, A. & Wedgwood, R. J. Activity of colistin against *Pseudomonas aeruginosa*: Inhibition by calcium. *Journal of Infectious Diseases* **124**, (1971).
402. Newton, B. A. The properties and mode of action of the polymyxins. *Bacteriological Reviews* **20**, (1956).
403. Koike, M., Iida, K. & Matsuo, T. Electron microscopic studies on mode of action of polymyxin. *J Bacteriol* **97**, (1969).
404. Pristovsek, P. & Kidric, J. The Search for Molecular Determinants of LPS Inhibition by Proteins and Peptides. *Current Topics in Medicinal Chemistry* **4**, (2005).
405. Bruch, M. D., Cajal, Y., Koh, J. T. & Jain, M. K. Higher-order structure of polymyxin B: The functional significance of topological flexibility. *J Am Chem Soc* **121**, (1999).
406. Nation, R. L., Velkov, T. & Li, J. Colistin and polymyxin B: Peas in a pod, or chalk and cheese? *Clinical Infectious Diseases* vol. 59 (2014).

407. Mares, J., Kumaran, S., Gobbo, M. & Zerbe, O. Interactions of lipopolysaccharide and polymyxin studied by NMR spectroscopy. *Journal of Biological Chemistry* **284**, (2009).
408. Khondker, A. & Rheinstädter, M. C. How do bacterial membranes resist polymyxin antibiotics? *Communications Biology* vol. 3 (2020).
409. Tangso, K. J., da Cunha, P. H. C. D., Spicer, P., Li, J. & Boyd, B. J. Antimicrobial Activity from Colistin-Heparin Lamellar-Phase Complexes for the Coating of Biomedical Devices. *ACS Applied Materials and Interfaces* **8**, (2016).
410. Bibi, M. *et al.* Combining Colistin and Fluconazole Synergistically Increases Fungal Membrane Permeability and Antifungal Cidalty. *ACS Infectious Diseases* **7**, (2021).
411. Bechinger, B. & Lohner, K. Detergent-like actions of linear amphipathic cationic antimicrobial peptides. *Biochimica et Biophysica Acta - Biomembranes* vol. 1758 (2006).
412. Zeth, K. & Sancho-Vaello, E. The human antimicrobial peptides dermcidin and LL-37 show novel distinct pathways in membrane interactions. *Frontiers in Chemistry* vol. 5 (2017).
413. Cajal, Y., Rogers, J., Berg, O. G. & Jain, M. K. Intermembrane molecular contacts by polymyxin B mediate exchange of phospholipids. *Biochemistry* **35**, (1996).
414. Clausell, A., Rabanal, F., Garcia-Subirats, M., Alsina, M. A. & Cajal, Y. Membrane association and contact formation by a synthetic analogue of polymyxin B and its fluorescent derivatives. *Journal of Physical Chemistry B* **110**, (2006).
415. Kracke, F., Vassilev, I. & Krömer, J. O. Microbial electron transport and energy conservation - The foundation for optimizing bioelectrochemical systems. *Frontiers in Microbiology* vol. 6 (2015).
416. Berrisford, J. M., Baradaran, R. & Sazanov, L. A. Structure of bacterial respiratory complex I. *Biochimica et Biophysica Acta - Bioenergetics* **1857**, (2016).
417. Gutiérrez-Fernández, J. *et al.* Key role of quinone in the mechanism of respiratory complex I. *Nature Communications* **11**, (2020).
418. Deris, Z. Z. *et al.* A secondary mode of action of polymyxins against Gram-negative bacteria involves the inhibition of NADH-quinone oxidoreductase activity. *Journal of Antibiotics* **67**, (2014).
419. Yu, Z., Zhu, Y., Fu, J., Qiu, J. & Yin, J. Enhanced NADH metabolism involves colistin-induced killing of *Bacillus subtilis* and *Paenibacillus polymyxa*. *Molecules* **24**, (2019).
420. Mogi, T. *et al.* Polymyxin B identified as an inhibitor of alternative NADH dehydrogenase and malate: Quinone oxidoreductase from the gram-positive bacterium *Mycobacterium smegmatis*. *Journal of Biochemistry* **146**, (2009).
421. Yu, Z., Qin, W., Lin, J., Fang, S. & Qiu, J. Antibacterial mechanisms of polymyxin and bacterial resistance. *BioMed Research International* vol. 2015 (2015).
422. Imlay, J. A. The molecular mechanisms and physiological consequences of oxidative stress: Lessons from a model bacterium. *Nature Reviews Microbiology* vol. 11 (2013).
423. Sampson, T. R. *et al.* Rapid killing of *Acinetobacter baumannii* by polymyxins is mediated by a hydroxyl radical death pathway. *Antimicrobial Agents and Chemotherapy* **56**, (2012).
424. Kohanski, M. A., Dwyer, D. J., Hayete, B., Lawrence, C. A. & Collins, J. J. A Common Mechanism of Cellular Death Induced by Bactericidal Antibiotics. *Cell* **130**, (2007).
425. Yeom, J., Imlay, J. A. & Park, W. Iron homeostasis affects antibiotic-mediated cell death in *Pseudomonas* species. *Journal of Biological Chemistry* **285**, (2010).

426. Dwyer, D. J., Kohanski, M. A., Hayete, B. & Collins, J. J. Gyrase inhibitors induce an oxidative damage cellular death pathway in *Escherichia coli*. *Molecular Systems Biology* **3**, (2007).
427. Nakajima, K. & Kawamata, J. Studies on the mechanism of action of colistin. IV. Activation of "latent" ribonuclease in *Escherichia coli* by colistin. *Biken J* **9**, 115–23 (1966).
428. McCoy, L. S. *et al.* Polymyxins and analogues bind to ribosomal RNA and interfere with eukaryotic translation *in vitro*. *ChemBioChem* **14**, (2013).
429. Loutet, S. A. & Valvano, M. A. Extreme Antimicrobial Peptide and Polymyxin B Resistance in the Genus *Burkholderia*. *Frontiers in Microbiology* **2**, (2011).
430. Xu, Y. *et al.* An evolutionarily conserved mechanism for intrinsic and transferable polymyxin resistance. *mBio* **9**, (2018).
431. Jen, F. E. C. *et al.* *Neisseria gonorrhoeae* Becomes Susceptible to Polymyxin B and Colistin in the Presence of PBT2. *ACS Infectious Diseases* **6**, (2020).
432. Stogios, P. J. *et al.* Substrate Recognition by a Colistin Resistance Enzyme from *Moraxella catarrhalis*. *ACS Chemical Biology* **13**, (2018).
433. Aquilini, E., Merino, S., Knirel, Y. A., Regué, M. & Tomás, J. M. Functional identification of *Proteus mirabilis* *eptC* gene encoding a core lipopolysaccharide phosphoethanolamine transferase. *International Journal of Molecular Sciences* **15**, (2014).
434. Jiang, S. S. *et al.* *Proteus mirabilis* *pmrI*, an RppA-regulated gene necessary for polymyxin B resistance, biofilm formation, and urothelial cell invasion. *Antimicrobial Agents and Chemotherapy* **54**, (2010).
435. Lin, Q. Y. *et al.* *Serratia marcescens* *arn*, a PhoP-regulated locus necessary for polymyxin B resistance. *Antimicrobial Agents and Chemotherapy* **58**, (2014).
436. Muyembe, T., Vandepitte, J. & Desmyter, J. Natural colistin resistance in *Edwardsiella tarda*. *Antimicrob Agents Chemother* **4**, (1973).
437. Samonis, G. *et al.* Trends of isolation of intrinsically resistant to colistin Enterobacteriaceae and association with colistin use in a tertiary hospital. *European Journal of Clinical Microbiology and Infectious Diseases* **33**, (2014).
438. Sidorchuk, Z., Zähringer, U. & Rietschel, E. T. Chemical structure of the lipid A component of the lipopolysaccharide from a *Proteus mirabilis* Re-mutant. *European Journal of Biochemistry* **137**, (1983).
439. Hase, S. & Rietschel, E. T. The Chemical Structure of the Lipid A Component of Lipopolysaccharides from *Chromobacterium violaceum* NCTC 9694. *European Journal of Biochemistry* **75**, (1977).
440. Sud, I. J. & Feingold, D. S. Mechanism of polymyxin B resistance in *Proteus mirabilis*. *Journal of Bacteriology* **104**, (1970).
441. Olaitan, A. O., Morand, S. & Rolain, J. M. Mechanisms of polymyxin resistance: Acquired and intrinsic resistance in bacteria. *Frontiers in Microbiology* vol. 5 (2014).
442. Baron, S., Hadjadj, L., Rolain, J. M. & Olaitan, A. O. Molecular mechanisms of polymyxin resistance: knowns and unknowns. *International Journal of Antimicrobial Agents* **48**, (2016).
443. Gunn, J. S. The *Salmonella* PmrAB regulon: lipopolysaccharide modifications, antimicrobial peptide resistance and more. *Trends in Microbiology* vol. 16 (2008).
444. Gunn, J. S. *et al.* PmrA-PmrB-regulated genes necessary for 4-aminoarabinose lipid A modification and polymyxin resistance. *Molecular Microbiology* **27**, (1998).



445. Zhou, Z. *et al.* Lipid A modifications in polymyxin-resistant *Salmonella typhimurium*: PmrA-dependent 4-amino-4-deoxy-L-arabinose, and phosphoethanolamine incorporation. *Journal of Biological Chemistry* **276**, (2001).
446. Vasconcelos, N. G. *et al.* Synergistic effects of *Cinnamomum cassia* L. essential oil in combination with polymyxin B against carbapenemase-producing *Klebsiella pneumoniae* and *Serratia marcescens*. *PLoS ONE* **15**, (2020).
447. Baron, S. *et al.* Inactivation of the *arn* operon and loss of aminoarabinose on lipopolysaccharide as the cause of susceptibility to colistin in an atypical clinical isolate of *Proteus vulgaris*. *International Journal of Antimicrobial Agents* **51**, (2018).
448. Huang, J. *et al.* Comparative analysis of phosphoethanolamine transferases involved in polymyxin resistance across 10 clinically relevant Gram-negative bacteria. *International Journal of Antimicrobial Agents* **51**, (2018).
449. Samantha, A. & Vrieling, A. Lipid A Phosphoethanolamine Transferase: Regulation, Structure and Immune Response. *Journal of Molecular Biology* **432**, (2020).
450. Tzeng, Y. L. *et al.* Cationic antimicrobial peptide resistance in *Neisseria meningitidis*. *Journal of Bacteriology* **187**, (2005).
451. McGee, D. J. *et al.* Cholesterol enhances *Helicobacter pylori* resistance to antibiotics and LL-37. *Antimicrobial Agents and Chemotherapy* **55**, (2011).
452. Ito-Kagawa, M. & Koyama, Y. Selective cleavage of a peptide antibiotic, colistin by colistinase. *The Journal of Antibiotics* **33**, (1980).
453. Ito, M. & Aida, T. Studies on the bacterial formation of a peptide antibiotic, colistin. *Agricultural and Biological Chemistry* **30**, (1966).
454. Hamel, M., Rolain, J. M. & Baron, S. A. The history of colistin resistance mechanisms in bacteria: Progress and challenges. *Microorganisms* **9**, (2021).
455. Dalebroux, Z. D. & Miller, S. I. Salmonellae PhoPQ regulation of the outer membrane to resist innate immunity. *Current Opinion in Microbiology* vol. 17 (2014).
456. Groisman, E. A. The pleiotropic two-component regulatory system PhoP-PhoQ. *Journal of Bacteriology* vol. 183 (2001).
457. Kier, L. D., Weppelman, R. M. & Ames, B. N. Regulation of nonspecific acid phosphatase in *Salmonella*: *phoN* and *phoP* genes. *Journal of Bacteriology* **138**, (1979).
458. Choi, J. & Groisman, E. A. Activation of master virulence regulator PhoP in acidic pH requires the *Salmonella*-specific protein UgtL. *Science Signaling* **10**, (2017).
459. Prost, L. R. *et al.* Activation of the Bacterial Sensor Kinase PhoQ by Acidic pH. *Molecular Cell* **26**, (2007).
460. García Vescovi, E., Soncini, F. C. & Groisman, E. A. Mg<sup>2+</sup> as an extracellular signal: Environmental regulation of *Salmonella* virulence. *Cell* **84**, (1996).
461. Bader, M. W. *et al.* Recognition of antimicrobial peptides by a bacterial sensor kinase. *Cell* **122**, (2005).
462. Miller, S. I., Kukral, A. M. & Mekalanos, J. J. A two-component regulatory system (*phoP/phoQ*) controls *Salmonella typhimurium* virulence. *Proc Natl Acad Sci U S A* **86**, (1989).
463. Alpuche Aranda, C. M., Swanson, J. A., Loomis, W. P. & Miller, S. I. *Salmonella typhimurium* activates virulence gene transcription within acidified macrophage phagosomes. *Proc Natl Acad Sci U S A* **89**, (1992).

464. Gunn, J. S., Belden, W. J. & Miller, S. I. Identification of PhoP-PhoQ activated genes within a duplicated region of the *Salmonella typhimurium* chromosome. *Microbial Pathogenesis* **25**, (1998).
465. Belden, W. J. & Miller, S. I. Further characterization of the PhoP regulon: Identification of new PhoP- activated virulence loci. *Infection and Immunity* **62**, (1994).
466. Choi, M. J., Kim, S. & Ko, K. S. Pathways regulating the *pbpP* operon and colistin resistance in *Klebsiella pneumoniae* strains. *Journal of Microbiology and Biotechnology* **26**, (2016).
467. Cianciulli Sesso, A. *et al.* Gene Expression Profiling of *Pseudomonas aeruginosa* Upon Exposure to Colistin and Tobramycin. *Frontiers in Microbiology* **12**, (2021).
468. Fernández, L. *et al.* Adaptive resistance to the “last hope” antibiotics polymyxin B and colistin in *Pseudomonas aeruginosa* is mediated by the novel two-component regulatory system ParR-ParS. *Antimicrobial Agents and Chemotherapy* **54**, (2010).
469. Jeddou, F. ben *et al.* Adaptive and mutational responses to peptide dendrimer antimicrobials in *Pseudomonas aeruginosa*. *Antimicrobial Agents and Chemotherapy* **64**, (2020).
470. Luo, Q. *et al.* Molecular epidemiology and colistin resistant mechanism of *mcr*-positive and *mcr*-negative clinical isolated *Escherichia coli*. *Frontiers in Microbiology* **8**, (2017).
471. Choi, Y. *et al.* Comparison of Fitness Cost and Virulence in Chromosome- and Plasmid-Mediated Colistin-Resistant *Escherichia coli*. *Frontiers in Microbiology* **11**, (2020).
472. Nirwan, P. K., Chatterjee, N., Panwar, R., Dudeja, M. & Jaggi, N. Mutations in two component system (PhoPQ and PmrAB) in colistin resistant *Klebsiella pneumoniae* from North Indian tertiary care hospital. *Journal of Antibiotics* **74**, (2021).
473. Hong, Y. K. & Ko, K. S. PmrAB and PhoPQ Variants in Colistin-Resistant *Enterobacter* spp. Isolates in Korea. *Current Microbiology* (2019).
474. Gunn, J. S., Ernst, R. K., McCoy, A. J. & Miller, S. I. Constitutive mutations of the *Salmonella enterica* serovar Typhimurium transcriptional virulence regulator *phoP*. *Infection and Immunity* **68**, (2000).
475. Gunn, J. S., Hohmann, E. L. & Miller, S. I. Transcriptional regulation of *Salmonella* virulence: A PhoQ periplasmic domain mutation results in increased net phosphotransfer to PhoP. *Journal of Bacteriology* **178**, (1996).
476. Miller, A. K. *et al.* PhoQ mutations promote lipid A modification and polymyxin resistance of *Pseudomonas aeruginosa* found in colistin-treated cystic fibrosis patients. *Antimicrobial Agents and Chemotherapy* **55**, (2011).
477. Wilton, M., Charron-Mazenod, L., Moore, R. & Lewenza, S. Extracellular DNA acidifies biofilms and induces aminoglycoside resistance in *Pseudomonas aeruginosa*. *Antimicrobial Agents and Chemotherapy* **60**, (2016).
478. Cannatelli, A. *et al.* *In vivo* evolution to Colistin resistance by PmrB sensor kinase mutation in KPC-producing *Klebsiella pneumoniae* is associated with low-dosage colistin treatment. *Antimicrobial Agents and Chemotherapy* **58**, (2014).
479. Wösten, M. M. S. M., Kox, L. F. F., Chamnongpol, S., Soncini, F. C. & Groisman, E. A. A signal transduction system that responds to extracellular iron. *Cell* **103**, (2000).
480. Helena Mäkelä, P., Sarvas, M., Calcagno, S. & Lounatmaa, K. Isolation and genetic characterization of polymyxin-resistant mutants of *Salmonella*. *FEMS Microbiology Letters* **3**, (1978).

481. Roland, K. L., Martin, L. E., Esther, C. R. & Spitznagel, J. K. Spontaneous *pmrA* mutants of *Salmonella typhimurium* LT2 define a new two- component regulatory system with a possible role in virulence. *Journal of Bacteriology* **175**, (1993).
482. Arroyo, L. A. *et al.* The *pmrCAB* operon mediates polymyxin resistance in *Acinetobacter baumannii* ATCC 17978 and clinical isolates through phosphoethanolamine modification of lipid A. *Antimicrobial Agents and Chemotherapy* **55**, (2011).
483. Soncini, F. C. & Groisman, E. A. Two-component regulatory systems can interact to process multiple environmental signals. *Journal of Bacteriology* **178**, (1996).
484. Lee, H., Hsu, F. F., Turk, J. & Groisman, E. A. The PmrA-regulated *pmrC* gene mediates phosphoethanolamine modification of lipid A and polymyxin resistance in *Salmonella enterica*. *Journal of Bacteriology* **186**, (2004).
485. Farizano, J. v., Pescaretti, M. D. L. M., López, F. E., Hsu, F. F. & Delgado, M. A. The PmrAB system-inducing conditions control both lipid A remodeling and O-antigen length distribution, influencing the *Salmonella typhimurium*-host interactions. *Journal of Biological Chemistry* **287**, (2012).
486. Marchal, K. *et al.* *In silico* identification and experimental validation of PmrAB targets in *Salmonella typhimurium* by regulatory motif detection. *Genome Biol* **5**, (2004).
487. Breazeale, S. D., Ribeiro, A. A. & Raetz, C. R. H. Origin of lipid A species modified with 4-amino-4-deoxy-L-arabinose in polymyxin-resistant mutants of *Escherichia coli*: An aminotransferase (ArnB) that generates UDP-4-amino-4-deoxy-L-arabinose. *Journal of Biological Chemistry* **278**, (2003).
488. Trent, M. S., Ribeiro, A. A., Lin, S., Cotter, R. J. & Raetz, C. R. H. An inner membrane enzyme in *Salmonella* and *Escherichia coli* that transfers 4-amino-4-deoxy-L-arabinose to lipid A: Induction in polymyxin-resistant mutants and role of a novel lipid-linked donor. *Journal of Biological Chemistry* **276**, (2001).
489. Azam, M. *et al.* Colistin Resistance Among Multiple Sequence Types of *Klebsiella pneumoniae* Is Associated With Diverse Resistance Mechanisms: A Report From India. *Frontiers in Microbiology* **12**, (2021).
490. Quesada, A. *et al.* Polymorphism of genes encoding PmrAB in colistin-resistant strains of *Escherichia coli* and *Salmonella enterica* isolated from poultry and swine. *Journal of Antimicrobial Chemotherapy* **70**, (2015).
491. Diene, S. M. *et al.* The rhizome of the multidrug-resistant *Enterobacter aerogenes* genome reveals how new “Killer Bugs” are created because of a sympatric lifestyle. *Molecular Biology and Evolution* **30**, (2013).
492. Lee, J. Y. & Ko, K. S. Mutations and expression of PmrAB and PhoPQ related with colistin resistance in *Pseudomonas aeruginosa* clinical isolates. *Diagnostic Microbiology and Infectious Disease* **78**, (2014).
493. Kox, L. F. F., Wösten, M. M. S. M. & Groisman, E. A. A small protein that mediates the activation of a two-component system by another two-component system. *EMBO Journal* **19**, (2000).
494. Kato, A., Latifi, T. & Groisman, E. A. Closing the loop: The PmrA/PmrB two-component system negatively controls expression of its posttranscriptional activator PmrD. *Proc Natl Acad Sci U S A* **100**, (2003).
495. Wright, M. S. *et al.* Genomic and transcriptomic analyses of colistin-resistant clinical isolates of *Klebsiella pneumoniae* reveal multiple pathways of resistance. *Antimicrobial Agents and Chemotherapy* **59**, (2015).

496. Cain, A. K. *et al.* Morphological, genomic and transcriptomic responses of *Klebsiella pneumoniae* to the last-line antibiotic colistin. *Scientific Reports* **8**, (2018).
497. Sun, L. *et al.* Proteomic Changes of *Klebsiella pneumoniae* in Response to Colistin Treatment and *crrB* Mutation-Mediated Colistin Resistance. *Antimicrobial Agents and Chemotherapy* **64**, (2020).
498. Cheng, Y. H., Lin, T. L., Lin, Y. T. & Wang, J. T. Amino acid substitutions of *crrB* responsible for resistance to colistin through *crrC* in *Klebsiella pneumoniae*. *Antimicrobial Agents and Chemotherapy* **60**, (2016).
499. Lippa, A. M. & Goulian, M. Feedback inhibition in the PhoQ/PhoP signaling system by a membrane peptide. *PLoS Genetics* **5**, (2009).
500. Salazar, M. E., Podgornaia, A. I. & Laub, M. T. The small membrane protein MgrB regulates PhoQ bifunctionality to control PhoP target gene expression dynamics. *Molecular Microbiology* **102**, (2016).
501. Cannatelli, A. *et al.* MgrB inactivation is a common mechanism of colistin resistance in KPC-producing *Klebsiella pneumoniae* of clinical origin. *Antimicrobial Agents and Chemotherapy* **58**, (2014).
502. Mhaya, A., Bégu, D., Tounsi, S. & Arpin, C. MgrB Inactivation Is Responsible for Acquired Resistance to Colistin in *Enterobacter hormaechei* subsp. *steigerwaltii*. *Antimicrobial Agents and Chemotherapy* **64**, (2020).
503. Esposito, E. P. *et al.* Molecular epidemiology and virulence profiles of colistin-resistant *Klebsiella pneumoniae* blood isolates from the hospital agency “Ospedale dei Colli,” Naples, Italy. *Frontiers in Microbiology* **9**, (2018).
504. Poirel, L. *et al.* The *mgrB* gene as a key target for acquired resistance to colistin in *Klebsiella pneumoniae*. *Journal of Antimicrobial Chemotherapy* **70**, (2015).
505. Gutu, A. D. *et al.* Polymyxin resistance of *Pseudomonas aeruginosa* phoQ mutants is dependent on additional two-component regulatory systems. *Antimicrobial Agents and Chemotherapy* **57**, (2013).
506. Lee, J. Y., Park, Y. K., Chung, E. S., Na, I. Y. & Ko, K. S. Evolved resistance to colistin and its loss due to genetic reversion in *Pseudomonas aeruginosa*. *Scientific Reports* **6**, (2016).
507. Fernández, L. *et al.* The two-component system CprRS senses cationic peptides and triggers adaptive resistance in *Pseudomonas aeruginosa* independently of ParRS. *Antimicrobial Agents and Chemotherapy* **56**, (2012).
508. Lee, J. Y. *et al.* Development of colistin resistance in *pmrA*-, *phoP*-, *parR*- and *cprR*-inactivated mutants of *Pseudomonas aeruginosa*. *Journal of Antimicrobial Chemotherapy* **69**, (2014).
509. Adams, M. D. *et al.* Resistance to colistin in *Acinetobacter baumannii* associated with mutations in the PmrAB two-component system. *Antimicrobial Agents and Chemotherapy* **53**, (2009).
510. Cheah, S. E. *et al.* Polymyxin Resistance in *Acinetobacter baumannii*: Genetic Mutations and Transcriptomic Changes in Response to Clinically Relevant Dosage Regimens. *Scientific Reports* **6**, (2016).
511. Adams, M. D. *et al.* Comparative genome sequence analysis of multidrug-resistant *Acinetobacter baumannii*. *Journal of Bacteriology* **190**, (2008).
512. Gerson, S. *et al.* Diversity of amino acid substitutions in PmrCAB associated with colistin resistance in clinical isolates of *Acinetobacter baumannii*. *International Journal of Antimicrobial Agents* **55**, (2020).

513. Park, Y. K., Choi, J. Y., Shin, D. & Ko, K. S. Correlation between overexpression and amino acid substitution of the PmrAB locus and colistin resistance in *Acinetobacter baumannii*. *International Journal of Antimicrobial Agents* **37**, (2011).
514. Zhang, W. *et al.* The role of LpxA/C/D and *pmrA/B* gene systems in colistin-resistant clinical strains of *Acinetobacter baumannii*. *Frontiers in Laboratory Medicine* **1**, (2017).
515. Zhou, P. & Zhao, J. Structure, inhibition, and regulation of essential lipid A enzymes. *Biochimica et Biophysica Acta - Molecular and Cell Biology of Lipids* vol. 1862 (2017).
516. Moffatt, J. H. *et al.* Colistin resistance in *Acinetobacter baumannii* is mediated by complete loss of lipopolysaccharide production. *Antimicrobial Agents and Chemotherapy* **54**, (2010).
517. Nhu, N. T. K. *et al.* The induction and identification of novel Colistin resistance mutations in *Acinetobacter baumannii* and their implications. *Scientific Reports* **6**, (2016).
518. Moffatt, J. H. *et al.* Insertion sequence *ISAbA11* is involved in colistin resistance and loss of lipopolysaccharide in *Acinetobacter baumannii*. *Antimicrobial Agents and Chemotherapy* **55**, (2011).
519. Boinett, C. J. *et al.* Clinical and laboratory-induced colistin-resistance mechanisms in *Acinetobacter baumannii*. *Microbial Genomics* **5**, (2019).
520. Pamp, S. J., Gjermansen, M., Johansen, H. K. & Tolker-Nielsen, T. Tolerance to the antimicrobial peptide colistin in *Pseudomonas aeruginosa* biofilms is linked to metabolically active cells, and depends on the *pmr* and *mexAB-oprM* genes. *Molecular Microbiology* **68**, (2008).
521. Chiang, W. C., Pamp, S. J., Nilsson, M., Givskov, M. & Tolker-Nielsen, T. The metabolically active subpopulation in *Pseudomonas aeruginosa* biofilms survives exposure to membrane-targeting antimicrobials via distinct molecular mechanisms. *FEMS Immunology and Medical Microbiology* **65**, (2012).
522. Young, M. L., Bains, M., Bell, A. & Hancock, R. E. W. Role of *Pseudomonas aeruginosa* outer membrane protein OprH in polymyxin and gentamicin resistance: Isolation of an OprH-deficient mutant by gene replacement techniques. *Antimicrobial Agents and Chemotherapy* vol. 36 (1992).
523. Macfarlane, E. L. A., Kwasnicka, A., Ochs, M. M. & Hancock, R. E. W. PhoP-PhoQ homologues in *Pseudomonas aeruginosa* regulate expression of the outer-membrane protein OprH and polymyxin B resistance. *Molecular Microbiology* **34**, (1999).
524. Srinivasan, V. B. & Rajamohan, G. KpnEF, a new member of the *Klebsiella pneumoniae* cell envelope stress response regulon, is an SMR-type efflux pump involved in broad-spectrum antimicrobial resistance. *Antimicrobial Agents and Chemotherapy* **57**, (2013).
525. McCoy, A. J., Liu, H., Falla, T. J. & Gunn, J. S. Identification of *Proteus mirabilis* mutants with increased sensitivity to antimicrobial peptides. *Antimicrobial Agents and Chemotherapy* **45**, (2001).
526. Sundaramoorthy, N. S., Suresh, P., Selva Ganesan, S., GaneshPrasad, A. K. & Nagarajan, S. Restoring colistin sensitivity in colistin-resistant *E. coli*: Combinatorial use of MarR inhibitor with efflux pump inhibitor. *Scientific Reports* **9**, (2019).
527. Parra-Lopez, C., Baer, M. T. & Groisman, E. A. Molecular genetic analysis of a locus required for resistance to antimicrobial peptides in *Salmonella typhimurium*. *EMBO Journal* **12**, (1993).
528. Baron, S. A. & Rolain, J. M. Efflux pump inhibitor CCCP to rescue colistin susceptibility in *mcr-1* plasmid-mediated colistin-resistant strains and Gram-negative bacteria. *Journal of Antimicrobial Chemotherapy* **73**, (2018).

529. Ni, W. *et al.* Effects of efflux pump inhibitors on colistin resistance in multidrug-resistant gram-negative bacteria. *Antimicrobial Agents and Chemotherapy* **60**, (2016).
530. Liu, Y. Y. *et al.* Emergence of plasmid-mediated colistin resistance mechanism MCR-1 in animals and human beings in China: A microbiological and molecular biological study. *The Lancet Infectious Diseases* **16**, (2016).
531. Lin, Y. *et al.* Metadata Analysis of *mcr-1*-Bearing Plasmids Inspired by the Sequencing Evidence for Horizontal Transfer of Antibiotic Resistance Genes Between Polluted River and Wild Birds. *Frontiers in Microbiology* **11**, (2020).
532. Shen, Z., Wang, Y., Shen, Y., Shen, J. & Wu, C. Early emergence of *mcr-1* in *Escherichia coli* from food-producing animals. *The Lancet Infectious Diseases* vol. 16 (2016).
533. Haenni, M. *et al.* Co-occurrence of extended spectrum  $\beta$  lactamase and MCR-1 encoding genes on plasmids. *The Lancet Infectious Diseases* vol. 16 (2016).
534. Wang, R. *et al.* The global distribution and spread of the mobilized colistin resistance gene *mcr-1*. *Nature Communications* **9**, (2018).
535. Zając, M. *et al.* Occurrence and Characterization of *mcr-1*-Positive *Escherichia coli* Isolated From Food-Producing Animals in Poland, 2011–2016. *Frontiers in Microbiology* **10**, (2019).
536. Mendes, A. C. *et al.* *mcr-1* in carbapenemase-producing *Klebsiella pneumoniae* with hospitalized patients, Portugal, 2016-2017. *Emerging Infectious Diseases* **24**, (2018).
537. Elbediwi, M. *et al.* Genomic Characterization of *mcr-1*-carrying *Salmonella enterica* Serovar ST 34 Clone Isolated From Pigs in China. *Frontiers in Bioengineering and Biotechnology* **8**, (2020).
538. Ma, Q. *et al.* Multidrug-resistant *Shigella sonnei* carrying the plasmid-mediated *mcr-1* gene in China. *International Journal of Antimicrobial Agents* **52**, (2018).
539. Zeng, K. J., Doi, Y., Patil, S., Huang, X. & Tian, G. B. Emergence of the plasmid-mediated *mcr-1* gene in colistin-resistant *Enterobacter aerogenes* and *Enterobacter cloacae*. *Antimicrobial Agents and Chemotherapy* vol. 60 (2016).
540. Li, X. P. *et al.* Emergence of the colistin resistance gene *mcr-1* in *Citrobacter freundii*. *International Journal of Antimicrobial Agents* vol. 49 (2017).
541. AbuOun, M. *et al.* *mcr-1* and *mcr-2* variant genes identified in *Moraxella* species isolated from pigs in Great Britain from 2014 to 2015. *Journal of Antimicrobial Chemotherapy* **72**, (2017).
542. McGann, P. *et al.* *Escherichia coli* harboring *mcr-1* and *blaCTX-M* on a novel IncF plasmid: First report of *mcr-1* in the United States. *Antimicrobial Agents and Chemotherapy* vol. 60 (2016).
543. Migura-Garcia, L. *et al.* *mcr*-Colistin Resistance Genes Mobilized by IncX4, IncHI2, and IncI2 Plasmids in *Escherichia coli* of Pigs and White Stork in Spain. *Frontiers in Microbiology* **10**, (2020).
544. Zhao, F., Feng, Y., Lü, X., McNally, A. & Zong, Z. IncP plasmid carrying colistin resistance gene *mcr-1* in *Klebsiella pneumoniae* from hospital sewage. *Antimicrobial Agents and Chemotherapy* **61**, (2017).
545. Zhang, C. *et al.* A phage-like IncY plasmid carrying the *mcr-1* gene in *Escherichia coli* from a pig farm in China. *Antimicrobial Agents and Chemotherapy* **61**, (2017).
546. Schrauwen, E. J. A. *et al.* High prevalence of the *mcr-1* gene in retail chicken meat in the Netherlands in 2015. *Antimicrobial Resistance and Infection Control* vol. 6 (2017).
547. Manageiro, V., Jones-dias, D., Ferreira, E. & Caniça, M. Plasmid-mediated colistin resistance (*Mcr-1*) in *Escherichia coli* from non-imported fresh vegetables for human consumption in Portugal. *Microorganisms* **8**, (2020).

548. Zhu, L. *et al.* Comprehensive Understanding of the Plasmid-Mediated Colistin Resistance Gene *mcr-1* in Aquatic Environments. *Environmental Science and Technology* **54**, (2020).
549. Zhao, F., Feng, Y., Lü, X., McNally, A. & Zong, Z. Remarkable diversity of *Escherichia coli* carrying *mcr-1* from hospital sewage with the identification of two new *mcr-1* variants. *Frontiers in Microbiology* **8**, (2017).
550. Zhang, X. F. *et al.* Possible transmission of *mcr-1*-harboring *Escherichia coli* between companion animals and human. *Emerging Infectious Diseases* vol. 22 (2016).
551. Ahmed, Z. S., Elshafiee, E. A., Khalefa, H. S., Kadry, M. & Hamza, D. A. Evidence of colistin resistance genes (*mcr-1* and *mcr-2*) in wild birds and its public health implication in Egypt. *Antimicrobial Resistance and Infection Control* **8**, (2019).
552. Torres, R. T. *et al.* Emergence of colistin resistance genes (*mcr-1*) in *Escherichia coli* among widely distributed wild ungulates. *Environmental Pollution* **291**, (2021).
553. Nakano, A. *et al.* Prevalence and Relatedness of *mcr-1*-Mediated Colistin-Resistant *Escherichia coli* Isolated From Livestock and Farmers in Japan. *Frontiers in Microbiology* **12**, (2021).
554. Catry, B. *et al.* Use of colistin-containing products within the European Union and European Economic Area (EU/EEA): development of resistance in animals and possible impact on human and animal health. *International Journal of Antimicrobial Agents* vol. 46 (2015).
555. Wang, Y. *et al.* Changes in colistin resistance and *mcr-1* abundance in *Escherichia coli* of animal and human origins following the ban of colistin-positive additives in China: an epidemiological comparative study. *The Lancet Infectious Diseases* **20**, (2020).
556. Usui, M. *et al.* Decreased colistin resistance and *mcr-1* prevalence in pig-derived *Escherichia coli* in Japan after banning colistin as a feed additive. *Journal of Global Antimicrobial Resistance* **24**, (2021).
557. Zhang, J. *et al.* Housefly (*Musca domestica*) and blow fly (*Protophormia terraenovae*) as vectors of bacteria carrying colistin resistance genes. *Applied and Environmental Microbiology* **84**, (2018).
558. Hu, M. *et al.* Crystal Structure of *Escherichia coli* originated MCR-1, a phosphoethanolamine transferase for Colistin Resistance. *Scientific Reports* **6**, (2016).
559. Ma, G., Zhu, Y., Yu, Z., Ahmad, A. & Zhang, H. High resolution crystal structure of the catalytic domain of MCR-1. *Scientific Reports* **6**, (2016).
560. Xu, Y., Lin, J., Cui, T., Srinivas, S. & Feng, Y. Mechanistic insights into transferable polymyxin resistance among gut bacteria. *Journal of Biological Chemistry* **293**, (2018).
561. Gao, R. *et al.* Dissemination and Mechanism for the MCR-1 Colistin Resistance. *PLoS Pathogens* **12**, (2016).
562. Kieffer, N., Nordmann, P. & Poirel, L. *Moraxella* species as potential sources of MCR-like polymyxin resistance determinants. *Antimicrobial Agents and Chemotherapy* **61**, (2017).
563. Khedher, M. Ben *et al.* Massive analysis of 64,628 bacterial genomes to decipher water reservoir and origin of mobile colistin resistance genes: is there another role for these enzymes? *Scientific Reports* **10**, (2020).
564. Wanty, C. *et al.* The structure of the neisserial lipooligosaccharide phosphoethanolamine transferase A (LptA) required for resistance to polymyxin. *Journal of Molecular Biology* **425**, (2013).

565. Fage, C. D., Brown, D. B., Boll, J. M., Keatinge-Clay, A. T. & Trent, M. S. Crystallographic study of the phosphoethanolamine transferase EptC required for polymyxin resistance and motility in *Campylobacter jejuni*. *Acta Crystallographica Section D: Biological Crystallography* **70**, (2014).
566. Stojanoski, V. *et al.* Structure of the catalytic domain of the colistin resistance enzyme MCR-1. *BMC Biology* **14**, (2016).
567. Hassan, J. *et al.* The mobile colistin resistance gene, *mcr-1.1*, is carried on Incx4 plasmids in multidrug resistant *E. coli* isolated from rainbow trout aquaculture. *Microorganisms* **8**, (2020).
568. Lv, D. *et al.* *bla*NDM and *mcr-1* to *mcr-5* gene distribution characteristics in gut specimens from different regions of China. *Antibiotics* **10**, (2021).
569. Liu, H. *et al.* A novel *mcr-1* variant carried by an IncI2-Type plasmid identified from a multidrug resistant enterotoxigenic *Escherichia coli*. *Frontiers in Microbiology* **9**, (2018).
570. Sun, J. *et al.* Deciphering MCR-2 colistin resistance. *mBio* **8**, (2017).
571. Yin, W. *et al.* Novel plasmid-mediated colistin resistance gene *mcr-3* in *Escherichia coli*. *mBio* **8**, (2017).
572. Zhang, H. *et al.* Action and mechanism of the colistin resistance enzyme MCR-4. *Communications Biology* **2**, (2019).
573. Ma, S. *et al.* Mobile colistin resistance gene *mcr-5* in porcine *Aeromonas hydrophila*. *Journal of Antimicrobial Chemotherapy* **73**, (2018).
574. Borowiak, M. *et al.* Development of a Novel *mcr-6* to *mcr-9* Multiplex PCR and Assessment of *mcr-1* to *mcr-9* Occurrence in Colistin-Resistant *Salmonella enterica* Isolates From Environment, Feed, Animals and Food (2011–2018) in Germany. *Frontiers in Microbiology* **11**, (2020).
575. dos Santos, L. D. R. *et al.* Co-occurrence of *mcr-1*, *mcr-3*, *mcr-7* and clinically relevant antimicrobial resistance genes in environmental and fecal samples. *Archives of Microbiology* **202**, (2020).
576. Wang, X. *et al.* Emergence of a novel mobile colistin resistance gene, *mcr-8*, in NDM-producing *Klebsiella pneumoniae*. *Emerging Microbes and Infections* **7**, (2018).
577. Carroll, L. M. *et al.* Identification of novel mobilized colistin resistance gene *mcr-9* in a multidrug-resistant, colistin-susceptible *Salmonella enterica* serotype Typhimurium isolate. *mBio* **10**, (2019).
578. Wang, C. *et al.* Identification of novel mobile colistin resistance gene *mcr-10*. *Emerging Microbes and Infections* **9**, (2020).
579. Xavier, B. B. *et al.* Identification of a novel plasmid-mediated colistin resistance gene, *mcr-2*, in *Escherichia coli*, Belgium, June 2016. *Eurosurveillance* **21**, (2016).
580. Lima, T., Domingues, S. & da Silva, G. J. Plasmid-mediated colistin resistance in *Salmonella enterica*: A review. *Microorganisms* vol. 7 (2019).
581. Ling, Z. *et al.* Epidemiology of mobile colistin resistance genes *mcr-1* to *mcr-9*. *Journal of Antimicrobial Chemotherapy* vol. 75 (2020).
582. Tyso, G. H. *et al.* The *mcr-9* gene of *Salmonella* and *Escherichia coli* is not associated with colistin resistance in the United States. *Antimicrobial Agents and Chemotherapy* **64**, (2020).
583. Kananizadeh, P. *et al.* Emergence of carbapenem-resistant and colistin-susceptible Enterobacter cloacae complex co-harboring *bla*IMP-1 and *mcr-9* in Japan. *BMC Infectious Diseases* **20**, (2020).



584. Kieffer, N. *et al.* *Mcr-9*, an Inducible Gene Encoding an Acquired Phosphoethanolamine Transferase in *Escherichia coli*, and Its Origin. *Antimicrobial Agents and Chemotherapy* **63**, (2019).
585. Olaitan, A. O., Chabou, S., Okdah, L., Morand, S. & Rolain, J. M. Dissemination of the *mcr-1* colistin resistance gene. *The Lancet Infectious Diseases* vol. 16 (2016).
586. Luk-in, S. *et al.* Occurrence of *mcr*-mediated colistin resistance in *Salmonella* clinical isolates in Thailand. *Scientific Reports* **11**, (2021).
587. Li, Y. *et al.* Characterization of the global distribution and diversified plasmid reservoirs of the colistin resistance gene *mcr-9*. *Scientific Reports* **10**, (2020).
588. Gelbíčová, T. *et al.* Dissemination and Comparison of Genetic Determinants of *mcr*-Mediated Colistin Resistance in Enterobacteriaceae via Retailed Raw Meat Products. *Frontiers in Microbiology* **10**, (2019).
589. Pan, Y. *et al.* Discovery of *mcr-3.1* gene carried by a prophage located in a conjugative IncA/C2 plasmid from a *Salmonella* Choleraesuis clinical isolate. *Journal of Infection* vol. 82 (2021).
590. Hatrongjit, R. *et al.* Genomic analysis of *Aeromonas veronii* C198, a novel *Mcr-3.41*-harboring isolate from a patient with septicemia in Thailand. *Pathogens* **9**, (2020).
591. Partridge, S. R. *et al.* Proposal for assignment of allele numbers for mobile colistin resistance (*mcr*) genes. *Journal of Antimicrobial Chemotherapy* **73**, (2018).
592. Zhang, J. *et al.* Molecular detection of colistin resistance genes (*mcr-1*, *mcr-2* and *mcr-3*) in nasal/oropharyngeal and anal/cloacal swabs from pigs and poultry. *Scientific Reports* **8**, (2018).
593. Yang, Y. Q., Li, Y. X., Lei, C. W., Zhang, A. Y. & Wang, H. N. Novel plasmid-mediated colistin resistance gene *mcr-7.1* in *Klebsiella pneumoniae*. *Journal of Antimicrobial Chemotherapy* **73**, (2018).
594. Shen, Y. *et al.* Prevalence and genetic analysis of *mcr-3*-positive *Aeromonas* species from humans, retail meat, and environmental water samples. *Antimicrobial Agents and Chemotherapy* **62**, (2018).
595. Wang, Y., Hou, N., Rasooly, R., Gu, Y. & He, X. Prevalence and Genetic Analysis of Chromosomal *mcr-3/7* in *Aeromonas* From U.S. Animal-Derived Samples. *Frontiers in Microbiology* **12**, (2021).
596. Partridge, S. R. *mcr-2* in the IncX4 plasmid pKP37-BE is flanked by directly oriented copies of ISEc69. *Journal of Antimicrobial Chemotherapy* vol. 72 (2017).
597. Diaconu, E. L. *et al.* Emergence of IncHI2 Plasmids With Mobilized Colistin Resistance (*mcr*)-9 Gene in ESBL-Producing, Multidrug-Resistant *Salmonella typhimurium* and Its Monophasic Variant ST34 From Food-Producing Animals in Italy. *Frontiers in Microbiology* **12**, (2021).
598. Rumi, M. V. *et al.* Co-occurrence of clinically relevant  $\beta$ -lactamases and MCR-1 encoding genes in *Escherichia coli* from companion animals in Argentina. *Veterinary Microbiology* **230**, (2019).
599. Dominguez, J. E. *et al.* Simultaneous carriage of *mcr-1* and other antimicrobial resistance determinants in *Escherichia coli* from poultry. *Frontiers in Microbiology* **9**, (2018).
600. Yamaguchi, T. *et al.* High Prevalence of Colistin-Resistant *Escherichia coli* with Chromosomally Carried *mcr-1* in Healthy Residents in Vietnam . *mSphere* **5**, (2020).
601. Singh, S. *et al.* Emergence of chromosome-borne colistin resistance gene *mcr-1* in clinical isolates of *Klebsiella pneumoniae* from India. *Antimicrobial Agents and Chemotherapy* vol. 62 (2018).

602. Pathak, A., Singh, S., Kumar, A. & Prasad, K. N. Emergence of chromosome borne colistin resistance gene, *mcr-1* in clinical isolates of *Pseudomonas aeruginosa*. *International Journal of Infectious Diseases* **101**, (2020).
603. Caselli, E., D'Accolti, M., Soffritti, I., Piffanelli, M. & Mazzacane, S. Spread of *mcr-1*-driven colistin resistance on hospital surfaces, Italy. *Emerging Infectious Diseases* vol. 24 (2018).
604. Gales, A. C., Reis, A. O. & Jones, R. N. Contemporary assessment of antimicrobial susceptibility testing methods for polymyxin B and colistin: Review of available interpretative criteria and quality control guidelines. *Journal of Clinical Microbiology* **39**, (2001).
605. Gales, A. C., Jones, R. N. & Sader, H. S. Contemporary activity of colistin and polymyxin B against a worldwide collection of Gram-negative pathogens: Results from the SENTRY antimicrobial surveillance program (2006-09). *Journal of Antimicrobial Chemotherapy* **66**, (2011).
606. Chew, K. L., La, M. van, Lin, R. T. P. & Teo, J. W. P. Colistin and polymyxin B susceptibility testing for carbapenem-resistant and *mcr*-positive Enterobacteriaceae: Comparison of Sensititre, MicroScan, Vitek 2, and Etest with broth microdilution. *Journal of Clinical Microbiology* **55**, (2017).
607. Pitt, T. L., Sparrow, M., Warner, M. & Stefanidou, M. Survey of resistance of *Pseudomonas aeruginosa* from UK patients with cystic fibrosis to six commonly prescribed antimicrobial agents. *Thorax* vol. 58 (2003).
608. Andrews, J. M. BSAC standardized disc susceptibility testing method (version 6). *Journal of Antimicrobial Chemotherapy* **60**, (2007).
609. Walkty, A. *et al.* Antimicrobial susceptibility of *Pseudomonas aeruginosa* isolates obtained from patients in Canadian intensive care units as part of the Canadian National Intensive Care Unit study. *Diagnostic Microbiology and Infectious Disease* **61**, (2008).
610. Keen, E. F. *et al.* Prevalence of multidrug-resistant organisms recovered at a military burn center. *Burns* **36**, (2010).
611. García-Castillo, M. *et al.* Wide dispersion of ST175 clone despite high genetic diversity of carbapenem-nonsusceptible *Pseudomonas aeruginosa* clinical strains in 16 Spanish hospitals. *Journal of Clinical Microbiology* **49**, (2011).
612. Wi, Y. M. *et al.* Emergence of colistin resistance in *Pseudomonas aeruginosa* ST235 clone in South Korea. *International Journal of Antimicrobial Agents* **49**, (2017).
613. Tahmasebi, H., Dehbashi, S. & Arabestani, M. R. Prevalence and molecular typing of colistin-resistant *Pseudomonas aeruginosa* (CRPA) among  $\beta$ -lactamase-producing isolates: A study based on high-resolution melting curve analysis method. *Infection and Drug Resistance* **13**, (2020).
614. Linden, P. K. *et al.* Use of parenteral colistin for the treatment of serious infection due to antimicrobial-resistant *Pseudomonas aeruginosa*. *Clin Infect Dis* **37**, (2003).
615. Hachem, R. Y. *et al.* Colistin is effective in treatment of infections caused by multidrug-resistant *Pseudomonas aeruginosa* in cancer patients. *Antimicrobial Agents and Chemotherapy* **51**, (2007).
616. Sabuda, D. M. *et al.* Utilization of colistin for treatment of multidrug-resistant *Pseudomonas aeruginosa*. *Canadian Journal of Infectious Diseases and Medical Microbiology* **19**, (2008).
617. Falagas, M. E. *et al.* Colistin therapy for microbiologically documented multidrug-resistant Gram-negative bacterial infections: a retrospective cohort study of 258 patients. *International Journal of Antimicrobial Agents* **35**, (2010).

618. Taccetti, G. *et al.* Early antibiotic treatment for *Pseudomonas aeruginosa* eradication in patients with cystic fibrosis: A randomised multicentre study comparing two different protocols. *Thorax* **67**, (2012).
619. Lu, Q. *et al.* Efficacy of high-dose nebulized colistin in ventilator-associated pneumonia caused by multidrug-resistant *Pseudomonas aeruginosa* and *Acinetobacter baumannii*. *Anesthesiology* **117**, (2012).
620. Haworth, C. S., Foweraker, J. E., Wilkinson, P., Kenyon, R. F. & Bilton, D. Inhaled colistin in patients with bronchiectasis and chronic *Pseudomonas aeruginosa* infection. *American Journal of Respiratory and Critical Care Medicine* **189**, (2014).
621. Blanco-Aparicio, M. *et al.* Eradication of *Pseudomonas aeruginosa* with inhaled colistin in adults with non-cystic fibrosis bronchiectasis. *Chronic Respiratory Disease* **16**, (2019).
622. Moni, M. *et al.* Clinical efficacy and pharmacokinetics of colistimethate sodium and colistin in critically ill patients in an Indian hospital with high endemic rates of multidrug-resistant Gram-negative bacterial infections: A prospective observational study. *International Journal of Infectious Diseases* **100**, (2020).
623. Wiegand, I., Hilpert, K. & Hancock, R. E. W. Agar and broth dilution methods to determine the minimal inhibitory concentration (MIC) of antimicrobial substances. *Nature Protocols* **3**, (2008).
624. Wind, C. M., de Vries, H. J. C. & van Dam, A. P. Determination of *in vitro* synergy for dual antimicrobial therapy against resistant *Neisseria gonorrhoeae* using Etest and agar dilution. *International Journal of Antimicrobial Agents* **45**, (2015).
625. Odds, F. C. Synergy, antagonism, and what the checkerboard puts between them. *Journal of Antimicrobial Chemotherapy* vol. 52 (2003).
626. Helander, I. M. & Mattila-Sandholm, T. Fluorometric assessment of Gram-negative bacterial permeabilization. *Journal of Applied Microbiology* **88**, (2000).
627. Bagge, N. *et al.* *Pseudomonas aeruginosa* Biofilms Exposed to Imipenem Exhibit Changes in Global Gene Expression and  $\beta$ -Lactamase and Alginate Production. *Antimicrobial Agents and Chemotherapy* **48**, (2004).
628. O'Callaghan, C. H., Morris, A., Kirby, S. M. & Shingler, A. H. Novel method for detection of beta-lactamases by using a chromogenic cephalosporin substrate. *Antimicrob Agents Chemother* **1**, (1972).
629. Pader, V. *et al.* *Staphylococcus aureus* inactivates daptomycin by releasing membrane phospholipids. *Nature Microbiology* **2**, (2016).
630. Sweeney, E., Sabnis, A., Edwards, A. M. & Harrison, F. Effect of host-mimicking medium and biofilm growth on the ability of colistin to kill *Pseudomonas aeruginosa*. *Microbiology (United Kingdom)* **166**, (2020).
631. Zupan, J. R., Cameron, T. A., Anderson-Furgeson, J. & Zambryski, P. C. Dynamic FtsA and FtsZ localization and outer membrane alterations during polar growth and cell division in *Agrobacterium tumefaciens*. *Proc Natl Acad Sci U S A* **110**, (2013).
632. Lam, J. S., Anderson, E. M. & Hao, Y. LPS quantitation procedures. *Methods in Molecular Biology* **1149**, (2014).
633. Tsuji, K., Steindler, K. A. & Harrison, S. J. Limulus amoebocyte lysate assay for detection and quantitation of endotoxin in a small volume parenteral product. *Applied and Environmental Microbiology* **40**, (1980).
634. Crosby, H. A., Bion, J. F., Penn, C. W. & Elliott, T. S. J. Antibiotic-induced release of endotoxin from bacteria *in vitro*. *Journal of Medical Microbiology* **40**, (1994).

635. Fomsgaard, A., Freudenberg, M. A. & Galanos, C. Modification of the silver staining technique to detect lipopolysaccharide in polyacrylamide gels. *Journal of Clinical Microbiology* **28**, (1990).
636. Rabilloud, T. Silver staining of 2D electrophoresis gels. *Methods in Molecular Biology* **893**, (2012).
637. Weiss, R. L. & Fraser, D. Surface structure of intact cells and spheroplasts of *Pseudomonas aeruginosa*. *Journal of Bacteriology* **113**, (1973).
638. Loh, L. N. & Ward, T. H. *Escherichia coli* K1 invasion of human brain microvascular endothelial cells. in *Methods in Enzymology* vol. 506 (2012).
639. Furniss, R. C. D. *et al.* Detection of colistin resistance in *Escherichia coli* by use of the MALDI Biotyper Sirius mass spectrometry system. *Journal of Clinical Microbiology* **57**, (2019).
640. Dortet, L. *et al.* Optimization of the MALDIxin test for the rapid identification of colistin resistance in *Klebsiella pneumoniae* using MALDI-TOF MS. *Journal of Antimicrobial Chemotherapy* **75**, (2020).
641. Furniss, C. R. D., Kostrzewa, M., Mavridou, D. A. I. & Larrouy-Maumus, G. The clue is in the lipid A: Rapid detection of colistin resistance. *PLoS Pathogens* **16**, (2020).
642. Müller, A. *et al.* Daptomycin inhibits cell envelope synthesis by interfering with fluid membrane microdomains. *Proc Natl Acad Sci U S A* **113**, (2016).
643. Jones, T. *et al.* Failures in clinical treatment of *Staphylococcus aureus* infection with daptomycin are associated with alterations in surface charge, membrane phospholipid asymmetry, and drug binding. *Antimicrobial Agents and Chemotherapy* **52**, (2008).
644. Machuca, J. *et al.* Interplay between plasmid-mediated and chromosomal-mediated fluoroquinolone resistance and bacterial fitness in *Escherichia coli*. *Journal of Antimicrobial Chemotherapy* **69**, (2014).
645. Clarke, T. B. Early innate immunity to bacterial infection in the lung is regulated systemically by the commensal microbiota via Nod-like receptor ligands. *Infection and Immunity* **82**, (2014).
646. Brown, R. L., Sequeira, R. P. & Clarke, T. B. The microbiota protects against respiratory infection via GM-CSF signaling. *Nature Communications* **8**, (2017).
647. Moradali, M. F., Ghods, S. & Rehm, B. H. A. *Pseudomonas aeruginosa* lifestyle: A paradigm for adaptation, survival, and persistence. *Frontiers in Cellular and Infection Microbiology* vol. 7 (2017).
648. Ibrahim, D., Jabbour, J. F. & Kanj, S. S. Current choices of antibiotic treatment for *Pseudomonas aeruginosa* infections. *Current Opinion in Infectious Diseases* vol. 33 (2020).
649. Horcajada, J. P. *et al.* Epidemiology and treatment of multidrug-resistant and extensively drug-resistant *Pseudomonas aeruginosa* infections. *Clinical Microbiology Reviews* **32**, (2019).
650. Billings, N. *et al.* The Extracellular Matrix Component Psl Provides Fast-Acting Antibiotic Defense in *Pseudomonas aeruginosa* Biofilms. *PLoS Pathogens* **9**, (2013).
651. Huang, J. X. *et al.* Mucin binding reduces colistin antimicrobial activity. *Antimicrobial Agents and Chemotherapy* **59**, (2015).
652. Lewenza, S. Extracellular DNA-induced antimicrobial peptide resistance mechanisms in *Pseudomonas aeruginosa*. *Frontiers in Microbiology* vol. 4 (2013).
653. Mulcahy, L. R., Burns, J. L., Lory, S. & Lewis, K. Emergence of *Pseudomonas aeruginosa* strains producing high levels of persister cells in patients with cystic fibrosis. *Journal of Bacteriology* **192**, (2010).

654. Chung, E. S., Wi, Y. M. & Ko, K. S. Variation in formation of persister cells against colistin in *Acinetobacter baumannii* isolates and its relationship with treatment failure. *Journal of Antimicrobial Chemotherapy* **72**, (2017).
655. Fisher, R. A., Gollan, B. & Helaine, S. Persistent bacterial infections and persister cells. *Nature Reviews Microbiology* vol. 15 (2017).
656. Lee, D. G. *et al.* Genomic analysis reveals that *Pseudomonas aeruginosa* virulence is combinatorial. *Genome Biology* **7**, (2006).
657. Mikkelsen, H., McMullan, R. & Filloux, A. The *Pseudomonas aeruginosa* reference strain PA14 displays increased virulence due to a mutation in *ladS*. *PLoS ONE* **6**, (2011).
658. Jacoby, G. A. AmpC B-Lactamases. *Clinical Microbiology Reviews* vol. 22 (2009).
659. Yang, Y., Xiang, Y. & Xu, M. From red to green: The propidium iodide-permeable membrane of *Shewanella decolorationis* S12 is repairable. *Scientific Reports* **5**, (2015).
660. Crompton, T., Peitsch, M. C., MacDonald, H. R. & Tschopp, J. Propidium iodide staining correlates with the extent of DNA degradation in isolated nuclei. *Biochemical and Biophysical Research Communications* **183**, (1992).
661. Rajnovic, D., Muñoz-Berbel, X. & Mas, J. Fast phage detection and quantification: An optical density-based approach. *PLoS ONE* **14**, (2019).
662. Band, V. I. *et al.* Antibiotic failure mediated by a resistant subpopulation in *Enterobacter cloacae*. *Nature Microbiology* **1**, (2016).
663. Jayol, A., Nordmann, P., Brink, A. & Poirel, L. Heteroresistance to colistin in *Klebsiella pneumoniae* associated with alterations in the PhoPQ regulatory system. *Antimicrobial Agents and Chemotherapy* **59**, (2015).
664. Karvanen, M., Malmberg, C., Lagerbäck, P., Friberg, L. E. & Cars, O. Colistin is extensively lost during standard in vitro experimental conditions. *Antimicrobial Agents and Chemotherapy* **61**, (2017).
665. Sabnis, A., Ledger, E. V. K., Pader, V. & Edwards, A. M. Antibiotic interceptors: Creating safe spaces for bacteria. *PLoS Pathogens* **14**, (2018).
666. El-Halfawy, O. M. *et al.* Antibiotic capture by bacterial lipocalins uncovers an extracellular mechanism of intrinsic antibiotic resistance. *mBio* **8**, (2017).
667. Lee, J. *et al.* *Staphylococcus aureus* extracellular vesicles carry biologically active  $\beta$ -lactamase. *Antimicrobial Agents and Chemotherapy* **57**, (2013).
668. Manning, A. J. & Kuehn, M. J. Contribution of bacterial outer membrane vesicles to innate bacterial defense. *BMC Microbiology* **11**, (2011).
669. Kulkarni, H. M., Nagaraj, R. & Jagannadham, M. V. Protective role of *E. coli* outer membrane vesicles against antibiotics. *Microbiological Research* **181**, (2015).
670. Llobet, E., Tomás, J. M. & Bengoechea, J. A. Capsule polysaccharide is a bacterial decoy for antimicrobial peptides. *Microbiology (NY)* **154**, (2008).
671. Schwechheimer, C. & Kuehn, M. J. Outer-membrane vesicles from Gram-negative bacteria: Biogenesis and functions. *Nature Reviews Microbiology* vol. 13 (2015).
672. MacDonald, I. A. & Kuehna, M. J. Stress-induced outer membrane vesicle production by *Pseudomonas aeruginosa*. *Journal of Bacteriology* **195**, (2013).
673. Jann, K. & Jann, B. Polysaccharide antigens of *Escherichia coli*. *Reviews of Infectious Diseases* vol. 9 Suppl 5 (1987).

674. Liberati, N. T. *et al.* An ordered, nonredundant library of *Pseudomonas aeruginosa* strain PA14 transposon insertion mutants. *Proc Natl Acad Sci U S A* **103**, (2006).
675. Franklin, M. J., Nivens, D. E., Weadge, J. T. & Lynne Howell, P. Biosynthesis of the *Pseudomonas aeruginosa* extracellular polysaccharides, alginate, Pel, and Psl. *Frontiers in Microbiology* vol. 2 (2011).
676. Jain, S. & Ohman, D. E. Role of an alginate lyase for alginate transport in mucoid *Pseudomonas aeruginosa*. *Infection and Immunity* **73**, (2005).
677. Mattsby-Baltzer, I., Lindgren, K., Lindholm, B. & Edebo, L. Endotoxin shedding by enterobacteria: Free and cell-bound endotoxin differ in Limulus activity. *Infection and Immunity* **59**, (1991).
678. Vanaja, S. K. *et al.* Bacterial Outer Membrane Vesicles Mediate Cytosolic Localization of LPS and Caspase-11 Activation. *Cell* **165**, (2016).
679. Kell, D. B. & Pretorius, E. On the translocation of bacteria and their lipopolysaccharides between blood and peripheral locations in chronic, inflammatory diseases: the central roles of LPS and LPS-induced cell death. *Integrative Biology (United Kingdom)* **7**, (2015).
680. Weinstein, J. R., Swarts, S., Bishop, C., Hanisch, U. K. & Möller, T. Lipopolysaccharide is a frequent and significant contaminant in microglia-activating factors. *GLIA* **56**, (2008).
681. Patra, K. P. *et al.* A Protein-Conjugate Approach to Develop a Monoclonal Antibody-Based Antigen Detection Test for the Diagnosis of Human Brucellosis. *PLoS Neglected Tropical Diseases* **8**, (2014).
682. Vozza, N. F. & Feldman, M. F. Glyco-engineering O-antigen-based vaccines and diagnostics in *E. coli*. *Methods in Molecular Biology* **1321**, (2015).
683. Zhang, H., Niesel, D. W., Peterson, J. W. & Klimpel, G. R. Lipoprotein release by bacteria: Potential factor in bacterial pathogenesis. *Infection and Immunity* **66**, (1998).
684. Ried, G., Hindennach, I. & Henning, U. Role of lipopolysaccharide in assembly of *Escherichia coli* outer membrane proteins OmpA, OmpC, and OmpF. *Journal of Bacteriology* **172**, (1990).
685. Rottem, S., Markowitz, O. & Razin, S. Cerulenin-Induced Changes in the Lipopolysaccharide Content and Phospholipid Composition of *Proteus mirabilis*. *European Journal of Biochemistry* **85**, (1978).
686. Roberts, J. L. *et al.* *In Vitro* Evaluation of the Interaction of Dextrin-Colistin Conjugates with Bacterial Lipopolysaccharide. *Journal of Medicinal Chemistry* **59**, (2016).
687. Jeannot, K. *et al.* Detection of Colistin Resistance in *Pseudomonas aeruginosa* Using the MALDIxin Test on the Routine MALDI Biotyper Sirius Mass Spectrometer. *Frontiers in Microbiology* **12**, (2021).
688. Keren, I., Kaldalu, N., Spoering, A., Wang, Y. & Lewis, K. Persister cells and tolerance to antimicrobials. *FEMS Microbiology Letters* **230**, (2004).
689. Ren, H. *et al.* Gradual increase in antibiotic concentration affects persistence of *Klebsiella pneumoniae*. *J Antimicrob Chemother* **70**, (2015).
690. Ojha, A. K. *et al.* Growth of *Mycobacterium tuberculosis* biofilms containing free mycolic acids and harbouring drug-tolerant bacteria. *Molecular Microbiology* **69**, (2008).
691. Ahmad, Z. *et al.* Biphasic kill curve of isoniazid reveals the presence of drug-tolerant, not drug-resistant, *Mycobacterium tuberculosis* in the guinea pig. *Journal of Infectious Diseases* **200**, (2009).
692. Prax, M. & Bertram, R. Metabolic aspects of bacterial persisters. *Frontiers in Cellular and Infection Microbiology* vol. 4 (2014).

693. Alkasir, R. *et al.* Characterization and transcriptome analysis of *Acinetobacter baumannii* persister cells. *Microbial Drug Resistance* **24**, (2018).
694. Yokota, S. ichi *et al.* Release of large amounts of lipopolysaccharides from *Pseudomonas aeruginosa* cells reduces their susceptibility to colistin. *International Journal of Antimicrobial Agents* **51**, (2018).
695. Schneider-Futschik, E. K. *et al.* Sputum Active Polymyxin Lipopeptides: Activity against Cystic Fibrosis *Pseudomonas aeruginosa* Isolates and Their Interactions with Sputum Biomolecules. *ACS Infectious Diseases* **4**, (2018).
696. Doroshenko, N. *et al.* Extracellular DNA impedes the transport of vancomycin in *Staphylococcus epidermidis* biofilms preexposed to subinhibitory concentrations of vancomycin. *Antimicrobial Agents and Chemotherapy* **58**, (2014).
697. Colvin, K. M. *et al.* The Pel and Psl polysaccharides provide *Pseudomonas aeruginosa* structural redundancy within the biofilm matrix. *Environmental Microbiology* **14**, (2012).
698. Knecht, L. E., Veljkovic, M. & Fieseler, L. Diversity and Function of Phage Encoded Depolymerases. *Frontiers in Microbiology* vol. 10 (2020).
699. Gorelik, A., Illes, K. & Nagar, B. Crystal structure of the mammalian lipopolysaccharide detoxifier. *Proc Natl Acad Sci U S A* **115**, (2018).
700. Moubareck, C. A. Polymyxins and bacterial membranes: A review of antibacterial activity and mechanisms of resistance. *Membranes* vol. 10 (2020).
701. Kaye, K. S., Pogue, J. M., Tran, T. B., Nation, R. L. & Li, J. Agents of Last Resort: Polymyxin Resistance. *Infectious Disease Clinics of North America* vol. 30 (2016).
702. Su, M. *et al.* Polymyxin derivatives as broad-spectrum antibiotic agents. *Chemical Communications* **55**, (2019).
703. Bradley, J. S., Pong, A., Franzon, D. & Duthie, S. Bacterial Infection, Antimicrobial Use, and Antibiotic-Resistant Organisms in the Pediatric Intensive Care Unit. in *Pediatric Critical Care* (2006).
704. Yang, Q. *et al.* Balancing *mcr-1* expression and bacterial survival is a delicate equilibrium between essential cellular defence mechanisms. *Nature Communications* **8**, (2017).
705. Mohamed, Y. F., Abou-Shleib, H. M., Khalil, A. M., El-Guink, N. M. & El-Nakeeb, M. A. Membrane permeabilization of colistin toward pan-drug resistant gram-negative isolates. *Brazilian Journal of Microbiology* **47**, (2016).
706. Yu, Z., Zhu, Y., Qin, W., Yin, J. & Qiu, J. Oxidative stress induced by polymyxin E is involved in rapid killing of *Paenibacillus polymyxa*. *BioMed Research International* **2017**, (2017).
707. van der Weide, H. *et al.* Antimicrobial activity of two novel antimicrobial peptides AA139 and SET-M33 against clinically and genotypically diverse *Klebsiella pneumoniae* isolates with differing antibiotic resistance profiles. *International Journal of Antimicrobial Agents* **54**, (2019).
708. He, Y. & Lazaridis, T. Activity Determinants of Helical Antimicrobial Peptides: A Large-Scale Computational Study. *PLoS ONE* **8**, (2013).
709. Shai, Y. Mechanism of the binding, insertion and destabilization of phospholipid bilayer membranes by  $\alpha$ -helical antimicrobial and cell non-selective membrane-lytic peptides. *Biochimica et Biophysica Acta - Biomembranes* vol. 1462 (1999).
710. Betts, J. W., Sharili, A. S., la Ragione, R. M. & Wareham, D. W. *In Vitro* Antibacterial Activity of Curcumin-Polymyxin B Combinations against Multidrug-Resistant Bacteria Associated with Traumatic Wound Infections. *Journal of Natural Products* **79**, (2016).

711. Berg, J. R., Spilker, C. M. & Lewis, S. A. Effects of polymyxin B on mammalian urinary bladder. *Journal of Membrane Biology* **154**, (1996).
712. Berg, J. R., Spilker, C. M. & Lewis, S. A. Modulation of polymyxin B effects on mammalian urinary bladder. *American Journal of Physiology - Renal Physiology* **275**, (1998).
713. Lewis, J. R. & Lewis, S. A. Colistin interactions with the mammalian urothelium. *American Journal of Physiology - Cell Physiology* **286**, (2004).
714. Fu, L., Wan, M., Zhang, S., Gao, L. & Fang, W. Polymyxin B Loosens Lipopolysaccharide Bilayer but Stiffens Phospholipid Bilayer. *Biophysical Journal* **118**, (2020).
715. Khadka, N. K., Aryal, C. M. & Pan, J. Lipopolysaccharide-Dependent Membrane Permeation and Lipid Clustering Caused by Cyclic Lipopeptide Colistin. *ACS Omega* **3**, (2018).
716. Voss, B. J. & Stephen Trent, M. LPS Transport: Flipping Out over MsbA. *Current Biology* vol. 28 (2018).
717. Whitfield, C., Williams, D. M. & Kelly, S. D. Lipopolysaccharide O-antigens-bacterial glycans made to measure. *Journal of Biological Chemistry* vol. 295 (2020).
718. Han, W. *et al.* Defining function of lipopolysaccharide O-antigen ligase *waaL* using chemoenzymatically synthesized substrates. *Journal of Biological Chemistry* **287**, (2012).
719. Clairfeuille, T. *et al.* Structure of the essential inner membrane lipopolysaccharide-PbgA complex. *Nature* **584**, (2020).
720. O'Driscoll, N. H., Cushnie, T. P. T., Matthews, K. H. & Lamb, A. J. Colistin causes profound morphological alteration but minimal cytoplasmic membrane perforation in populations of *Escherichia coli* and *Pseudomonas aeruginosa*. *Archives of Microbiology* **200**, (2018).
721. Lima, F. C. G. de *et al.* Ultrastructural changes caused by the combination of intravenous immunoglobulin with meropenem, amikacin and colistin in multidrug-resistant *Acinetobacter baumannii*. *Microbial Pathogenesis* **149**, (2020).
722. Watt, S. R. & Clarke, A. J. Role of autolysins in the EDTA-induced lysis of *Pseudomonas aeruginosa*. *FEMS Microbiology Letters* **124**, (1994).
723. Banin, E., Brady, K. M. & Greenberg, E. P. Chelator-induced dispersal and killing of *Pseudomonas aeruginosa* cells in a biofilm. *Applied and Environmental Microbiology* **72**, (2006).
724. Evans, D. J., Brown, M. R. W., Allison, D. G. & Gilbert, P. Susceptibility of bacterial biofilms to tobramycin: Role of specific growth rate and phase in the division cycle. *Journal of Antimicrobial Chemotherapy* **25**, (1990).
725. Lee, A. J. *et al.* Robust, linear correlations between growth rates and  $\beta$ -lactam-mediated lysis rates. *Proc Natl Acad Sci U S A* **115**, (2018).
726. Martini, C. L. *et al.* Cellular Growth Arrest and Efflux Pumps Are Associated With Antibiotic Persists in *Streptococcus pyogenes* Induced in Biofilm-Like Environments. *Frontiers in Microbiology* **12**, (2021).
727. David, H. L. & Rastogi, N. Antibacterial action of colistin (polymyxin E) against *Mycobacterium aurum*. *Antimicrobial Agents and Chemotherapy* **27**, (1985).
728. Metruccio, M. M. E., Evans, D. J., Gabriel, M. M., Kadurugamuwa, J. L. & Fleiszig, S. M. J. *Pseudomonas aeruginosa* outer membrane vesicles triggered by human mucosal fluid and lysozyme can prime host tissue surfaces for bacterial adhesion. *Frontiers in Microbiology* **7**, (2016).
729. Cannatelli, A. *et al.* An allelic variant of the PmrB sensor kinase responsible for colistin resistance in an *Escherichia coli* strain of clinical origin. *Scientific Reports* **7**, (2017).



730. Goldberg, S. D., Clinthorne, G. D., Goulian, M. & DeGrado, W. F. Transmembrane polar interactions are required for signaling in the *Escherichia coli* sensor kinase PhoQ. *Proc Natl Acad Sci U S A* **107**, (2010).
731. Choi, J. & Groisman, E. A. The lipopolysaccharide modification regulator PmrA limits *Salmonella* virulence by repressing the type three-secretion system Spi/Ssa. *Proc Natl Acad Sci U S A* **110**, (2013).
732. Kato, A., Chen, H. D., Latifi, T. & Groisman, E. A. Reciprocal Control between a Bacterium's Regulatory System and the Modification Status of Its Lipopolysaccharide. *Molecular Cell* **47**, (2012).
733. Rao, M. S. *et al.* Novel Computational Approach to Predict Off-Target Interactions for Small Molecules. *Frontiers in Big Data* **2**, (2019).
734. Tsubery, H., Ofek, I., Cohen, S. & Fridkin, M. Structure - Function studies of Polymyxin B nonapeptide: Implications to sensitization of Gram-negative bacteria. *Journal of Medicinal Chemistry* **43**, (2000).
735. Vaara, M. & Viljanen, P. Binding of polymyxin B nonapeptide to gram-negative bacteria. *Antimicrobial Agents and Chemotherapy* **27**, (1985).
736. Moison, E. *et al.* A Fluorescent Probe Distinguishes between Inhibition of Early and Late Steps of Lipopolysaccharide Biogenesis in Whole Cells. *ACS Chemical Biology* **12**, (2017).
737. Soon, R. L. *et al.* Design, synthesis, and evaluation of a new fluorescent probe for measuring polymyxin-lipopolysaccharide binding interactions. *Analytical Biochemistry* **409**, (2011).
738. Figueroa, D. M., Wade, H. M., Montales, K. P., Elmore, D. E. & Darling, L. E. O. Production and visualization of bacterial spheroplasts and protoplasts to characterize antimicrobial peptide localization. *Journal of Visualized Experiments* **2018**, (2018).
739. Panta, P. R. & Doerrler, W. T. A link between pH homeostasis and colistin resistance in bacteria. *Scientific Reports* **11**, (2021).
740. Green, D. A. *et al.* Evaluation of calcium-enhanced media for colistin susceptibility testing by gradient agar diffusion and broth microdilution. *Journal of Clinical Microbiology* **58**, (2020).
741. Vaara, M. Polymyxins and their potential next generation as therapeutic antibiotics. *Frontiers in Microbiology* vol. 10 (2019).
742. Heath, R. J., Yu, Y. T., Shapiro, M. A., Olson, E. & Rock, C. O. Broad spectrum antimicrobial biocides target the FabI component of fatty acid synthesis. *Journal of Biological Chemistry* **273**, (1998).
743. Heath, R. J. *et al.* Mechanism of triclosan inhibition of bacterial fatty acid synthesis. *Journal of Biological Chemistry* **274**, (1999).
744. Sivaraman, S. *et al.* Inhibition of the Bacterial Enoyl Reductase FabI by Triclosan: A Structure-Reactivity Analysis of FabI Inhibition by Triclosan Analogues. *Journal of Medicinal Chemistry* **47**, (2004).
745. Huang, Y. H., Lin, J. S., Ma, J. C. & Wang, H. H. Functional characterization of triclosan-resistant enoyl-acyl-carrier protein reductase (*fabV*) in *Pseudomonas aeruginosa*. *Frontiers in Microbiology* **7**, (2016).
746. Lobritz, M. A. *et al.* Antibiotic efficacy is linked to bacterial cellular respiration. *Proc Natl Acad Sci U S A* **112**, (2015).
747. Kawai, Y. *et al.* Crucial role for central carbon metabolism in the bacterial L-form switch and killing by  $\beta$ -lactam antibiotics. *Nature Microbiology* **4**, (2019).

748. Hurdle, J. G., O'Neill, A. J., Chopra, I. & Lee, R. E. Targeting bacterial membrane function: An underexploited mechanism for treating persistent infections. *Nature Reviews Microbiology* vol. 9 (2011).
749. Chen, X., Zhang, M., Zhou, C., Kallenbach, N. R. & Ren, D. Control of bacterial persister cells by Trp/Arg-containing antimicrobial peptides. *Applied and Environmental Microbiology* 77, (2011).
750. Grassi, L. *et al.* Generation of persister cells of *Pseudomonas aeruginosa* and *Staphylococcus aureus* by chemical treatment and evaluation of their susceptibility to membrane-targeting agents. *Frontiers in Microbiology* 8, (2017).
751. Chua, S. L. *et al.* Selective labelling and eradication of antibiotic-tolerant bacterial populations in *Pseudomonas aeruginosa* biofilms. *Nature Communications* 7, (2016).
752. Petrosillo, N., Ioannidou, E. & Falagas, M. E. Colistin monotherapy vs. combination therapy: Evidence from microbiological, animal and clinical studies. *Clinical Microbiology and Infection* vol. 14 (2008).
753. Durante-Mangoni, E. *et al.* Colistin and rifampicin compared with colistin alone for the treatment of serious infections due to extensively drug-resistant *Acinetobacter baumannii*: A multicenter, randomized clinical trial. *Clinical Infectious Diseases* 57, (2013).
754. Park, H. J. *et al.* Colistin monotherapy versus colistin/rifampicin combination therapy in pneumonia caused by colistin-resistant *Acinetobacter baumannii*: A randomised controlled trial. *Journal of Global Antimicrobial Resistance* 17, (2019).
755. Osborn, M. J., Gander, J. E., Parisi, E. & Carson, J. Mechanism of assembly of the outer membrane of *Salmonella typhimurium*. Isolation and characterization of cytoplasmic and outer membrane. *Journal of Biological Chemistry* 247, (1972).
756. Gharaibeh, M. H. & Shatnawi, S. Q. An overview of colistin resistance, mobilized colistin resistance genes dissemination, global responses, and the alternatives to colistin: A review. *Veterinary World* vol. 12 (2019).
757. Haas, G. J. & Sevag, M. G. Critical role of amino acids on the sensitivity and development of resistance to polymyxin B. *Archives of Biochemistry and Biophysics* 43, (1953).
758. Li, Z., Cao, Y., Yi, L., Liu, J. H. & Yang, Q. Emergent Polymyxin Resistance: End of an Era? *Open Forum Infectious Diseases* vol. 6 (2019).
759. Rossi, F. *et al.* Emergence of colistin resistance in the largest university hospital complex of São Paulo, Brazil, over five years. *Brazilian Journal of Infectious Diseases* 21, (2017).
760. Battikh, H. *et al.* Clonal Spread of Colistin-Resistant *Klebsiella pneumoniae* Coproducing KPC and VIM Carbapenemases in Neonates at a Tunisian University Hospital. *Microbial Drug Resistance* 23, (2017).
761. Giacobbe, D. R. *et al.* Risk factors for bloodstream infections due to colistin-resistant KPC-producing *Klebsiella pneumoniae*: Results from a multicenter case-control study. *Clinical Microbiology and Infection* 21, (2015).
762. Walia, K., Sharma, M., Vijay, S. & Shome, B. R. Understanding policy dilemmas around antibiotic use in food animals & offering potential solutions. *Indian Journal of Medical Research* vol. 149 (2019).
763. Davies, M. & Walsh, T. R. A colistin crisis in India. *The Lancet. Infectious diseases* vol. 18 (2018).
764. Kuo, S. C. *et al.* Colistin resistance gene *mcr-1* in *Escherichia coli* isolates from humans and retail meats, Taiwan. *Journal of Antimicrobial Chemotherapy* vol. 71 (2016).

765. European Centre for Disease Prevention and Control. Surveillance of antimicrobial resistance in Europe—annual report of the European antimicrobial resistance surveillance network (EARS-Net) 2017. *ECDC: Surveillance Report* (2018).
766. Liu, C., Sun, D., Zhu, J. & Liu, W. Two-component signal transduction systems: A major strategy for connecting input stimuli to biofilm formation. *Frontiers in Microbiology* vol. 10 (2019).
767. Bretl, D. J., Demetriadou, C. & Zahrt, T. C. Adaptation to Environmental Stimuli within the Host: Two-Component Signal Transduction Systems of *Mycobacterium tuberculosis*. *Microbiology and Molecular Biology Reviews* **75**, (2011).
768. Choi, E., Groisman, E. A. & Shin, D. Activated by different signals, the PhoP/PhoQ two-component system differentially regulates metal uptake. *Journal of Bacteriology* **191**, (2009).
769. Yuan, J., Jin, F., Glatter, T. & Sourjik, V. Osmosensing by the bacterial PhoQ/PhoP two-component system. *Proc Natl Acad Sci U S A* **114**, (2017).
770. Sinha, A. *et al.* PmrC (EptA) and CptA negatively affect outer membrane vesicle production in *Citrobacter rodentium*. *Journal of Bacteriology* **201**, (2019).
771. Aghapour, Z. *et al.* Molecular mechanisms related to colistin resistance in Enterobacteriaceae. *Infection and Drug Resistance* vol. 12 (2019).
772. Zelendova, M. *et al.* Characterization of the Complete Nucleotide Sequences of *mcr-1*-Encoding Plasmids From Enterobacterales Isolates in Retailed Raw Meat Products From the Czech Republic. *Frontiers in Microbiology* **11**, (2021).
773. Strepis, N. *et al.* Genetic Analysis of *mcr-1*-Carrying Plasmids From Gram-Negative Bacteria in a Dutch Tertiary Care Hospital: Evidence for Intrapatient and Interspecies Transmission Events. *Frontiers in Microbiology* **12**, (2021).
774. Hussein, N. H., AL-Kadmy, I. M. S., Taha, B. M. & Hussein, J. D. Mobilized colistin resistance (*mcr*) genes from 1 to 10: a comprehensive review. *Molecular Biology Reports* vol. 48 (2021).
775. Macesic, N. *et al.* Silent spread of mobile colistin resistance gene *mcr-9.1* on IncHI2 ‘superplasmids’ in clinical carbapenem-resistant Enterobacterales. *Clinical Microbiology and Infection* **27**, (2021).
776. Torres, D. A. *et al.* Colistin resistance in Gram-negative bacteria analysed by five phenotypic assays and inference of the underlying genomic mechanisms. *BMC Microbiology* **21**, (2021).
777. El-Halfawy, O. M. & Valvano, M. A. Antimicrobial heteroresistance: An emerging field in need of clarity. *Clinical Microbiology Reviews* vol. 28 (2015).
778. Band, V. I. *et al.* Colistin heteroresistance is largely undetected among carbapenem-resistant Enterobacterales in the United States. *mBio* **12**, (2021).
779. Sherman, E. X., Wozniak, J. E. & Weiss, D. S. Methods to evaluate colistin heteroresistance in *Acinetobacter baumannii*. in *Methods in Molecular Biology* vol. 1946 (2019).
780. Napier, B. A., Band, V., Burd, E. M. & Weiss, D. S. Colistin heteroresistance in *Enterobacter cloacae* is associated with cross-resistance to the host antimicrobial lysozyme. *Antimicrobial Agents and Chemotherapy* **58**, (2014).
781. Cheong, H. S., Kim, S. Y., Wi, Y. M., Peck, K. R. & Ko, K. S. Colistin heteroresistance in *Klebsiella pneumoniae* isolates and diverse mutations of PmrAB and PhoPQ in resistant subpopulations. *Journal of Clinical Medicine* **8**, (2019).
782. Band, V. I. & Weiss, D. S. Heteroresistance: A cause of unexplained antibiotic treatment failure? *PLoS Pathogens* **15**, (2019).

783. Band, V. I. *et al.* Carbapenem-resistant *Klebsiella pneumoniae* exhibiting clinically undetected colistin heteroresistance leads to treatment failure in a murine model of infection. *mBio* **9**, (2018).
784. Simpson, B. W. & Trent, M. S. Pushing the envelope: LPS modifications and their consequences. *Nature Reviews Microbiology* vol. 17 (2019).
785. Hinchliffe, P. *et al.* Insights into the Mechanistic Basis of Plasmid-Mediated Colistin Resistance from Crystal Structures of the Catalytic Domain of MCR-1. *Scientific Reports* **7**, (2017).
786. Li, B. *et al.* Colistin Resistance Gene *mcr-1* Mediates Cell Permeability and Resistance to Hydrophobic Antibiotics. *Frontiers in Microbiology* **10**, (2020).
787. Yan, A., Guan, Z. & Raetz, C. R. H. An undecaprenyl phosphate-aminoarabinose flippase required for polymyxin resistance in *Escherichia coli*. *Journal of Biological Chemistry* **282**, (2007).
788. Dortet, L. *et al.* Rapid detection and discrimination of chromosome-And MCR-plasmid-mediated resistance to polymyxins by MALDI-TOF MS in *Escherichia coli*: The MALDIxin test. *Journal of Antimicrobial Chemotherapy* **73**, (2018).
789. Luo, Q., Wang, Y. & Xiao, Y. Prevalence and transmission of mobilized colistin resistance (*mcr*) gene in bacteria common to animals and humans. *Biosafety and Health* vol. 2 (2020).
790. Andrews, J. M. BSAC standardized disc susceptibility testing method (version 4). *Journal of Antimicrobial Chemotherapy* vol. 56 (2005).
791. Joo, H. S., Fu, C. I. & Otto, M. Bacterial strategies of resistance to antimicrobial peptides. *Philosophical Transactions of the Royal Society B: Biological Sciences* **371**, (2016).
792. Mishra, N. N. *et al.* Carotenoid-related alteration of cell membrane fluidity impacts *Staphylococcus aureus* susceptibility to host defense peptides. *Antimicrobial Agents and Chemotherapy* **55**, (2011).
793. Chapman, M. R., Lam, K. L. H., Waring, A. J., Lehrer, R. I. & Lee, K. Y. C. The Origin of Antimicrobial Resistance and Fluidity Dependent Membrane Structural Transformation by Antimicrobial Peptide Protegrin-1. *Biophysical Journal* **96**, (2009).
794. Simcock, P. W. *et al.* Membrane Binding of Antimicrobial Peptides Is Modulated by Lipid Charge Modification. *Journal of Chemical Theory and Computation* **17**, (2021).
795. Etzerodt, T., Henriksen, J. R., Rasmussen, P., Clausen, M. H. & Andresen, T. L. Selective acylation enhances membrane charge sensitivity of the antimicrobial peptide mastoparan-X. *Biophysical Journal* **100**, (2011).
796. Bayer, A. S., Schneider, T. & Sahl, H. G. Mechanisms of daptomycin resistance in *Staphylococcus aureus*: Role of the cell membrane and cell wall. *Ann N Y Acad Sci* **1277**, (2013).
797. Zhou, H., Fang, J., Tian, Y. & Lu, X. Y. Mechanisms of nisin resistance in Gram-positive bacteria. *Annals of Microbiology* vol. 64 (2014).
798. Chen, Y. F., Sun, T. L., Sun, Y. & Huang, H. W. Interaction of daptomycin with lipid bilayers: A lipid extracting effect. *Biochemistry* **53**, (2014).
799. Moll, G. N., Konings, W. N. & Driessen, A. J. M. The lantibiotic nisin induces transmembrane movement of a fluorescent phospholipid. *Journal of Bacteriology* **180**, (1998).
800. Bitar, I. *et al.* Detection of Five *mcr-9*-Carrying Enterobacterales Isolates in Four Czech Hospitals. *mSphere* **5**, (2020).
801. Landman, D., Salamera, J. & Quale, J. Irreproducible and uninterpretable polymyxin B MICs for *Enterobacter cloacae* and *Enterobacter aerogenes*. *Journal of Clinical Microbiology* **51**, (2013).

802. Turlej-Rogacka, A. *et al.* Evaluation of colistin stability in agar and comparison of four methods for MIC testing of colistin. *European Journal of Clinical Microbiology and Infectious Diseases* **37**, (2018).
803. Matuschek, E., Åhman, J., Webster, C. & Kahlmeter, G. Antimicrobial susceptibility testing of colistin – evaluation of seven commercial MIC products against standard broth microdilution for *Escherichia coli*, *Klebsiella pneumoniae*, *Pseudomonas aeruginosa*, and *Acinetobacter* spp. *Clinical Microbiology and Infection* **24**, (2018).
804. Mirajkar, C. J. & Gebhart, C. J. Comparison of agar dilution and antibiotic gradient strip test with broth microdilution for susceptibility testing of swine *Brachyspira* species. *Journal of Veterinary Diagnostic Investigation* **28**, (2016).
805. Guérin, F. *et al.* Cluster-dependent colistin hetero-resistance in *Enterobacter cloacae* complex. *Journal of Antimicrobial Chemotherapy* **71**, (2016).
806. Satola, S. W., Farley, M. M., Anderson, K. F. & Patel, J. B. Comparison of detection methods for heteroresistant vancomycin-intermediate *Staphylococcus aureus*, with the population analysis profile method as the reference method. *Journal of Clinical Microbiology* **49**, (2011).
807. Wootton, M. *et al.* A modified population analysis profile (PAP) method to detect hetero-resistance to vancomycin in *Staphylococcus aureus* in a UK hospital. *Journal of Antimicrobial Chemotherapy* **47**, (2001).
808. da Costa, T. M. *et al.* Clinical and microbiological characteristics of heteroresistant and vancomycin-intermediate *Staphylococcus aureus* from bloodstream infections in a Brazilian teaching hospital. *PLoS ONE* **11**, (2016).
809. Pascucci, M. *et al.* AI-based mobile application to fight antibiotic resistance. *Nature Communications* **12**, (2021).
810. Luria, S. E. & Delbrück, M. Mutations of bacteria from virus sensitivity to virus resistance. *Genetics* **28**, (1943).
811. Bachl, J., Dessing, M., Olsson, C., von Borstel, R. C. & Steinberg, C. An experimental solution for the Luria-Delbrück fluctuation problem in measuring hypermutation rates. *Proc Natl Acad Sci U S A* **96**, (1999).
812. Jones, M. E., Thomas, S. M. & Rogers, A. Luria-Delbruck fluctuation experiments: Design and analysis. *Genetics* **136**, (1994).
813. Lea, D. E. & Coulson, C. A. The distribution of the numbers of mutants in bacterial populations. *Journal of Genetics* **49**, (1949).
814. Cairns, J., Overbaugh, J. & Miller, S. The origin of mutants. *Nature* vol. 335 (1988).
815. Dalmolin, T., Lima-Morales, D. & Barth, A. Plasmid-mediated Colistin Resistance: What Do We Know? *Journal of Infectiology* **1**, (2018).
816. Binsker, U., Käsbohrer, A. & Hammerl, J. A. Global colistin use: a review of the emergence of resistant Enterobacterales and the impact on their genetic basis. *FEMS Microbiology Reviews* **46**, (2022).
817. Perez, F. & Bonomo, R. A. Colistin resistance in China: from outer membrane to One Health. *The Lancet Infectious Diseases* vol. 20 (2020).
818. Mmatli, M., Mbelle, N. M., Maningi, N. E. & Osei Sekyere, J. Emerging Transcriptional and Genomic Mechanisms Mediating Carbapenem and Polymyxin Resistance in Enterobacteriaceae : a Systematic Review of Current Reports . *mSystems* **5**, (2020).
819. MacNair, C. R. *et al.* Overcoming *mcr-1* mediated colistin resistance with colistin in combination with other antibiotics. *Nature Communications* **9**, (2018).

820. Li, X. *et al.* The Attenuated Protective Effect of Outer Membrane Vesicles Produced by a *mcr-1* Positive Strain on Colistin Sensitive *Escherichia coli*. *Frontiers in Cellular and Infection Microbiology* **11**, (2021).
821. Kim, S. *et al.* Characterization of chromosome-mediated colistin resistance in *Escherichia coli* isolates from livestock in Korea. *Infection and Drug Resistance* **12**, (2019).
822. Suzuki, S., Horinouchi, T. & Furusawa, C. Prediction of antibiotic resistance by gene expression profiles. *Nature Communications* **5**, (2014).
823. Witzky, A., Tollerson, R. & Ibba, M. Translational control of antibiotic resistance. *Open Biology* vol. 9 (2019).
824. Malik, A., Mueller-Schickert, A. & Bardwell, J. C. A. Cytosolic selection systems to study protein stability. *Journal of Bacteriology* **196**, (2014).
825. Paul, M. *et al.* Effectiveness and safety of colistin: Prospective comparative cohort study. *Journal of Antimicrobial Chemotherapy* **65**, (2010).
826. Bian, X. *et al.* Dose optimization of colistin combinations against carbapenem-resistant *Acinetobacter baumannii* from patients with hospital-acquired pneumonia in China by using an *in vitro* pharmacokinetic/pharmacodynamic model. *Antimicrobial Agents and Chemotherapy* **63**, (2019).
827. Falagas, M. E., Rafailidis, P. I., Kasiakou, S. K., Hatzopoulou, P. & Michalopoulos, A. Effectiveness and nephrotoxicity of colistin monotherapy vs. colistin-meropenem combination therapy for multidrug-resistant Gram-negative bacterial infections. *Clinical Microbiology and Infection* **12**, (2006).
828. Zhou, Y. F. *et al.* Colistin Combined With Tigecycline: A Promising Alternative Strategy to Combat *Escherichia coli* Harboring *bla*NDM-5 and *mcr-1*. *Frontiers in Microbiology* **10**, (2020).
829. Dickstein, Y. *et al.* Colistin resistance development following colistin-meropenem combination therapy versus colistin monotherapy in patients with infections caused by carbapenem-resistant organisms. *Clinical Infectious Diseases* **71**, (2020).
830. MacGowan, A. P. *et al.* *In vitro* assessment of colistin's antipseudomonal antimicrobial interactions with other antibiotics. *Clinical Microbiology and Infection* **5**, (1999).
831. Gunderson, B. W. *et al.* Synergistic activity of colistin and ceftazidime against multiantibiotic-resistant *Pseudomonas aeruginosa* in an *in vitro* pharmacodynamic model. *Antimicrobial Agents and Chemotherapy* **47**, (2003).
832. Timurkaynak, F. *et al.* *In vitro* activities of non-traditional antimicrobials alone or in combination against multidrug-resistant strains of *Pseudomonas aeruginosa* and *Acinetobacter baumannii* isolated from intensive care units. *International Journal of Antimicrobial Agents* **27**, (2006).
833. Cirioni, O. *et al.* Efficacy of colistin/rifampin combination in experimental rat models of sepsis due to a multiresistant *Pseudomonas aeruginosa* strain. *Critical Care Medicine* **35**, (2007).
834. Hill, D. *et al.* Antibiotic susceptibilities of *Pseudomonas aeruginosa* isolates derived from patients with cystic fibrosis under aerobic, anaerobic, and biofilm conditions. *Journal of Clinical Microbiology* **43**, (2005).
835. Giamarellos-Bourboulis, E. J., Sambatakou, H., Galani, I. & Giamarellou, H. *In vitro* interaction of colistin and rifampin on multidrug-resistant *Pseudomonas aeruginosa*. *Journal of Chemotherapy* **15**, (2003).

836. Tascini, C. *et al.* Microbiological activity and clinical efficacy of a colistin and rifampin combination in multidrug-resistant *Pseudomonas aeruginosa* infections. *Journal of Chemotherapy* **16**, (2004).
837. Giamarellos-Bourboulis, E. J., Xirouchaki, E. & Giamarellou, H. Interactions of colistin and rifampin on multidrug-resistant *Acinetobacter baumannii*. *Diagnostic Microbiology and Infectious Disease* **40**, (2001).
838. Hogg, G. M., Barr, J. G. & Webb, C. H. *In-vitro* activity of the combination of colistin and rifampicin against multidrug-resistant strains of *Acinetobacter baumannii*. *Journal of Antimicrobial Chemotherapy* vol. 41 (1998).
839. Tascini, C., Menichetti, F., Bozza, S., del Favero, A. & Bistoni, F. Evaluation of the activities of two-drug combinations of rifampicin, polymyxin B and ampicillin/sulbactam against *Acinetobacter baumannii*. *Journal of Antimicrobial Chemotherapy* vol. 42 (1998).
840. Lenhard, J. R., Nation, R. L. & Tsuji, B. T. Synergistic combinations of polymyxins. *International Journal of Antimicrobial Agents* **48**, (2016).
841. Saslaw, S., Carlisle, H. N. & Moheimani, M. Comparison of colistin-carbenicillin, colistin, and carbenicillin in *Pseudomonas* sepsis in monkeys. *Antimicrob Agents Chemother* **3**, (1973).
842. Cirioni, O. *et al.* Efficacy of tachyplesin III, colistin, and imipenem against a multiresistant *Pseudomonas aeruginosa* strain. *Antimicrobial Agents and Chemotherapy* **51**, (2007).
843. Montero, A. *et al.* Antibiotic combinations for serious infections caused by carbapenem-resistant *Acinetobacter baumannii* in a mouse pneumonia model. *Journal of Antimicrobial Chemotherapy* **54**, (2004).
844. Pantopoulou, A. *et al.* Colistin offers prolonged survival in experimental infection by multidrug-resistant *Acinetobacter baumannii*: the significance of co-administration of rifampicin. *International Journal of Antimicrobial Agents* **29**, (2007).
845. Giacometti, A. *et al.* Antiendotoxin activity of antimicrobial peptides and glycopeptides. *Journal of Chemotherapy* **15**, (2003).
846. Tascini, C. *et al.* Clinical and microbiological efficacy of colistin therapy alone or in combination as treatment for multidrug resistant *Pseudomonas aeruginosa* diabetic foot infections with or without osteomyelitis. *Journal of Chemotherapy* **18**, (2006).
847. Vaara, M. & Vaara, T. Sensitization of Gram-negative bacteria to antibiotics and complement by a nontoxic oligopeptide. *Nature* **303**, (1983).
848. Macnair, C. R. & Brown, E. D. Outer membrane disruption overcomes intrinsic, acquired, and spontaneous antibiotic resistance. *mBio* **11**, (2020).
849. Meletiadis, J., Pournaras, S., Roilides, E. & Walsh, T. J. Defining fractional inhibitory concentration index cutoffs for additive interactions based on self-drug additive combinations, Monte Carlo simulation analysis, and *in vitro-in vivo* correlation data for antifungal drug combinations against *Aspergillus fumigatus*. *Antimicrobial Agents and Chemotherapy* **54**, (2010).
850. Bononi, I., Balatti, V., Gaeta, S. & Tognon, M. Gram-negative bacterial lipopolysaccharide retention by a positively charged new-generation filter. *Applied and Environmental Microbiology* **74**, (2008).
851. Schromm, A. B. *et al.* The charge of endotoxin molecules influences their conformation and IL-6-inducing capacity. *J Immunol* **161**, (1998).
852. Emiola, A., Andrews, S. S., Heller, C. & George, J. Crosstalk between the lipopolysaccharide and phospholipid pathways during outer membrane biogenesis in *Escherichia coli*. *Proc Natl Acad Sci U S A* **113**, (2016).

853. Bertani, B. & Ruiz, N. Function and Biogenesis of Lipopolysaccharides. *EcoSal Plus* **8**, (2018).
854. Jensen, T. *et al.* Colistin inhalation therapy in cystic fibrosis patients with chronic *Pseudomonas aeruginosa* lung infection. *Journal of Antimicrobial Chemotherapy* **19**, (1987).
855. Hodson, M. E., Gallagher, C. G. & Govan, J. R. W. A randomised clinical trial of nebulised tobramycin or colistin in cystic fibrosis. *European Respiratory Journal* **20**, (2002).
856. Haseeb, A. *et al.* Dose Optimization of Colistin: A Systematic Review. *Antibiotics* vol. 10 (2021).
857. Lambert, P. A. Cellular impermeability and uptake of biocides and antibiotics in Gram-positive bacteria and mycobacteria. in *Journal of Applied Microbiology Symposium Supplement* vol. 92 (2002).
858. Drapeau, C. M. J., Grilli, E. & Petrosillo, N. Rifampicin combined regimens for Gram-negative infections: data from the literature. *International Journal of Antimicrobial Agents* **35**, (2010).
859. Mohammadi, M. *et al.* Synergistic Effect of Colistin and Rifampin Against Multidrug Resistant *Acinetobacter baumannii*: A Systematic Review and Meta-Analysis. *The Open Microbiology Journal* **11**, (2017).
860. Lee, H. J. *et al.* Synergistic activity of colistin and rifampin combination against multidrug-resistant *Acinetobacter baumannii* in an *in vitro* pharmacokinetic/pharmacodynamic model. *Antimicrobial Agents and Chemotherapy* **57**, (2013).
861. Zhang, H. & Zhang, Q. Clinical efficacy and safety of colistin treatment in patients with pulmonary infection caused by *Pseudomonas aeruginosa* or *Acinetobacter baumannii*: A meta-analysis. *Archives of Medical Science* vol. 11 (2015).
862. Zaidi, S. T. R., al Omran, S., al Aithan, A. S. M. & al Sultan, M. Efficacy and safety of low-dose colistin in the treatment for infections caused by multidrug-resistant gram-negative bacteria. *Journal of Clinical Pharmacy and Therapeutics* **39**, (2014).
863. Theuretzbacher, U., Outtersson, K., Engel, A. & Karlén, A. The global preclinical antibacterial pipeline. *Nature Reviews Microbiology* vol. 18 (2020).
864. Venkatesan, P. WHO 2020 report on the antibacterial production and development pipeline. *The Lancet Microbe* **2**, (2021).
865. Ordooei Javan, A., Shokouhi, S. & Sahraei, Z. A review on colistin nephrotoxicity. *European Journal of Clinical Pharmacology* vol. 71 (2015).
866. Dijksteel, G. S., Ulrich, M. M. W., Middelkoop, E. & Boekema, B. K. H. L. Review: Lessons Learned From Clinical Trials Using Antimicrobial Peptides (AMPs). *Frontiers in Microbiology* vol. 12 (2021).
867. Gai, Z., Samodelov, S. L., Kullak-Ublick, G. A. & Visentin, M. Molecular Mechanisms of Colistin-Induced Nephrotoxicity. *Molecules (Basel, Switzerland)* vol. 24 (2019).
868. Michalopoulos, A. & Papadakis, E. Inhaled anti-infective agents: Emphasis on colistin. *Infection* vol. 38 (2010).
869. Mouton, J. W. Combination therapy as a tool to prevent emergence of bacterial resistance. in *Infection* vol. 27 (1999).
870. Angst, D. C., Tepekule, B., Sun, L., Bogos, B. & Bonhoeffer, S. Comparing treatment strategies to reduce antibiotic resistance in an *in vitro* epidemiological setting. *Proc Natl Acad Sci U S A* **118**, (2021).
871. Guest, R. L., Guerra, D. S., Wissler, M., Grimm, J. & Silhavy, T. J. YejM modulates activity of the YciM/FtsH protease complex to prevent lethal accumulation of lipopolysaccharide. *mBio* **11**, (2020).



872. Fivenson, E. M. & Bernhardt, T. G. An essential membrane protein modulates the proteolysis of LpxC to control lipopolysaccharide synthesis in *Escherichia coli*. *mBio* **11**, (2020).
873. O'Rourke, A. *et al.* Mechanism-of-action classification of antibiotics by global transcriptome profiling. *Antimicrobial Agents and Chemotherapy* **64**, (2020).
874. Mishra, N. N. & Bayer, A. S. Correlation of cell membrane lipid profiles with daptomycin resistance in methicillin-resistant *Staphylococcus aureus*. *Antimicrobial Agents and Chemotherapy* **57**, (2013).
875. Mishra, N. N. *et al.* *In Vitro* cross-resistance to daptomycin and host defense cationic antimicrobial peptides in clinical methicillin-resistant *Staphylococcus aureus* isolates. *Antimicrobial Agents and Chemotherapy* **55**, (2011).
876. Casadei, M. A., Mañas, P., Niven, G., Needs, E. & Mackey, B. M. Role of membrane fluidity in pressure resistance of *Escherichia coli* NCTC 8164. *Applied and Environmental Microbiology* **68**, (2002).
877. Romano, K. P. *et al.* Mutations in *pmrB* Confer Cross-Resistance between the LptD Inhibitor POL7080 and Colistin in *Pseudomonas aeruginosa*. *Antimicrobial Agents and Chemotherapy* **63**, (2019).
878. Brennan-Krohn, T., Pironti, A. & Kirby, J. E. Synergistic activity of colistin-containing combinations against colistin-resistant Enterobacteriaceae. *Antimicrobial Agents and Chemotherapy* **62**, (2018).
879. Gogry, F. A., Siddiqui, M. T., Sultan, I. & Haq, Q. M. R. Current Update on Intrinsic and Acquired Colistin Resistance Mechanisms in Bacteria. *Frontiers in Medicine* vol. 8 (2021).
880. Ma, W. *et al.* Biophysical Impact of Lipid A Modification Caused by Mobile Colistin Resistance Gene on Bacterial Outer Membranes. *Journal of Physical Chemistry Letters* **12**, (2021).
881. Sondhi, P., Maruf, M. H. U. & Stine, K. J. Nanomaterials for biosensing lipopolysaccharide. *Biosensors* vol. 10 (2020).
882. Powers, M. J. & Trent, M. S. Phospholipid retention in the absence of asymmetry strengthens the outer membrane permeability barrier to last-resort antibiotics. *Proc Natl Acad Sci U S A* **115**, (2018).
883. Malinverni, J. C. & Silhavy, T. J. An ABC transport system that maintains lipid asymmetry in the Gram-negative outer membrane. *Proc Natl Acad Sci U S A* **106**, (2009).
884. Sutterlin, H. A. *et al.* Disruption of lipid homeostasis in the Gram-negative cell envelope activates a novel cell death pathway. *Proc Natl Acad Sci U S A* **113**, (2016).
885. Tune, B. M. Nephrotoxicity of beta-lactam antibiotics: Mechanisms and strategies for prevention. in *Pediatric Nephrology* vol. 11 (1997).
886. Simpson, B. W., Douglass, M. v. & Stephen Trent, M. Restoring balance to the outer membrane: YejM's role in LPS regulation. *mBio* **11**, (2020).
887. Klein, G. & Raina, S. Regulated assembly of LPS, its structural alterations and cellular response to LPS defects. *International Journal of Molecular Sciences* vol. 20 (2019).
888. Huan, Y., Kong, Q., Mou, H. & Yi, H. Antimicrobial Peptides: Classification, Design, Application and Research Progress in Multiple Fields. *Frontiers in Microbiology* vol. 11 (2020).
889. Stark, M., Liu, L. P. & Deber, C. M. Cationic hydrophobic peptides with antimicrobial activity. *Antimicrobial Agents and Chemotherapy* **46**, (2002).
890. Brogden, K. A. Antimicrobial peptides: Pore formers or metabolic inhibitors in bacteria? *Nature Reviews Microbiology* vol. 3 (2005).

891. Duwadi, D. *et al.* Identification and screening of potent antimicrobial peptides in arthropod genomes. *Peptides (N.Y.)* **103**, (2018).
892. Hanson, M. A. *et al.* Synergy and remarkable specificity of antimicrobial peptides *in vivo* using a systematic knockout approach. *Elife* **8**, (2019).
893. Dobias, J., Poirel, L. & Nordmann, P. Cross-resistance to human cationic antimicrobial peptides and to polymyxins mediated by the plasmid-encoded MCR-1? *Clinical Microbiology and Infection* **23**, (2017).
894. Muhlebach, M. S. & Noah, T. L. Endotoxin activity and inflammatory markers in the airways of young patients with cystic fibrosis. *American Journal of Respiratory and Critical Care Medicine* **165**, (2002).
895. Tsubery, H., Ofek, I., Cohen, S. & Fridkin, M. N-terminal modifications of Polymyxin B nonapeptide and their effect on antibacterial activity. *Peptides (N.Y.)* **22**, (2001).
896. Vaara, M. Polymyxin derivatives that sensitize Gram-negative bacteria to other antibiotics. *Molecules* vol. 24 (2019).
897. Bauldoff, G. S., Nunley, D. R., Manzetti, J. D., Dauber, J. H. & Keenan, R. J. Use of aerosolized colistin sodium in cystic fibrosis patients awaiting lung transplantation. *Transplantation* **64**, (1997).
898. Porro, C. *et al.* Pro-inflammatory effect of cystic fibrosis sputum microparticles in the murine lung. *Journal of Cystic Fibrosis* **12**, (2013).
899. Cantin, A. M., Hartl, D., Konstan, M. W. & Chmiel, J. F. Inflammation in cystic fibrosis lung disease: Pathogenesis and therapy. *Journal of Cystic Fibrosis* vol. 14 (2015).
900. Brown, R. L., Yeung Larkinson, M. L. & Clarke, T. B. Immunological design of commensal communities to treat intestinal infection and inflammation. *PLoS Pathogens* **17**, (2021).
901. Yao, J. & Rock, C. O. How bacterial pathogens eat host lipids: Implications for the development of fatty acid synthesis therapeutics. *Journal of Biological Chemistry* vol. 290 (2015).
902. Baker, L. Y. *et al.* *Pseudomonas aeruginosa* responds to exogenous polyunsaturated fatty acids (PUFAs) by modifying phospholipid composition, membrane permeability, and phenotypes associated with virulence. *BMC Microbiology* **18**, (2018).